

# PSEUDO-NATURAL PRODUCTS VIA PICTET-SPENGLER REACTION AND DEAROMATIZATION

Dissertation

zur Erlangung des akademischen Grades eines  
Doktors der Naturwissenschaften (Dr. rer. nat.)  
der Fakultät für Chemie und Chemische Biologie  
an der Technischen Universität Dortmund

vorgelegt von

**M. Sc. Annina Burhop**

Geboren am 09.03.1992  
in Hoya (Weser), Niedersachsen

Dortmund 2020



Die vorliegende Arbeit entstand im Zeitraum von April 2017 bis November 2020 unter der Anleitung von Prof. Dr. Dr. h.c. Herbert Waldmann an der Fakultät für Chemie und Chemische Biologie der Technischen Universität Dortmund und dem Max-Planck-Institut für molekulare Physiologie Dortmund.

1. Gutachter: Prof. Dr. Dr. h.c. Herbert Waldmann

2. Gutachter: Dr. Andreas Brunschweiler



Results presented in this dissertation contributed to the following publications:

A. Burhop, M. Grigalunas, S. Bag, A. Pahl, S. Sievers, A. P. Antonchick, H. Waldmann, "Synthesis of Indofulvin Pseudo-Natural Products Yields a New Autophagy Inhibitor Chemotype", *in preparation*

M. Grigalunas, A. Burhop, S. Zinken, A. Pahl, S. Sievers, D. J. Foley, A. P. Antonchick, H. Waldmann, "Natural Product Fragment Combination to Performance-Diverse Pseudo-Natural Products", *Nat. Commun.*, *under revision*

T. Schneidewind, A. Brause, A. Pahl, A. Burhop, T. Mejuch, S. Sievers, H. Waldmann, S. Ziegler, "Morphological Profiling Identifies a Common Mode of Action for Small Molecules with Different Targets", *Chem. Bio. Chem.*, **2020**, <https://doi.org/10.1002/cbic.202000381>

Results presented in this dissertation may also be found in the following bachelor/ master theses:

J. Hoock, "Synthesis of Complex Indoline Pseudo-Natural products", Master Thesis, 2020

S. Woitalla, "Derivatisierung und biologische Evaluierung eines spiro-Indolygriseofulvin-Pseudonaturstoffes", *Bachelor Thesis*, **2019**

P. Bodenbinder, Synthese einer Substanzbibliothek von Derivaten eines Pseudo-Naturstoffs mit biologischer Aktivität durch *de novo* Kombination von Naturstofffragmenten, *Bachelor Thesis*, **2018**



# ACKNOWLEDGEMENT

I had a great time at the Max Planck institute over the last years and will hold it in grateful memory. For me, it was the best place that I could have imagined to perform my Ph.D., and I would like to thank everyone responsible for this.

Starting with Prof. Dr. Dr. h. c. Herbert Waldmann, my supervisor, who enabled my doctoral studies in his group and all the privileges connected to this. I could not have wished for a better supervisor and am very grateful for the opportunities that were presented to me in this position. While working very independently I learned more than I could have thought of, but I felt always assured that his support would be there if needed. The access to the outstanding scientific environment of the Max Planck Institute and the latest state-of-the-art equipment played a crucial role in my scientific development and enabled my project to be where it is today.

Additionally, I am grateful to Dr. Andreas Brunschweiger for taking over the responsibilities as my second examiner. I appreciated our collaboration on different natural product fragments for potential immobilization on DNA.

A special thanks goes to Dr. Michael Grigalunas for his great company and daily support. Over the last three years you have not only been my labmate and supporter, but become a really good friend of mine. I truly hope we never lose sight of each other.

My deep gratitude goes to the students and trainees that worked together with me. Joseph Hooch was mainly responsible for all the advances with the  $\gamma$ -pyrone annulation on indole-containing libraries. Patrick Eisenberg, Pia Bodenbinder, and Sophie Woitalla were involved in the pseudo-natural product library synthesis via oxa-Pictet-Spengler reaction. I was blessed with all the help in the lab and without them I would never been able to generate such a comprehensive compound collection. I wish you all the best.

I want to acknowledge the whole pseudo-natural product team which has grown a lot over the last three years. Thanks for every helpful scientific discussion, the mutual support, and every starting material that was shared or provided. In this context, I want to emphasize Dr. Sukdev Bag who derivatized the chlorine on my pseudo-natural product.

Furthermore, I would like to express my gratitude to the whole cell painting taskforce, including Dr. Andreas Christoforow, Dr. Gregor Cremosnik, Dr. Michael Grigalunas, Dr. Axel Pahl, Tabea Schneidewind, Julian Wilke, Dr. Slava Ziegler, and Sarah Zinken, for all the fruitful discussion. I really enjoyed working on this project, and the team was a major reason for this.

I would like to thank every member of the Compound Management and Screening Center for the implementation of the biological evaluation of my compounds. A special thanks goes to Dr. Sonja Sievers who was a great contact for all biology related questions and Dr. Axel Pahl who was primarily responsible for the cell painting assay and the corresponding analysis.

I knew that I was never alone when it came to scientific questions and that I always had a number of contacts available. In this context, I would like to highlight Dr. Andrey Antonchick and Dr. Luis Bering for their helpful support with chemical issues and Julian Wilke, Tabea Schneidewind, Jana Flegel, as well as Dr. Slava Ziegler for answering any biological questions.

I would like to thank everyone responsible for the analytic support with the Max Planck Institute Dortmund. Therefore, I would like to highlight Jens Warmers for the maintenance of almost all instruments, Dr. Petra Janning and her team for HRMS measurements and Bernhard Griewel, as well as the NMR-Team of the TU Dortmund for the performance of all NMR experiments.

Moreover, I really enjoyed my functions in different organizations, such as the International Chemical Biology Society (ICBS) Student Chapter Dortmund and the PhDnet of our institute. Namely, I would like to thank Dr. Elena Reckzeh, Dr. Michael Winzker, Jana Flegel, Tabea Schneidewind, and Elisabeth Hennes for their great work.

I am fortunate to perform my Ph.D. in a highly international and collegial environment. I am glad to have gotten to know each and every one of colleges at the Max Planck Institute, but especially everyone from department IV. The regular barbeque parties and the evenings on the roof terrace will remain in my memory for a long time. Even though I am looking forward to everything the future holds for me, I am going to miss my great colleagues.

I even count some of my colleagues among my friends today including Jana Flegel, Tabea Schneidewind, Nadine Kaiser, Michael Grigalunas, Andreas Christoforow, and Stefan Zimmermann. I am so glad to have met you. For this alone it was worthwhile to come to the Ruhr area.

Am Schluss möchte ich mich bei Gerrit bedanken, dessen Ermutigung, Bestätigung und Unterstützung so viel wert sind. Ich kann mich immer auf dich verlassen und du bist jederzeit für mich da! Die letzten Worte des Dankes möchte ich an meine Familie, meine Eltern und meine Schwester, richten. Ich möchte, dass ihr wisst, wie unschätzbar wertvoll eure Unterstützung für mich ist. Ohne euch hätte ich es nicht geschafft, heute hier zu stehen.







# Contents

Acknowledgement.....	VII
Abstract.....	3
Kurzzusammenfassung.....	5
1. Introduction.....	7
1.1. Design approaches for small molecule libraries.....	7
1.1.1. Pseudo-Natural products.....	13
1.2. Complexity-generating reactions.....	17
1.2.1. Pictet-Spengler reaction.....	18
1.2.2. Dearomatization.....	19
1.3. Biological evaluation.....	21
1.3.1. Phenotypic screening.....	21
1.3.2. Morphological Profiling: Cell Painting Assay.....	22
1.4. Autophagy and its regulation.....	24
2. Aim of the thesis.....	27
3. Results and Discussion.....	28
3.1. Pseudo-NPs via Pictet-Spengler reaction.....	28
3.1.1. Library Design.....	28
3.1.2. Method development.....	31
3.1.3. Substrate Scope.....	33
3.1.4. Diastereoselectivity.....	54
3.1.5. Cheminformatics.....	55
3.2. Dearomatisation.....	57
3.2.1. Library Design.....	58
3.2.2. $\gamma$ -Pyrone annulation.....	59
3.2.3. Cheminformatics.....	70
3.3. Biological evaluation.....	72
3.3.1. Indofulvins: New Bioactivity.....	72
3.3.2. Indofulvins: Fragment Bioactivity.....	88
3.3.3. Morphological Profiling of indolenines.....	91
3.3.4. Pseudo-NPs in biological space.....	93
3.3.5. Morphological Investigation of structural Features.....	96
4. Summary.....	101

5. Experimental.....	104
5.1. Materials for Organic Synthesis .....	104
5.2. Chemical synthesis .....	105
5.2.1. $\beta$ -aryl ethanol starting materials .....	105
5.2.2. Carbonyl starting materials .....	118
5.2.3. Pseudo-NPs via Pictet-Spengler reaction .....	121
5.2.4. Dearomatisation.....	206
5.3. Materials for biological experiments .....	227
5.4. Biological methods.....	229
5.5. Morphological profiling .....	234
5.5.1. Compounds used for the analysis (Well IDs).....	236
Abbreviations .....	244
References .....	250
Curriculum Vitae (Lebenslauf).....	258
Eidesstattliche Versicherung (Affidavit) .....	260

## ABSTRACT

Natural Products (NPs) represent an important origin of inspiration in drug discovery. Historically the most productive source, NPs remain highly relevant for the treatment of human disease and for chemical biology studies investigating biological coherences. Their privileged molecular scaffolds constitute “prevalidated” representations of nature’s exploration of biologically relevant chemical space. Therefore, NPs have served as inspiration for many design approaches for small molecule collections. Likewise, the recently proposed pseudo-Natural Product (pseudo-NP) concept has recourse to the biological relevance of NPs. In this concept, novel scaffolds are generated by merging biosynthetically unrelated NP fragments. Pseudo-NPs resemble NPs but the unprecedented combinations may provide compounds that are chemically and biologically significantly different from NPs.

Herein, the design and synthesis of new pseudo-NPs compound classes accessible through the oxa-Pictet-Spengler reaction are described. Triflic acid immobilized on silica as a catalyst enabled the reaction of complex cyclic ketones with several different annulation partners, including multiple isomeric variants. The simple reaction conditions and broad substrate scope allowed for the rapid synthesis of a diverse compound collection. A further degree of derivatization was achieved by indole dearomatization.  $\gamma$ -Pyrone annulation of indole compounds derived from the oxa-Pictet-Spengler reaction as well as the Fischer indole reaction gave efficient access to novel classes of pseudo-NPs. Cheminformatic analyses characterized the pseudo-NP libraries with both NP- and drug-like characteristics, suggesting the resemblance of NPs while expanding nature’s chemical space. In a target-agnostic cell-based assay, indofulvins were found to have a new bioactivity as potent autophagy inhibitors (Figure 1). Further investigations identified mitochondrial respiration as a potential target. The simultaneous gain in new bioactivity while losing one of the fragment’s original activities provides a proof of concept of the pseudo-NP method as a viable design principle for bioactive small molecules.

To characterize the pseudo-NP in a broader biological context, all classes were screened in the cell painting assay. Morphological profiling evaluates phenotypic changes in cells upon compound treatment and condenses them into characteristic “fingerprints”. The indofulvins appeared to show morphological changes that are similar to the ones induced by oligomycin, a known inhibitor of mitochondrial respiration. On the other hand, the indofulvins had a low biosimilarity to the parent NP griseofulvin, which demonstrates the loss of the fragment’s original activity on phenotype level.

## Abstract

Additionally, morphological profiling enabled an evaluation of chemically relevant features for the phenotype by comparing a large compound collection with more than 240 compounds. The investigation revealed the combination of two fragments can lead to a new morphological effect. From the analyses, it was concluded that both fragments of the indofulvins, indole and griseofulvin, are not dominating the fingerprint. The connection type between the two fragments, as well as different regioisomers can also result in scaffold dependent biological effects.

These results suggest that the pseudo-NP concept in combination with the cell painting assay may be able to be used to rationally design new compound classes and therefore further explore chemical space with biological relevance.

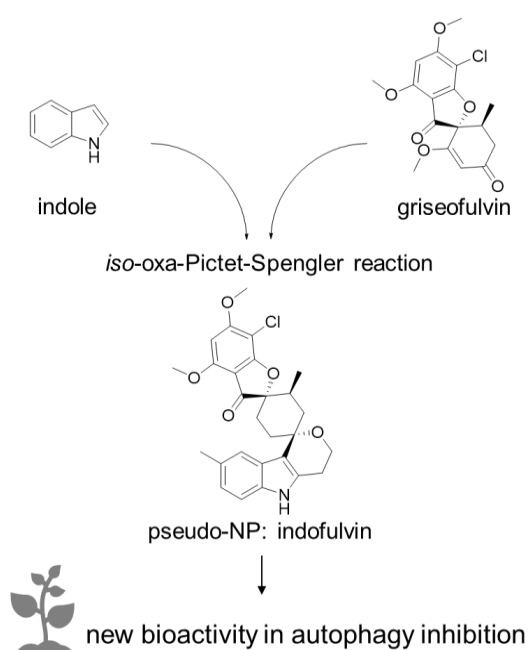


Figure 1: Conceptual overview of the pseudo-natural product indofulvin and its bioactivity.

## KURZZUSAMMENFASSUNG

Naturstoffe (NPs) stellen einen wichtigen Ursprung von Leitstrukturen in der Arzneimittelforschung dar. Historisch sind sie eine der ergiebigsten Quellen der Medizinalchemie und auch heute haben NPs für die Behandlung von Krankheiten und für die Untersuchung biologischer Zusammenhänge eine hohe Bedeutung. Ihre privilegierten molekularen Strukturen repräsentieren „prävalidierte“ Vertreter von biologisch relevanten chemischen Raum. Damit dienen NPs bereits häufig als Inspiration für neue Designansätze von Substanzbibliotheken. Auch das kürzlich veröffentlichte Pseudo-Naturstoff-Konzept greift auf die biologische Relevanz von NPs zurück. Bei diesem Konzept werden neuartige Molekülgerüste durch die Fusion von biosynthetisch nicht verwandten NP-Fragmenten erzeugt. Zwar ähneln Pseudo-NPs NPs in vielen Eigenschaften, können durch die beispiellose Kombination jedoch vollkommen neue Verbindungen ergeben, die sich chemisch sowie biologisch signifikant von NPs unterscheiden.

Im Folgenden werden das Design und die Synthese neuer Pseudo-NP Klassen, die durch die Oxa-Pictet-Spengler Reaktion zugänglich sind, vorgestellt. Auf Kieselgel immobilisierte Trifluormethansulfonsäure ermöglichte als Katalysator die Reaktion komplexer zyklischer Ketone mit mehreren verschiedenen Anullierungspartnern, einschließlich isomerer Varianten. Die einfachen Reaktionsbedingungen und breite Substrattoleranz erlaubten die schnelle Synthese einer vielfältigen Substanzbibliothek. Ein höherer Grad der Derivatisierung wurde durch die Dearomatisierung von Indolen erreicht. Die  $\gamma$ -Pyrrol-Anullierung von Indolverbindungen, die sowohl von der Oxa-Pictet-Spengler-Reaktion, als auch von der Fischer-Indol-Reaktion abgeleitet sind, lieferte einen effizienten Zugang zu neuen Pseudo-NP Klassen. Cheminformatische Analysen wiesen den Pseudo-NPs NP- und medikamentenähnliche Charakteristika zu, was auf eine Ähnlichkeit zu NPs bei gleichzeitiger Erweiterung des chemischen Raumes schließen lässt. In einem zellbasierten Assay wurde eine neue Bioaktivität der Indofulvine als potente Inhibitoren der Autophagie nachgewiesen (Abbildung 1). Weitere Untersuchungen identifizierten die mitochondriale Atmung als ein potentiell Target. Der gleichzeitige Verlust der ursprünglichen Fragmentaktivität liefert als Machbarkeitsnachweis einen Erfolg für das Pseudo-NP-Konzept.

Um das Pseudo-NP Konzept in einem breiteren biologischen Kontext zu evaluieren, wurden alle Klassen im Cell Painting Assay untersucht. Diese morphologische Analyse bewertet die phänotypischen zellulären Veränderungen nach der Zugabe einer Verbindung und überführt sie in charakteristische "Fingerabdrücke". Die Indofulvine wiesen ähnliche morphologische Veränderungen wie von Oligomycin, einem bekannten Inhibitor der mitochondrialen Atmung, induziert auf. Weiter war die biologische Ähnlichkeit der Indofulvine zum Ausgangs-NP

## Kurzzusammenfassung

Griseofulvin gering, was den Verlust der ursprünglichen Fragmentaktivität auf morphologischer Ebene zeigt.

Zusätzlich ermöglichte die morphologische Analyse einer Substanzbibliothek von mehr als 240 Verbindungen eine Bewertung chemischer Merkmale, die relevant für den Phänotyp scheinen. Die Untersuchung ergab, dass die Kombination von zwei Fragmenten zu einem neuen morphologischen Effekt führen kann, da Fragmente wie Indol und Griseofulvin, den Fingerabdruck nicht zu dominieren scheinen. Die Art der Kombination sowie Regioisomere können ebenfalls zu klassenabhängigen biologischen Effekten führen.

Diese Ergebnisse deuten darauf hin, dass das Pseudo-NP-Konzept in Kombination mit der morphologischen Analyse in der Lage sein könnte, neue Verbindungsklassen rational zu entwerfen und damit den biologisch verwendeten chemischen Raum zu erweitern.

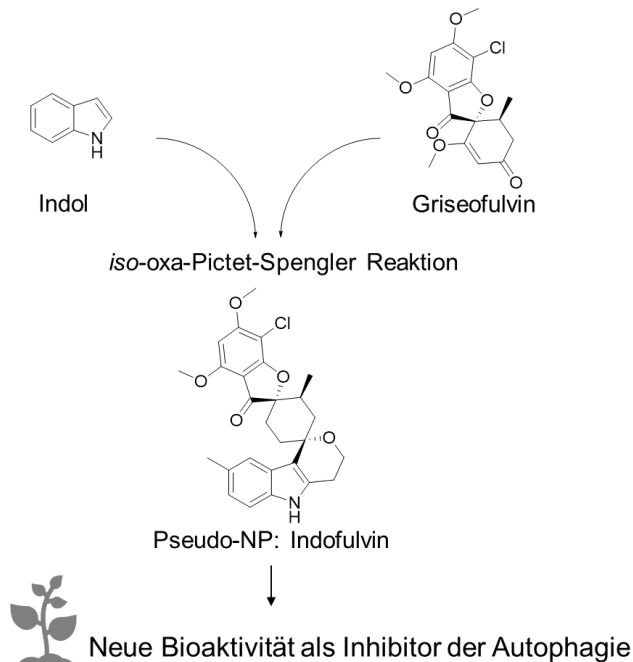


Abbildung 1: Konzeptioneller Überblick über den pseudo-NP Indofulvin und seine biologische Bedeutung.



# 1. INTRODUCTION

## 1.1. DESIGN APPROCHES FOR SMALL MOLECULE LIBRARIES

Small molecules are excellent tools for the study of complex biological networks and the development of new drugs. Compared to genetic approaches, the usage of small molecules is beneficial as they can show a rapid effect that is dose-dependent and reversible.<sup>[1]</sup> However, the supply of selective, bioactive molecules is often limited. The identification of chemical space in order to guide the design of compounds with biological relevance remains one of the greatest challenges. The potential number of small molecules is over  $10^{60}$  which is too high to synthesize or biologically evaluate.<sup>[2]</sup> In this context, diversity within biologically relevant chemical space is more important than library size. It is crucial to focus on approaches that significantly increase the chance of bioactivity.

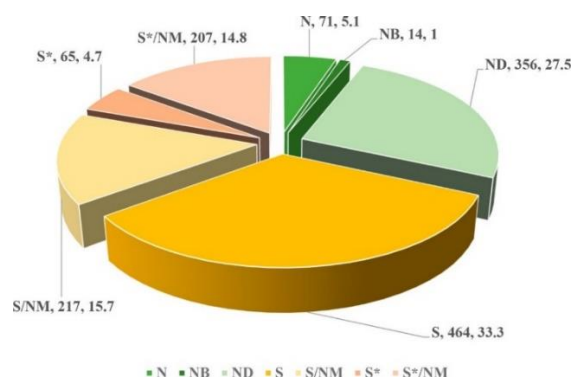


Figure 2: Pie chart of all 1394 small molecule approved drugs from 1981 to 2019 sorted by their sources.<sup>[3]</sup> N: unaltered natural product, NB: botanical drug, ND: natural product derivative, S: synthetic drug, S\*: synthetic drug (NP pharmacophore), /NM: mimic of natural product.

Natural products show a distinct advantage, as they inherently cover areas of biologically relevant chemical space.<sup>[4]</sup> They have served as therapeutics and as fruitful inspirations for valuable NP derivatives over the last decades. 32% (441 out of 1394) of small molecules approved by the US Food and Drug Administration (FDA) between 1981 and 2019 that were based on small molecules were NPs or direct derivatives (Figure 2).<sup>[3]</sup> NPs are often endowed with inherent bioactivity that cover a broad range of effects: anti-cancer, anti-infective, anti-diabetic, among others. Beyond their bioactivity, NPs show an improved delivery to their intracellular site of action as they are compared to synthetic drugs more likely to be substrates for transporter systems. NPs represent a great diversity of chemical structures with high complexity and a high degree of stereochemistry. As NPs co-evolved with their interaction partners, relevant structural parameters for binding to conserved proteins may be deposited in them. Consequently, their scaffolds may not only be

## Introduction

prevalidated for their targets, but also privileged representations of Nature's exploration of biologically relevant chemical space.<sup>[5]</sup>

Despite immense interest in NPs, the availability of NPs can be problematic as these complex structures often require multistep syntheses or time-consuming isolations.<sup>[6]</sup> The difficult access can have a major influence on following studies including the synthesis of a broad structure-activity-relationship (SAR). To address this restriction, several NP-inspired design principles have been employed, including the diversity-oriented synthesis (DOS), ring distortion strategy (CtD) and biology-oriented synthesis.

### DIVERSITY-ORIENTED SYNTHESIS (DOS)

The DOS approach is aiming to explore chemically underrepresented space with small but highly diverse chemical libraries. By systematic mixing and matching of various chemical building blocks the diversity of compound libraries is maximized. Synthesis pathways are therefore compared to target-oriented synthesis approaches not linear but branched and divergent (Figure 3).<sup>[7]</sup>

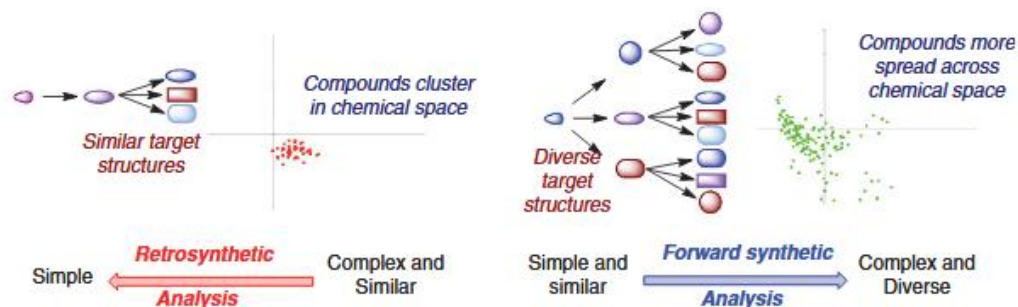


Figure 3: Synthetic strategy in target-oriented synthesis approaches (left) compared to diversity-oriented synthesis approaches (right).<sup>[7a]</sup>

The DOS approach is pursuing two concepts: From simple starting materials to complex products and from similar starting materials to diverse products. The forward-synthetic planning has to fulfill the requirements of increasing complexity and diversity and can be divided in a build-, couple and pair-phase (Figure 4). Initially, multifunctional building blocks (**1**) are generated by robust asymmetric reactions. The following couple phase is increasing complexity by combining various building blocks (**2**) and diversifying them ideally under full stereo control (**3a-c**). The pair-phase is transforming the collection of relatively similar substrates into a collection of more diverse products by intramolecular coupling reactions (**4a-c**). The resulting small molecule libraries, similar to NPs are enriched in bioactivity and  $sp^3$ -hybridised centers.<sup>[7b, 8]</sup>

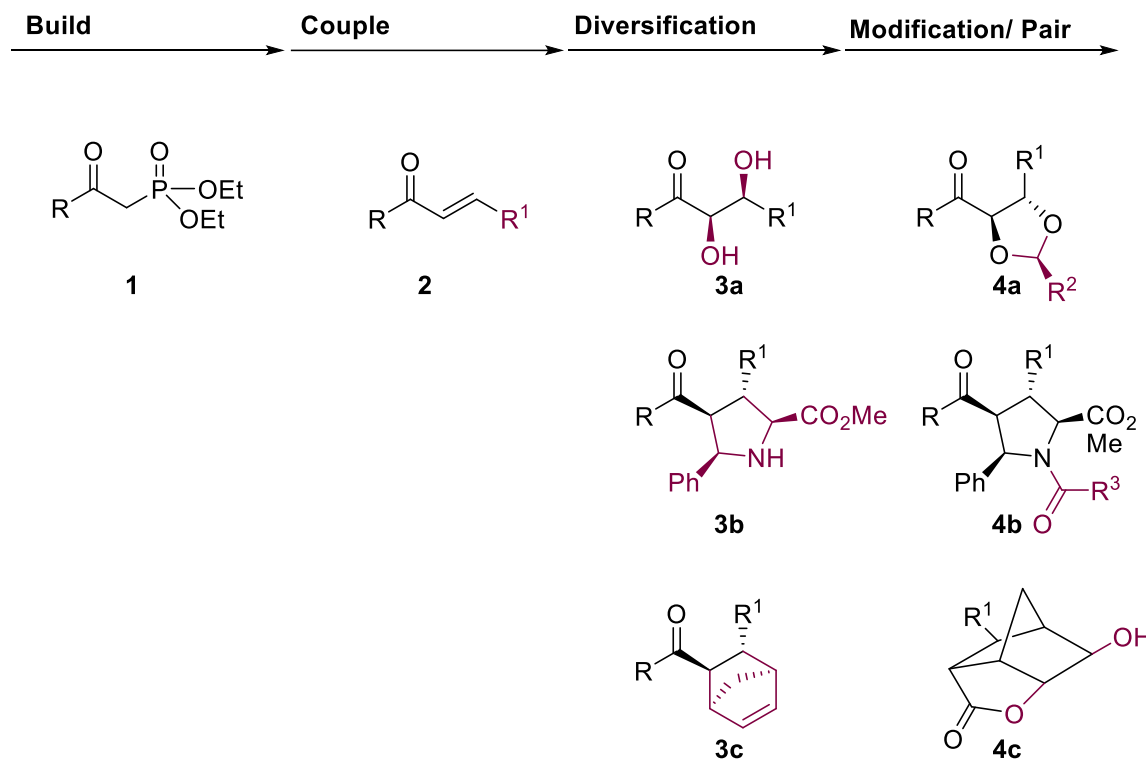


Figure 4: DOS approach: simple starting materials **1** are transformed in complex structures **4a-c** while simultaneously increasing diversity.<sup>[7a]</sup>

#### RING DISTORTION STRATEGY (CTD)

The ring distortion strategy is inspired by nature, where common intermediates are used for the synthesis of various NPs. Instead of directly aiming for an improvement in potency or pharmacokinetics, this concept pursues the goal to generate highly diverse scaffolds from a structurally complex NP and can therefore also be termed as the complexity-to-diversity (CtD) strategy. In contrast to other approaches, NPs are not simplified or reduced to smaller fragments but significantly modified to change its overall topology. While aiming for a high degree of diversity, different reaction types, such as ring-cleavage, ring-expansion or -contraction, ring-fusion, and ring-rearrangements, can be applied.<sup>[9]</sup>

Examples including gibberellic acid, adrenosterone, quinine, abietic acid, and yohimbine among others proved its application in a diverse library synthesis.<sup>[9-10]</sup> The recently published derivatization of pleuromutilin demonstrates proof of concept for generating bioactive molecules (Figure 5). A highly complex ring-contraction product was identified as having anticancer activity. A subsequent modification of the primary hit resulted in ferroptocide, a potent inhibitor of thioredoxin and therefore rapid inducer of ferroptotic cell death.<sup>[11]</sup>

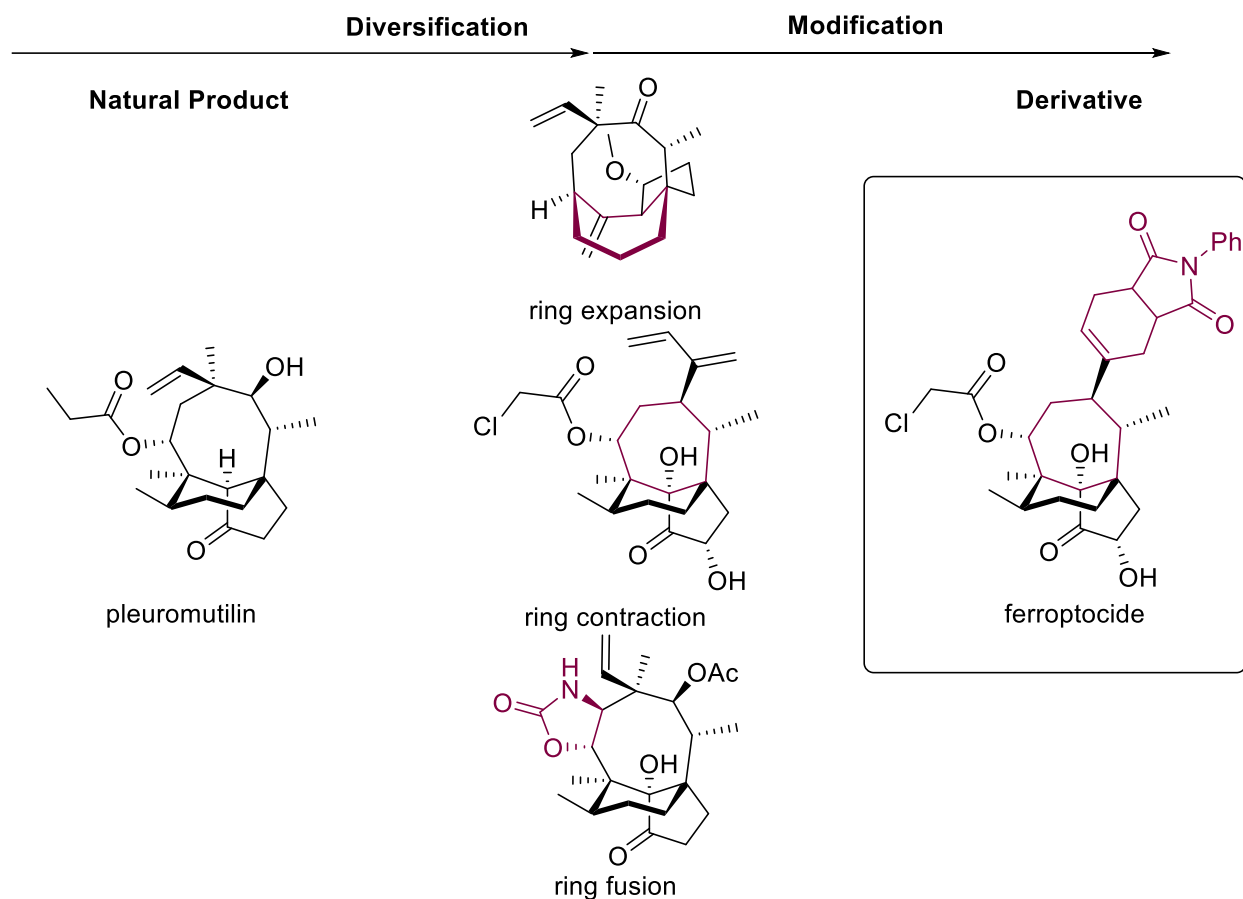


Figure 5: Ring distortion strategy on pleuromutilin yielding ferroptocide after diversification and modification.<sup>[11]</sup>

While this strategy opens up many possibilities to synthesize structurally challenging compound libraries, it is highly dependent on the access to the guiding natural products. The complex derivatization requires sufficient amounts of starting materials, which limits its application.<sup>[12]</sup> Additionally, the modification of complex NPs can be challenging in terms of many possible side reactions. In this context, it is essential to focus on starting materials with orthogonal functional groups for selective derivatization. Furthermore, a considerable practical expenditure can be necessary for the search of suitable reaction conditions and restrict the approach opportunities.

#### BIOLOGY-ORIENTED SYNTHESIS (BIOS)

Another way to use the structural information from NPs to focus on biological relevant areas of chemical space is the BIOS concept. For this method, NPs are used as prevalidated starting points and are reduced to simplified core scaffolds.<sup>[5]</sup> The simplification is based on chemoinformatic structural analysis of NPs and visualized in a tree-like structural classification of

NPs (SCONP).<sup>[13]</sup> The smaller fragments are likely to constitute biological relevance and allow an easy selection of related structures to base the library synthesis on. The simplified NP core stays conserved whereas the surrounding substitution pattern can be highly diverse.<sup>[5]</sup> The derivatization can optimize the NPs original bioactivity in terms of potency and pharmacodynamic properties and lead to highly selective compounds. The BIOS approach proved its success in many examples, such as in the development of a neurite growth promoter (Figure 6). The NP rynchophylline's known bioactivity is the promotion of neurite growth.<sup>[14]</sup> After the simplification to the *spiro*-core structure followed by a diverse modification, five derivatives with activity in neurite growth assays were identified.<sup>[15]</sup>

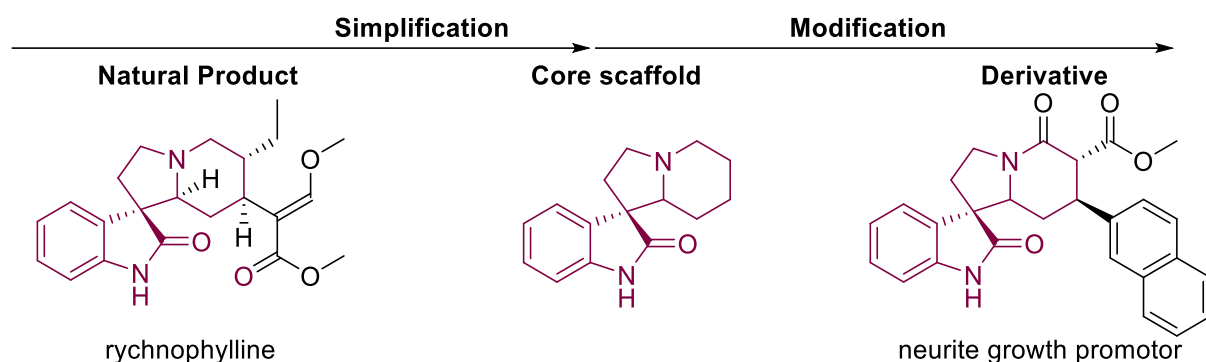


Figure 6: Visualization of the BIOS approach covering simplification and modification of natural products to yield optimized derivatives. Example: Rynchophylline, which provided active neurite growth promoters.<sup>[15]</sup>

However, the focus on selected NPs and their scaffolds restricts the exploration of chemical and biological space. Although NPs are chemically highly diverse, the chemical space is larger and cannot be significantly extended by this approach. On the biological side, the resulting compound library may retain similar biological effects to structurally related NPs rather than showing new bioactivity.<sup>[12]</sup>

#### FRAGMENT-BASED DRUG DESIGN (FBDD)

Fragment-based drug design (FBDD) describes the screening of small fragments to find low-affinity binders and combine them to provide potent interaction partners. Known ligands of interesting target proteins or other known drugs or drug candidates provide the concept's starting point. They can be fragmented into smaller scaffolds that fulfill the rule-of-three for their lead-likeness. Additionally, the fragments' solubility, and structural diversity are of great importance to avoid accumulating and cover broad chemical space.<sup>[16]</sup> Relatively weak interactions can be identified with biophysical techniques like target-based NMR, mass spectrometry, and thermal shift assay. The following optimization of each interaction in the binding site and reconstruction

## Introduction

into a single molecule results in a potent compound with high binding affinity as sum of the fragments individual interaction.<sup>[17]</sup>

Guided by this concept, the new glucokinase activator **5** were rationally designed and resulted in a five times increased activity. The analysis identified benzamide as key fragment of GKA50 and the cyclopropylsulfonyl and aminothiazolyl moieties as beneficial from the clinical candidate PSN-GK1 (Figure 7).<sup>[18]</sup>

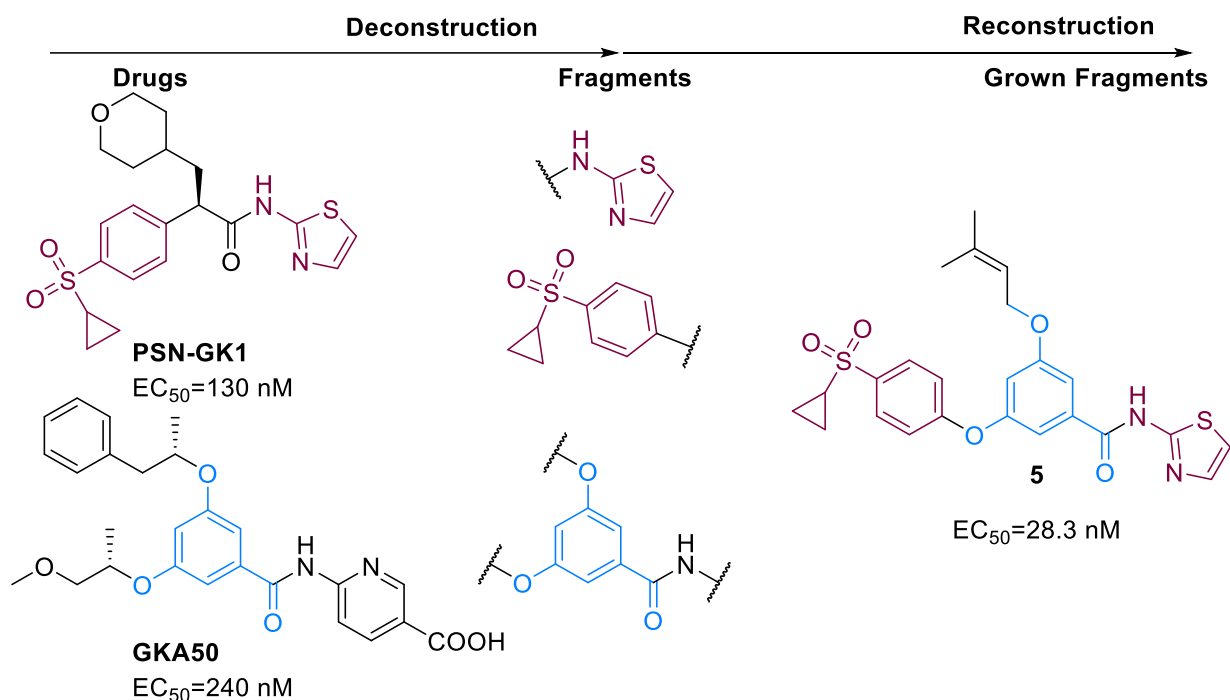


Figure 7: Fragment-based drug design with the glucokinase activator using the deconstruction-reconstruction approach through a privileged fragment-merging strategy.<sup>[18]</sup>

However, FBDD mainly focus on flat,  $sp^2$ -rich fragments and are derived from known chemical space. Over et al.<sup>[19]</sup> addressed this limitation by analyzing >180,000 natural products in order to gain fragments with high three-dimensional character. 2,000 clusters of natural-product-derived fragments were identified which were not only structurally diverse and readily accessible but also cover different chemical space than the six times larger commercially available fragment subset annotated in the ZINC database. The number of  $sp^3$ -hybridized centers is significantly increased compared to synthetic scaffolds and provides a high three-dimensional character for the NP-fragments. A high potential of NP-structures in the FBDD is suggested as their fragments appear to sufficiently represent NPs in complexity and diversity.<sup>[17, 19]</sup> Its application in drug discovery demonstrated by the development of novel fragment-sized p38aMAP kinase inhibitors and new, unprecedented phosphatase inhibitors.

### 1.1.1. PSEUDO-NATURAL PRODUCTS

While the guiding strategies to generate biologically relevant small-molecule libraries above show successful applications, they may also be restricted by limitations. A high structural diversification generated in the DOS covers a broad chemical space, but biological relevance and synthetic strategies constitute a great challenge. The Ctd strategy uses NPs as starting points to rapidly access complex scaffolds and are therefore highly dependent on the NPs availability. The simplification and derivatization of NPs in the BIOS approach usually results in compounds covering similar chemical and biological space relative to their parent NP. Consequently, an interaction with similar targets may be more presumable than novel bioactivity. FBDD identifies low-binding fragments for biological relevant targets and extends them to potent interaction partners. However, this approach requires a known target and predominantly employs  $sp^2$ -rich compounds, leaving out the biological relevant, high  $sp^3$  fraction represented by NPs.<sup>[12]</sup>

More recently, a new design approach based on the NP-fragment classes<sup>[19]</sup> was introduced to increase discovery productivity. As the NP-like chemical space appears to be larger than covered by nature, the guiding strategy is to synthetically combine unrelated NP building fragments to provide novel scaffolds. These compounds are called pseudo-NPs as they share structural features but are not accessible through existing biosynthetic pathways. The resulting chemotypes are suggested to explore new chemical space while simultaneously resembling the complexity of NPs. Thereby, pseudo-NPs may retain biological relevance of the NPs, but have the chance to reveal unknown bioactivity and lead to the identification of new targets. Compound libraries derived from this approach are in contrast to the relatively flat molecular skeletons from combinatorial chemistry.<sup>[12, 20]</sup>

One of the first examples for this design approach are the chromopyrones derived from the fusion of chromanes to tetrahydropyrimidinones (Figure 8a).<sup>[21]</sup> Both fragments can be found in nature, where chromans cover a broad range of bioactivities and tetrahydropyrimidinones represent a natural product class of antibiotics. The combination of the two fragments to a pseudo-NP revealed the expansion of chemical space, as well as a new bioactivity in glucose uptake inhibition. The compounds selectively target both glucose transporters GLUT-1 and -3 and thereby reduce tumor cell growth. Interestingly, this bioactivity appears to truly be the result of the fragment combination as neither the chromane nor tetrahydropyrimidinones substructures show any glucose uptake inhibition.

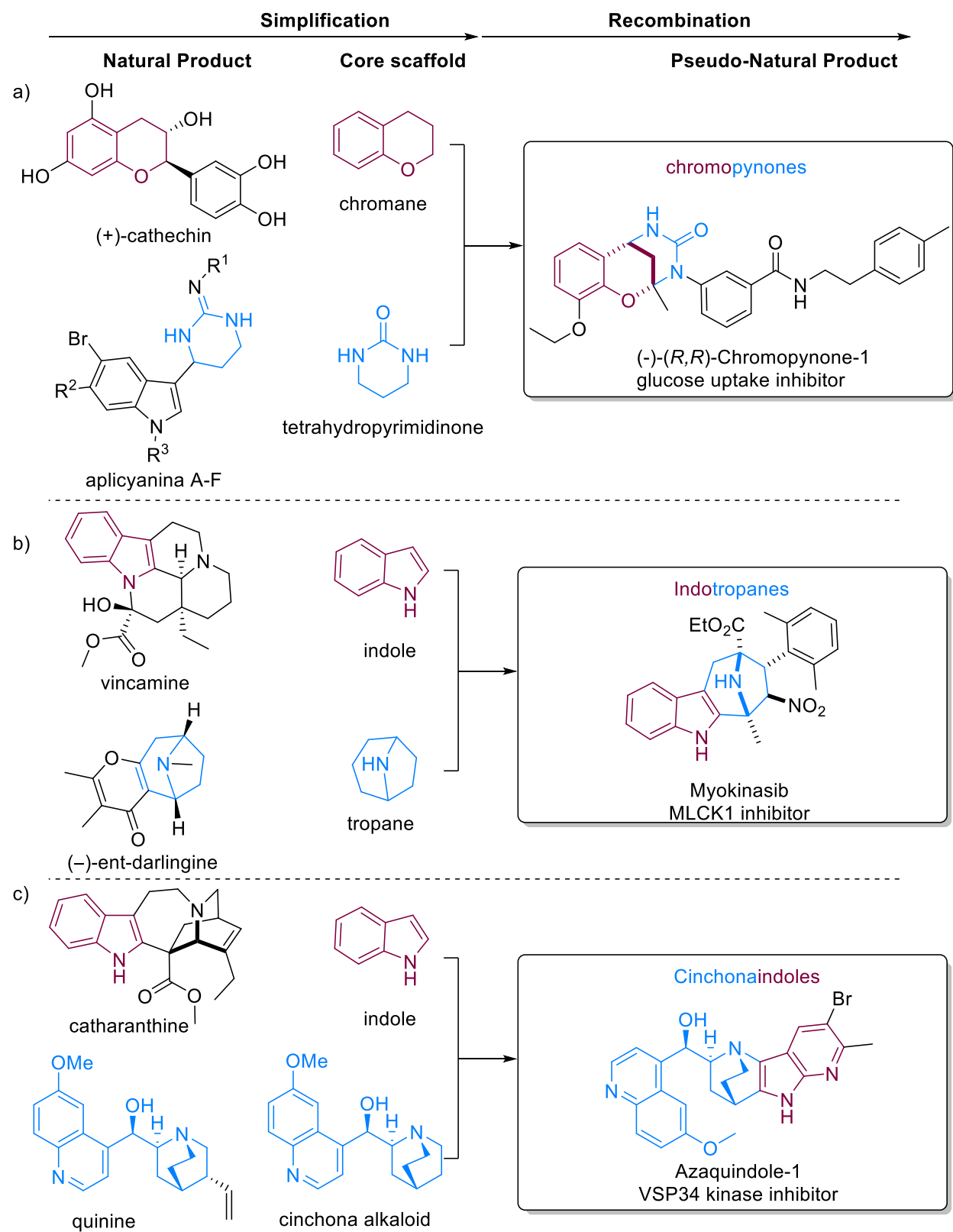


Figure 8: Pseudo-natural product approach<sup>[12]</sup> with a) chromopyrones revealed a new glucose uptake inhibitor<sup>[21]</sup>, b) indotropanes as MLCK1 inhibitors<sup>[22]</sup> and c) azaquindoles as VSP34 kinase inhibitors<sup>[23]</sup>.

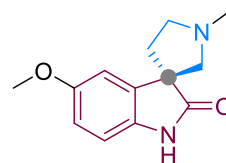
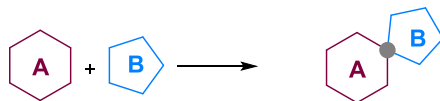


Furthermore, indotropanes structurally combine the ubiquitous NP-fragment indole and a tropane via copper-catalyzed 3+2 cycloaddition reaction (Figure 8b).<sup>[22]</sup> Members of the complex pseudo-NP library showed an interesting multinucleated phenotype. Target identification revealed an inhibition of myosin light chain kinase 1 (MLCK1), which was isoform-specific. The fragment-sized cinchona alkaloids and indoles comprise several unique structures and biological activities. The fusion of both fragments in a Pd-catalyzed Heck coupling led to a complex pseudo-NP library (Figure 8c).<sup>[23]</sup> The azaindole derivative Azaquindole-1 represents a very potent autophagy inhibitor, which interacts with the VSP34 kinase and therefore suppresses the lipidation of the phagophore inducer LC3.

Three-dimensionality is of major importance for spatial binding to proteins<sup>[24]</sup> and to resemble NPs complexity, the fragment combination ideally generates stereogenic centers. Therefore, different connection types can be found in NPs and is used in pseudo-NP collections. A connectivity of two fragments in just one point generate a complex spiro center like in (-)-horsfiline (Figure 9a). A monopodal or linear connection is shown in tambjamine A (Figure 9b), where the pyrrole is attached to the cyclopentadiene via a simple bond. A connection in two points can be achieved through an edge fusion (Figure 9c) for example in murraya alkaloids. Additional complexity can be generated by the fusion of two fragments with three atoms shared (Figure 9d). The bridged fusion can be found in sespenine. A connection of two fragments in four points is called bipodal connection (Figure 9e) or bridged bipodal connection (Figure 9f).<sup>[20]</sup> In this case two connection points can be linked through either one or multiple bonds and introduce a third fragment. The size and functionalities of the newly generated fragment may influence the properties of the resulting pseudo-NP library and has to be considered carefully.

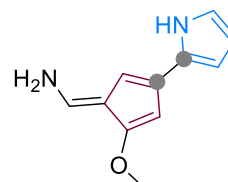
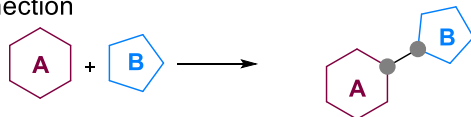
## Introduction

a) Spiro fusion



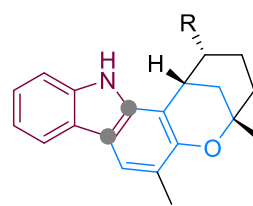
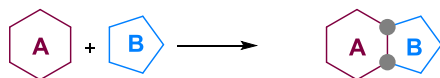
(-)-horsfiline

b) Monopodal connection



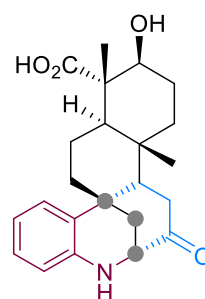
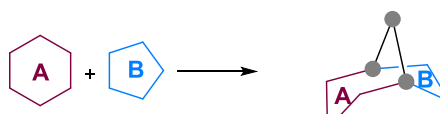
tambjamine A

c) Edge fusion



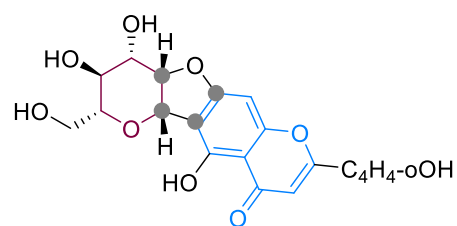
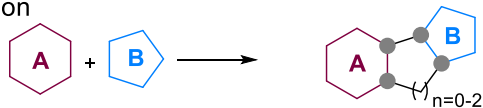
murraya alkaloids

d) Bridged fusion



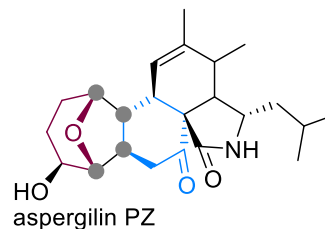
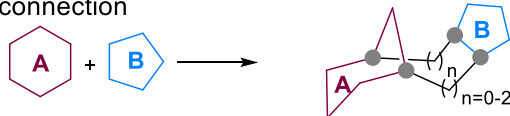
sespenine

e) Bipodal connection



chafuroside A

f) Bridged bipodal connection



aspergillin PZ

Figure 9: Different connection types for the fusion of two fragments including one NP example for each connectivity.<sup>[20]</sup>

## 1.2.COMPLEXITY-GENERATING REACTIONS

Since NPs have a high structural complexity which can be attributed to target interaction and specificity, our goal is to access small molecules with more globular or spherical molecular skeletons. Whereas the percentage of  $sp^3$ -hybridized carbons in NPs is high at around 68%, the fraction of  $sp^3$  carbons in synthetic and commercially available compounds is significantly lower at 37%.<sup>[25]</sup> Complexity-generating reactions, for example cycloadditions and multicomponent reactions, are valuable for accessing three-dimensionality in an efficient manner. Nevertheless, medicinal chemistry is dominated by a small set of standard reactions falling into few different categories. More than 80% of the performed synthetic steps can be assigned to either amide formation, Suzuki-Miyaura reaction, aromatic nucleophilic substitution, amine Boc-deprotections, or electrophilic reactions of amines (Figure 10)<sup>[26]</sup>. Reasons for the limited diversity are the availability of starting materials, the desired robustness of the reactions regarding their velocity, efficiency, and reliability, as well as the introduction of unfavored for example lipophilic moieties through some other reactions. Furthermore, the functional group tolerance of new methodologies usually requires protecting groups. Accordingly, these complex reactions prove to not be efficient and applicable to medicinal chemistry when they require multiple steps of protection and deprotection. As a consequence of the dominance of amide bonds and reactions including aromatic scaffolds, the resulting molecules have an increased linear and  $sp^2$  character. Additionally, nitrogen is more represented than oxygen in synthetic compounds which also does not reflect NPs.<sup>[20]</sup>

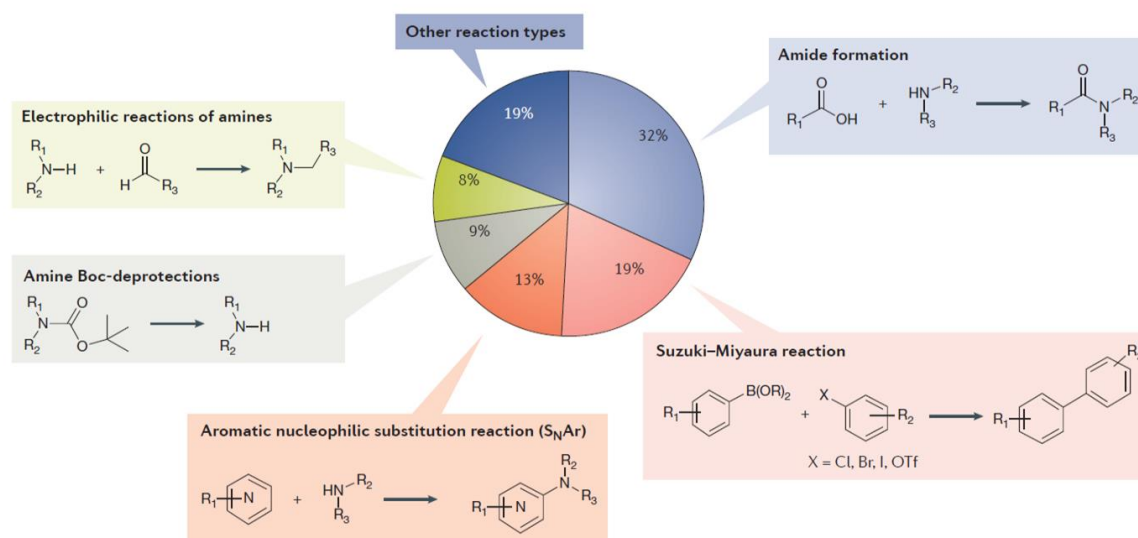


Figure 10: Dominant reaction types in medicinal chemistry in a pie chart<sup>[26]</sup>: The five widely used reactions are amide formation, Suzuki-Miyaura reactions, aromatic nucleophilic substitutions, Boc-deprotections and electrophilic reactions of amines.

## Introduction

To best depict nature's complexity an expansion of the synthetic toolbox in medicinal chemistry is required.<sup>[27]</sup> Ideal reactions for the library synthesis of complex molecules therefore must be efficient, tolerant of diverse functional groups, robust, reproducible, operationally simple operational procedure without high-risk or sensitive materials, and have facile access to starting materials.

### 1.2.1. PICTET-SPENGLER REACTION

In 1911 Amè Pictet and Theodor Spengler described a cycloaddition after heating  $\beta$ -phenylethylamine and formaldehyde dimethylacetal under hydrochloric acid catalysis.<sup>[28]</sup> Due to its value in alkaloid synthesis and its broad applicability to pharmaceuticals, the Pictet-Spengler reaction has been developed into a powerful synthetic strategy over the last 100 years.<sup>[29]</sup> Thereby, the method underwent constant advancements, such as a broader substrate scope, identification of correlating enzymes in 1977<sup>[30]</sup>, and stereoselective methods. Furthermore, a modification of the Pictet-Spengler reaction led to its oxygen variant, in which aryl alcohols and carbonyl functionalized components generate 1, (1'-di)-substituted pyrans. Just as for the amino version, the oxa-Pictet-Spengler reaction is promoted by Lewis or Brønsted acids, such as boron trifluoride etherate and trifluoroacetic acid.<sup>[31]</sup> The resulting pyrans fused to an aromatic ring system can be found in many NPs. One of the most famous representatives is the isochromane framework, which has attracted attention over the last few decades. Examples include *Penicillium* PSU-F40 isolated penicisochromane D<sup>[31]</sup>, the alkaloid excentricine<sup>[32]</sup> from the roots of *Stephania excentrica* and the structurally complex cytosporolides A<sup>[33]</sup> which was obtained from *Cytospora sp* (Figure 11).<sup>[31]</sup>

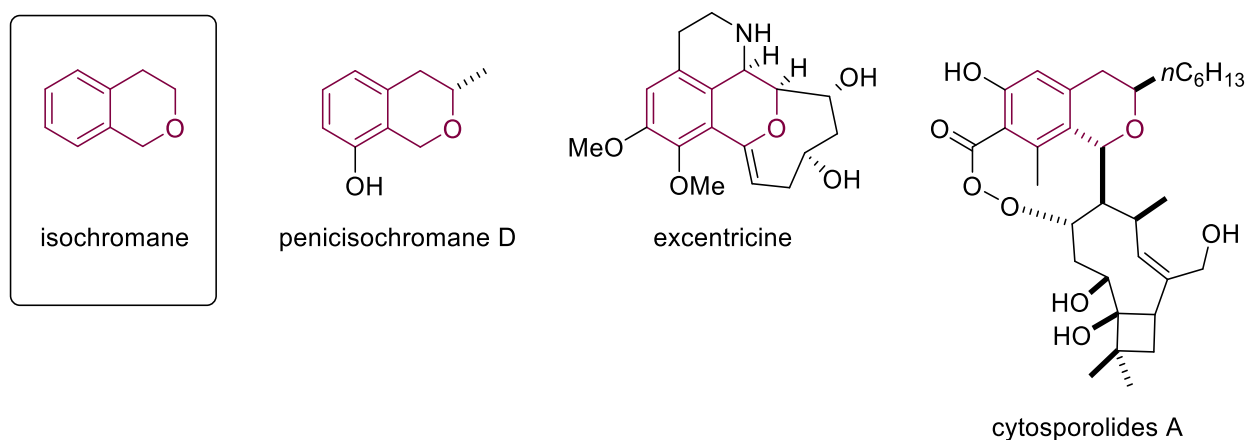


Figure 11: Selected NPs bearing the isochromane scaffold.<sup>[31]</sup>

More recently, asymmetric variants of the oxa-Pictet-Spengler reaction were developed. For a long time, the control of the enantioselective addition to oxacarbenium ions provided a challenge.<sup>[34]</sup> Chiral amine/hydrogen bond donors and bifunctional Brønstedt acids<sup>[35]</sup>, similarly to imidodiphosphate catalysts<sup>[36]</sup> proved to efficiently affect the products enantioselectivity. The substrate scope of these reactions is comprised of different aryl alcohols including indoles, benzofurans, and thiophenes, as well as a wide range of aldehydes, ketones, or their masked derivatives. However, the oxa-Pictet-Spengler reaction with more complex cyclic ketones remains a challenge.

### 1.2.2. DEAROMATIZATION

Dearomatization reactions proved to be an excellent tool in the synthesis of polycyclic scaffolds of various complex NPs including salvileucalin B, (-)-acutumine, (+)-fendleridine and (+)-cannabisativine (Figure 12a). The overcoming of aromatic stabilization results in highly reactive intermediates, which subsequently enable carbon-carbon and carbon-heteroatom bond formation, as well as cycloadditions and other cascade reactions. The vast majority of dearomatization reactions are represented by phenols as substrates.<sup>[37]</sup> The NP (±)-cleroindicin D for example is synthesized by oxidative dearomatization of a phenol starting material **6** (Figure 12b). The first step uses oxone and leads to the corresponding para-peroxyquinol **7**, which cyclizes under acidic conditions (**8**) and yields the natural product after diastereoselective rearrangement. The dearomatization of electron-rich heteroarenes including furans pyrroles and benzofurans constitutes often a key step in total synthesis. Especially the dearomative Diels-Alder reaction with furans is described extensively in the literature to generate complex structures. Electron-rich indoles also proved to be excellent starting materials for dearomatization reactions. Indolic alkaloid frameworks either react via Diels-Alder cycloaddition or a stepwise Michael-Mannich sequence to give their indoline analogs. Porco et al.<sup>[38]</sup> described the synthesis of pleiomaltinine through an  $\gamma$ -pyrone annulation with maltol derivative **10** in the last step (Figure 12c). The method for the access to unusual alkaloid-pyrone structures has been extended by an asymmetric version using a chiral thiourea catalyst.<sup>[39]</sup> Although asymmetric dearomatization strategies have a high potential for chemical synthesis, they still remain underdeveloped.

## Introduction

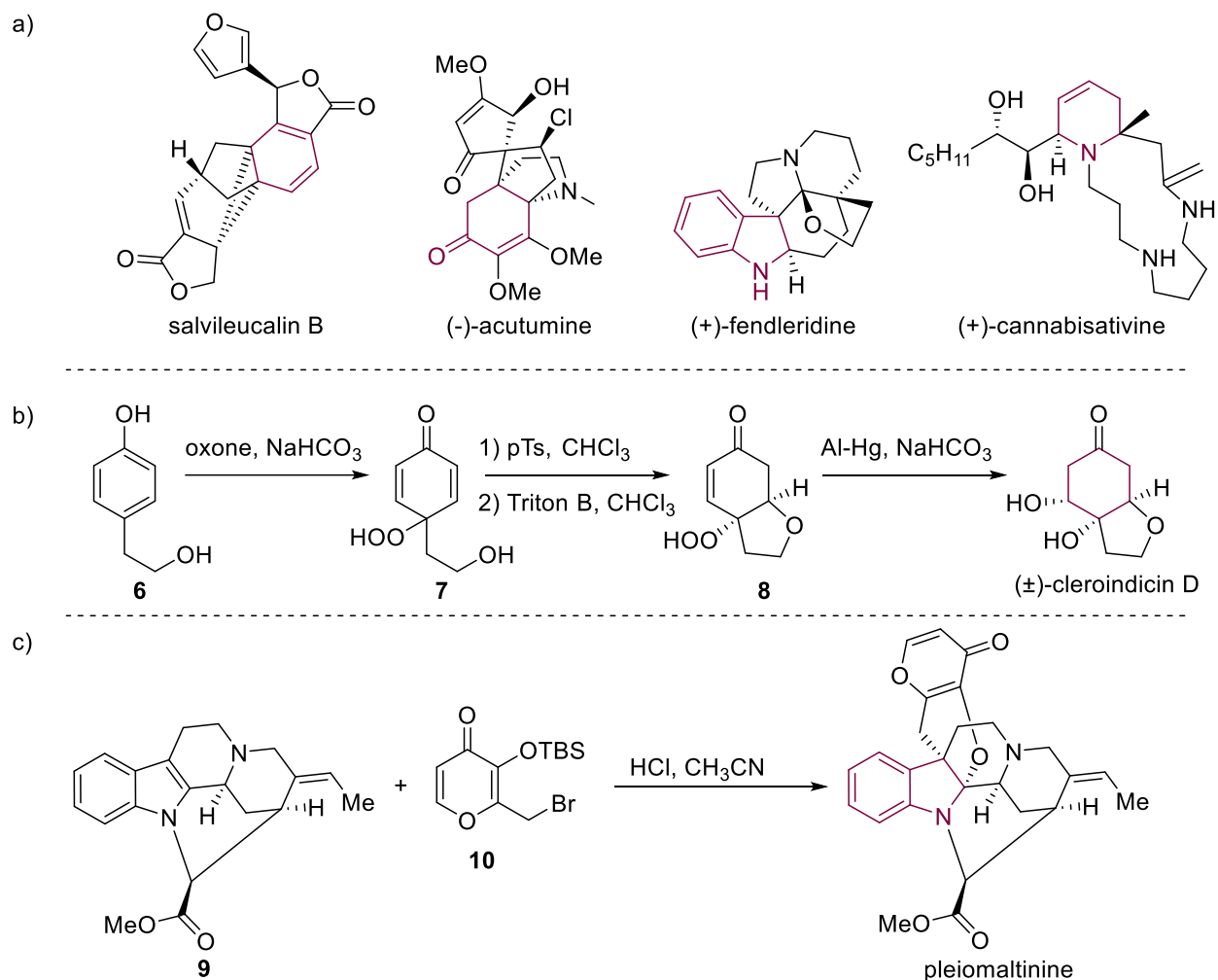


Figure 12: Dearomatization in natural product total synthesis. a) Selected syntheses through dearomatization. The former aromatic ring is colored in magenta.<sup>[37]</sup> b) Total synthesis of (±)-cleroindicin D involving an oxidative dearomatization through oxone.<sup>[40]</sup> c) Dearomative alkaloid-pyrone annulation in the synthesis of pleiomaltinine.<sup>[38]</sup>

### 1.3. BIOLOGICAL EVALUATION

To support the identification of bioactive molecules, methodologies that allow a fast and meaningful analysis of compound libraries are required. A major contributory factor to be able to test a large number of molecules is automated image acquisition in a high-throughput manner. Most target-based assays need to test relatively large compound (>100,000) libraries to generate a satisfactory hit rate. With an increased quality of prevalidated NP-inspired collections, less than 1,000 compounds are sufficient.<sup>[41]</sup> However, compounds might address different targets of a similar process. In order to enable a comprehensive biological analysis, assays which cover a broad range of bioactivities are beneficial. In contrast to the reverse chemical genetic approach, which searches for interaction partners for a known target, discovery in forward chemical genetics can be based on a phenotype of interest. Comparable to mutants in classical genetics, compound libraries are investigated regarding their phenotypic effects in cells or their extracts. However, instead of acting on gene level by deleting or impairing protein function, small molecules can inhibit or activate proteins by direct interaction. The forward chemical genetics can be divided into three inevitable components: a compound collection, a biological assay with the ability of detecting the phenotype of interest, and a target identification strategy.<sup>[42]</sup> The least systematic target identification usually includes methods such as proteomic hit identification strategies, cellular thermal shift assays, thermal proteome profiling as a combination of both, and genetic hit identification.<sup>[43]</sup> Thereby, the forward chemical genetic approach may not only deliver proteins that regulate distinct cellular processes, but also increase the number of relevant tool compounds.<sup>[42]</sup> Interestingly, approved drugs identified through phenotypic assays appear to attain a greater success over target-based approaches. About 37% of clinically approved compounds from 1999 to 2008 were identified via forward chemical genetics, where just 23% were derived from the reverse chemical genetics.<sup>[44]</sup>

#### 1.3.1. PHENOTYPIC SCREENING

Phenotypic screening may allow an unbiased identification of bioactive molecules by translating phenotypic changes into physiologically relevant results. Therefore, it can be especially beneficial for the identification of novel targets as multiple possible interactions are covered in a phenotypic response. Recent advances in technology and robotics allow parallel screening of various compounds and is increasing its efficiency. Usually these biological assays are performed in cells where complex cellular extracts or organelles and fluorescently labeled proteins or antibodies are used for quantification of the phenotypic output.<sup>[42, 45]</sup> Due to the usage of phenotypic assays on

## Introduction

cells or model organisms, the compound's bioavailability plays an earlier role compared to primary assays with isolated proteins.<sup>[46]</sup>

The phenotype for pathways or cellular processes, including mitosis, is specific and can be used for the investigation of novel interactors. Cell division involves large structural rearrangements which can, for example, be visualized by a fluorescent antibody against phosphorylated histone H3. This prometaphase marker selectively labels mitotic cells and can therefore identify inhibitors of this cellular process.<sup>[47]</sup>

Furthermore, autophagy as catabolic process in correlation with the recovery of cellular building blocks can be investigated via phenotypic screening. A relevant autophagy marker of autophagosomes, protein microtubule associated light chain 3 (LC3), is tagged with the enhanced green fluorescent protein (eGFP).<sup>[48]</sup> Once autophagy is induced, LC3 localizes in the autophagosome membrane and is subsequently degraded. The labeling allows the tracking and, in addition with the degradation inhibitor chloroquine, autophagosome quantification for the identification of autophagy inhibitors. The resulting signal directly correlates with the pathway activity. While autophagy induces the formation of autophagosomes, autophagy inhibitors are supposed to show a reduced signal correlating with fewer autophagosomes.<sup>[45]</sup>

The cell viability can also be investigated by fluorescent dyes including propidium iodide. This intercalating agent stains nucleic acids, but is not membrane permeable. As distinct from living cells, dying or dead cells have a damaged membrane, which can be overcome by propidium iodide. Therefore, it can be used as viability marker as it selectively stains dead cells.<sup>[49]</sup>

### 1.3.2. MORPHOLOGICAL PROFILING: CELL PAINTING ASSAY

Morphological profiling is advancing phenotypic screening to the next level. Instead of screening for a specific phenotype, multiparameter investigations enable access to diverse bioactivities and many potential targets.<sup>[50]</sup> Technological advancements in microscopy, robotics, and computer analysis has enabled the coverage of a broad phenotypic spectrum in a high-through put manner. The phenotypic traits of cells can be described by hundreds of parameters. A perturbation through compound treatment may involve morphological changes, which can be extracted during image analysis and transformed into specific morphological profiles.<sup>[46, 51]</sup> Upon comparison with reference compounds or other research molecules, these data can be used to generate a target or mode-of-action hypothesis<sup>[23, 52]</sup>, SAR analysis<sup>[53]</sup>, and to investigate the influence of chemical differences on a biological level.<sup>[50, 54]</sup> Furthermore, a broad clustering of reference compounds with a common mode-of-action but different targets enables the identification of so far



uncharacterized small molecules predicted to share the same mode-of-action. A defined cluster of structural unrelated iron chelators and cell cycle modulators were shown to share a common mode-of-action and enabled the identification of three new representatives of this bioactivity.<sup>[55]</sup>

Morphological profiling, for example the cell painting assay, is especially powerful for the investigation of compound libraries with unknown biological effects including molecules from the pseudo-NP approach. The unbiased way of investigating the perturbed biological system and wide range of covered bioactivities potentially allows the identification of unexpected or unprecedented bioactivity.<sup>[56]</sup> In contrast to commonly used target identification methods, the morphological profiling is potentially capable to reveal non-protein targets.<sup>[52]</sup> In the cell painting assay, human osteosarcoma (U-2OS) cells are treated with research compounds, as well as annotated references (Figure 13). Six dyes are multiplexed to stain different cellular compartments (nuclei, endoplasmic reticulum, nucleoli, RNA, actin, Golgi apparatus and mitochondria), followed by image analysis and feature extraction to generate morphological fingerprints, that represent changes induced by the compound collection compared to the DMSO control.<sup>[57]</sup> The comparison to other profiles, for example from references with known target, target hypothesis can be deduced.

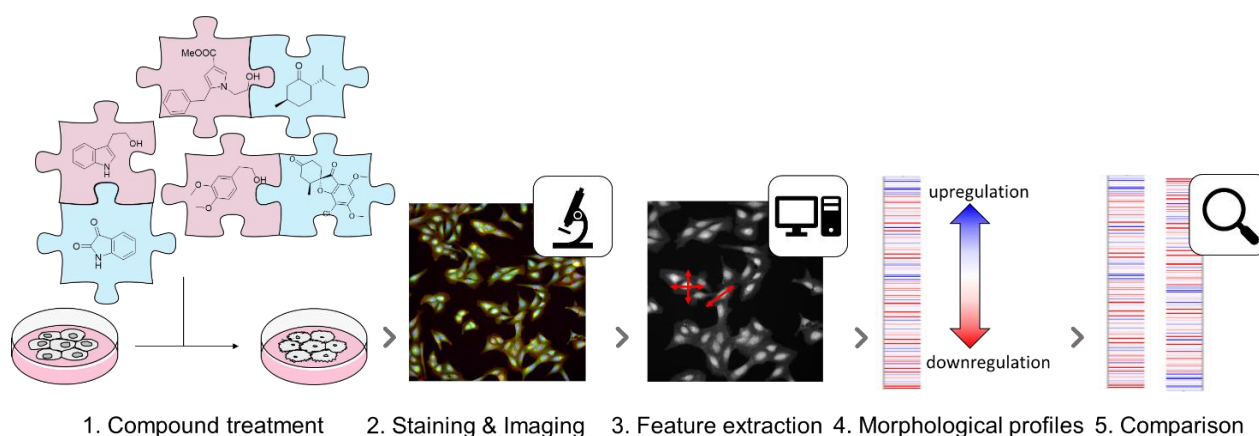


Figure 13: Overview of the cell painting assay.

The high potential of the cell painting assay to investigate bioactivity was already recognized in the pioneering report of Carpenter et al. in 2013.<sup>[57]</sup> In addition to the supposed applications in identifying new targets and mode-of-actions, Clemons et al. demonstrated its application for compound selection in order to maximize a collection's heterogeneity.<sup>[50, 58]</sup> In combination with other phenotypic high-throughput screens, the cell painting assay delivered important information to enrich the collection hit rate. Furthermore, stereomeric investigations with disubstituted azetidines revealed morphological differences derived from different mode-of-actions.<sup>[54b]</sup>

## 1.4. AUTOPHAGY AND ITS REGULATION

Autophagy is a highly conserved mechanism of eukaryotic cells to maintain the organismal homeostasis in both physiological and pathological situations. The catabolic process accounts for the cell's degradation of cytosolic components including metabolism products that are correlated with cytotoxicity upon accumulation, redox-active protein aggregates, pathogens, and damaged mitochondria.<sup>[59]</sup> The clearance of dysfunctional mitochondria prevents the release of reactive oxygen species and defends the cell against these toxic effects. Thereby, autophagy often represents a stress reaction, which is caused by intracellular or extracellular perturbations such as infections, starvation, or other metabolic, physical or chemical challenges.<sup>[60]</sup> Nutrient deprivation induces autophagy and allows a temporary compensation for the lack of extracellular nutrients by providing relevant building blocks through degradation.<sup>[61]</sup> A misbalance between formation and degradation of macromolecules is associated with various diseases as cancer<sup>[62]</sup> and neurodegenerative disorders including Alzheimer's, Huntington's, and Parkinson's disease.<sup>[63]</sup> Autophagy's clinical relevance has led to a considerable attention in the past decade and the development of several tool compounds and pharmaceutical drugs.<sup>[64]</sup>

Autophagy is divided into three forms depending on the delivery of substrates for degradation to the lysosomes: microautophagy, chaperone-mediated autophagy, and macroautophagy. The latter as main route to the lysosome is the best characterized and the most prominent form of autophagy. Upon induction via different stimuli, macroautophagy (hereafter annotated as autophagy) is initiated through the formation of phagophores, which are cytosolic membrane structures (Figure 14). Phagophores encompass the autophagic cargo consisting of various macromolecules targeted for degradation, as well as the autophagy receptor protein p62/SQSTM1<sup>[65]</sup> and elongate to double-walled vesicles called autophagosomes. After the fusion with the lysosome, the initially formed autolysosome contains acidic lysosomal enzymes that facilitate the degradation of the autophagic cargo. Additionally, the inner membrane is degraded and finally, permeases release the building blocks into the cytosol.<sup>[61, 64b]</sup>

Autophagy relies on complex machinery coordinated by various regulators at numerous stages. The first autophagy-related gene (ATG) was published in 1997<sup>[66]</sup> and represents the start of an unprecedented increase in the number of papers about autophagy.<sup>[64b]</sup>

The multistep formation of autophagosomes is mediated by complex signal transduction (Figure 14)<sup>[64a]</sup>. Comprehensive genetic studies identified ATG1 kinase as an essential autophagy regulator in yeast. The mammalian homologue to ATG1 is the ULK1 complex, consisting of ULK1, ATG13, FIP200 and ATG101. The key energy sensor AMP activated protein kinase (AMPK)

phosphorylates the ULK1 complex, which subsequently regulates the class III PI3K complex and consequently induces autophagy. The classical mammalian autophagy regulation is via the mammalian target of rapamycin complex 1 (mTORC1) pathway, which has an inhibitory effect on the ULK1 complex and therefore on autophagy induction. Respectively, the addition of rapamycin as a natural mTORC1 inhibitor induces autophagy. The mTORC1-independent regulation relies on the intracellular levels of inositol 1,4,5-trisphosphate (IP<sub>3</sub>), Ca<sup>2+</sup> ions and cAMP. As all second messengers effect autophagy negatively, reduced levels can induce the pathway.<sup>[64a]</sup>

In mammalian autophagy, several ATG proteins are involved in the formation of key protein LC3, which takes an essential part in the phagophore elongation and closure. To fulfill its function, LC3 is activated through lipidation with phosphatidylethanolamine (PE). The active form LC3-II is able to localize in membranes and allow its recruitment to the phagophore. LC3-II represents a marker for the autophagy process as it remains on the autophagosome through its whole lifespan. Additionally, the ATG12-ATG5-ATG16L1 complex is also located on the phagophore and plays a relevant role in autophagosome formation. However, upon autophagosome formation and following maturation, the complex dissociates.

The late stage of autophagy is characterized by the autophagosome maturation. This process is mediated by diverse factors such as different SNAREs (syntaxin 17 and SNAP29 on autophagosomes, and VAMP8 on lysosomes), homotypic fusion and protein sorting (HOPS) complex, Rab7, GABARAPs, and Beclin1-interacting partners such as ATG14L, amongst others.<sup>[64a]</sup>

## Introduction

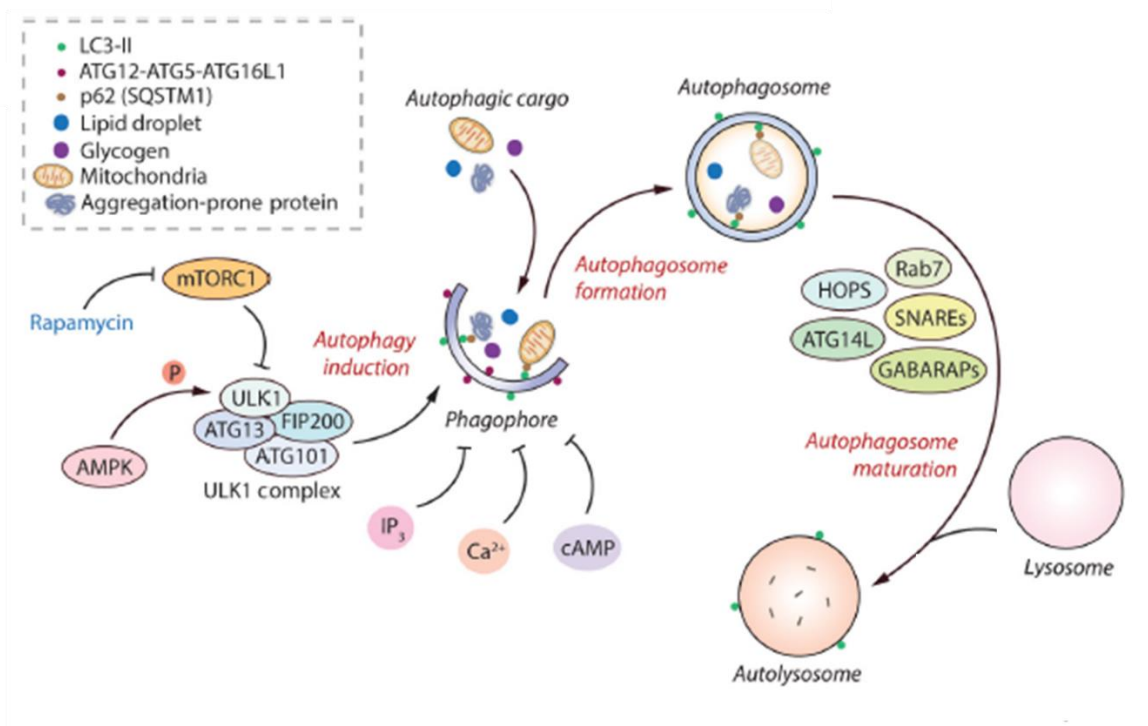


Figure 14: Regulation of macro autophagy in mammalian cells (adapted from <sup>[64a]</sup>).

Due to its importance in several cellular functions, the autophagy pathway is a target of interest for small molecules. Over the past years, several autophagy modulators were investigated as tool compounds for enlightenment of the molecular mechanism of the pathway and also for clinical applications.<sup>[62, 64a]</sup> The mTORC1 inhibitor rapamycin is a known autophagy inducer and has proven to reduce accumulation of amyloid- $\beta$ .<sup>[67]</sup> In this context rapamycin similarly to the AMPK activator resveratrol has shown beneficial effects on Alzheimer's disease in a mouse model. Autophagy inhibitors on the other side may apply in cancer therapy.<sup>[62]</sup> Wortmannin<sup>[68]</sup> as a rather unselective PI3K inhibitor and several other selective VPS34 inhibitors including VPS34-IN1<sup>[69]</sup>, autophinib<sup>[70]</sup>, and azaquindole-1<sup>[23]</sup> appear to interfere with autophagosome biogenesis. Chloroquine and its derivative hydroxychloroquine effect the autolysosome formation by preventing the autophagosome-lysosome fusion. The accumulation of autophagosomes negatively effects the autophagic flux.<sup>[71]</sup> Both modulators derived from quinoline represent important tool compounds in the study of autophagy and are employed in clinics as FDA approved drugs. Due to its autophagy inhibition chloroquine is used in combination with other chemotherapeutics for several anti-cancer treatments.

## 2. AIM OF THE THESIS

Despite decades of research and great advances through new technologies, many diseases and their stimuli are still insufficiently understood for the development of effective therapeutics, not to mention a cure. New tool compounds have the potential to resolve biological coherences and close remaining gaps in knowledge.

For this purpose, the aim of this thesis is to generate new chemical entities that can act as modulators of relevant biological pathways. The new compound classes are based on the pseudo-NP approach which is the fusion of biosynthetically unrelated NP fragments.<sup>[12, 20-23, 53]</sup> These fragments can be considered as prevalidated by nature and might bear biological relevance that enhances the hit rates in bioassays. Employing an oxa-Pictet-Spengler reaction as a means to merge an aryl ethanol fragment with a cyclic NP fragment having a ketone functionality should give access to new, complex spiro pseudo-NP classes. Beyond the three-dimensional complexity, the diversity of the library can be increased by different fragments, both carbonyl-containing compounds and aromatic nucleophiles, as well as utilizing isomeric variants, including the unreported *iso*-oxa-Pictet-Spengler reaction. A further level of complexity and diversity is gained by the dearomatization<sup>[37, 72]</sup> of indole-containing pseudo-NP classes through the incorporation of an additional fragment. This approach should provide interesting indolenine and indoline pseudo-NP collections.

After the establishment of the complexity generating reactions and the exploration of the scope, the compounds are supposed to be investigated regarding their new chemical and biological properties. Cheminformatic analyses should clarify the pseudo-NPs coverage in the Lipinski's-like space<sup>[73]</sup>, their three-dimensionality<sup>[74]</sup> and NP-likeness score<sup>[75]</sup>. Furthermore, the collections are evaluated in diverse phenotypic screenings including a morphological profiling assay<sup>[46, 57-58, 76]</sup> for their potential as new tools in chemical biology and drug discovery. Novel effects can be investigated from the analysis of a structure-activity-relationship study to determine the most active compound for mode-of-action and target identification. Morphological profiling can be applied for a deeper analysis of structural influences on the phenotype including different connection types, regioisomers or fragment combinations. In addition to the investigation of new bioactivities, it might be interesting to evaluate the fragment's original activities, especially when they represent a relevant part of the active molecules. Analyses of the new pseudo-NP classes could not only generate new bioactivity, but also result in loss of the biological properties of their parent fragments and may provide a deeper understanding of the pseudo-NPs concept in the discovery of entirely novel tool compounds.

## 3. RESULTS AND DISCUSSION

### 3.1. PSEUDO-NPS VIA PICTET-SPENGLER REACTION

#### 3.1.1. LIBRARY DESIGN

Based on the pseudo-NP concept (chapter 1.1.1), the compound library is supposed to have broad structural diversity and increased complexity through the combination of NP fragments. The Pictet-Spengler reaction constitutes a good opportunity to combine two fragments as it generates complexity to mimic the high stereogenic content observed in NPs.<sup>[20]</sup> This method can be used to fuse privileged aromatic fragments, such as indoles, pyrroles, or chromans which are ubiquitous in nature for example in the NPs yohimbine, pyrrolostatin, and blapsin B, to carbonyl-containing fragments (Figure 15). Ketones are particularly advantageous combination partners as a diverse range of NPs bearing this functionality are either commercially available or readily accessible in a few synthetic steps, including (-)-menthone, griseofulvin, and cholestanone.

Employing cyclic ketones yields a cyclic structure fused at a central carbon representing a new spirocyclic center. The spiro connection of two fragments results in sterically more demanding structures with a high degree of three-dimensionality. Molecular complexity has been associated with target selectivity, compound safety and therefore a greater chance of success in clinical development.<sup>[77]</sup> Furthermore, the spiro center represents a new stereogenic center and the asymmetric characteristics of the molecule is one important criterium of biological activities. Constrained spiro motifs occur in many alkaloid, lactone or terpenoid NPs fulfilling diverse bioactivities, including antimicrobial, antitumor, and antibiotic activity.<sup>[78]</sup> Therefore, a connection via spiro center may be advantageous as it increases the complexity and is present in several NPs constituting a broad spectrum of bioactivities.

The combination of the two NP fragments via oxa-Pictet-Spengler reaction generates diverse subclasses depending on the applied aryl alcohol, for example spiro indole tetrahydropyrans, spiro benzofuran tetrahydropyrans, spiro pyrrole oxazines, spiro thiophene tetrahydropyrans, and spiro chromans, among others.

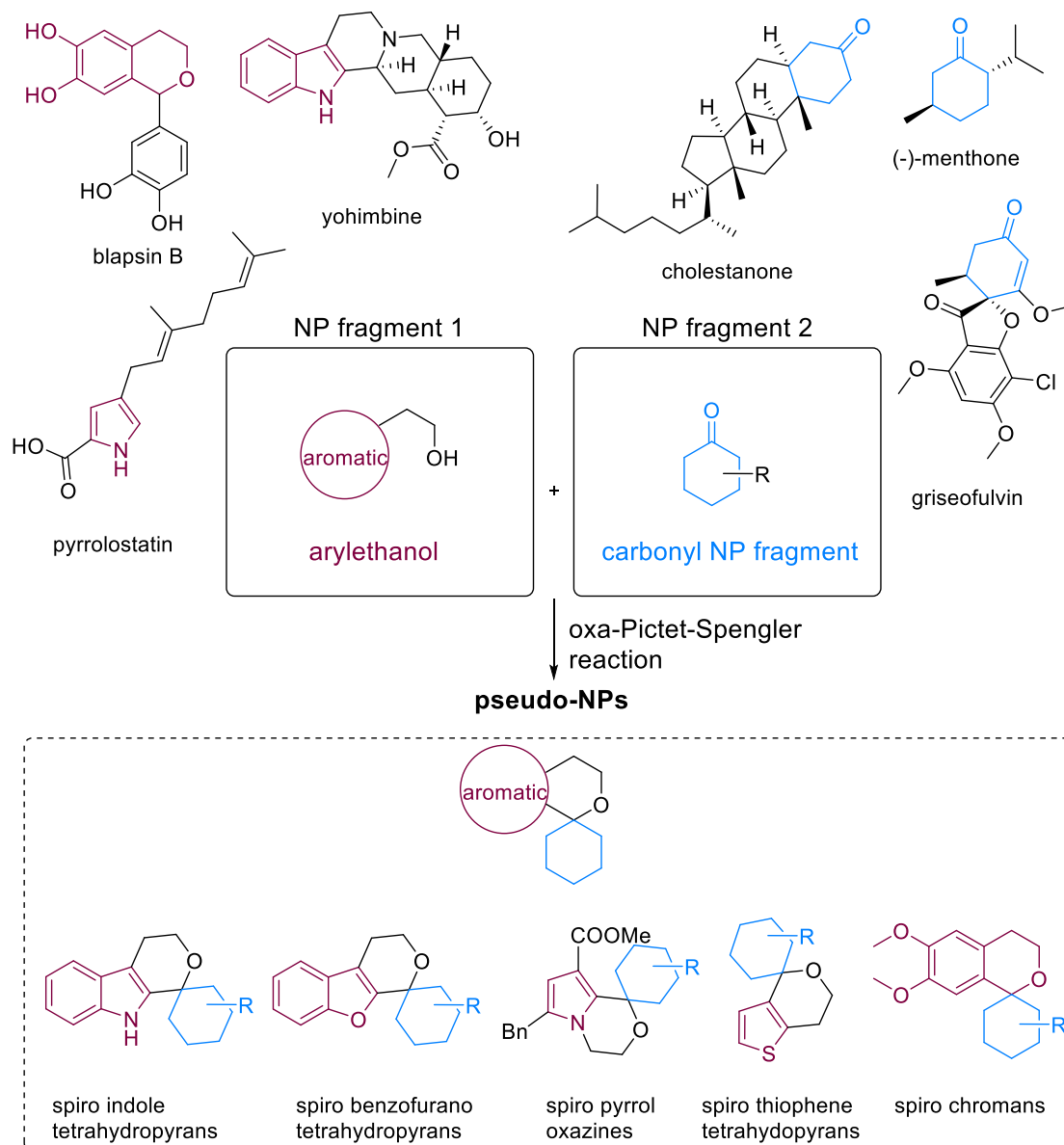


Figure 15: Library design based on the combination of aryl ethanol with cyclic ketone fragments via Pictet-Spengler reaction. Three different fragment representations in nature are shown, such as for the aryl fragments blapsin B, pyrrolostatin, and yohimbine and griseofulvin, cholestanone, and menthone for carbonyl compounds. A high level of diversity is achieved by the application of diverse aromatic compounds including indole, benzofurans, pyrroles, thiophenes, among others to generate pseudo-NP classes as spiro indole/benzofuran tetrahydropyrans, spiro pyrrole oxazines, spiro thiophen tetrahydropyrans, and spiro chromans.

Structural diversity can be employed by using very diverse aryl alcohols, such as indoles, benzofurans, pyrroles, thiophenes, and different phenol derivatives. Additionally, diversity can be increased by employing different isomeric variants of the same aryl alcohol (Figure 16). For instance, an indole **11** can be functionalized in three positions. Tryptophol **12** with a functionalization in the C3 position represents the starting material for the standard oxa-Pictet-Spengler reaction and yields  $\beta$ -spiro indole tetrahydropyrans. The *iso*-oxa-Pictet-Spengler reaction with indoles bearing the ethanol in the C2 position (**13**) results in  $\gamma$ -spiro indole tetrahydropyrans, which differ in the orientation of the indole. This *iso*-version and consequently the connection type are unknown through existing biosynthetic pathways and therefore, provide interesting, new scaffold variants. Furthermore, a functionalization on the indole nitrogen is conceivable (**14**), which leads to spiro indole oxazines. The second level of diversity is achieved by employing various carbonyl fragments differing from fragment-sized NPs such as griseofulvin to smaller building blocks, including isatin or (-)-menthone.

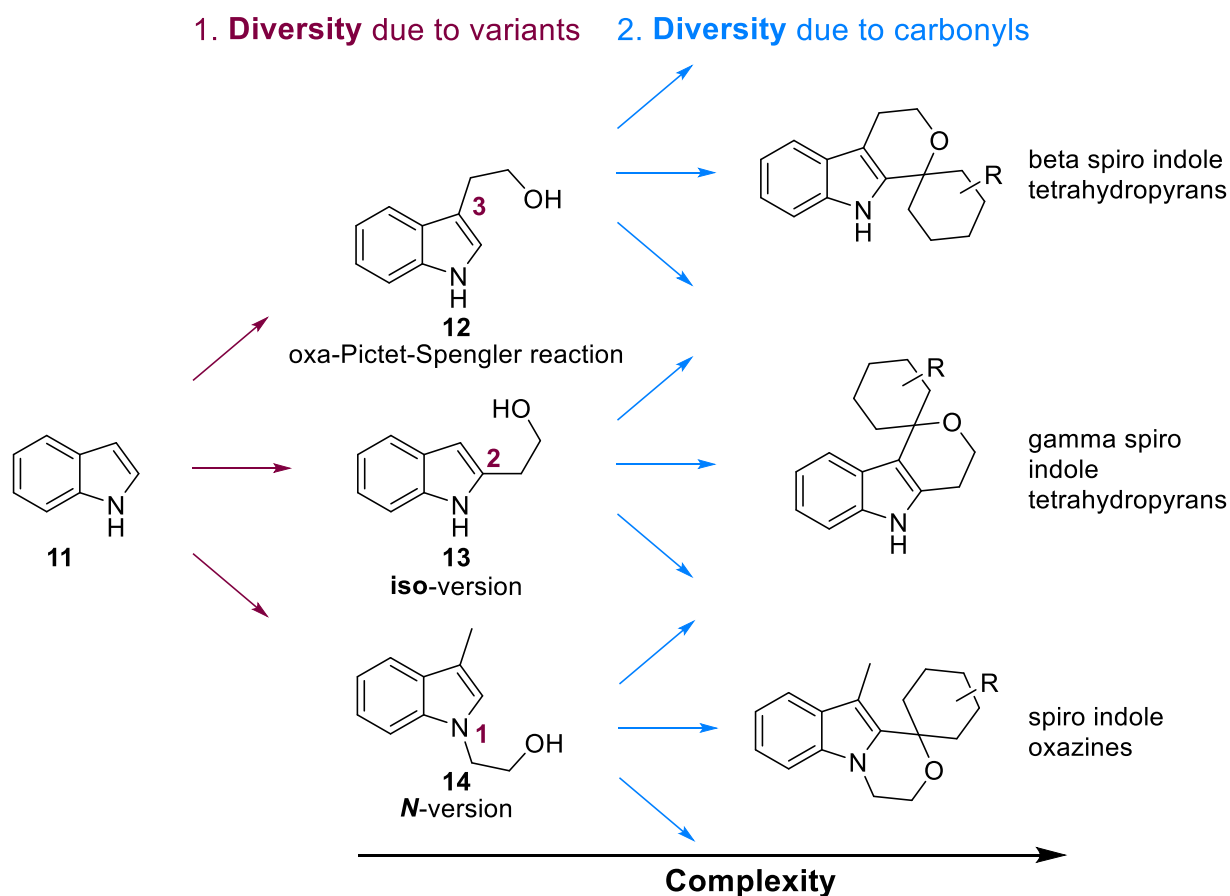


Figure 16: Strategy to increase diversity and complexity of the compound library using the indole as an example by the application of different variants and carbonyl fragments while simultaneously raising complexity.



The current state of the oxa-Pictet-Spengler especially the *iso*-version is underdeveloped and many substrate combinations either result in low yields, have extensive reaction times<sup>[79]</sup> at elevated temperatures<sup>[80]</sup>, or are not present in the literature. Our goal was to first develop a robust, general method that can then be applied for a diverse library synthesis.

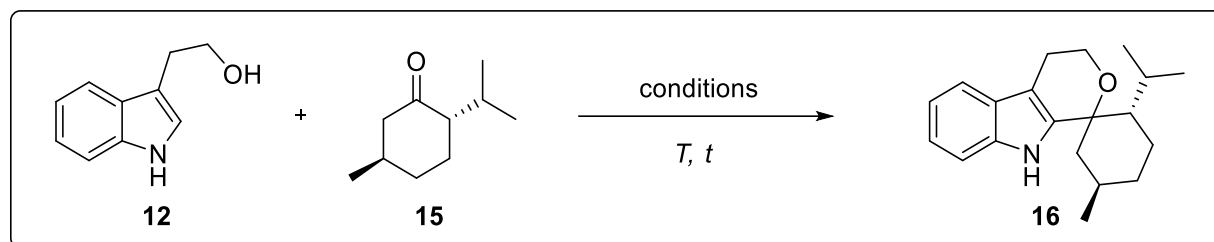
### 3.1.2. METHOD DEVELOPMENT

As synthetic methodology often limits the complexity and diversity of compound libraries, there is a need for new reactions especially those that enable non-traditional connections.<sup>[27]</sup> The Pictet-Spengler reaction (chapter 1.2.1.) was chosen to connect aryl ethanol and cyclic ketones. Although the reaction itself has been known for over one hundred years, its oxa-version with sterically demanding cyclic ketones and the isomeric variants still remain underdeveloped.

To enable the oxa-Pictet-Spengler reaction with challenging starting materials, the method was investigated on the commercially available model substrates tryptophol **12** and (-)-menthone **15** (Table 1). First optimization attempts with employing previously reported<sup>[31]</sup> successful Brønsted acids, including para-toluene sulfonic acid (pTs) and trifluoroacetic acid (TFA), did not deliver the product **16** in a desired yield (Table 1, entry 1-3). The Lewis acid boron trifluoride etherate (BF<sub>3</sub>·Et<sub>2</sub>O) showed a yield of 27% of the desired product **16** after five days (Table 1, entry 4). However, neither further extending the reaction time nor varying the temperature and/or the solvent increased the yield. Also, the addition of dehydrating agents, as sodium sulfate, did not improve the yield to an extent which can be used for the synthesis of a compound library. After substantial experimentation, triflic acid adsorbed on silica gel (TfOH·SiO<sub>2</sub>) was identified as suitable catalyst for the oxa-Pictet-Spengler reaction with cyclic ketones. A reaction time of just 30 min was sufficient to deliver the desired cyclized product **16** in almost quantitative yield of 98% (Table 1, entry 5, hereafter referred as optimal reaction conditions). These conditions are a significant improvement to those currently in the literature. The triflic acid supported on silica gel is readily prepared, safe to handle, easily removed from the reaction mixture via filtration, and can even be recycled after the reaction. In literature, TfOH·SiO<sub>2</sub> is mainly applied for alkylation reactions<sup>[81]</sup> for instance of β-dicarbonyl compounds through the direct reaction with alcohols or alkenes<sup>[82]</sup>. Interestingly, neither triflic acid (TfOH) nor silica (SiO<sub>2</sub>) alone showed a similar effect, indicating the importance of the adsorption (Table 1, entry 6 and 7).

## Results and Discussion

Table 1: Method development by screening various different reaction conditions.



Entry	Conditions	Additives	$t$ [h]	Yield* <b>16</b> [%]
1	pTs (10 mol%), MeOH	-	120	no conversion
2	pTs (10 mol%), MeOH	Na <sub>2</sub> SO <sub>4</sub>	120	7
3	TFA (10 mol%), MeOH	Na <sub>2</sub> SO <sub>4</sub>	120	11
4	BF <sub>3</sub> ·Et <sub>2</sub> O (10 mol%), MeCN	Na <sub>2</sub> SO <sub>4</sub>	120	27
5	TfOH·SiO <sub>2</sub> (6.5 mol%), CH <sub>2</sub> Cl <sub>2</sub>	-	0.5	98
6	TfOH (10 mol%), CH <sub>2</sub> Cl <sub>2</sub>	-	120	traces
7	SiO <sub>2</sub> (10 mol%), CH <sub>2</sub> Cl <sub>2</sub>	-	120	no conversion

\*Yield determined by NMR.

Under the optimal reaction conditions one diastereomer (>20:1) was detected for the model reaction with (-)-menthone. It was observed that this diastereoselectivity is derived from the steric hindrance of the carbonyl fragment. Sterically demanding residues in the  $\alpha$  position result in high selectivity during the cyclization, whereas the oxa-Pictet-Spengler reaction with 3-methyl cyclohexanone led to the formation of both diastereomers (further discussion in 3.1.4.).

### 3.1.3. SUBSTRATE SCOPE

The robustness of the developed oxa-Pictet-Spengler reaction conditions was investigated for various aryl alcohols and carbonyl fragments while aiming for a versatile pseudo-NP library.

#### STARTING MATERIALS

For the first NP fragment, different aryl alcohols were commercially available or were obtained in a few synthetic steps. The starting materials for the oxa-Pictet-Spengler reaction, its *iso*- and *N*-version were derived from the same indole derivatives (Figure 17). The functionalization was performed under basic conditions to some extent with a catalyst for regioselectivity.

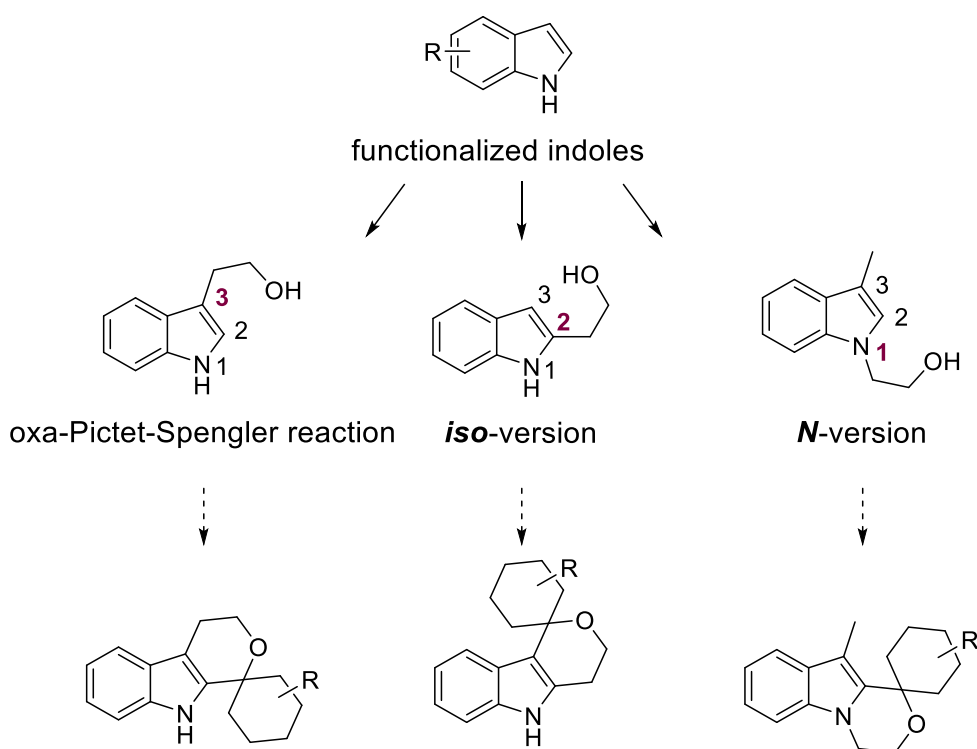


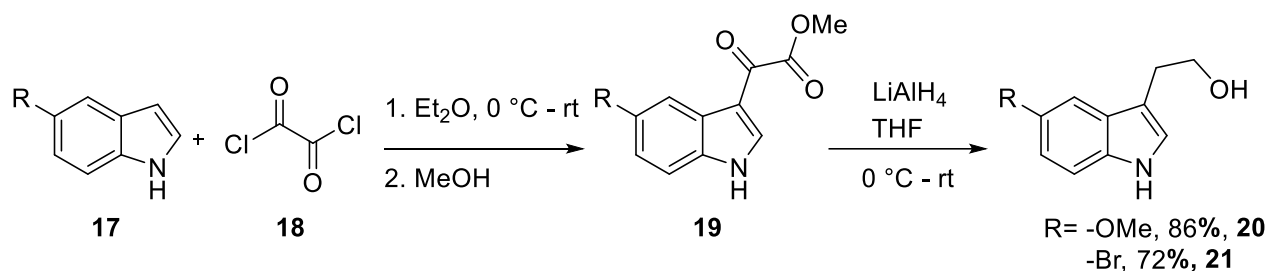
Figure 17: Isomeric variants for the enhancement of structural diversity. Three different functionalization positions on the indole result in two types of spiro indole tetrahydropyrans differing in the orientation of the indole and spiro indoles oxazines.

The indole as planar heteroaromatic molecule shows an inconsistent distribution of the electron density. Whereas the heterocyclic nitrogen atom is acidic due to the delocalization of its free electron pair into the  $\pi$ -system, the resonance results in a relatively high electron density on C3.<sup>[83]</sup> Consequently, this position is nucleophilic and activated for electrophilic substitution reactions.

In order to synthesize indole derivatives with different residues on the indole ring, the respective indoles were used as starting materials for the introduction of the alcohol. A functionalization in

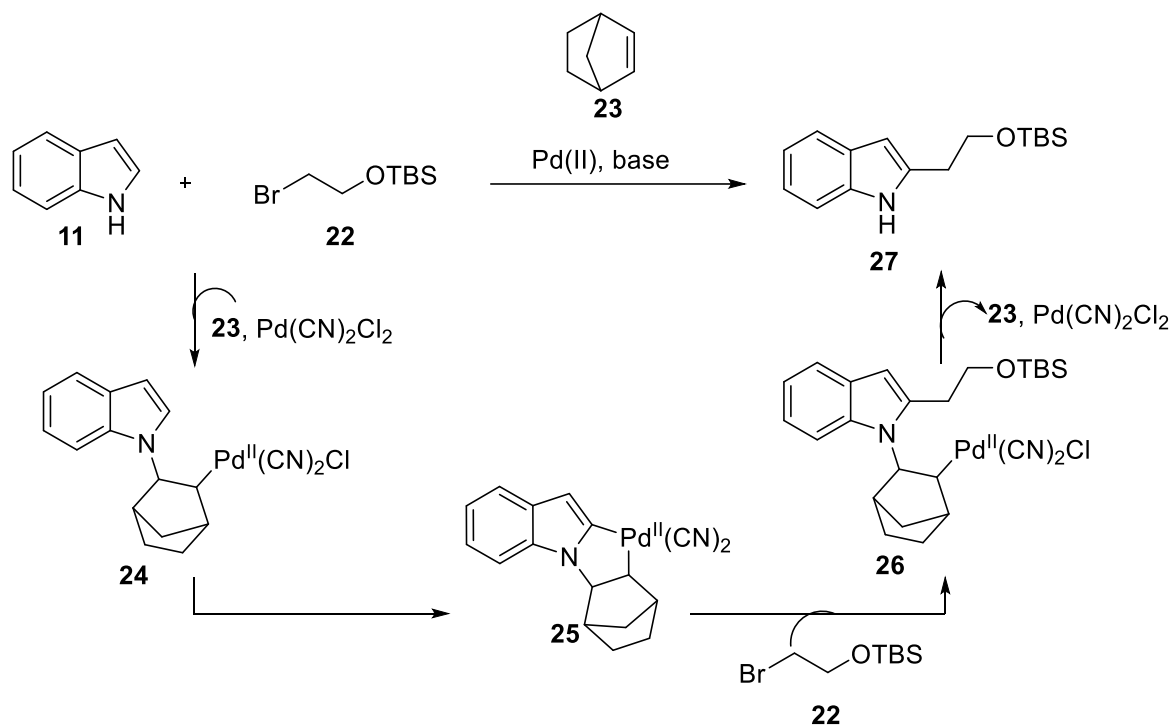
## Results and Discussion

C3 position requires due to its naturally nucleophilicity next to oxalyl chloride **18** no further addition of a base to form adduct **19** in high regioselectivity (Scheme 1). After reduction with lithium aluminum hydride (LiAlH<sub>4</sub>), two indole derivatives with a functionalization in C3 **20** and **21** were generated in good yields over two steps (72-86%).



Scheme 1: Two step introduction of an alcohol in the indole C3 position with oxalyl chloride. Isolated yield in percent (%).

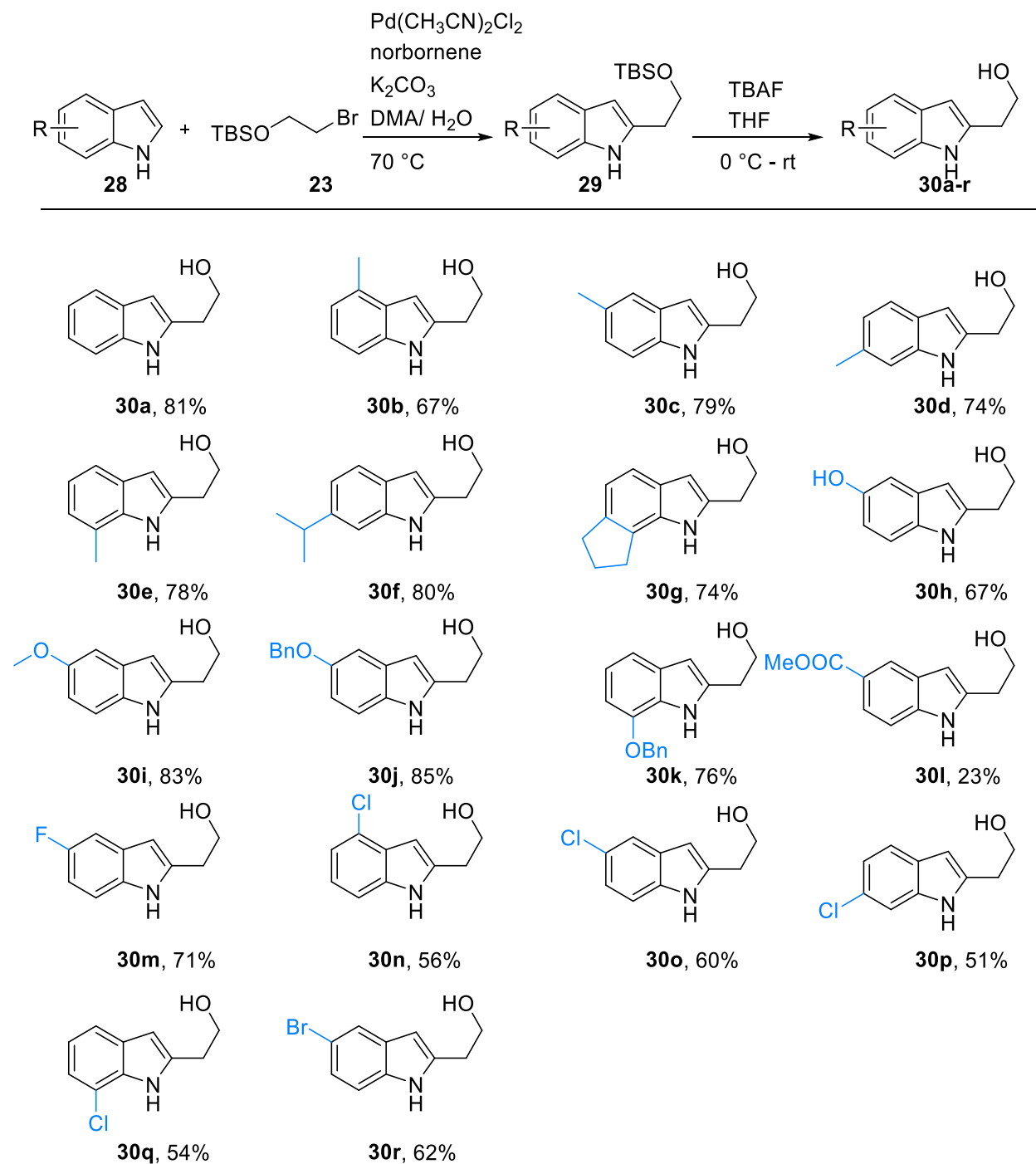
Whereas a regioselective installation of alkyl residues on the more electron-rich C3 position does not cause any problems<sup>[84]</sup>, only few methods enable a similar functionalization on C2 by direct C-H substitution<sup>[85]</sup>. Inspired by the Catellani reaction<sup>[86]</sup>, Bach et al. developed a process to access  $\alpha$ -alkyl-substituted indoles through palladium(II)/norbornene-cocatalysis.<sup>[87]</sup> In the first step, the indole interacts with the palladium(II) catalyst and norbornene **23** to give intermediate **24** (Scheme 2). After a base-catalyzed intramolecular *ortho*-palladation, the resulting palladaheterocycle **25** reacts with the TBS protected bromoethanol **22** by oxidative addition, reductive elimination, followed by norbornene expulsion, and protodepalladation to give the alkyl-substituted heterocycle **27**. Norbornene **23** represents a transpositional cocatalyst that assists palladium in activating the  $\alpha$ -C-H bond of NH indoles, providing excellent regioselectivities for the alkylation in C2.



Scheme 2: Proposed mechanism of the indole functionalization in the C2 position.<sup>[87]</sup>

The method<sup>[87]</sup> was applied to various commercially available indoles **28** with different residues on *C4-C7* yielding TBS protected indolyethanols **29**. Subsequently, the adducts **29** were deprotected by employing tetrabutylammonium fluoride (TBAF) solution to give diverse starting materials for the *iso*-oxa-Pictet-Spengler reaction **30a-r** (Scheme 3). In general different functionalities were well tolerated and the yields over the two-step synthesis were moderate to high (23-85%). Especially alkyl substituents, including methyl groups in **30b**, **30c**, **30d**, and **30e**, as well as isopropyl in **30f** and cyclopentyl in **30g**, gave high yields of the desired aryl ethanol (67-80%). Ethers, such as a methoxy group in **30i** or benzoyl groups in **30j** and **30k** are also well tolerated and result in good yields of 76-85%. A hydroxy group as in **30h** and halogens (**30m-30r**) result in slightly lower yields (51-71%). A plausible reason is the potential interaction of the Pd-catalyst with the halogens. However, a methyl ester **30l** gave the lowest yield at 23% and a carboxy functionality on *C5* resulted in no product formation, indicating a negative influence of electron withdrawing groups.

## Results and Discussion

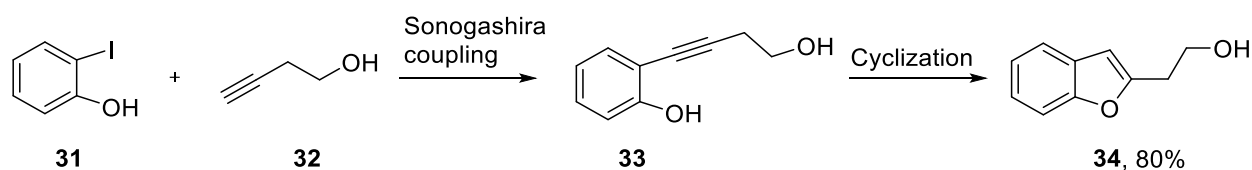


Scheme 3: Two-step syntheses<sup>[87]</sup> of different indolylethanol functionalized in C2 position. Isolated yield in percent (%).

Similar to the functionalization in the C2 position, TBS protected bromoethanol was applied for the synthesis of an indole-*N*-ethanol **14**. However, no catalyst for regioselectivity and just the

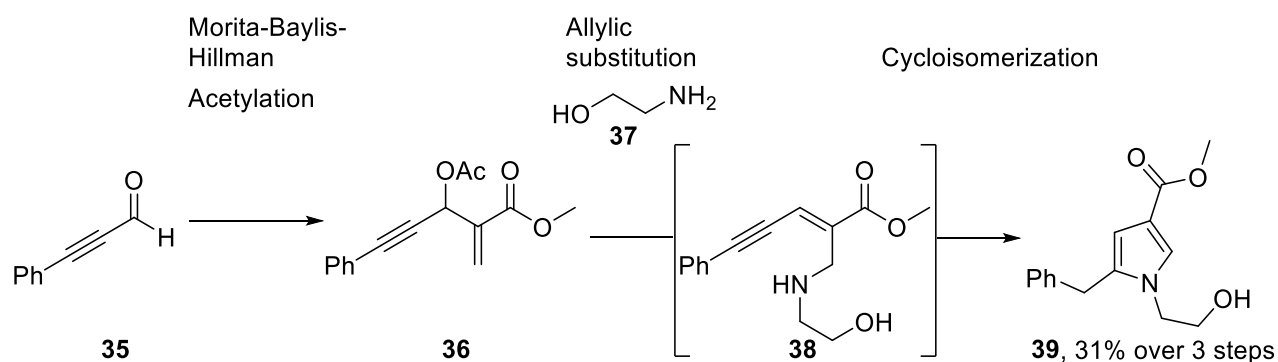
addition of sodium hydride as base was required to yield the desired indole starting material after deprotection in 83% over two steps.

2-Benzofuranoethanol **34**, the oxygen analog to the *iso* indole starting materials, was synthesized through a recently reported Sonogashira coupling followed by an intramolecular cyclization of 2-alkynyl phenols (Scheme 4).<sup>[88]</sup> Starting from 2-halophenol **31** and alkyne **32**, the 2-(phenylethynyl) phenol **33** was generated by Sonogashira coupling through Pd-catalysis. Commercially available copper(I) iodide enabled the mild cyclization of adduct **33** to form the desired 2-substituted benzofuran **34** in excellent yield (80%).



Scheme 4: Synthesis of 2-benzofuranoethanol **34** through Sonogashira coupling, followed by intramolecular cyclization.<sup>[88]</sup> Isolated yield in percent (%).

The access to the substituted pyrrole 2-(1*H*-pyrrol-1-yl)ethan-1-ol **39** was enabled by applying a procedure reported by Reddy et al. (Scheme 5).<sup>[89]</sup> First, the acetylenic aldehyde, phenylpropargyl aldehyde **35**, was submitted to a Morita-Baylis-Hillman (MBH) reaction and subsequently acetylated to give the MBH-acetate **36**.<sup>[89]</sup> A  $K_2CO_3$ -mediated tandem reaction involving allylic substitution/cycloisomerization with 2-amino-ethanol **37** led to the formation of 2-(1*H*-pyrrol-1-yl)ethan-1-ol **39**. The substituted pyrrole **39** was obtained in a good overall yield of 31% over three steps.



Scheme 5: Synthesis of the substituted pyrrole 2-(1*H*-pyrrol-1-yl)ethan-1-ol **39** from Morita-Baylis-Hillman acetates through a metal-free tandem reaction.<sup>[89-90]</sup> Isolated yield in percent (%).

Aryl ethanols, including benzothiophen-3-ethanol **53** and the phenol derivatives **62** and **64**, were generated in high yields (79-85%) through the reduction of their respective carboxylic acid with  $LiAlH_4$ .

### OXA-PICTET-SPENGLER REACTION ON INDOLES

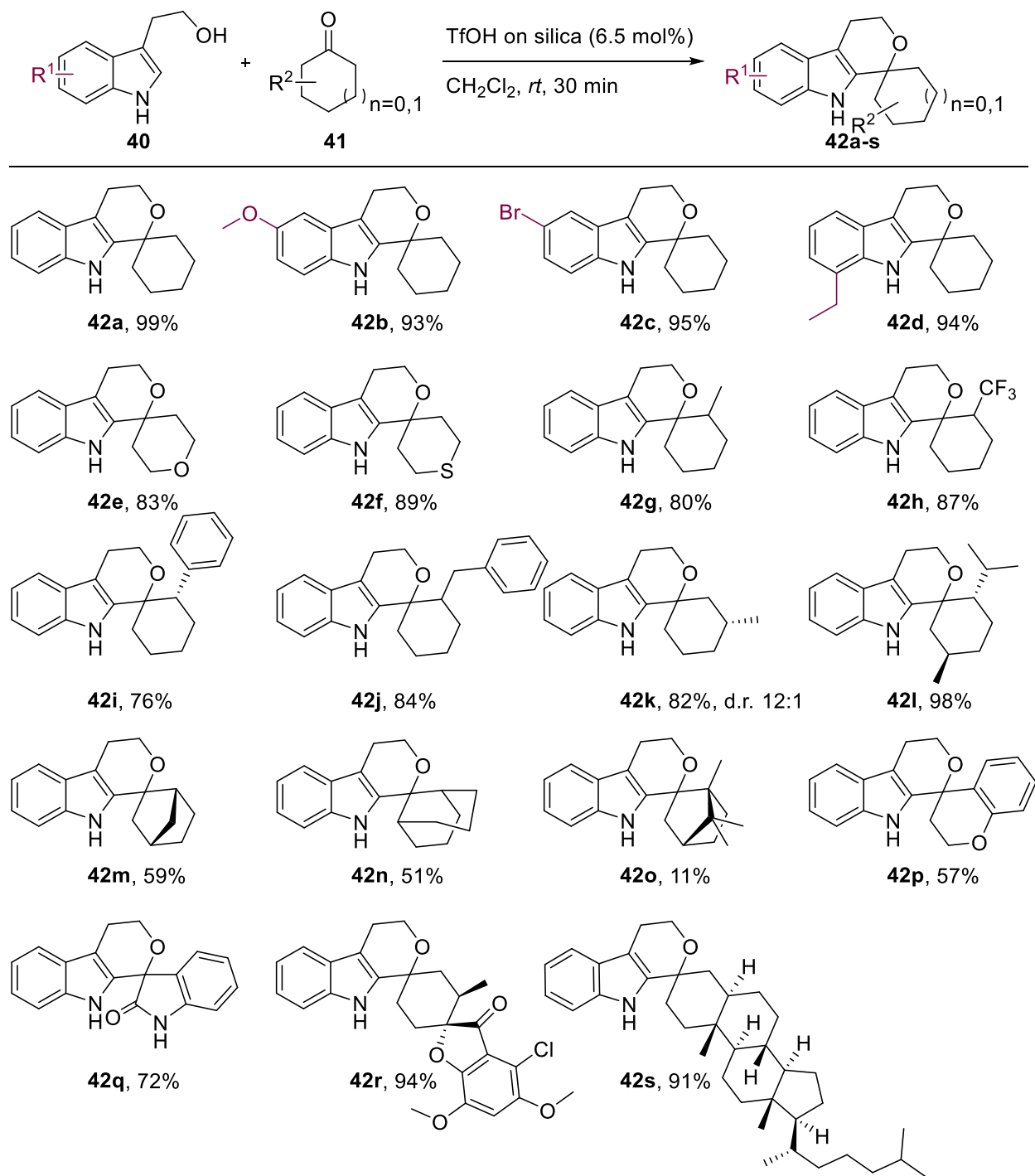
The substrate scope of the oxa-Pictet-Spengler reaction was investigated with 3-indolyethanol. The optimal reaction conditions were transferred to a number of different indoles with variations on the benzene ring and cyclic ketones varying in their substitution pattern (Scheme 6).

According to expectation, the oxa-Pictet-Spengler reaction of 3-indolyethanol **12** with the simplest cyclic ketone, cyclohexanone, resulted in an almost quantitative conversion to the desired spiro product **42a** (99%). The three derivatives of 3-indolyethanol with either a methoxy group, halogens or alkyl substitutions on the aromatic system led to a similarly high yield of **42b**, **42c**, and **42d** of 93-95%.

Cyclohexanone derivatives, including a pyran and its sulphur variant, gave the desired cyclized products **42e** and **42f** in very good yields of 83 and 98%. Alkyl substituents in the  $\alpha$  position of the carbonyl function, such as in **42g**, **42h**, **42i**, and **42j** were also tolerated. The increased steric demand directly next to the reaction center resulted in slightly reduced yields (76-87%). The  $\alpha$  position of carbonyl compounds is generally acidic and is subjected to keto-enol tautomerism, which usually rapidly interconvert stereoisomers. Consequently, the applied cyclic ketones, as well as the oxa-Pictet-Spengler products are racemic mixtures. The application of the enantiopure 3-methyl cyclohexanone delivered besides a high yield of **42k** (82%), separable diastereomers with a diastereomeric ratio (d.r.) of 12:1. However, for the oxa-Pictet-Spengler reaction with the NP (-)-menthone no formation of diastereomers was detected (**42l**). In comparison to a single methyl group in the  $\beta$  position, the sterically demanding *iso*-propyl in the  $\alpha$  position appears to induce diastereoselectivity. The same holds true for the bicyclic systems of norcamphor in **42m** and (-)-camphor in **42o**, where just one diastereomer was detected.

Bridged ketones resulting in **42m** and **42n** were also tolerated in the oxa-Pictet-Spengler reaction (51-59%). Even the reaction with the NP camphor with high three-dimensional character and steric hinderance gave the desired spiro compound **42o**, even though the yield was significantly reduced to 11%. Products derived from less electrophilic aromatic ketones, such as 4-chromanone and isatin, could be obtained in moderate to good yields (**42p** and **42q**). The optimized conditions were applied to the fragment-sized<sup>[19, 91]</sup> NP griseofulvin and the steroid NP 5 $\alpha$ -cholestan-3-one to provide **42r** and **42s** in excellent yield (91-94%).

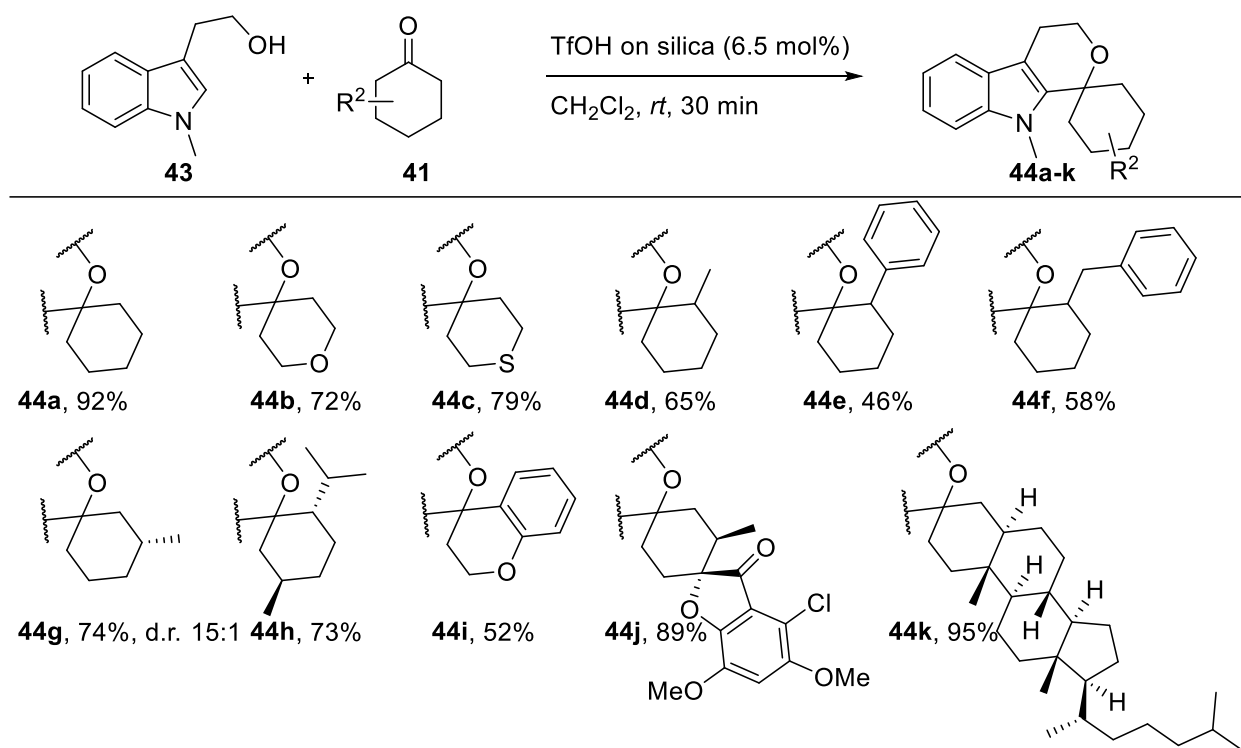




Scheme 6: Substrate scope of the optimized reaction conditions (ketone (1.5 eq.), TfOH-SiO<sub>2</sub> (6.5 mol%), CH<sub>2</sub>Cl<sub>2</sub>, *rt*, 30 min) of the oxa-Pictet-Spengler reaction on 3-indolylethanol and a variety of cyclic ketones differing degrees of steric hindrance, functional groups, and complexities. Isolated yield in percent (%). If not further indicated, the diastereomeric ratio (d.r.) is above 20:1.

## Results and Discussion

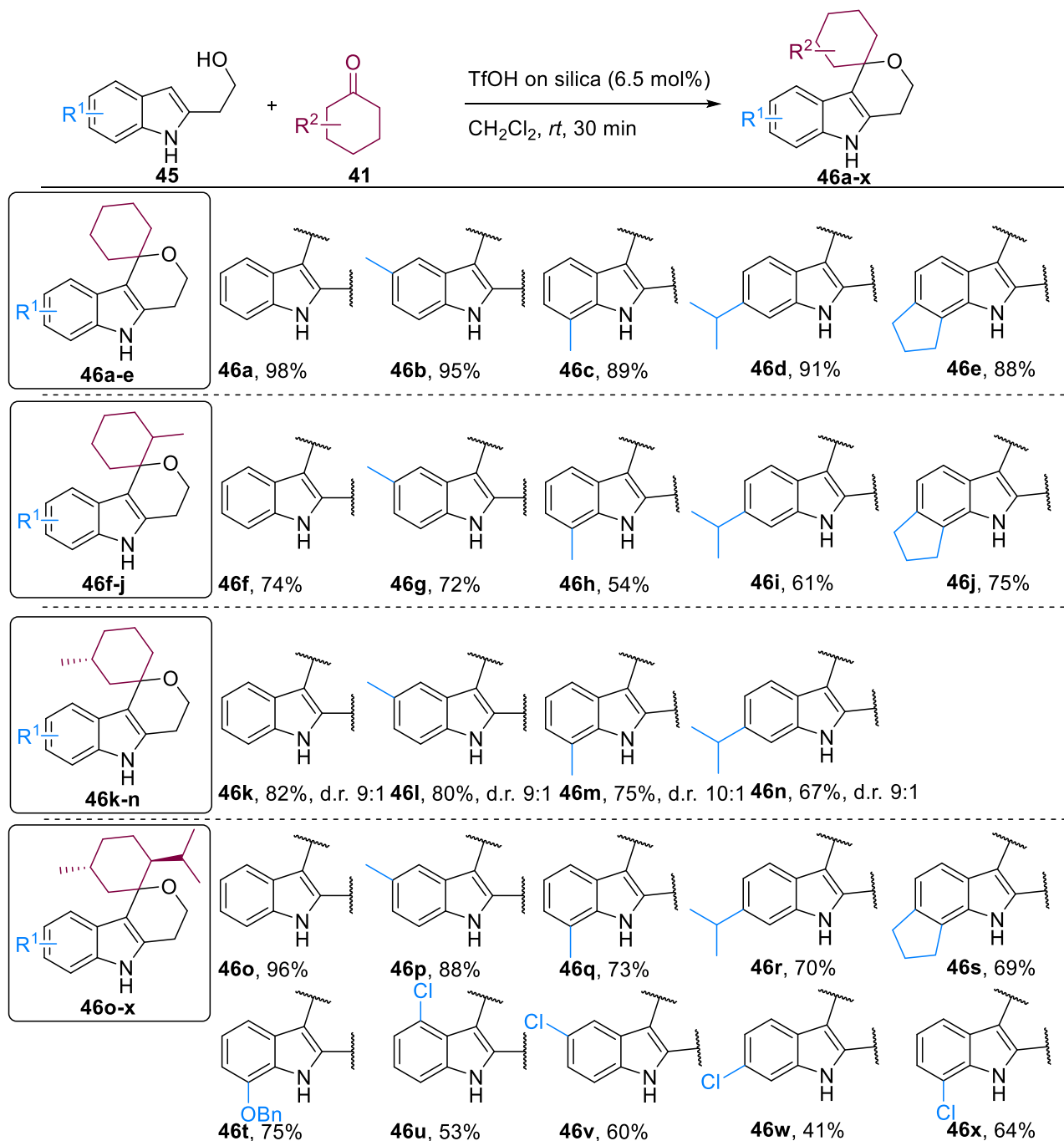
The oxa-Pictet-Spengler reaction with a substitution on the indole nitrogen was investigated for *N*-methyl 3-indolyethanol **43** and a selection of cyclic ketones (Scheme 7). Unhindered carbonyl compounds such as cyclohexanone, tetrahydro-4*H*-pyran-4-one, and 3-methyl-cyclohexanone reacted to give high yields between 72-92% of the desired products (**44a-c**). Even when more sterically hindered ketones were employed, moderate to high yields (46-74%) were obtained (**44d-g**). The oxa-Pictet-Spengler reaction was also tolerated with NPs or their derivatives, including (-)-menthone, chromanone, griseofulvin, and 5 $\alpha$ -cholestan-3-one to provide the desired pseudo-NPs **44h**, **44i**, **44j**, and **44k**. Excluding **44g**, all examples gave a diastereoselective ratio above 20:1.



Scheme 7: Oxa-Pictet-Spengler reaction on *N*-methyl 3-indolyethanol **43**. Isolated yield in percent (%). If not further indicated, the diastereomeric ratio (d.r.) is above 20:1.

To generate diversity, the isomeric variant was explored by employing the *iso*-oxa-Pictet-Spengler reaction on 2-indolyethanol derivatives. The optimized reaction conditions were applicable to several different cyclic ketones with various degrees of steric hindrance, functional groups, and complexities. First, the influence of substituents on the aromatic system of the indole was investigated on four cyclic ketones, including cyclohexanone, 2- and 3-methyl cyclohexanone and the NP (-)-menthone (Scheme 8). The unsubstituted indole as well as different alkyl residues on the indole were tolerated over all ketones and resulted in high yields (**46a-s**). Chloride derivatives

showed a slightly lower yield in the *iso*-oxa-Pictet-Spengler reaction (**46u-x**). Due to its negative inductive effect, the halogen reduces the electron density of the aromatic system, which may impair the conversion. In comparison,  $\alpha$  substituents were less tolerated, resulting in higher yields for (3-methyl) cyclohexanone (**46k-n**).

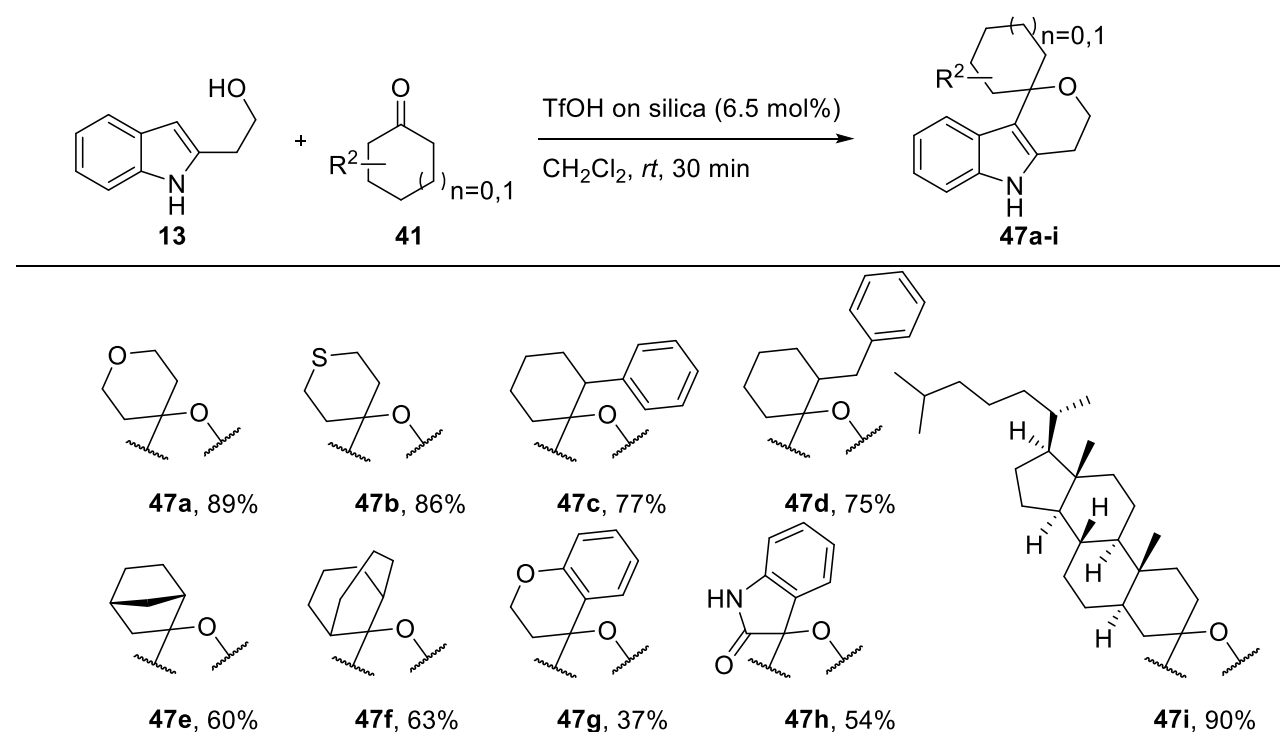


Scheme 8: *iso*-oxa-Pictet-Spengler reaction with diverse 2-indolylethanol with substituents on the aromatic system. Isolated yield in percent (%). If not further indicated, the diastereomeric ratio (d.r.) is above 20:1.

## Results and Discussion

As observed for the 3-indolylethanol derivative, the formation of diastereomers was only detected for the reaction with 3-methyl cyclohexanone (**46k-n**). For all indole derivatives, a diastereomeric ratio of about 9:1 was identified, indicating still a high preference for the formation of one stereoisomer. Nevertheless, (-)-menthone showed a high diastereoselectivity, which appears to be induced by the substituent in the  $\alpha$  position.

Afterwards, another nine cyclic ketones with varying degrees of complexity were employed in the *iso*-oxa-Pictet-Spengler reaction on the unsubstituted indole **13** (Scheme 9). Overall, a similar trend as for the 3-indolylethanol was observed. Cyclic ketones with no sterically demanding residues resulted in high yields (**47a** and **b**), whereas substituents in  $\alpha$  position slightly decreased the yield (**47c** and **d**). Bicyclic carbonyl scaffolds with a high ring strain and a high three-dimensional character showed a moderate yield of around 60% (**47e** and **f**). The less electrophilic carbonyl compounds as 4-chromanone and isatin resulted in a reduced yield (**47g** and **47h**). However, the complex NP 5 $\alpha$ -cholestan-3-one reacted to give an excellent yield of 90% of the desired product (**47i**).



Scheme 9: *iso*-oxa-Pictet-Spengler reaction of the unsubstituted 2-indolylethanol **13** with nine cyclic ketones with different complexities, including the NPs norcamphor, 4-chromanone, isatin, and the steroid derivative 5 $\alpha$ -cholestan-3-one. Isolated yield in percent (%). If not further indicated, the diastereomeric ratio (d.r.) is above 20:1.

The robustness of the developed oxa-Pictet-Spengler reaction conditions enabled access to various different indofulvins derived from the fragment-sized<sup>[19, 91]</sup> NP griseofulvin (Scheme 10).

Different substituents varying in electronic properties on the indole provided the desired pseudo-NPs in high yields. However, small differences were observed which corresponds to the trends reported before: More electron-rich aromatic systems lead to higher isolated yields. Thereby, the conversion of the *iso*-oxa-Pictet-Spengler reaction appears to be directly correlated to the activating or deactivating influence of substituents as electron-rich aromatic compounds promote electrophilic aromatic substitutions (Figure 18).<sup>[92]</sup> Beside hydrogen, all residues show a positive or negative inductive effect (+I or -I effect), as it is determined by the substituent's influence on the aromatic reactivity in comparison to benzene. However, substituents may display an additional mesomeric effect (+M or -M effect), which can have the same or opposite sign as its inductive effect. The activating or deactivating influence of a substituent results from the sum of its inductive and the potential mesomeric effect. Alkyl substituents, which slightly increase the electron density with their positive inductive effect<sup>[93]</sup>, were well tolerated and provided high yields (**50b-f** and **50n-o**). Ethers, including the methoxy group and the benzyl ether, as well as hydroxy groups share a positive mesomeric effect that is considerably stronger than its negative inductive effect. Therefore, ethers and hydroxy groups act as activating substituents, which are beneficial for electrophilic aromatic substitutions and provided excellent yields in the *iso*-oxa-Pictet-Spengler reaction (**50g-i**). In contrast, the negative inductive effect of chlorine and bromine exceeds their positive mesomeric effect. Thus, the halogens are deactivating substituents, indicated by the slightly reduced yield (**50j-l**). The methyl ester represents an electron withdrawing group which is dominated by its negative mesomeric effect. The reduced electron density became noticeable in the slightly reduced yield of indofulvin **50m**.

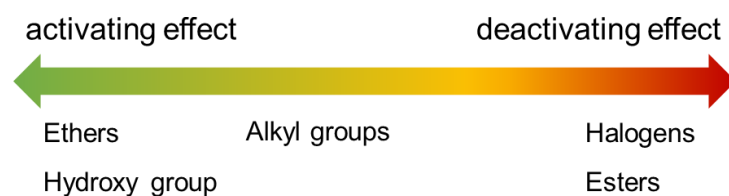
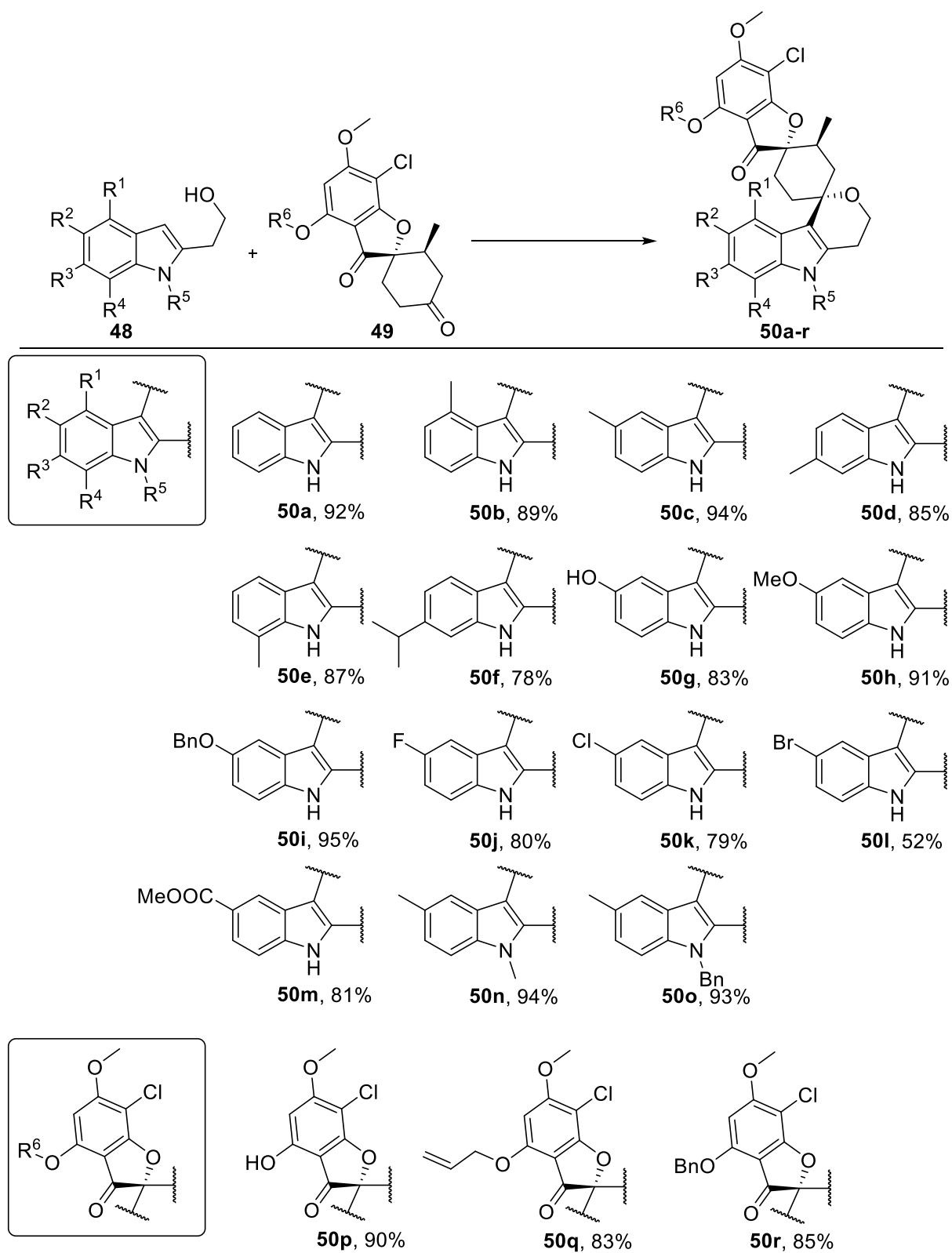


Figure 18: Activating or deactivating influence of substituents in electrophilic aromatic substitutions.<sup>[92]</sup>

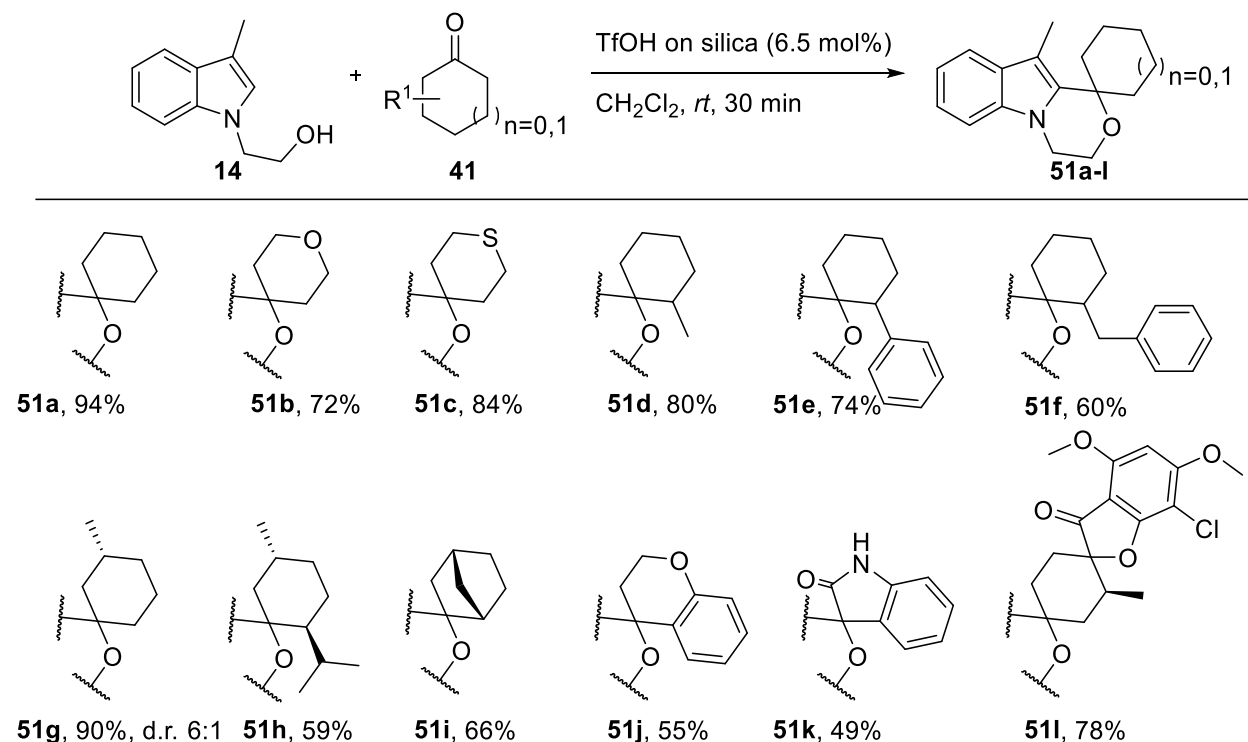
Derivatization on the indole nitrogen was generally well tolerated and resulted in excellent yields (**50n-o**). The griseofulvin ketone itself was derivatized by selective demethylation of one methoxy group and all three variants resulted in excellent yields (**50p-r**).

## Results and Discussion



Scheme 10: Substrate scope of indofulvins **50a-r** derived from 2-indolylethanol and griseofulvin derivatives. Isolated yield in percent (%).

The last investigated isomeric variant of the oxa-Pictet-Spengler reaction on indoles was the *N*-oxa-Pictet-Spengler. 2-(3-methyl-1*H*-indol-1-yl)ethan-1-ol **14** was subjected to the reaction with previously used cyclic ketones under the optimized reaction conditions (Scheme 11). Simple, unsubstituted carbonyl compounds, including cyclohexanone, tetrahydro-4*H*-pyran-4-one, and tetrahydro-4*H*-thiopyran-4-one, expectably provided the desired spiro compounds (**51a-c**) in high yields. Cyclic ketones with substituents in  $\alpha$  and  $\beta$  position, as well as the bicyclic NP norcamphor were also tolerated and gave moderate to excellent yields (**51d-i**). Experience with the other isomeric variants of the oxa-Pictet-Spengler reaction has shown that 4-chromanone and isatin had a slightly reduced yield which was also true for the reaction with 2-(3-methyl-1*H*-indol-1-yl)ethan-1-ol **14** (**51j** and **k**). The reaction with the derivative of griseofulvin resulted in a good yield of 78% (**51l**).

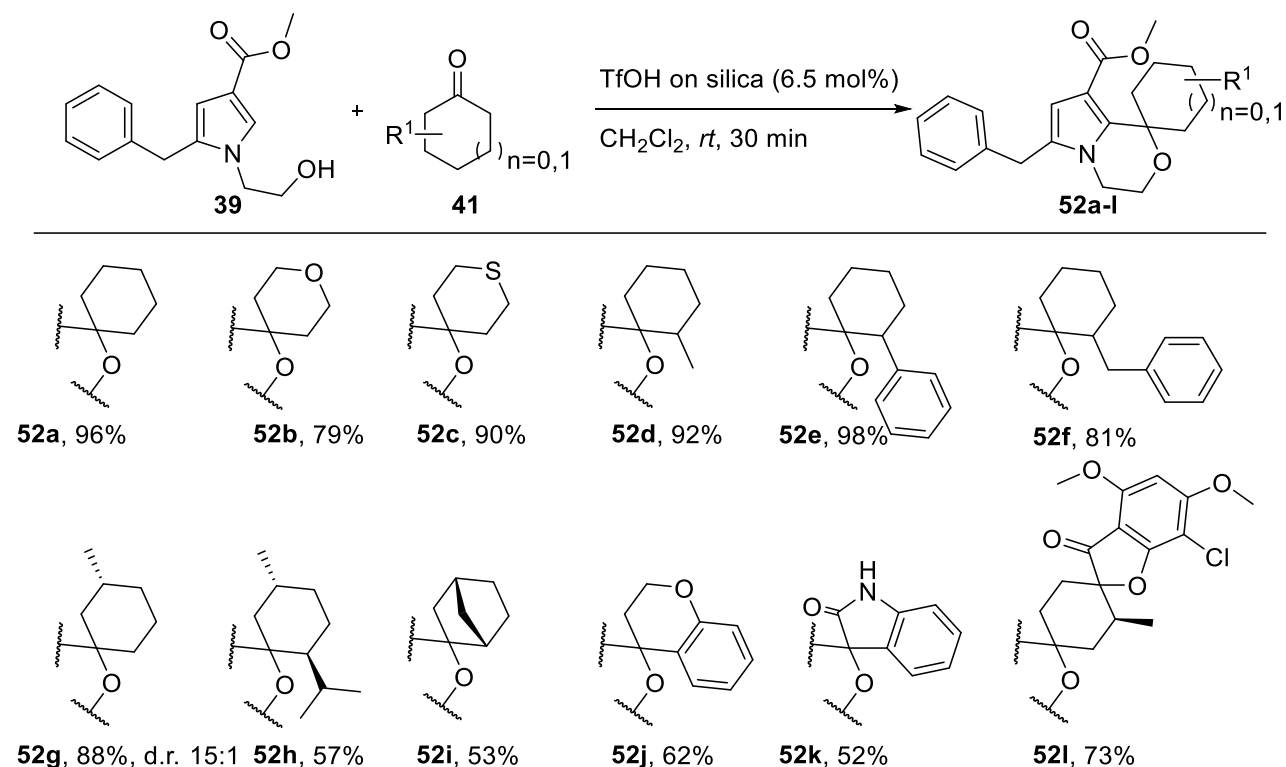


Scheme 11: *N*-oxa-Pictet-Spengler reaction of 2-(3-methyl-1*H*-indol-1-yl)ethan-1-ol **14** with a selection of cyclic ketones. Isolated yield in percent (%). If not further indicated, the diastereomeric ratio (d.r.) is above 20:1.

Altogether, indoles in several different variations turned out to be excellent coupling partners in the oxa-Pictet-Spengler reaction. Not only the common oxa-Pictet-Spengler reaction with 3-indolylethanol, but also the in nature unknown *iso*- and *N*-version enabled the synthesis of small and diverse compound libraries in high yields. Additionally, the optimal reaction conditions provided the pseudo-NPs class of indofulvins.

## OXA-PICTET-SPENGLER REACTION ON PYRROLES

The biologically interesting<sup>[94]</sup> pyrrole oxazine framework can be constructed via an oxa-Pictet-Spengler reaction with 2-(1*H*-pyrrol-1-yl)ethan-1-ol **39**. The previously reported method<sup>[89b]</sup> involved long reaction times of more 9-12 h for cyclic ketones to generate the desired spiro compounds in moderate to good yields (71-86%). Employing 2-(1*H*-pyrrol-1-yl)ethan-1-ol **39** with cyclohexanone under the optimized reaction conditions enabled the formation of the desired spiro compound **52a** in excellent yield (90%) after only 30 min at room temperature (Scheme 12). Also, other cyclic carbonyl scaffolds, including unsubstituted tetrahydro-4*H*-pyran-4-one and tetrahydro-4*H*-thiopyran-4-one, different ketones with substituents in  $\alpha$  and/or  $\beta$  position were tolerated (**52b-g**). NPs and their derivatives were also investigated in the oxa-Pictet-Spengler reaction and provided the pseudo-NPs in moderate yield (**52h-l**). Thus, the application of TfOH·SiO<sub>2</sub> immobilized on silica represents a significant improvement of the reaction conditions<sup>[89b]</sup> currently available in the literature.



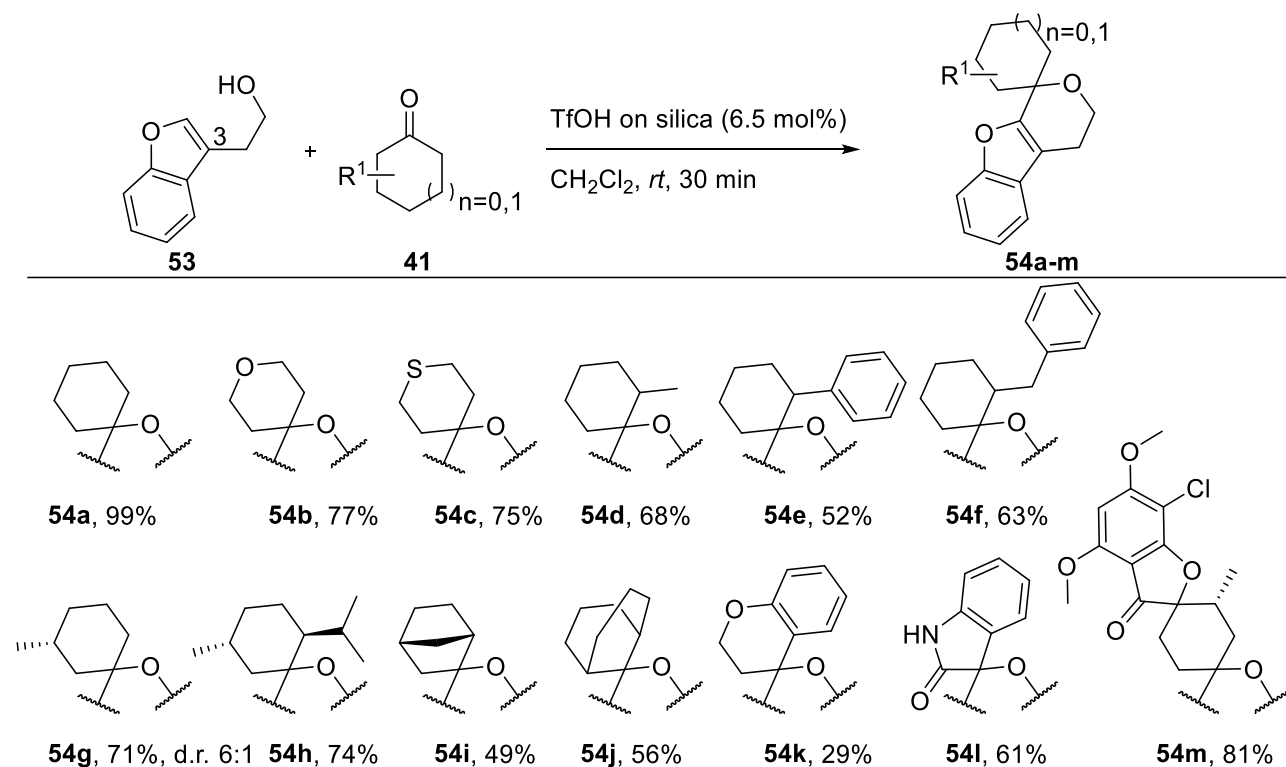
Scheme 12: Pyrrolooxazines **52a-l** derived from the oxa-Pictet-Spengler reaction of 2-(1*H*-pyrrol-1-yl)ethan-1-ol **39** with different cyclic ketones. Isolated yield in percent (%). If not further indicated, the diastereomeric ratio (d.r.) is above 20:1.



## OXA-PICTET-SPENGLER REACTION ON BENZOFURANS

Benzofuran is a privileged heterocycle in nature and for medicinal chemistry and potentially suitable for the Pictet-Spengler reaction. Gharpure et al.<sup>[95]</sup> reported a stepwise synthesis from vinylogous carbonate precursors through a oxa-Pictet-Spengler type reaction to generate C-fused pyranobenzofurans. However, the direct cyclization from benzofuranoethanols remain challenging.

The optimized reaction conditions for the oxa-Pictet-Spengler reaction proved to be successful for the synthesis of diverse spiro benzofurans derived from 3-benzofurano ethanol **53** (Scheme 13). Both unsubstituted cyclic ketones, including cyclohexanone, tetrahydro-4*H*-pyran-4-one and tetrahydro-4*H*-thiopyran-4-one, and diverse ketones with alkyl residues in the  $\alpha$  and/or  $\beta$  position yielded the desired spiro compounds (**54a-h**). Larger residues especially in the  $\alpha$  position, for instance in **54e** and **54f**, tended to show a slightly reduced yield of 52-63%. Bicyclic systems in **54i** and **54j** were also tolerated, as well as a selection of NPs and their derivatives, such as 4-chromanone, isatin and a griseofulvin ketone (**54k-m**). Overall, the yield was comparable to the results for the indole analogs.

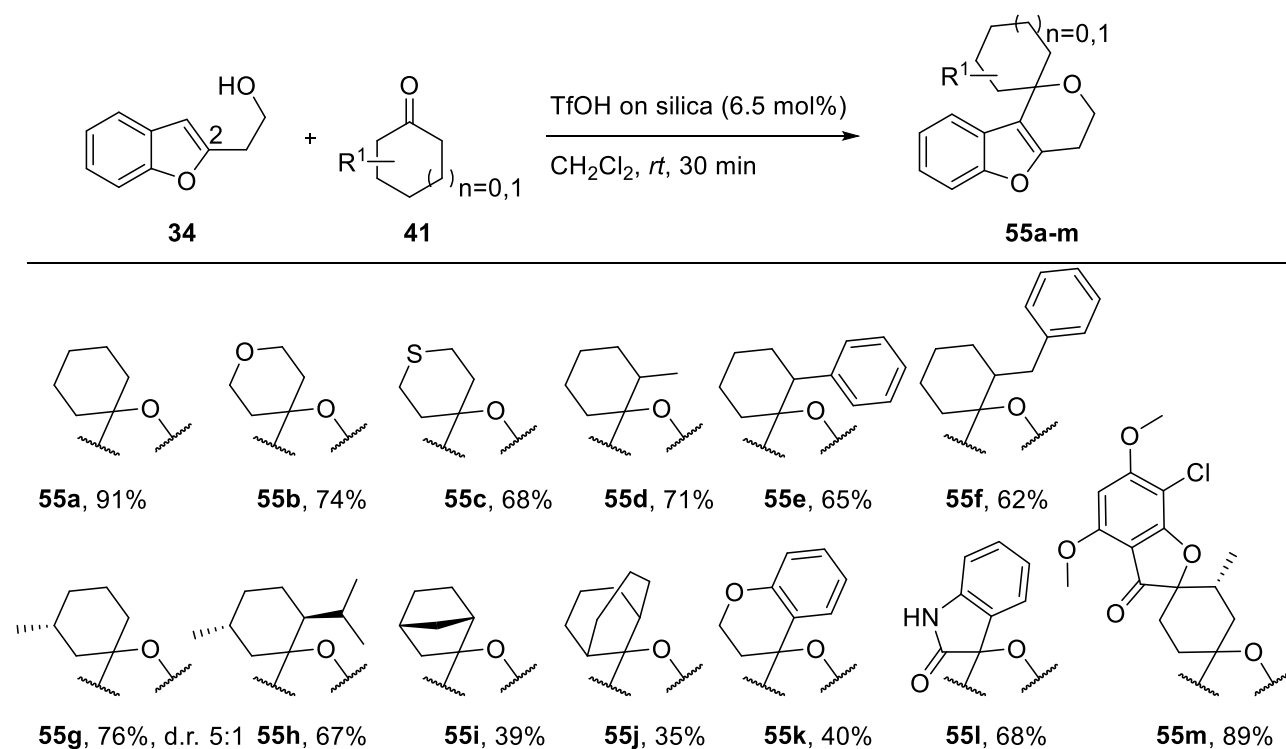


Scheme 13: Oxa-Pictet-Spengler reaction on 3-benzofurano ethanol **53** with a variation of cyclic ketones. Isolated yield in percent (%). If not further indicated, the diastereomeric ratio (d.r.) is above 20:1.

## Results and Discussion

Similar to the *iso*-oxa-Pictet-Spengler reaction of indoles, an isomeric variant might be feasible with benzofuranoethanol **34**, which is functionalized in the C2 position. The reaction conditions were transferred to a diverse collection of cyclic ketones with various degrees of steric hindrance and complexities (Scheme 14).

The desired spiro compounds were generated in moderate to good yields depending on the steric demand of the ketone fragment. According to expectation, the use of simple cyclohexanone analogs resulted in high yields (**55a-c**). Cyclic ketones with various alkyl substituents showed a slightly reduced yield (**55d-h**), whereas the application of bicyclic carbonyl compounds with a high three-dimensional character had a significantly decreased yield of 35-39% (**55i-j**). 4-Chromanone and isatin provided the corresponding pseudo-NPs **55k** and **55l** in a moderate yield. The griseofulvin ketone as a fragment-sized<sup>[19]</sup> spiro NP gave the desired bispiro pseudo-NP **55m** in an excellent yield of 89%. In comparison to the oxa-Pictet-Spengler reaction with 3-benzofurano ethanol **34**, no major differences regarding yield and diastereoselectivity were detected.

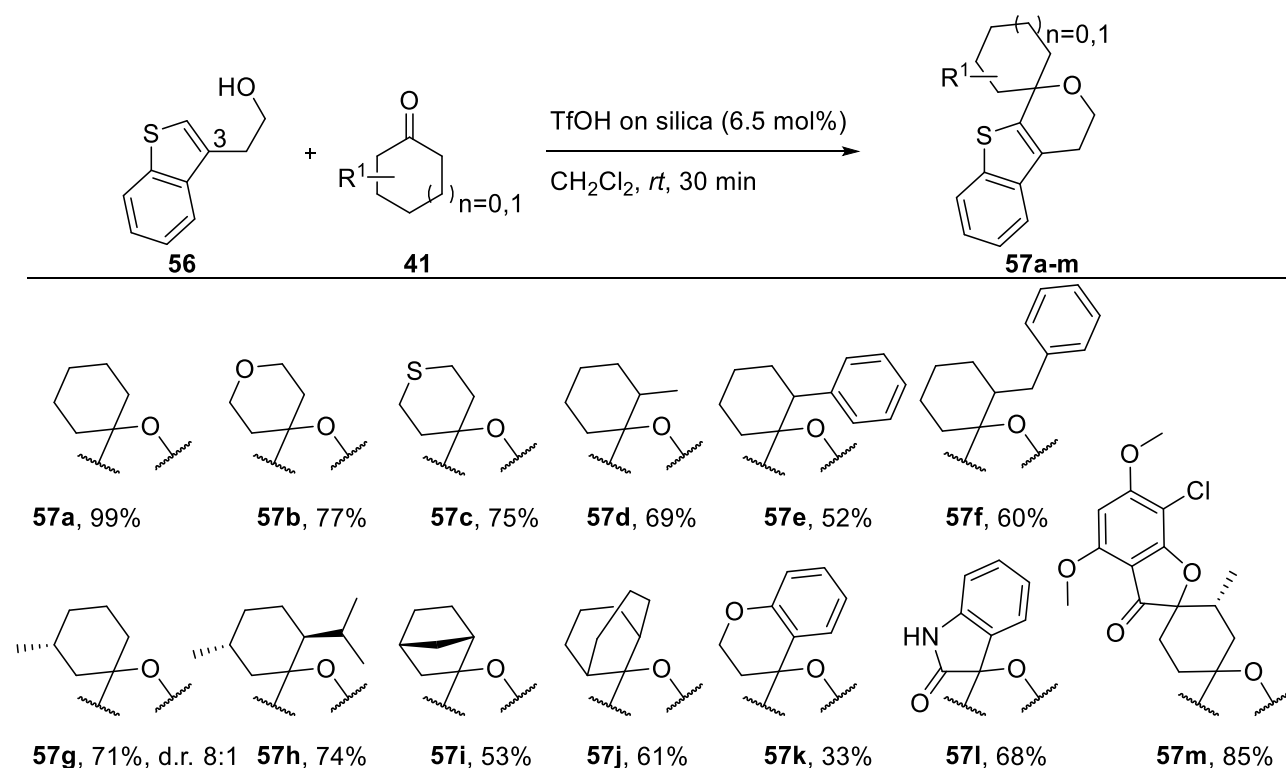


Scheme 14: Spiro compounds **55a-m** derived from the *iso*-oxa-Pictet-Spengler reaction with 2-benzofurano ethanol **34** with diverse cyclic ketones. Isolated yield in percent (%). If not further indicated, the diastereomeric ratio (d.r.) is above 20:1.

## OXA-PICTET-SPENGLER REACTION ON (BENZO)THIOPHENES

The substrate scope of the oxa-Pictet-Spengler reaction was extended to benzothiophenes, the sulphur analog to benzofurans. The addition of triflic acid on silica under the optimal reaction conditions to 2-(benzothiophen-3-yl)ethan-1-ol **56** and cyclic ketones resulted in a diverse library (Scheme 15).

The reaction with the simplest cyclic ketone, cyclohexanone, resulted in an almost quantitative conversion (**57a**). The pyran and thiopyran analog showed a slightly reduced reactivity with good yields (**57b-c**). Substituents in  $\beta$ , as well as in  $\alpha$  positions were tolerated and gave the desired spiro thiophenes in moderate yield (**57d-h**). Three-dimensionally demanding bicycles, including norcamphor and bicyclo[3.3.1]nonan-9-one, provided the corresponding Pictet-Spengler products in yield between 53-61% (**57i-j**). NP fragments, such as 4-chromanone, isatin and the more complex griseofulvin derivative, enabled the synthesis of different pseudo-NPs (**57k-m**).

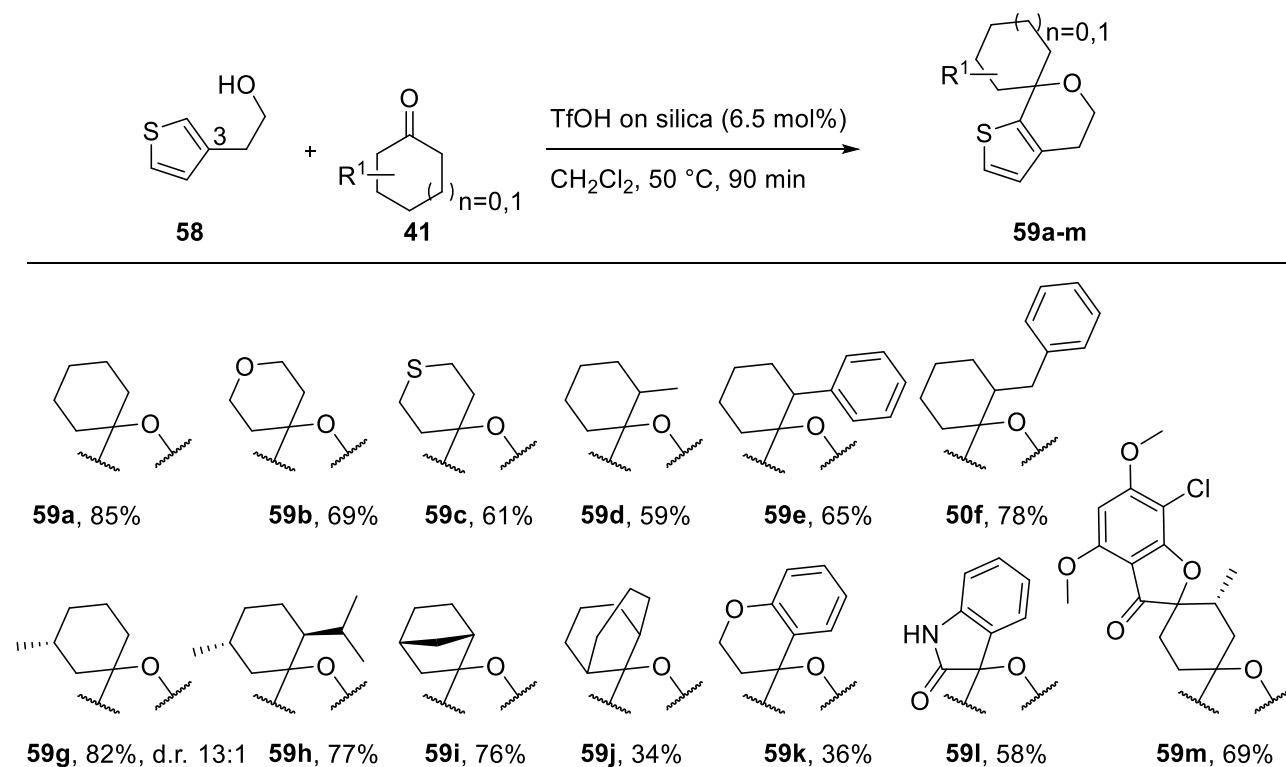


Scheme 15: Oxa-Pictet-Spengler reaction on 2-(benzothiophen-3-yl)ethan-1-ol **56** with various ketones. Isolated yield in percent (%). If not further indicated, the diastereomeric ratio (d.r.) is above 20:1.

## Results and Discussion

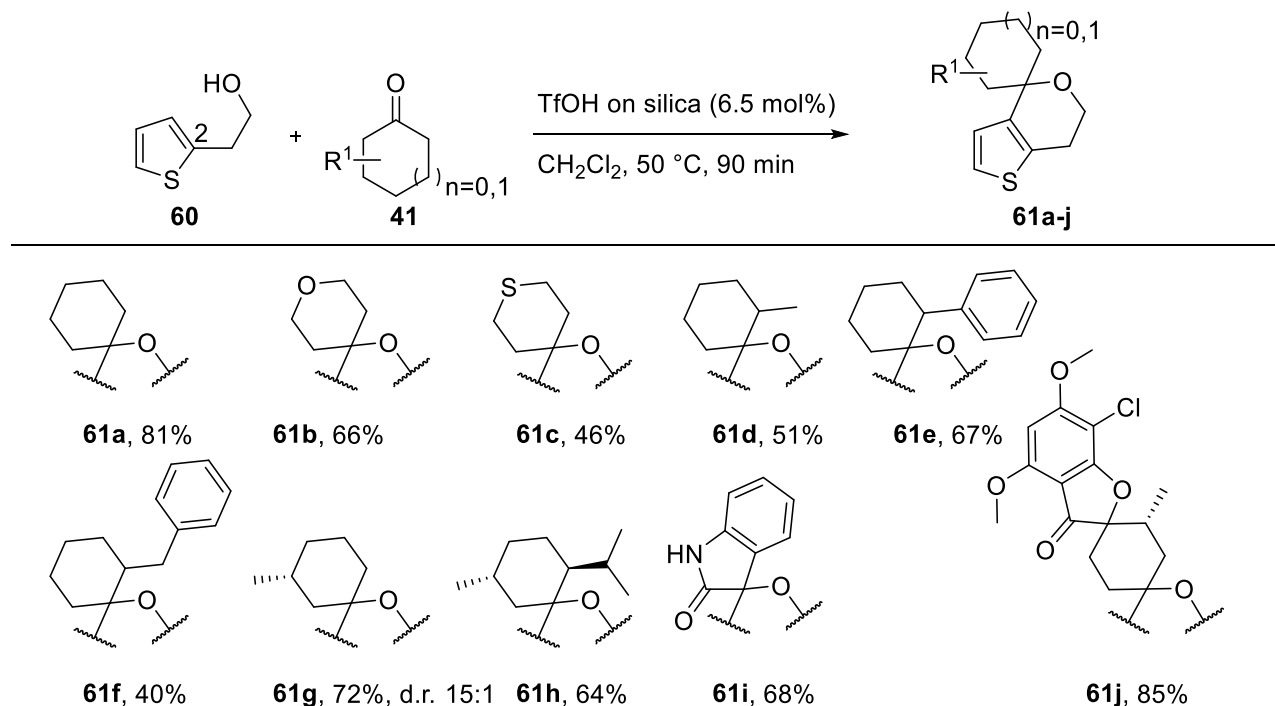
Thiophenes are structurally similar to benzothiophenes and pyrroles and generate interesting spiro compounds in the oxa-Pictet-Spengler reaction. However, the standard reaction conditions showed no or very low conversion after 30 min at room temperature. A following optimization of the reaction conditions revealed a significant improvement upon increasing the temperature to 50 °C. The best results were generated after a reaction time of 90 min.

The oxa-Pictet-Spengler reaction of 2-(thiophen-3-yl)ethan-1-ol **58** with diverse cyclic ketones resulted in the desired spiro compounds (Scheme 16). All unsubstituted and  $\alpha$ ,  $\beta$ -alkyl substituted cyclohexanone analogs of the collection of cyclic ketones were tolerated in the reaction and gave moderate to good yields (**59a-h**). Bicyclic carbonyl compounds, as well as the NP fragments 4-chromanone, isatin, and griseofulvin, gave the desired spiro thiophenes (**59i-m**).



Scheme 16: Oxa-Pictet-Spengler reaction on the thiophene 2-(thiophen-3-yl)ethan-1-ol **58**. Isolated yield in percent (%). If not further indicated, the diastereomeric ratio (d.r.) is above 20:1.

Thiophene **60** with a functionalization in the C2 position represents an isomeric variant to 2-(thiophen-3-yl)ethan-1-ol **58**. In the oxa-Pictet-Spengler reaction, the 2-(thiophen-2-yl)ethan-1-ol **60** appeared to be less reactive compared to the starting material functionalized in the C3 position **58** (Scheme 17). In comparison, the yields for the cyclohexanone derivatives were slightly reduced (**60a-g**). The oxa-Pictet-Spengler products **60h**, **60i** and **60j** derived from (-)-menthone, isatin and griseofulvin were generated in moderate to good yield (64-85%). However, the bicyclic ketones norcamphor and bicyclo[3.3.1]nonan-9-one, as well as 4-chromanone showed no conversion.

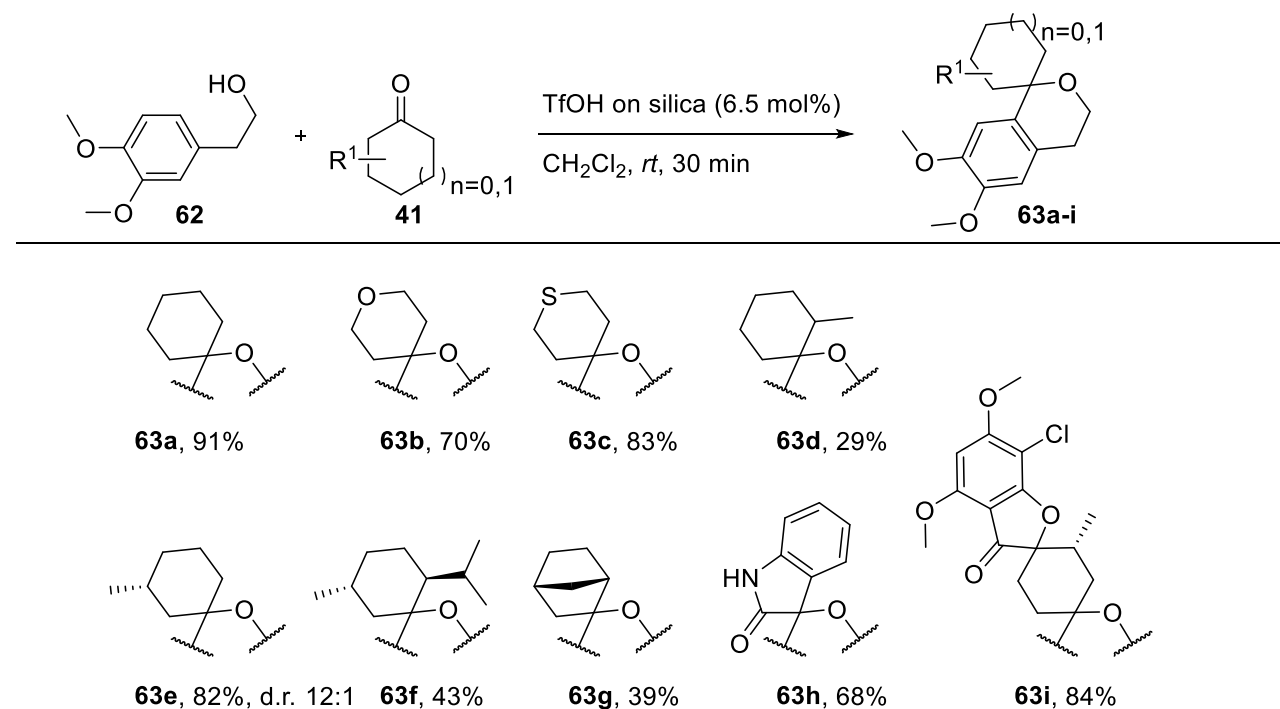


Scheme 17: The oxa-Pictet-Spengler reaction on 2-(thiophen-2-yl)ethan-1-ol **60** with cyclic ketones is yielding different spiro compounds (**61a-j**). Isolated yield in percent (%). If not further indicated, the diastereomeric ratio (d.r.) is above 20:1.

## OXA-PICTET-SPENGLER REACTION ON PHENYLETHANOLS

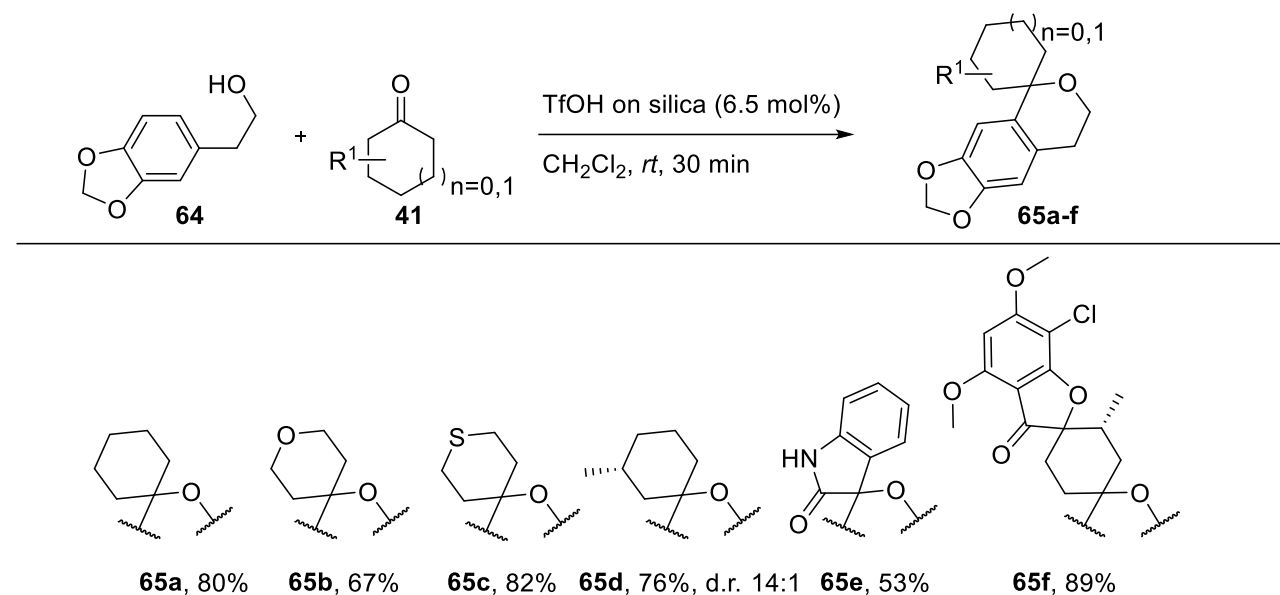
The Pictet-Spengler reaction, including the oxa-version, is well studied on phenylethanols to give diverse chromans. Even a reaction with cyclic ketones to generate novel  $\sigma$  receptor ligands is known in literature.<sup>[80a]</sup> However, the method only covers simple,  $\alpha$ ,  $\beta$ -unsubstituted carbonyl compounds and still requires long reaction times of 6 h.

The oxa-Pictet-Spengler reaction on 3,4-dimethoxyphenylethanol **62** under the catalysis of triflic acid on silica successfully delivered the desired spiro chromans in only 30 min (Scheme 18). Unsubstituted cyclohexanone analogs resulted in high yields (**63a-c**), whereas the reaction appeared to be more impaired by substituents in the  $\alpha$  position. Even small residues, such as a methyl group, reduced the yield to 29% (**63d**). Cyclic ketones with sterically more demanding phenyl and benzyl groups showed no conversion at all. Whereas a methyl substitution in the  $\beta$  position gave the spiro chroman **63e** in high yield, (-)-menthone also led to a decreased yield compared to indoles and its analogs (**63f**). The NP fragments norcamphor, isatin, and griseofulvin resulted in the corresponding pseudo-NPs in moderate to high yields (**63g-i**).



Scheme 18: Oxa-Pictet-Spengler reaction 3,4-dimethoxyphenylethanol **62** with a collection of cyclic ketones under the catalysis of triflic acid on silica. Isolated yield in percent (%). If not further indicated, the diastereomeric ratio (d.r.) is above 20:1.

2-(benzo[1,3]dioxol-5-yl)ethan-1-ol **64** showed the same tendency as its derivative 3,4-dimethoxy-phenylethanol **62** in the oxa-Pictet-Spengler reaction (Scheme 19). Unsubstituted or substituents in the  $\beta$  position on the cyclic ketone were accepted and resulted in moderate to high yields (**65a-d**). Isatin and the griseofulvin ketone as NP fragments provided the respective pseudo NPs in good yield (**65e-f**). However, residues in the  $\alpha$  position to the carbonyl were not tolerated. Cyclic ketones, including 2-methyl cyclohexanone, 2-phenyl cyclohexanone, 2-benzyl cyclohexanone and (-)-menthone, showed no conversion. All attempts to adjust the reaction conditions by extending the reaction time up to five days and increasing the temperature to 50 °C did not improve the conversion.



Scheme 19: Spiro chromans **65a-f** derived from the oxa-Pictet-Spengler reaction of 2-(benzo[1,3]dioxol-5-yl)ethan-1-ol **64** with diverse cyclic ketones. Isolated yield in percent (%). If not further indicated, the diastereomeric ratio (d.r.) is above 20:1.

### 3.1.4. DIASTEREOSELECTIVITY

The developed method for the oxa-Pictet-Spengler reaction on cyclic ketones showed a high diastereoselectivity. The applied catalyst itself does not introduce stereoselectivity. The selectivity is therefore substrate controlled. Out of the diverse carbonyl fragments which differ in substituents and complexity, for only one ketone the formation of diastereomers was detected. 3-Methyl cyclohexanone represents the exception over the other cyclic ketones and generated stereoisomers in the (*iso*)-oxa-Pictet-Spengler reaction (d.r. 5-15:1). In comparison, it exhibits the least sterically demanding substituent in proximity to the reactive center. The methyl group in  $\beta$  position appears to be not effectively introduce high d.r. above 20:1.

Determination of the stereochemistry of the novel generated stereogenic center of the spiro connection proved to be challenging. A direct assignment via different NMR methods could not deliver information about the isomer as no interaction between the pyran ring and the carbonyl fragment can be detected. Therefore, the method of choice for the determination of the stereochemistry is x-ray crystallography. The relevant indofulvin **50c** was selected as model compound and its stereogenic center was resolved to be the (*S*)-enantiomer (Figure 19). Under the assumption of the same transition state, the stereochemistry was transferred to the other Pictet-Spengler products.

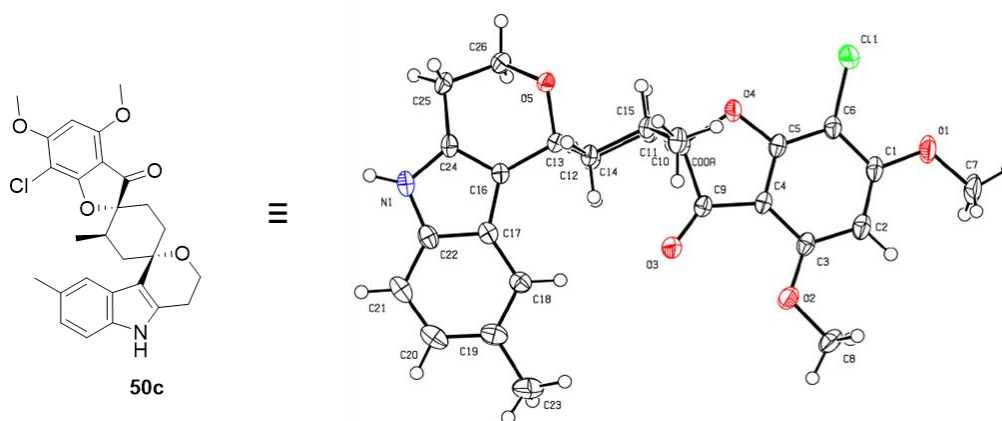


Figure 19: Crystal structure of indofulvin **50c** to determine the stereochemistry of the new stereogenic center.



### 3.1.5. CHEMINFORMATICS

To gain insight into the structural and physiochemical properties of the compound library derived from the oxa-Pictet-Spengler reaction, cheminformatic methods were employed. The plotting of the pseudo-NPs regarding their Alog P values versus the molecular weight (Figure 20a)<sup>[74]</sup> showed them to cover a preferable chemical space for drug discovery. Most of the spiro aryl compounds (79%, 165 out of 210 compounds) displayed an Alog P < 5 and a molecular weight < 500 and therefore fell into the Lipinski's rule-of-five space. In addition, the pseudo-NPs three-dimensional shape was characterized in a principal moments of inertia (PMI) plot (Figure 20b)<sup>[74]</sup>. The spiro aryl compounds derived from the oxa-Pictet-Spengler reaction showed a wide structural diversity represented by a broad distribution within the triangle, where each corner constitutes a different shape. The compounds showed a significant shift away from the rod/disk-like axis extending into a more spherical shape, which is likely due to the spirocyclic connection of the fragments. The abundance in three-dimensionality indicates an imitation of NPs' overall shape compared to synthetic compound collections and suggests the conservation of NPs' molecular diversities through the process of reduction into NP-fragments followed by the recombination into pseudo-NPs.

In comparison to the ketone and aryl starting materials, the chemical properties of the oxa-Pictet-Spengler products drastically changed. The lead-likeness plot determined differences regarding their relative molecular mass and hydrophobicity (Figure 20a). As the Pictet-Spengler reaction combines two fragments, the molecular weight is increased, indicated by a shift to the right towards higher molecular mass. Furthermore, an ethanol and a carbonyl function are converted to a pyran with a spiro connection to an aliphatic cycle resulting in a higher hydrophobic fraction which is represented by an increased Alog P value. In the investigation of the three-dimensionality a clear difference of the spiro compounds to their starting materials was visible (Figure 20b). Especially, aryl ethanols showed a limited range of three-dimensionality as they tend to be flat and linear. In combination with the cyclic ketones, the Pictet-Spengler products showed a significant increase in three-dimensionality. Thereby, the newly generated spiro center appears to play an important role for the more spherical shape.

## Results and Discussion

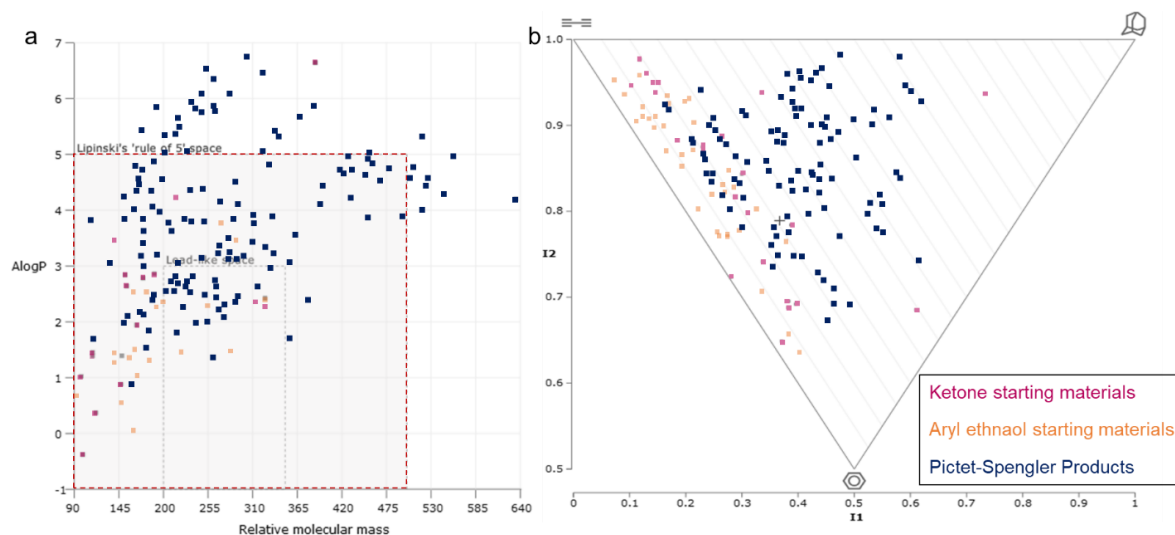


Figure 20: Cheminformatics of oxa-Pictet-Spengler products (blue) compared to their starting materials (aryl ethanol (orange) and cyclic ketones (pink)). a: Lead-likeness-plot, Alog P versus the relative molecular mass.<sup>[74]</sup> b: PMI plot<sup>[74]</sup> of the pseudo-NP collection displays a broad diversity of three-dimensional space similar to NPs.

To chemically characterize the pseudo-NPs, indofulvins **50a-r** were chemoinformatically analyzed using a NP-likeness score introduced by Ertl et al.<sup>[96]</sup> Comparison of the pseudo-NP library to compounds from the DrugBank<sup>[97]</sup> and ChEMBL NPs<sup>[98]</sup> revealed a consilience with both sets by falling in between them (Figure 21a)<sup>[99]</sup>. The pseudo-NP collection appears to resemble NPs and show drug-like characteristics. Favorable properties for drug discovery were additionally investigated via the quantitative estimation of drug-likeness (QED), where the pseudo-NPs showed a high drug-like fraction (Figure 21b). The drug-likeness could be attributed to the mixed heteroatom content and/or regioisomeric connections not observed in nature.

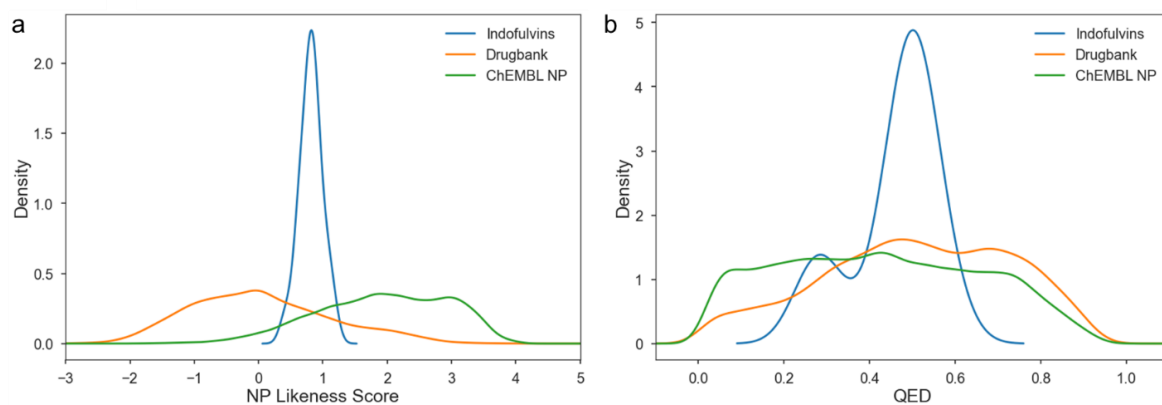
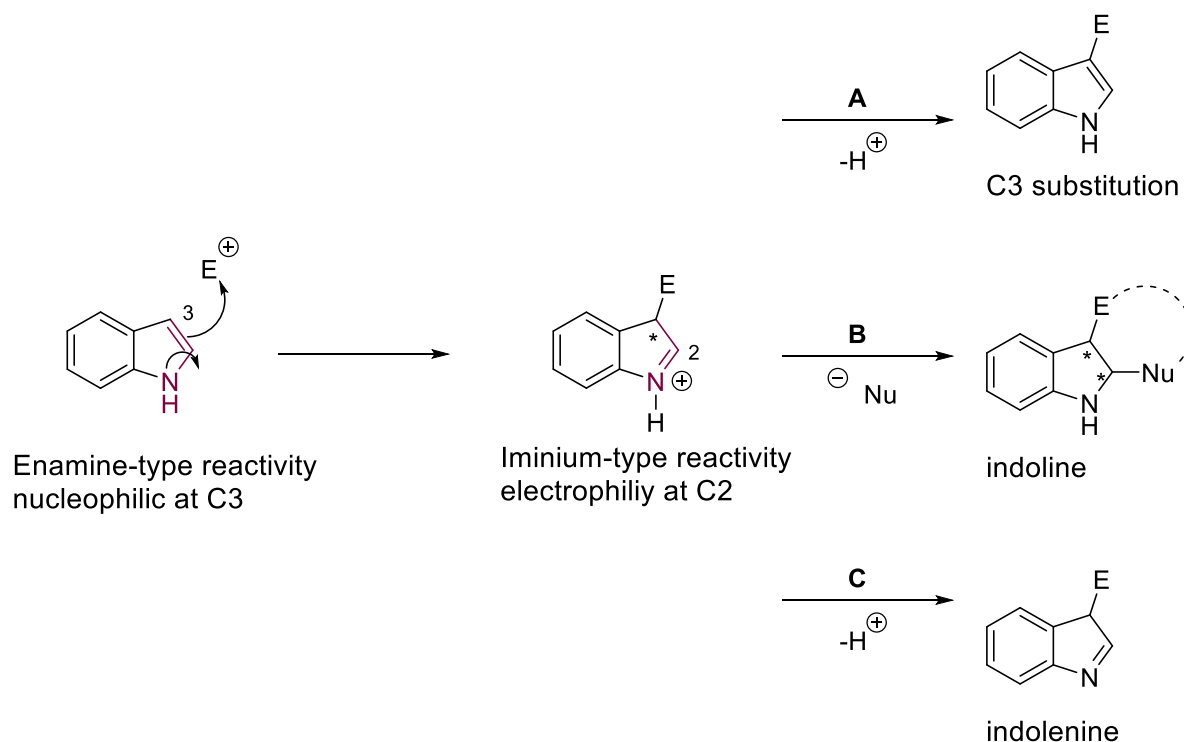


Figure 21: Chemoinformatic analysis of the indofulvin pseudo-NP collection. a: NP-likeness score<sup>[96]</sup> and b: quantitative estimation of drug-likeness (QED). Indofulvins (blue curve) compared to the DrugBank<sup>[97]</sup> compound collection (orange curve) and ChEMBL NPs<sup>[98]</sup> (green curve).

### 3.2. DEAROMATISATION

Indoles are ubiquitous in nature and fulfill various bioactivities. Many pseudo-NP collections including the compound collection derived from the Fischer indole reaction and in parts the library via Pictet-Spengler reaction, are based on the scaffold. Additionally, the indole provides the opportunity for further functionalization through different reactive sites. The nucleophilicity at C3 position results in an enamine-type reactivity that can lead to a substitution (Scheme 20a).<sup>[100]</sup> An alternative reaction type of indoles is the iminium type reactivity which is generated as soon as the scaffold cannot be rearomatized after the nucleophilic attack. The iminium ion intermediate can be trapped by a nucleophilic attack resulting in an indoline with contiguous stereocenters (Scheme 20b) or alternatively by deprotonation leading to indolenines (Scheme 20c).<sup>[72]</sup>

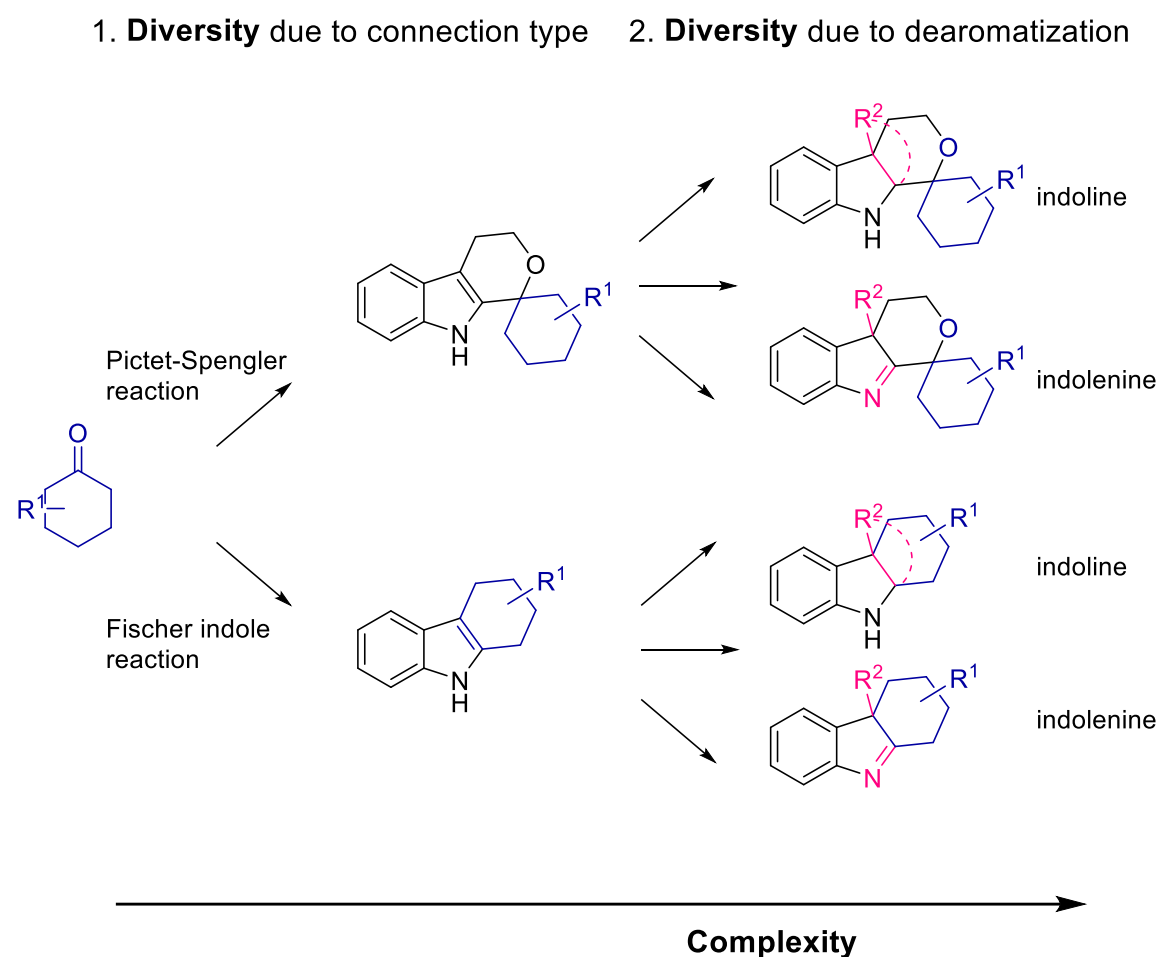


Scheme 20: Overview of the different reactivities of indoles covering the enamine-type reactivity, which enables the nucleophilic attack of the C3 position and the resulting iminium intermediate, which can be trapped via nucleophilic attack at the C2 position to give indolines or deprotonation yielding in indolenines.<sup>[100]</sup>

The wide range of reactivity enables the potential access to indoline and indolenine scaffolds. Both structures share therapeutically relevance for the treatments of cancer, inflammation, and hypertension and are therefore interesting motives for compound collections.<sup>[101]</sup>

## 3.2.1. LIBRARY DESIGN

Pseudo-NP collections bearing a dearomatized indoline or indolenine scaffold are an asset as they show interesting bioactivities, provide a significantly increased complexity with the  $sp^3$  hybridized stereocenters<sup>[72]</sup> and already existing pseudo-NP compounds can be employed as starting materials. NP fragments with a carbonyl functionality can first be used for the formation of diverse libraries through an oxa-Pictet-Spengler or a Fischer indole reaction. The complexity as well as the diversity is further increased by the following dearomatization of the indole. The incorporation of an additional NP fragment in C2/C3 position introduces further complexity (Scheme 21).



Scheme 21: Library design based on indole containing pseudo-NP collections derived from Pictet-Spengler or Fischer indole reaction. A next level of complexity and diversity is introduced by the incorporation of an additional NP fragment in C2/C3 position of the indole resulting in indolines or indolenines.

### 3.2.2. $\gamma$ -PYRONE ANNULATION

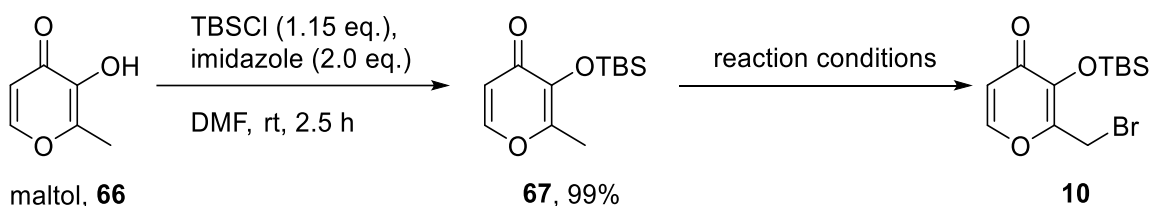
The synthesis of the dearomatized indole compounds was realized by Joseph Hoock. The Fischer indole starting materials were partially provided by Dr. Michael Grigalunas.

The incorporation of maltol as a new NP fragment through dearomative  $\gamma$ -pyrone annulation can be performed on indoles. Maltol is known for its antineoplastic bioactivity against different cancer cell models via ROS induction<sup>[102]</sup> and represents an interesting NP fragment. The pioneering methodology was developed by Porco et. al.<sup>[38]</sup> to provide the unusual alkaloid scaffold of pleiomaltinine (chapter 1.2.2.). Additionally, an asymmetric version is known in the literature<sup>[39]</sup> that generates functionalized indolenines stereoselectively. This reaction may provide a great opportunity to generate a diverse cyclized indoline and open indolenine collection.

#### STARTING MATERIALS

For the  $\gamma$ -pyrone annulation a reactive maltol derivative **10** was synthesized in two steps from the commercially available NP **66**. After a TBS-protection in the first step, the literature procedure<sup>[38]</sup> employs the hazardous<sup>[103]</sup> and costly solvent carbon tetrachloride (CCl<sub>4</sub>) for the bromination in the second step. In order to replace the solvent with a less harmful alternative, different reaction conditions were screened (Table 2).

Table 2: Investigation of different reaction conditions in order to replace carbon tetrachloride (CCl<sub>4</sub>) in the second reaction step of the synthesis of the reactive maltol species **10**.



Entry	Reagents	Solvent	T [°C]	t [min]	Yield* [%]
1	NBS (1.05 eq.), AIBN (0.13 eq.)	CCl <sub>4</sub>	105	60	32
2	NBS (1.05 eq.), AIBN (0.13 eq.)	CHCl <sub>3</sub>	85	60	7
3	NBS (1.05 eq.), AIBN (0.13 eq.)	DCE	105	60	5 <sup>a</sup>
4	NBS (1.05 eq.), AIBN (0.13 eq.)	DMC	105	120	15 <sup>a</sup>
5	DBDMH (1.05 eq.), AIBN (0.13 eq.)	DMC	105	120	-
6	NBS (1.05 eq.), AIBN (0.13 eq.)	DMC	105	60	66 <sup>b</sup>
7	NBS (1.05 eq.), AIBN (0.13 eq.), mw	DMC	105	1	75 <sup>b</sup>

\*Yield determined by NMR. After isolation <sup>a</sup> via silica flash chromatography or <sup>b</sup> aqueous work up.

## Results and Discussion

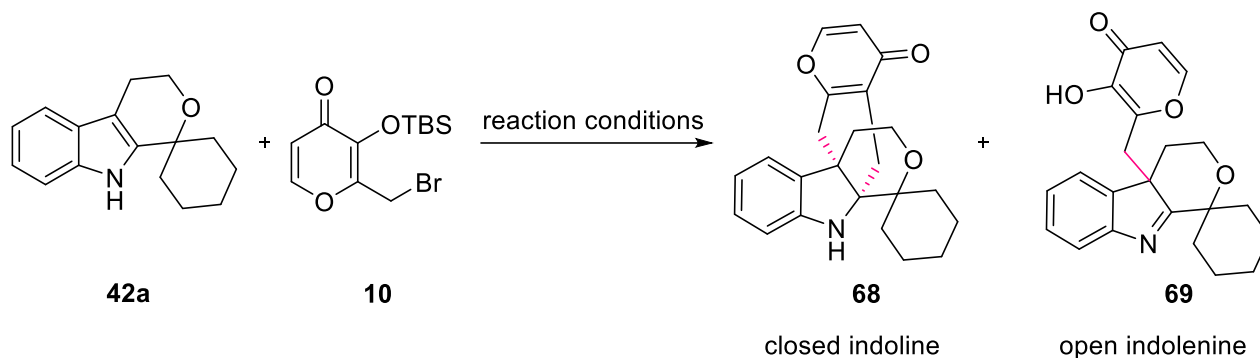
The original literature procedure<sup>[104]</sup> was tested and gave a yield of 32% (Table 2, entry 1), whereas the application of other chlorinated solvents including chloroform and dichloroethane (DCE) was not successful. Dimethyl carbonate is reported as alternative to halogenated solvents with similar physical properties as the boiling temperature is 90 °C.<sup>[105]</sup> However, stability issues resulted in a relatively low yield of 15% after purification via flash column chromatography (Table 2, entry 4). An adjusted purification via aqueous work-up led to a significant improvement of the yield (66%, table 2, entry 6). The transfer to the microwave gave a good yield of 75% as well as excellent reaction conditions with a reaction time of just 1 min (Table 2, entry 7). Thereby, these optimized reaction conditions are not only replacing the toxic CCl<sub>4</sub>, but also nearly doubling the yield with a significant shorter reaction time.

### METHOD OPTIMIZATION

The reliable synthesis of the activated maltol **10**, enabled the start of the method development for the  $\gamma$ -pyrone annulation itself. Ideally, the reaction can give access to both dearomatized scaffolds: the closed, sterically demanding indoline **68** and the open indolenine **69**. The reproducibility of the reaction conditions published in literature<sup>[38]</sup> was confirmed on the simple 2,3-dimethyl indole by NMR.

The investigation of different reaction conditions was performed on the sterically least hindered spiro indolyl tetrahydropyran **42a** derived from the Pictet-Spengler reaction. The brominated maltol **10** was freshly generated before each experiment to avoid effects due to its instability. The literature procedure<sup>[38]</sup> using an excess of hydrochloric acid in dioxane gave a low yield of 11% separated on the two products in a ratio of 3:1 for the indolenine (Table 3, entry 1). A fast decomposition of the brominated maltol **10** was observed upon acid addition, leaving no active species after 5 min. Therefore, the influence of the acid was investigated by the addition of TfOH·SiO<sub>2</sub> as an alternative and no addition of acid in different solvents. Whereas the addition of TfOH·SiO<sub>2</sub> and pure acetonitrile (MeCN) resulted in only traces of product formation (Table 3, entry 2 and 3), the  $\gamma$ -pyrone annulation in methanol afforded 40% conversion (Table 3, entry 4). However, the major product formed was the open indolenine **69** over the closed indoline **68** (3:1).

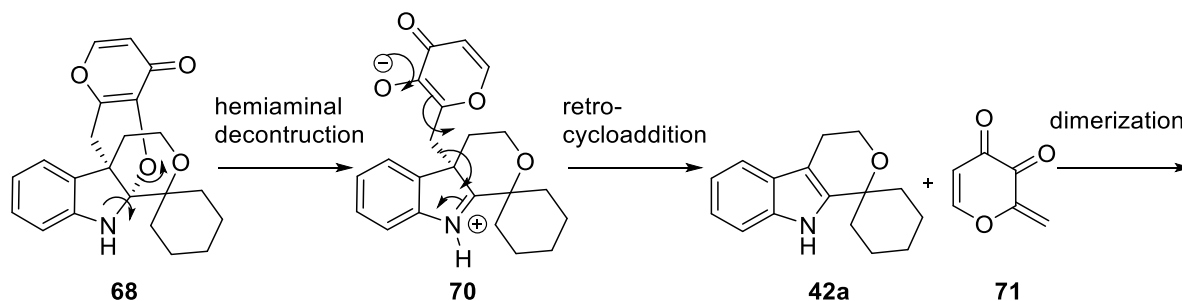
Table 3: Screening of different reaction conditions for the investigation of the  $\gamma$ -pyrone annulation on the sterically least demanding pseudo-NP **42a** derived from the Pictet-Spengler reaction. The brominated maltol **10** was freshly prepared with NBS and AIBN in DMC in the microwave at 105 °C for 1 min.



Entry	Reagents	Solvent	Ratio 68:69	<i>t</i> [min]	Yield [%]
1	HCl in dioxane(3.0 eq.)	MeCN	1:3	60	11 <sup>b</sup>
2	TfOH · SiO <sub>2</sub>	CH <sub>2</sub> Cl <sub>2</sub>	-	60	traces <sup>a</sup>
3	-	MeCN	-	180	traces <sup>a</sup>
4	-	MeOH	1:3	60	40 <sup>b</sup>

<sup>a</sup>Observation determined by uHPLC. <sup>b</sup>After isolation via silica flash chromatography.

Further structure elucidations revealed the indoline's instability and decomposition to the starting material and the maltol dimer or maltol. The mechanism of decomposition was proposed to be initiated by the free electron pair of the indoline's nitrogen resulting in the deconstruction of the hemiaminal and C-O bond cleavage at C2 (Scheme 22). The iminium intermediate **70** performs a retro-cycloaddition to give the starting material **42a** and a reactive maltol species **71**, which undergoes dimerization. A similar decomposition is reported in the presence of Lewis acid or after heating the product.<sup>[38]</sup>



Scheme 22: Proposed decomposition of the indoline scaffold **68**.

## Results and Discussion

To prevent the indoline decomposition, a stabilization of the hemiaminal through *in-situ* acetylation of the nitrogen was proposed. The most efficient acetylation conditions employed acetic anhydride ((Ac)<sub>2</sub>O), triethylamine (Et<sub>3</sub>N) and dimethylamino-pyridine (DMAP) showing a quantitative conversion after 30 min. Although the acetylation was supposed to functionalize and stabilize the indolenine, 2D NMR data and x-ray crystallography revealed an acetylation of the free maltol hydroxy group of the open indolenine **69**. The crystal structure shows the (*S*)-enantiomer of the racemic indolenines **74a** (Figure 22).

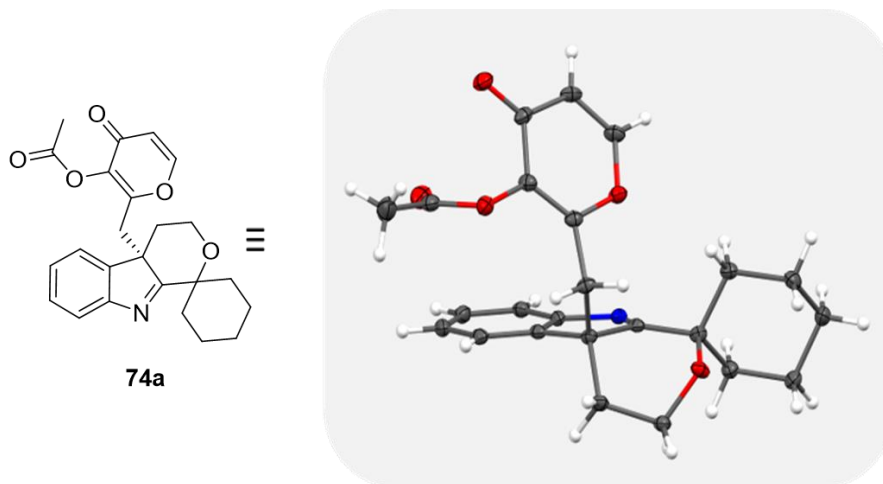
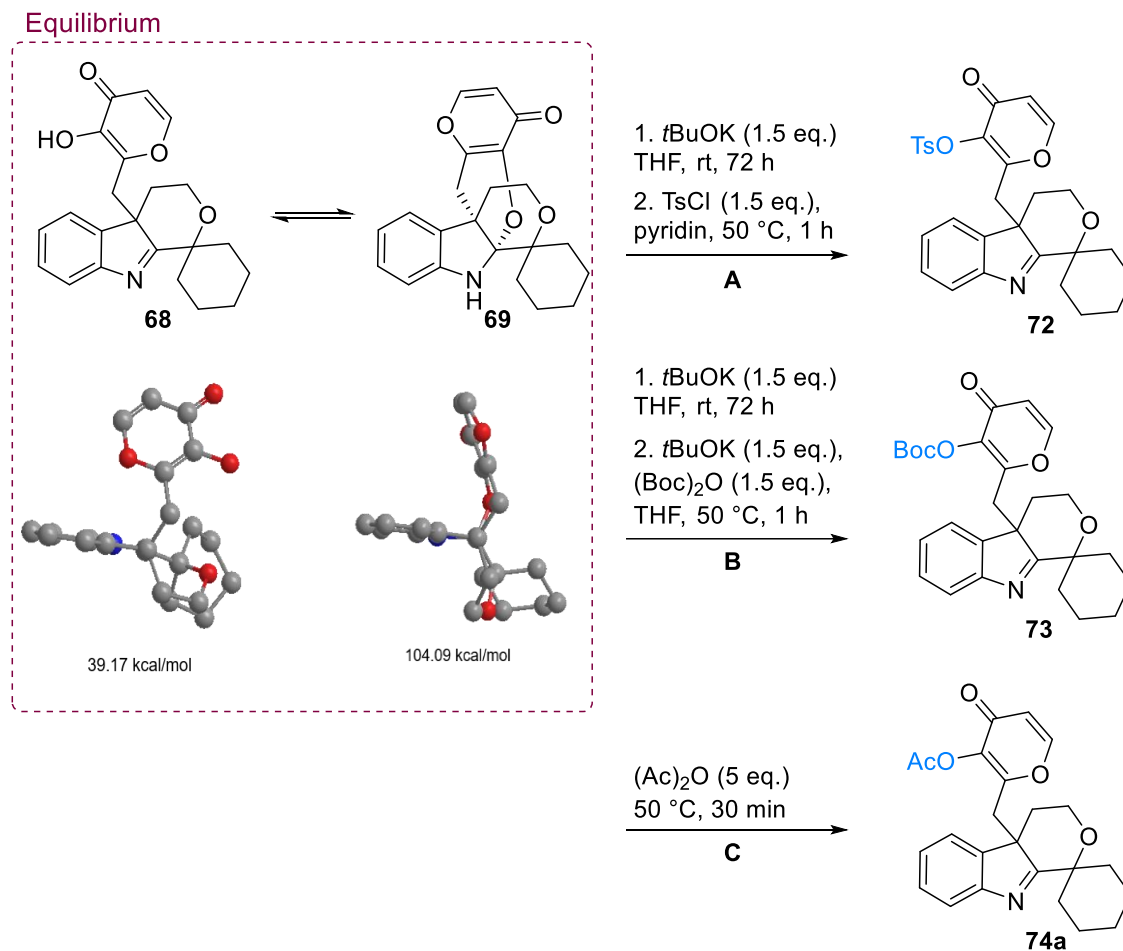


Figure 22: The x-ray crystallography confirmed the acetylated indolenine structure.

In advanced investigations an equilibrium between the closed indoline and open indolenine scaffold was determined, which is dependent on the residues in the new stereocenter of the Pictet-Spengler reaction. The more sterically demanding the ketone, the more the equilibrium is shifted towards the open indolenine scaffold. Spiro compounds derived from cyclic ketones favor the open indolenine scaffold over the closed indoline scaffold as the total energy is significantly lower for the indolenines (Scheme 23). Two sp<sup>3</sup> hybridized, tetrahedral centers and the spiro center in close proximity appear to be disadvantageous for the indoline formation. All experiments trying to stabilize the closed indoline form and shift the equilibrium towards this scaffold remained unsuccessful (Scheme 23). Neither the treatment with a stronger base like potassium *tert*-butoxide (*t*BuOK) to increase the hydroxy group's nucleophilicity for the attack on the iminium ion followed by different protecting groups for the indoline's nitrogen nor the waiver of base to circumvent a benefited retro-cycloaddition by deprotonating the nitrogen yielded in the desired product. The reaction always resulted in the formation of the opened indolenine scaffold.





Scheme 23: Efforts to access the closed indoline structure via  $\gamma$ -pyrone annulation resulted in only the formation of the open indolenine scaffold.

## INDOLENINES

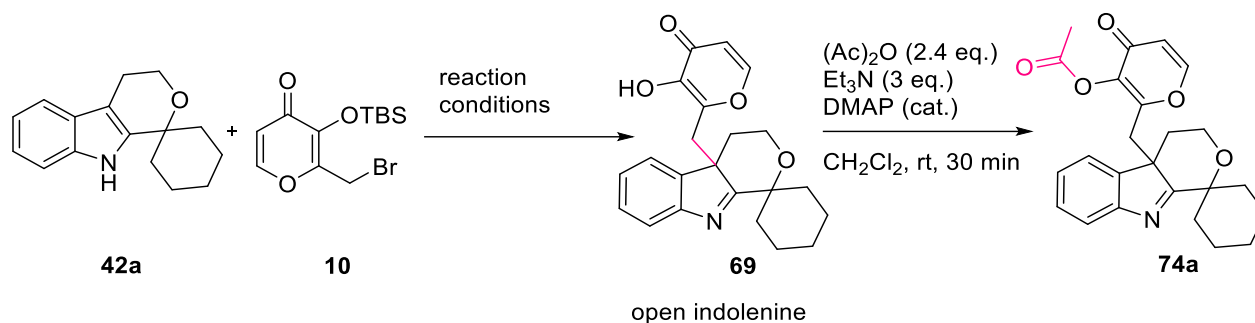
As the indolenine scaffold is still an interesting motif, the reaction conditions were optimized for the open version **74** (Table 4). The  $\gamma$ -pyrone annulation is also followed by an acetylation with acetic anhydride ((Ac)<sub>2</sub>O), triethylamine (Et<sub>3</sub>N) and dimethylamino-pyridine (DMAP) as the acetylation appeared to deliver more stable compounds.

The reaction without reagents in methanol resulted in a moderate yield of 40% after 30 min and constituted a good basis for further optimization (Table 4, entry 1). The substitution of the solvent to a solvent system of methanol with dichloromethane (3:1) significantly improved the yield to 70%. Presumably, as the polarity of the starting materials vary widely, a solvent mixture created an advantage for the solubility of both components. The solvent system between acetonitrile (MeCN) and dichloromethane (3:1) resulted in a reduced conversion to the desired product (Table

## Results and Discussion

4, entry 3). However, a mixture of trifluoroethanol (TFE) with dichloromethane (3:1) generated the best results with a yield of 86% after 30 min at room temperature and even quantitative conversion in the microwave (50 °C for 10 min, Table 4, entry 4 and 5).

Table 4: Optimization of the reaction conditions for acetylated indolenines.



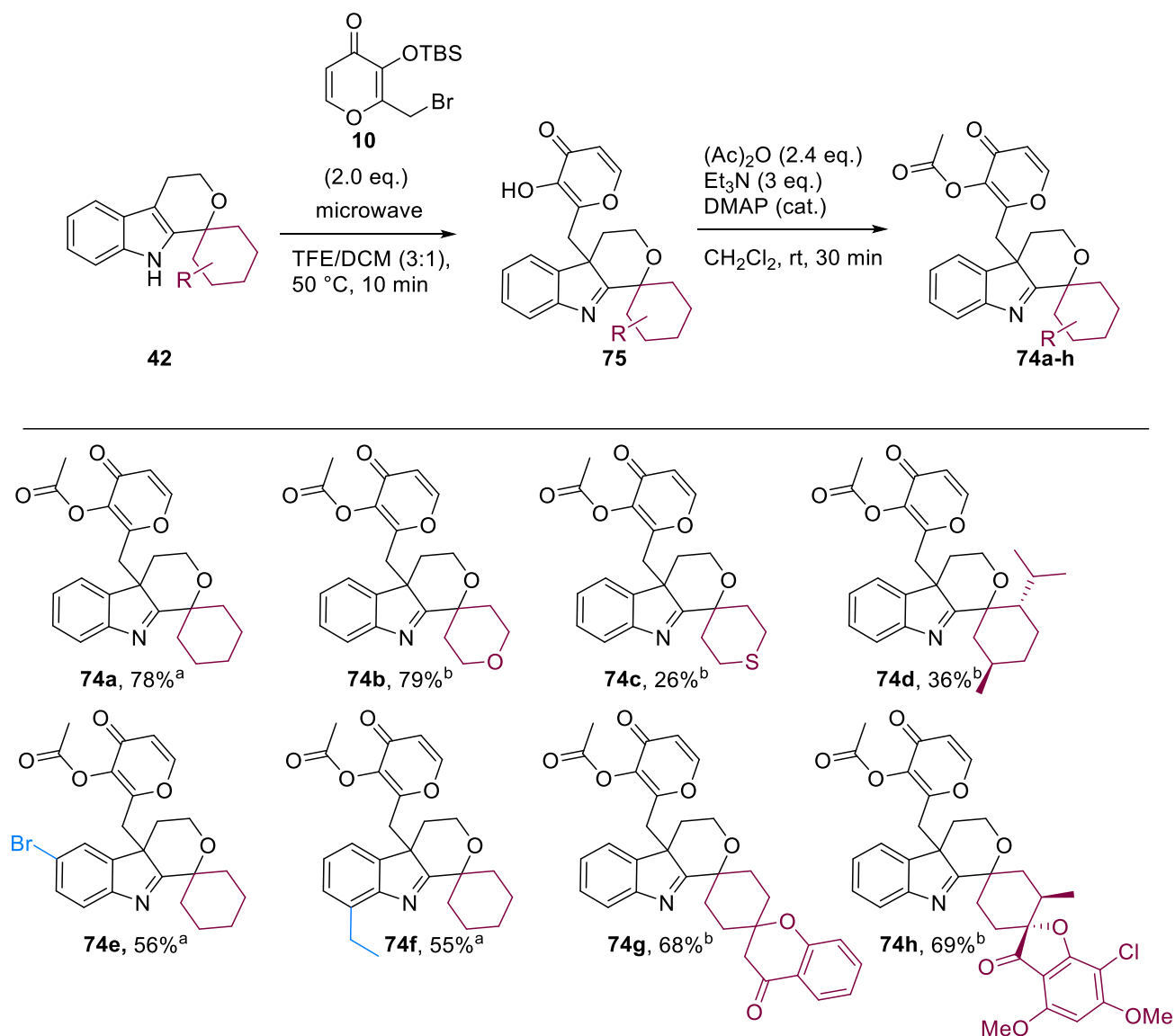
Entry	Solvent system	$T$ [°C]	$t$ [min]	Yield* [%]
1	MeOH	22	30	40
2	MeOH/CH <sub>2</sub> Cl <sub>2</sub> (3:1)	22	30	70
3	MeCN/ CH <sub>2</sub> Cl <sub>2</sub> (3:1)	22	30	5
4	TFE/CH <sub>2</sub> Cl <sub>2</sub> (3:1)	22	30	86
5	TFE/CH <sub>2</sub> Cl <sub>2</sub> (3:1)	50 (mw)	10	quant.

\*Yield determined by NMR.

Depending on the substituents on the indole and the carbonyl fragment, the acetylated  $\gamma$ -pyrone product shares a similar polarity to maltol and its dimer. Consequently, the application of silica flash column chromatography led to a problematic purification of the desired products. Additionally, decomposition on the column was observed for pseudo-NPs, including **74a**. By employing a purification via gel perfusion chromatography (GPC) the yield of the acetylated  $\gamma$ -pyrone product **74a** was improved from 25% after silica chromatography to 78% after GPC. GPC systems function as a size exclusion chromatography, separating compounds by their molecular weight. Maltol compared to the pseudo-NP is significantly lighter in molecular weight and size, resulting in an ideal separation from the desired product. No decomposition of the pseudo-NP was observed, leading to the high isolated yield of 78% after 2 reactions.

The optimal reaction conditions and purification methods enabled the synthesis of a spiro indolenine based on pseudo-NPs derived from the Pictet-Spengler reaction (Scheme 24). The vast majority of the spiro starting materials gave good yields (55-79%) after two reaction steps. Only the sulphur derivative **74c** and the sterically demanding menthone derivative **74d** led to a moderate yield of 26 or 36%. Interestingly, purification of derivative **74b**, **74g** and **74h** via silica

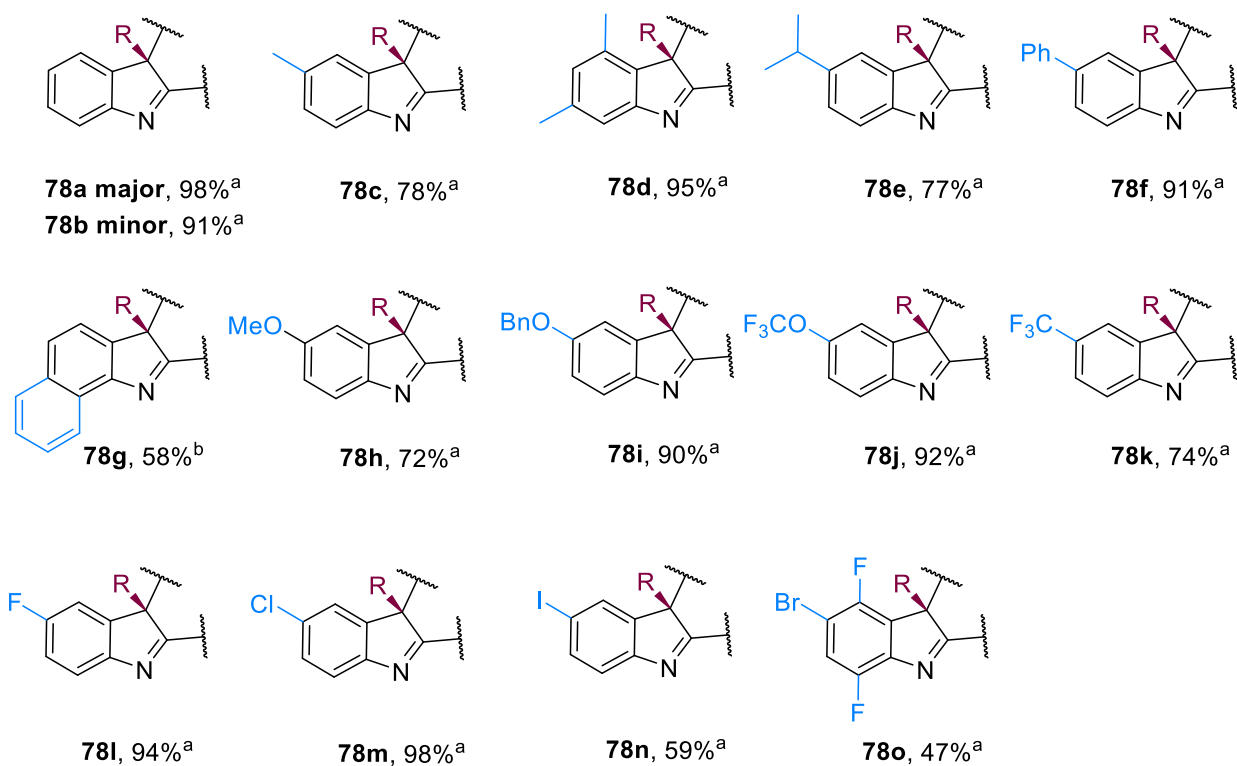
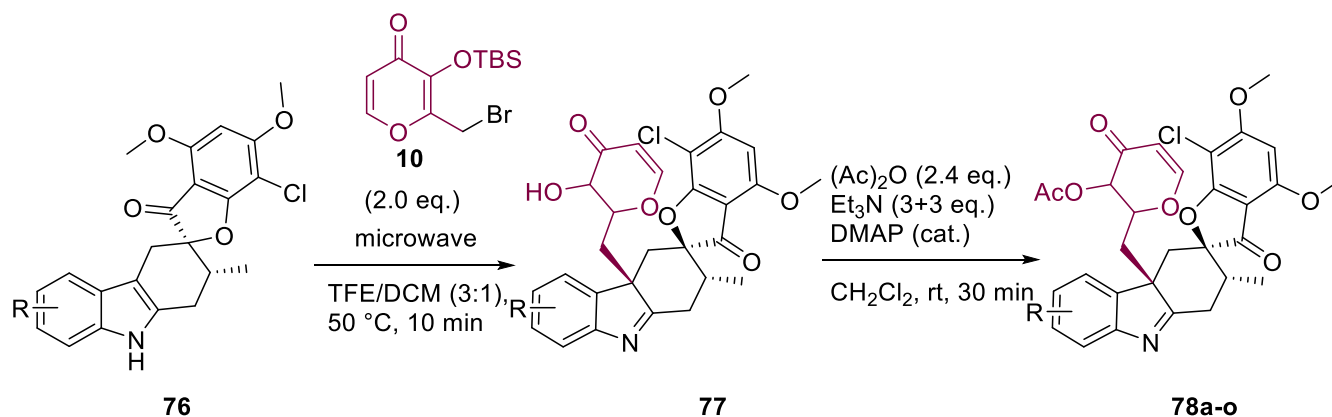
flash column chromatography resulted in a good separation from the starting materials and therefore, yields above 68%. The griseofulvin derivative **74h** was obtained as diastereomeric mixture (0.85:0.15). All other compounds were formed as racemic mixture which was confirmed via optical rotation measurements. Although the method was transferable to all  $\beta$ -indole tetrahydropyrans and gave overall good yields,  $\gamma$ -derivatives derived from indoles functionalized in the C2 position of the indole did not lead to the desired product formation.



Scheme 24: Substrate scope for the  $\gamma$ -pyrone annulation followed by acetylation of different spiro indole tetrahydropyrans derived from the oxa-Pictet-Spengler reaction. Isolated yield in percent. Purification via <sup>a</sup>GPC or <sup>b</sup>flash column chromatography.

## Results and Discussion

Additionally, the  $\gamma$ -pyrone annulation was performed on multiple griseofulvin indoles **76** derived from the Fischer indole reaction (Scheme 25). The method of the acetylation was slightly adjusted by repeatably adding the equivalent portion of acetic anhydride and triethylamine after 15 min.



Scheme 25: Substrate scope for the  $\gamma$ -pyrone annulation followed by acetylation on griseofulvin indoles derived from the Fischer indole reaction. Isolated yield in percent. Purification via <sup>a</sup>GPC or <sup>b</sup>flash column chromatography. Residue R corresponds to the acylated maltol moiety.

The  $\gamma$ -pyrone annulation was suitable for all griseofulvin indoles **76** and resulted in good to excellent yields (47-95%) over two steps. All different substituents on the indole from various alkyl **66**

residues, ethers and halogens were tolerated (**78c-o**). Even the triple halogenated derivative which is reduced in aromatic electron density gave a moderate yield of 47% of the desired product **78o**. However, the reaction conditions were not applicable to different sinomenine indoles and quinine indoles.

The stereochemistry of the newly generated stereocenter of the annulated griseofulvin indoles was determined as (*S*)-enantiomer by x-ray crystallography of compound **78i** (Figure 23). Only one diastereomer of the reaction was observed, indicating a substrate-induced selectivity. The molecular shape of the chiral indoles appears to shield the *si*-side of the molecule, which favors an attack from the *re*-side.

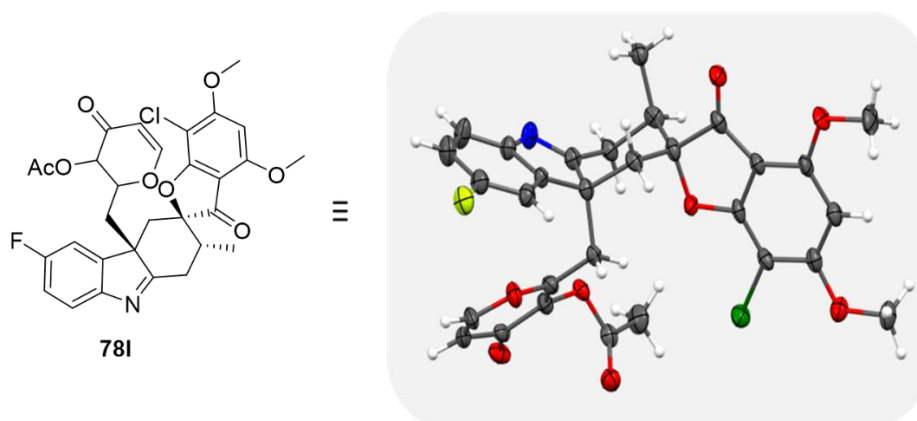


Figure 23: Crystal structure of the acetylated  $\gamma$ -pyrone annulation product **78i** identified the stereochemistry of the new stereogenic center as (*S*)-enantiomer.

Although the acetylation of the  $\gamma$ -pyrone annulation products improved their stability, decomposition of some compounds was observed after a few days in chloroform. Therefore, a comprehensive stability analysis was performed to identify compounds which could decompose. The compounds were dissolved in deuterated chloroform, DMSO, and DMSO with the addition of hydrochloric acid and was analyzed by  $^1\text{H}$  NMR. Satisfyingly, the vast majority of the compounds appeared to be stable without showing decomposition for up to five weeks. However, different electronic effects on the indole could influence the compounds stability (Figure 24). Pseudo-NPs with residues that result in a negative inductive effect ( $-I$ ), including  $-\text{OCF}_3$ ,  $-\text{CF}_3$ , and halogens, showed no decomposition and are considered stable. Compounds having a positive inductive effect ( $+I$ ), such as methyl- or phenyl groups, appeared to show minor decomposition after two months. Compounds with a strong positive inductive effect ( $+I$ ) as the naphthyl derivative **78g** or

## Results and Discussion

with a positive mesomeric effect (+M), including ethers, exhibited decomposition after a few days. Consequently, the three compounds **78g**, **78h**, and **78i** were excluded from biological investigations.

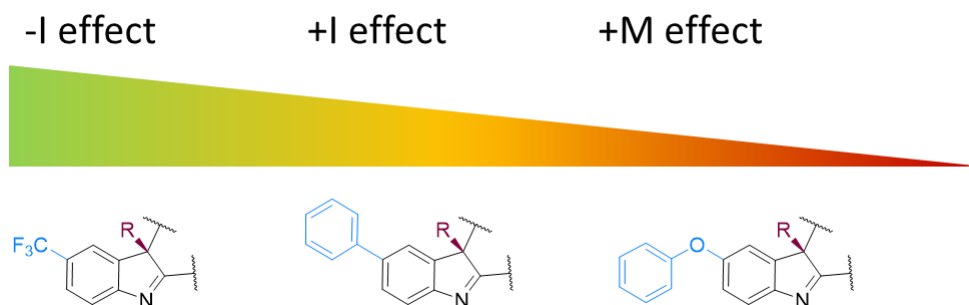
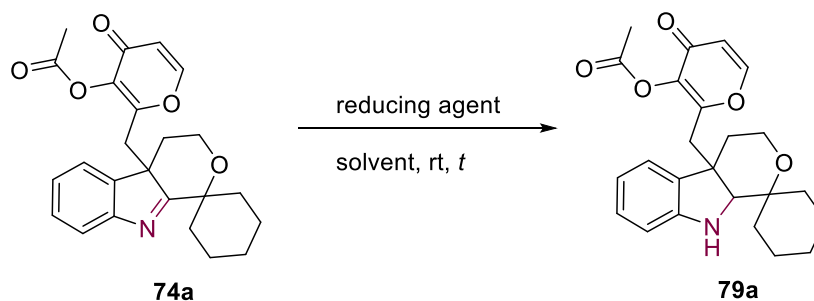


Figure 24: Stability trend of annulated griseofulvin indoles.

### INDOLINE

Closed indolines appeared to not be directly accessible through  $\gamma$ -pyrone annulation. However, indolines can also be generated via the reduction of the imine functionality of indolenines.<sup>[37]</sup> Different reducing agents including the triacetoxyborohydride (STAB-H)<sup>[106]</sup> and the less sterically demanding sodium cyanoborohydride (NaBH<sub>3</sub>CN) were used on the  $\gamma$ -pyrone annulation product **74a** (Table 5). Both reagents selectively reduced the indolenine in the desired indoline **79a**. The highest yield with almost quantitative conversion was observed employing NaBH<sub>3</sub>CN in methanol after 15 min. The isolated yield of spiro compound **79a** derived from the Pictet-Spengler reaction over three reaction steps amounted to 40%.

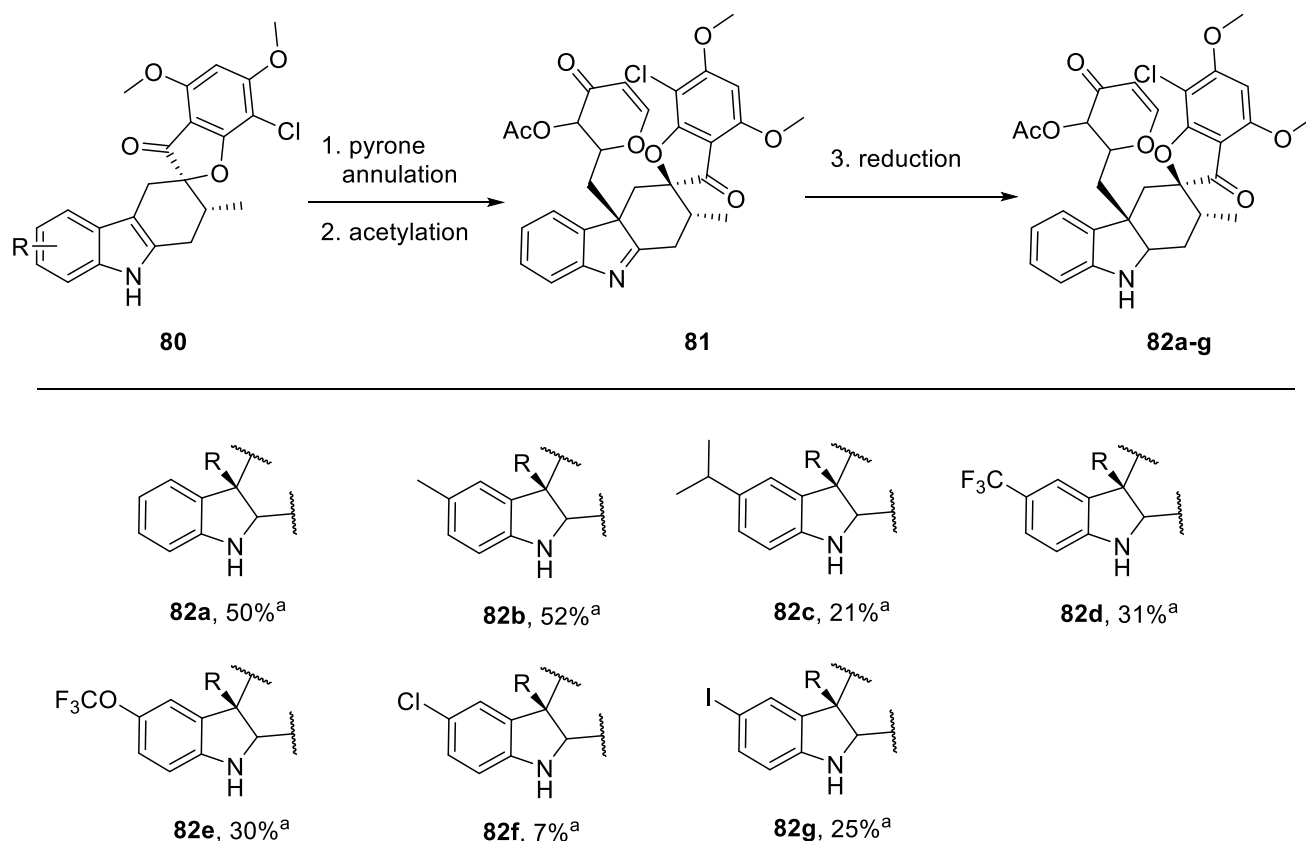
Table 5: Optimization of the reaction conditions for the reduction of the indolenines to indolines on the unfunctionalized Pictet-Spengler product with cyclohexanone **74a**.



Entry	Reducing agent	Solvent	$t$ [min]	Yield* [%]
1	STAB-H (4 eq.)	DCE	30	87
2	NaBH <sub>3</sub> CN (2 eq.)	MeOH	30	98
5	NaBH <sub>3</sub> CN (1.5 eq.)	MeOH	15	99

\*Yield determined by NMR.

The three-step synthesis of  $\gamma$ -pyrone annulation followed by acetylation and reduction enabled access to a small collection of indolines **82a-g** (Scheme 26). As expected, the isolated yields were relatively low (7-52%) as they involved two purification steps. The purification of the chlorine substituted indole **82f** gave problems due to mixed fractions with maltol that led to the reduced yield of 7% over three steps. However, overall all substituents from halogens and alkyl residues, among others were tolerated in the complete sequence and resulted in stable indolines **82a-g**.



Scheme 26: Substrate scope for the  $\gamma$ -pyrone annulation followed by acetylation and reduction to indolines **82a-g**. Isolated yield in percent over three steps. Purification via <sup>a</sup>GPC. Residue R corresponds to the acylated maltol moiety. 1.  $\gamma$ -pyrone annulation: **10** (2.0 eq.), TFE, 50 °C, 30 min, 2. acetylation: (Ac)<sub>2</sub>O (2.4 eq.), Et<sub>3</sub>N (3.0 eq.), DMAP (cat.), CH<sub>2</sub>Cl<sub>2</sub>, 22 °C, 30 min, 3. reduction: NaBH<sub>3</sub>CN (1.5 eq.), MeOH, 22 °C, 15 min.

In summary, a  $\gamma$ -pyrone annulation method for the dearomatization of indole-containing pseudo-NP was developed. The equilibrium is shifted to the open indolenine with a lower energy than to the closed indoline version. Based on this hypothesis, it was not possible to stabilize the closed indoline form. Nevertheless, a diverse indolenine collection was synthesized and stabilized via acetylation. Without this stabilization the  $\gamma$ -pyrone products slowly decomposed to their starting materials. The indolenines could furthermore be reduced to stable indolines.

### 3.2.3. CHEMINFORMATICS

The new classes of dearomatized pseudo-NPs were evaluated regarding their physicochemical properties by employing cheminformatics.

The lead-likeness plot assigns compounds regarding their hydrophobicity and molecular weight with drug-like properties (Figure 25a). The plot indicated that the dearomatized compounds mostly share a beneficial AlogP value as parameter for hydrophobicity. However, due to the addition of another fragment the pseudo-NPs have a relatively high molecular weight which shifts the majority of the compounds out of the Lipinski's rule of five space. The original guideline for Lipinski's rule of drug-likeness was proposed in the early 1990s.<sup>[73]</sup> The concept should to some extent not be overemphasized as many natural products or biologicals do not fall into the required limits and can therefore not be included.<sup>[75]</sup>

Characterization of shape by a principal moments of inertia plot<sup>[74]</sup> (Figure 25b) revealed that both the indolenines and the indolines are shifted away from the rod/disk-like axis towards a more spherical shape. Compared to the indole starting materials, the dearomatized compounds showed even higher three-dimensional character. This indicates a three-dimensionality that coincides more closely to the shape of NPs than synthetic drug-like compounds.

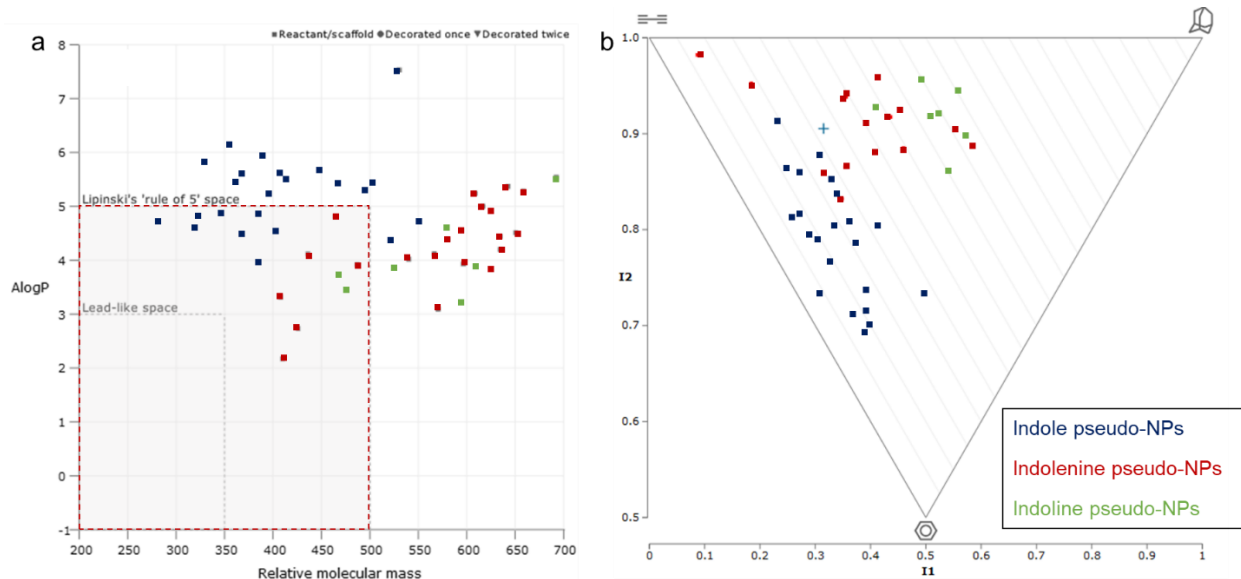


Figure 25: Cheminformatics of dearomatized indoles in comparison to the pseudo-NP starting materials (indole pseudo-NPs (blue), indolenine pseudo-NPs (red), indoline pseudo-NPs (green)). a: Lead-likeness plot, Alog P versus the relative molecular mass.<sup>[74]</sup> b: PMI plot<sup>[74]</sup> of the pseudo-NP collection displays a broad diversity of three-dimensional space similar to NPs.



Atom connectivity was evaluated by a NP-likeness score<sup>[96]</sup> (Figure 26) and compared to NPs in the ChEMBL database<sup>[98]</sup> and compounds in the DrugBank<sup>[97]</sup>, which characterizes marketed and experimental drugs. The pseudo-NP collection is represented by the area where drugs and NPs intersect, indicating that some NP-identity is conserved while also suggesting the fragment combinations do not occur in nature.

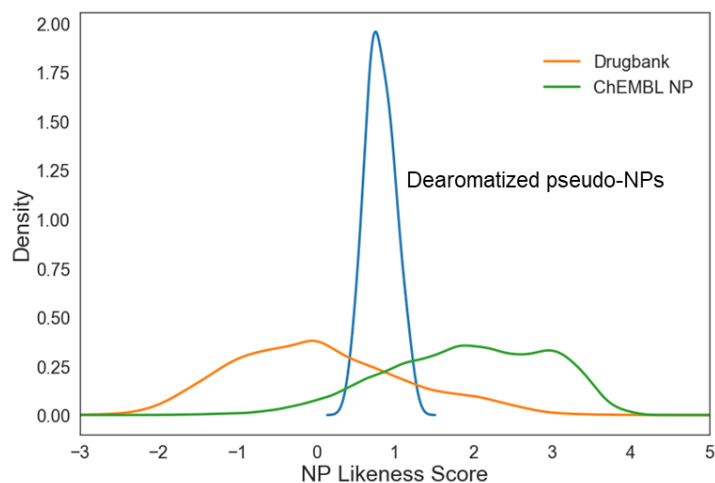


Figure 26: NP-likeness score<sup>[96]</sup> of the dearomatized indoles and indolenines. Dearomatized pseudo-NPs (blue curve) compared to the DrugBank<sup>[97]</sup> compound collection (orange curve) and ChEMBL NPs<sup>[98]</sup> (green curve).

### 3.3. BIOLOGICAL EVALUATION

The identification of specific modulators is highly important for the study of biological phenomena and is a basis for the development of effective therapeutics. Given the unprecedented structures, the pseudo-NP library was biologically investigated in multiple phenotypic assays covering different relevant pathways including glucose uptake, reactive oxygen species (ROS) formation, kynurenine pathway, osteogenesis, and autophagy modulation. Additionally, unbiased morphological profiling was employed to investigate potential bioactivity. All initial assays and their half maximal inhibitory concentration ( $IC_{50}$ ) calculation were performed by the Compound Management and Screening Center (COMAS) of the Max Planck Institute of Molecular Physiology in a medium- or high-throughput manner.

#### 3.3.1. INDOFULVINS: NEW BIOACTIVITY

##### AUTOPHAGY INHIBITION THROUGH INDOFULVINS

The phenotypic autophagy assay identifies new inhibitors of this pathway based on the procedure established by Balgi et al.<sup>[107]</sup> Thereby, human MCF7 breast carcinoma cells are stably transfected with a plasmid bearing an eGFP-LC3 conjugate and therefore express fluorescently labeled LC3. The basal autophagy level is depicted by cells under fed conditions. The marker protein is present in the non-membrane bound LC3-I version, which is equally distributed throughout the cytoplasm. Therefore, the fluorescence comprises the complete cells under the microscope (Figure 27). Autophagy is artificially induced by either the application of Earle's balanced salt solution (EBSS) representing an amino acid starvation or the addition of the mTOR inhibitor rapamycin.<sup>[67a]</sup> The lipidation of LC3-I to LC3-II and its following localization in the autophagosome membrane is visualized as green puncta. Chloroquine as an inhibitor of the autophagosome-lysosome fusion prevents the autophagosome degradation and consequently enhances the fluorescent signal.<sup>[71]</sup> The number puncta, which is representing the autophagosomes, is a direct measurable parameter for a functional autophagy. Autophagy inhibitors are supposed to reverse this phenotypic effect and thereby, reduce the puncta formation.

The investigation of two different induction methods allows to draw conclusions about the compound's mode-of-action relative to the autophagy pathway. An inhibition upon both conditions suggests an interference downstream of mTOR. A reduced signal only under amino acid starvation indicates an inhibition upstream or independently of mTOR.<sup>[107]</sup>

Initially, the pseudo-NPs were tested at a single concentration of 10  $\mu\text{M}$  in the autophagy assay. An inhibition of the pathway by  $\geq 70\%$  qualifies them for retesting. A confirmation in activity results in the dose-dependent investigation and the determination of the  $\text{IC}_{50}$ . Compounds with  $\text{IC}_{50}$  below 10  $\mu\text{M}$  in at least one of the induction methods are considered to be active.

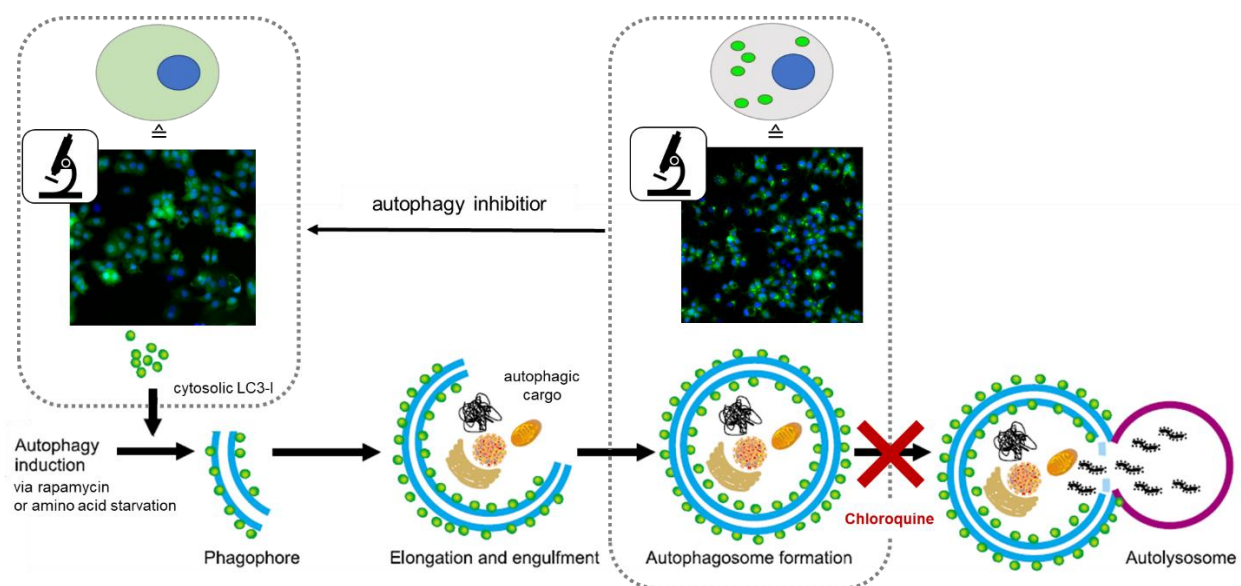


Figure 27: Cell-based assay to monitor autophagy in MCF7 cells using with eGFP-labelled LC3 for microscopic readout. (Scheme adapted from <sup>[63]</sup>) Before autophagy induction eGFP labelled LC3-I is equally distributed throughout the cytoplasm. Upon autophagy induction via amino acid starvation or addition of rapamycin, LC3-II is generated by the lipidation of LC3-I and relocated to the phagophore membrane. The addition of chloroquine prevents the fusion with the lysosome and therefore stops the autophagy process on the level of the autophagosome. Due to the eGFP labelling of LC3-II, the autophagosomes are visualized as green puncta. Autophagy inhibitors are supposed to reverse this effect and lead to a diffuse fluorescence signal.

This phenotypic screen identified the indofulvins as a promising new chemotype of autophagy inhibitors. The unsubstituted  $\gamma$ -indofulvin **50a** showed an inhibitory effect with an  $\text{IC}_{50} = 3.39 \pm 0.38 \mu\text{M}$  and served as starting point for the synthesis of a small SAR collection varying in the substitution of the indole in different positions including the indole nitrogen, as well as one methoxy group and the chlorine of the griseofulvin moiety (Table 6). For the diverse functionalization of the C4-7 position of the indole, the respective indole was functionalized on C2 through regioselective Pd-catalysis. The subsequently performed Pictet-Spengler reaction gave high to excellent yields for all derivatives (**50a-m**, 79-94%). Small residues including fluorine and a methyl group were broadly tolerated on the indole (**50b-e**, **50j**). The introduction of a methyl group in the C5 position improved the autophagy activity to an  $\text{IC}_{50} = 0.82 \pm 0.20 \mu\text{M}$  (**50c**).

## Results and Discussion

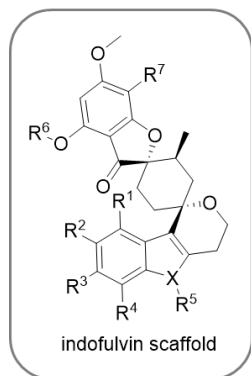
Sterically more demanding residues such as a benzyl group and methyl ester lead to a loss of bioactivity (**50i** and **50m**). A hydroxy group as well as a methoxy group were also not tolerated and caused a significant drop in activity to a more than ten times higher  $IC_{50}$  (**50g-h**).

A derivatization on the indole nitrogen with a methyl or benzyl group resulted in a significant reduction of bioactivity (**50n-o**). A benzofuran moiety instead of an indole also showed no improvement in bioactivity (**55m**).

Furthermore, the griseofulvin part was derivatized by removing regioselective the methoxy group in close proximity to the carbonyl function with magnesium iodide and subsequent submitting it for nucleophilic substitution with organo halide compounds (**50p-r**). However, different residues on  $R^6$  did not give more active inhibitors of autophagy, the Pictet-Spengler reaction gave excellent yields of the desired compounds. Lastly, the griseofulvin chlorine was substituted by hydrogen, a methyl and benzyl group through Pd-catalyzed cross coupling (**50s-u**). The potency in the autophagy assay of the resulting derivatives was lower than of indofulvin **50c**.

Table 6: Structure-activity-study of indofulvins in autophagy inhibition.

Indofulvin	R <sup>1</sup>	R <sup>2</sup>	R <sup>3</sup>	R <sup>4</sup>	R <sup>5</sup>	R <sup>6</sup>	R <sup>7</sup>	X	IC <sub>50</sub> (μM)
<b>50a</b>	H	H	H	H	H	Me	Cl	N	3.39 ± 0.38
<b>50b</b>	Me	H	H	H	H	Me	Cl	N	3.03 ± 0.76
<b>50c</b>	H	Me	H	H	H	Me	Cl	N	0.82 ± 0.20
<b>50d</b>	H	H	Me	H	H	Me	Cl	N	4.16 ± 1.19
<b>50e</b>	H	H	H	Me	H	Me	Cl	N	1.01 ± 0.46
<b>50j</b>	H	F	H	H	H	Me	Cl	N	1.41 ± 0.27
<b>50k</b>	H	Cl	H	H	H	Me	Cl	N	4.18 ± 0.44
<b>50h</b>	H	OMe	H	H	H	Me	Cl	N	>10
<b>50i</b>	H	OBn	H	H	H	Me	Cl	N	>10
<b>50m</b>	H	COOMe	H	H	H	Me	Cl	N	>10
<b>50g</b>	H	OH	H	H	H	Me	Cl	N	>10
<b>50n</b>	H	Me	H	H	Me	Me	Cl	N	7.42 ± 0.65
<b>50l</b>	H	Me	H	H	Bn	Me	Cl	N	>10
<b>55m</b>	H	H	H	H	-	Me	Cl	O	7.42 ± 1.23
<b>50p</b>	H	Me	H	H	H	H	Cl	N	4.86 ± 1.12
<b>50q</b>	H	Me	H	H	H	allyl	Cl	N	4.67 ± 1.36
<b>50r</b>	H	Me	H	H	H	Bn	Cl	N	>10
<b>50s</b>	H	Me	H	H	H	Me	H	N	>10
<b>50t</b>	H	Me	H	H	H	Me	Me	N	3.69 ± 0.92
<b>50u</b>	H	Me	H	H	H	Me	Ph	N	>10



Indofulvin **50c** (COMAS ID= 409328) showed the strongest inhibitory effect in autophagy with an  $IC_{50} = 0.82 \pm 0.20 \mu\text{M}$  upon amino acid starvation (Figure 28a). The images indicated a reversal effect: After compound treatment, the staining was distributed throughout the cell and resembled the phenotype under fed conditions (Figure 28b).<sup>[107]</sup> The green puncta representing the autophagosomes, which are visible upon amino acid starvation with EBSS and CQ, could not be found upon addition of indofulvin **50c**. As the addition of indofulvin **50c** showed no inhibitory effect on the autophagy activity induced by rapamycin, the compound is likely to act either downstream or independently of mTOR.

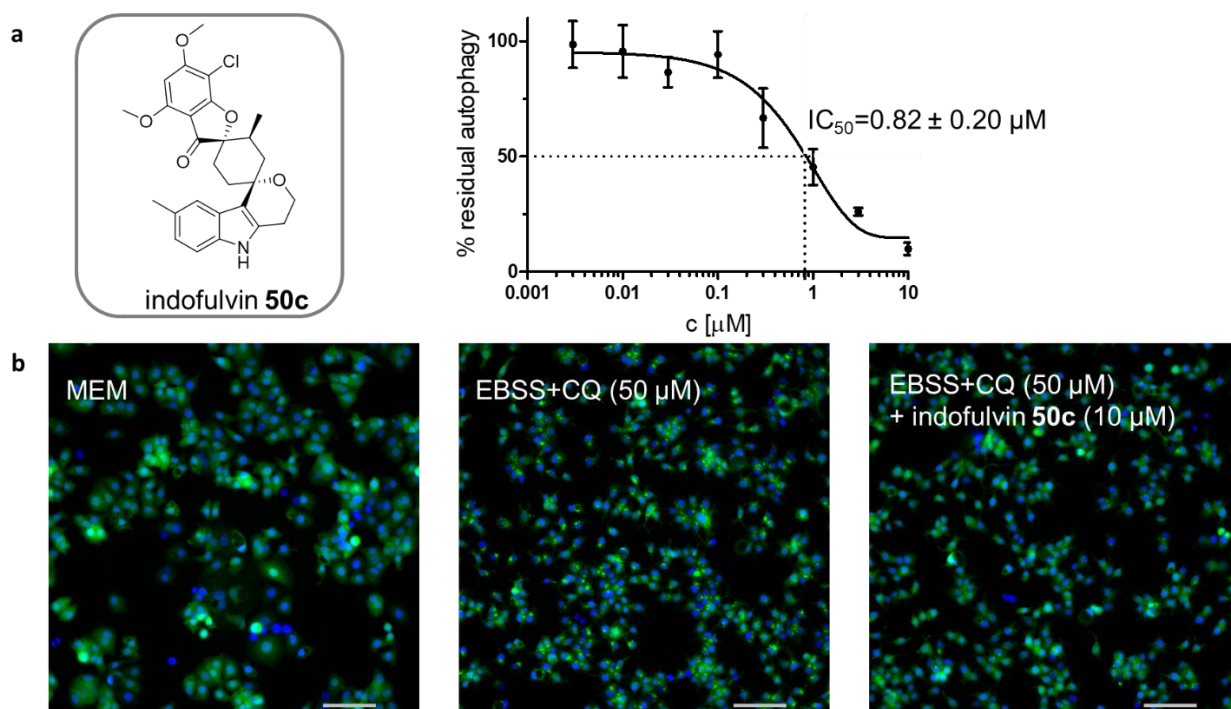


Figure 28: Influence of indofulvin **50c** on the autophagic flux. a) Dose dependency of indofulvin **50c** on autophagy inhibition in the phenotypic assay quantified by the number of autophagosomes per cell.  $IC_{50} = 0.82 \pm 0.20 \mu\text{M}$ , ( $n=3$ ). b) Resulting microscopic pictures from the screening with media MEM for the basal level of autophagy, EBSS+CQ as negative control and after compound treatment. Nuclear DNA was stained with Hoechst, the green color is attributable to eGFP labeled LC3.

## VALIDATION OF THE INDOFULVINS AS AUTOPHAGY INHIBITORS ON PROTEIN LEVEL

The indofulvins as new chemotype of autophagy inhibitors required further validation. However, phenotypic investigations based on GFP-conjugates involve limitations such as its proteolytic degradation by the lysosome.<sup>[108]</sup> As a consequence, a reduced fluorescence signal can arise from an increased autophagosome-lysosome fusion and can lead to false positive hits.<sup>[109]</sup> Additionally, the conjugation to GFP might influence the activity of LC3 due to its size. The GFP signal might also be reduced due to its increased proteasomal degradation as non-native protein.<sup>[108]</sup> Therefore, indofulvins were further evaluated in a GFP-independent assay.

A GFP-LC3 independent investigation of autophagy is the quantification of relevant autophagy proteins including the native proteins LC3-I, LC3-II and p62 using immunoblotting methodology. As upon autophagy induction the level of LC3-II is increased via lipidation, inhibitors are supposed to show the opposite effect and reduce the phosphatidylethanolamine adduct.<sup>[61]</sup> Under starved conditions with EBSS, a slight difference between the DMSO control and indofulvin **50c** at 10  $\mu\text{M}$  was visible indicating a higher level of LC3-II in the negative control (Figure 29). The treatment with chloroquine (CQ) showed a significantly higher amount of LC3-II for the autophagy induced cells. As CQ is inhibiting the autophagosome-lysosome fusion, but not the autophagosome formation, an enrichment in LC3-II meets the expectations. The other autophagy marker, protein p62 ( $\cong$  sequestosome-1), is degraded upon pathway activation.<sup>[65]</sup> In comparison to modified eagle medium (MEM), the negative control with DMSO under starvation showed a lower level of p62. However, with increasing concentration of indofulvin **50c** the amount of p62 raised suggesting an inhibition of autophagy. Therewith, both markers showed the expected effect for autophagy inhibition on protein level and confirmed the compound's bioactivity.

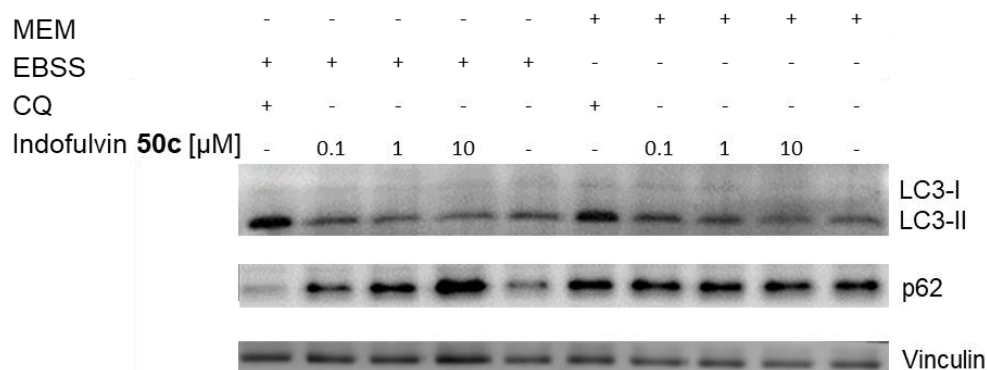


Figure 29: Immunoblot of indofulvin **50c** for the autophagy marker LC3-II and p62 with vinculin as control. Upon autophagy induction the level of LC3-II is slightly reduced after compound treatment compared to the DMSO control. The indofulvin **50c** significantly inhibits the degradation of p62. Representative immunoblot, n=4.

## GLUCOSE-DEPENDENT VIABILITY INVESTIGATIONS

Examination of a compound's potential cytotoxicity is important as it can produce false positive hits and therefore needed to be excluded for further investigations. In addition to the analysis under fed conditions, the exploration of the cell viability under starved conditions provides further validation of autophagy inhibitors. Without autophagy, starved cells fail to gain energy for homeostasis and are unfit to compensate the lack of nutrition.<sup>[61]</sup> Consequently, autophagy inhibitors are supposed to show a selective viability such as inducing apoptosis under starved conditions, but ideally causing no cell death under nutrient rich conditions.

A viability assay under fed and starved conditions for nine different concentrations (0.39-10  $\mu\text{M}$ ) and over a period of 72h was performed with an IncuCyte Zoom® analysis system (Figure 30). This live-cell imaging and analysis platform allowed a time-resolved quantification of cell viability. Propidium iodide was employed as fluorescent agent for the selective staining of dead cells.<sup>[49]</sup> The tubulin binder nocodazole was used as positive control and the negative control is represented by MCF7 cells treated with DMSO.<sup>[110]</sup>

At 10  $\mu\text{M}$  indofulvin **50c** showed a slightly increased fraction of dead cells of almost 4% after 72 h (Figure 30a). A concentration of 6.67  $\mu\text{M}$  resulted in no increased cell death relative to DMSO, suggesting indofulvin **50c** is not toxic in its relevant concentration. Conversely, under starved conditions, the pseudo-NP appeared to have a significant influence on the cell viability (Figure 30b). Concentrations of 0.88  $\mu\text{M}$  and higher showed a distinctly higher fraction of dead cells. Without glucose, the percentage number of dead cells was between 50-80% after 72 h. Indofulvin **50c** induced cell death under starved conditions in a dose-dependent manner with an  $\text{EC}_{50}=1.38 \pm 0.45 \mu\text{M}$  (Figure 30c). These results suggest a nutrient-dependent toxicity of indofulvin **50c** by autophagy inhibition, but no toxic effects for the relevant concentrations below 10  $\mu\text{M}$  on MCF7 cells under fed conditions.

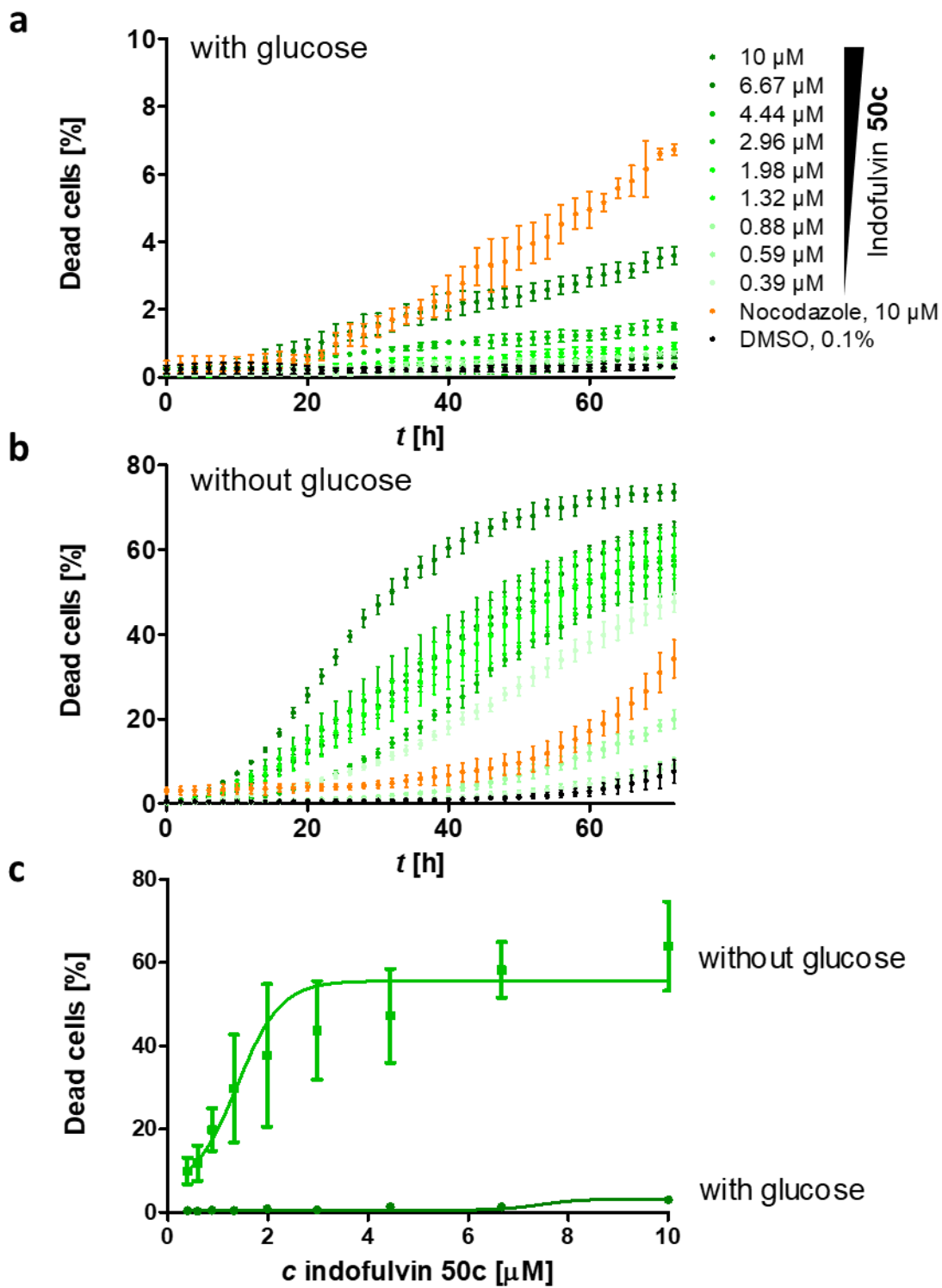


Figure 30: Influence of indofulvin 50c on the selective viability of MCF7 cells. Staining of dead cells with propidium iodide. Representative graph of three independent replicates shown. (n= 3, N=3) Cell viability under a) fed conditions and b) starved conditions. c) Fraction of dead cells for both conditions.



## MORPHOLOGICAL PROFILING FOR TARGET HYPOTHESIS

Unbiased morphological profiling was employed as a means to investigate a wide range of biological space for target identification. In a single experiment a large number of phenotypic features are deduced from image analysis and can be used to evaluate bioactivity and generate a target hypothesis by the comparison to annotated references.<sup>[46]</sup>

The COMAS established the cell painting assay based on the pioneering work of the Carpenter group.<sup>[46, 76]</sup> After treatment of cells with a compound collection, six dyes are employed to selectively stain different cell components. Subsequent automated image acquisition of the cells allows the extraction of 579 morphological features. The quantification of the phenotypic change of each feature can be translated into a characteristic fingerprint that represents the compound's bioactivity. Induction determines the fraction of significantly changed features in percent relative to the DMSO control and thereby represents a unit for bioactivity in the cell painting assay. A morphological change is considered to be significant once its difference is +/- three-fold of the median for the negative control. A low induction below 5% indicates that less than 29 features are significantly changed. These low inducing compounds reflect a low bioactivity in the cell painting assay and are not further analyzed. A high induction indicates major morphological differences relative to DMSO. High inducing compounds may interact with multiple targets or have pleiotropic activity. Additionally, compounds with very high induction values appear to share a high similarity in their profiles. As overactivity might no longer be related to the compound's primary bioactivity, compounds with inductions above 70% were excluded from the analyses. This overactivity profile is not yet completely understood and is still under investigation. Consequently, compounds with an induction greater than 5%, but below 70% were used for further investigations such as the comparison to other compounds. If necessary, compounds were screened at additional concentrations to deliver fingerprints that are within the desired induction window.<sup>[53]</sup>

The similarity of two morphological profiles is specified as one minus the correlation distances between the profiles. Empirically, biosimilarities greater 75% are considered biosimilar whereas a percentage below indicates a relevant difference between the compounds and is therefore considered as dissimilar. For the comparison of more than two profiles the cross-similarity, which describes the median biosimilarity percentage (MBP) for larger compound sets, was introduced. In addition, a dimension reduction analysis (Principal Component Analysis, short PCA) was employed for the evaluation of compound sets in which all morphological information from the profiles are reduced and arranged in three-dimensional space. Each spot represents one morphological profile from the CPA. The similarity of profiles is depicted by the distance between

## Results and Discussion

spots. A close proximity represents a high biological similarity, whereas a greater distance between compounds is translated to differences in the morphological profiling.

For a meaningful comparison and to avoid false positive matching in phenotypic similarity, it appeared to be important to compare compounds in a certain induction window. While comparing classes with broad induction ranges, compounds were found to form clusters due to similar induction rather than true biosimilarity.<sup>[111]</sup> In the PCA analysis component 1 is especially induction-dependent if a wide induction range is employed (Figure 31). Based on experience, induction ranges below 25% showed sufficient mixing relative to the induction. However, some data sets required smaller induction windows while others tolerated large ranges with adequate mixing. Therefore, it is necessary to compare compounds in a variety of induction ranges.

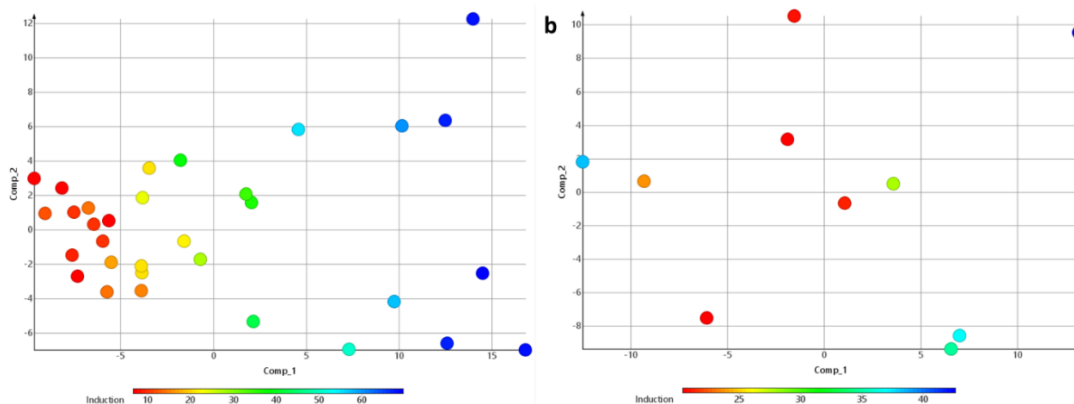


Figure 31: Induction effect on component 1. a) PCA plot with a broad induction range from 6.6% to 69.8% and b) a defined induction window of 20-45% (right). Induction is represented by color. Component 1 is heavily influenced by the induction unless reducing the induction range to 25%.<sup>[111]</sup>

For the first analysis, the phenotypic profiles from the pseudo-NP were compared to the known autophagy inhibitors chloroquine<sup>[71]</sup>, aumitin<sup>[112]</sup>, autophinib<sup>[70]</sup>, autogramin<sup>[113]</sup>, azaquindole<sup>[23]</sup> and wortmannin<sup>[68]</sup> (Figure 32). All modulators shared at least one concentration in a comparable induction window to indofulvin **50c**. However, the biosimilarity was overall low compared to the references ( $\leq 55\%$ ), indicating a dissimilar mode-of-action.

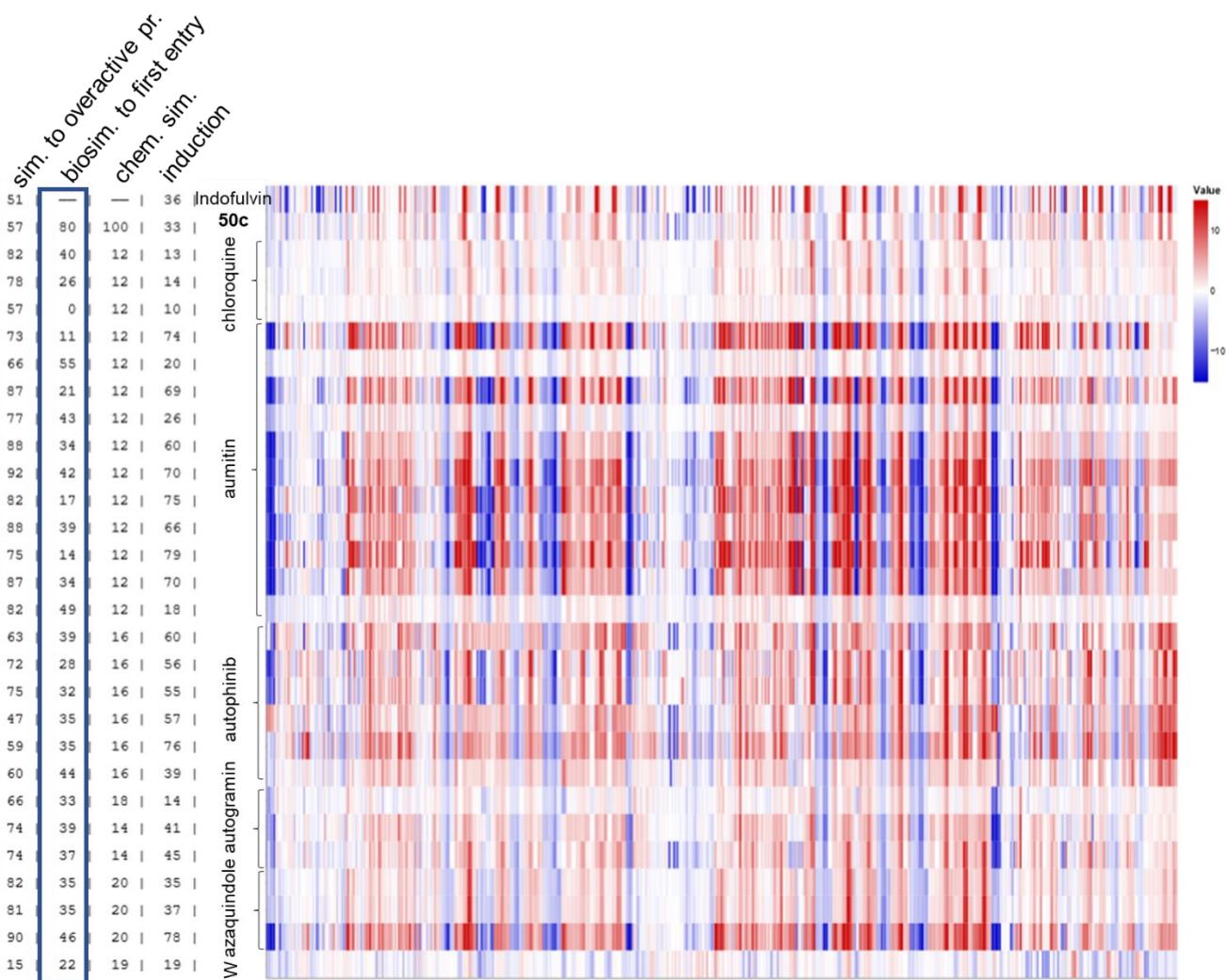


Figure 32: Morphological fingerprint comparison of indofulvin **50c** to the known autophagy inhibitors chloroquine, aumitin, autophinib, autogramin, azaquindole and wortmannin (W). Biological similarity (Bio. Sim) was calculated to the first entry (indofulvin **50c**).

Although the biosimilarity to the known complex I inhibitor of the mitochondrial respiration aumitin<sup>[112]</sup> was with maximal 55% relatively low (Figure 32), especially the features connected with the mitochondria were affected by the indofulvin **50c**. The mitochondria showed significant differences to the DMSO control (Figure 33a). These morphological changes might indicate an interference with the mitochondrial metabolism, such as mitochondrial respiration. The morphological biosimilarity of indofulvin **50c** to four known interactors<sup>[112]</sup> with the mitochondrial respiration was analyzed (Figure 33b). Rotenone, oligomycin, and carbonyl cyanide-4 (trifluoromethoxy) phenylhydrazone (FCCP) induced sufficient morphological changes with an induction range of 33-52% that is comparable to the 36% induction of indofulvin **50c**. Antimycin A

## Results and Discussion

appeared to be a low inducing compound with a maximal induction of 23% that could be used for the comparison. The similarity of the morphological profiles of indofilvin **50c** was extremely low to rotenone, antimycin A and FCCP (0-25%). However, the pseudo-NP showed a significantly higher biosimilarity of 87% to oligomycin. Consequently, indofilvin **50c** was hypothesized to share a similar mode-of-action by targeting mitochondrial respiration.

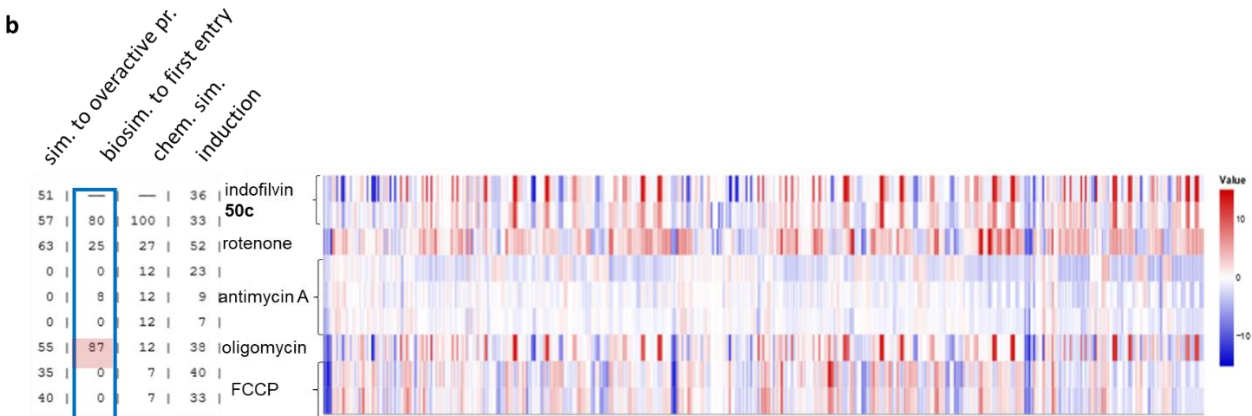
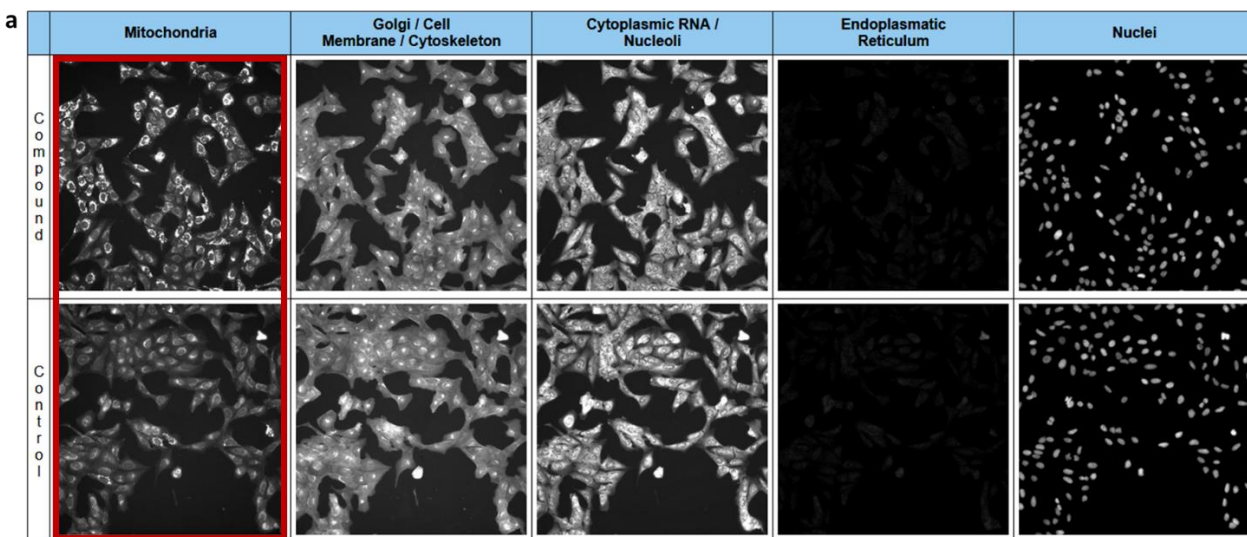


Figure 33: Influence of indofilvin **50c** on mitochondrial phenotype. a) Representative cell painting images of the stained organelles revealed significant morphological changes on mitochondria after compound treatment with indofilvin **50c** relative to DMSO. b) Morphological fingerprint comparison between indofilvin **50c** and known interactors of the mitochondrial respiration: rotenone, antimycin A, oligomycin, and FCCP. Biological similarity (Bio. Sim) was calculated to the first entry (indofilvin **50c**).

## INDOFULVINS INFLUENCE ON MITOCHONDRIAL RESPIRATION

As autophagy regulates the degradation of damaged or nonfunctional mitochondria, a correlation between the interference in mitochondrial metabolism and autophagy inhibitors has been reported before.<sup>[112, 114]</sup> Moreover, an inhibitory effect on mitochondrial respiration affects the autophagic flux.<sup>[115]</sup> Potent inhibitors of the mitochondrial metabolism including rotenone, oligomycin, and FCCP show simultaneously an inhibitory effect on autophagy and demonstrate the close interplay of both pathways.<sup>[112, 116]</sup> Due to the high biosimilarity of indofulvin **50c** to complex V inhibitor oligomycin<sup>[117]</sup>, the influence of the pseudo-NP on the mitochondrial respiration was investigated in the Seahorse XF Extracellular Flux Analyzer.

The Mito Stress Test<sup>[53, 112]</sup> investigates the mitochondrial respiration by the time-dependent measurement of the oxygen consumption rate (OCR) and the extracellular acidification rate (ECAR) of cells with two fluorophores.<sup>[118]</sup> The OCR is a direct parameter for mitochondrial respiration as oxygen is converted to water through complex IV (Figure 34a). The extracellular acidification indicates the cells anaerobic glycolysis level as alternative energy source once the mitochondrial respiration is inhibited. By the addition of known inhibitors, key parameters of mitochondrial function can be investigated (Figure 34b). Initially, a base line without chemical perturbation representing the basal respiration is recorded. The subsequent addition of the complex V inhibitor oligomycin inhibits the ATP-linked respiration<sup>[117]</sup> and therefore reduces the OCR. The difference to the non-mitochondrial oxygen consumption exist due to the remaining basal respiration, which is not coupled to ATP production. FCCP as uncoupling agents disrupts the mitochondrial membrane potential and results in the maximal level of the OCR indicating the maximal respiration. The higher potential compared to the basal respiration terms as spare capacity. The final addition of the complex I and III inhibitors rotenone and antimycin A completely shuts down mitochondrial respiration resulting in the minimal oxygen level.<sup>[118]</sup>

An inhibitor of mitochondrial respiration is supposed to affect both the OCR and the ECAR. Upon compound treatment, the OCR was reduced in a dose-dependent manner (Figure 34c). The ECAR on the other side increased as the cells are shifting their energy metabolism towards anaerobic glycolysis.

## Results and Discussion

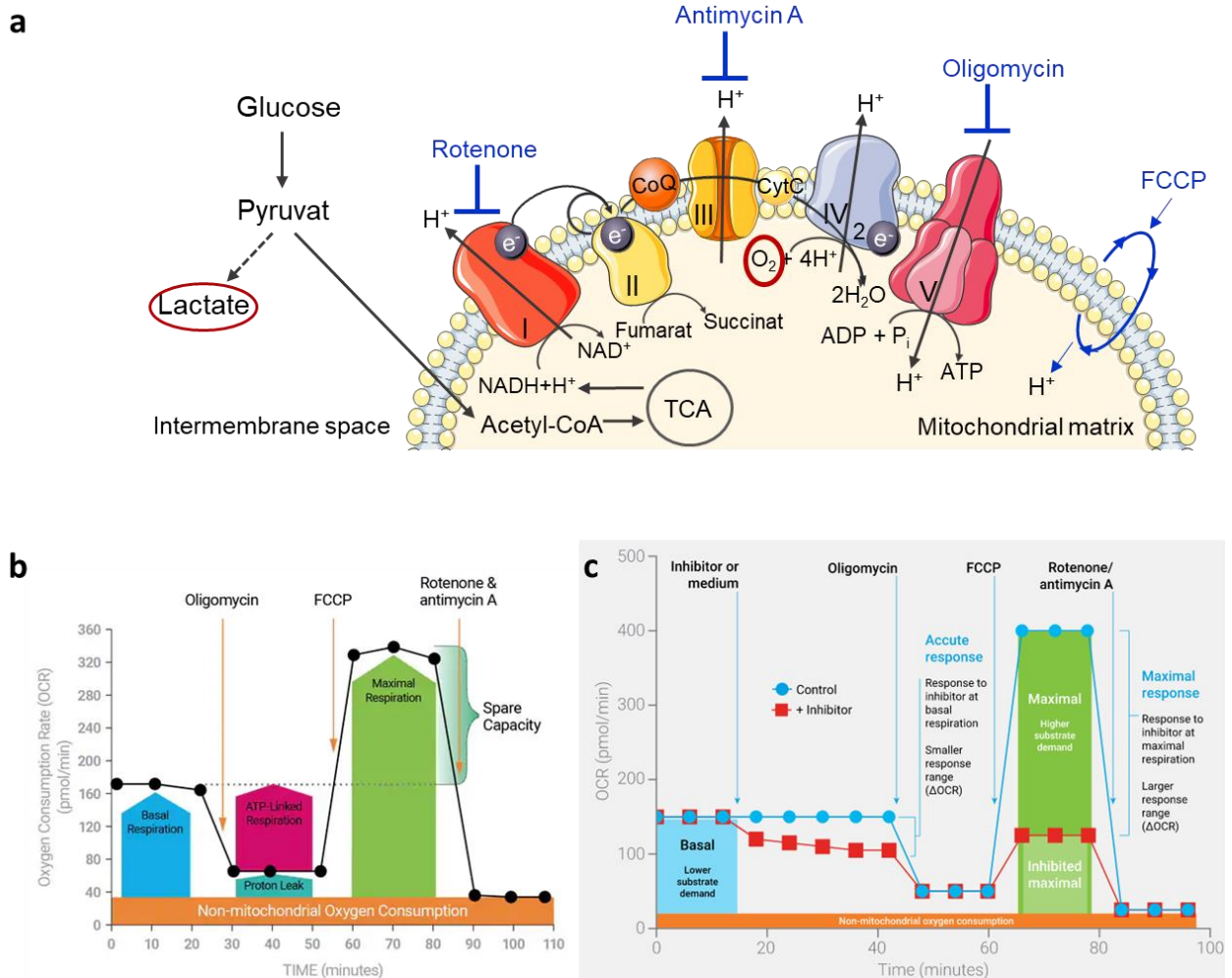


Figure 34: Mitochondrial respiration and its measurement via the Mito Stress Test. a) Scheme of the process of mitochondrial respiration including the known inhibitors rotenone, antimycin A, oligomycin, and FCCP with their targets. Initially, complex I of the electron transport chain utilizes the product from the tricarboxylic acid cycle (TCA)  $\text{NADH} + \text{H}^+$  and complex II  $\text{FADH}_2$  to transfer an electron each onto ubiquinone (CoQ). CoQ passes the electron to complex III, which subsequently transfers them to complex IV. Complex IV reduces oxygen to water. During this process complex I, III, and IV transfer protons to the intermembrane space and consequently decrease the pH of the mitochondrial matrix. The proton gradient is used by complex V to generate ATP. b) Mito Stress Test profile of the oxygen consumption rate (OCR) including the key parameters of the mitochondrial respiration. c) Mito Stress Test profile of the oxygen consumption rate (OCR) with an inhibitor.<sup>[118]</sup>

Indofulvin **50c** was analyzed for its influence on the mitochondrial respiration employing a Mito Stress Test in two cell lines (Figure 35). Upon compound treatment after 30 min, the OCR was significantly reduced for concentrations greater than 1  $\mu\text{M}$  in HeLa cells (Figure 35a). At the highest concentration of 30  $\mu\text{M}$ , the OCR dropped to 35%, which is almost the same level as after the addition of oligomycin. The ECAR simultaneously was dose-dependently increased up to 135%, indicating the alternative energy gain via anaerobic glycolysis due to the blocked mitochondrial respiration (Figure 35b). In MCF7 cells a similar effect was observed showing slightly less sensitivity (Figure 35c and d). This analysis revealed indofulvin **50c** as an inhibitor of mitochondrial respiration.

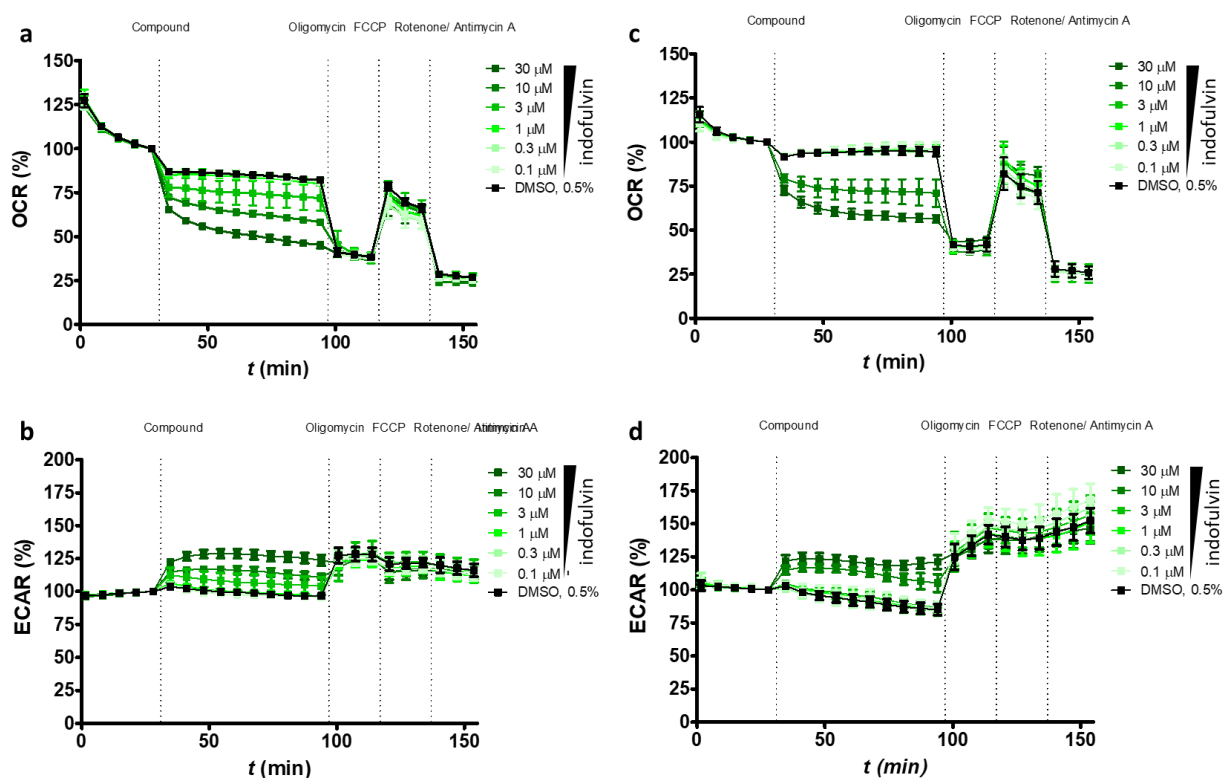


Figure 35: Influence of indofulvin **50c** on mitochondrial respiration in HeLa (a and b) and MCF7 cells (c and d). The oxygen consumption rate (OCR, a and c) and extracellular acidification rate (ECAR, b and d) are measured over time. Addition of indofulvin **50c** in six concentrations varying from 0.1 to 30  $\mu\text{M}$ . Subsequent injection of oligomycin (1  $\mu\text{M}$ ), FCCP (0.25  $\mu\text{M}$ ) and rotenone/antimycin A (0.5  $\mu\text{M}$ ). (n=3, N=2)

The correlation of the indofulvins activity in autophagy inhibition and the interference with the mitochondrial respiration was investigated by analyzing the most active autophagy hit indofulvin **50c**, a less active derivative **65f**, and an inactive derivative **50o** as well as the parent NP griseofulvin in the Mito Stress Test (Figure 36). The most active compound in the autophagy

## Results and Discussion

assay also showed the strongest effect on mitochondrial respiration. The chroman derivative **65f** (Figure 36a, blue) had a moderate  $IC_{50} = 4.00 \pm 0.29 \mu\text{M}$  in autophagy inhibition and also showed a reduced OCR and therefore an inhibitory effect on the mitochondrial metabolism. The griseofulvin indole with a benzyl-group on the indole nitrogen **50o** (Figure 36a, orange), similar to griseofulvin (Figure 36a, violet), was inactive in the autophagy assay and showed no significant impact on mitochondrial respiration relative to DMSO. Consequently, this trend not only confirms a correlation between the activity in autophagy and mitochondrial respiration of the pseudo-NPs, but also proved the generation of new bioactivity of griseofulvin-based pseudo-NPs, whereas griseofulvin showed no effect on both pathways.

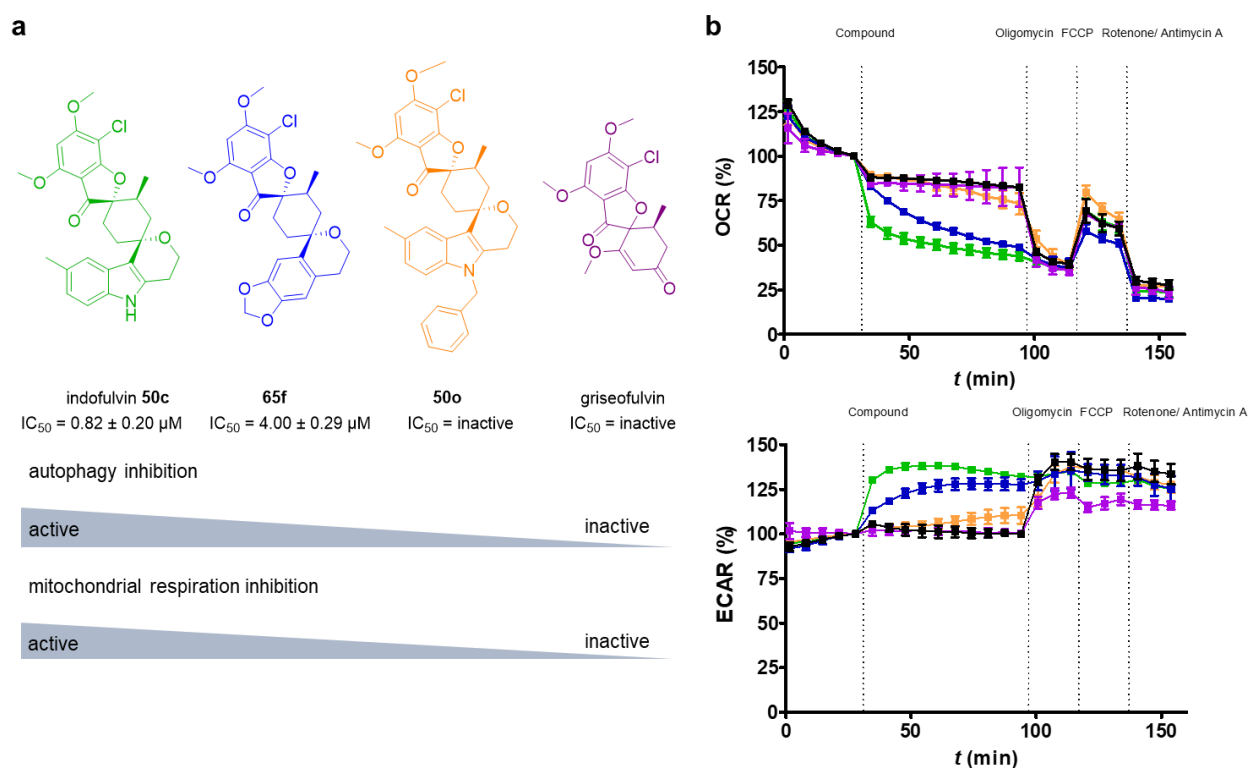


Figure 36: The bioactivity of different pseudo-NPs and griseofulvin revealed a clear correlation between the activity in the autophagy assay and the Mito Stress Test. The most potent inhibitor of autophagy, indofulvin **50c** (green), had the highest effect on the mitochondrial metabolism. The chromane derivative **65f** (blue) showed a moderate effect in both assays and both the benzylated pseudo-NP **50o** (orange) and NP griseofulvin (violet) were inactive for autophagy inhibition and showed no interference with mitochondrial respiration. a) Overview of the investigated compounds and their bioactivities. b) Mito Stress Test of the three pseudo-NPs and griseofulvin including the addition of oligomycin (1  $\mu\text{M}$ ), FCCP (0.25  $\mu\text{M}$ ), rotenone/antimycin A (0.5  $\mu\text{M}$ ). (n=3, N=2)



## INVESTIGATION FOR LYSOSOMOTROPISM

One mode-of-action of autophagy inhibitors is the prevention of the autophagosome-lysosome fusion. Lysosomotropic compounds, including chloroquine and chlorpromazine interfere with the lysosome and act therefore mTOR-independently.<sup>[52]</sup> A biosimilarity to the overactive profile may be related to lysosomotropism as is a common effect for compounds. A morphological similarity to the reference smoothed agonist (SAG)<sup>[119]</sup> above 70% suggested a potential accumulation in the lysosome and was further analyzed in the LysoTracker™ Red DND-99 assay in MCF7 cells.<sup>[120]</sup> The assay employs a fluorescent dye that is enriched in the acidic lysosome. After addition of a lysosomotropic compound, the pH of the lysosome is increased to release the LysoTracker™ Red DND-99 staining. The negative controls with DMSO and water showed the characteristic red color under the microscope, whereas the lysosomotropic compounds CQ (50  $\mu$ M) and chlorpromazine (5  $\mu$ M) had a reduced signal (Figure 37a). The treatment with indofulvin **50c** gave a similar picture under the microscope compared to the DMSO control without any reduction in the LysoTracker™ Red DND-99 staining (Figure Xa). After quantification of the dye's intensity, indofulvin **50c** exhibited the same level of LysoTracker™ Red DND-99, whereas the positive controls showed a dose-dependent effect (Figure 37b). These results suggest that indofulvin **50c** is not lysosomotropic and likely does not interfere with the lysosome's function.

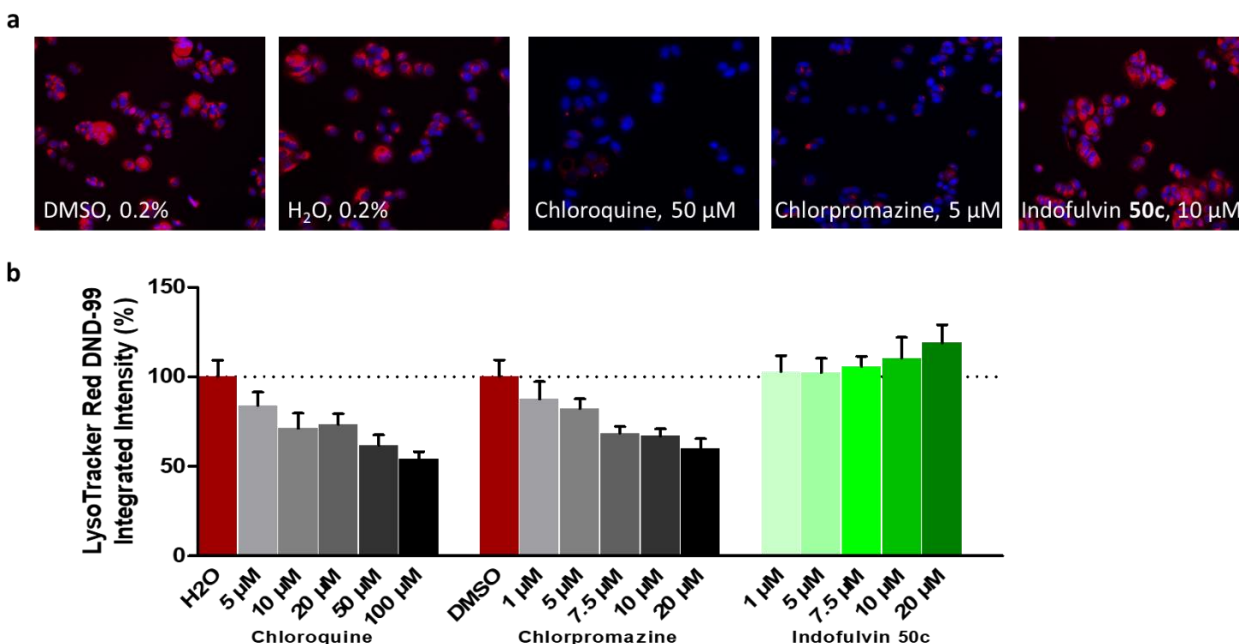


Figure 37: Investigation regarding the lysosomotropism of indofulvin **50c** via LysoTracker™ Red DND-99 assay.<sup>[120]</sup> a) Representative microscope pictures of the negative controls DMSO and water, as well as the positive controls chloroquine and chlorpromazine and indofulvin **50c**. b) Quantification of the LysoTracker™ Red DND-99 assay showing the integrated intensity (in %) for each sample. (n=3, N=3)

### 3.3.2. INDOFULVINS: FRAGMENT BIOACTIVITY

Griseofulvin represents a major moiety of the bioactive pseudo-NP indofulvin **50c**. The fragment-sized<sup>[19]</sup> NP is known for its tubulin binding and is used for several applications including antifungal medication.<sup>[121]</sup> This raises the question, if the new pseudo-NP is still interacting with tubulin or the fragment's original activity has been lost. Ideally, the bioactivity of the indofulvin **50c** is derived from the combination of the griseofulvin fragment with an indole and not from the original fragment alone. This analysis extends to an evaluation of the pseudo-NP approach as the concept that aims to overcome the limitation of BIOS in which compounds interact with similar targets. In order to answer the question, a biochemical and a cell-based tubulin-binding assay were performed.

#### TUBULIN-BINDING ASSAYS

The *in-vitro* assay follows the tubulin polymerization upon GTP addition by the measurement of the absorbance at 340 nm.<sup>[122]</sup> A direct interference with tubulin is supposed to result in either stabilization or destabilization of tubulin polymerization leading to a deviation in the course of the curve compared to the DMSO control. Taxol showed an enhancement in tubulin polymerization while nocodazole and griseofulvin inhibited tubulin polymerization (Figure 38a).<sup>[110, 121b, 123]</sup> In the presence of indofulvin **50c**, no interference with tubulin was detected at concentrations up to 50  $\mu$ M as the polymerization curve showed no difference relative to the DMSO control.

To investigate potential tubulin interaction of the compound in a cellular context in which tubulin associated proteins are also involved, a histone staining for the detection of mitotic cells was performed.<sup>[47]</sup> Compounds which interfere with tubulin are known to prevent cell division and induce mitotic arrest. Consequently, tubulin interactors, for example taxol and nocodazole, increased the percentage of mitotic cells compared to the negative control DMSO (Figure 38b). The parent NP griseofulvin also showed a dose-dependent higher fraction of cells in mitotic arrest. At a concentration of 20  $\mu$ M, griseofulvin led to > 30% mitotic cells, a value six times higher than the DMSO control. However, indofulvin's **50c** percentage of mitotic cells was comparable to DMSO for concentrations up to 30  $\mu$ M. The pseudo-NP therefore could not be associated with tubulin interaction in the *in-vitro* and *in-cell* assay, suggesting a loss of griseofulvin's original tubulin-binding activity.

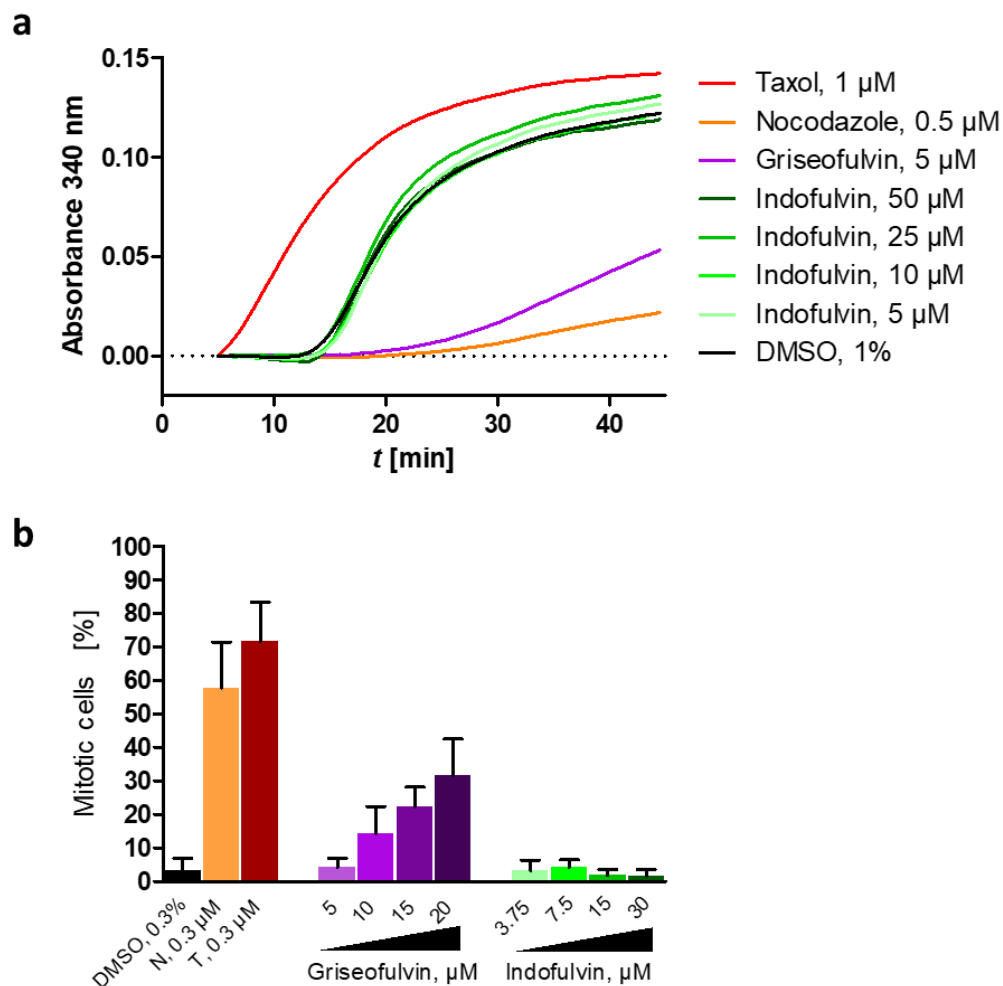


Figure 38: Investigation of indofulvin's **50c** potential interaction with tubulin due to its relationship to the known tubulin binder griseofulvin. a) *In-vitro* assay<sup>[122]</sup> analyzing the tubulin polymerization upon addition of GTP via absorbance at 340 nm, suggesting no tubulin interaction due to no significant deviation from the DMSO control. Representative graph shown. (n=3, N=2) b) Influence of indofulvin **50c** on the number of mitotic cells in MCF7 cells assessed by phospho-Histone 3 staining revealed no tubulin interference (green). Positive controls: N= Nocodazole (orange), T= Taxol (red) and griseofulvin. (n=3, N=3).<sup>[47]</sup>

#### COMPARISON ON A MORPHOLOGICAL LEVEL

The cell painting assay affords the opportunity to compare pseudo-NPs with their parent NPs on a morphological level.<sup>[51]</sup> Clusters in the PCA demonstrate phenotypic differences between compound classes, whereas no clusters, for example in a scatter plot, are considered to cover a biological space, which is not scaffold dependent.

## Results and Discussion

Via PCA analyses all  $\gamma$ -indofulvins were plotted against four different concentrations of their parent NP griseofulvin (Figure 39a). The indofulvins formed a clear cluster that appeared to be morphologically significantly different to griseofulvin. This is also represented by a low MBP of 30% between the two compound classes. The analysis of morphological fingerprints from indofulvin **50c** and griseofulvin also possessed a low biosimilarity of 34% by few shared features (Figure 39b). The PCA analysis of the  $\gamma$ -indofulvins and representative tubulin interactors from the reference compound set revealed clear scaffold-dependent clustering. Although the distance between both clusters is closer, the investigation indicated phenotypic differences between indofulvins and tubulin-binders. In conclusion, the cell painting assay was able to identify biological distinctions on a morphological level between the indofulvins and their fragment-sized parent NP griseofulvin.

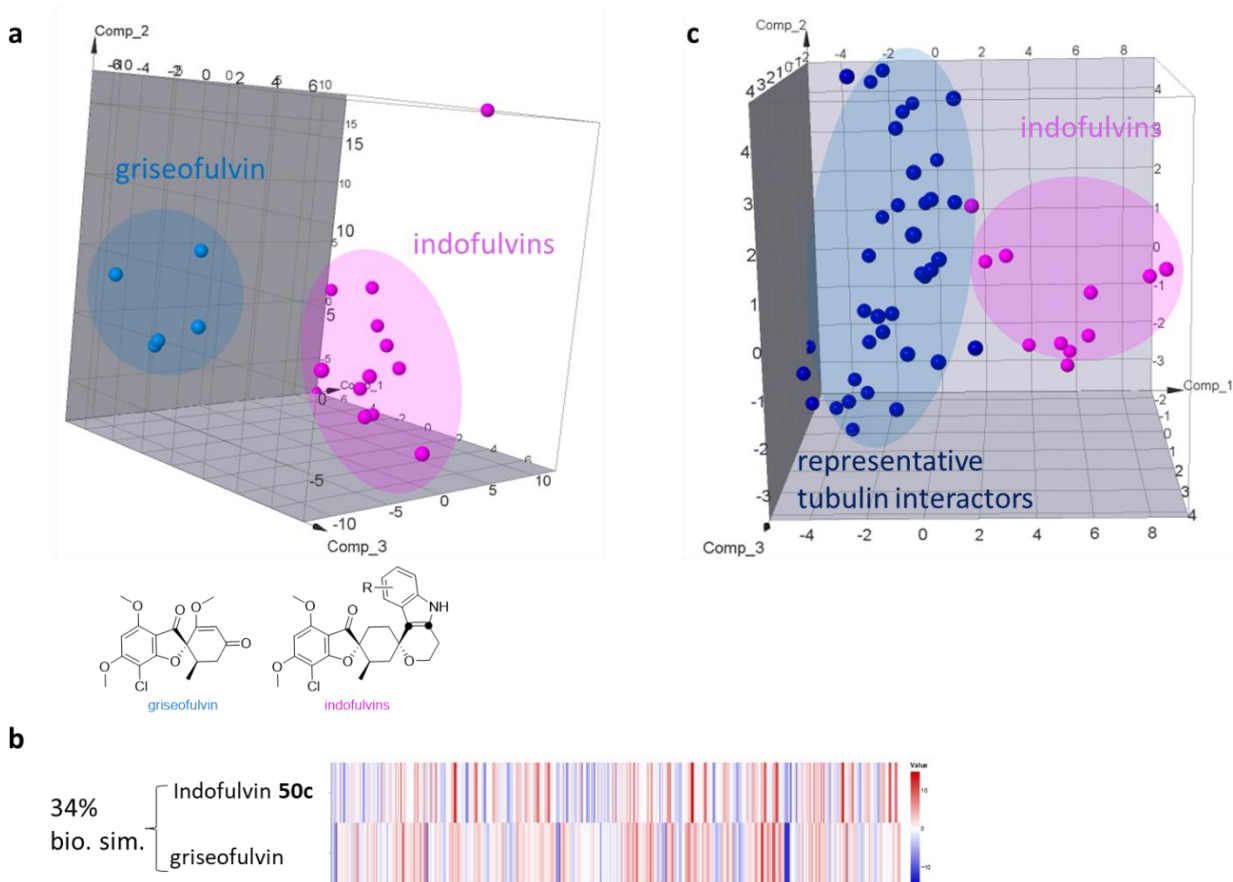


Figure 39: Morphological investigation of indofulvins regarding their parent NP bioactivity of tubulin binding. a) PCA plot of indofulvins and griseofulvin showed clear scaffold-dependent clustering. Induction window: 20-45, Expl. Var.: PC1 (69.2%), PC2 (12.7%), PC3 (5.6%). b) Morphological profile of indofulvin **50c** in comparison to griseofulvin with a biosimilarity of 34% representing differences between the two profiles. c) PCA plot of indofulvins and references with annotated tubulin interaction resulting in clear scaffold-dependent clusters. Induction window: 20-45%, Expl. Var.: PC1 (45.0%), PC2 (20.8%), PC3 (7.1%).

### 3.3.3. MORPHOLOGICAL PROFILING OF INDOLENINES

Similar to the indofulvins, the dearomatized indolenines are based on griseofulvin indoles that are derived from the Fischer indole reaction and can be compared to related compounds employing the cell painting assay. The indolenines are also bearing parts of the fragment-sized NP griseofulvin and are closely related to griseofulvin indole pseudo-NPs from which the product is derived. To investigate whether the  $\gamma$ -pyrone annulation results in a different bioactivity, the compound classes were analyzed on morphological level. The PCA plot of the indolenines in comparison to their direct parent molecules from the Fischer indole reaction revealed clear clusters (Figure 40). Although the compound classes showed no overlap, the compound classes shared compounds with higher biosimilarity, which is also represented by a MBP of 72%. In comparison to the griseofulvin indoles, the indolenines shared a higher intraclass similarity demonstrated by the less widespread cluster. Consequently, different substitutions on the indole might have a greater influence on the griseofulvin indoles than on the indolenines. Overall, the addition of the  $\gamma$ -pyrone fragment seems to have an influence on the bioactivity and appears to change the phenotypic profile compared to their aromatized starting materials.

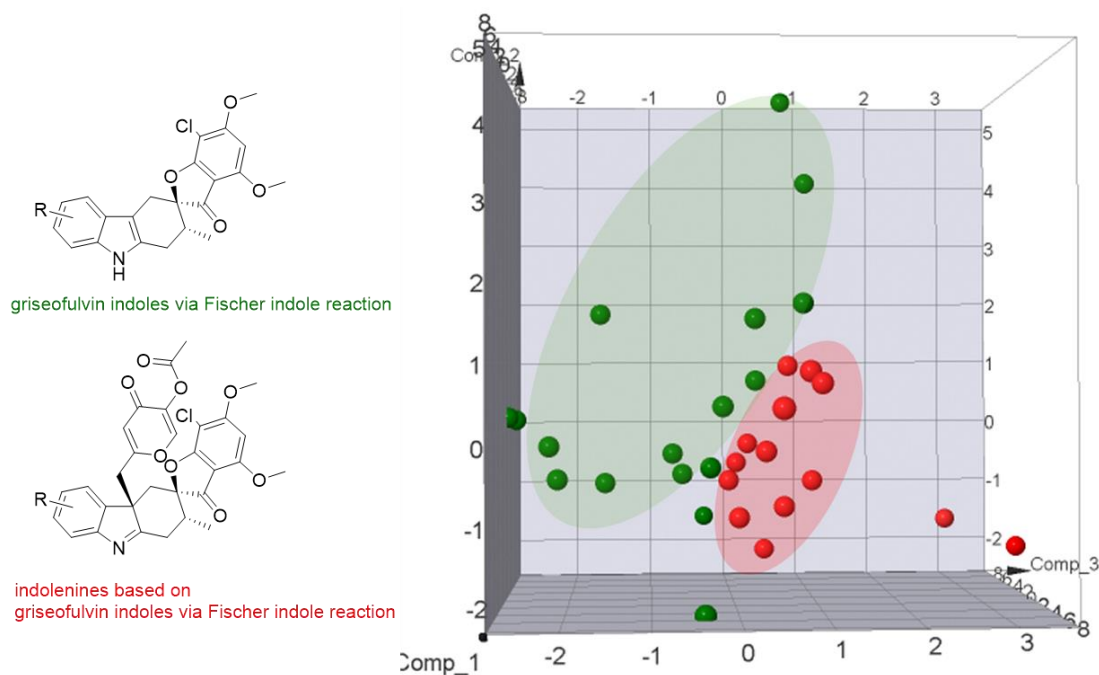


Figure 40: Comparison of the indolenines based on griseofulvin indoles via Fischer indole reaction (red) to their dearomatized starting materials (green) shows clear clusters in morphological profiling. Induction window: 20-45%, Expl. Var.: PC1 (56.5%), PC2 (10.6%), PC3 (7.7%).

## Results and Discussion

Moreover, the indofulvins have a significant part in common with the NP griseofulvin, which possesses annotated tubulin-binding activity. Morphological profiling enabled the investigation if next to their structural features the pseudo-NPs also share griseofulvin's bioactivity. The PCA plot indicated a compound class-dependent clustering with griseofulvin falling into the expected cluster of tubulin interactors (Figure 41). These phenotypic differences suggested a bioactivity that differs from an interference with tubulin. Thereby, not only the indofulvins, but also the indolenines derived from griseofulvin indoles seem to have lost their ability to bind tubulin.

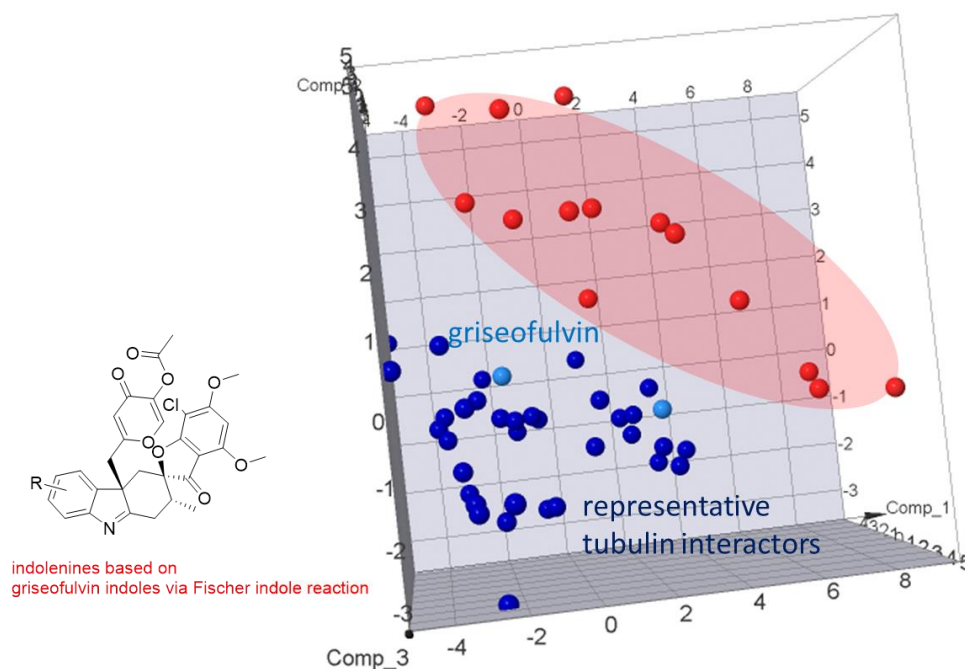


Figure 41: Comparison of the indolenines based on griseofulvin indoles via Fischer indole reaction (red) to griseofulvin and other references annotated with tubulin interaction activity indicates phenotypic differences between the compound classes. Induction window: 20-45%, Expl. Var.: PC1 (43.0%), PC2 (16.3%), PC3 (13.4%).

### 3.3.4. PSEUDO-NPs IN BIOLOGICAL SPACE

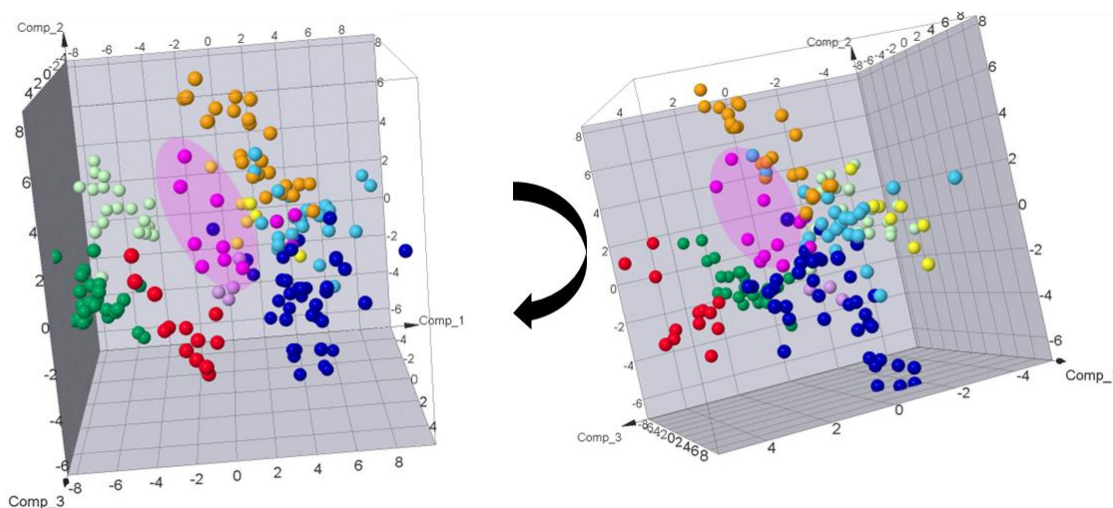
*The reference's target assignment and composition of relevant representations was performed by Dr. Slava Ziegler.*

The unprecedented scaffolds of pseudo-NP provide an opportunity to interact with new, currently maybe even unknown targets and thereby expand known biological space. The morphological profiling may give insights whether the pseudo-NPs share a phenotype with known references or occupy areas of biological space that are underexplored. Relevant representations with annotated bioactivities of eight pathways or targets serve as biological clusters<sup>[55]</sup> to determine and extent the pseudo-NPs relate. The PCA plot of the indofulvins in comparison to the references showed a complex cluster formation with differences in the range of distribution and a degree of overlapping between clusters (Figure 42a). For instance, representatives involved in the DNA synthesis formed a clear and isolated cluster, whereas references annotated with activity against histone deacetylases (HDAC) spread out more broadly and slightly overlapped with lysosomotropic compounds. The indofulvins formed a cluster that differs from the eight other clusters indicating a different bioactivity on morphological level. The PCA plot of the indolenines and the eight reference classes revealed a new cluster that is separated from the others and therefore could interact with other targets (Figure 42b).

Both pseudo-NP classes, the indofulvins and the indolenines, showed phenotypical differences to the eight reference clusters and occupy areas, which are not covered by their representatives. These results suggest that the pseudo-NPs may extend into new areas of the biological space.

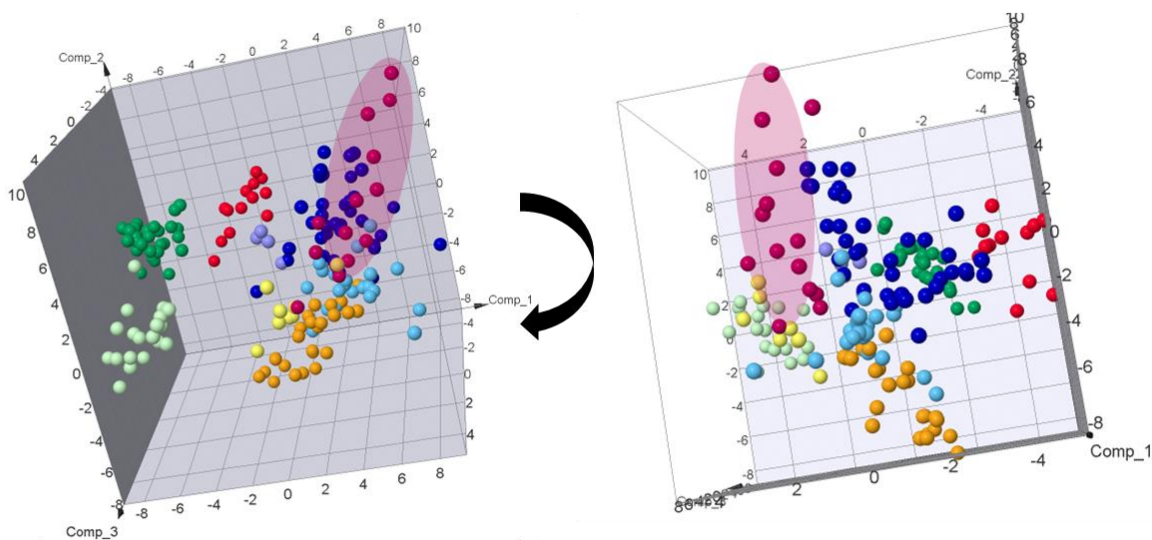
## Results and Discussion

**a**



AKT\_P13K\_MTOR Aurora DNA synth HDAC HSP90 Lysosomotrop Tubulin Uncopler indofulvins

**b**



AKT\_P13K\_MTOR Aurora DNA synth HDAC HSP90 Lysosomotrop Tubulin Uncopler indolenines

Figure 42: Comparison of morphological changes of pseudo-NPs to eight reference clusters. a) Indofulvins (pink) form a new cluster, which is not overlapping with the pathway-dependent clusters derived from the references. Induction window: 20-45%, Expl. Var.: PC1 (47.9%), PC2 (18.9%), PC3 (9.2%). b) Indolenines (dark red) build a cluster by extending into uncovered biological space. Induction window: 20-45, Expl. Var.: PC1 (50.1%), PC2 (21.7%), PC3 (7.3%).



In the context of a broad morphological investigation, different pseudo-NPs classes derived from the combination of the fragment-sized NPs griseofulvin, cinchona alkaloids, and sinomenine with indoles or chromanones,  $\beta$ -indofulvins acquired an exceptional position.<sup>[111]</sup> The plot of the interclass MBP over all compound classes showed the griseofulvin tetrahydropyrano indoles with remarkably low biosimilarities to the other pseudo-NPs classes (Figure 43). Whereas cinchona alkaloid indoles and chromanones (QD-C/I, QN-C/I), as well as sinomenine derivatives (S-C/I) shared relatively many phenotypic features, represented by high interclass MBP above 65%, the  $\beta$ -indofulvins had a biosimilarity of less than 11% to every other class. Even the intraclass MBP was relatively low at 44%, indicating a wide range of phenotypes and a major influence by different substitution on the indole on morphological level.

In summary, the connection of griseofulvin to indoles through Pictet-Spengler reaction appeared to generate interesting compound classes that show considerable differences to other references and pseudo-NP classes.

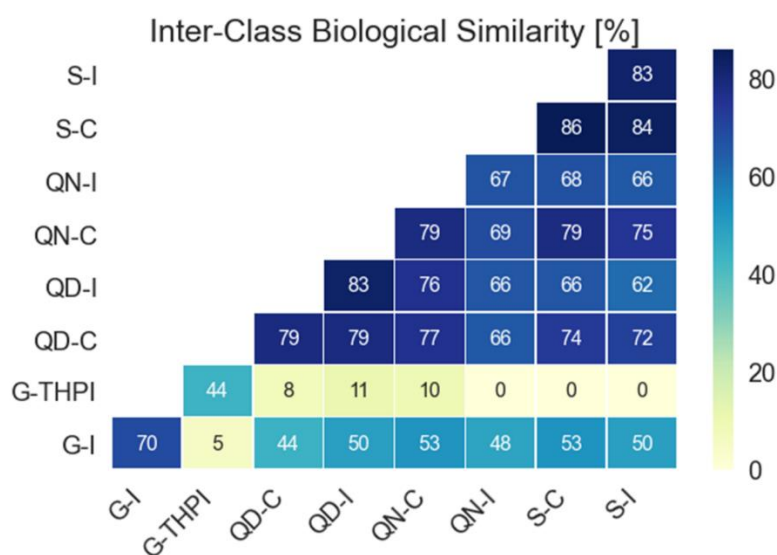


Figure 43: Inter-class biosimilarity of pseudo-NPs derived from the combination of fragment-sized NPs with indoles or chromanones. Induction: 15-45%; G-I: griseofulvin indoles derived from the Fischer indole reaction, G-THPI: indofulvins, QD-C: quinidine chromanones, QD-I: quinidine indoles, QN-C: quinine chromanones, QN-I: quinine indoles, S-C: sinomenine chromanones, S-I: sinomenine indoles.

### 3.3.5. MORPHOLOGICAL INVESTIGATION OF STRUCTURAL FEATURES

The cell painting assay proved to be a great tool in the exploration of the pseudo-NPs potential. While morphological profiling already suggested the parent fragment's bioactivity is lost upon combination with an indole or the indolenines, the influence of different structural features on the phenotype was investigated.

To examine the differences between two compound classes that have the same fragment combination but different fusion patterns, the griseofulvin indoles derived from the Pictet-Spengler and Fischer indole reaction were compared. Both pseudo-NPs share the griseofulvin and indole moiety. However, a connection via Pictet-Spengler reaction yields in spiro-fused compounds, whereas the Fischer indole reaction generates a direct connection via edge fusion.<sup>[20]</sup> The PCA of both compound classes revealed a clear clustering dependent on their connection type (Figure 44a). Therefore, a differentiation of the combination of the same fragment via different fusion pattern can be possible on morphological level.

Furthermore, a comparison of  $\beta$ - and  $\gamma$ -indofulvins might enlighten the role of different regioisomeric variants and allow a conclusion if structural differences like this can be relevant for the phenotype. The indofulvins differ in the indole orientation and showed in the PCA plot a clear separation depending on the regioisomeric variant (Figure 44b). Consequently, regioisomeric differences can have a great influence on the phenotype and might change them in a distinct direction. However, there are examples in the literature can be found including regioisomers from the Fischer indole reaction, where isomeric differences do not induce selective morphological changes.<sup>[111]</sup>

Furthermore, the role of fragments themselves were analyzed regarding their influence on the morphological profile, and this information was used for the design of future pseudo-NP libraries. NP fragments showing a major influence on the phenotype that are independent of fragment combination might not represent a preferred starting point for a biologically diverse compound collection. This may be especially important when fragment-sized NPs, including griseofulvin, which represent the biggest part of the pseudo-NP might have the potential to dominate the profile. As pseudo-NPs bearing griseofulvin could be influenced by the connection type and regioisomeric variants a dominance from the NP appears very unlikely. Additionally, the significant morphological difference upon fragment combination to the original NP indicates the potential to generate novel phenotypes with griseofulvin. To further investigate a potential fragment dominance, griseofulvin was compared with different smaller fragments' connections, namely indoles and indolenines, but sharing the griseofulvin NP.

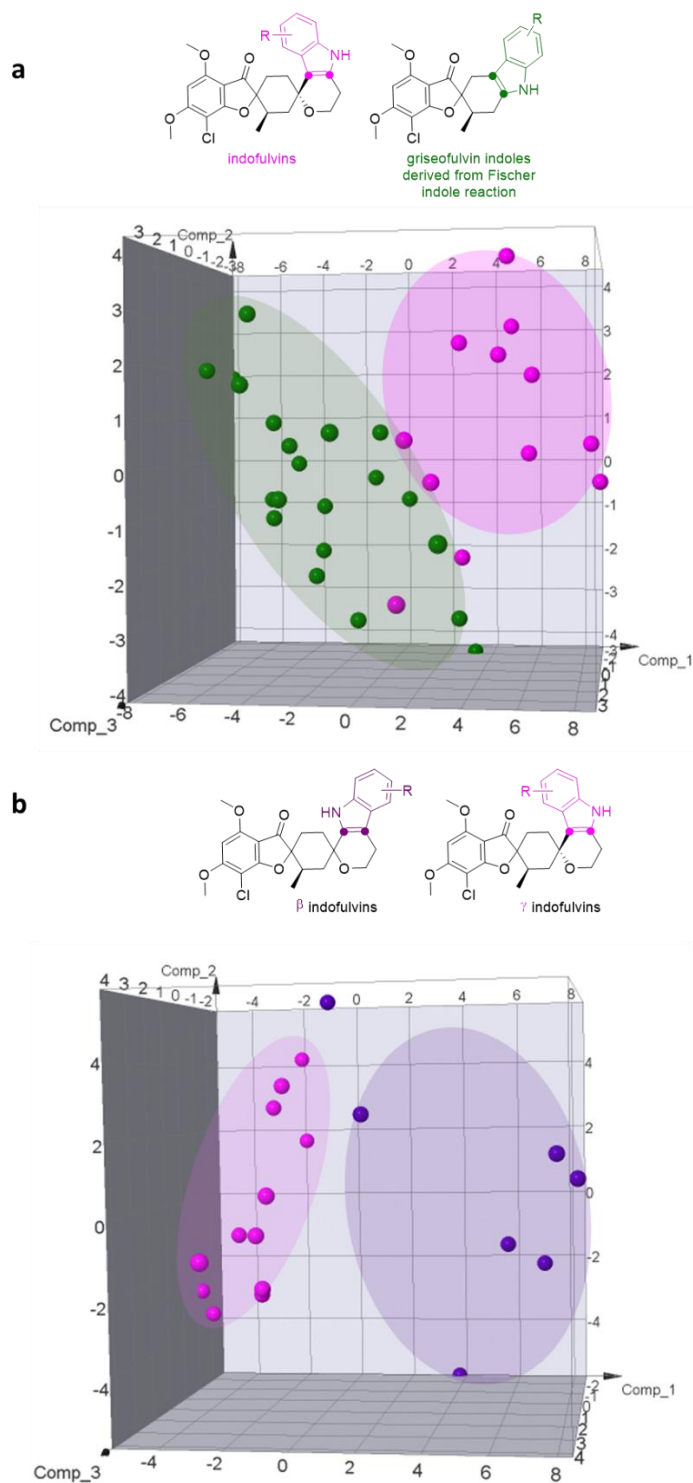


Figure 44: PCA plot of morphological profiles of pseudo-NP classes which differ in structural features. a) Differentiation of different connection types of the same fragments indicates fusion pattern-derived clustering. Induction window: 20-45%, Expl. Var.: PC1 (64.9%), PC2 (11.7%), PC3 (6.4%). b) Differentiation between regioisomeric variants  $\beta$ - and  $\gamma$ -indofulvins show selective morphological changes depending on the indole orientation. Induction window: 20-45, Expl. Var.: PC1 (53.1%), PC2 (23.7%), PC3 (8.5%).

## Results and Discussion

The PCA plot showed a clustering dependent on the fragment that is fused to griseofulvin (Figure 45a). The indoles differed from the indolenines and both pseudo-NP classes indicate significant morphological differences to griseofulvin itself suggesting, the phenotype derived from griseofulvin can be influenced and is therefore not dominating.

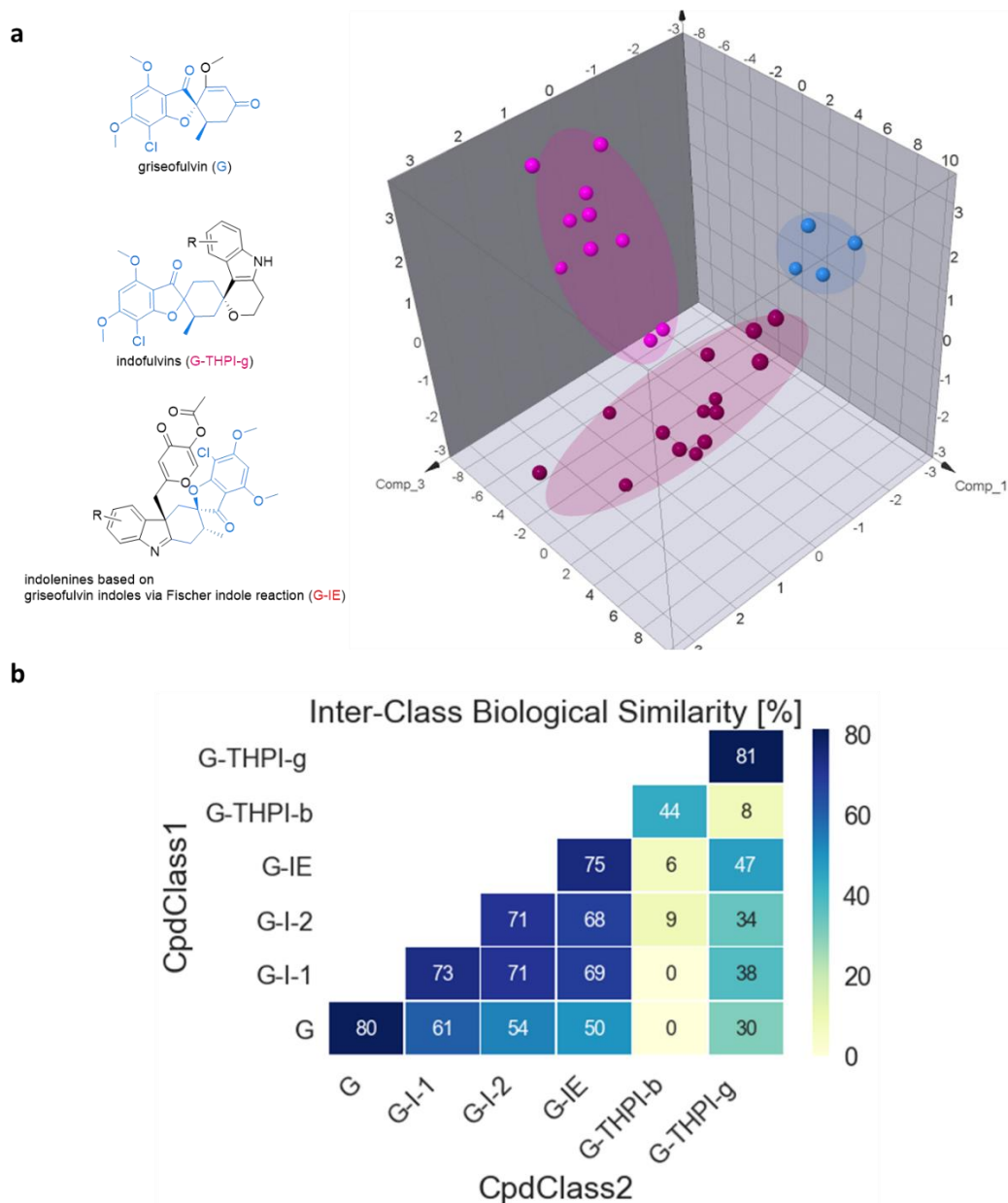


Figure 45: Morphological investigation of griseofulvin. a) PCA plot of griseofulvin containing compound classes indicate a morphological change that is not dominated by the griseofulvin fragment. Induction window: 20-45%, Expl. Var.: PC1 (67.9%), PC2 (10.1%), PC3 (5.8%). b) Inter-class biosimilarity of all griseofulvin containing classes. G= griseofulvin, G-I-1, G-I-2: griseofulvin indoles from the Fischer indole reaction, G-IE: griseofulvin indolenines, G-THPI-b, G-THPI-g: griseofulvin indoles from the Pictet-Spengler reaction.

The inter class biosimilarity of all griseofulvin containing classes including the NP itself is below 71% for all classes (Figure 45b), indicating no significant similarity on morphological level. The griseofulvin indoles derived from the Pictet-Spengler reaction in both regioisomeric variants (G-THPI-b and G-THPI-g) appeared to be particularly different from the other classes, sharing maximal 47% of the features. On the contrary, griseofulvin indoles from the Fischer indole reaction (G-I-1 and G-I-2) and the indolenines (G-IE) had more features in common and shared a biosimilarity of around 70%. The possibility to affect griseofulvin's morphological profile by the combination with different fragments which results in very different phenotypes, indicates the NP as non-dominating.

Furthermore, a potential influence by the indole fragment was investigated by comparing indole containing compound classes which are combined with completely different fragments including quinidine, sinomenine and griseofulvin. The PCA of the three compound classes revealed a clear clustering dependent on the second fragment (Figure 46a). Thereby, the indole fragment appears to be not dominating as its morphological profile can be changed by the combination with other fragments. On this basis, it was hypothesized that the combination of indole with a different fragment would generate a new cluster that differs from the other indole-containing classes. Compounds containing both chromanone and indole fragments (chromanone indoles) were synthesized and screened for their morphological changes in the cell painting assay. The comparison to all other indole containing compound classes revealed the generation of a novel phenotype that shares less than 65% with the other classes (Figure 46b). This correctly predicted dissimilarity of the non-dominating indole collection demonstrates the possibility of the cell painting assay as a tool for the design of phenotypically different compound collections.

## Results and Discussion

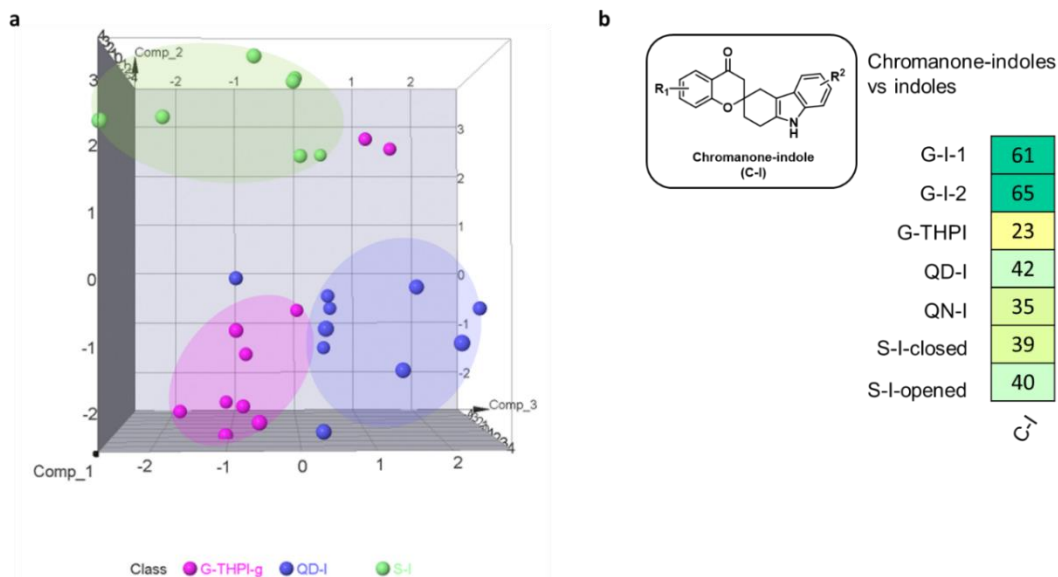


Figure 46: Morphological profiling of indole containing compound classes with the prediction of the novel chromanone indoles. a) PCA plot of indofulvins (pink), quinidine indoles (blue), and sinomenine indoles (green). Induction window: 20-45%, Expl. Var.: PC1 (39.7%), PC2 (25.2%), PC3 (8.4%). b) Interclass biosimilarity to the newly synthesized chromanone indoles confirmed the prediction of a new cluster with low biosimilarity to the other clusters.

Overall, the phenotype of the pseudo-NP collection appears to be dependent on several factors, including structural features. The combination of two fragments appeared to have a significant impact on the phenotype as for instance the biosimilarity of indofulvin **50c** to its parent NP griseofulvin drops to 34%. But the fusion itself is not the only important factor, the connection type, for instance for griseofulvin indoles derived from Pictet-Spengler or Fischer indole reaction, could also influence the morphological profile. Regioisomeric variations could also lead to differences on morphological level. An investigation for the fragment's dominance revealed that indoles and griseofulvin can be influenced by different fragment combinations and are therefore considered to be non-dominating. Employing non-dominating fragments in future pseudo-NP libraries may be beneficial for the coverage of a broad biological range. Sinomenine on the other side was reported<sup>[111]</sup> to have a great influence on the pseudo-NPs and thereby limiting the potential of addressing new targets. The cell painting assay could be used to characterize bioactivity in a broader cellular context and enable a biological differentiation of structurally related pseudo-NP classes. The potential to predict morphological trends of a new compound classes may prove to be a useful approach in the future.

## 4. SUMMARY

The optimization of the complexity-generating oxa-Pictet-Spengler reaction with cyclic ketones enabled the synthesis of a diverse pseudo-natural product (pseudo-NP) compound library by combining biosynthetically unrelated fragments. The developed procedure is operationally simple, safe, fast, and can be conducted under ambient conditions by employing an immobilized triflic acid (TfOH-SiO<sub>2</sub>) catalyst. The reaction was applicable to various aryl ethanol, including isomeric variants as the underdeveloped *iso*-oxa-Pictet-Spengler reaction. Even previously challenging cyclic ketone substrates reacted rapidly to provide access to a multifaceted spiro compound library (Figure 47). In this context, the extended (*iso*)-oxa-Pictet-Spengler reaction as synthetic methodology may spark the pharmaceutical industry to make and explore structures that were previously inaccessible.

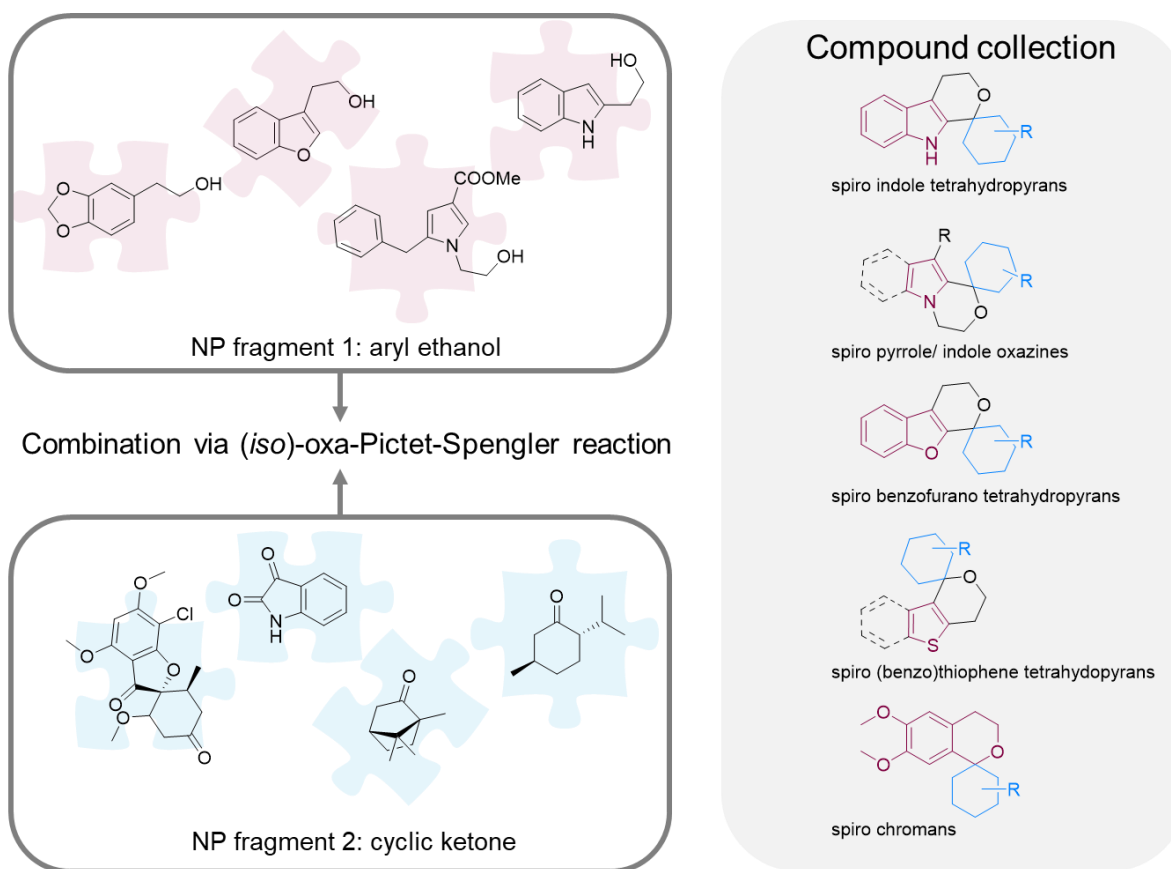


Figure 47: Summary of the compound collection derived from the (*iso*)-oxa-Pictet-Spengler reaction.

Cheminformatic analyses connected the compound collection with beneficial chemical properties including high three-dimensionality and drug-like features. An investigation of the NP-likeness-score classified the indofulvins in between natural products (NPs) and drugs, indicating shared characteristics with both of them.

## Summary

An even higher degree of complexity was achieved by the dearomatization of indole-containing pseudo-NP collections. The direct  $\gamma$ -pyrone annulation of oxa-Pictet-Spengler products and diverse griseofulvin indoles derived from the Fischer indole reaction provided access to highly three-dimensional indolenines. A subsequent reduction of the indolenines to indolines generated another new pseudo-NP class.

Biological investigations revealed that the pseudo-NP class of indofulvins exhibit a new chemotype of potent autophagy inhibitors. The most active representative showed a high biological similarity to oligomycin in morphological profiling, suggesting a similar mode-of-action by targeting mitochondrial respiration. Additional analyses identified an influence of indofulvins on the oxygen consumption rate (OCR) and extracellular acidification rate (ECAR), indicating a correlation between the inhibition of autophagy and mitochondrial respiration (Figure 48).

The pseudo-NP class of indofulvins showed new bioactivity compared to the parent NP griseofulvin. While griseofulvin does not affect the autophagy pathway, several indofulvins were found to be autophagy inhibitors. Additionally, griseofulvin interacts with tubulin whereas the pseudo-NPs neither affect tubulin polymerization nor increases mitotic arrest in cells. The differences were also shown by low morphological similarities in the Cell Painting Assay between the pseudo-NPs and the NP fragments from which they are derived. Consequently, the new bioactivity may be a result of the fusion of two unrelated NP fragments while the combination of fragments may also simultaneously diminish the native bioactivity of the individual fragments (Figure 48).

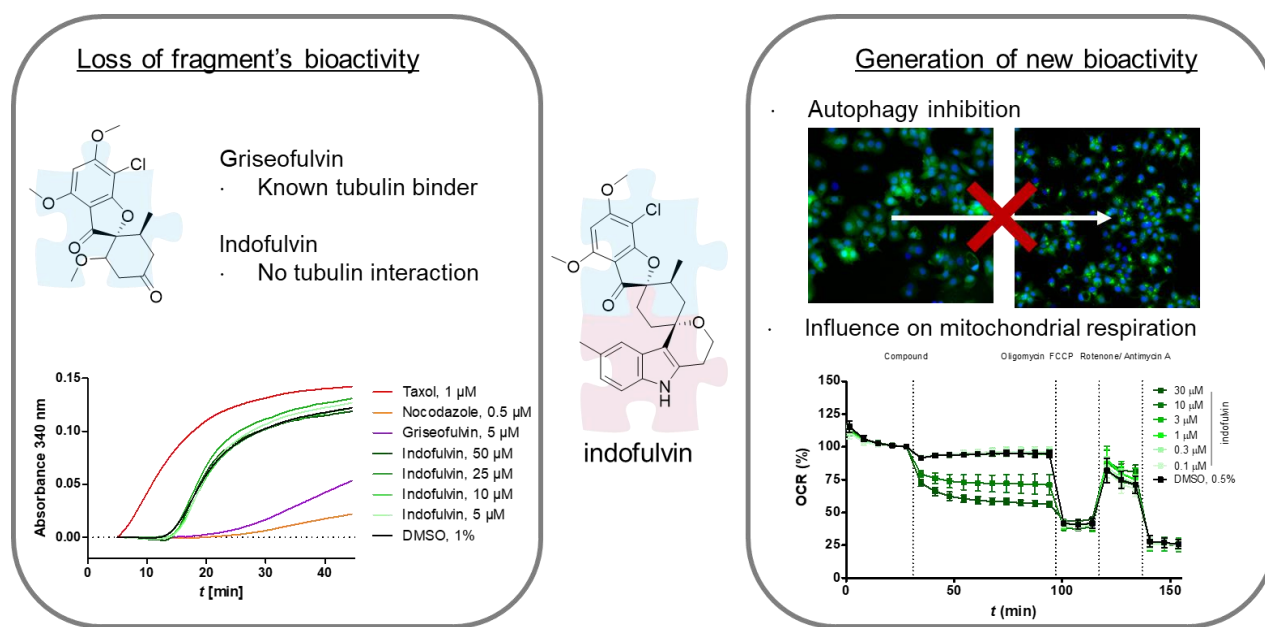


Figure 48: Summary of the biological effects of the pseudo-NP indofulvin.



Morphological profiling as unbiased analysis of bioactivity was employed to evaluate the compound library regarding relevant structural features. Chemical variations, including different connection types of the same fragments and regioisomers, can influence the phenotypic profiles to show scaffold-dependent clustering. Additionally, the role of fragments themselves were analyzed regarding their influence on the morphological profile and categorized as either phenotypically dominating fragments or suitable combination partners for novel bioactivity. On this basis, a newly pseudo-NP class was designed and correctly predicted to have novel biological profiles relative to the existing compound set.

These results provide a proof of principle for the pseudo-NP approach as an advanced design concept for bioactive small molecule libraries. The *de-novo* combination of NP fragments demonstrates the opportunity to overcome limitations of other approaches, for instance biology-oriented syntheses (BIOS). BIOS is restricted by the limited chemical space and retention of biological targets, whereas the pseudo-NPs not only extended the chemical space but also retain biological relevance without exhibiting similar bioactivity to the parent compound. In this context, the morphological profiling proved to be a valuable method for the unbiased evaluation of bioactivity, which resulted in target hypotheses and might also guide the design of future compound collections.

## 5. EXPERIMENTAL

### 5.1. MATERIALS FOR ORGANIC SYNTHESIS

All reactions with air or moisture sensitive reagents or intermediates were carried out under an argon atmosphere, and all the glassware was dried by heat gun under high vacuum prior to use. Commercial reagents were used without further purification. Dry solvents were received from Acros, Sigma Aldrich and VWR in anhydrous quality and used without any further purification. All other solvents or reagents were purified according to standard procedures or were used as received from Sigma Aldrich, Alfa Aesar, Acros, Fisher Scientific, Merck and TCI.

Qualitative thin-layer chromatography (TLC) was performed on silica coated aluminum plates (Merck 60 F254) and visualized by UV irradiation (254 nm) or potassium permanganate stain (1.5 g  $\text{KMnO}_4$ , 10 g  $\text{K}_2\text{CO}_3$ , 1.25 mL 10% aqueous NaOH solution and 200 mL  $\text{H}_2\text{O}$ ) with additional heating with a heat gun.

Analytical uHPLC-MS and LCMS was carried out on an Agilent 1290 Infinity system equipped followed by a mass detector (column: Zorbax Eclipse C18 Rapid Resolution 2.1x50 mm 1.8 $\mu\text{m}$ ).

Flash column chromatography was performed with silica gel from Acros Organics (40-65  $\mu\text{m}$ , 230-400 mesh) or using an automatic medium pressure liquid chromatography Reveleris® X2 Flash System (Büchi) and GraceResolve™ cartridges.

Preparative HPLC-MS was performed on an Agilent 1100 preparative HPLC system equipped with a mass detector (1100/LC/MSD VL, Agilent Series) with a C18 column (Nucleodur C18 gravity VP 125/10 5  $\mu\text{m}$ , Nucleodur C18 gravity VP 125/21 5  $\mu\text{m}$ , Nucleodur C4 gravity VP 125/10 5  $\mu\text{m}$ ).

NMR samples were measured on Bruker AV 400 Avance III HD (NanoBay), Agilent Technologies DD2, Bruker AV 500 Avance III HD (Prodigy), Bruker AV 600 Avance III HD (CryoProbe) or Bruker AV 700 Avance III HD (CryoProbe) spectrometers. The detected data from the spectra was reported in ppm in relation to a deuterated solvent ( $\text{CDCl}_3$ = 7.26, 77.16 ppm;  $\text{DMSO-d}_6$ = 2.50, 39.52 ppm;  $\text{MeOH-d}_4$ = 3.31, 49.00 ppm). 2D NMR correlations, including  $^1\text{H}/^1\text{H}$  COSY,  $^1\text{H}/^1\text{H}$  NOESY,  $^1\text{H}/^{13}\text{C}$  HSQC,  $^1\text{H}/^{13}\text{C}$  HMBC, were applied for the assignment of the signals.

HR-MS spectra were recorded on a LTQ Orbitrap mass spectrometer coupled to an Accela HPLC-System (HPLC column= Hypersyl GOLD, 50 mm x 1 mm, particle size 1.9  $\mu\text{m}$ , ionization method= electron spray ionization (ESI)).

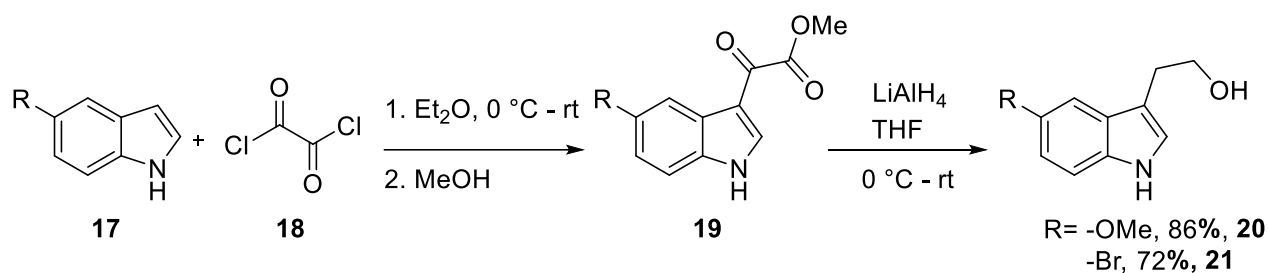
Microwave reactions were performed on a CEM Discover SP Activent device.

## 5.2. CHEMICAL SYNTHESIS

### 5.2.1. $\beta$ -ARYL ETHANOL STARTING MATERIALS

#### TRYPTOPHOL DERIVATIVES

General procedure A: Synthesis of 3-indolyethanol derivatives

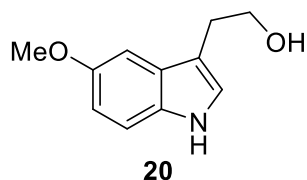


Indole **17** (10 mmol, 1 eq.) was dissolved in dry ethyl ether (50 mL) and oxalyl chloride (2.7 mL, 30 mmol, 3 eq.) was added dropwise at 0 °C. The reaction mixture is allowed to warm up to room temperature and stirred for 6 h. After quenching the reaction mixture with methanol (2 mL, 50 mmol, 5 eq.), the crude mixture was filtered over celite, washed with cold ethyl ether and directly used in the next step without further purification.

The methyl 2-(1H-indol-3-yl)-2-oxoacetate derivative was dissolved in THF (20 mL) and carefully added to a suspension of LiAlH<sub>4</sub> (1.52 g, 40 mmol, 4 eq.) in THF (40 mL) at 0 °C. After stirring at 80 °C for 2 h, the reaction mixture was quenched with water (1.5 mL), aqueous NaOH (10%, 3 mL) and water (4.5 mL) at 0 °C. The solution was filtered and washed with ethyl acetate (2x, 15 mL). After combining the organic layers, drying and concentrating the crude mixture *in vacuo*, the product was purified via flash column chromatography (EtOAc in CycHex).

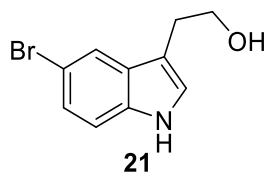
## Experimental

### 2-(5-methoxy-1*H*-indol-3-yl)ethan-1-ol **20**



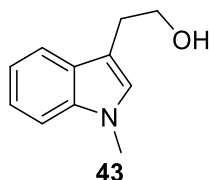
1.65 g, 86%. **<sup>1</sup>H NMR** (400 MHz, Chloroform-*d*)  $\delta$  7.98 (s, 1H), 7.30-7.21 (m, 1H), 7.06 (d,  $J = 2.2$  Hz, 2H), 6.88 (ddt,  $J = 8.8, 2.4, 0.4$  Hz, 1H), 3.89 (t,  $J = 6.7$  Hz, 2H) – 3.87 (s, 3H), 3.01 (t,  $J = 6.7$  Hz, 2H) ppm. **<sup>13</sup>C NMR** (101 MHz, Chloroform-*d*)  $\delta$  154.3, 123.5, 112.7, 112.2, 100.9, 77.6, 77.2, 76.9, 62.8, 56.2, 29.0 ppm. **HRMS-ESI** ( $m/z$ ):  $[M + H]^+$  calculated for  $C_{11}H_{13}O_2N^+$  192.0946; found 192.0945.

### 2-(5-bromo-1*H*-indol-3-yl)ethan-1-ol **21**



1.72 g, 72%. **<sup>1</sup>H NMR** (600 MHz, Chloroform-*d*)  $\delta$  8.19 (s, 1H), 7.77 (d,  $J = 1.9$  Hz, 1H), 7.30 (dd,  $J = 8.6, 1.9$  Hz, 1H), 7.25 (d,  $J = 8.6$  Hz, 1H), 7.10 (d,  $J = 2.3$  Hz, 1H), 3.91 (t,  $J = 6.4$  Hz, 2H), 3.00 (td,  $J = 6.4, 0.8$  Hz, 2H) ppm. **<sup>13</sup>C NMR** (151 MHz, Chloroform-*d*)  $\delta$  135.3, 129.6, 125.4, 124.0, 121.8, 113.1, 113.0, 112.5, 62.9, 28.9 ppm. **HRMS-ESI** ( $m/z$ ):  $[M + H]^+$  calculated for  $C_{10}H_{10}ONBr^+$  239.9946 and 241.9925, found 239.9941 and 241.9920.

### 2-(1-methyl-1*H*-indol-3-yl)ethan-1-ol **43**



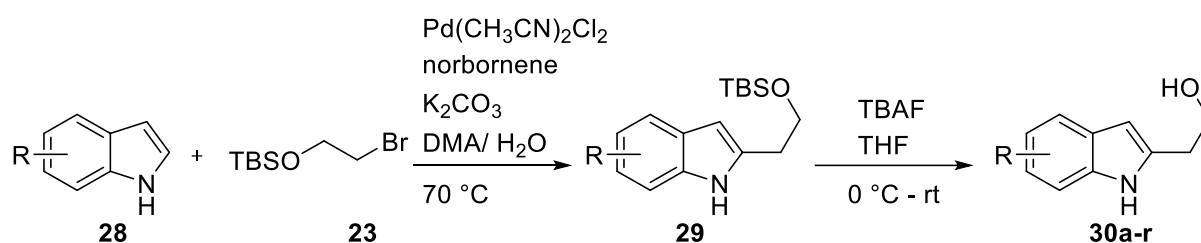
To a solution of tryptophol **12** (1.5 g, 9.31 mmol, 1 eq.) in DCM (25 mL), tetrabutyl ammonium bisulfate (0.28 g, 0.83 mmol, 0.09 eq.) and potassium hydroxide solution (50%, 1.25 mL) were added. After stirring for 5 min, methyl iodide (0.7 g, 11.06 mmol, 1.2 eq.) was added and the resulting mixture was stirred for another 24 h. Sat.  $NH_4Cl$  (25 mL) was added and the aqueous phase was extracted with DCM (3x, 30 mL). After combining the organic phases, drying over  $Na_2SO_4$  and concentration under reduced pressure, the crude reaction mixture was purified via

flash column chromatography (EtOAc in CycHex) to give the desired product as a white solid (1.22 g, 75%).

**<sup>1</sup>H NMR** (600 MHz, Chloroform-*d*)  $\delta$  7.62 (d, *J* = 7.9 Hz, 1H), 7.32 (d, *J* = 8.2 Hz, 1H), 7.24 (d, *J* = 7.2 Hz, 1H), 7.13 (t, *J* = 7.8 Hz, 1H), 6.95 (s, 1H), 3.90 (t, *J* = 6.3 Hz, 2H), 3.77 (s, 3H), 3.03 (t, *J* = 6.3 Hz, 2H) ppm. **<sup>13</sup>C NMR** (151 MHz, Chloroform-*d*)  $\delta$  137.5, 128.2, 127.7, 122.1, 119.3, 119.3, 111.0, 109.6, 63.1, 33.0, 29.0 ppm. **HRMS-ESI** (*m/z*): [M + H]<sup>+</sup> calculated for C<sub>11</sub>H<sub>13</sub>ON<sup>+</sup> 176.0997; found 176.0995.

## 2-INDOLYLETHANOL DERIVATIVES

General procedure B: Synthesis of 2-indolylethanol derivatives

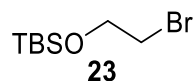


Indole **28** (1 eq.), norbornene (1.61 g, 0.02 mol, 2 eq.), potassium carbonate (2.36 g, 0.02 mol, 2 eq.), palladium(II) chloride diacetonitrile complex (0.22 g, 0.85 mmol, 10 mol%) and a solution of dimethylacetamide (11.2 mL) and water (0.1 mL) was added to a three-neck flask. The resulting reaction mixture was briefly evacuated and backfilled with argon (3x) and (2-bromoethoxy)(*tert*-butyl)dimethylsilane **23** (1.83 mL, 0.01 mol, 1 eq.) was added. The mixture was heated to 70 °C and stirred for 20 h under argon. After completion, the solution was cooled to room temperature and diethyl ether (150 mL) was added. The mixture was filtrated, dried over MgSO<sub>4</sub> and concentrated *in vacuo* with the water bath set to 70 °C. The product **29** was purified via flash column chromatography and directly submitted to the next step.

The TBS-protected 2-indolylethanol **29** (1 eq.) was dissolved in dry THF (0.1 M) and cooled to 0 °C. After adding TBAF in THF (1 M, 12 mL, 2.5 eq.) dropwise, the solution was stirred until completion (rt, 4 h). Aqueous NaHCO<sub>3</sub> (10 mL) was added and the aqueous phase was extracted with ethyl acetate (5x, 15 mL). After the organic phases were combined, dried over MgSO<sub>4</sub> and concentrated, the products **30a-r** were purified via flash column chromatography (EtOAc in CycHex).

## Experimental

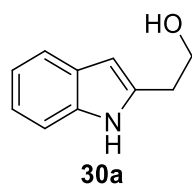
### (2-bromoethoxy)(*tert*-butyl)dimethylsilane **23**



Bromoethanol (2.84 mL, 40 mmol, 1 eq.) and imidazole (5.45 g, 80 mmol, 2 eq.) were dissolved in DMF (50 mL). After *tert*-butyldimethylsilyl chlorid (6.03 g, 40 mmol, 1 eq.) was added, the resulting mixture was stirred (rt, 2 h). The solution was washed with sat. NaCl and subsequently extracted with dichloromethane (3x, 20 mL). The combined organic layers were dried over Na<sub>2</sub>SO<sub>4</sub> and concentrated to give the desired product **23** as a colorless liquid (8.56 g, 90%).

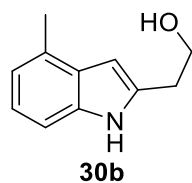
**<sup>1</sup>H NMR** (400 MHz, Chloroform-*d*)  $\delta$  3.80 (dd,  $J$  = 6.4 Hz, 2H), 3.31 (t,  $J$  = 6.5 Hz, 2H), 0.82 (s, 9H), 0.02 (s, 5H) ppm. **<sup>13</sup>C NMR** (151 MHz, Chloroform-*d*)  $\delta$  69.2, 32.0, 30.6, 25.9, 0.01 ppm. **HRMS-ESI** ( $m/z$ ): [M + H]<sup>+</sup> calculated for C<sub>8</sub>H<sub>19</sub>BrOSi<sup>+</sup> 239.0389 and 241.0368 ; found 239.0386 and 241.0367.

### 2-(1*H*-indol-2-yl)ethan-1-ol **30a**



682 mg, 81%. **<sup>1</sup>H NMR** (400 MHz, Chloroform-*d*)  $\delta$  8.35 (s, 1H), 7.47 (ddt,  $J$  = 7.7, 1.5, 0.8 Hz, 1H), 7.25 (dq,  $J$  = 8.0, 0.9 Hz, 1H), 7.15 – 6.95 (m, 2H), 6.22 (dq,  $J$  = 1.8, 0.9 Hz, 1H), 3.90 (t,  $J$  = 5.8 Hz, 2H), 2.94 (td,  $J$  = 5.8, 0.8 Hz, 2H) ppm. **<sup>13</sup>C NMR** (176 MHz, Chloroform-*d*)  $\delta$  137.24, 136.29, 128.72, 121.43, 120.08, 119.88, 110.93, 100.26, 77.52, 77.34, 77.16, 62.21, 31.35 ppm. **HRMS-ESI** ( $m/z$ ): [M + H]<sup>+</sup> calculated for C<sub>10</sub>H<sub>11</sub>NO<sup>+</sup> 162.0841; found 162.0841.

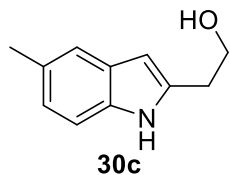
### 2-(4-methyl-1*H*-indol-2-yl)ethan-1-ol **30b**



281 mg, 67%. **<sup>1</sup>H NMR** (600 MHz, Chloroform-*d*)  $\delta$  8.42 (s, 1H), 7.17 (d,  $J$  = 8.1 Hz, 1H), 7.05 (t,  $J$  = 7.6 Hz, 1H), 6.88 (d,  $J$  = 7.1 Hz, 1H), 6.31 (s, 1H), 3.97 (t,  $J$  = 5.8 Hz, 2H), 3.03 (t,  $J$  = 5.8 Hz, 2H), 2.53 (s, 3H) ppm. **<sup>13</sup>C NMR** (151 MHz, Chloroform-*d*)  $\delta$  136.4, 135.9, 129.5, 128.5, 121.6,

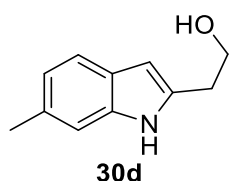
120.0, 108.3, 99.0, 62.5, 31.4, 18.9 ppm. **HRMS-ESI** ( $m/z$ ):  $[M + H]^+$  calculated for  $C_{11}H_{13}NO^+$  176.0997; found 176.0996.

2-(5-methyl-1*H*-indol-2-yl)ethan-1-ol **30c**



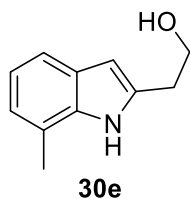
775 mg, 79%. **<sup>1</sup>H NMR** (700 MHz, Chloroform-*d*)  $\delta$  8.31 (s, 1H), 7.34 (s, 1H), 7.20 (d,  $J = 8.2$  Hz, 1H), 6.97 (d,  $J = 8.1$  Hz, 1H), 6.21 (s, 1H), 3.93 (t,  $J = 5.8$  Hz, 2H), 2.98 (t,  $J = 5.8$  Hz, 2H), 2.44 (s, 3H) ppm. **<sup>13</sup>C NMR** (176 MHz, Chloroform-*d*)  $\delta$  137.3, 134.7, 129.2, 129.1, 123.1, 119.9, 110.5, 100.1, 62.6, 31.6, 21.8 ppm. **HRMS-ESI** ( $m/z$ ):  $[M + H]^+$  calculated for  $C_{11}H_{13}NO^+$  176.0997; found 176.0995.

2-(6-methyl-1*H*-indol-2-yl)ethan-1-ol **30d**



592 mg, 74%. **<sup>1</sup>H NMR** (400 MHz, Chloroform-*d*)  $\delta$  8.25 (s, 1H), 7.43 (d,  $J = 8.0$  Hz, 1H), 7.11 (dq,  $J = 1.6, 0.8$  Hz, 1H), 6.93 (ddt,  $J = 8.0, 1.5, 0.6$  Hz, 1H), 6.24 (dd,  $J = 2.1, 1.0$  Hz, 1H), 4.04 – 3.80 (m, 2H), 2.97 (t,  $J = 5.8$  Hz, 2H), 2.46 (t,  $J = 0.7$  Hz, 3H) ppm. **<sup>13</sup>C NMR** (151 MHz Chloroform-*d*)  $\delta$  136.1, 128.5, 123.1, 122.3, 120.3, 119.4, 118.0, 101.2, 62.8, 31.7, 17.1 ppm. **HRMS-ESI** ( $m/z$ ):  $[M + H]^+$  calculated for  $C_{11}H_{13}NO^+$  176.0997; found 176.0995.

2-(7-methyl-1*H*-indol-2-yl)ethan-1-ol **30e**



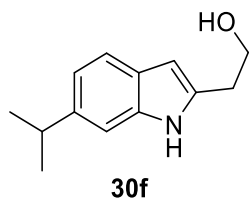
468 mg, 78%. **<sup>1</sup>H NMR** (400 MHz, Chloroform-*d*)  $\delta$  8.32 (s, 1H), 7.40 (ddt,  $J = 7.8, 1.3, 0.7$  Hz, 1H), 7.07 – 6.97 (m, 1H), 6.94 (dp,  $J = 7.1, 0.9$  Hz, 1H), 6.31 (dt,  $J = 2.1, 0.8$  Hz, 1H), 3.98 (t,  $J = 5.2$  Hz, 2H), 3.04 (td,  $J = 5.8, 0.8$  Hz, 2H), 2.56 – 2.40 (m, 3H) ppm. **<sup>13</sup>C NMR** (151 MHz,

## Experimental

Chloroform-*d*  $\delta$  136.2, 133.6, 129.2, 123.1, 120.5, 120.1, 117.9, 99.2, 61.7, 30.1, 16.4 ppm.

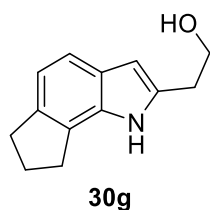
**HRMS-ESI** ( $m/z$ ):  $[M + H]^+$  calculated for  $C_{11}H_{13}NO^+$  176.0997; found 176.0992.

### 2-(6-isopropyl-1*H*-indol-2-yl)ethan-1-ol **30f**



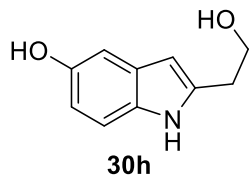
397 mg, 80%.  **$^1H$  NMR** (500 MHz, Chloroform-*d*)  $\delta$  8.57 (s, 1H), 7.58 (d,  $J = 8.2$  Hz, 1H), 7.24 (d,  $J = 1.6$  Hz, 1H), 7.13 (d,  $J = 8.2$  Hz, 1H), 6.30 (d,  $J = 2.3$  Hz, 1H), 3.86 (t,  $J = 6.1$  Hz, 2H), 3.22 – 3.05 (m, 1H), 2.96 – 2.88 (m, 3H), 1.46 – 1.41 (m, 6H) ppm.  **$^{13}C$  NMR** (126 MHz, Chloroform-*d*)  $\delta$  142.61, 136.86, 136.72, 126.90, 119.77, 119.14, 108.23, 99.93, 62.28, 34.60, 31.50, 27.20, 24.86 ppm. **HRMS-ESI** ( $m/z$ ):  $[M + H]^+$  calculated for  $C_{13}H_{17}NO^+$  204.1310; found 204.1310.

### 2-(1,6,7,8-tetrahydrocyclopenta[*g*]indol-2-yl)ethan-1-ol **30g**



232 mg, 74%.  **$^1H$  NMR** (700 MHz, Chloroform-*d*)  $\delta$  8.37 (s, 1H), 7.44 (d,  $J = 8.0$  Hz, 1H), 7.10 (dd,  $J = 8.0, 2.5$  Hz, 1H), 6.33 (d,  $J = 2.2$  Hz, 1H), 3.90 (t,  $J = 6.0$  Hz, 2H), 3.09 (dt,  $J = 23.4, 7.4$  Hz, 4H), 2.96 (t,  $J = 6.0$  Hz, 2H), 2.27 (p,  $J = 7.3$  Hz, 2H) ppm.  **$^{13}C$  NMR** (176 MHz, Chloroform-*d*)  $\delta$  137.98, 136.20, 133.51, 127.33, 125.23, 118.07, 116.79, 100.91, 77.52, 77.34, 77.16, 62.47, 33.33, 31.54, 30.16, 25.73 ppm. **HRMS-ESI** ( $m/z$ ):  $[M + H]^+$  calculated for  $C_{13}H_{15}NO^+$  202.1154; found 202.1152.

### 2-(2-hydroxyethyl)-1*H*-indol-5-ol **30h**

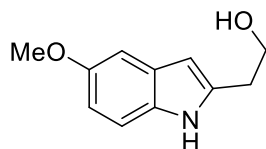


172 mg, 67%.  **$^1H$  NMR** (700 MHz, Methanol-*d*<sub>4</sub>)  $\delta$  7.11 (d,  $J = 8.6$  Hz, 1H), 6.84 (d,  $J = 2.4$  Hz, 1H), 6.60 (dd,  $J = 8.6, 2.4$  Hz, 1H), 6.07 (s, 1H), 4.12 (q,  $J = 7.1$  Hz, 1H), 3.87 (t,  $J = 7.1$  Hz, 2H),



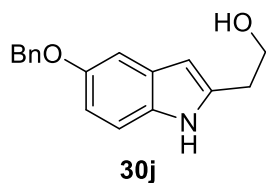
2.98 – 2.92 (m, 2H), 2.04 (s, 1H), 1.26 (t,  $J = 7.1$  Hz, 1H) ppm.  $^{13}\text{C NMR}$  (176 MHz, Methanol- $d_4$ )  $\delta$  151.6, 139.2, 133.2, 131.3, 112.2, 111.5, 105.2, 100.2, 63.0, 33.1 ppm. **HRMS-ESI** ( $m/z$ ):  $[\text{M} + \text{H}]^+$  calculated for  $\text{C}_{10}\text{H}_{11}\text{NO}_2^+$  178.0790; found 178.0790.

2-(5-methoxy-1*H*-indol-2-yl)ethan-1-ol **30i**



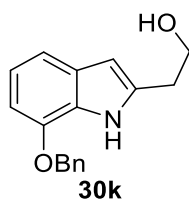
355 mg, 83%.  $^1\text{H NMR}$  (700 MHz, Chloroform- $d$ )  $\delta$  8.33 (s, 1H), 7.20 (d,  $J = 8.7$  Hz, 1H), 7.02 (d,  $J = 2.3$  Hz, 1H), 6.80 (dd,  $J = 8.7, 2.3$  Hz, 1H), 6.22 (s, 1H), 3.95 (t,  $J = 5.8$  Hz, 2H), 3.84 (s, 3H), 2.99 (t,  $J = 5.8$  Hz, 2H) ppm.  $^{13}\text{C NMR}$  (176 MHz, Chloroform- $d$ )  $\delta$  154.5, 138.1, 131.6, 129.3, 111.6, 102.3, 100.5, 62.6, 56.2, 31.6, 27.2 ppm. **HRMS-ESI** ( $m/z$ ):  $[\text{M} + \text{H}]^+$  calculated for  $\text{C}_{11}\text{H}_{13}\text{NO}_2^+$  192.0946; found 192.0945.

2-(5-(benzyloxy)-1*H*-indol-2-yl)ethan-1-ol **30j**



291 mg, 85%.  $^1\text{H NMR}$  (700 MHz, Chloroform- $d$ )  $\delta$  8.33 (s, 1H), 7.47 (d,  $J = 7.5$  Hz, 2H), 7.38 (t,  $J = 7.5$  Hz, 2H), 7.31 (t,  $J = 7.5$  Hz, 1H), 7.21 (d,  $J = 8.7$  Hz, 1H), 7.10 (d,  $J = 2.3$  Hz, 1H), 6.88 (dd,  $J = 8.7, 2.3$  Hz, 1H), 6.21 (s, 1H), 5.10 (s, 2H), 3.95 (t,  $J = 5.8$  Hz, 2H), 2.99 (t,  $J = 5.8$  Hz, 2H) ppm.  $^{13}\text{C NMR}$  (176 MHz, Chloroform- $d$ )  $\delta$  152.3, 136.8, 136.8, 130.4, 127.9, 127.5, 126.7, 126.5, 111.0, 110.2, 102.7, 99.2, 70.0, 30.3, 25.9 ppm. **HRMS-ESI** ( $m/z$ ):  $[\text{M} + \text{H}]^+$  calculated for  $\text{C}_{17}\text{H}_{17}\text{NO}_2^+$  268.1259; found 268.1255.

2-(7-(benzyloxy)-1*H*-indol-2-yl)ethan-1-ol **30k**

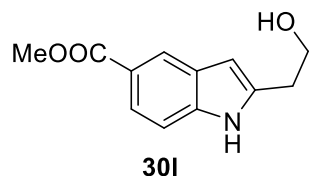


355 mg, 76%.  $^1\text{H NMR}$  (700 MHz, Chloroform- $d$ )  $\delta$  8.65 (s, 1H), 7.51 – 7.47 (m, 2H), 7.44 – 7.39 (m, 2H), 7.39 – 7.36 (m, 1H), 7.20 (d,  $J = 7.9$  Hz, 1H), 7.00 (t,  $J = 7.8$  Hz, 1H), 6.69 (d,  $J = 7.7$  Hz,

## Experimental

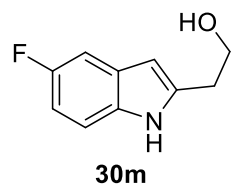
1H), 6.29 – 6.26 (m, 1H), 5.19 (s, 2H), 3.84 (ddt,  $J = 6.0, 3.1, 1.6$  Hz, 2H), 2.94 – 2.89 (m, 2H) ppm.  $^{13}\text{C}$  NMR (176 MHz, Chloroform-*d*)  $\delta$  145.04, 137.23, 136.48, 130.14, 128.73, 128.25, 128.05, 126.69, 120.09, 113.13, 102.78, 100.80, 77.34, 77.16, 76.98, 70.35, 62.19, 31.41. **HRMS-ESI** ( $m/z$ ):  $[\text{M} + \text{H}]^+$  calculated for  $\text{C}_{17}\text{H}_{17}\text{NO}_2^+$  268.1259; found 268.1256.

methyl 2-(2-hydroxyethyl)-1*H*-indole-5-carboxylate **30l**



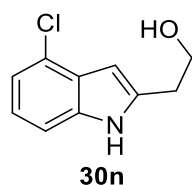
61 mg, 23%.  $^1\text{H}$  NMR (500 MHz, Chloroform-*d*)  $\delta$  8.82 (s, 1H), 8.30 (s, 1H), 7.83 (s, 1H), 7.32 (s, 1H), 6.36 (s, 1H), 4.00 (s, 2H), 3.92 (s, 3H), 3.03 (s, 2H) ppm.  $^{13}\text{C}$  NMR (126 MHz, Chloroform-*d*)  $\delta$  168.8, 139.3, 139.1, 128.4, 123.2, 123.1, 122.0, 110.6, 101.8, 62.6, 52.2 ppm. **HRMS-ESI** ( $m/z$ ):  $[\text{M} + \text{H}]^+$  calculated for  $\text{C}_{12}\text{H}_{13}\text{NO}_3^+$  220.0895; found 220.0895.

2-(5-fluoro-1*H*-indol-2-yl)ethan-1-ol **30m**



310 mg, 71%.  $^1\text{H}$  NMR (700 MHz, Chloroform-*d*)  $\delta$  7.22 (dd,  $J = 8.7, 4.4$  Hz, 1H), 7.18 (dd,  $J = 9.6, 2.4$  Hz, 1H), 6.87 (td,  $J = 9.1, 2.5$  Hz, 1H), 6.25 (s, 1H), 3.99 (t,  $J = 5.7$  Hz, 2H), 3.01 (t,  $J = 5.7$  Hz, 2H) ppm.  $^{13}\text{C}$  NMR (176 MHz, Chloroform-*d*)  $\delta$  158.9, 139.4, 132.9, 129.2, 111.4, 109.8, 105.1, 100.8, 62.6, 31.5 ppm. **HRMS-ESI** ( $m/z$ ):  $[\text{M} + \text{H}]^+$  calculated for  $\text{C}_{10}\text{H}_{10}\text{FNO}^+$  180.0746; found 180.0744.

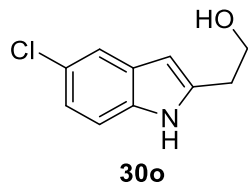
2-(4-chloro-1*H*-indol-2-yl)ethan-1-ol **30n**



129 mg, 56%.  $^1\text{H}$  NMR (400 MHz, Chloroform-*d*)  $\delta$  7.41 – 7.35 (m, 1H), 7.30 (d,  $J = 3.2$  Hz, 1H), 7.25 (d,  $J = 1.6$  Hz, 1H), 6.75 (dd,  $J = 3.1, 0.9$  Hz, 1H), 4.34 (dd,  $J = 5.6, 4.9$  Hz, 2H), 4.00 (dd,  $J = 5.7, 4.9$  Hz, 2H) ppm.  $^{13}\text{C}$  NMR (126 MHz, Chloroform-*d*)  $\delta$  137.2, 129.3, 127.8, 126.7, 122.6, 112

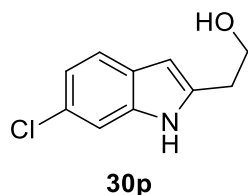
119.7, 108.4, 100.6, 77.7, 77.6, 77.4, 77.2, 62.3, 49.4 ppm. **HRMS-ESI** ( $m/z$ ):  $[M + H]^+$  calculated for  $C_{10}H_{10}ClNO^+$  196.0451 and 198.0421; found 196.0448 and 198.0420.

2-(5-chloro-1*H*-indol-2-yl)ethan-1-ol **30o**



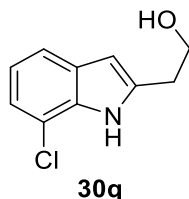
213 mg, 60%.  **$^1H$  NMR** (700 MHz, Chloroform-*d*)  $\delta$  8.60 (s, 1H), 7.49 (d,  $J = 2.0$  Hz, 1H), 7.21 (d,  $J = 8.6$  Hz, 1H), 7.07 (dd,  $J = 8.6, 2.0$  Hz, 1H), 6.22 (s, 1H), 3.96 (t,  $J = 5.7$  Hz, 2H), 2.98 (t,  $J = 5.7$  Hz, 2H) ppm.  **$^{13}C$  NMR** (176 MHz, Chloroform-*d*)  $\delta$  134.6, 129.7, 125.3, 121.6, 119.4, 111.6, 100.0, 62.3, 31.2 ppm. **HRMS-ESI** ( $m/z$ ):  $[M + H]^+$  calculated for  $C_{10}H_{10}ClNO^+$  196.0451 and 198.0421; found 196.0450 and 198.0419.

2-(6-chloro-1*H*-indol-2-yl)ethan-1-ol **30p**



198 mg, 51%.  **$^1H$  NMR** (400 MHz, Chloroform-*d*)  $\delta$  8.45 (s, 1H), 7.36 (dd,  $J = 8.4, 0.7$  Hz, 1H), 7.23 (dt,  $J = 1.9, 0.7$  Hz, 1H), 6.97 (dd,  $J = 8.4, 1.9$  Hz, 1H), 6.18 (dt,  $J = 2.1, 0.9$  Hz, 1H), 3.91 (dd,  $J = 6.0, 5.4$  Hz, 2H), 2.97 – 2.86 (m, 2H) ppm.  **$^{13}C$  NMR** (176 MHz, Chloroform-*d*)  $\delta$  138.5, 136.8, 127.4, 121.0, 120.7, 110.9, 100.6, 62.6, 31.4 ppm. **HRMS-ESI** ( $m/z$ ):  $[M + H]^+$  calculated for  $C_{10}H_{10}ClNO^+$  196.0451 and 198.0421; found 196.0449 and 198.0419.

2-(7-chloro-1*H*-indol-2-yl)ethan-1-ol **30q**

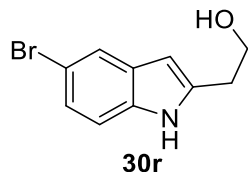


190 mg, 54%.  **$^1H$  NMR** (500 MHz, Chloroform-*d*)  $\delta$  7.51 (dd,  $J = 7.9, 1.2$  Hz, 1H), 7.16 (dd,  $J = 7.6, 1.2$  Hz, 1H), 7.11 (d,  $J = 3.2$  Hz, 1H), 7.00 (t,  $J = 7.7$  Hz, 1H), 6.49 (d,  $J = 3.2$  Hz, 1H), 4.61 (t,  $J = 5.4$  Hz, 2H), 3.93 (t,  $J = 5.3$  Hz, 2H) ppm.  **$^{13}C$  NMR** (126 MHz, Chloroform-*d*)  $\delta$  132.5, 132.1,

## Experimental

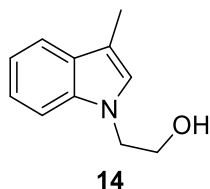
131.3, 123.8, 120.6, 120.2, 116.8, 102.1, 63.7, 51.2 ppm. **HRMS-ESI** ( $m/z$ ):  $[M + H]^+$  calculated for  $C_{10}H_{10}ClNO^+$  196.0451 and 198.0421; found 196.0449 and 198.0419.

### 2-(5-bromo-1*H*-indol-2-yl)ethan-1-ol **30r**



545 mg, 62%. **<sup>1</sup>H NMR** (600 MHz, Chloroform-*d*)  $\delta$  7.76 (d,  $J = 1.9$  Hz, 1H), 7.29 (dd,  $J = 8.7$ , 1.9 Hz, 1H), 7.24 (d,  $J = 8.7$  Hz, 1H), 7.16 (d,  $J = 3.1$  Hz, 1H), 6.46 (dd,  $J = 3.1$ , 0.8 Hz, 1H), 4.26 (t,  $J = 5.3$  Hz, 2H), 3.95 (t,  $J = 5.3$  Hz, 2H) ppm. **<sup>13</sup>C NMR** (151 MHz, Chloroform-*d*)  $\delta$  135.2, 130.7, 129.8, 124.9, 123.9, 113.2, 111.2, 101.6, 62.3, 49.2 ppm. **HRMS-ESI** ( $m/z$ ):  $[M + H]^+$  calculated for  $C_{10}H_{10}BrNO^+$  239.9946 and 241.9925; found 239.9945 and 241.9925.

### 2-(3-methyl-1*H*-indol-1-yl)ethan-1-ol **14**

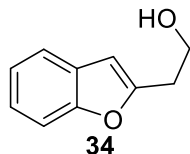


3-methylindole (1.750 g, 13.3 mmol, 1 eq.) and potassium hydroxide (1.5 g, 26.7 mmol, 2 eq.) were dissolved in DMSO (50 mL). (3-bromoethoxy)(*tert*-butyl)dimethylsilane (5.7 mL, 26.7 mmol, 2 eq.) was added and the resulting mixture was stirred for 12 h at room temperature. After quenching the mixture with water (70 mL) at 0 °C, the aqueous layer was extracted with ethyl acetate (4x, 30 mL). The combined organic layers were dried over  $MgSO_4$ , filtered and concentrated under reduced pressure. Flash column chromatography gave the desired intermediate which was subsequently deprotected.

1-(2-((*tert*-butyldimethylsilyl)oxy)ethyl)-3-methyl-1*H*-indole (1.67 g, 5.77 mmol, 1 eq.) was dissolved in THF (50 mL). TBAF in THF (15.17 mL, 15.17 mmol, 1M, 2.6 eq.) was added at 0 °C and the resulting mixture was stirred for 24 h at room temperature. After adding sat.  $NaHCO_3$  solution (60 mL), the mixture was extracted with ethyl acetate (5x, 20 mL). The combined organic layers were dried over  $MgSO_4$ , filtered and concentrated *in vacuo*. The crude mixture was purified via flash column chromatography to give the desired product **14** as light-yellow solid (1.01 g, 44% over two steps).

**<sup>1</sup>H NMR** (700 MHz, Chloroform-*d*)  $\delta$  7.58 (dt,  $J = 7.9, 1.0$  Hz, 1H), 7.33 (dt,  $J = 8.2, 0.9$  Hz, 1H), 7.21 (ddd,  $J = 8.2, 7.0, 1.2$  Hz, 1H), 7.12 (ddd,  $J = 7.9, 7.0, 1.0$  Hz, 1H), 6.93 (q,  $J = 1.1$  Hz, 1H), 4.23 (t,  $J = 5.3$  Hz, 2H), 3.94 (dd,  $J = 5.7, 4.9$  Hz, 2H), 2.33 (d,  $J = 1.1$  Hz, 3H) ppm. **<sup>13</sup>C NMR** (176 MHz, Chloroform-*d*)  $\delta$  136.8, 129.3, 126.2, 121.9, 119.5, 119.2, 111.15, 109.5, 62.5, 48.8, 9.9 ppm. **HRMS-ESI** ( $m/z$ ):  $[M + H]^+$  calculated for  $C_{11}H_{13}O^+$  176.0997; found 176.0995.

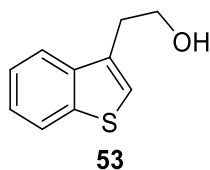
2-(benzofuran-2-yl)ethan-1-ol **34**



2-iodophenol (500 mg, 2.27 mmol, 1 eq.), palladium acetate (25.6 mg, 0.11 mmol, 0.05 eq.), copper(I) iodide (21.7 mg, 0.11 mmol, 0.05 eq.) and triphenylphosphine (29.8 mg, 0.11 mmol, 0.05 eq.) was dissolved in anhydrous triethylamine (20 mL). 3-butyne-1-ol (189.3  $\mu$ L, 2.50 mmol, 1.1 eq.) was added and the resulting reaction mixture was stirred for 12 h at room temperature.<sup>[88b]</sup> The solution was concentrated under reduced pressure and the residue was diluted with ethyl acetate (10 mL). After the organic layer was washed with water (10 mL) and sat. NaCl (10 mL) and dried over  $Na_2SO_4$ , the solvent was removed *in vacuo*. The desired product was isolated as light-yellow oil (288 mg, 80%) from flash column chromatography (EtOAc in CycHex).

**<sup>1</sup>H NMR** (700 MHz, Chloroform-*d*)  $\delta$  7.50 (ddd,  $J = 7.5, 1.5, 0.7$  Hz, 1H), 7.43 (dq,  $J = 8.1, 0.9$  Hz, 1H), 7.25 – 7.17 (m, 2H), 6.51 (q,  $J = 0.9$  Hz, 1H), 4.00 (t,  $J = 6.2$  Hz, 2H), 3.05 (td,  $J = 6.2, 0.9$  Hz, 2H) ppm. **<sup>13</sup>C NMR** (176 MHz, Chloroform-*d*)  $\delta$  156.3, 155.2, 129.0, 123.9, 123.0, 120.8, 111.2, 104.0, 61.1, 32.4 ppm. **HRMS-ESI** ( $m/z$ ):  $[M + H]^+$  calculated for  $C_{10}H_{10}O_2^+$  163.0681; found 163.0673.

2-(benzo[*b*]thiophen-3-yl)ethan-1-ol **53**



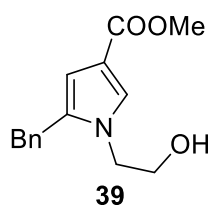
2-(benzo[*b*]thiophen-3-yl)acetic acid (300 mg, 1.56 mmol, 1 eq.) in THF (2.5 mL) was added to a suspension of  $LiAlH_4$  (118.5 mg, 3.12 mmol, 2 eq.) in anhydrous THF (5 mL). The resulting mixture was stirred for 12 h at room temperature and quenched with methanol (1 mL) and aqueous NaOH (10%, 2 mL). After neutralization with hydrochloric acid (2 mL), the mixture was extracted with

## Experimental

ethyl acetate (3x, 15 mL). The combined organic layers were washed with sat. NaCl, dried over NaSO<sub>4</sub>, filtered and concentrated *in vacuo*. After purification via flash column chromatography, the product was isolated as yellow solid (218 mg, 79%).

**<sup>1</sup>H NMR** (700 MHz, Chloroform-*d*)  $\delta$  7.88 (dt, *J* = 7.9, 0.9 Hz, 1H), 7.83 – 7.72 (m, 1H), 7.38 (dddd, *J* = 25.2, 8.2, 7.0, 1.2 Hz, 2H), 7.23 (d, *J* = 1.0 Hz, 1H), 3.97 (t, *J* = 6.5 Hz, 2H), 3.14 (td, *J* = 6.5, 1.0 Hz, 2H) ppm. **<sup>13</sup>C NMR** (176 MHz, Chloroform-*d*)  $\delta$  140.9, 139.2, 133.2, 124.7, 124.3, 123.3, 123.2, 122.0, 62.3, 32.3 ppm. **HRMS-ESI** (*m/z*): [M + H]<sup>+</sup> calculated for C<sub>10</sub>H<sub>10</sub>OS<sup>+</sup> 179.0452 and 180.0486; found 179.0451 and 180.0483.

methyl 5-benzyl-1-(2-hydroxyethyl)-1*H*-pyrrole-3-carboxylate **39**



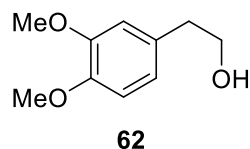
Propargyl aldehyde (5.0 g, 38.4 mmol, 1.0 eq.), methyl acrylate (4.0 g, 46.1 mmol, 1.2 eq.) and DABCO (2.2 g, 19.2 mmol, 0.5 eq.) were dissolved in anhydrous DMSO (35 mL). The resulting mixture was stirred for 3 h at room temperature and subsequently diluted with water (200 mL). After extraction with ethyl acetate (3x, 200 mL), the combined organic layers were dried over MgSO<sub>4</sub>, filtered and concentrated under reduced pressure.<sup>[90]</sup>

The resulting MBH alcohol (3.7 g, 16.9 mmol, 1 eq.) was purified via flash column chromatography (EtOAc in CycHex) and subsequently dissolved in anhydrous dichloromethane (25 mL). Acetic anhydride (2.6 g, 30 mmol, 1.5 eq.) and DMAP (0.62 g, 5.1 mmol, 0.3 eq.) were added and the resulting solution was stirred for 30 min at 0 °C. After the addition of water (10 mL), the solution was extracted with dichloromethane (3x, 15 mL), dried over MgSO<sub>4</sub>, filtered and concentrated *in vacuo*.

The MBH acetate (3.2 g, 12 mmol, 1 eq.) was purified via flash column chromatography (CycHex) and dissolved in DMF (15 mL). 2-aminoethanol (0.73 g, 12 mmol, 1 eq.) and potassium carbonate (1.7 g, 12 mmol, 1 eq.) were added and the resulting mixture was heated for 4 h at 45 °C. After the addition of water (10 mL), the solution was extracted with ethyl acetate (3x, 10 mL). The combined organic layers were washed with sat. NaCl, dried over Na<sub>2</sub>SO<sub>4</sub>, filtered and concentrated *in vacuo*. The crude mixture was purified via flash column chromatography (EtOAc in CycHex) to give the desired product as a yellow solid (2.9 g, 31% over three steps).<sup>[89]</sup>

**$^1\text{H NMR}$**  (500 MHz, Chloroform-*d*)  $\delta$  7.34 (d,  $J$  = 1.9 Hz, 1H), 7.31 – 7.26 (m, 2H), 7.25 – 7.19 (m, 1H), 7.18 – 7.11 (m, 2H), 6.35 (d,  $J$  = 1.8 Hz, 1H), 3.95 (s, 2H), 3.87 (t,  $J$  = 5.4 Hz, 2H), 3.77 (s, 3H), 3.68 (t,  $J$  = 5.4 Hz, 2H) ppm.  **$^{13}\text{C NMR}$**  (126 MHz, Chloroform-*d*)  $\delta$  165.8, 138.8, 133.1, 129.1, 128.8, 127.3, 127.0, 115.1, 110.1, 62.5, 51.4, 49.6, 33.1 ppm. **HRMS-ESI** ( $m/z$ ):  $[\text{M} + \text{H}]^+$  calculated for  $\text{C}_{15}\text{H}_{17}\text{NO}_3^+$  259.1208; found 259.1206.

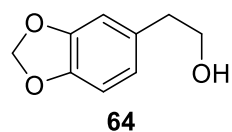
#### 2-(3,4-dimethoxyphenyl)ethan-1-ol **62**



To a suspension of  $\text{LiAlH}_4$  (0.67 g, 17.72 mmol, 3 eq.) in THF (25 mL) was added 3,4-dihydroxy-1-benzenecarboxylic acid (1 g, 5.95 mmol, 1 eq.) at 0 °C. After refluxing the mixture for 6 h, it was cooled to 0 °C and quenched with water (13 mL) and hydrochloric acid (10%, 13 mL). The mixture was extracted with ethyl acetate, dried over  $\text{MgSO}_4$  and concentrated under reduced pressure. Flash column chromatography (EtOAc in CycHex) gave the desired product **62** as colorless oil (0.73 g, 80%).

**$^1\text{H NMR}$**  (600 MHz, Chloroform-*d*)  $\delta$  = 6.78 (d,  $J$  = 6.8 Hz, 1 H), 6.70–6.78 (m, 2 H), 3.82 (s, 3 H), 3.83 (s, 3 H), 3.79 (t,  $J$  = 6.6 Hz, 2 H), 2.77 (t,  $J$  = 6.6 Hz, 2 H), 2.25 (s, 1 H) ppm.  **$^{13}\text{C NMR}$**  (151 MHz, Chloroform-*d*)  $\delta$  = 148.8, 147.2, 131.1, 121.0, 112.2, 111.3, 63.4, 55.7, 55.1, 38.7 ppm. **HRMS-ESI** ( $m/z$ ):  $[\text{M} + \text{H}]^+$  calculated for  $\text{C}_{10}\text{H}_{14}\text{O}_3^+$  183.0943; found 183.0942.

#### 2-(benzo[*d*][1,3]dioxol-5-yl)ethan-1-ol **64**



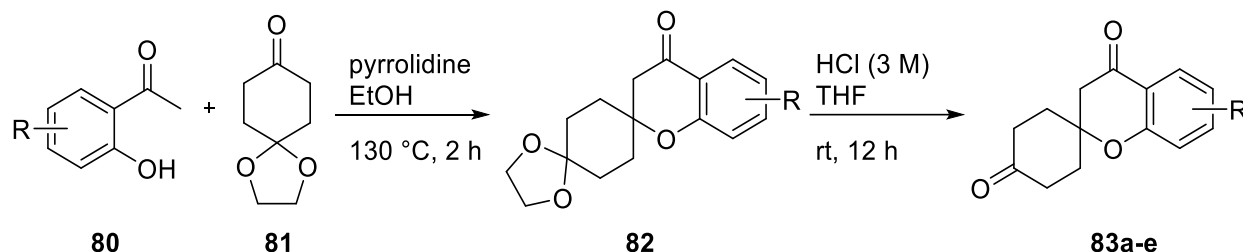
To a suspension of  $\text{LiAlH}_4$  (210.67 mg, 5.55 mmol, 1 eq.) in anhydrous THF (40 mL), a solution of 2-(benzo[*d*][1,3]dioxol-5-yl)acetic acid (1 g, 5.55 mmol, 1 eq.) in anhydrous THF (20 mL) was added dropwise. The resulting mixture was stirred (4 h) and subsequently quenched with methanol (1 mL) and NaOH solution (10%, 2 mL) and neutralized with aqueous hydrochloric acid (10%, 2 mL). The aqueous layer was extracted with ethyl acetate (3x, 15 mL). The combined organic layers were washed with sat. NaCl solution, dried over  $\text{Na}_2\text{SO}_4$  and concentrated under reduced pressure. The desired product **64** was purified via flash column chromatography as a light-yellow solid (0.78 g, 85%).

## Experimental

**<sup>1</sup>H NMR** (400 MHz, Chloroform-*d*)  $\delta$  = 6.66–6.73 (m, 2 H), 6.62 (dd,  $J$  = 7.9, 1.6 Hz, 1 H), 5.87 (s, 2 H), 3.74 (t,  $J$  = 6.5 Hz, 2 H), 2.71 (t,  $J$  = 6.5 Hz, 2 H), 2.29 (s, 1 H) ppm. **<sup>13</sup>C NMR** (151 MHz, Chloroform-*d*)  $\delta$  = 147.6, 146.1, 132.4, 121.9, 109.3, 108.2, 101.0, 63.6, 38.8 ppm. **HRMS-ESI** ( $m/z$ ):  $[M + H]^+$  calculated for C<sub>9</sub>H<sub>10</sub>O<sub>3</sub><sup>+</sup> 167.0630; found 167.0629.

### 5.2.2. CARBONYL STARTING MATERIALS

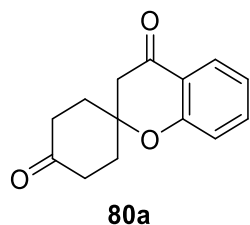
Chromanone derivatives



Acetophenone **80** (2.5 mmol, 1.1 eq.), 1,4-dioxaspiro[4.5]decan-8-one (350 mg, 2.25 mmol, 1 eq.) and pyrrolidine (398 mg, 0.01 mol, 2.5 eq.) were dissolved in anhydrous ethanol (4 mL) and stirred at 130 °C for 2 h in the microwave. The reaction mixture was concentrated under reduced pressure, diluted with ethyl acetate and washed with hydrochloric acid (3 M, 3x, 5 mL), NaOH (1 M, 1x, 5 mL). After drying over MgSO<sub>4</sub> and concentrating *in vacuo*, the intermediate was directly used without further purification in the next step.

The spiro compound was dissolved in anhydrous THF (10 mL) and hydrochloric acid (3 M, 10 mL) was added to the solution. After stirring over night at room temperature, the reaction mixture was neutralized with NaHCO<sub>3</sub> (5 mL) and extracted with ethyl acetate (3x, 10 mL). The combined organic layers were dried over MgSO<sub>4</sub>, concentrated and purified via flash column chromatography (EtOAc in CycHex).

spiro[chromane-2,1'-cyclohexane]-4,4'-dione **80a**

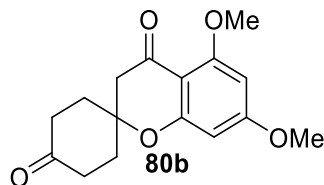


379 mg, 73%. **<sup>1</sup>H NMR** (700 MHz, Chloroform-*d*)  $\delta$  7.90 (dd,  $J$  = 7.8, 1.8 Hz, 1H), 7.53 (ddd,  $J$  = 8.3, 7.2, 1.8 Hz, 1H), 7.09 – 6.99 (m, 2H), 2.80 (s, 2H), 2.79 – 2.70 (m, 2H), 2.51 – 2.40 (m, 2H), 2.31 (ddt,  $J$  = 15.2, 4.7, 2.1 Hz, 2H), 1.90 (td,  $J$  = 13.8, 5.0 Hz, 2H) ppm. **<sup>13</sup>C NMR** (176 MHz, 118



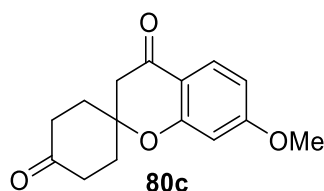
Chloroform-*d*)  $\delta$  209.9, 191.6, 159.2, 136.9, 127.2, 122.0, 121.1, 118.5, 78.4, 47.8, 36.6, 34.4 ppm. **HRMS-ESI** ( $m/z$ ):  $[M + H]^+$  calculated for  $C_{14}H_{14}O_3$  231.0943; found 231.0940.

5,7-dimethoxyspiro[chromane-2,1'-cyclohexane]-4,4'-dione **80b**



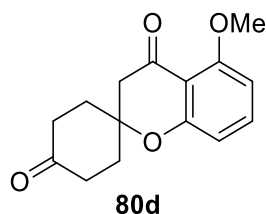
523 mg, 80%.  **$^1H$  NMR** (700 MHz, Chloroform-*d*)  $\delta$  6.12 (d,  $J = 1.4$  Hz, 1H), 6.09 (d,  $J = 1.4$  Hz, 1H), 3.88 (s, 3H), 3.84 (s, 3H), 2.75 – 2.67 (m, 4H), 2.46 – 2.39 (m, 2H), 2.34 – 2.27 (m, 2H), 1.88 (td,  $J = 13.6, 5.0$  Hz, 2H) ppm.  **$^{13}C$  NMR** (176 MHz, Chloroform-*d*)  $\delta$  209.8, 188.6, 166.4, 162.5, 162.3, 105.6, 94.1, 93.1, 77.8, 56.3, 55.8, 48.6, 36.5, 34.2 ppm. **HRMS-ESI** ( $m/z$ ):  $[M + H]^+$  calculated for  $C_{16}H_{18}O_5$  291.1154; found 291.1154.

7-methoxyspiro[chromane-2,1'-cyclohexane]-4,4'-dione **80c**



393 mg, 67%.  **$^1H$  NMR** (400 MHz, Chloroform-*d*)  $\delta$  7.82 (d,  $J = 8.8$  Hz, 1H), 6.59 (d,  $J = 6.4$  Hz, 1H), 6.46 (d,  $J = 2.4$  Hz, 1H), 3.85 (s, 3H), 2.81 – 2.66 (m, 4H), 2.52 – 2.38 (m, 2H), 2.38 – 2.22 (m, 2H), 1.88 (td,  $J = 13.8, 5.2$  Hz, 2H) ppm.  **$^{13}C$  NMR** (176 MHz, Chloroform-*d*)  $\delta$  209.8, 190.0, 166.7, 161.0, 128.8, 114.7, 110.0, 101.5, 78.6, 55.9, 47.3, 36.5, 34.4 ppm. **HRMS-ESI** ( $m/z$ ):  $[M + H]^+$  calculated for  $C_{15}H_{16}O_4$  261.1049; found 261.1047.

5-methoxyspiro[chromane-2,1'-cyclohexane]-4,4'-dione **80d**



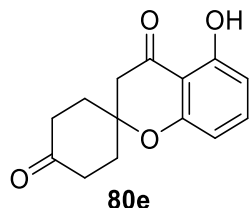
475 mg, 81%.  **$^1H$  NMR** (400 MHz, Chloroform-*d*)  $\delta$  7.41 (t,  $J = 8.4$  Hz, 1H), 6.62 (dd,  $J = 8.3, 1.0$  Hz, 1H), 6.54 (dd,  $J = 8.5, 0.9$  Hz, 1H), 3.91 (s, 3H), 2.81 – 2.63 (m, 4H), 2.49 – 2.36 (m, 2H), 2.29 (ddt,  $J = 15.2, 4.9, 2.1$  Hz, 2H), 1.96 – 1.82 (m, 2H) ppm.  **$^{13}C$  NMR** (126 MHz, Chloroform-

## Experimental

d)  $\delta$  209.9, 190.2, 160.7, 160.6, 136.5, 111.1, 110.4, 104.2, 77.6, 56.4, 48.9, 36.4, 34.1 ppm.

**HRMS-ESI** ( $m/z$ ):  $[M + H]^+$  calculated for  $C_{15}H_{16}O_4^+$  261.1049; found 261.1046.

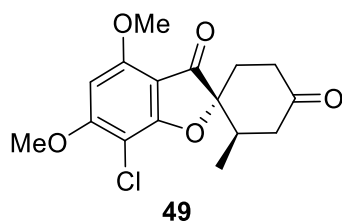
5-hydroxyspiro[chromane-2,1'-cyclohexane]-4,4'-dione **80e**



420 mg, 76%. **<sup>1</sup>H NMR** (500 MHz, Chloroform-*d*)  $\delta$  11.60 (s, 1H), 7.40 (t,  $J = 8.3$  Hz, 1H), 6.55 (dd,  $J = 8.4, 0.9$  Hz, 1H), 6.50 (dd,  $J = 8.2, 1.0$  Hz, 1H), 2.82 (s, 2H), 2.80 – 2.69 (m, 2H), 2.52 – 2.43 (m, 2H), 2.32 (ddt,  $J = 15.2, 4.6, 2.1$  Hz, 2H), 1.90 (td,  $J = 13.8, 5.1$  Hz, 2H) ppm. **<sup>13</sup>C NMR** (126 MHz, Chloroform-*d*)  $\delta$  209.5, 197.3, 162.2, 158.9, 138.8, 110.0, 107.9, 107.9, 77.9, 46.9, 36.3, 34.3 ppm. **HRMS-ESI** ( $m/z$ ):  $[M + H]^+$  calculated for  $C_{14}H_{14}O_4^+$  246.0892; found 246.0893.

(2*R*,2'*R*)-7-Chloro-4,6-dimethoxy-2'-methyl-3*H*-spiro[benzofuran-2,1'-cyclohexane]-3,4'-dione **49**

*The griseofulvin ketone was kindly provided by Dr. Michael Grigalunas.*



To an oven-dried three-neck flask was added griseofulvin (10.583 g, 30 mmol), Pd/C (500 mg, 10%) and anhydrous ethyl acetate (100 ml). The reaction mixture was purged with hydrogen (10 min), then a balloon of  $H_2$  was attached and the reaction was stirred at 22 °C. After 54 h, the reaction was purged with Argon (10 min). The mixture was filtered through celite and washed with dichloromethane. The eluent was concentrated and used in the next step without further purification.

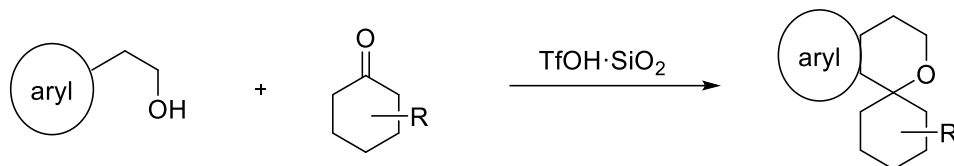
To a flask containing the crude hydrogenated product was added AcOH (200 ml) and an aqueous solution of  $H_2SO_4$  (60 ml, 2M). The reaction was heated to 80 °C for 16 h. After this time, the reaction was cooled to room temperature and diluted with EtOAc (200 ml) and poured into ice water (200 ml). The organic layer was washed with water (3x, 80 mL), dried over  $Na_2SO_4$  and concentrated *in vacuo*. The crude product was used in the next step without further purification.

To the enone, Pd/C (600 mg, 10%) and anhydrous ethyl acetate (80 ml) was added under an atmosphere of Ar. The reaction mixture was purged with H<sub>2</sub> (10 min), then a balloon of H<sub>2</sub> was attached and the reaction was stirred. After 6 h, the reaction was purged with argon (10 min). The mixture was filtered through celite, washed with dichloromethane, and concentrated. Purification by MPLC (silica gel, 10-36% EtOAc in CyHex) afforded 4.7g (48% over three steps) of the title compound as a white solid.

**<sup>1</sup>H NMR** (400 MHz, Chloroform-*d*) δ 6.10 (s, 1H), 4.00 (s, 3H), 3.97 (s, 3H), 2.98 (dt, *J* = 15.2, 8.9 Hz, 1H), 2.87 (dd, *J* = 16.0, 12.5 Hz, 1H), 2.54 – 2.42 (m, 3H), 2.20 (dd, *J* = 8.8, 5.2 Hz, 2H), 0.92 (d, *J* = 6.5 Hz, 3H) ppm. **<sup>13</sup>C NMR** (101 MHz, Chloroform-*d*) δ 209.1, 197.5, 168.1, 164.4, 157.8, 105.5, 97.4, 90.6, 89.2, 57.0, 56.4, 44.0, 38.4, 36.2, 31.2, 15.2 ppm. **HRMS-ESI** (*m/z*): [M + H]<sup>+</sup> calculated for C<sub>16</sub>H<sub>16</sub>O<sub>5</sub>Cl<sup>+</sup> 325.08373 and 327.08078, found 325.08375 and 327.08073.

### 5.2.3. PSEUDO-NPS VIA PICTET-SPENGLER REACTION

#### GENERAL PROCEDURE C/D: PICTET-SPENGLER REACTION WITH CYCLIC KETONES



#### C: Standard procedure

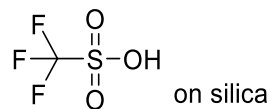
To an oven-dried microwave vial β-aryl ethanol (1.0 eq.) was added. After dissolving in anhydrous dichloromethane (3 ml), TfOH·SiO<sub>2</sub> (6.5 mol%) and cyclic ketone (1.5 eq.) were added. The reaction tube was flushed with argon and the reaction mixture was stirred at room temperature for 30 min. The mixture was filtered and rinsed with ethyl acetate. The combined organic layers were concentrated *in vacuo* and subsequently purified via flash column chromatography (EtOAc in CycHex (0-50%)) to give the desired product.

#### D: Adjusted procedure

β-aryl ethanol (1.0 eq.) was dissolved in anhydrous dichloromethane (3 mL) and subsequently, TfOH·SiO<sub>2</sub> (6.5 mol%) and cyclic ketone (1.5 eq.) were added. After flushing the reaction tube with argon, the reaction mixture was heated to 50 °C for 2 h. The reaction mixture was filtered, rinsed with ethyl acetate and concentrated *in vacuo*. The desired product was purified via flash column chromatography (EtOAc in CycHex (0-50%)).

## Experimental

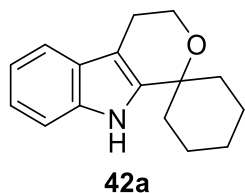
Catalyst: Triflic acid on silica



To a suspension of silica (10 g, predried at 110 °C for 30 min) in ethyl ether (100 mL), triflic acid (0.45 mL, 5.0 mmol) was added carefully. The resulting mixture was stirred for 1 h under argon and subsequently ethyl ether was removed in vacuo. The residue was dried for 2 h at 110 °C to afford the catalyst triflic acid immobilized on silica as a white powder (0.5 mmol/g).

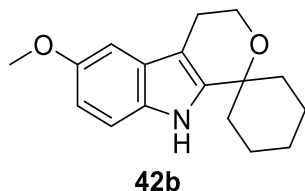
### $\beta$ -TETRAHYDROPYRANOINDOLES

4',9'-dihydro-3'*H*-spiro[cyclohexane-1,1'-pyrano[3,4-*b*]indole] **42a**



Synthesized via procedure C, 23.9 mg, 99%. **<sup>1</sup>H NMR** (400 MHz, Chloroform-*d*)  $\delta$  7.78 (s, 1H), 7.54 (ddt,  $J = 7.5, 1.5, 0.7$  Hz, 1H), 7.34 (ddd,  $J = 8.0, 1.3, 0.8$  Hz, 1H), 7.25 – 7.10 (m, 2H), 4.05 (t,  $J = 5.5$  Hz, 2H), 2.84 (t,  $J = 5.5$  Hz, 2H), 2.15 – 2.02 (m, 2H), 1.93 – 1.75 (m, 3H), 1.73 – 1.56 (m, 4H) ppm. **<sup>13</sup>C NMR** (126 MHz, Chloroform-*d*)  $\delta$  139.7, 135.7, 127.2, 121.7, 119.7, 118.4, 110.9, 107.0, 72.6, 59.8, 35.9, 25.6, 22.6, 21.5 ppm. **HRMS-ESI** ( $m/z$ ):  $[M + H]^+$  calculated for C<sub>16</sub>H<sub>19</sub>NO  $[M+H]^+$ : 242.1539, found 242.1539.

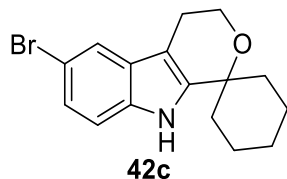
6'-methoxy-4',9'-dihydro-3'*H*-spiro[cyclohexane-1,1'-pyrano[3,4-*b*]indole] **42b**



Synthesized via procedure C, 25.3 mg, 93%. **<sup>1</sup>H NMR** (500 MHz, Chloroform-*d*)  $\delta$  7.77 (s, 1H), 7.10 (d,  $J = 8.7$  Hz, 1H), 6.88 (d,  $J = 2.5$  Hz, 1H), 6.72 (dd,  $J = 8.7, 2.4$  Hz, 1H), 3.91 (t,  $J = 5.5$  Hz, 2H), 3.77 (s, 3H), 2.68 (t,  $J = 5.5$  Hz, 2H), 2.26 (t,  $J = 6.7$  Hz, 1H), 1.99 – 1.86 (m, 2H), 1.85 – 1.74 (m, 2H), 1.74 – 1.58 (m, 2H), 1.51 (ddt,  $J = 14.1, 9.2, 4.1$  Hz, 3H) ppm. **<sup>13</sup>C NMR** (126 MHz, Chloroform-*d*)  $\delta$  154.1, 140.6, 130.7, 127.5, 111.6, 111.4, 106.6, 100.5, 72.7, 59.7, 56.0, 42.1,

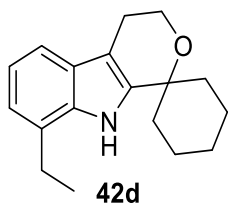
35.7, 27.0, 25.5, 22.6, 21.4 ppm. **HRMS-ESI** ( $m/z$ ):  $[M + H]^+$  calculated for  $C_{17}H_{21}NO_2$   $[M+H]^+$ : 272.1576, found 272.1577.

6'-bromo-4',9'-dihydro-3'H-spiro[cyclohexane-1,1'-pyrano[3,4-b]indole] **42c**



Synthesized via procedure C, 30.4 mg, 95%.  **$^1H$  NMR** (400 MHz, Chloroform-*d*)  $\delta$  7.70 (s, 1H), 7.61 (dt,  $J = 1.9, 0.6$  Hz, 1H), 7.23 (dd,  $J = 8.6, 1.9$  Hz, 1H), 7.18 (dd,  $J = 8.6, 0.6$  Hz, 1H), 3.99 (t,  $J = 5.5$  Hz, 2H), 2.74 (t,  $J = 5.5$  Hz, 2H), 2.04 (m, 2H), 1.77 (dddd,  $J = 14.9, 7.1, 3.9, 1.9$  Hz, 3H), 1.62 (m, 4H), 1.29 (m, 1H) ppm.  **$^{13}C$  NMR** (126 MHz, Chloroform-*d*)  $\delta$  140.6, 130.7, 127.5, 111.6, 111.4, 106.6, 100.5, 72.7, 59.7, 56.0, 42.1, 35.7, 27.0, 25.5, 22.6, 21.4 ppm. **HRMS-ESI** ( $m/z$ ):  $[M + H]^+$  calculated for  $C_{16}H_{18}BrNO$   $[M+H]^+$ : 320.0572 and 321.0551, found 320.0570 and 321.0548.

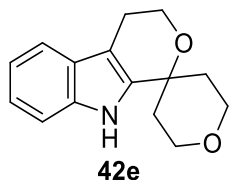
8'-ethyl-4',9'-dihydro-3'H-spiro[cyclohexane-1,1'-pyrano[3,4-b]indole] **42d**



Synthesized via procedure C, 25.3 mg, 94%.  **$^1H$  NMR** (400 MHz, Chloroform-*d*)  $\delta$  7.52 (s, 1H), 7.36 (dd,  $J = 7.7, 1.2$  Hz, 1H), 7.08 (m, 1H), 7.01 (d,  $J = 7.2$  Hz, 1H), 4.01 (t,  $J = 5.4$  Hz, 2H), 2.87 (q,  $J = 7.6$  Hz, 2H), 2.80 (t,  $J = 5.4$  Hz, 2H), 2.06 (m, 2H), 1.80 (td,  $J = 10.2, 3.9$  Hz, 3H), 1.66 (m, 4H), 1.38 (t,  $J = 7.6$  Hz, 3H), 1.33 (m, 1H) ppm.  **$^{13}C$  NMR** (101 MHz Chloroform-*d*)  $\delta$  139.3, 134.4, 127.0, 126.3, 120.4, 120.0, 116.1, 107.6, 72.6, 59.9, 35.9, 27.1, 25.6, 24.2, 22.7, 21.5, 14.0 ppm. **HRMS-ESI** ( $m/z$ ):  $[M + H]^+$  calculated for  $C_{15}H_{23}NO$   $[M+H]^+$ : 270.1780, found 270.1759.

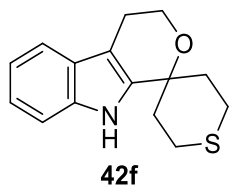
## Experimental

### 2,3,4',5,6,9'-hexahydro-3*H*-spiro[pyran-4,1'-pyrano[3,4-*b*]indole] **42e**



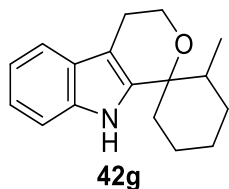
Synthesized via procedure C, 20.2 mg, 83%. **<sup>1</sup>H NMR** (700 MHz, Chloroform-*d*)  $\delta$  7.78 (s, 1H), 7.50 (d,  $J = 7.8$  Hz, 1H), 7.35 (d,  $J = 8.0$  Hz, 1H), 7.18 (td,  $J = 7.5, 6.9, 1.2$  Hz, 1H), 7.12 (t,  $J = 7.4$  Hz, 1H), 4.02 (t,  $J = 5.4$  Hz, 2H), 3.93 (td,  $J = 11.9, 1.9$  Hz, 2H), 3.88 (dd,  $J = 11.5, 5.1$  Hz, 2H), 2.82 (t,  $J = 5.4$  Hz, 2H), 2.04 (td,  $J = 13.8, 12.9, 5.3$  Hz, 2H), 1.90 (d,  $J = 13.8$  Hz, 2H) ppm. **<sup>13</sup>C NMR** (176 MHz, Chloroform-*d*)  $\delta$  137.8, 135.9, 127.1, 122.2, 119.9, 118.5, 111.1, 107.9, 70.2, 63.5, 60.2, 36.0, 22.6 ppm. **HRMS-ESI** ( $m/z$ ):  $[M + H]^+$  calculated for C<sub>15</sub>H<sub>18</sub>NO<sub>2</sub>  $[M+H]^+$ : 244.1332, found 244.1333.

### 2',3',4,5',6',9'-hexahydro-3*H*-spiro[pyrano[3,4-*b*]indole-1,4'-thiopyran] **42f**



Synthesized via procedure C, 23.1 mg, 89%. **<sup>1</sup>H NMR** (700 MHz, Chloroform-*d*)  $\delta$  7.68 (s, 1H), 7.50 (d,  $J = 7.8$  Hz, 1H), 7.34 (d,  $J = 8.1$  Hz, 1H), 7.18 (t,  $J = 7.6$  Hz, 1H), 7.12 (t,  $J = 7.4$  Hz, 1H), 3.99 (t,  $J = 5.4$  Hz, 2H), 3.21 (m, 2H), 2.80 (t,  $J = 5.4$  Hz, 2H), 2.44 (dt,  $J = 15.7, 3.4$  Hz, 2H), 2.29 (d,  $J = 14.1$  Hz, 2H), 2.01 (td,  $J = 13.5, 3.6$  Hz, 2H) ppm. **<sup>13</sup>C NMR** (176 MHz, Chloroform-*d*)  $\delta$  138.6, 135.8, 127.1, 119.9, 118.5, 111.1, 107.3, 71.0, 59.8, 36.7, 31.1, 23.7, 22.5 ppm. **HRMS-ESI** ( $m/z$ ):  $[M + H]^+$  calculated for C<sub>15</sub>H<sub>18</sub>NOS  $[M+H]^+$ : 260.1104, found 260.1106.

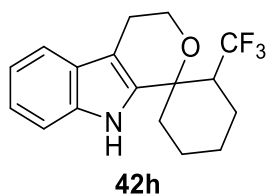
### 2-methyl-4',9'-dihydro-3*H*-spiro[cyclohexane-1,1'-pyrano[3,4-*b*]indole] **42g**



Synthesized via procedure C, 20.4 mg, 80%. **<sup>1</sup>H NMR** (700 MHz, Chloroform-*d*)  $\delta$  7.54 (s, 1H), 7.42 (ddt,  $J = 7.7, 1.4, 0.7$  Hz, 1H), 7.25 (dt,  $J = 8.0, 0.9$  Hz, 1H), 7.05 (dddd,  $J = 31.6, 7.9, 7.1, 1.1$  Hz, 2H), 4.08 – 3.99 (m, 1H), 3.81 (td,  $J = 11.2, 3.4$  Hz, 1H), 2.82 (ddd,  $J = 15.0, 11.2, 5.7$  Hz,

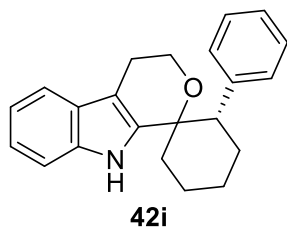
1H), 2.56 (ddd,  $J = 15.0, 3.4, 1.3$  Hz, 1H), 2.19 – 2.13 (m, 1H), 1.71 (tdd,  $J = 10.9, 5.4, 3.1$  Hz, 2H), 1.68 – 1.60 (m, 1H), 1.57 – 1.51 (m, 1H), 1.40 – 1.33 (m, 3H), 1.29 (dt,  $J = 13.1, 4.0$  Hz, 1H), 0.60 (d,  $J = 6.7$  Hz, 3H) ppm.  $^{13}\text{C NMR}$  (176 MHz, Chloroform-*d*)  $\delta$  137.4, 134.6, 126.1, 120.4, 118.4, 117.1, 109.7, 107.4, 74.0, 58.8, 39.8, 33.8, 28.5, 25.2, 21.4, 20.2, 14.8 ppm. **HRMS-ESI** ( $m/z$ ):  $[\text{M} + \text{H}]^+$  calculated for  $\text{C}_{17}\text{H}_{21}\text{NO}$   $[\text{M}+\text{H}]^+$ : 256.1623, found 256.1623.

2-(trifluoromethyl)-4',9'-dihydro-3'*H*-spiro[cyclohexane-1,1'-pyrano[3,4-*b*]indole] **42h**



Synthesized via procedure C, 26.9 mg, 87%.  $^1\text{H NMR}$  (700 MHz, Chloroform-*d*)  $\delta$  7.54 (s, 1H), 7.42 (ddt,  $J = 7.7, 1.4, 0.7$  Hz, 1H), 7.25 (dt,  $J = 8.0, 0.9$  Hz, 1H), 7.05 (dddd,  $J = 31.6, 7.9, 7.1, 1.1$  Hz, 2H), 4.08 – 3.99 (m, 1H), 3.81 (td,  $J = 11.2, 3.4$  Hz, 1H), 2.82 (ddd,  $J = 15.0, 11.2, 5.7$  Hz, 1H), 2.56 (ddd,  $J = 15.0, 3.4, 1.3$  Hz, 1H), 2.19 – 2.13 (m, 1H), 1.71 (tdd,  $J = 10.9, 5.4, 3.1$  Hz, 2H), 1.68 – 1.60 (m, 1H), 1.57 – 1.51 (m, 1H), 1.40 – 1.33 (m, 3H), 1.29 (dt,  $J = 13.1, 4.0$  Hz, 1H) ppm.  $^{13}\text{C NMR}$  (176 MHz, Chloroform-*d*)  $\delta$  138.9, 135.3, 127.5, 121.4, 119.0, 118.2, 110.3, 108.1, 74.7, 59.6, 40.1, 34.6, 29.2, 26.0, 21.4, 21.2, 20.7 ppm. **HRMS-ESI** ( $m/z$ ):  $[\text{M} + \text{H}]^+$  calculated for  $\text{C}_{17}\text{H}_{18}\text{F}_3\text{NO}$   $[\text{M}+\text{H}]^+$ : 310.1340, found 310.1341.

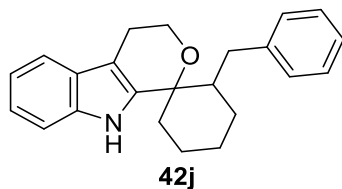
(2*S*)-2-phenyl-4',9'-dihydro-3'*H*-spiro[cyclohexane-1,1'-pyrano[3,4-*b*]indole] **42i**



Synthesized via procedure C, 24.1 mg, 76%.  $^1\text{H NMR}$  (700 MHz, Chloroform-*d*)  $\delta$  7.99 (s, 1H), 7.59 (ddt,  $J = 8.2, 3.3, 1.0$  Hz, 2H), 7.42 – 7.36 (m, 3H), 7.32 – 7.22 (m, 4H), 4.30 (ddd,  $J = 11.1, 5.2, 1.8$  Hz, 1H), 4.04 (td,  $J = 10.9, 3.4$  Hz, 1H), 3.17 (dd,  $J = 12.8, 3.6$  Hz, 1H), 2.71 (ddd,  $J = 14.8, 3.4, 1.8$  Hz, 1H), 2.67 – 2.60 (m, 1H), 2.57 (dd,  $J = 13.0, 3.7$  Hz, 1H), 2.55 – 2.50 (m, 1H), 2.24 – 2.19 (m, 1H), 2.19 – 2.13 (m, 1H), 2.06 – 1.99 (m, 1H), 1.97 – 1.87 (m, 2H), 1.81 – 1.71 (m, 1H) ppm.  $^{13}\text{C NMR}$  (176 MHz, Chloroform-*d*)  $\delta$  141.4, 136.6, 134.5, 127.8, 126.2, 124.9, 120.1, 118.1, 117.0, 109.7, 107.8, 74.2, 59.4, 52.0, 34.6, 27.6, 25.4, 24.0, 21.0, 20.2 ppm. **HRMS-ESI** ( $m/z$ ):  $[\text{M} + \text{H}]^+$  calculated for  $\text{C}_{22}\text{H}_{23}\text{NO}$   $[\text{M}+\text{H}]^+$ : 318.1780, found 318.1777.

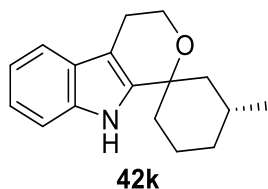
## Experimental

### 2-benzyl-4',9'-dihydro-3'*H*-spiro[cyclohexane-1,1'-pyrano[3,4-*b*]indole] **42j**



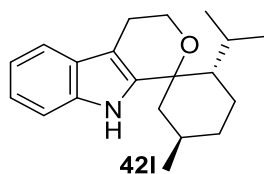
Synthesized via procedure C, 27.9 mg, 84%. **<sup>1</sup>H NMR** (700 MHz, Chloroform-*d*)  $\delta$  7.71 (s, 1H), 7.51 (dq,  $J = 7.8, 0.9$  Hz, 1H), 7.37 (dt,  $J = 8.1, 0.9$  Hz, 1H), 7.20 – 7.18 (m, 1H), 7.16 – 7.14 (m, 3H), 7.10 – 7.07 (m, 1H), 6.95 – 6.91 (m, 2H), 4.16 (ddd,  $J = 11.2, 5.6, 1.1$  Hz, 1H), 3.92 (td,  $J = 11.3, 3.4$  Hz, 1H), 3.24 (dd,  $J = 14.0, 4.9$  Hz, 1H), 3.02 – 2.93 (m, 1H), 2.69 (ddd,  $J = 15.1, 3.4, 1.1$  Hz, 1H), 2.59 – 2.51 (m, 1H), 2.38 – 2.28 (m, 2H), 2.12 – 1.98 (m, 2H), 1.83 (dddd,  $J = 14.5, 5.6, 3.5, 1.8$  Hz, 2H), 1.78 – 1.74 (m, 1H), 1.74 – 1.64 (m, 2H) ppm. **<sup>13</sup>C NMR** (176 MHz, Chloroform-*d*)  $\delta$  140.8, 137.0, 134.8, 128.1, 127.3, 124.9, 120.6, 119.7, 118.5, 109.9, 74.5, 58.9, 51.4, 47.5, 41.2, 35.87, 27.0, 25.2, 24.0, 21.4, 20.2 ppm. **HRMS-ESI** ( $m/z$ ):  $[M + H]^+$  calculated for  $C_{23}H_{25}NO$   $[M+H]^+$ : 332.1936, found 332.1934.

### (3*R*)-3-methyl-4',9'-dihydro-3'*H*-spiro[cyclohexane-1,1'-pyrano[3,4-*b*]indole] **42k**

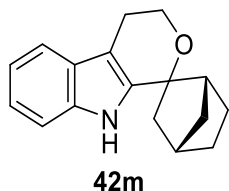


Synthesized via procedure C, 20.9 mg, 82%, d.r. 12:1. **<sup>1</sup>H NMR** (700 MHz, Chloroform-*d*)  $\delta$  7.76 (s, 1H), 7.52 (dt,  $J = 7.8, 1.0$  Hz, 1H), 7.32 (dt,  $J = 8.0, 1.0$  Hz, 1H), 7.16 (dddd,  $J = 31.4, 8.0, 7.1, 1.2$  Hz, 2H), 4.08 – 3.96 (m, 2H), 2.82 (qdd,  $J = 15.1, 6.0, 4.7$  Hz, 2H), 2.11 – 2.01 (m, 2H), 2.01 – 1.91 (m, 1H), 1.87 – 1.76 (m, 2H), 1.69 – 1.60 (m, 1H), 1.58 – 1.49 (m, 1H), 1.46 (s, 1H), 1.29 (dd,  $J = 13.6, 12.0$  Hz, 1H), 0.94 (d,  $J = 6.6$  Hz, 3H) ppm. **<sup>13</sup>C NMR** (176 MHz, Chloroform-*d*)  $\delta$  139.6, 135.9, 127.5, 121.9, 119.8, 118.5, 111.1, 107.2, 73.6, 60.1, 44.7, 35.3, 34.6, 27.7, 22.8, 22.8, 21.6 ppm. **HRMS-ESI** ( $m/z$ ):  $[M + H]^+$  calculated for  $C_{17}H_{21}NO$   $[M+H]^+$ : 256.1623, found 256.1622.



**(2*S*,5*R*)-2-isopropyl-5-methyl-4',9'-dihydro-3'*H*-spiro[cyclohexane-1,1'-pyrano[3,4-*b*]indole] 42l**

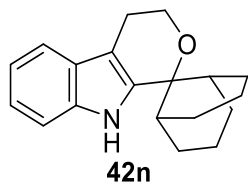
Synthesized via procedure C, 29.2 mg, 98%. **<sup>1</sup>H NMR** (400 MHz, Chloroform-*d*)  $\delta$  7.61 (s, 1H), 7.50 (ddt,  $J = 7.4, 1.5, 0.7$  Hz, 1H), 7.33 (ddd,  $J = 7.9, 1.3, 0.8$  Hz, 1H), 7.14 (m, 2H), 4.09 (ddd,  $J = 11.2, 5.7, 1.1$  Hz, 1H), 3.86 (td,  $J = 11.3, 3.4$  Hz, 1H), 2.91 (ddd,  $J = 15.1, 11.3, 5.7$  Hz, 1H), 2.64 (ddd,  $J = 15.1, 3.4, 1.1$  Hz, 1H), 2.23 (m, 1H), 1.87 (dtd,  $J = 12.0, 3.6, 2.1$  Hz, 2H), 1.71 (m, 1H), 1.59 (dq,  $J = 13.2, 3.4$  Hz, 1H), 1.48 (m, 2H), 1.12 (dd,  $J = 14.0, 11.9$  Hz, 1H), 1.01 (m, 2H), 0.94 (dd,  $J = 7.8, 6.6$  Hz, 1H), 0.90 (d,  $J = 6.5$  Hz, 3H), 0.86 (m, 3H), 0.74 (d,  $J = 7.0$  Hz, 3H) ppm. **<sup>13</sup>C NMR** (101 MHz, Chloroform-*d*)  $\delta$  138.8, 135.8, 127.3, 121.5, 119.6, 118.2, 111.0, 108.7, 77.5, 59.8, 51.0, 44.2, 35.4, 27.8, 27.7, 24.0, 22.6, 22.4, 20.9, 18.9 ppm. **HRMS-ESI** ( $m/z$ ):  $[M + H]^+$  calculated for C<sub>20</sub>H<sub>28</sub>NO  $[M+H]^+$ : 298.2165, found 298.2168.

**(1*R*,4*S*)-4',9'-dihydro-3'*H*-spiro[bicyclo[2.2.1]heptane-2,1'-pyrano[3,4-*b*]indole] 42m**

Synthesized via procedure C, 14.9 mg, 59%. **<sup>1</sup>H NMR** (500 MHz, Chloroform-*d*)  $\delta$  7.76 (s, 1H), 7.54 – 7.47 (m, 1H), 7.34 (ddd,  $J = 8.0, 2.5, 1.5$  Hz, 1H), 7.21 – 7.07 (m, 2H), 4.13 – 3.87 (m, 2H), 3.02 – 2.86 (m, 1H), 2.77 – 2.57 (m, 2H), 2.49 – 2.38 (m, 1H), 2.10 – 1.98 (m, 2H), 1.88 – 1.71 (m, 2H), 1.71 – 1.55 (m, 4H), 1.49 – 1.37 (m, 3H) ppm. **<sup>13</sup>C NMR** (126 MHz, Chloroform-*d*)  $\delta$  139.8, 136.0, 127.3, 122.2, 122.0, 120.0, 118.5, 111.2, 107.0, 81.0, 62.5, 46.1, 39.9, 36.5, 28.1, 27.3, 22.9 ppm. **HRMS-ESI** ( $m/z$ ):  $[M + H]^+$  calculated for C<sub>17</sub>H<sub>19</sub>NO  $[M+H]^+$ : 254.1467, found 254.1467.

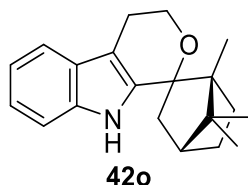
## Experimental

### 4',9'-dihydro-3'-*H*-spiro[bicyclo[3.3.1]nonane-9,1'-pyrano[3,4-*b*]indole] **42n**



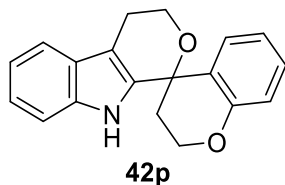
Synthesized via procedure C, 14.3 mg, 51%. **<sup>1</sup>H NMR** (500 MHz, Chloroform-*d*)  $\delta$  8.08 (s, 1H), 7.55 (s, 1H), 7.39 (s, 1H), 7.17 (d,  $J = 39.4$  Hz, 2H), 4.05 (s, 2H), 2.86 (s, 2H), 2.42 – 2.30 (m, 2H), 2.29 – 2.20 (m, 1H), 2.15 – 2.11 (m, 2H), 2.08 (q,  $J = 5.3, 4.6$  Hz, 3H), 1.97 (dd,  $J = 14.8, 6.5$  Hz, 2H), 1.88 – 1.80 (m, 1H), 1.69 – 1.60 (m, 1H), 1.54 – 1.49 (m, 2H) ppm. **<sup>13</sup>C NMR** (126 MHz, Chloroform-*d*)  $\delta$  138.9, 135.0, 126.5, 121.7, 119.4, 118.2, 110.7, 108.7, 75.7, 58.1, 46.7, 35.8, 34.4, 29.0, 27.9, 27.0, 22.7, 20.7, 20.5 ppm **HRMS-ESI** ( $m/z$ ):  $[M + H]^+$  calculated for C<sub>19</sub>H<sub>23</sub>NO  $[M+H]^+$ : 282.1780, found 282.1781.

### (1*R*,4*R*)-1,7,7-trimethyl-4',9'-dihydro-3'-*H*-spiro[bicyclo[2.2.1]heptane-2,1'-pyrano[3,4]indole] **42o**



Synthesized via procedure C, 3.5 mg, 11%. **<sup>1</sup>H NMR** (500 MHz, Chloroform-*d*)  $\delta$  7.81 (s, 1H), 7.62 – 7.49 (m, 1H), 7.40 – 7.35 (m, 1H), 7.29 – 7.10 (m, 2H), 4.21 – 3.96 (m, 2H), 3.21 – 2.93 (m, 1H), 2.87 – 2.61 (m, 2H), 2.50 – 2.42 (m, 1H), 1.88 – 1.67 (m, 2H), 1.61 – 1.48 (m, 3H), 1.45 – 1.30 (m, 3H), 1.27 (s, 6H) ppm. **<sup>13</sup>C NMR** (126 MHz, Chloroform-*d*)  $\delta$  139.8, 135.6, 127.0, 121.6, 119.6, 110.8, 80.6, 61.9, 57.8, 49.2, 43.3, 39.6, 38.8, 36.5, 29.9, 27.1, 26.5, 22.2, 19.8, 15.8 ppm. **HRMS-ESI** ( $m/z$ ):  $[M + H]^+$  calculated for C<sub>20</sub>H<sub>25</sub>NO  $[M+H]^+$ : 296.1936, found 296.1932.

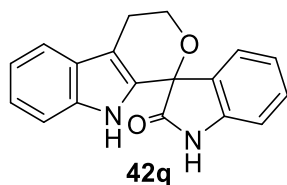
### 4',9'-dihydro-3'-*H*-spiro[chromane-4,1'-pyrano[3,4-*b*]indole] **42p**



Synthesized via procedure C, 16.6 mg, 57%. **<sup>1</sup>H NMR** (400 MHz, Chloroform-*d*)  $\delta$  7.56 – 7.44 (m, 1H), 7.40 (s, 1H), 7.14 – 7.02 (m, 4H), 6.82 (dd,  $J = 8.3, 1.2$  Hz, 1H), 6.76 (dd,  $J = 7.7, 1.7$  Hz, 1H), 6.68 – 6.58 (m, 1H), 4.43 (ddd,  $J = 10.9, 9.1, 6.1$  Hz, 1H), 4.30 – 4.18 (m, 1H), 4.11 – 3.84

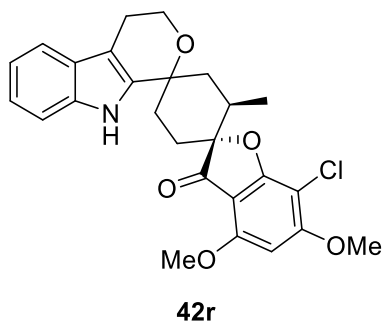
(m, 2H), 2.94 (ddd,  $J = 15.4, 6.8, 4.9$  Hz, 1H), 2.81 (ddd,  $J = 15.4, 5.4, 4.6$  Hz, 1H), 2.35 – 2.16 (m, 2H).  $^{13}\text{C NMR}$  (176 MHz, Chloroform-*d*)  $\delta$  155.3, 136.4, 135.7, 130.5, 130.3, 127.0, 124.1, 122.6, 120.7, 120.1, 118.7, 117.7, 111.4, 110.77, 70.2, 62.5, 60.4, 34.1, 22.7. **HRMS-ESI** ( $m/z$ ):  $[\text{M} + \text{H}]^+$  calculated for  $\text{C}_{19}\text{H}_{17}\text{NO}_2$   $[\text{M} + \text{H}]^+$ : 292.1259, found 292.1261.

4',9'-dihydro-3'-*H*-spiro[indoline-3,1'-pyrano[3,4-*b*]indol]-2-one **42q**



Synthesized via procedure C, 20.9 mg, 72%.  $^1\text{H NMR}$  (700 MHz, Methanol-*d*4)  $\delta$  7.42 – 7.26 (m, 2H), 7.18 – 6.97 (m, 4H), 6.87 – 6.72 (m, 1H), 6.65 – 6.50 (m, 1H), 4.88 – 4.82 (m, 1H), 4.35 – 4.26 (m, 1H), 3.19 (d,  $J = 1.9$  Hz, 1H), 3.05 – 2.96 (m, 1H) ppm.  $^{13}\text{C NMR}$  (176 MHz, Methanol-*d*4)  $\delta$  181.7, 144.1, 138.5, 136.2, 133.7, 132.1, 127.6, 126.5, 124.9, 123.1, 121.1, 119.1, 113.0, 112.2, 107.6, 80.0, 63.2, 25.4 ppm. **HRMS-ESI** ( $m/z$ ):  $[\text{M} + \text{H}]^+$  calculated for  $\text{C}_{18}\text{H}_{14}\text{N}_2\text{O}_2$   $[\text{M} + \text{H}]^+$ : 291.1055, found 291.1051.

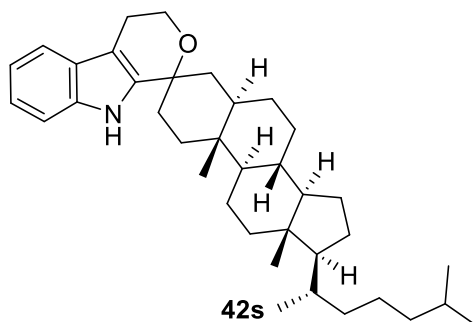
(2*R*,2'*R*)-7-chloro-4,6-dimethoxy-2'-methyl-4'',9''-dihydro-3*H*,3''*H*-dispiro[benzofuran-2,1'-cyclohexane-4',1''-pyrano[3,4-*b*]indol]-3-one **42r**



Synthesized via procedure C, 43.9 mg, 94%.  $^1\text{H NMR}$  (400 MHz, Chloroform-*d*)  $\delta$  8.06 (s, 1H), 7.49 (ddt,  $J = 7.7, 1.3, 0.7$  Hz, 1H), 7.33 (m, 1H), 7.17 (ddd,  $J = 8.1, 7.1, 1.3$  Hz, 1H), 7.10 (ddd,  $J = 8.1, 7.1, 1.1$  Hz, 1H), 6.10 (s, 1H), 4.02 (s, 3H), 3.99 (s, 3H), 2.82 (m, 2H), 2.72 (ddd,  $J = 13.0, 6.7, 4.2$  Hz, 1H), 2.54 (m, 3H), 2.02 (m, 3H), 1.79 (ddd,  $J = 12.8, 4.0, 2.6$  Hz, 1H), 1.43 (s, 1H), 0.82 (d,  $J = 6.7$  Hz, 3H) ppm.  $^{13}\text{C NMR}$  (176 MHz, Chloroform-*d*)  $\delta$  199.4, 168.7, 164.3, 157.7, 138.1, 135.9, 127.0, 121.8, 119.5, 118.3, 111.1, 107.3, 106.1, 92.6, 88.9, 72.4, 60.2, 57.0, 56.3, 38.8, 33.9, 30.1, 28.7, 27.0, 22.6, 14.8 ppm. **HRMS-ESI** ( $m/z$ ):  $[\text{M} + \text{H}]^+$  calculated for  $\text{C}_{26}\text{H}_{27}\text{ClNO}_5$   $[\text{M} + \text{H}]^+$ : 468.1572, found 468.1568.

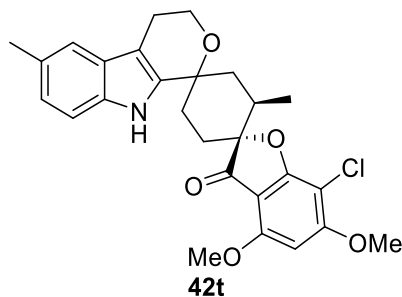
## Experimental

(5*R*,8*S*,9*R*,10*R*,13*S*,14*R*,17*S*)-10,13-dimethyl-17-((*S*)-6-methylheptan-2-yl)-1,2,4,4',5,6,7,8,9,9',10,11,12,13,14,15,16,17-octadecahydro-3'*H*-spiro[cyclopenta[*a*]phenanthrene-3,1'-pyrano[3,4-*b*]indole] **42s**



Synthesized via procedure C, 48.2 mg, 91%. **<sup>1</sup>H NMR** (500 MHz, Chloroform-*d*)  $\delta$  7.57 (s, 1H), 7.42 (dd,  $J = 7.7, 1.2$  Hz, 1H), 7.29 – 7.23 (m, 1H), 7.08 (ddd,  $J = 8.1, 7.0, 1.3$  Hz, 1H), 7.03 (ddd,  $J = 8.0, 7.0, 1.1$  Hz, 1H), 4.02 – 3.81 (m, 2H), 2.85 – 2.60 (m, 2H), 1.90 (ddt,  $J = 16.8, 14.5, 2.6$  Hz, 2H), 1.71 (d,  $J = 4.5$  Hz, 1H), 1.63 – 1.57 (m, 3H), 1.47 – 1.38 (m, 3H), 1.31 – 1.23 (m, 6H), 1.17 (d,  $J = 10.2$  Hz, 4H), 1.04 (ddd,  $J = 16.6, 10.4, 5.5$  Hz, 6H), 0.97 – 0.91 (m, 3H), 0.86 (s, 3H), 0.84 (dd,  $J = 6.6, 3.2$  Hz, 3H), 0.80 (dt,  $J = 6.7, 2.2$  Hz, 9H), 0.60 (s, 3H) ppm. **<sup>13</sup>C NMR** (126 MHz, Chloroform-*d*)  $\delta$  139.1, 135.6, 127.1, 121.7, 119.6, 118.2, 110.8, 107.2, 76.8, 73.1, 59.7, 54.1, 42.6, 40.2, 40.0, 39.5, 38.8, 36.2, 35.8, 35.6, 35.3, 33.5, 31.9, 31.3, 28.4, 28.3, 28.0, 26.9, 24.2, 23.8, 22.9, 22.6, 22.5, 21.0, 18.7, 12.1, 11.7 ppm. **HRMS-ESI** ( $m/z$ ):  $[M + H]^+$  calculated for C<sub>37</sub>H<sub>55</sub>NO  $[M+H]^+$ : 530.4284, found 530.4280.

(2*R*,2'*R*)-7-chloro-4,6-dimethoxy-2',6''-dimethyl-4''',9''-dihydro-3*H*,3''*H*-dispiro[benzofuran-2,1'-cyclohexane-4',1''-pyrano[3,4-*b*]indol]-3-one **42t**

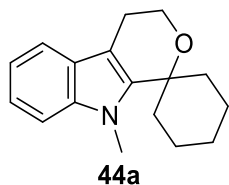


Synthesized via procedure C, 40.0 mg, 83%. **<sup>1</sup>H NMR** (400 MHz, Chloroform-*d*)  $\delta$  7.84 (s, 1H), 7.20 (dd,  $J = 1.6, 0.8$  Hz, 1H), 7.14 (dd,  $J = 8.1, 0.6$  Hz, 1H), 6.91 (ddd,  $J = 8.2, 1.6, 0.6$  Hz, 1H), 6.02 (s, 1H), 3.94 – 3.92 (m, 8H), 2.74 – 2.68 (m, 2H), 2.63 (dtd,  $J = 13.4, 7.0, 4.5$  Hz, 1H), 2.54 – 2.47 (m, 1H), 2.45 – 2.38 (m, 1H), 2.37 (s, 3H), 1.97 (dd,  $J = 13.1, 2.7$  Hz, 1H), 1.90 (ddd,  $J =$

14.2, 4.2, 2.4 Hz, 1H), 1.71 (ddd,  $J = 12.8, 4.0, 2.6$  Hz, 1H), 0.74 (d,  $J = 6.8$  Hz, 3H) ppm.  $^{13}\text{C}$  NMR (101 MHz, Chloroform-*d*)  $\delta$  199.5, 168.8, 164.4, 157.8, 138.3, 134.2, 128.9, 127.3, 123.4, 118.1, 110.8, 106.9, 92.7, 89.0, 72.5, 60.4, 57.1, 56.5, 38.9, 34.0, 30.2, 28.9, 22.7, 21.7, 14.9. HRMS-ESI ( $m/z$ ):  $[\text{M} + \text{H}]^+$  calculated for  $\text{C}_{27}\text{H}_{28}\text{ClNO}_5$   $[\text{M} + \text{H}]^+$ : 482.1656 and 484.1627, found 482.1652 and 484.1626.

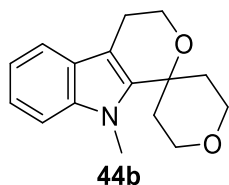
#### *N*-METHYL- $\beta$ -TETRAHYDROPYRANOINDOLES

9'-methyl-4',9'-dihydro-3'*H*-spiro[cyclohexane-1,1'-pyrano[3,4-*b*]indole] **44a**



Synthesized via procedure C, 23.5 mg, 92%.  $^1\text{H}$  NMR (500 MHz, Chloroform-*d*)  $\delta$  7.41 (dd,  $J = 7.8, 1.2$  Hz, 1H), 7.18 (d,  $J = 8.2$  Hz, 1H), 7.12 (ddd,  $J = 8.3, 6.9, 1.2$  Hz, 1H), 7.07 – 6.97 (m, 1H), 3.87 (t,  $J = 5.5$  Hz, 2H), 3.70 (s, 3H), 2.73 (t,  $J = 5.4$  Hz, 2H), 1.99 – 1.87 (m, 2H), 1.87 – 1.65 (m, 4H), 1.59 – 1.48 (m, 2H), 1.34 (s, 1H), 1.21 (qt,  $J = 12.8, 4.0$  Hz, 1H) ppm.  $^{13}\text{C}$  NMR (126 MHz, Chloroform-*d*)  $\delta$  140.2, 137.7, 126.7, 121.7, 119.5, 118.5, 109.2, 107.9, 73.8, 59.6, 34.4, 32.0, 25.9, 23.3, 21.7 ppm. HRMS-ESI ( $m/z$ ):  $[\text{M} + \text{H}]^+$  calculated for  $\text{C}_{17}\text{H}_{21}\text{NO}$   $[\text{M} + \text{H}]^+$ : 256.1623, found 256.1620.

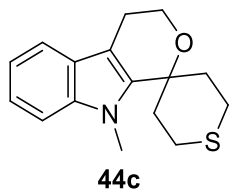
9'-methyl-2,3,4',5,6,9'-hexahydro-3'*H*-spiro[pyran-4,1'-pyrano[3,4-*b*]indole] **44b**



Synthesized via procedure C, 18.5 mg, 72%.  $^1\text{H}$  NMR (500 MHz, Chloroform-*d*)  $\delta$  7.52 (dt,  $J = 7.8, 1.0$  Hz, 1H), 7.30 (dt,  $J = 8.3, 0.9$  Hz, 1H), 7.24 (ddd,  $J = 8.2, 7.0, 1.2$  Hz, 1H), 7.13 (ddd,  $J = 7.9, 6.9, 1.0$  Hz, 1H), 3.98 (t,  $J = 5.4$  Hz, 4H), 3.91 – 3.85 (m, 2H), 3.83 (s, 3H), 2.85 (t,  $J = 5.4$  Hz, 2H), 2.33 (ddd,  $J = 14.2, 12.3, 5.5$  Hz, 2H), 1.85 (dt,  $J = 14.1, 1.3$  Hz, 2H) ppm.  $^{13}\text{C}$  NMR (126 MHz, Chloroform-*d*)  $\delta$  137.9, 137.5, 126.1, 121.8, 119.4, 118.3, 109.0, 108.2, 71.0, 63.5, 59.6, 34.5, 31.6, 22.9 ppm. HRMS-ESI ( $m/z$ ):  $[\text{M} + \text{H}]^+$  calculated for  $\text{C}_{16}\text{H}_{19}\text{NO}_2$   $[\text{M} + \text{H}]^+$ : 258.1416, found 258.1418.

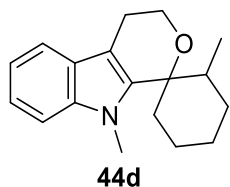
## Experimental

### 9-methyl-2',3',4,5',6',9-hexahydro-3*H*-spiro[pyrano[3,4-*b*]indole-1,4'-thiopyran] **44c**

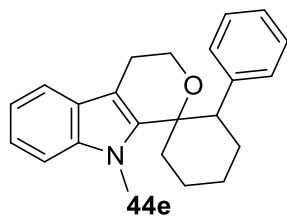


Synthesized via procedure C, 21.6 mg, 79%. **<sup>1</sup>H NMR** (500 MHz, Chloroform-*d*)  $\delta$  7.52 (dt,  $J$  = 7.8, 1.0 Hz, 1H), 7.31 (dt,  $J$  = 8.2, 1.0 Hz, 1H), 7.24 (ddd,  $J$  = 8.2, 7.0, 1.2 Hz, 1H), 7.13 (ddd,  $J$  = 7.9, 7.0, 1.1 Hz, 1H), 3.97 (t,  $J$  = 5.5 Hz, 2H), 3.85 (s, 3H), 3.34 – 3.22 (m, 2H), 2.84 (t,  $J$  = 5.4 Hz, 2H), 2.45 (dddd,  $J$  = 13.6, 4.0, 2.8, 1.5 Hz, 2H), 2.38 – 2.20 (m, 4H) ppm. **<sup>13</sup>C NMR** (126 MHz, Chloroform-*d*)  $\delta$  139.3, 137.8, 126.5, 122.1, 119.7, 118.7, 109.4, 108.0, 72.2, 59.6, 35.5, 32.2, 24.0, 23.1 ppm. **HRMS-ESI** ( $m/z$ ):  $[M + H]^+$  calculated for C<sub>16</sub>H<sub>19</sub>NOS  $[M+H]^+$ : 274.1187, found 274.1185.

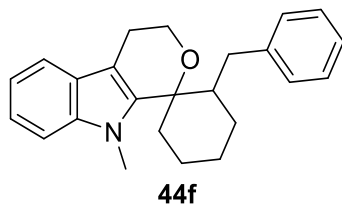
### 2,9'-dimethyl-4',9'-dihydro-3'*H*-spiro[cyclohexane-1,1'-pyrano[3,4-*b*]indole] **44d**



Synthesized via procedure C, 17.5 mg, 65%. **<sup>1</sup>H NMR** (500 MHz, Chloroform-*d*)  $\delta$  7.50 (d,  $J$  = 7.8 Hz, 1H), 7.29 (dt,  $J$  = 8.2, 0.9 Hz, 1H), 7.20 (ddd,  $J$  = 8.2, 7.0, 1.2 Hz, 1H), 7.10 (ddd,  $J$  = 7.9, 7.0, 1.0 Hz, 1H), 4.07 (ddd,  $J$  = 11.1, 5.8, 1.1 Hz, 1H), 3.83 (td,  $J$  = 11.3, 3.3 Hz, 1H), 3.79 (s, 3H), 2.98 – 2.85 (m, 1H), 2.65 (ddd,  $J$  = 15.0, 3.3, 1.0 Hz, 1H), 2.28 – 2.11 (m, 2H), 1.83 – 1.61 (m, 4H), 1.60-1.51 (m, 2H), 1.45 – 1.33 (m, 1H), 0.68 (d,  $J$  = 6.7 Hz, 3H) ppm. **<sup>13</sup>C NMR** (126 MHz, Chloroform-*d*)  $\delta$  138.8, 137.4, 126.3, 121.2, 119.0, 118.0, 109.0, 108.8, 76.2, 59.2, 39.0, 33.1, 31.6, 29.5, 26.3, 22.8, 21.2, 15.9 ppm. **HRMS-ESI** ( $m/z$ ):  $[M + H]^+$  calculated for C<sub>18</sub>H<sub>23</sub>NO  $[M+H]^+$ : 270.1780, found 270.1785.

9'-methyl-2-phenyl-4',9'-dihydro-3'*H*-spiro[cyclohexane-1,1'-pyrano[3,4-*b*]indole] **44e**

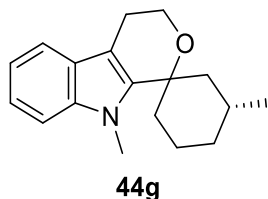
Synthesized via procedure C, 15.2 mg, 46%. **<sup>1</sup>H NMR** (500 MHz, Chloroform-*d*)  $\delta$  7.24 (dt,  $J$  = 7.8, 0.9 Hz, 1H), 7.16 (dt,  $J$  = 8.2, 0.9 Hz, 1H), 7.13 – 7.02 (m, 3H), 6.98 – 6.85 (m, 3H), 3.98 (ddd,  $J$  = 11.0, 4.0, 2.9 Hz, 1H), 3.87 (s, 3H), 3.67 (ddd,  $J$  = 11.0, 7.9, 6.8 Hz, 1H), 3.19 (dd,  $J$  = 12.5, 3.7 Hz, 1H), 2.46 – 2.37 (m, 2H), 2.25 (qd,  $J$  = 13.0, 3.6 Hz, 1H), 2.20 – 2.13 (m, 1H), 1.91 – 1.74 (m, 3H), 1.71 – 1.52 (m, 2H) ppm. **<sup>13</sup>C NMR** (126 MHz, Chloroform-*d*)  $\delta$  143.0, 138.2, 137.3, 128.6, 127.3, 126.2, 126.0, 121.0, 118.8, 117.9, 109.0, 108.7, 76.3, 59.6, 51.4, 33.7, 31.9, 29.0, 26.5, 22.5, 21.2 ppm. **HRMS-ESI** ( $m/z$ ):  $[M + H]^+$  calculated for C<sub>23</sub>H<sub>25</sub>NO  $[M+H]^+$ : 332.1936, found 332.1935.

2-benzyl-9'-methyl-4',9'-dihydro-3'*H*-spiro[cyclohexane-1,1'-pyrano[3,4-*b*]indole] **44f**

Synthesized via procedure C, 20.0 mg, 58%. **<sup>1</sup>H NMR** (500 MHz, Chloroform-*d*)  $\delta$  7.45 (dt,  $J$  = 7.9, 1.0 Hz, 1H), 7.22 (dt,  $J$  = 8.3, 0.9 Hz, 1H), 7.15 (ddd,  $J$  = 8.2, 7.0, 1.2 Hz, 1H), 7.09 – 6.98 (m, 4H), 6.87 – 6.75 (m, 2H), 4.14 – 3.98 (m, 1H), 3.80 (td,  $J$  = 11.4, 3.3 Hz, 1H), 3.72 (s, 3H), 2.92 (ddd,  $J$  = 15.0, 11.6, 5.8 Hz, 1H), 2.64 (ddd,  $J$  = 15.0, 3.3, 1.0 Hz, 1H), 2.42 – 2.25 (m, 3H), 2.23 – 2.10 (m, 2H), 1.78 – 1.54 (m, 4H), 1.25 – 1.09 (m, 2H) ppm. **<sup>13</sup>C NMR** (126 MHz, Chloroform-*d*)  $\delta$  141.9, 138.4, 137.5, 129.1, 128.0, 126.4, 125.4, 121.4, 119.2, 118.0, 109.5, 108.9, 76.6, 59.3, 46.8, 37.1, 33.1, 31.8, 26.4, 26.1, 22.9, 21.2 ppm. **HRMS-ESI** ( $m/z$ ):  $[M + H]^+$  calculated for C<sub>24</sub>H<sub>27</sub>NO  $[M+H]^+$ : 346.2093, found 346.2090.

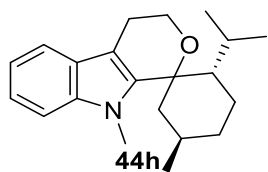
## Experimental

### (3*R*)-3,9'-dimethyl-4',9'-dihydro-3'*H*-spiro[cyclohexane-1,1'-pyrano[3,4-*b*]indole] **44g**



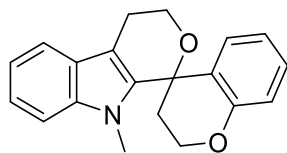
Synthesized via procedure C, 19.9 mg, 74%, d.r. 15:1. **<sup>1</sup>H NMR** (400 MHz, Chloroform-*d*)  $\delta$  7.50 (dt,  $J = 7.8, 1.0$  Hz, 1H), 7.28 (dt,  $J = 8.3, 1.0$  Hz, 1H), 7.21 (ddd,  $J = 8.2, 7.0, 1.2$  Hz, 1H), 7.11 (ddd,  $J = 8.0, 7.0, 1.1$  Hz, 1H), 4.05 – 3.89 (m, 2H), 3.80 (s, 3H), 2.90 – 2.75 (m, 2H), 2.08 – 1.93 (m, 3H), 1.92 – 1.75 (m, 3H), 1.70 – 1.61 (m, 1H), 1.61 – 1.50 (m, 2H), 0.94 (d,  $J = 6.5$  Hz, 3H) ppm. **<sup>13</sup>C NMR** (126 MHz, Chloroform-*d*)  $\delta$  139.0, 137.2, 126.2, 120.6, 118.7, 116.4, 109.0, 105.3, 76.2, 59.2, 39.1, 30.3, 31.7, 29.5, 26.3, 19.8, 20.2, 15.6 ppm. **HRMS-ESI** ( $m/z$ ):  $[M + H]^+$  calculated for C<sub>18</sub>H<sub>23</sub>NO  $[M+H]^+$ : 270.1780, found 270.1781.

### (2*S*,5*R*)-2-isopropyl-5,9'-dimethyl-4',9'-dihydro-3'*H*-spiro[cyclohexane-1,1'-pyrano[3,4]indole]**44h**

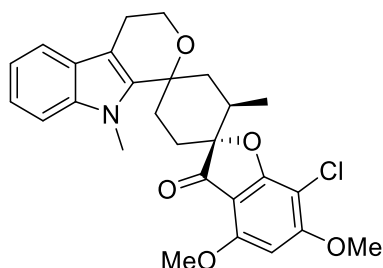


Synthesized via procedure C, 22.7 mg, 73%. **<sup>1</sup>H NMR** (500 MHz, Chloroform-*d*)  $\delta$  7.59 – 7.45 (m, 1H), 7.29 (d,  $J = 8.2$  Hz, 1H), 7.21 (ddd,  $J = 8.1, 7.0, 1.3$  Hz, 1H), 7.11 (td,  $J = 7.5, 7.0, 1.0$  Hz, 1H), 4.05 (dd,  $J = 11.1, 5.7$  Hz, 1H), 3.85 – 3.74 (m, 4H), 2.93 (ddd,  $J = 14.9, 11.7, 5.8$  Hz, 1H), 2.65 (dd,  $J = 14.9, 3.2$  Hz, 1H), 2.27 – 2.15 (m, 1H), 1.99 – 1.85 (m, 1H), 1.78 (qd,  $J = 12.7, 3.5$  Hz, 1H), 1.56 (td,  $J = 8.2, 7.0, 3.5$  Hz, 2H), 1.48 (hd,  $J = 6.9, 1.8$  Hz, 1H), 1.35 – 1.24 (m, 2H), 1.02 (qd,  $J = 12.7, 3.8$  Hz, 1H), 0.92 (d,  $J = 6.6$  Hz, 3H), 0.84 (d,  $J = 6.9$  Hz, 3H), 0.75 (d,  $J = 7.0$  Hz, 3H) ppm. **<sup>13</sup>C NMR** (126 MHz, Chloroform-*d*)  $\delta$  139.0, 137.3, 126.4, 121.2, 119.0, 117.9, 109.0, 108.8, 78.6, 59.0, 49.1, 42.4, 35.4, 31.6, 27.9, 27.5, 23.5, 22.8, 22.4, 20.6, 18.8 ppm. **HRMS-ESI** ( $m/z$ ):  $[M + H]^+$  calculated for C<sub>21</sub>H<sub>29</sub>NO  $[M+H]^+$ : 312.2249, found 312.2236.



9'-methyl-4',9'-dihydro-3'*H*-spiro[chromane-4,1'-pyrano[3,4-*b*]indole] **44i****44i**

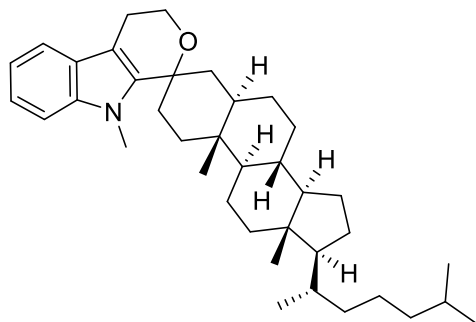
Synthesized via procedure C, 15.9 mg, 52%. **<sup>1</sup>H NMR** (700 MHz, Chloroform-*d*)  $\delta$  7.59 (d,  $J$  = 7.9 Hz, 1H), 7.22 (dd,  $J$  = 13.2, 2.8 Hz, 3H), 7.16 (dq,  $J$  = 7.9, 4.4, 4.0 Hz, 1H), 6.98 – 6.84 (m, 2H), 6.77 (t,  $J$  = 7.4 Hz, 1H), 4.52 (ddd,  $J$  = 13.1, 10.9, 2.2 Hz, 1H), 4.45 – 4.31 (m, 1H), 4.11 (dd,  $J$  = 13.1, 5.9 Hz, 1H), 4.05 (dd,  $J$  = 8.0, 4.0 Hz, 1H), 3.15 (s, 3H), 3.12 – 3.05 (m, 1H), 2.90 (dt,  $J$  = 15.2, 4.2 Hz, 1H), 2.51 – 2.34 (m, 2H) ppm. **<sup>13</sup>C NMR** (176 MHz, Chloroform-*d*)  $\delta$  155.1, 137.4, 136.0, 130.1, 129.6, 126.1, 123.9, 121.9, 120.8, 119.3, 118.3, 117.3, 109.8, 109.0, 70.2, 62.4, 59.9, 32.7, 30.5, 22.7 ppm. **HRMS-ESI** ( $m/z$ ):  $[M + H]^+$  calculated for C<sub>20</sub>H<sub>19</sub>NO<sub>2</sub>  $[M+H]^+$ : 306.1416, found 306.1417.

(2*R*,2'*R*)-7-chloro-4,6-dimethoxy-2',9"-dimethyl-4",9"-dihydro-3*H*,3"*H*-dispiro[benzofuran-2,1'-cyclohexane-4',1"-pyrano[3,4-*b*]indol]-3-one **44j****44j**

Synthesized via procedure C, 42.8 mg, 89%. **<sup>1</sup>H NMR** (700 MHz, Chloroform-*d*)  $\delta$  7.50 (d,  $J$  = 7.7 Hz, 1H), 7.32 (d,  $J$  = 8.2 Hz, 1H), 7.24 – 7.19 (m, 1H), 7.10 (t,  $J$  = 7.4 Hz, 1H), 6.11 (d,  $J$  = 6.5 Hz, 1H), 4.03 – 3.96 (m, 11H), 2.90 – 2.84 (m, 1H), 2.86 – 2.75 (m, 2H), 2.70 (dd,  $J$  = 14.1, 12.6 Hz, 1H), 2.58 – 2.50 (m, 1H), 2.23 (dd,  $J$  = 8.9, 5.3 Hz, 1H), 2.06 – 1.99 (m, 1H), 1.94 (ddd,  $J$  = 14.2, 4.2, 2.4 Hz, 1H), 1.78 (ddd,  $J$  = 12.9, 4.3, 2.5 Hz, 1H), 0.84 (d,  $J$  = 6.8 Hz, 3H) ppm. **<sup>13</sup>C NMR** (176 MHz, Chloroform-*d*)  $\delta$  199.7, 168.8, 164.5, 157.8, 138.6, 137.9, 126.5, 121.8, 119.4, 118.3, 109.4, 107.9, 106.1, 93.0, 89.0, 73.5, 59.8, 57.2, 57.2, 56.6, 37.5, 33.5, 31.9, 28.2, 28.5, 23.1, 15.0. ppm. **HRMS-ESI** ( $m/z$ ):  $[M + H]^+$  calculated for C<sub>27</sub>H<sub>28</sub>ClNO<sub>5</sub>  $[M+H]^+$ : 481.1656 and 483.1627, found 481.1654 and 483.1623.

## Experimental

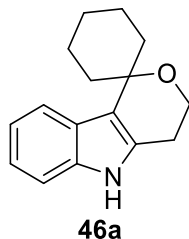
(5*R*,8*S*,9*R*,10*R*,13*S*,14*R*,17*S*)-9',10,13-trimethyl-17-((*S*)-6-methylheptan-2-yl)-1,2,4,4',5,6,7,8,9,9',10,11,12,13,14,15,16,17-octadecahydro-3'*H*-spiro[cyclopenta[*a*]phenanthrene-3,1'-pyrano[3,4-*b*]indole] **44k**



Synthesized via procedure C, 51.7 mg, 95%. **<sup>1</sup>H NMR** (500 MHz, Chloroform-*d*)  $\delta$  7.50 (d,  $J$  = 7.8 Hz, 1H), 7.29 (d,  $J$  = 8.2 Hz, 1H), 7.21 (ddd,  $J$  = 8.2, 6.9, 1.2 Hz, 1H), 7.17 – 7.05 (m, 1H), 4.05 – 3.88 (m, 2H), 3.82 (s, 3H), 2.94 – 2.72 (m, 2H), 2.06 – 1.96 (m, 2H), 1.95 – 1.87 (m, 2H), 1.87 – 1.74 (m, 2H), 1.68 (dq,  $J$  = 12.8, 3.4 Hz, 1H), 1.55 (dddd,  $J$  = 33.6, 17.4, 9.5, 3.5 Hz, 7H), 1.44 (s, 1H), 1.41 – 1.31 (m, 4H), 1.25 (qd,  $J$  = 12.7, 11.8, 3.5 Hz, 3H), 1.20 – 1.08 (m, 5H), 1.08 – 0.97 (m, 4H), 0.95 (s, 3H), 0.92 (d,  $J$  = 6.5 Hz, 3H), 0.88 (dd,  $J$  = 6.6, 2.5 Hz, 6H), 0.69 (s, 3H) ppm. **<sup>13</sup>C NMR** (126 MHz, Chloroform-*d*)  $\delta$  139.5, 137.4, 126.3, 121.4, 119.2, 118.1, 108.9, 107.9, 74.1, 59.2, 56.5, 56.3, 54.0, 42.6, 40.2, 40.0, 39.6, 37.4, 36.2, 35.9, 35.6, 35.4, 33.5, 32.0, 31.5, 29.7, 28.5, 28.3, 28.1, 24.2, 23.8, 23.0, 22.9, 22.6, 21.0, 18.7, 12.4, 12.2 ppm. **HRMS-ESI** ( $m/z$ ): [M + H]<sup>+</sup> calculated for C<sub>38</sub>H<sub>57</sub>NO [M+H]<sup>+</sup>: 544.4440, found 544.4434.

## $\gamma$ -TETRAHYDROPYRANOINDOLES

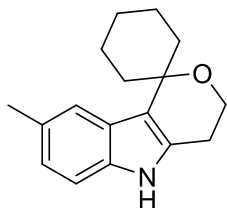
4',5'-dihydro-3'*H*-spiro[cyclohexane-1,1'-pyrano[4,3-*b*]indole] **46a**



Synthesized via procedure C, 23.7 mg, 98%. **<sup>1</sup>H NMR** (500 MHz, Chloroform-*d*)  $\delta$  7.92 (s, 1H), 7.67 – 7.53 (m, 1H), 7.31 (dd,  $J$  = 7.4, 1.4 Hz, 1H), 7.20 – 7.07 (m, 2H), 4.02 (t,  $J$  = 5.4 Hz, 2H), 2.79 (t,  $J$  = 5.5 Hz, 2H), 2.14 – 2.02 (m, 2H), 1.97 (dq,  $J$  = 14.2, 2.1 Hz, 2H), 1.87 – 1.75 (m, 4H), 1.64 (dt,  $J$  = 12.7, 3.2 Hz, 2H) ppm. **<sup>13</sup>C NMR** (126 MHz, Chloroform-*d*)  $\delta$  136.0, 131.2, 125.1, 136

121.3, 119.7, 119.4, 117.2, 111.2, 74.7, 58.6, 35.8, 26.1, 24.9, 22.0 ppm. **HRMS-ESI** ( $m/z$ ):  $[M + H]^+$  calculated for  $C_{16}H_{19}NO$   $[M+H]^+$ : 242.1467, found 242.1462.

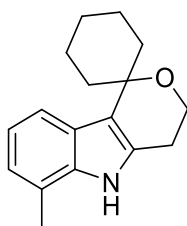
8'-methyl-4',5'-dihydro-3'*H*-spiro[cyclohexane-1,1'-pyrano[4,3-*b*]indol] **46b**



**46b**

Synthesized via procedure C, 24.2 mg, 95%.  **$^1H$  NMR** (700 MHz, Chloroform-*d*)  $\delta$  7.70 (s, 1H), 7.32 (s, 1H), 7.20 (d,  $J = 8.2$  Hz, 1H), 6.95 (d,  $J = 9.3$  Hz, 1H), 3.99 (t,  $J = 5.4$  Hz, 2H), 2.78 (t,  $J = 5.4$  Hz, 2H), 2.45 (s, 3H), 2.36 – 2.31 (m, 1H), 2.04 (td,  $J = 13.8, 4.2$  Hz, 2H), 1.95 – 1.91 (m, 2H), 1.81 – 1.74 (m, 3H), 1.62 (s, 2H), 1.43 (s, 1H) ppm.  **$^{13}C$  NMR** (176 MHz, Chloroform-*d*)  $\delta$  134.3, 131.2, 128.8, 125.3, 122.8, 119.1, 116.8, 110.8, 74.6, 58.6, 42.3, 35.7, 27.4, 26.1, 24.9, 22.0, 21.9 ppm. **HRMS-ESI** ( $m/z$ ):  $[M + H]^+$  calculated for  $C_{17}H_{21}NO$   $[M+H]^+$ : 255.1623, found 255.1620.

6'-methyl-4',5'-dihydro-3'*H*-spiro[cyclohexane-1,1'-pyrano[4,3-*b*]indol] **46c**

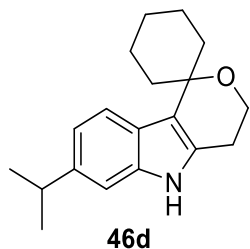


**46c**

Synthesized via procedure C, 22.6 mg, 89%.  **$^1H$  NMR** (700 MHz, Chloroform-*d*)  $\delta$  7.86 (s, 1H), 7.44 (d,  $J = 7.9$  Hz, 1H), 7.03 (t,  $J = 7.5$  Hz, 1H), 6.95 (d,  $J = 7.1$  Hz, 1H), 4.02 (t,  $J = 5.4$  Hz, 2H), 2.83 (d,  $J = 5.4$  Hz, 2H), 2.48 (s, 3H), 2.35 (t,  $J = 6.8$  Hz, 1H), 2.11 – 2.02 (m, 2H), 1.96 (d,  $J = 14.0$  Hz, 2H), 1.81 (t,  $J = 11.7$  Hz, 2H), 1.63 (d,  $J = 13.8$  Hz, 2H) ppm.  **$^{13}C$  NMR** (176 MHz, Chloroform-*d*)  $\delta$  135.4, 130.8, 124.5, 122.0, 120.3, 119.8, 117.7, 117.1, 74.6, 58.6, 42.3, 35.7, 27.3, 26.0, 24.9, 22.0, 17.0 ppm. **HRMS-ESI** ( $m/z$ ):  $[M + H]^+$  calculated for  $C_{17}H_{21}NO$   $[M+H]^+$ : 255.1623, found 255.1618.

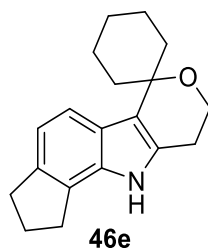
## Experimental

### 7'-isopropyl-4',5'-dihydro-3'*H*-spiro[cyclohexane-1,1'-pyrano[4,3-*b*]indole] **46d**

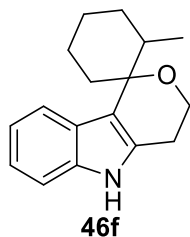


Synthesized via procedure C, 25.8 mg, 91%. **<sup>1</sup>H NMR** (700 MHz, Chloroform-*d*)  $\delta$  7.78 (s, 1H), 7.47 (d,  $J = 8.2$  Hz, 1H), 7.17 (d,  $J = 1.4$  Hz, 1H), 6.99 (dd,  $J = 8.2, 1.4$  Hz, 1H), 3.99 (t,  $J = 5.4$  Hz, 2H), 2.99 (p,  $J = 6.9$  Hz, 1H), 2.77 (t,  $J = 5.4$  Hz, 2H), 2.35 (t,  $J = 6.8$  Hz, 1H), 1.94 (d,  $J = 13.9$  Hz, 2H), 1.61 (d,  $J = 12.8$  Hz, 2H), 1.44 (s, 1H), 1.30 (d,  $J = 6.9$  Hz, 6H), 1.26 (dd,  $J = 6.9, 0.9$  Hz, 3H) ppm. **<sup>13</sup>C NMR** (176 MHz, Chloroform-*d*)  $\delta$  142.6, 136.3, 130.6, 123.2, 119.0, 118.9, 117.0, 108.5, 74.6, 58.7, 42.3, 35.8, 34.6, 27.3, 27.3, 26.1, 24.9, 24.9, 22.0 ppm. **HRMS-ESI** ( $m/z$ ):  $[M + H]^+$  calculated for C<sub>19</sub>H<sub>25</sub>NO  $[M+H]^+$ : 284.1936, found 284.1939.

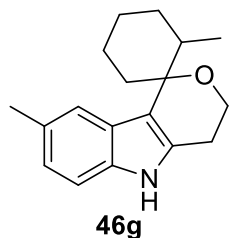
### 1',2',3',8',9',10'-hexahydrospiro[cyclohexane-1,6'-cyclopenta[*g*]pyrano[4,3-*b*]indole] **46e**



Synthesized via procedure C, 24.8 mg, 88%. **<sup>1</sup>H NMR** (700 MHz, Chloroform-*d*)  $\delta$  7.66 (s, 1H), 7.38 (d,  $J = 8.0$  Hz, 1H), 7.03 (d,  $J = 8.0$  Hz, 1H), 4.00 (t,  $J = 5.4$  Hz, 2H), 3.06 – 2.97 (m, 4H), 2.80 (t,  $J = 5.4$  Hz, 2H), 2.21 – 2.15 (m, 2H), 2.06 (td,  $J = 13.8, 4.3$  Hz, 2H), 1.97 – 1.90 (m, 2H), 1.84 – 1.73 (m, 3H), 1.64 – 1.56 (m, 2H), 1.26 (d,  $J = 2.3$  Hz, 2H) ppm. **<sup>13</sup>C NMR** (176 MHz, Chloroform-*d*)  $\delta$  138.0, 132.9, 130.2, 125.6, 123.6, 117.7, 117.4, 116.5, 74.7, 58.7, 35.7, 33.3, 30.3, 26.1, 25.8, 24.9, 22.0 ppm. **HRMS-ESI** ( $m/z$ ):  $[M + H]^+$  calculated for C<sub>19</sub>H<sub>23</sub>NO  $[M+H]^+$ : 282.1780, found 282.1789.

2-methyl-4',5'-dihydro-3'*H*-spiro[cyclohexane-1,1'-pyrano[4,3-*b*]indole] **46f**

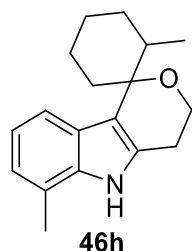
Synthesized via procedure C, 18.9 mg, 74%. **<sup>1</sup>H NMR** (700 MHz, Chloroform-*d*)  $\delta$  7.83 (s, 1H), 7.55 (d,  $J = 7.9$  Hz, 1H), 7.32 (dt,  $J = 8.1, 0.9$  Hz, 1H), 7.13 (ddd,  $J = 8.1, 7.0, 1.2$  Hz, 1H), 7.08 (ddd,  $J = 8.1, 7.1, 1.1$  Hz, 1H), 4.11 – 4.05 (m, 1H), 3.93 – 3.88 (m, 1H), 2.99 (ddd,  $J = 15.4, 11.2, 5.9$  Hz, 1H), 2.52 (ddd,  $J = 15.4, 3.3, 1.2$  Hz, 1H), 2.43 – 2.36 (m, 1H), 2.25 (ddd,  $J = 11.5, 6.7, 4.3$  Hz, 1H), 2.19 – 2.13 (m, 1H), 2.12 – 2.04 (m, 1H), 1.87 – 1.79 (m, 2H), 1.77 – 1.60 (m, 3H), 0.62 (d,  $J = 6.8$  Hz, 3H) ppm. **<sup>13</sup>C NMR** (176 MHz, Chloroform-*d*)  $\delta$  136.0, 132.1, 125.0, 121.3, 115.7, 111.1, 77.1, 58.7, 40.0, 34.6, 30.1, 26.9, 24.8, 22.0, 16.2 ppm. **HRMS-ESI** ( $m/z$ ): [M + H]<sup>+</sup> calculated for C<sub>17</sub>H<sub>21</sub>NO [M+H]<sup>+</sup>: 256.1623, found 256.1620.

2,8'-dimethyl-4',5'-dihydro-3'*H*-spiro[cyclohexane-1,1'-pyrano[4,3-*b*]indole] **46g**

Synthesized via procedure C, 19.4 mg, 72%. **<sup>1</sup>H NMR** (700 MHz, Chloroform-*d*)  $\delta$  7.77 (s, 1H), 7.33 (s, 1H), 7.20 (d,  $J = 8.2$  Hz, 1H), 6.96 (d,  $J = 8.2$  Hz, 1H), 4.08 (dd,  $J = 11.2, 5.8$  Hz, 1H), 3.90 (td,  $J = 11.2, 3.1$  Hz, 1H), 3.02 – 2.93 (m, 1H), 2.51 (d,  $J = 4.2$  Hz, 1H), 2.49 (s, 1H), 2.47 (s, 3H), 1.89 – 1.81 (m, 3H), 1.45 (s, 3H), 1.06 (d,  $J = 6.6$  Hz, 1H), 0.65 (d,  $J = 6.7$  Hz, 3H) ppm. **<sup>13</sup>C NMR** (176 MHz, Chloroform-*d*)  $\delta$  134.3, 132.3, 128.6, 125.3, 122.7, 119.2, 115.2, 110.7, 77.1, 58.7, 39.9, 34.5, 30.1, 27.2, 26.8, 24.8, 22.0, 21.9, 16.3 ppm. **HRMS-ESI** ( $m/z$ ): [M + H]<sup>+</sup> calculated for C<sub>18</sub>H<sub>23</sub>NO [M+H]<sup>+</sup>: 270.1780, found 270.1777.

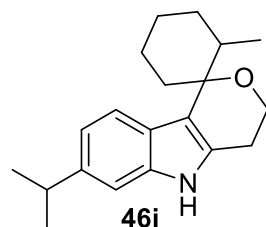
## Experimental

### 2,6'-dimethyl-4',5'-dihydro-3'*H*-spiro[cyclohexane-1,1'-pyrano[4,3-*b*]indole] **46h**

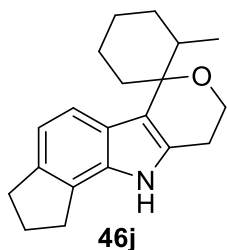


Synthesized via procedure C, 14.5 mg, 54%. **<sup>1</sup>H NMR** (700 MHz, Chloroform-*d*)  $\delta$  7.77 (s, 1H), 7.41 (d,  $J = 7.9$  Hz, 1H), 7.01 (t,  $J = 7.5$  Hz, 1H), 6.95 (d,  $J = 7.1$  Hz, 1H), 4.09 (dd,  $J = 11.2, 5.8$  Hz, 1H), 3.91 (td,  $J = 11.2, 3.3$  Hz, 1H), 3.04 – 2.97 (m, 1H), 2.58 – 2.54 (m, 1H), 2.48 (s, 3H), 2.19 – 2.11 (m, 1H), 1.90 – 1.79 (m, 2H), 1.57 (dd,  $J = 12.6, 3.5$  Hz, 2H), 1.44 (s, 2H), 1.04 (d,  $J = 6.6$  Hz, 1H), 0.63 (d,  $J = 6.7$  Hz, 3H) **<sup>13</sup>C NMR** (176 MHz, Chloroform-*d*)  $\delta$  135.4, 131.8, 124.5, 122.0, 120.2, 119.7, 117.2, 116.2, 58.7, 40.0, 34.5, 30.1, 27.2, 26.9, 24.8, 22.0, 17.1, 16.2 ppm. **HRMS-ESI** ( $m/z$ ): [M + H]<sup>+</sup> calculated for C<sub>18</sub>H<sub>23</sub>NO [M+H]<sup>+</sup>: 270.1780, found 270.1779.

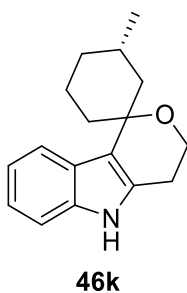
### 7'-isopropyl-2-methyl-4',5'-dihydro-3'*H*-spiro[cyclohexane-1,1'-pyrano[4,3-*b*]indole] **46i**



Synthesized via procedure C, 18.1 mg, 61%. **<sup>1</sup>H NMR** (700 MHz, Chloroform-*d*)  $\delta$  7.71 (s, 1H), 7.45 (d,  $J = 8.2$  Hz, 1H), 7.17 (d,  $J = 1.4$  Hz, 1H), 6.97 (dd,  $J = 8.2, 1.4$  Hz, 1H), 4.10 – 4.03 (m, 1H), 3.88 (td,  $J = 11.1, 3.2$  Hz, 1H), 3.03 – 2.93 (m, 2H), 2.49 (dd,  $J = 15.3, 4.3$  Hz, 1H), 2.23 (ddd,  $J = 11.6, 6.7, 4.5$  Hz, 1H), 1.81 (td,  $J = 13.9, 3.9$  Hz, 2H), 1.72 (ddd,  $J = 16.8, 8.5, 3.7$  Hz, 2H), 1.58 – 1.53 (m, 2H), 1.31 (d,  $J = 6.9$  Hz, 7H), 0.63 (d,  $J = 6.7$  Hz, 3H) ppm. **<sup>13</sup>C NMR** (176 MHz, Chloroform-*d*)  $\delta$  142.4, 136.4, 131.6, 123.2, 119.1, 118.8, 115.5, 108.4, 77.1, 58.8, 40.1, 34.6, 34.5, 30.1, 26.9, 24.9, 24.8, 24.8, 22.0, 16.3 ppm. **HRMS-ESI** ( $m/z$ ): [M + H]<sup>+</sup> calculated for C<sub>20</sub>H<sub>27</sub>NO [M+H]<sup>+</sup>: 298.2093, found 298.2051.

2-methyl-1',2',3',8',9',10'-hexahydrospiro[cyclohexane-1,6'-cyclopenta[*g*]pyrano[4,3-*b*]indole] **46j**

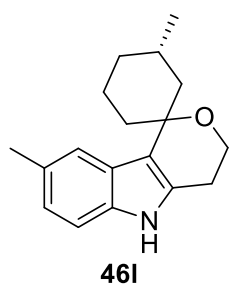
Synthesized via procedure C, 22.2 mg, 75%. **<sup>1</sup>H NMR** (700 MHz, Chloroform-*d*)  $\delta$  7.62 (s, 1H), 7.36 (d,  $J = 8.0$  Hz, 1H), 7.01 (d,  $J = 8.0$  Hz, 1H), 4.09 – 4.05 (m, 1H), 3.89 (td,  $J = 11.2, 3.3$  Hz, 1H), 3.02 (dq,  $J = 13.0, 6.8, 5.9$  Hz, 5H), 2.57 – 2.49 (m, 1H), 2.29 – 2.24 (m, 1H), 2.23 – 2.17 (m, 2H), 1.88 – 1.80 (m, 3H), 1.60 (dd,  $J = 14.4, 2.3$  Hz, 1H), 1.52 – 1.45 (m, 1H), 1.26 (s, 3H), 0.63 (d,  $J = 6.7$  Hz, 3H) ppm. **<sup>13</sup>C NMR** (176 MHz, Chloroform-*d*)  $\delta$  137.9, 133.0, 131.3, 125.5, 123.6, 117.5, 116.4, 116.2, 58.8, 40.0, 34.5, 33.4, 30.3, 30.1, 26.9, 25.8, 24.9, 22.0, 16.3 ppm. **HRMS-ESI** ( $m/z$ ):  $[M + H]^+$  calculated for C<sub>20</sub>H<sub>25</sub>NO  $[M+H]^+$ : 296.1936, found 296.1930.

(3*S*)-3-methyl-4',5'-dihydro-3'*H*-spiro[cyclohexane-1,1'-pyrano[4,3-*b*]indole] **46k**

Synthesized via procedure C, 20.9 mg, 82%, d.r. 9:1. **<sup>1</sup>H NMR** (700 MHz, Chloroform-*d*)  $\delta$  7.78 (s, 1H), 7.33 (dd,  $J = 8.0, 1.0$  Hz, 1H), 7.32 – 7.28 (m, 1H), 7.13 (d,  $J = 8.0$  Hz, 1H), 6.89 (dd,  $J = 8.0, 1.0$  Hz, 1H), 3.99 – 3.87 (m, 2H), 2.78 – 2.65 (m, 2H), 1.93 – 1.87 (m, 4H), 1.80 – 1.69 (m, 2H), 1.65 – 1.60 (m, 1H), 1.55 – 1.49 (m, 1H), 1.00 (d,  $J = 6.0$  Hz, 1H), 0.87 (d,  $J = 6.0$  Hz, 3H) ppm. **<sup>13</sup>C NMR** (176 MHz, Chloroform-*d*)  $\delta$  133.2, 130.7, 127.8, 124.6, 121.5, 118.8, 115.9, 111.0, 74.4, 57.4, 43.8, 33.8, 27.7, 24.0, 21.8, 21.4, 20.1 ppm. **HRMS-ESI** ( $m/z$ ):  $[M + H]^+$  calculated for C<sub>17</sub>H<sub>21</sub>NO  $[M+H]^+$ : 256.1624, found 256.1629.

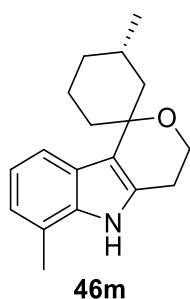
## Experimental

### (3*S*)-3,8'-dimethyl-4',5'-dihydro-3'*H*-spiro[cyclohexane-1,1'-pyrano[4,3-*b*]indole] **46l**



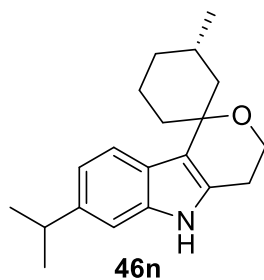
Synthesized via procedure C, 21.6 mg, 80%, d.r. 9:1. **<sup>1</sup>H NMR** (700 MHz, Chloroform-*d*)  $\delta$  7.80 (s, 1H), 7.32 (s, 1H), 7.19 (d,  $J = 8.2$  Hz, 1H), 6.96 (dd,  $J = 8.2, 1.1$  Hz, 1H), 4.03 – 3.94 (m, 2H), 2.82 – 2.70 (m, 2H), 2.48 (s, 3H), 1.98 – 1.91 (m, 4H), 1.82 (ddd,  $J = 14.7, 10.0, 4.1$  Hz, 2H), 1.73 – 1.68 (m, 1H), 1.68 – 1.64 (m, 1H), 1.04 (d,  $J = 6.5$  Hz, 1H), 0.95 (d,  $J = 6.5$  Hz, 3H) ppm. **<sup>13</sup>C NMR** (176 MHz, Chloroform-*d*)  $\delta$  134.3, 131.2, 128.8, 125.2, 122.8, 119.0, 116.4, 110.8, 75.4, 58.6, 44.6, 35.0, 34.9, 28.0, 24.9, 22.9, 22.0, 21.9 ppm. **HRMS-ESI** ( $m/z$ ): [M + H]<sup>+</sup> calculated for C<sub>18</sub>H<sub>23</sub>NO [M+H]<sup>+</sup>: 270.1780, found 270.1768.

### (3*S*)-3,6'-dimethyl-4',5'-dihydro-3'*H*-spiro[cyclohexane-1,1'-pyrano[4,3-*b*]indole] **46m**

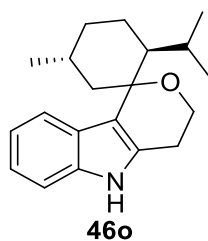


Synthesized via procedure C, 20.2 mg, 75%, d.r. 10:1. **<sup>1</sup>H NMR** (700 MHz, Chloroform-*d*)  $\delta$  7.86 (s, 1H), 7.42 (d,  $J = 7.9$  Hz, 1H), 7.03 (t,  $J = 7.5$  Hz, 1H), 6.95 (d,  $J = 7.1$  Hz, 1H), 4.05 – 3.97 (m, 2H), 2.88 – 2.77 (m, 2H), 2.48 (s, 3H), 1.95 (dd,  $J = 15.9, 8.3$  Hz, 4H), 1.82 – 1.79 (m, 2H), 1.45 (s, 1H), 1.03 (d,  $J = 6.5$  Hz, 2H), 0.94 (d,  $J = 6.5$  Hz, 3H) ppm. **<sup>13</sup>C NMR** (176 MHz, Chloroform-*d*)  $\delta$  135.4, 130.8, 124.5, 122.0, 120.3, 119.8, 117.4, 117.1, 75.3, 58.7, 44.7, 35.0, 34.9, 27.9, 24.9, 22.9, 22.0, 17.0 ppm. **HRMS-ESI** ( $m/z$ ): [M + H]<sup>+</sup> calculated for C<sub>18</sub>H<sub>23</sub>NO [M+H]<sup>+</sup>: 270.1780, found 270.1773.



**(3S)-7'-isopropyl-3-methyl-4',5'-dihydro-3'*H*-spiro[cyclohexane-1,1'-pyrano[4,3-*b*]indole] 46n**

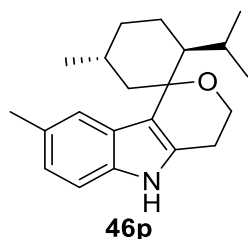
Synthesized via procedure C, 19.9 mg, 67%, d.r. 9:1. **<sup>1</sup>H NMR** (700 MHz, Chloroform-*d*)  $\delta$  7.74 (s, 1H), 7.45 (d,  $J = 8.2$  Hz, 1H), 7.17 (d,  $J = 1.3$  Hz, 1H), 6.99 (d,  $J = 8.2$  Hz, 1H), 4.02 – 3.94 (m, 2H), 3.02 – 2.96 (m, 1H), 2.83 – 2.77 (m, 1H), 2.77 – 2.72 (m, 1H), 2.40 (dd,  $J = 4.2, 2.1$  Hz, 1H), 1.95 – 1.89 (m, 3H), 1.79 (td,  $J = 12.3, 3.0$  Hz, 2H), 1.30 (d,  $J = 6.9$  Hz, 7H), 1.03 (d,  $J = 6.5$  Hz, 2H), 0.92 (d,  $J = 6.5$  Hz, 3H) ppm. **<sup>13</sup>C NMR** (176 MHz, Chloroform-*d*)  $\delta$  142.6, 136.3, 130.6, 123.2, 119.0, 118.9, 116.8, 108.5, 75.3, 58.8, 44.8, 35.0, 34.9, 34.6, 28.0, 24.9, 24.8, 22.9, 22.0 ppm. **HRMS-ESI** ( $m/z$ ):  $[M + H]^+$  calculated for C<sub>20</sub>H<sub>27</sub>NO  $[M+H]^+$ : 298.2093, found 298.2100.

**(2S,5R)-2-isopropyl-5-methyl-4',5'-dihydro-3'*H*-spiro[cyclohexane-1,1'-pyrano[4,3-*b*]indole] 46o**

Synthesized via procedure C, 28.6 mg, 96%. **<sup>1</sup>H NMR** (500 MHz, Chloroform-*d*)  $\delta$  7.81 (s, 1H), 7.51 (d,  $J = 7.8$  Hz, 1H), 7.32 (d,  $J = 8.0$  Hz, 1H), 7.09 (dt,  $J = 28.6, 7.5$  Hz, 2H), 4.06 (d,  $J = 17.0$  Hz, 1H), 3.90 (d,  $J = 22.5$  Hz, 1H), 2.99 (d,  $J = 32.8$  Hz, 1H), 2.52 (d,  $J = 15.5$  Hz, 1H), 2.13 (d,  $J = 16.5$  Hz, 1H), 1.95 (d,  $J = 12.5$  Hz, 1H), 1.87 (s, 2H), 1.77 – 1.66 (m, 1H), 1.50 (d,  $J = 62.0$  Hz, 3H), 1.11 (td,  $J = 12.9, 3.8$  Hz, 1H), 0.89 (d,  $J = 6.4$  Hz, 3H), 0.82 (d,  $J = 6.9$  Hz, 3H), 0.66 (d,  $J = 7.0$  Hz, 3H) ppm. **<sup>13</sup>C NMR** (126 MHz, Chloroform-*d*)  $\delta$  135.6, 131.8, 124.8, 121.0, 119.3, 119.1, 115.6, 110.8, 79.1, 58.1, 49.5, 43.6, 35.6, 27.9, 27.4, 24.5, 23.9, 22.4, 20.7, 18.8 ppm. **HRMS-ESI** ( $m/z$ ):  $[M + H]^+$  calculated for C<sub>20</sub>H<sub>27</sub>NO  $[M+H]^+$ : 298.2093, found 298.1095.

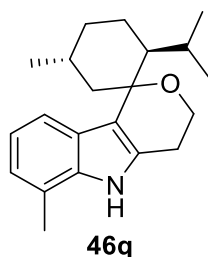
## Experimental

(2*S*,5*R*)-2-isopropyl-5,8'-dimethyl-4',5'-dihydro-3'*H*-spiro[cyclohexane-1,1'-pyrano[4,3]indole]**46p**



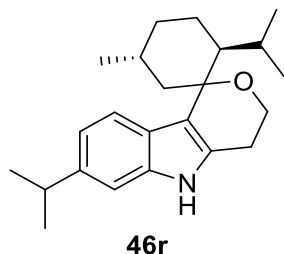
Synthesized via procedure C, 27.4 mg, 88%. **<sup>1</sup>H NMR** (700 MHz, Chloroform-*d*)  $\delta$  7.69 (s, 1H), 7.27 (s, 1H), 7.19 (d,  $J = 8.2$  Hz, 1H), 6.94 (d,  $J = 8.2$  Hz, 1H), 4.04 (dd,  $J = 11.2, 5.4$  Hz, 1H), 3.88 (td,  $J = 11.2, 3.2$  Hz, 1H), 3.02 – 2.94 (m, 1H), 2.50 (d,  $J = 15.3$  Hz, 1H), 2.45 (s, 3H), 2.12 (dd,  $J = 15.5, 4.3$  Hz, 1H), 1.94 (dd,  $J = 13.5, 4.2$  Hz, 1H), 1.91 – 1.86 (m, 2H), 1.77 – 1.68 (m, 2H), 1.48 – 1.41 (m, 1H), 1.26 (s, 3H), 0.90 (d,  $J = 6.5$  Hz, 3H), 0.82 (d,  $J = 6.9$  Hz, 3H), 0.68 (d,  $J = 7.0$  Hz, 3H) ppm. **<sup>13</sup>C NMR** (176 MHz, Chloroform-*d*)  $\delta$  134.3, 132.2, 128.8, 125.4, 122.8, 119.2, 115.5, 110.7, 79.5, 58.4, 49.7, 43.9, 35.9, 28.2, 27.7, 24.9, 24.3, 22.7, 22.0, 21.0, 19.2 ppm. **HRMS-ESI** ( $m/z$ ):  $[M + H]^+$  calculated for C<sub>21</sub>H<sub>29</sub>NO  $[M+H]^+$ : 312.2249, found 312.2247.

(2*S*,5*R*)-2-isopropyl-5,6'-dimethyl-4',5'-dihydro-3'*H*-spiro[cyclohexane-1,1'-pyrano[4,3]indole]**46q**



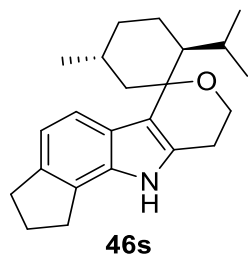
Synthesized via procedure C, 22.7 mg, 73%. **<sup>1</sup>H NMR** (700 MHz, Chloroform-*d*)  $\delta$  7.65 (s, 1H), 7.29 (d,  $J = 7.9$  Hz, 1H), 6.94 – 6.90 (m, 1H), 6.86 (d,  $J = 7.1$  Hz, 1H), 3.99 (dd,  $J = 11.2, 5.6$  Hz, 1H), 3.83 (td,  $J = 11.2, 3.3$  Hz, 1H), 2.96 – 2.91 (m, 1H), 2.47 (dd,  $J = 15.1, 2.8$  Hz, 2H), 2.40 (s, 3H), 2.10 (s, 1H), 2.08 – 2.02 (m, 1H), 1.90 – 1.86 (m, 1H), 1.42 – 1.36 (m, 1H), 1.02 (t,  $J = 13.1, 3.6$  Hz, 1H), 0.94 (d,  $J = 6.5$  Hz, 1H), 0.81 (d,  $J = 6.4$  Hz, 3H), 0.78 (dd,  $J = 6.8, 3.4$  Hz, 2H), 0.75 (d,  $J = 6.9$  Hz, 3H), 0.59 (d,  $J = 7.0$  Hz, 3H) ppm. **<sup>13</sup>C NMR** (176 MHz, Chloroform-*d*)  $\delta$  135.4, 131.7, 124.6, 122.1, 120.1, 119.9, 117.2, 116.4, 79.5, 58.5, 49.8, 44.0, 35.9, 28.2, 27.7, 24.8, 24.2, 22.7, 21.0, 19.1, 17.1 ppm. **HRMS-ESI** ( $m/z$ ):  $[M + H]^+$  calculated for C<sub>21</sub>H<sub>29</sub>NO  $[M+H]^+$ : 312.2249, found 312.2245.

(2*S*,5*R*)-2,7'-diisopropyl-5-methyl-4',5'-dihydro-3'*H*-spiro[cyclohexane-1,1'-pyrano[4,3]indole] **46r**



Synthesized via procedure C, 23.8 mg, 70%. **<sup>1</sup>H NMR** (700 MHz, Chloroform-*d*)  $\delta$  7.69 (s, 1H), 7.40 (d,  $J = 8.2$  Hz, 1H), 7.16 (d,  $J = 7.3$  Hz, 1H), 6.96 – 6.93 (m, 1H), 3.92 – 3.85 (m, 2H), 3.01 – 2.94 (m, 2H), 2.89 – 2.83 (m, 1H), 2.17 (s, 1H), 2.05 (s, 1H), 1.30 (ddd,  $J = 7.0, 4.3, 2.7$  Hz, 8H), 1.26 (d,  $J = 2.3$  Hz, 3H), 1.01 (d,  $J = 6.5$  Hz, 1H), 0.98 (d,  $J = 6.6$  Hz, 1H), 0.95 (d,  $J = 6.5$  Hz, 1H), 0.91 (d,  $J = 6.8$  Hz, 1H), 0.88 (d,  $J = 6.3$  Hz, 2H), 0.86 – 0.81 (m, 6H), 0.68 (d,  $J = 7.0$  Hz, 1H) ppm. **<sup>13</sup>C NMR** (176 MHz, Chloroform-*d*)  $\delta$  119.1, 119.0, 118.8, 108.4, 79.5, 63.00, 62.9, 58.5, 56.3, 51.2, 49.9, 44.09, 35.9, 35.8, 34.6, 34.5, 34.3, 28.2, 27.7, 24.9, 24.3, 22.7, 19.1 ppm. **HRMS-ESI** ( $m/z$ ):  $[M + H]^+$  calculated for C<sub>23</sub>H<sub>33</sub>NO  $[M+H]^+$ : 340.2562, found 340.2561.

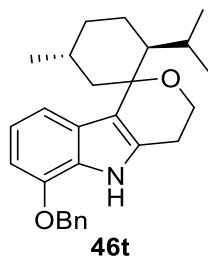
(2*S*,5*R*)-2-isopropyl-5-methyl-1',2',3',8',9',10'-hexahydrospiro[cyclohexane-1,6'-cyclopenta[*g*]pyrano[4,3-*b*]indole] **46s**



Synthesized via procedure C, 23.3 mg, 69%. **<sup>1</sup>H NMR** (700 MHz, Chloroform-*d*)  $\delta$  7.61 (s, 1H), 7.32 (d,  $J = 8.0$  Hz, 1H), 7.00 (d,  $J = 8.0$  Hz, 1H), 4.05 (dd,  $J = 11.2, 5.4$  Hz, 1H), 3.89 (dd,  $J = 11.2, 3.3$  Hz, 1H), 3.05 – 2.97 (m, 6H), 2.52 (dd,  $J = 15.3, 2.4$  Hz, 1H), 2.23 – 2.15 (m, 3H), 2.05 (s, 1H), 1.26 (d,  $J = 2.6$  Hz, 3H), 0.88 (d,  $J = 6.4$  Hz, 3H), 0.85 (dd,  $J = 6.7, 3.2$  Hz, 2H), 0.83 (d,  $J = 6.9$  Hz, 3H), 0.68 (d,  $J = 7.0$  Hz, 3H) ppm. **<sup>13</sup>C NMR** (176 MHz, Chloroform-*d*)  $\delta$  137.9, 133.0, 131.1, 125.5, 123.7, 117.5, 116.5, 116.5, 79.5, 58.5, 49.8, 44.0, 35.9, 33.4, 30.3, 28.2, 27.7, 25.7, 24.9, 24.3, 22.7, 21.0, 19.1 ppm. **HRMS-ESI** ( $m/z$ ):  $[M + H]^+$  calculated for C<sub>23</sub>H<sub>31</sub>NO  $[M+H]^+$ : 338.2406, found 338.2400.

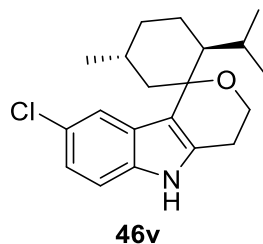
## Experimental

(2*S*,5*R*)-6'-(benzyloxy)-2-isopropyl-5-methyl-4',5'-dihydro-3'*H*-spiro[cyclohexane-1,1'-pyrano[4,3-*b*]indole] **46t**



Synthesized via procedure C, 30.3 mg, 75%. **<sup>1</sup>H NMR** (700 MHz, Chloroform-*d*)  $\delta$  8.08 (s, 1H), 7.51 – 7.46 (m, 2H), 7.41 (t,  $J$  = 7.5 Hz, 2H), 7.37 (d,  $J$  = 7.3 Hz, 1H), 7.14 (d,  $J$  = 8.0 Hz, 1H), 6.97 (t,  $J$  = 7.8 Hz, 1H), 6.69 (d,  $J$  = 7.7 Hz, 1H), 5.22 – 5.16 (m, 2H), 4.04 (dd,  $J$  = 11.2, 5.6 Hz, 1H), 3.92 – 3.86 (m, 1H), 3.00 – 2.94 (m, 1H), 2.51 (dd,  $J$  = 15.4, 2.6 Hz, 1H), 1.48 – 1.42 (m, 1H), 1.26 (s, 3H), 1.09 (dd,  $J$  = 13.0, 3.6 Hz, 1H), 1.01 (d,  $J$  = 6.5 Hz, 1H), 0.97 (d,  $J$  = 6.5 Hz, 1H), 0.92 (d,  $J$  = 6.8 Hz, 1H), 0.89 (d,  $J$  = 6.4 Hz, 3H), 0.87 – 0.84 (m, 3H), 0.82 (d,  $J$  = 6.9 Hz, 3H), 0.67 (d,  $J$  = 7.0 Hz, 2H) ppm. **<sup>13</sup>C NMR** (176 MHz, Chloroform-*d*)  $\delta$  145.5, 137.5, 131.7, 128.9, 128.5, 128.2, 126.5, 126.2, 119.9, 112.6, 102.8, 79.5, 70.5, 58.5, 49.9, 44.1, 35.9, 28.2, 27.7, 24.8, 24.2, 22.7, 21.0, 19.1 ppm. **HRMS-ESI** ( $m/z$ ):  $[M + H]^+$  calculated for C<sub>27</sub>H<sub>33</sub>NO<sub>2</sub>  $[M+H]^+$ : 404.2511, found 404.2510.

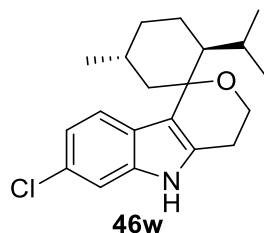
(2*S*,5*R*)-8'-chloro-2-isopropyl-5-methyl-4',5'-dihydro-3'*H*-spiro[cyclohexane-1,1'-pyrano[4,3-*b*]indole] **46v**



Synthesized via procedure C, 19.9 mg, 60%. **<sup>1</sup>H NMR** (500 MHz, Chloroform-*d*)  $\delta$  7.86 (s, 1H), 7.44 (d,  $J$  = 1.9 Hz, 1H), 7.22 (d,  $J$  = 8.6 Hz, 1H), 7.07 (dd,  $J$  = 8.6, 2.0 Hz, 1H), 4.05 (dd,  $J$  = 11.2, 5.4 Hz, 1H), 3.87 (td,  $J$  = 11.3, 3.2 Hz, 1H), 2.98 (ddd,  $J$  = 15.7, 11.4, 6.1 Hz, 1H), 2.55 – 2.48 (m, 1H), 2.10 (dt,  $J$  = 14.0, 3.3 Hz, 2H), 1.70 (dd,  $J$  = 12.9, 3.3 Hz, 2H), 1.42 (d,  $J$  = 1.6 Hz, 1H), 1.33 (s, 1H), 1.00 (dd,  $J$  = 8.5, 6.5 Hz, 2H), 0.90 (d,  $J$  = 6.4 Hz, 3H), 0.81 (d,  $J$  = 6.9 Hz, 3H), 0.68 (d,  $J$  = 7.0 Hz, 3H) ppm. **<sup>13</sup>C NMR** (126 MHz, Chloroform-*d*)  $\delta$  134.3, 133.8, 126.2, 125.3, 121.6, 118.8, 115.9, 112.0, 79.3, 58.4, 49.9, 43.9, 35.8, 28.2, 27.8, 24.3, 22.7, 21.0, 19.2 ppm. **HRMS-**

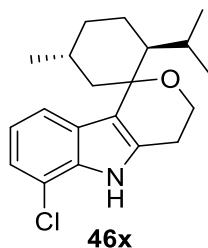
ESI ( $m/z$ ):  $[M + H]^+$  calculated for  $C_{20}H_{26}NOCl$   $[M+H]^+$ : 332.1703 and 334.1673, found 332.1702 and 334.1671.

(2*S*,5*R*)-7'-chloro-2-isopropyl-5-methyl-4',5'-dihydro-3'*H*-spiro[cyclohexane-1,1'-pyrano[4,3-*b*]indole] **46w**



Synthesized via procedure C, 13.6 mg, 41%.  $^1H$  NMR (700 MHz, Chloroform-*d*)  $\delta$  7.37 (d,  $J = 8.4$  Hz, 1H), 7.33 (d,  $J = 1.7$  Hz, 1H), 7.04 (dd,  $J = 8.4, 1.8$  Hz, 1H), 6.87 (s, 1H), 4.21 (t,  $J = 5.3$  Hz, 2H), 4.00 – 3.95 (m, 2H), 2.63 (p,  $J = 6.9$  Hz, 1H), 2.37 – 2.32 (m, 1H), 2.29 (q,  $J = 9.4, 8.5$  Hz, 1H), 1.32 – 1.19 (m, 10H), 0.98 (d,  $J = 6.5$  Hz, 3H), 0.90 – 0.85 (m, 8H) ppm.  $^{13}C$  NMR (176 MHz, Chloroform-*d*)  $\delta$  141.0, 128.0, 126.9, 126.2, 122.3, 121.3, 120.0, 109.6, 62.3, 49.0, 42.0, 39.1, 34.8, 32.3, 31.6, 31.1, 30.0, 29.7, 29.4, 23.2, 23.0, 22.0, 21.8, 21.3, 14.5 ppm. HRMS-ESI ( $m/z$ ):  $[M + H]^+$  calculated for  $C_{20}H_{26}NOCl$   $[M+H]^+$ : 332.1703 and 334.1673, found 332.1700 and 334.1669.

(2*S*,5*R*)-6'-chloro-2-isopropyl-5-methyl-4',5'-dihydro-3'*H*-spiro[cyclohexane-1,1'-pyrano[4,3-*b*]indole] **46x**

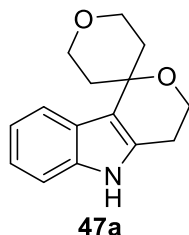


Synthesized via procedure C, 21.2 mg, 64%.  $^1H$  NMR (700 MHz, Chloroform-*d*)  $\delta$  7.36 (d,  $J = 1.0$  Hz, 1H), 7.15 (s, 1H), 6.97 (t,  $J = 7.7$  Hz, 1H), 6.87 (s, 1H), 4.64 (t,  $J = 5.5$  Hz, 2H), 4.01 (t,  $J = 5.4$  Hz, 2H), 2.59 (p,  $J = 6.9$  Hz, 1H), 2.27 (dd,  $J = 17.0, 4.9$  Hz, 1H), 2.20 (dt,  $J = 17.4, 2.7$  Hz, 1H), 2.14 – 2.07 (m, 1H), 1.91 – 1.85 (m, 2H), 1.85 – 1.76 (m, 2H), 1.34 – 1.25 (m, 3H), 0.98 (d,  $J = 6.5$  Hz, 1H), 0.88 (d,  $J = 6.9$  Hz, 6H) ppm.  $^{13}C$  NMR (176 MHz, Chloroform-*d*)  $\delta$  141.3, 131.7, 128.8, 123.6, 122.3, 120.0, 119.2, 119.2, 116.6, 63.9, 50.9, 41.9, 31.7, 31.2, 29.7, 23.1, 22.0,

## Experimental

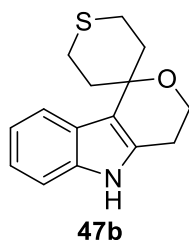
21.7, 21.3 ppm. **HRMS-ESI** ( $m/z$ ):  $[M + H]^+$  calculated for  $C_{20}H_{26}NOCl$   $[M+H]^+$ : 332.1703 and 334.1673, found 332.1703 and 334.1672.

2,3,4',5,5',6-hexahydro-3'*H*-spiro[pyran-4,1'-pyrano[4,3-*b*]indole] **47a**

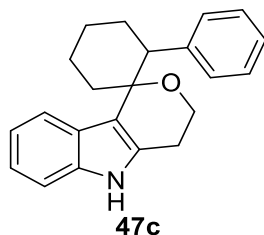


Synthesized via procedure C, 21.7 mg, 89%. **<sup>1</sup>H NMR** (500 MHz, Chloroform-*d*)  $\delta$  7.94 (s, 1H), 7.53 (d,  $J = 7.8$  Hz, 1H), 7.29 – 7.22 (m, 1H), 7.06 (dtd,  $J = 21.8, 7.2, 1.2$  Hz, 2H), 3.99 – 3.77 (m, 6H), 2.74 (t,  $J = 5.4$  Hz, 2H), 2.45 – 2.32 (m, 2H), 1.71 (d,  $J = 14.1$  Hz, 2H) ppm. **<sup>13</sup>C NMR** (126 MHz, Chloroform-*d*)  $\delta$  135.6, 131.2, 124.5, 121.3, 119.6, 118.7, 115.2, 111.0, 71.8, 63.7, 58.6, 35.7, 24.5 ppm. **HRMS-ESI** ( $m/z$ ):  $[M + H]^+$  calculated for  $C_{15}H_{17}NO_2$   $[M+H]^+$ : 244.1259, found 244.1255.

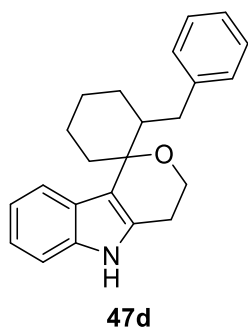
2',3',4,5,5',6'-hexahydro-3'*H*-spiro[pyrano[4,3-*b*]indole-1,4'-thiopyran] **47b**



Synthesized via procedure C, 22.3 mg, 86%. **<sup>1</sup>H NMR** (500 MHz, Chloroform-*d*)  $\delta$  7.94 (s, 1H), 7.64 (d,  $J = 7.7$  Hz, 1H), 7.32 (d,  $J = 7.9$  Hz, 1H), 7.21 – 7.06 (m, 2H), 3.99 (t,  $J = 5.4$  Hz, 2H), 3.30 – 3.17 (m, 2H), 2.80 (t,  $J = 5.4$  Hz, 2H), 2.51 – 2.35 (m, 4H), 2.28 – 2.13 (m, 2H) ppm. **<sup>13</sup>C NMR** (126 MHz, Chloroform-*d*)  $\delta$  135.9, 131.1, 124.7, 121.7, 119.9, 119.3, 116.6, 111.3, 72.9, 58.6, 36.7, 24.7, 24.2 ppm. **HRMS-ESI** ( $m/z$ ):  $[M + H]^+$  calculated for  $C_{15}H_{17}NOS$   $[M+H]^+$ : 260.1031, found 260.1029.

2-phenyl-4',5'-dihydro-3'*H*-spiro[cyclohexane-1,1'-pyrano[4,3-*b*]indole] **47c**

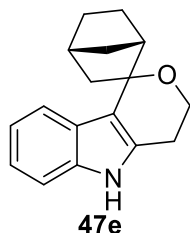
Synthesized via procedure C, 24.4 mg, 77%. **<sup>1</sup>H NMR** (500 MHz, Chloroform-*d*)  $\delta$  7.64 (d,  $J$  = 7.7 Hz, 1H), 7.38 (s, 1H), 7.26 (t,  $J$  = 7.5 Hz, 2H), 7.20 – 7.17 (m, 1H), 7.10 – 7.06 (m, 2H), 6.92 – 6.89 (m, 1H), 6.86 (d,  $J$  = 7.5 Hz, 2H), 3.91 (ddd,  $J$  = 11.1, 5.5, 1.7 Hz, 1H), 3.70 (td,  $J$  = 10.8, 3.3 Hz, 1H), 3.53 (dd,  $J$  = 12.3, 5.4 Hz, 1H), 3.25 (dd,  $J$  = 13.0, 3.6 Hz, 1H), 2.50 – 2.42 (m, 1H), 2.38 (s, 1H), 2.30 – 2.17 (m, 3H), 2.03 – 1.98 (m, 1H), 1.94 (ddd,  $J$  = 16.2, 7.7, 3.6 Hz, 2H), 1.90 – 1.84 (m, 1H) ppm. **<sup>13</sup>C NMR** (126 MHz, Chloroform-*d*)  $\delta$  143.6, 138.8, 135.4, 131.9, 129.2, 128.4, 126.7, 125.5, 120.7, 119.3, 114.8, 110.9, 76.7, 58.9, 57.5, 51.9, 42.3, 35.2, 27.9, 25.4, 24.1, 21.7 ppm. **HRMS-ESI** ( $m/z$ ):  $[M + H]^+$  calculated for C<sub>22</sub>H<sub>23</sub>NO  $[M+H]^+$ : 318.1780, found 318.1785.

2-benzyl-4',5'-dihydro-3'*H*-spiro[cyclohexane-1,1'-pyrano[4,3-*b*]indole] **47d**

Synthesized via procedure C, 24.9 mg, 75%. **<sup>1</sup>H NMR** (500 MHz, Chloroform-*d*)  $\delta$  7.91 (s, 1H), 7.72 – 7.58 (m, 1H), 7.35 (dd,  $J$  = 7.1, 1.8 Hz, 1H), 7.28 (t,  $J$  = 7.5 Hz, 1H), 7.20 – 7.12 (m, 5H), 7.09 – 7.05 (m, 1H), 6.85 (d,  $J$  = 7.2 Hz, 2H), 4.14 (dd,  $J$  = 11.3, 5.9 Hz, 1H), 3.97 (td,  $J$  = 11.3, 3.3 Hz, 1H), 3.24 (dd,  $J$  = 13.9, 4.8 Hz, 1H), 3.05 (ddd,  $J$  = 15.8, 11.3, 6.0 Hz, 1H), 2.58 (dd,  $J$  = 15.5, 3.1 Hz, 1H), 2.45 – 2.40 (m, 1H), 2.34 – 2.21 (m, 2H), 2.05 (ddd,  $J$  = 5.4, 3.7, 2.1 Hz, 1H), 1.90 – 1.83 (m, 1H), 1.76 – 1.67 (m, 2H), 1.63 – 1.59 (m, 1H) ppm. **<sup>13</sup>C NMR** (126 MHz, Chloroform-*d*)  $\delta$  142.4, 135.8, 132.1, 129.3, 128.3, 127.9, 126.0, 125.2, 121.2, 119.5, 110.9, 58.4, 52.5, 47.5, 42.2, 37.0, 35.5, 34.3, 33.4, 28.1, 26.3, 25.9, 25.1, 24.5, 21.7 ppm. **HRMS-ESI** ( $m/z$ ):  $[M + H]^+$  calculated for C<sub>23</sub>H<sub>25</sub>NO  $[M+H]^+$ : 332.1936, found 332.1929.

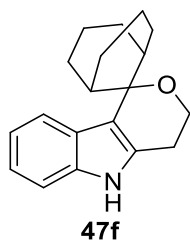
## Experimental

### (1*S*,4*R*)-4',5'-dihydro-3'*H*-spiro[bicyclo[2.2.1]heptane-2,1'-pyrano[4,3-*b*]indole] **47e**



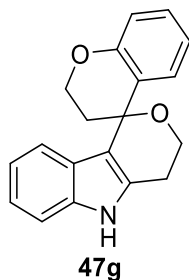
Synthesized via procedure C, 15.2 mg, 60%. **<sup>1</sup>H NMR** (500 MHz, Chloroform-*d*)  $\delta$  7.76 (s, 1H), 7.54 – 7.47 (m, 1H), 7.34 (ddd,  $J = 8.0, 2.5, 1.5$  Hz, 1H), 7.21 – 7.07 (m, 2H), 4.13 – 3.87 (m, 2H), 3.02 – 2.86 (m, 1H), 2.77 – 2.57 (m, 2H), 2.49 – 2.38 (m, 1H), 2.10 – 1.98 (m, 2H), 1.88 – 1.71 (m, 2H), 1.71 – 1.55 (m, 4H), 1.49 – 1.37 (m, 3H) ppm. **<sup>13</sup>C NMR** (126 MHz, Chloroform-*d*)  $\delta$  139.8, 136.0, 127.3, 122.2, 122.0, 120.0, 118.5, 111.2, 107.0, 81.0, 62.5, 46.1, 39.9, 36.5, 28.1, 27.3, 22.9 ppm. **HRMS-ESI** ( $m/z$ ):  $[M + H]^+$  calculated for C<sub>17</sub>H<sub>19</sub>NO  $[M+H]^+$ : 254.1467, found 254.1470.

### 4',5'-dihydro-3'*H*-spiro[bicyclo[3.3.1]nonane-9,1'-pyrano[4,3-*b*]indole] **47f**

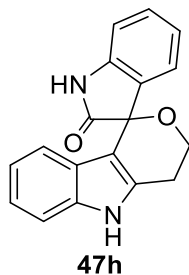


Synthesized via procedure C, 17.7 mg, 63%. **<sup>1</sup>H NMR** (500 MHz, Chloroform-*d*)  $\delta$  8.49 (s, 1H), 7.54 (d,  $J = 7.8$  Hz, 1H), 7.32 (d,  $J = 8.0$  Hz, 1H), 7.17 – 7.03 (m, 2H), 3.98 (t,  $J = 5.7$  Hz, 2H), 3.02 (t,  $J = 5.7$  Hz, 2H), 2.45 – 2.41 (m, 2H), 2.14 – 2.04 (m, 10H), 1.58 – 1.53 (m, 2H) ppm. **<sup>13</sup>C NMR** (126 MHz, Chloroform-*d*)  $\delta$  137.4, 136.5, 128.8, 121.7, 120.3, 120.1, 110.9, 100.7, 62.7, 47.0, 34.8, 31.6, 31.4, 30.1, 21.0 ppm. **HRMS-ESI** ( $m/z$ ):  $[M + H]^+$  calculated for C<sub>19</sub>H<sub>23</sub>NO  $[M+H]^+$ : 282.1780, found 281.1777.



4',5'-dihydro-3'-*H*-spiro[chromane-4,1'-pyrano[4,3-*b*]indole] **47g**

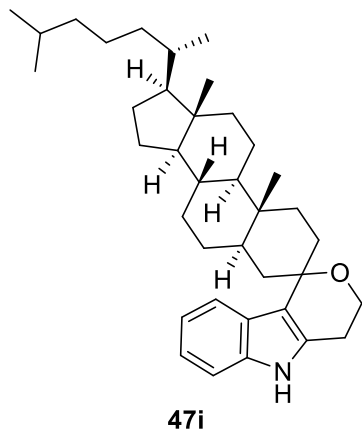
Synthesized via procedure C, 10.8 mg, 37%. **<sup>1</sup>H NMR** (500 MHz, Chloroform-*d*)  $\delta$  7.99 (s, 1H), 7.33 (d,  $J = 8.1$  Hz, 1H), 7.15 (dddd,  $J = 38.1, 8.2, 7.1, 1.5$  Hz, 2H), 6.99 – 6.89 (m, 3H), 6.85 (d,  $J = 7.9$  Hz, 1H), 6.70 (td,  $J = 7.4, 1.2$  Hz, 1H), 4.59 (ddd,  $J = 13.2, 10.8, 2.0$  Hz, 1H), 4.38 (ddd,  $J = 10.8, 4.4, 2.2$  Hz, 1H), 4.19 – 4.02 (m, 2H), 3.13 – 2.98 (m, 1H), 2.97 – 2.82 (m, 1H), 2.68 (ddd,  $J = 14.6, 13.5, 4.4$  Hz, 1H), 2.26 (dt,  $J = 14.6, 2.1$  Hz, 1H) ppm. **<sup>13</sup>C NMR** (126 MHz, Chloroform-*d*)  $\delta$  155.2, 136.0, 133.2, 130.0, 125.2, 125.0, 121.9, 120.5, 120.1, 119.4, 117.3, 113.3, 111.1, 71.3, 62.9, 59.0, 33.8, 27.3, 24.7 ppm. **HRMS-ESI** ( $m/z$ ):  $[M + H]^+$  calculated for C<sub>19</sub>H<sub>17</sub>NO<sub>2</sub>  $[M+H]^+$ : 292.1259, found 292.1254.

4',5'-dihydro-3'-*H*-spiro[indoline-3,1'-pyrano[4,3-*b*]indol]-2-one **47h**

Synthesized via procedure C, 15.7 mg, 54%. **<sup>1</sup>H NMR** (700 MHz, Methanol-*d*<sub>4</sub>)  $\delta$  7.39 – 7.26 (m, 2H), 7.14 – 6.93 (m, 4H), 6.83 – 6.67 (m, 1H), 6.60 – 6.48 (m, 1H), 4.85 – 4.77 (m, 1H), 4.27 (ddd,  $J = 7.5, 5.4, 2.7$  Hz, 1H), 3.17 (ddd,  $J = 15.8, 8.7, 5.3$  Hz, 1H), 2.97 (dt,  $J = 15.9, 4.0$  Hz, 1H) ppm. **<sup>13</sup>C NMR** (176 MHz, Methanol-*d*<sub>4</sub>)  $\delta$  181.0, 143.5, 137.9, 135.6, 133.1, 131.5, 127.0, 125.9, 124.3, 122.5, 120.4, 118.5, 112.4, 111.6, 106.9, 79.3, 62.6, 24.8 ppm. **HRMS-ESI** ( $m/z$ ):  $[M + H]^+$  calculated for C<sub>18</sub>H<sub>14</sub>N<sub>2</sub>O<sub>2</sub>  $[M+H]^+$ : 291.1055, found 291.1056.

## Experimental

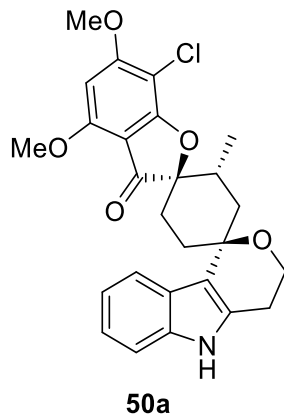
(5*R*,8*S*,9*R*,10*R*,13*S*,14*R*,17*S*)-10,13-dimethyl-17-((*S*)-6-methylheptan-2-yl)-1,2,4,4',5,5',6,7,8,9,10,11,12,13,14,15,16,17-octadecahydro-3'*H*-spiro[cyclopenta[*a*]phenanthrene-3,1'-pyrano[4,3-*b*]indole] **47i**



Synthesized via procedure C, 47.7 mg, 90%. **<sup>1</sup>H NMR** (500 MHz, Chloroform-*d*)  $\delta$  7.84 (s, 1H), 7.55 (dd,  $J = 7.2, 1.7$  Hz, 1H), 7.37 – 7.29 (m, 1H), 7.13 (pd,  $J = 7.2, 1.4$  Hz, 2H), 4.10 – 3.89 (m, 2H), 2.90 – 2.68 (m, 2H), 2.25 – 2.15 (m, 1H), 2.15 – 2.05 (m, 1H), 2.00 (dt,  $J = 12.5, 3.4$  Hz, 1H), 1.84 (ddt,  $J = 13.8, 6.3, 3.7$  Hz, 2H), 1.69 (ddd,  $J = 16.1, 9.6, 3.5$  Hz, 2H), 1.64 – 1.45 (m, 6H), 1.42 – 1.20 (m, 9H), 1.19 – 1.08 (m, 6H), 1.05 (s, 5H), 0.93 (d,  $J = 6.5$  Hz, 4H), 0.88 (dd,  $J = 6.6, 2.4$  Hz, 6H), 0.70 (s, 3H) ppm. **<sup>13</sup>C NMR** (126 MHz, Chloroform-*d*)  $\delta$  134.5, 129.9, 123.7, 120.0, 118.4, 117.6, 115.4, 109.9, 73.8, 57.2, 55.6, 55.2, 53.2, 41.6, 39.6, 39.1, 38.5, 37.6, 35.2, 34.8, 34.6, 34.4, 32.8, 31.0, 29.8, 27.5, 27.5, 27.0, 23.5, 23.2, 22.8, 21.8, 21.6, 20.0, 17.7, 11.1, 11.1 ppm. **HRMS-ESI** ( $m/z$ ): [M + H]<sup>+</sup> calculated for C<sub>37</sub>H<sub>55</sub>NO [M+H]<sup>+</sup>: 530.4284, found 530.4276.

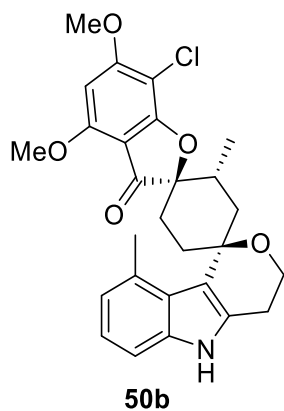
## INDOFULVINS

(2*R*,2'*R*,4'*S*)-7-chloro-4,6-dimethoxy-2'-methyl-4'',5''-dihydro-3*H*,3''*H*-dispiro[benzofuran-2,1'-cyclohexane-4',1''-pyrano[4,3-*b*]indol]-3-one **50a**



Synthesized via procedure C, 43.0 mg, 92%. **<sup>1</sup>H NMR** (400 MHz, Chloroform-*d*)  $\delta$  8.16 – 8.13 (m, 1H), 7.83 (s, 1H), 7.32 – 7.28 (m, 1H), 7.20 – 7.11 (m, 2H), 6.11 (s, 1H), 4.02 (d,  $J = 3.9$  Hz, 8H), 3.04 – 2.70 (m, 5H), 2.51 (ddd,  $J = 14.1, 12.9, 4.2$  Hz, 1H), 1.98 – 1.75 (m, 3H), 0.83 (d,  $J = 6.7$  Hz, 3H) ppm. **<sup>13</sup>C NMR** (126 MHz, Chloroform-*d*)  $\delta$  199.3, 168.5, 163.9, 157.5, 135.5, 130.8, 124.7, 121.3, 120.1, 120.0, 115.4, 110.5, 106.0, 93.1, 88.6, 74.0, 58.7, 56.9, 56.4, 38.4, 33.6, 31.0, 29.5, 28.6, 24.5, 14.8 ppm. **HRMS-ESI** ( $m/z$ ):  $[M + H]^+$  calculated for  $C_{26}H_{26}ClNO_5$   $[M+H]^+$ : 468.1500 and 470.1470, found 468.1500 and 470.1467.

(2*R*,2'*R*,4'*S*)-7-chloro-4,6-dimethoxy-2',9''-dimethyl-4'',5''-dihydro-3*H*,3''*H*-dispiro[benzofuran-2,1'-cyclohexane-4',1''-pyrano[4,3-*b*]indol]-3-one **50b**

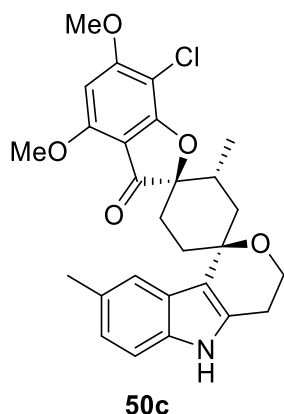


Synthesized via procedure C, 42.8 mg, 89%. **<sup>1</sup>H NMR** (700 MHz, Chloroform-*d*)  $\delta$  7.98 (s, 1H), 7.17 – 7.11 (m, 1H), 7.04 (t,  $J = 7.6$  Hz, 1H), 6.94 (dt,  $J = 7.2, 1.1$  Hz, 1H), 6.09 (s, 1H), 4.03 – 3.94 (m, 8H), 3.06 (s, 3H), 2.96 – 2.86 (m, 3H), 2.84 (dt,  $J = 5.4, 3.8$  Hz, 2H), 2.58 – 2.53 (m, 1H),

## Experimental

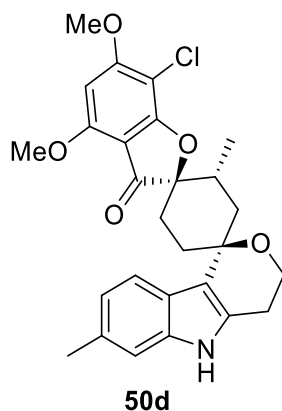
2.01 (dt,  $J = 14.5, 2.3$  Hz, 1H), 1.97 – 1.90 (m, 1H), 1.78 (ddd,  $J = 13.1, 4.2, 2.5$  Hz, 1H), 0.83 (d,  $J = 6.1$  Hz, 3H) ppm.  $^{13}\text{C}$  NMR (176 MHz, Chloroform- $d$ )  $\delta$  198.3, 167.4, 162.8, 156.6, 135.1, 130.9, 129.3, 123.4, 121.6, 120.3, 114.6, 107.3, 104.8, 92.1, 87.6, 74.1, 56.4, 55.8, 55.3, 39.2, 32.3, 30.2, 27.5, 25.9, 24.1, 23.3, 13.2 ppm. HRMS-ESI ( $m/z$ ):  $[\text{M} + \text{H}]^+$  calculated for  $\text{C}_{27}\text{H}_{28}\text{ClNO}_5$   $[\text{M} + \text{H}]^+$ : 482.1656 and 484.1627, found 482.1653 and 484.1626.

(2*R*,2'*R*,4'*S*)-7-chloro-4,6-dimethoxy-2',8''-dimethyl-4'',5''-dihydro-3*H*,3''*H*-dispiro[benzofuran-2,1'-cyclohexane-4',1''-pyrano[4,3-*b*]indol]-3-one **50c**



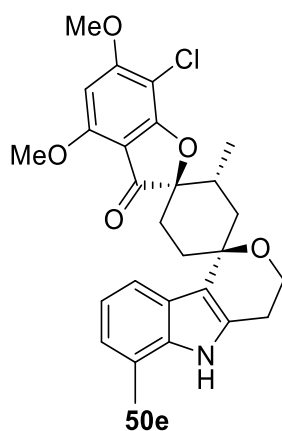
Synthesized via procedure C, 45.3 mg, 94%.  $^1\text{H}$  NMR (400 MHz, Chloroform- $d$ )  $\delta$  7.89 (s, 1H), 7.84 – 7.66 (m, 1H), 7.19 (dd,  $J = 8.1, 0.7$  Hz, 1H), 6.97 (ddd,  $J = 8.3, 1.6, 0.6$  Hz, 1H), 6.11 (s, 1H), 4.06 – 3.89 (m, 8H), 3.02 – 2.71 (m, 5H), 2.57 – 2.46 (m, 4H), 2.00 – 1.73 (m, 3H), 0.83 (d,  $J = 6.7$  Hz, 3H).  $^{13}\text{C}$  NMR (176 MHz, Chloroform- $d$ )  $\delta$  199.7, 168.8, 164.2, 157.8, 134.1, 131.2, 129.5, 125.2, 119.8, 115.2, 110.5, 106.4, 97.5, 93.5, 88.9, 74.4, 58.9, 57.2, 56.6, 38.7, 33.8, 29.8, 28.9, 27.2, 24.9, 22.1, 15.0 ppm. HRMS-ESI ( $m/z$ ):  $[\text{M} + \text{H}]^+$  calculated for  $\text{C}_{27}\text{H}_{28}\text{ClNO}_5$   $[\text{M} + \text{H}]^+$ : 482.1656 and 484.1627, found 482.1655 and 484.1626.

(2*R*,2'*R*,4'*S*)-7-chloro-4,6-dimethoxy-2',7''-dimethyl-4'',5''-dihydro-3*H*,3''*H*-dispiro[benzofuran-2,1'-cyclohexane-4',1''-pyrano[4,3-*b*]indol]-3-one **50d**



Synthesized via procedure C, 40.9 mg, 85%. <sup>1</sup>H NMR (700 MHz, Chloroform-*d*) δ 8.00 (d, *J* = 8.1 Hz, 1H), 7.69 (s, 1H), 7.10 (s, 1H), 6.99 (dd, *J* = 8.1, 1.5 Hz, 1H), 6.11 (s, 1H), 4.06 – 3.96 (m, 8H), 2.98 – 2.85 (m, 2H), 2.85 – 2.79 (m, 1H), 2.79 – 2.72 (m, 2H), 2.53 – 2.47 (m, 1H), 2.45 (s, 3H), 1.99 – 1.88 (m, 1H), 1.85 (ddd, *J* = 14.4, 4.2, 2.6 Hz, 1H), 1.78 (ddd, *J* = 13.0, 4.1, 2.6 Hz, 1H), 0.82 (d, *J* = 6.8 Hz, 3H) ppm. <sup>13</sup>C NMR (176 MHz, Chloroform-*d*) δ 199.5, 168.8, 164.2, 157.8, 136.3, 131.4, 130.3, 122.9, 121.9, 120.0, 115.5, 110.9, 106.4, 93.4, 88.9, 74.3, 59.0, 57.2, 56.7, 38.8, 33.9, 29.8, 28.9, 27.2, 24.8, 22.0, 15.1 ppm. HRMS-ESI (*m/z*): [M + H]<sup>+</sup> calculated for C<sub>27</sub>H<sub>28</sub>ClNO<sub>5</sub> [M+H]<sup>+</sup>: 482.1656 and 484.1627, found 482.1653 and 484.1624.

(2*R*,2'*R*,4'*S*)-7-chloro-4,6-dimethoxy-2',6''-dimethyl-4'',5''-dihydro-3*H*,3''*H*-dispiro[benzofuran-2,1'-cyclohexane-4',1''-pyrano[4,3-*b*]indol]-3-one **50e**

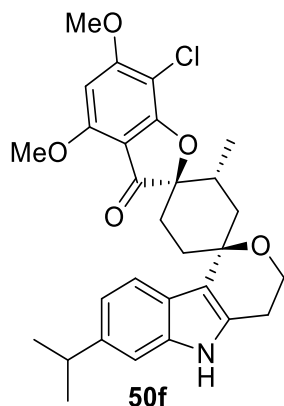


Synthesized via procedure C, 42.1 mg, 87%. <sup>1</sup>H NMR (700 MHz, Chloroform-*d*) δ 8.01 (d, *J* = 7.9 Hz, 1H), 7.77 (d, *J* = 3.7 Hz, 1H), 7.26 (s, 1H), 7.10 (t, *J* = 7.5 Hz, 1H), 6.96 (d, *J* = 6.9 Hz, 1H), 6.11 (s, 1H), 4.06 – 4.00 (m, 6H), 4.01 – 3.96 (m, 2H), 2.98 – 2.94 (m, 1H), 2.84 – 2.78 (m, 2H),

## Experimental

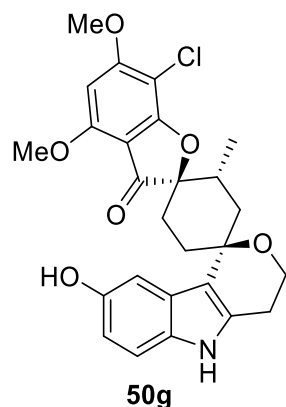
2.54 – 2.47 (m, 1H), 2.46 (s, 3H), 2.26 – 2.20 (m, 1H), 1.96 – 1.91 (m, 1H), 1.85 (ddd,  $J = 14.4, 4.2, 2.6$  Hz, 1H), 1.78 (ddd,  $J = 13.0, 4.2, 2.6$  Hz, 1H), 0.82 (d,  $J = 6.8$  Hz, 3H) ppm.  $^{13}\text{C NMR}$  (176 MHz, Chloroform- $d$ )  $\delta$  198.2, 167.5, 162.9, 156.5, 133.9, 129.5, 123.2, 121.0, 119.2, 118.5, 116.8, 114.9, 105.06, 96.2, 92.1, 87.6, 73.0, 57.6, 55.8, 55.3, 37.4, 32.6, 28.5, 27.6, 25.9, 23.5, 15.7, 13.2 ppm. **HRMS-ESI** ( $m/z$ ):  $[\text{M} + \text{H}]^+$  calculated for  $\text{C}_{27}\text{H}_{28}\text{ClNO}_5$   $[\text{M} + \text{H}]^+$ : 482.1656 and 484.1627, found 482.1654 and 484.1623.

(2*R*,2'*R*,4'*S*)-7-chloro-7"-isopropyl-4,6-dimethoxy-2'-methyl-4",5"-dihydro-3*H*,3"*H*-dispiro[benzofuran-2,1'-cyclohexane-4',1"-pyrano[4,3-*b*]indol]-3-one **50f**



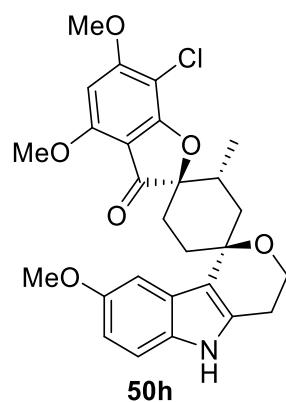
Synthesized via procedure C, 39.7 mg, 78%.  $^1\text{H NMR}$  (500 MHz, Chloroform- $d$ )  $\delta$  8.30 (s, 1H), 7.97 (d,  $J = 8.2$  Hz, 1H), 7.69 (s, 1H), 7.46 – 7.32 (m, 1H), 7.08 (dd,  $J = 5.5, 1.5$  Hz, 2H), 7.03 – 6.86 (m, 2H), 6.03 (s, 1H), 3.94 (d,  $J = 4.1$  Hz, 6H), 2.82 – 2.72 (m, 2H), 2.70 – 2.63 (m, 2H), 2.47 – 2.36 (m, 1H), 1.85 (ddt,  $J = 14.6, 4.6, 2.6$  Hz, 1H), 1.79 – 1.73 (m, 1H), 1.71 – 1.65 (m, 1H), 1.22 (d,  $J = 2.9$  Hz, 6H), 0.74 (d,  $J = 6.8$  Hz, 3H) ppm.  $^{13}\text{C NMR}$  (126 MHz, Chloroform- $d$ )  $\delta$  199.5, 168.8, 164.2, 157.9, 142.9, 136.2, 130.6, 123.3, 120.0, 119.6, 115.5, 108.2, 106.4, 93.5, 89.0, 74.4, 62.7, 59.1, 57.2, 56.7, 38.9, 34.7, 33.9, 31.7, 29.9, 29.0, 27.3, 24.9, 15.1 ppm. **HRMS-ESI** ( $m/z$ ):  $[\text{M} + \text{H}]^+$  calculated for  $\text{C}_{29}\text{H}_{32}\text{ClNO}_5$   $[\text{M} + \text{H}]^+$ : 510.1969 and 512.1940, found 510.1968 and 512.1938.

(2*R*,2'*R*,4'*S*)-7-chloro-8''-hydroxy-4,6-dimethoxy-2'-methyl-4'',5''-dihydro-3*H*,3''*H*-dispiro[benzofuran-2,1'-cyclohexane-4',1''-pyrano[4,3-*b*]indol]-3-one **50g**



Synthesized via procedure C, 40.1 mg, 83%. **<sup>1</sup>H NMR** (700 MHz, Methanol-*d*<sub>4</sub>) δ 7.49 (d, *J* = 2.3 Hz, 1H), 7.13 (d, *J* = 8.6 Hz, 1H), 6.62 (dd, *J* = 8.6, 2.3 Hz, 1H), 6.41 (s, 1H), 4.06 (s, 3H), 4.04 (s, 3H), 2.90 (td, *J* = 14.4, 4.2 Hz, 1H), 2.85 – 2.74 (m, 3H), 2.67 – 2.60 (m, 1H), 2.42 (td, *J* = 13.7, 4.2 Hz, 1H), 2.05 – 2.00 (m, 1H), 1.90 (d, *J* = 14.4 Hz, 1H), 1.84 (d, *J* = 13.5 Hz, 1H), 1.76 (d, *J* = 11.7 Hz, 1H), 1.38 – 1.30 (m, 3H), 0.79 (d, *J* = 6.8 Hz, 3H) ppm. **<sup>13</sup>C NMR** (176 MHz, Methanol-*d*<sub>4</sub>) δ 200.9, 169.7, 166.3, 159.5, 151.3, 112.2, 111.0, 104.3, 94.2, 90.7, 75.4, 60.0, 57.7, 56.9, 49.4, 39.3, 35.1, 30.6, 29.8, 25.4, 15.2 ppm. **HRMS-ESI** (*m/z*): [M + H]<sup>+</sup> calculated for C<sub>26</sub>H<sub>26</sub>ClNO<sub>6</sub> [M+H]<sup>+</sup>: 484.1449 and 486.1419, found 484.1447 and 486.1416.

(2*R*,2'*R*,4'*S*)-7-chloro-8''-methoxy-4,6-dimethoxy-2'-methyl-4'',5''-dihydro-3*H*,3''*H*-dispiro[benzofuran-2,1'-cyclohexane-4',1''-pyrano[4,3-*b*]indol]-3-one **50h**

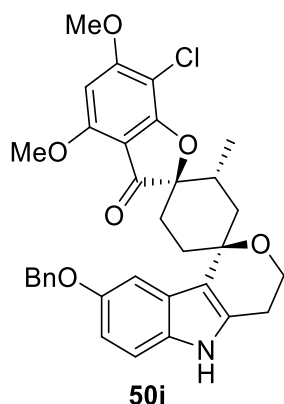


Synthesized via procedure C, 45.3 mg, 91%. **<sup>1</sup>H NMR** (700 MHz, Chloroform-*d*) δ 7.71 (s, 1H), 7.66 (d, *J* = 2.3 Hz, 1H), 7.19 (d, *J* = 8.7 Hz, 1H), 6.81 (dd, *J* = 8.7, 2.4 Hz, 1H), 6.09 (s, 1H), 4.03 (s, 3H), 4.01 (s, 4H), 4.00 (s, 3H), 2.95 (td, *J* = 14.4, 4.2 Hz, 1H), 2.91 – 2.86 (m, 1H), 2.86 – 2.80

## Experimental

(m, 1H), 2.79 – 2.72 (m, 2H), 2.51 (td,  $J = 13.7, 4.3$  Hz, 1H), 1.93 (d,  $J = 14.8$  Hz, 1H), 1.86 (dt,  $J = 14.3, 3.3$  Hz, 1H), 1.81 – 1.76 (m, 1H), 0.83 (d,  $J = 6.8$  Hz, 3H) ppm.  $^{13}\text{C}$  NMR (176 MHz, Chloroform-*d*)  $\delta$  199.4, 168.6, 164.0, 157.6, 154.4, 131.8, 130.7, 125.3, 115.4, 111.5, 111.3, 106.3, 102.2, 97.4, 93.2, 88.8, 74.1, 58.8, 56.4, 38.3, 33.7, 29.4, 28.7, 27.1, 24.7, 14.9 ppm. HRMS-ESI ( $m/z$ ):  $[\text{M} + \text{H}]^+$  calculated for  $\text{C}_{27}\text{H}_{28}\text{ClNO}_6$   $[\text{M} + \text{H}]^+$ : 498.1605 and 500.1576, found 498.1602 and 500.1573.

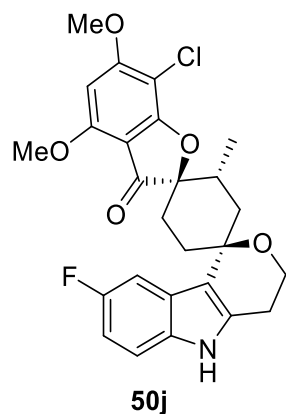
(2*R*,2'*R*,4'*S*)-7-chloro-8''-benzoyl-4,6-dimethoxy-2'-methyl-4'',5''-dihydro-3*H*,3''*H*-dispiro[benzofuran-2,1'-cyclohexane-4',1''-pyrano[4,3-*b*]indol]-3-one **50i**



Synthesized via procedure C, 54.5 mg, 95%.  $^1\text{H}$  NMR (500 MHz, Chloroform-*d*)  $\delta$  7.71 (s, 1H), 7.60 (d,  $J = 7.1$  Hz, 2H), 7.37 (t,  $J = 7.5$  Hz, 2H), 7.29 (t,  $J = 7.4$  Hz, 1H), 7.19 (d,  $J = 8.7$  Hz, 1H), 6.87 (dd,  $J = 8.7, 2.4$  Hz, 1H), 6.09 (s, 1H), 5.39 – 5.28 (m, 2H), 3.99 (d,  $J = 18.4$  Hz, 8H), 2.96 (td,  $J = 14.3, 4.2$  Hz, 1H), 2.91 – 2.80 (m, 2H), 2.80 – 2.70 (m, 2H), 2.50 (td,  $J = 13.7, 4.3$  Hz, 1H), 1.93 (d,  $J = 14.8$  Hz, 1H), 1.85 (dt,  $J = 14.2, 3.2$  Hz, 1H), 1.82 – 1.76 (m, 1H), 0.83 (d,  $J = 6.8$  Hz, 3H) ppm.  $^{13}\text{C}$  NMR (126 MHz, Chloroform-*d*)  $\delta$  168.8, 164.2, 157.9, 153.7, 138.5, 132.0, 131.0, 128.6, 128.4, 127.9, 125.5, 115.7, 112.4, 111.6, 103.6, 97.5, 93.4, 89.0, 74.3, 71.1, 59.0, 57.2, 56.6, 38.6, 34.0, 29.6, 29.0, 25.0, 15.1 ppm. HRMS-ESI ( $m/z$ ):  $[\text{M} + \text{H}]^+$  calculated for  $\text{C}_{33}\text{H}_{32}\text{ClNO}_6$   $[\text{M} + \text{H}]^+$ : 574.1918 and 575.1952, found 574.1916 and 575.1950.

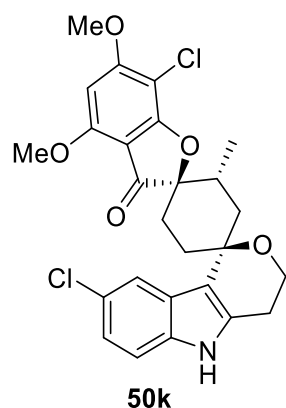


(2*R*,2'*R*,4'*S*)-7-chloro-8''-fluoro-4,6-dimethoxy-2'-methyl-4'',5''-dihydro-3*H*,3''*H*-dispiro[benzofuran-2,1'-cyclohexane-4',1''-pyrano[4,3-*b*]indol]-3-one **50j**



Synthesized via procedure C, 38.8 mg, 80%. <sup>1</sup>H NMR (700 MHz, Chloroform-*d*) δ 7.83 (dd, *J* = 9.9, 2.4 Hz, 2H), 7.20 (dd, *J* = 8.7, 4.3 Hz, 1H), 6.88 (td, *J* = 9.0, 2.4 Hz, 1H), 6.11 (s, 1H), 4.03 (s, 3H), 4.02 (s, 3H), 3.99 (s, 2H), 2.90 (td, *J* = 14.3, 4.2 Hz, 1H), 2.87 – 2.80 (m, 2H), 2.80 – 2.71 (m, 2H), 2.50 (td, *J* = 13.6, 4.2 Hz, 1H), 1.92 (d, *J* = 14.7 Hz, 1H), 1.84 (dt, *J* = 14.2, 3.5 Hz, 1H), 1.78 (dt, *J* = 12.9, 3.2 Hz, 1H), 0.83 (d, *J* = 6.8 Hz, 3H) ppm. <sup>13</sup>C NMR (176 MHz, Chloroform-*d*) δ 199.4, 164.2, 157.8, 133.0, 132.3, 111.2, 109.8, 106.4, 105.4, 97.5, 93.2, 89.0, 74.2, 58.9, 57.2, 56.7, 38.5, 33.9, 29.6, 28.9, 24.9, 15.0 ppm. HRMS-ESI (*m/z*): [M + H]<sup>+</sup> calculated for C<sub>26</sub>H<sub>25</sub>ClFNO<sub>5</sub> [M+H]<sup>+</sup>: 486.1405 and 488.1376, found 486.1401 and 488.1372.

(2*R*,2'*R*,4'*S*)-7-chloro-8''-chloro-4,6-dimethoxy-2'-methyl-4'',5''-dihydro-3*H*,3''*H*-dispiro[benzofuran-2,1'-cyclohexane-4',1''-pyrano[4,3-*b*]indol]-3-one **50k**

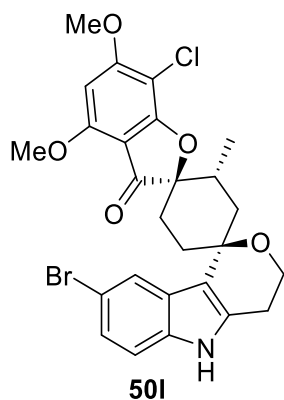


Synthesized via procedure C, 39.6 mg, 79%. <sup>1</sup>H NMR (700 MHz, Chloroform-*d*) δ 8.10 – 8.07 (m, 1H), 7.87 (s, 1H), 7.21 (d, *J* = 8.5 Hz, 1H), 7.10 (dd, *J* = 8.5, 1.9 Hz, 1H), 6.11 (s, 1H), 4.02 (d, *J* = 4.4 Hz, 8H), 2.89 (td, *J* = 14.3, 4.2 Hz, 1H), 2.87 – 2.81 (m, 2H), 2.80 – 2.71 (m, 2H), 2.49 (td,

## Experimental

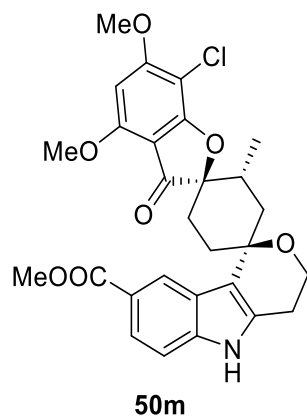
$J = 13.6, 4.2$  Hz, 1H), 1.92 (d,  $J = 14.8$  Hz, 1H), 1.84 (dt,  $J = 14.2, 3.7$  Hz, 1H), 1.81 – 1.76 (m, 1H), 0.83 (d,  $J = 6.8$  Hz, 3H) ppm.  $^{13}\text{C NMR}$  (176 MHz, Chloroform- $d$ )  $\delta$  199.3, 164.1, 157.7, 134.0, 132.5, 126.0, 125.8, 121.8, 119.3, 115.5, 111.6, 93.0, 88.8, 74.0, 58.6, 57.0, 56.5, 38.5, 33.7, 29.6, 28.6, 24.6, 14.8 ppm. **HRMS-ESI** ( $m/z$ ):  $[\text{M} + \text{H}]^+$  calculated for  $\text{C}_{26}\text{H}_{25}\text{Cl}_2\text{NO}_5$   $[\text{M} + \text{H}]^+$ : 502.1110 and 504.1080, found 502.1108 and 504.1079.

(2*R*,2'*R*,4'*S*)-7-chloro-8''-bromo-4,6-dimethoxy-2'-methyl-4'',5''-dihydro-3*H*,3''*H*-dispiro[benzofuran-2,1'-cyclohexane-4',1''-pyrano[4,3-*b*]indol]-3-one **50I**



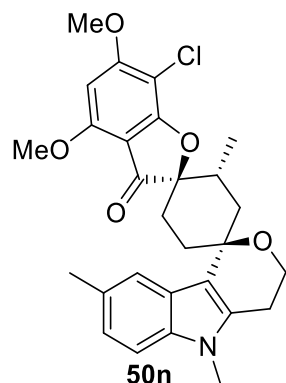
Synthesized via procedure C, 28.3 mg, 52%.  $^1\text{H NMR}$  (700 MHz, Chloroform- $d$ )  $\delta$  8.02 (dd,  $J = 4.9, 1.8$  Hz, 1H), 7.30 (dd,  $J = 8.7, 1.7$  Hz, 1H), 7.22 (d,  $J = 8.7$  Hz, 1H), 7.17 (d,  $J = 5.3$  Hz, 1H), 6.09 (s, 1H), 4.24 (t,  $J = 5.1$  Hz, 2H), 4.01 (s, 3H), 3.96 (d,  $J = 3.1$  Hz, 6H), 2.89 – 2.82 (m, 1H), 2.77 – 2.71 (m, 1H), 2.64 (t,  $J = 17.5$  Hz, 2H), 2.36 (dd,  $J = 13.2, 6.9$  Hz, 1H), 1.43 (s, 1H), 1.09 (d,  $J = 6.9$  Hz, 3H) ppm.  $^{13}\text{C NMR}$  (176 MHz, Chloroform- $d$ )  $\delta$  197.8, 168.1, 164.0, 157.8, 135.8, 130.1, 127.9, 126.7, 125.0, 123.7, 117.4, 116.7, 113.5, 111.1, 97.5, 91.9, 62.1, 57.0, 56.4, 48.9, 34.3, 30.3, 14.4 ppm. **HRMS-ESI** ( $m/z$ ):  $[\text{M} + \text{H}]^+$  calculated for  $\text{C}_{26}\text{H}_{25}\text{BrClNO}_5$   $[\text{M} + \text{H}]^+$ : 546.0605 and 547.0584, found 546.0602 and 547.0582.

methyl-(2*R*,2'*R*,4'*S*)-7-chloro-4,6-dimethoxy-2'-methyl-3-oxo-4'',5''-dihydro-3*H*,3''*H*-dispiro[benzofuran-2,1'-cyclohexane-4',1''-pyrano[4,3-*b*]indole]-8''-carboxylate **50m**



Synthesized via procedure C, 42.6 mg, 81%. **<sup>1</sup>H NMR** (700 MHz, Chloroform-*d*)  $\delta$  8.93 (s, 1H), 8.06 (s, 1H), 7.89 (dd,  $J = 8.5, 1.5$  Hz, 1H), 7.32 (d,  $J = 8.5$  Hz, 1H), 6.10 (s, 1H), 4.01 (d,  $J = 1.0$  Hz, 9H), 2.99 (td,  $J = 14.3, 4.2$  Hz, 1H), 2.94 – 2.88 (m, 1H), 2.88 – 2.78 (m, 2H), 2.78 – 2.71 (m, 1H), 2.50 (td,  $J = 13.6, 4.3$  Hz, 1H), 1.93 (d,  $J = 14.8$  Hz, 1H), 1.87 (dt,  $J = 14.3, 3.8$  Hz, 1H), 1.80 (dt,  $J = 12.9, 3.9$  Hz, 1H), 1.26 (s, 1H), 0.84 (d,  $J = 6.8$  Hz, 3H) ppm. **<sup>13</sup>C NMR** (176 MHz, Chloroform-*d*)  $\delta$  199.1, 168.5, 164.0, 157.8, 138.3, 132.4, 124.6, 123.2, 122.6, 122.2, 116.9, 110.4, 106.4, 93.0, 88.9, 74.1, 57.0, 56.4, 52.3, 38.6, 33.8, 30.0, 28.8, 24.6, 14.8 ppm. **HRMS-ESI** ( $m/z$ ):  $[M + H]^+$  calculated for  $C_{28}H_{28}ClNO_7$   $[M+H]^+$ : 526.1554 and 527.1525, found 526.1553 and 527.1522.

(2*R*,2'*R*,4'*S*)-7-chloro-4,6-dimethoxy-2',5'',8''-trimethyl-4'',5''-dihydro-3*H*,3''*H*-dispiro[benzofuran-2,1'-cyclohexane-4',1''-pyrano[4,3-*b*]indol]-3-one **50n**

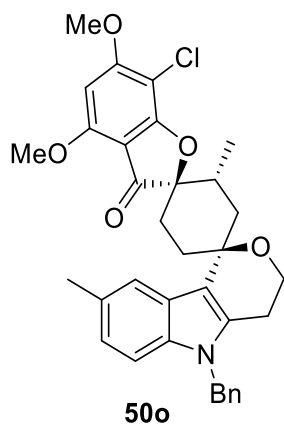


Synthesized via procedure C, 46.6 mg, 94%. **<sup>1</sup>H NMR** (700 MHz, Chloroform-*d*)  $\delta$  7.93 – 7.88 (m, 1H), 7.20 – 7.15 (m, 1H), 7.01 (dd,  $J = 8.3, 1.6$  Hz, 1H), 6.11 (s, 1H), 4.03 (d,  $J = 1.3$  Hz, 3H),

## Experimental

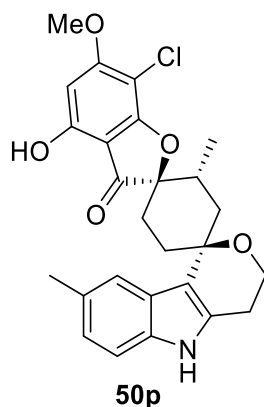
4.02 (s, 3H), 4.02 – 3.96 (m, 2H), 3.61 (s, 3H), 3.00 – 2.86 (m, 2H), 2.82 – 2.70 (m, 3H), 2.54 (d,  $J = 5.7$  Hz, 3H), 2.51 (ddd,  $J = 14.1, 12.8, 4.2$  Hz, 1H), 1.96 – 1.88 (m, 1H), 1.88 – 1.80 (m, 1H), 1.81 – 1.75 (m, 1H), 0.82 (d,  $J = 6.8$  Hz, 3H) ppm.  $^{13}\text{C}$  NMR (176 MHz, Chloroform-*d*)  $\delta$  199.8, 168.8, 164.3, 157.8, 135.4, 132.9, 129.0, 124.8, 122.7, 119.8, 114.3, 108.7, 106.4, 93.5, 88.9, 74.4, 59.0, 57.2, 56.6, 38.9, 33.9, 30.0, 29.3, 28.9, 27.3, 23.7, 22.1, 15.1 ppm. HRMS-ESI ( $m/z$ ):  $[\text{M} + \text{H}]^+$  calculated for  $\text{C}_{28}\text{H}_{30}\text{ClNO}_5$   $[\text{M} + \text{H}]^+$ : 496.1813 and 498.1783, found 496.1810 and 498.1781.

(2*R*,2'*R*,4'*S*)-5''-benzyl-7-chloro-4,6-dimethoxy-2',8''-dimethyl-4'',5''-dihydro-3*H*,3'*H*-dispiro[benzofuran-2,1'-cyclohexane-4',1''-pyrano[4,3-*b*]indol]-3-one **50o**



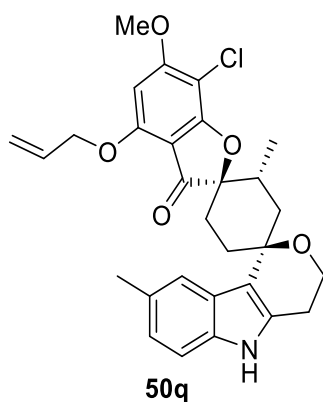
Synthesized via procedure C, 53.1 mg, 93%.  $^1\text{H}$  NMR (700 MHz, Chloroform-*d*)  $\delta$  7.97 – 7.88 (m, 1H), 7.27 – 7.24 (m, 3H), 7.23 – 7.19 (m, 1H), 7.13 (d,  $J = 8.3$  Hz, 1H), 7.03 – 6.98 (m, 2H), 6.96 (dd,  $J = 8.4, 1.6$  Hz, 1H), 6.11 (s, 1H), 5.24 (d,  $J = 2.9$  Hz, 2H), 4.03 (s, 3H), 4.02 (s, 3H), 4.01 (s, 2H), 3.00 (td,  $J = 14.3, 4.2$  Hz, 1H), 2.96 – 2.85 (m, 1H), 2.79 – 2.64 (m, 2H), 2.55 (s, 3H), 2.54 – 2.49 (m, 1H), 1.96 (ddd,  $J = 11.9, 4.3, 2.0$  Hz, 1H), 1.88 (ddd,  $J = 14.3, 4.1, 2.6$  Hz, 1H), 1.80 (ddd,  $J = 12.9, 4.1, 2.6$  Hz, 1H), 0.84 (d,  $J = 6.9$  Hz, 3H) ppm.  $^{13}\text{C}$  NMR (176 MHz, Chloroform-*d*)  $\delta$  199.7, 168.8, 164.2, 157.8, 138.2, 135.2, 132.8, 129.3, 129.1, 127.6, 126.5, 125.2, 122.9, 119.9, 115.0, 109.2, 106.4, 97.6, 93.5, 88.9, 74.4, 58.9, 57.2, 56.6, 46.6, 38.9, 33.9, 29.9, 28.9, 23.8, 22.1, 15.1 ppm. HRMS-ESI ( $m/z$ ):  $[\text{M} + \text{H}]^+$  calculated for  $\text{C}_{34}\text{H}_{34}\text{ClNO}_5$   $[\text{M} + \text{H}]^+$ : 572.2126 and 573.2159, found 572.2123 and 573.2155.

(2*R*,2'*R*,4'*S*)-7-chloro-4-hydroxy-6-methoxy-2',8''-dimethyl-4'',5''-dihydro-3*H*,3''*H*-dispiro[benzofuran-2,1'-cyclohexane-4',1''-pyrano[4,3-*b*]indol]-3-one **50p**



Synthesized via procedure C, 42.1 mg, 90%. **<sup>1</sup>H NMR** (400 MHz, Chloroform-*d*)  $\delta$  8.11 (s, 1H), 7.73 (dd,  $J = 1.7, 0.9$  Hz, 1H), 7.64 (s, 1H), 7.11 (dd,  $J = 8.2, 0.7$  Hz, 1H), 6.96 – 6.81 (m, 1H), 6.05 (s, 1H), 3.98 – 3.87 (m, 2H), 3.86 (s, 3H), 2.86 – 2.63 (m, 5H), 2.51 – 2.36 (m, 4H), 1.95 (s, 1H), 1.92 – 1.82 (m, 1H), 1.78 (dd,  $J = 10.1, 2.6$  Hz, 1H), 1.71 (ddd,  $J = 12.9, 4.1, 2.7$  Hz, 1H), 0.79 – 0.69 (m, 3H) ppm. **<sup>13</sup>C NMR** (101 MHz, Chloroform-*d*)  $\delta$  184.1, 166.4, 165.1, 156.4, 134.1, 131.2, 129.3, 125.2, 123.0, 119.4, 115.0, 110.6, 105.0, 94.6, 92.9, 74.1, 58.9, 57.3, 38.7, 33.7, 29.9, 28.7, 27.1, 24.7, 22.1, 15.1 ppm. **HRMS-ESI** ( $m/z$ ):  $[M + H]^+$  calculated for  $C_{26}H_{26}ClNO_5$   $[M+H]^+$ : 468.1500 and 470.1470, found 468.1497 and 470.1468.

(2*R*,2'*R*,4'*S*)-4-(allyloxy)-7-chloro-6-methoxy-2',8''-dimethyl-4'',5''-dihydro-3*H*,3''*H*-dispiro[benzofuran-2,1'-cyclohexane-4',1''-pyrano[4,3-*b*]indol]-3-one **50q**

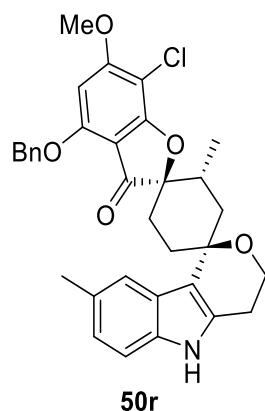


Synthesized via procedure C, 42.1 mg, 83%. **<sup>1</sup>H NMR** (700 MHz, Chloroform-*d*)  $\delta$  7.90 (d,  $J = 1.5$  Hz, 1H), 7.78 (s, 1H), 7.19 (d,  $J = 8.2$  Hz, 1H), 6.97 (dd,  $J = 8.3, 1.6$  Hz, 1H), 6.14 (s, 1H), 5.55 (dd,  $J = 17.3, 1.5$  Hz, 1H), 5.40 (dd,  $J = 10.6, 1.4$  Hz, 1H), 4.85 – 4.76 (m, 2H), 4.03 – 3.98 (m,

## Experimental

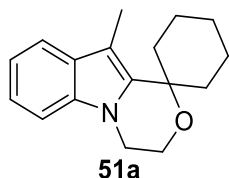
1H), 3.97 (s, 3H), 2.98 – 2.86 (m, 2H), 2.80 – 2.71 (m, 2H), 2.53 (s, 3H), 2.51 – 2.47 (m, 1H), 2.04 (s, 3H), 1.97 – 1.89 (m, 1H), 1.85 (ddd,  $J = 14.4, 4.2, 2.6$  Hz, 1H), 1.79 (ddd,  $J = 13.0, 4.2, 2.6$  Hz, 1H), 0.83 (d,  $J = 6.9$  Hz, 3H) ppm.  $^{13}\text{C}$  NMR (176 MHz, Chloroform- $d$ )  $\delta$  198.9, 168.4, 163.6, 156.5, 132.4, 130.9, 129.1, 122.8, 119.6, 118.8, 118.7, 110.2, 93.0, 90.4, 77.2, 77.1, 76.9, 74.1, 70.3, 58.6, 56.8, 38.4, 33.6, 29.6, 28.6, 26.9, 24.6, 21.8, 14.7 ppm. HRMS-ESI ( $m/z$ ):  $[\text{M} + \text{H}]^+$  calculated for  $\text{C}_{29}\text{H}_{30}\text{ClNO}_5$   $[\text{M} + \text{H}]^+$ : 508.1813 and 510.1783, found 508.1811 and 510.1782.

(2*R*,2'*R*,4'*S*)-4-(benzyloxy)-7-chloro-6-methoxy-2',8''-dimethyl-4'',5''-dihydro-3*H*,3''*H*-dispiro[benzofuran-2,1'-cyclohexane-4',1''-pyrano[4,3-*b*]indol]-3-one **50r**

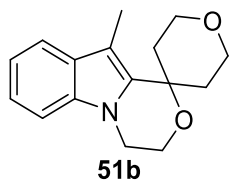


Synthesized via procedure C, 47.4 mg, 85%.  $^1\text{H}$  NMR (700 MHz, Chloroform- $d$ )  $\delta$  7.97 (d,  $J = 1.6$  Hz, 1H), 7.79 (s, 1H), 7.59 – 7.53 (m, 2H), 7.42 (dd,  $J = 8.4, 7.0$  Hz, 2H), 7.35 (td,  $J = 7.0, 1.9$  Hz, 1H), 7.20 (d,  $J = 8.2$  Hz, 1H), 6.99 (dd,  $J = 8.3, 1.5$  Hz, 1H), 6.12 (s, 1H), 5.34 (d,  $J = 5.2$  Hz, 2H), 4.05 – 3.97 (m, 2H), 3.88 (s, 3H), 3.02 – 2.96 (m, 1H), 2.93 (dd,  $J = 14.4, 13.0$  Hz, 1H), 2.82 (dd,  $J = 6.5, 4.8$  Hz, 1H), 2.80 – 2.73 (m, 2H), 2.56 (s, 3H), 2.51 (dd,  $J = 4.2, 1.3$  Hz, 1H), 1.94 (ddt,  $J = 14.5, 4.4, 2.6$  Hz, 1H), 1.87 (ddd,  $J = 14.4, 4.1, 2.5$  Hz, 1H), 1.81 (ddd,  $J = 12.9, 4.1, 2.5$  Hz, 1H), 0.85 (d,  $J = 6.8$  Hz, 3H) ppm.  $^{13}\text{C}$  NMR (176 MHz, Chloroform- $d$ )  $\delta$  198.9, 168.7, 163.8, 156.7, 136.3, 134.1, 131.2, 129.3, 129.2, 129.1, 128.5, 127.2, 127.1, 125.3, 123.1, 119.9, 115.3, 110.5, 93.3, 91.5, 74.4, 71.5, 58.9, 57.0, 38.7, 34.0, 29.9, 28.9, 24.8, 22.1, 15.1 ppm. HRMS-ESI ( $m/z$ ):  $[\text{M} + \text{H}]^+$  calculated for  $\text{C}_{33}\text{H}_{32}\text{ClNO}_5$   $[\text{M} + \text{H}]^+$ : 558.1969, found 558.1967.

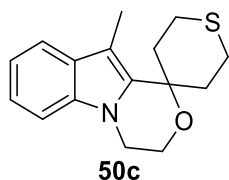
## INDOLE OXAZINES

10'-methyl-3',4'-dihydrospiro[cyclohexane-1,1'-[1,4]oxazino[4,3-a]indole] **51a**

Synthesized via procedure C, 24.0 mg, 94%. **<sup>1</sup>H NMR** (400 MHz, Chloroform-*d*)  $\delta$  7.54 (ddd,  $J = 7.7, 1.3, 0.7$  Hz, 1H), 7.24 (ddd,  $J = 8.0, 1.3, 0.8$  Hz, 1H), 7.21 – 7.15 (m, 1H), 7.15 – 7.09 (m, 1H), 4.13 – 4.00 (m, 4H), 2.39 (s, 3H), 2.10 – 1.91 (m, 4H), 1.78 (tdd,  $J = 8.8, 5.0, 2.1$  Hz, 3H), 1.67 – 1.57 (m, 2H), 1.35 (dt,  $J = 13.9, 3.9$  Hz, 1H) ppm. **<sup>13</sup>C NMR** (101 MHz, Chloroform-*d*)  $\delta$  134.9, 126.8, 121.1, 119.4, 118.3, 115.2, 108.5, 103.4, 75.0, 58.4, 42.1, 34.4, 25.7, 21.5, 10.3 ppm. **HRMS-ESI** ( $m/z$ ):  $[M + H]^+$  calculated for C<sub>17</sub>H<sub>21</sub>NO  $[M+H]^+$ : 256.1623, found 256.1622.

10'-methyl-2,3,3',4',5,6-hexahydrospiro[pyran-4,1'-[1,4]oxazino[4,3-a]indole] **51b**

Synthesized via procedure C, 18.5 mg, 72%. **<sup>1</sup>H NMR** (700 MHz, Chloroform-*d*)  $\delta$  7.55 (dt,  $J = 7.8, 1.0$  Hz, 1H), 7.25 (dt,  $J = 8.1, 1.0$  Hz, 1H), 7.20 (ddd,  $J = 8.1, 6.9, 1.2$  Hz, 1H), 7.13 (ddd,  $J = 7.9, 6.9, 1.1$  Hz, 1H), 4.14 – 4.04 (m, 4H), 3.95 – 3.82 (m, 4H), 2.41 (s, 3H), 2.41 – 2.34 (m, 2H), 1.95 – 1.84 (m, 2H) ppm. **<sup>13</sup>C NMR** (176 MHz, Chloroform-*d*)  $\delta$  133.7, 133.0, 127.6, 120.3, 118.4, 117.3, 107.3, 102.9, 71.3, 62.2, 57.6, 40.8, 33.6, 8.9 ppm. **HRMS-ESI** ( $m/z$ ):  $[M + H]^+$  calculated for C<sub>16</sub>H<sub>19</sub>NO<sub>2</sub>  $[M+H]^+$ : 258.1416, found 258.1425.

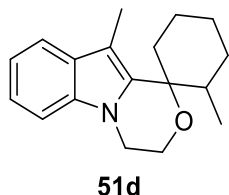
10'-methyl-2,3,3',4',5,6-hexahydrospiro[thiopyran-4,1'-[1,4]oxazino[4,3-a]indole] **50c**

Synthesized via procedure C, 23.0 mg, 84%. **<sup>1</sup>H NMR** (700 MHz, Chloroform-*d*)  $\delta$  7.55 (dt,  $J = 7.9, 1.0$  Hz, 1H), 7.24 (dt,  $J = 8.1, 0.9$  Hz, 1H), 7.20 (ddd,  $J = 8.1, 6.9, 1.2$  Hz, 1H), 7.13 (ddd,  $J = 7.9, 6.9, 1.1$  Hz, 1H), 4.12 – 4.02 (m, 4H), 3.22 (ddd,  $J = 13.6, 12.5, 2.7$  Hz, 2H), 2.47 – 2.40 (m,

## Experimental

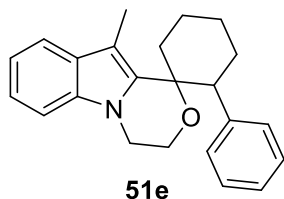
5H), 2.36 (ddd,  $J = 14.1, 12.6, 3.7$  Hz, 2H), 2.32 – 2.27 (m, 2H) ppm.  $^{13}\text{C}$  NMR (176 MHz, Chloroform- $d$ )  $\delta$  134.9, 134.7, 128.6, 121.3, 119.4, 118.4, 108.4, 103.8, 73.1, 58.2, 41.7, 35.2, 23.6, 10.1 ppm. HRMS-ESI ( $m/z$ ):  $[\text{M} + \text{H}]^+$  calculated for  $\text{C}_{16}\text{H}_{19}\text{NOS}$   $[\text{M}+\text{H}]^+$ : 274.1187, found 274.1193.

2,10'-dimethyl-3',4'-dihydrospiro[cyclohexane-1,1'-[1,4]oxazino[4,3-a]indole] **51d**



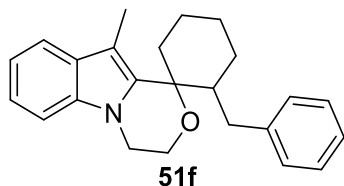
Synthesized via procedure C, 21.5 mg, 80%.  $^1\text{H}$  NMR (400 MHz, Chloroform- $d$ )  $\delta$  7.46 (ddd,  $J = 7.7, 1.3, 0.8$  Hz, 1H), 7.16 (ddd,  $J = 8.0, 1.3, 0.7$  Hz, 1H), 7.13 – 6.99 (m, 2H), 4.07 – 3.98 (m, 1H), 3.98 – 3.89 (m, 3H), 2.27 (s, 3H), 2.20 – 2.07 (m, 2H), 1.74 – 1.28 (m, 7H), 0.63 (d,  $J = 6.7$  Hz, 3H) ppm.  $^{13}\text{C}$  NMR (176 MHz, Chloroform- $d$ )  $\delta$  135.6, 135.1, 129.1, 120.9, 119.4, 118.4, 108.5, 103.1, 77.9, 58.7, 42.1, 39.8, 33.1, 29.7, 26.5, 21.6, 16.3, 10.3 ppm. HRMS-ESI ( $m/z$ ):  $[\text{M} + \text{H}]^+$  calculated for  $\text{C}_{18}\text{H}_{23}\text{NO}$   $[\text{M}+\text{H}]^+$ : 270.1780, found 270.1878.

10'-methyl-2-phenyl-3',4'-dihydrospiro[cyclohexane-1,1'-[1,4]oxazino[4,3-a]indole] **51e**

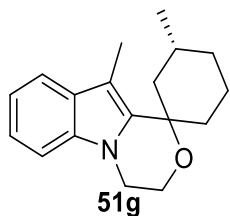


Synthesized via procedure C, 24.5 mg, 74%.  $^1\text{H}$  NMR (400 MHz, Chloroform- $d$ )  $\delta$  7.57 – 7.43 (m, 1H), 7.13 – 7.08 (m, 2H), 7.07 – 7.03 (m, 2H), 7.03 – 6.99 (m, 1H), 6.99 – 6.95 (m, 3H), 4.05 (ddd,  $J = 11.6, 4.1, 1.5$  Hz, 1H), 3.88 (td,  $J = 11.4, 2.8$  Hz, 1H), 3.76 (ddd,  $J = 11.4, 2.9, 1.5$  Hz, 1H), 3.42 – 3.31 (m, 1H), 3.27 (dd,  $J = 12.8, 3.7$  Hz, 1H), 2.53 (s, 3H), 2.26 (ddd,  $J = 21.7, 12.6, 3.0$  Hz, 2H), 2.06 – 1.79 (m, 4H), 1.78 – 1.61 (m, 2H) ppm.  $^{13}\text{C}$  NMR (176 MHz, Chloroform- $d$ )  $\delta$  142.6, 134.4, 134.3, 129.0, 128.6, 127.1, 125.9, 120.4, 118.7, 118.0, 107.9, 102.7, 77.6, 59.1, 51.1, 41.2, 33.5, 28.2, 26.2, 21.3, 10.6 ppm. HRMS-ESI ( $m/z$ ):  $[\text{M} + \text{H}]^+$  calculated for  $\text{C}_{23}\text{H}_{25}\text{NO}$   $[\text{M}+\text{H}]^+$ : 332.1936, found 332.1936.



2-benzyl-10'-methyl-3',4'-dihydrospiro[cyclohexane-1,1'-[1,4]oxazino[4,3-a]indole] **51f**

Synthesized via procedure C, 20.7 mg, 60%. **<sup>1</sup>H NMR** (700 MHz, Chloroform-*d*)  $\delta$  7.59 (dt,  $J$  = 7.8, 1.0 Hz, 1H), 7.27 (t,  $J$  = 0.9 Hz, 1H), 7.22 – 7.16 (m, 3H), 7.14 (ddd,  $J$  = 7.9, 6.9, 1.0 Hz, 1H), 7.12 – 7.09 (m, 1H), 6.99 – 6.96 (m, 2H), 4.16 (ddd,  $J$  = 10.7, 3.0, 1.4 Hz, 1H), 4.12 – 4.03 (m, 4H), 2.46 (s, 4H), 2.37 (dd,  $J$  = 13.4, 10.7 Hz, 1H), 2.30 – 2.26 (m, 2H), 1.81 – 1.76 (m, 1H), 1.76 – 1.68 (m, 3H), 1.52 (dd,  $J$  = 8.8, 3.7 Hz, 2H) ppm. **<sup>13</sup>C NMR** (176 MHz, Chloroform-*d*)  $\delta$  142.0, 135.3, 135.2, 129.6, 129.2, 128.3, 125.8, 121.1, 119.5, 118.5, 108.5, 103.2, 78.4, 58.7, 47.5, 42.1, 37.7, 33.1, 26.2, 26.1, 21.7, 10.6 ppm. **HRMS-ESI** ( $m/z$ ):  $[M + H]^+$  calculated for C<sub>24</sub>H<sub>27</sub>NO  $[M+H]^+$ : 346.2093, found 346.2095.

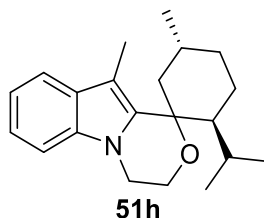
(3*R*)-3,10'-dimethyl-3',4'-dihydrospiro[cyclohexane-1,1'-[1,4]oxazino[4,3-a]indole] **51g**

Synthesized via procedure C, 24.3 mg, 90%, d.r. 6:1. **<sup>1</sup>H NMR** (700 MHz, Chloroform-*d*)  $\delta$  7.54 (dt,  $J$  = 7.9, 1.0 Hz, 1H), 7.24 (dt,  $J$  = 8.1, 0.9 Hz, 1H), 7.18 (ddd,  $J$  = 8.1, 6.9, 1.2 Hz, 1H), 7.12 (ddd,  $J$  = 7.9, 7.0, 1.1 Hz, 1H), 4.11 – 4.01 (m, 4H), 2.37 (s, 3H), 2.07 – 1.98 (m, 2H), 1.96 – 1.84 (m, 2H), 1.77 (ddt,  $J$  = 10.5, 5.8, 3.4 Hz, 2H), 1.66 – 1.61 (m, 2H), 1.03 (s, 1H), 0.94 (d,  $J$  = 6.7 Hz, 3H). **<sup>13</sup>C NMR** (176 MHz, Chloroform-*d*)  $\delta$  136.0, 135.0, 129.1, 121.2, 119.5, 118.5, 108.6, 103.5, 75.8, 58.6, 43.3, 42.1, 34.6, 33.9, 27.7, 22.8, 21.6, 10.4 ppm. **HRMS-ESI** ( $m/z$ ):  $[M + H]^+$  calculated for C<sub>18</sub>H<sub>23</sub>NO  $[M+H]^+$ : 270.1780, found 270.1880.

## Experimental

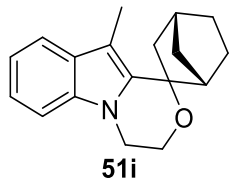
(2*S*,5*R*)-2-isopropyl-5,10'-dimethyl-3',4'-dihydrospiro[cyclohexane-1,1'-[1,4]oxazino[4,3-*a*]indole]

### 51h

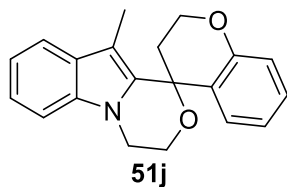


Synthesized via procedure C, 18.4 mg, 59%. **<sup>1</sup>H NMR** (700 MHz, Chloroform-*d*)  $\delta$  7.55 (dt,  $J$  = 7.8, 1.0 Hz, 1H), 7.26 – 7.24 (m, 1H), 7.15 (dddd,  $J$  = 36.8, 7.9, 7.0, 1.1 Hz, 2H), 4.13 – 4.07 (m, 1H), 4.07 – 3.95 (m, 3H), 2.34 (s, 3H), 2.21 (ddd,  $J$  = 14.3, 3.5, 2.4 Hz, 1H), 1.94 (ddd,  $J$  = 12.6, 3.7, 1.8 Hz, 1H), 1.91 – 1.82 (m, 2H), 1.72 (dd,  $J$  = 12.9, 3.4 Hz, 1H), 1.57 (dtd,  $J$  = 12.4, 7.1, 6.4, 2.8 Hz, 3H), 1.38 (dd,  $J$  = 14.3, 11.8 Hz, 1H), 0.92 (d,  $J$  = 6.5 Hz, 3H), 0.85 (d,  $J$  = 6.9 Hz, 3H), 0.76 (d,  $J$  = 7.0 Hz, 3H) ppm. **<sup>13</sup>C NMR** (176 MHz, Chloroform-*d*)  $\delta$  135.3, 134.8, 128.8, 120.6, 119.1, 118.1, 108.2, 102.8, 80.0, 58.1, 49.1, 42.0, 41.7, 35.2, 27.8, 27.6, 23.7, 22.2, 20.6, 18.7, 10.0 ppm. **HRMS-ESI** ( $m/z$ ):  $[M + H]^+$  calculated for C<sub>21</sub>H<sub>29</sub>NO  $[M+H]^+$ : 312.2249, found 312.2248.

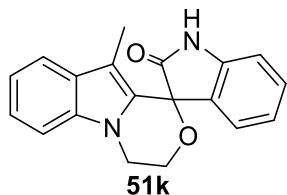
(1*S*,4*R*)-10'-methyl-3',4'-dihydrospiro[bicyclo[2.2.1]heptane-2,1'-[1,4]oxazino[4,3-*a*]indole] **51i**



Synthesized via procedure C, 17.6 mg, 66%. **<sup>1</sup>H NMR** (400 MHz, Chloroform-*d*)  $\delta$  7.46 (dd,  $J$  = 7.8, 3.7 Hz, 1H), 7.13 (ddd,  $J$  = 7.8, 2.3, 1.1 Hz, 2H), 7.08 – 7.03 (m, 1H), 4.08 – 3.91 (m, 3H), 3.90 – 3.75 (m, 1H), 2.82 – 2.49 (m, 2H), 2.37 (d,  $J$  = 11.5 Hz, 4H), 2.34 – 2.26 (m, 1H), 2.02 – 1.88 (m, 1H), 1.81 (d,  $J$  = 3.5 Hz, 1H), 1.45 – 1.30 (m, 4H), 1.30 – 1.22 (m, 1H), 1.22 – 1.13 (m, 1H) ppm. **<sup>13</sup>C NMR** (176 MHz, Chloroform-*d*)  $\delta$  128.4, 120.7, 118.4, 117.4, 107.5, 104.8, 82.5, 58.9, 57.2, 45.5, 42.2, 41.0, 40.9, 35.8, 34.7, 28.4, 21.7, 10.7 ppm. **HRMS-ESI** ( $m/z$ ):  $[M + H]^+$  calculated for C<sub>18</sub>H<sub>21</sub>NO  $[M+H]^+$ : 268.1623, found 268.1622.

10'-methyl-3',4'-dihydrospiro[chromane-4,1'-[1,4]oxazino[4,3-a]indole] **51j**

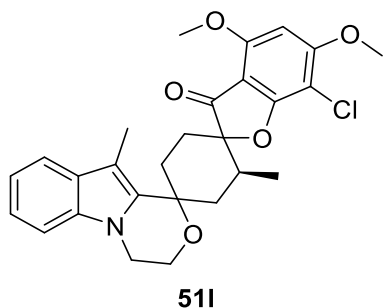
Synthesized via procedure C, 16.8 mg, 55%. **<sup>1</sup>H NMR** (700 MHz, Chloroform-*d*)  $\delta$  7.54 (dt,  $J = 7.9, 1.0$  Hz, 1H), 7.35 (dt,  $J = 8.2, 0.9$  Hz, 1H), 7.26 (td,  $J = 7.8, 1.1$  Hz, 1H), 7.23 (ddd,  $J = 8.3, 7.1, 1.7$  Hz, 1H), 7.17 (ddd,  $J = 7.9, 7.0, 1.0$  Hz, 1H), 6.94 (ddd,  $J = 9.5, 8.0, 1.4$  Hz, 2H), 6.78 (ddd,  $J = 7.8, 7.1, 1.2$  Hz, 1H), 4.53 (ddd,  $J = 13.1, 10.8, 2.1$  Hz, 1H), 4.36 (ddd,  $J = 10.9, 4.3, 2.3$  Hz, 1H), 4.26 – 4.19 (m, 4H), 2.55 (ddd,  $J = 14.6, 13.3, 4.3$  Hz, 1H), 2.41 (dt,  $J = 14.6, 2.2$  Hz, 1H), 1.81 (s, 3H) ppm. **<sup>13</sup>C NMR** (176 MHz, Chloroform-*d*)  $\delta$  138.3, 133.9, 128.7, 128.0, 123.4, 123.0, 120.6, 120.2, 119.3, 118.0, 115.9, 108.1, 106.2, 106.0, 74.9, 58.6, 45.9, 39.6, 24.2, 9.8 ppm. **HRMS-ESI** ( $m/z$ ):  $[M + H]^+$  calculated for C<sub>20</sub>H<sub>19</sub>NO<sub>2</sub>  $[M+H]^+$ : 306.1416, found 306.1410.

10'-methyl-3',4'-dihydrospiro[indoline-3,1'-[1,4]oxazino[4,3-a]indol]-2-one **51k**

Synthesized via procedure C, 14.9 mg, 49%. **<sup>1</sup>H NMR** (700 MHz, Chloroform-*d*)  $\delta$  7.53 (s, 1H), 7.48 (dt,  $J = 7.9, 1.0$  Hz, 1H), 7.36 – 7.30 (m, 2H), 7.24 (ddd,  $J = 8.2, 7.0, 1.2$  Hz, 1H), 7.22 – 7.18 (m, 1H), 7.12 (ddd,  $J = 8.0, 7.0, 1.0$  Hz, 1H), 7.05 (td,  $J = 7.6, 1.0$  Hz, 1H), 6.92 (dt,  $J = 7.9, 0.8$  Hz, 1H), 5.18 – 5.11 (m, 1H), 4.33 – 4.23 (m, 3H), 1.68 (s, 3H). **<sup>13</sup>C NMR** (176 MHz, Chloroform-*d*)  $\delta$  174.3, 139.9, 134.7, 129.6, 128.6, 127.3, 125.0, 124.5, 122.5, 120.9, 118.6, 117.7, 109.0, 107.6, 106.4, 75.5, 59.6, 40.3, 6.8 ppm. **HRMS-ESI** ( $m/z$ ):  $[M + H]^+$  calculated for C<sub>19</sub>H<sub>16</sub>N<sub>2</sub>O<sub>2</sub>  $[M+H]^+$ : 305.1212, found 305.1211.

## Experimental

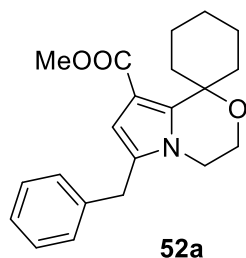
(2'*S*)-7-chloro-4,6-dimethoxy-2',10''-dimethyl-3'',4''-dihydro-3*H*-dispiro[benzofuran-2,1'-cyclohexane-4',1''-[1,4]oxazino[4,3-*a*]indol]-3-one **51I**



Synthesized via procedure C, 37.5 mg, 78%. **<sup>1</sup>H NMR** (400 MHz, Chloroform-*d*)  $\delta$  7.64 – 7.50 (m, 1H), 7.24 (dt, *J* = 8.0, 0.8 Hz, 1H), 7.21 – 7.16 (m, 1H), 7.15 – 7.09 (m, 1H), 6.10 (s, 1H), 4.15 – 4.03 (m, 4H), 4.01 (d, *J* = 5.1 Hz, 6H), 2.95 – 2.67 (m, 3H), 2.58 (s, 3H), 2.56 – 2.42 (m, 1H), 2.02 (ddt, *J* = 28.4, 13.2, 2.7 Hz, 2H), 1.78 (ddd, *J* = 12.9, 4.1, 2.5 Hz, 1H), 0.84 (d, *J* = 6.5 Hz, 3H) ppm. **<sup>13</sup>C NMR** (176 MHz, Chloroform-*d*)  $\delta$  199.3, 168.7, 164.3, 157.9, 135.2, 134.4, 129.1, 121.4, 119.6, 118.7, 108.5, 106.2, 105.0, 92.9, 89.0, 74.8, 58.8, 57.2, 56.6, 42.1, 37.7, 33.4, 29.1, 28.4, 27.2, 15.0, 10.0 ppm. **HRMS-ESI** (*m/z*): [*M* + *H*]<sup>+</sup> calculated for C<sub>27</sub>H<sub>28</sub>ClNO<sub>5</sub> [*M*+*H*]<sup>+</sup>: 482.1656 and 484.1627, found 482.1655 and 484.1627.

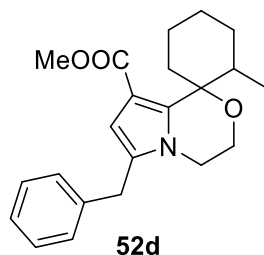
## PYRROLOOXAZINES

methyl 6'-benzyl-3',4'-dihydrospiro[cyclohexane-1,1'-pyrrolo[2,1][1,4]oxazine]-8'-carboxylate **52a**



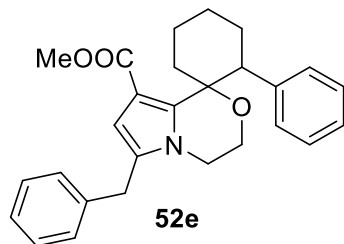
Synthesized via procedure C, 32.6 mg, 96%. **<sup>1</sup>H NMR** (500 MHz, Chloroform-*d*)  $\delta$  7.30 (dd, *J* = 8.0, 6.7 Hz, 2H), 7.23 (d, *J* = 7.4 Hz, 1H), 7.16 – 7.12 (m, 2H), 6.35 (d, *J* = 0.9 Hz, 1H), 3.94 – 3.83 (m, 4H), 3.76 (s, 3H), 3.66 – 3.58 (m, 2H), 2.60 (td, *J* = 13.5, 4.7 Hz, 2H), 1.76 (dq, *J* = 13.8, 1.9 Hz, 2H), 1.71 – 1.41 (m, 6H) ppm. **<sup>13</sup>C NMR** (126 MHz, Chloroform-*d*)  $\delta$  164.9, 140.5, 138.1, 129.1, 128.7, 128.5, 126.6, 110.5, 108.3, 76.2, 57.3, 50.9, 42.8, 32.3, 32.1, 24.7, 21.4 ppm. **HRMS-ESI** (*m/z*): [*M* + *H*]<sup>+</sup> calculated for C<sub>21</sub>H<sub>25</sub>NO<sub>3</sub> [*M*+*H*]<sup>+</sup>: 340.1834, found 340.1833.

methyl 6'-benzyl-2-methyl-3',4'-dihydrospiro[cyclohexane-1,1'-pyrrolo[2,1-c][1,4]oxazine]-8'-carboxylate **52d**



Synthesized via procedure C, 32.5 mg, 92%. **<sup>1</sup>H NMR** (500 MHz, Chloroform-*d*)  $\delta$  7.24 – 7.19 (m, 2H), 7.17 – 7.10 (m, 1H), 7.08 – 6.99 (m, 2H), 6.33 (d,  $J$  = 0.9 Hz, 1H), 3.89 – 3.70 (m, 4H), 3.68 (s, 3H), 3.55 – 3.43 (m, 2H), 2.74 (ddd,  $J$  = 11.4, 6.7, 4.7 Hz, 1H), 2.46 – 2.34 (m, 1H), 1.90 (dt,  $J$  = 14.2, 2.1 Hz, 1H), 1.60 (d,  $J$  = 3.8 Hz, 1H), 1.51-1.41 (m, 3H) 1.42 – 1.29 (m, 2H), 0.51 (d,  $J$  = 6.8 Hz, 3H) ppm. **<sup>13</sup>C NMR** (126 MHz, Chloroform-*d*)  $\delta$  164.9, 140.0, 138.3, 128.9, 128.7, 128.3, 126.5, 110.8, 108.1, 79.0, 57.6, 50.9, 42.9, 37.1, 32.2, 30.3, 29.7, 25.5, 21.3, 16.3 ppm. **HRMS-ESI** ( $m/z$ ): [M + H]<sup>+</sup> calculated for C<sub>22</sub>H<sub>27</sub>NO<sub>3</sub> [M+H]<sup>+</sup>: 354.1991, found 354.1990.

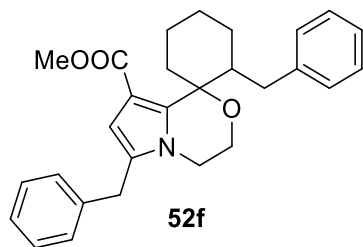
methyl 6'-benzyl-2-phenyl-3',4'-dihydrospiro[cyclohexane-1,1'-pyrrolo[2,1-c][1,4]oxazine]-8'-carboxylate **52e**



Synthesized via procedure C, 40.7 mg, 98%. **<sup>1</sup>H NMR** (400 MHz, Chloroform-*d*)  $\delta$  7.44 (s, 1H), 7.37 – 7.30 (m, 4H), 7.30 – 7.27 (m, 1H), 7.25 (d,  $J$  = 4.5 Hz, 4H), 6.83 – 6.72 (m, 2H), 6.57 (d,  $J$  = 0.7 Hz, 1H), 4.23 (dd,  $J$  = 13.0, 3.7 Hz, 1H), 4.04 (s, 4H), 3.85 – 3.73 (m, 1H), 3.41 (ddd,  $J$  = 12.2, 2.6, 1.2 Hz, 1H), 2.91 (dddd,  $J$  = 28.2, 14.1, 12.0, 4.4 Hz, 2H), 2.40 – 2.27 (m, 1H), 2.23 – 2.12 (m, 1H), 2.09 – 1.97 (m, 1H), 1.98 – 1.77 (m, 4H) ppm. **<sup>13</sup>C NMR** (126 MHz, Chloroform-*d*)  $\delta$  165.2, 143.2, 138.9, 138.2, 129.6, 128.5, 128.1, 127.7, 127.0, 126.1, 125.8, 110.8, 108.5, 78.9, 58.2, 51.0, 48.4, 42.6, 31.7, 30.8, 27.7, 25.5, 21.3 ppm. **HRMS-ESI** ( $m/z$ ): [M + H]<sup>+</sup> calculated for C<sub>27</sub>H<sub>29</sub>NO<sub>3</sub> [M+H]<sup>+</sup>: 416.2147, found 416.2145.

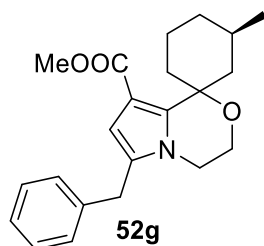
## Experimental

methyl 2,6'-dibenzyl-3',4'-dihydrospiro[cyclohexane-1,1'-pyrrolo[2,1-c][1,4]oxazine]-8'-carboxylate **52f**



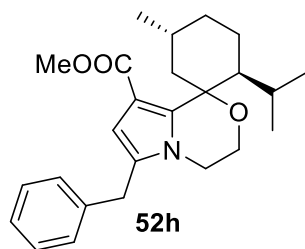
Synthesized via procedure C, 34.8 mg, 81%. **<sup>1</sup>H NMR** (400 MHz, Chloroform-*d*)  $\delta$  7.32 – 7.26 (m, 4H), 7.25 – 7.07 (m, 8H), 7.01 – 6.93 (m, 2H), 6.42 (d,  $J$  = 0.9 Hz, 1H), 4.02 – 3.83 (m, 2H), 3.80 (s, 3H), 3.67 – 3.59 (m, 2H), 3.24 (dd,  $J$  = 13.9, 4.8 Hz, 1H), 3.11 – 2.98 (m, 1H), 2.60 – 2.24 (m, 3H), 2.12 – 1.97 (m, 3H), 1.90 – 1.78 (m, 1H) ppm. **<sup>13</sup>C NMR** (126 MHz, Chloroform-*d*)  $\delta$  165.3, 142.3, 140.8, 139.8, 138.6, 129.5, 129.1, 128.7, 128.3, 126.9, 126.3, 125.7, 111.4, 108.9, 79.7, 57.9, 52.9, 51.3, 42.6, 35.8, 33.8, 28.4, 25.5, 21.7 ppm. **HRMS-ESI** ( $m/z$ ): [M + H]<sup>+</sup> calculated for C<sub>28</sub>H<sub>31</sub>NO<sub>3</sub> [M+H]<sup>+</sup>: 430.2304, found 430.2301.

methyl (3*R*)-6'-benzyl-3-methyl-3',4'-dihydrospiro[cyclohexane-1,1'-pyrrolo[2,1-c][1,4]oxazine]-8'-carboxylate **52g**



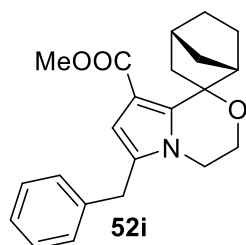
Synthesized via procedure C, 31.1 mg, 88%, d.r. 15:1 **<sup>1</sup>H NMR** (500 MHz, Chloroform-*d*)  $\delta$  7.32 – 7.27 (m, 2H), 7.25 – 7.19 (m, 1H), 7.16 – 7.11 (m, 2H), 6.35 (d,  $J$  = 0.8 Hz, 1H), 3.94 – 3.82 (m, 4H), 3.75 (s, 3H), 3.63 (t,  $J$  = 5.1 Hz, 2H), 2.52 (td,  $J$  = 13.6, 5.0 Hz, 1H), 2.27 (dd,  $J$  = 13.4, 11.9 Hz, 1H), 1.78 – 1.71 (m, 3H), 1.71 – 1.62 (m, 2H), 1.61 – 1.52 (m, 1H), 1.16 (dd,  $J$  = 12.1, 3.8 Hz, 1H), 0.90 (d,  $J$  = 6.5 Hz, 3H) ppm. **<sup>13</sup>C NMR** (126 MHz, Chloroform-*d*)  $\delta$  164.8, 140.2, 138.1, 129.1, 128.7, 128.5, 126.5, 110.6, 108.4, 76.9, 57.4, 50.9, 42.8, 40.7, 33.5, 32.4, 31.4, 27.5, 22.4, 21.5 ppm. **HRMS-ESI** ( $m/z$ ): [M + H]<sup>+</sup> calculated for C<sub>22</sub>H<sub>27</sub>NO<sub>3</sub> [M+H]<sup>+</sup>: 354.1991, found 354.1993.

methyl(2*S*,5*R*)-6'-benzyl-2-isopropyl-5-methyl-3',4'-dihydrospiro[cyclohexane-1,1'-pyrrolo[2,1-*c*][1,4]oxazine]-8'-carboxylate **52h**



Synthesized via procedure C, 22.5 mg, 57%. **<sup>1</sup>H NMR** (500 MHz, Chloroform-*d*)  $\delta$  7.29 (dd,  $J = 8.0, 6.7$  Hz, 2H), 7.23 (d,  $J = 7.3$  Hz, 1H), 7.17 – 7.10 (m, 2H), 6.39 (d,  $J = 0.9$  Hz, 1H), 3.92 – 3.78 (m, 4H), 3.75 (s, 3H), 3.61 – 3.53 (m, 2H), 2.62 (ddd,  $J = 12.1, 4.5, 2.0$  Hz, 1H), 2.12 (dd,  $J = 14.0, 11.9$  Hz, 1H), 1.96 (ddd,  $J = 14.0, 3.6, 2.3$  Hz, 1H), 1.80 – 1.65 (m, 2H), 1.31 – 1.17 (m, 4H), 0.89 (d,  $J = 6.4$  Hz, 3H), 0.79 (d,  $J = 6.9$  Hz, 3H), 0.69 (d,  $J = 7.0$  Hz, 3H) ppm. **<sup>13</sup>C NMR** (126 MHz, Chloroform-*d*)  $\delta$  165.2, 140.2, 138.7, 129.2, 129.0, 128.7, 126.9, 111.3, 108.6, 81.7, 57.7, 51.3, 46.4, 43.2, 40.1, 34.8, 32.6, 28.9, 28.0, 24.1, 22.5, 21.6, 19.5 ppm. **HRMS-ESI** ( $m/z$ ):  $[M + H]^+$  calculated for C<sub>25</sub>H<sub>33</sub>NO<sub>3</sub>  $[M+H]^+$ : 396.2460, found 396.2463.

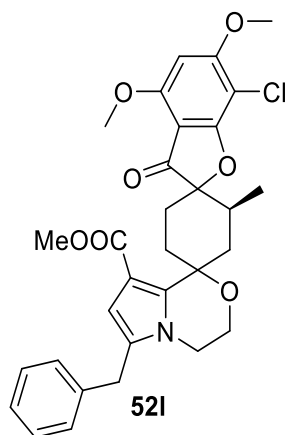
methyl(1*S*,4*R*)-6'-benzyl-3',4'-dihydrospiro[bicyclo[2.2.1]heptane-2,1'-pyrrolo[2,1-*c*][1,4]oxazine]-8'-carboxylate **52i**



Synthesized via procedure C, 18.6 mg, 53%. **<sup>1</sup>H NMR** (400 MHz, Chloroform-*d*)  $\delta$  7.30 (t,  $J = 7.5$  Hz, 2H), 7.23 (d,  $J = 7.2$  Hz, 1H), 7.19 – 7.11 (m, 2H), 6.38 (d,  $J = 0.8$  Hz, 1H), 3.98 – 3.79 (m, 4H), 3.74 (s, 3H), 3.73 – 3.56 (m, 2H), 3.38 (ddd,  $J = 13.1, 4.8, 2.7$  Hz, 1H), 2.49 (d,  $J = 3.7$  Hz, 1H), 2.37 (t,  $J = 5.1$  Hz, 1H), 2.26 (dt,  $J = 10.2, 2.2$  Hz, 1H), 1.85 – 1.69 (m, 1H), 1.59 (dd,  $J = 13.2, 3.3$  Hz, 1H), 1.46 – 1.31 (m, 2H), 1.26 (ddd,  $J = 16.0, 12.4, 2.5$  Hz, 2H) ppm. **<sup>13</sup>C NMR** (126 MHz, Chloroform-*d*)  $\delta$  165.9, 138.1, 129.7, 128.7, 128.7, 128.6, 128.5, 126.6, 126.5, 111.6, 110.7, 84.0, 59.2, 51.2, 47.9, 43.8, 41.8, 37.1, 36.4, 32.5, 29.0, 23.5 ppm. **HRMS-ESI** ( $m/z$ ):  $[M + H]^+$  calculated for C<sub>22</sub>H<sub>25</sub>NO<sub>3</sub>  $[M+H]^+$ : 352.1834, found 352.1834.

## Experimental

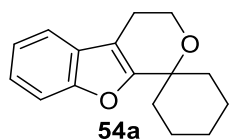
methyl(2'*S*)-6''-benzyl-7-chloro-4,6-dimethoxy-2'-methyl-3-oxo-3'',4''-dihydro-3*H*-dispiro[benzofuran-2,1'-cyclohexane-4',1''-pyrrolo[2,1-*c*][1,4]oxazine]-8''-carboxylate **52i**



Synthesized via procedure C, 41.2 mg, 73%. **<sup>1</sup>H NMR** (500 MHz, Chloroform-*d*)  $\delta$  7.26 – 7.19 (m, 2H), 7.16 (d,  $J$  = 7.5 Hz, 1H), 7.07 (dd,  $J$  = 8.1, 1.5 Hz, 2H), 6.37 (s, 1H), 6.00 (s, 1H), 3.96 – 3.87 (m, 10H), 3.60 (dt,  $J$  = 7.8, 5.0 Hz, 2H), 3.24 – 3.09 (m, 3H), 2.60 (ddd,  $J$  = 13.0, 6.8, 4.3 Hz, 1H), 2.46 – 2.37 (m, 1H), 2.31 (td,  $J$  = 13.6, 4.4 Hz, 1H), 1.82 – 1.64 (m, 4H), 0.73 (d,  $J$  = 6.9 Hz, 3H) ppm. **<sup>13</sup>C NMR** (126 MHz, Chloroform-*d*)  $\delta$  198.1, 168.2, 164.8, 163.6, 157.7, 138.1, 136.4, 129.6, 128.7, 128.7, 128.6, 128.5, 126.5, 111.2, 110.1, 105.8, 92.5, 88.7, 75.8, 57.3, 56.8, 56.2, 51.5, 42.8, 36.4, 32.8, 32.5, 28.0, 27.9, 26.9, 14.7 ppm. **HRMS-ESI** ( $m/z$ ):  $[M + H]^+$  calculated for C<sub>31</sub>H<sub>32</sub>ClNO<sub>7</sub>  $[M+H]^+$ : 566.1867, found 566.1880.

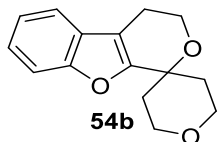
## TETRAHYDROPYRANO BENZOFURANS

3',4'-dihydrospiro[cyclohexane-1,1'-pyrano[3,4-*b*]benzofuran] **54a**

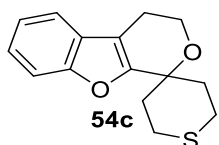


Synthesized via procedure C, 24.0 mg, 99%. **<sup>1</sup>H NMR** (700 MHz, Chloroform-*d*)  $\delta$  7.47 – 7.41 (m, 2H), 7.26 – 7.19 (m, 2H), 3.99 (t,  $J$  = 5.4 Hz, 2H), 2.75 (t,  $J$  = 5.4 Hz, 2H), 1.95 – 1.85 (m, 4H), 1.73 (dddd,  $J$  = 13.1, 8.1, 6.6, 3.0 Hz, 3H), 1.66 (dtd,  $J$  = 12.8, 4.2, 2.9 Hz, 2H), 1.42 – 1.35 (m, 1H) ppm. **<sup>13</sup>C NMR** (176 MHz, Chloroform-*d*)  $\delta$  156.8, 153.2, 127.0, 122.4, 121.4, 117.8, 110.2, 108.4, 72.3, 58.3, 32.8, 24.3, 21.6, 20.2 ppm. **HRMS-ESI** ( $m/z$ ):  $[M + H]^+$  calculated for C<sub>16</sub>H<sub>18</sub>O<sub>2</sub>  $[M+H]^+$ : 243.1307, found 243.1300.

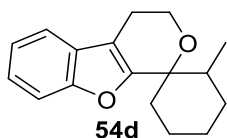


2,3,3',4',5,6-hexahydrospiro[pyran-4,1'-pyrano[3,4-*b*]benzofuran] **54b**

Synthesized via procedure C, 18.8 mg, 77%. **<sup>1</sup>H NMR** (700 MHz, Chloroform-*d*)  $\delta$  7.44 – 7.30 (m, 2H), 7.23 – 7.08 (m, 2H), 3.93 (t,  $J$  = 5.4 Hz, 2H), 3.86 – 3.76 (m, 4H), 2.70 (t,  $J$  = 5.4 Hz, 2H), 2.18 (ddd,  $J$  = 13.9, 10.8, 6.2 Hz, 2H), 1.71 (dq,  $J$  = 14.2, 2.6 Hz, 2H) ppm. **<sup>13</sup>C NMR** (176 MHz, Chloroform-*d*)  $\delta$  154.9, 153.4, 126.8, 122.8, 121.6, 118.0, 110.4, 109.3, 69.8, 62.2, 58.6, 33.1, 21.6 ppm. **HRMS**-ESI ( $m/z$ ):  $[M + H]^+$  calculated for C<sub>15</sub>H<sub>16</sub>O<sub>3</sub>  $[M+H]^+$ : 245.1099, found 245.10989.

2',3,3',4,5',6'-hexahydrospiro[pyrano[3,4-*b*]benzofuran-1,4'-thiopyran] **54c**

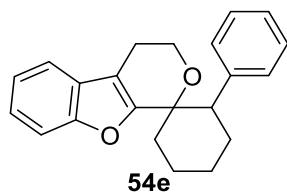
Synthesized via procedure C, 19.5 mg, 75%. **<sup>1</sup>H NMR** (700 MHz, Chloroform-*d*)  $\delta$  7.52 – 7.42 (m, 2H), 7.28 – 7.21 (m, 2H), 3.99 (t,  $J$  = 5.4 Hz, 2H), 3.14 (ddd,  $J$  = 13.6, 12.3, 2.7 Hz, 2H), 2.76 (t,  $J$  = 5.4 Hz, 2H), 2.52 (dt,  $J$  = 14.2, 4.0 Hz, 2H), 2.27 (ddd,  $J$  = 13.9, 12.3, 3.7 Hz, 2H), 2.17 (dt,  $J$  = 13.8, 3.3 Hz, 2H) ppm. **<sup>13</sup>C NMR** (176 MHz, Chloroform-*d*)  $\delta$  155.8, 153.3, 126.7, 122.8, 121.6, 118.0, 110.4, 108.8, 70.6, 58.3, 33.7, 22.3, 21.5 ppm. **HRMS**-ESI ( $m/z$ ):  $[M + H]^+$  calculated for C<sub>15</sub>H<sub>16</sub>O<sub>2</sub>S  $[M+H]^+$ : 261.0871, found 261.0870.

2-methyl-3',4'-dihydrospiro[cyclohexane-1,1'-pyrano[3,4-*b*]benzofuran] **54d**

Synthesized via procedure C, 17.4 mg, 68%. **<sup>1</sup>H NMR** (500 MHz, Chloroform-*d*)  $\delta$  7.49 – 7.42 (m, 2H), 7.26 – 7.19 (m, 2H), 4.13 – 3.95 (m, 2H), 2.93 – 2.81 (m, 1H), 2.67 – 2.52 (m, 1H), 2.35 (dddd,  $J$  = 12.8, 4.9, 3.3, 1.3 Hz, 1H), 2.15 – 2.01 (m, 1H), 1.92 – 1.69 (m, 4H), 1.69 – 1.63 (m, 1H), 1.55 (ddt,  $J$  = 15.8, 7.9, 3.9 Hz, 3H), 0.79 (d,  $J$  = 6.2 Hz, 2H), 0.67 (d,  $J$  = 6.7 Hz, 1H) ppm. **<sup>13</sup>C NMR** (126 MHz, Chloroform-*d*)  $\delta$  155.8, 153.2, 126.9, 122.3, 121.4, 117.7, 110.7, 109.9, 76.5, 74.7, 58.4, 39.5, 37.4, 31.6, 28.3, 24.9, 21.6 ppm. **HRMS**-ESI ( $m/z$ ):  $[M + H]^+$  calculated for C<sub>17</sub>H<sub>20</sub>O<sub>2</sub>  $[M+H]^+$ : 257.1463, found 257.1460.

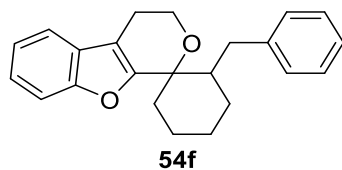
## Experimental

### 2-phenyl-3',4'-dihydrospiro[cyclohexane-1,1'-pyrano[3,4-*b*]benzofuran] **54e**

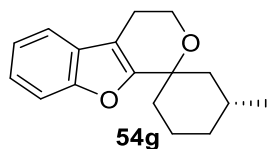


Synthesized via procedure C, 16.5 mg, 52%. **<sup>1</sup>H NMR** (500 MHz, Chloroform-*d*)  $\delta$  7.46 (dt,  $J$  = 8.2, 0.9 Hz, 1H), 7.24 (ddd,  $J$  = 7.6, 1.5, 0.7 Hz, 1H), 7.20 (ddd,  $J$  = 8.3, 7.2, 1.4 Hz, 1H), 7.17 – 7.07 (m, 3H), 7.05 – 6.93 (m, 3H), 3.96 (ddd,  $J$  = 11.3, 5.2, 1.9 Hz, 1H), 3.76 (ddd,  $J$  = 11.3, 10.3, 3.6 Hz, 1H), 3.21 (dd,  $J$  = 13.1, 3.6 Hz, 1H), 2.34 (ddd,  $J$  = 15.2, 3.6, 1.9 Hz, 1H), 2.31 – 2.20 (m, 2H), 2.20 – 2.10 (m, 1H), 1.97 – 1.63 (m, 4H), 1.61 – 1.47 (m, 2H) ppm. **<sup>13</sup>C NMR** (126 MHz, Chloroform-*d*)  $\delta$  154.9, 153.0, 141.4, 127.9, 126.7, 126.1, 124.9, 122.1, 121.2, 117.6, 110.2, 110.0, 74.8, 58.9, 49.7, 32.4, 26.6, 25.1, 21.1, 20.0 ppm. **HRMS-ESI** ( $m/z$ ): [M + H]<sup>+</sup> calculated for C<sub>22</sub>H<sub>22</sub>O<sub>2</sub> [M+H]<sup>+</sup>: 319.1620, found 319.1614.

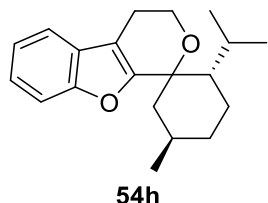
### 2-benzyl-3',4'-dihydrospiro[cyclohexane-1,1'-pyrano[3,4-*b*]benzofuran] **54f**



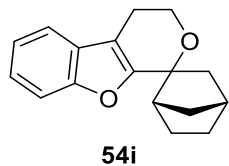
Synthesized via procedure C, 20.9 mg, 63%. **<sup>1</sup>H NMR** (500 MHz, Chloroform-*d*)  $\delta$  7.55 – 7.41 (m, 2H), 7.32 – 7.27 (m, 1H), 7.26 – 7.19 (m, 2H), 7.19 – 7.05 (m, 3H), 7.03 – 6.98 (m, 1H), 4.20 – 4.10 (m, 1H), 4.10 – 3.88 (m, 1H), 3.11 (dd,  $J$  = 13.2, 2.8 Hz, 1H), 2.93 (dddd,  $J$  = 15.0, 11.2, 5.8, 4.0 Hz, 1H), 2.63 (dddd,  $J$  = 15.1, 13.2, 3.5, 1.3 Hz, 1H), 2.48 – 2.29 (m, 1H), 2.25 – 2.14 (m, 1H), 1.99 – 1.88 (m, 1H), 1.88 – 1.76 (m, 2H), 1.76 – 1.63 (m, 2H), 1.61 (dd,  $J$  = 12.8, 4.1 Hz, 1H), 1.57 (s, 3H) ppm. **<sup>13</sup>C NMR** (126 MHz, Chloroform-*d*)  $\delta$  155.5, 153.3, 140.6, 128.2, 126.9, 124.4, 122.5, 121.5, 117.8, 110.9, 58.4, 47.5, 44.8, 36.0, 31.7, 28.7, 26.3, 24.8, 24.0, 21.7, 20.0 ppm. **HRMS-ESI** ( $m/z$ ): [M + H]<sup>+</sup> calculated for C<sub>23</sub>H<sub>24</sub>O<sub>2</sub> [M+H]<sup>+</sup>: 333.1776, found 333.1772.

(3*R*)-3-methyl-3',4'-dihydrospiro[cyclohexane-1,1'-pyrano[3,4-*b*]benzofuran] **54g**

Synthesized via procedure C, 18.2 mg, 71%. **<sup>1</sup>H NMR** (500 MHz, Chloroform-*d*)  $\delta$  7.51 – 7.36 (m, 2H), 7.32 – 7.14 (m, 2H), 4.09 – 3.88 (m, 2H), 2.86 – 2.63 (m, 2H), 1.97 – 1.82 (m, 3H), 1.82 – 1.70 (m, 3H), 1.69 – 1.51 (m, 2H), 1.05 – 0.96 (m, 1H), 0.93 (d,  $J$  = 6.4 Hz, 3H) ppm. **<sup>13</sup>C NMR** (126 MHz, Chloroform-*d*)  $\delta$  157.5, 154.2, 128.1, 123.5, 122.5, 118.9, 111.2, 109.5, 73.9, 59.5, 42.2, 34.1, 32.9, 27.2, 22.6, 22.5, 21.1 ppm. **HRMS-ESI** ( $m/z$ ):  $[M + H]^+$  calculated for C<sub>17</sub>H<sub>20</sub>O<sub>2</sub>  $[M+H]^+$ : 257.1463, found 257.1462.

(2*S*,5*R*)-2-isopropyl-5-methyl-3',4'-dihydrospiro[cyclohexane-1,1'-pyrano[3,4-*b*]benzofuran] **54h**

Synthesized via procedure C, 22.0 mg, 74%. **<sup>1</sup>H NMR** (400 MHz, Chloroform-*d*)  $\delta$  7.52 (ddt,  $J$  = 7.3, 1.2, 0.6 Hz, 1H), 7.35 (ddd,  $J$  = 7.3, 1.2, 0.6 Hz, 1H), 7.20 – 7.11 (m, 2H), 4.11 (ddd,  $J$  = 12.0, 6.0, 1.0 Hz, 1H), 3.91 (td,  $J$  = 12.0, 3.3 Hz, 1H), 3.00 – 2.91 (m, 1H), 2.73 (dd,  $J$  = 15.0, 3.3 Hz, 1H), 2.33 – 2.20 (m, 1H), 1.92 (dtd,  $J$  = 12.0, 3.6, 2.1 Hz, 2H), 1.80 – 1.75 (m, 1H), 1.61 (dq,  $J$  = 13.2, 3.3 Hz, 1H), 1.12 – 1.09 (m, 1H), 1.08 (m, 2H), 0.99 (dd,  $J$  = 7.8, 6.5 Hz, 1H), 0.93 (d,  $J$  = 6.5 Hz, 3H), 0.90 – 0.83 (m, 3H), 0.79 (d,  $J$  = 7.0 Hz, 3H) ppm. **<sup>13</sup>C NMR** (101 MHz, Chloroform-*d*)  $\delta$  138.6, 135.3, 127.0, 121.4, 119.2, 117.9, 110.6, 108.3, 77.0, 59.2, 50.4, 44.0, 35.4, 27.5, 27.2, 23.6, 22.1, 22.0, 21.2, 18.4 ppm. **HRMS-ESI** ( $m/z$ ):  $[M + H]^+$  calculated for C<sub>20</sub>H<sub>26</sub>O<sub>2</sub>  $[M+H]^+$ : 299.1933, found 299.1933.

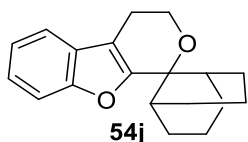
(1*S*,4*R*)-3',4'-dihydrospiro[bicyclo[2.2.1]heptane-2,1'-pyrano[3,4-*b*]benzofuran] **54i**

Synthesized via procedure C, 12.4 mg, 49%. **<sup>1</sup>H NMR** (500 MHz, Chloroform-*d*)  $\delta$  7.48 – 7.40 (m, 2H), 7.26 – 7.17 (m, 2H), 4.09 – 3.96 (m, 1H), 3.89 (ddd,  $J$  = 11.4, 8.2, 4.4 Hz, 1H), 2.94 – 2.78

## Experimental

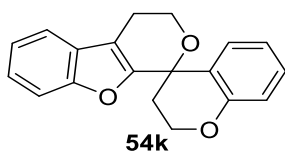
(m, 1H), 2.72 – 2.61 (m, 1H), 2.53 (dt,  $J = 4.1, 1.4$  Hz, 1H), 2.45 – 2.34 (m, 1H), 2.27 (dp,  $J = 9.7, 1.9$  Hz, 1H), 2.19 (ddd,  $J = 12.9, 4.6, 3.0$  Hz, 1H), 2.08 – 1.98 (m, 1H), 1.98 – 1.86 (m, 1H), 1.70 – 1.49 (m, 1H), 1.49 – 1.32 (m, 2H), 1.31 – 1.22 (m, 1H) ppm.  $^{13}\text{C}$  NMR (126 MHz, Chloroform-*d*)  $\delta$  156.5, 154.5, 153.3, 126.9, 122.5, 117.8, 110.5, 107.8, 80.8, 60.9, 45.1, 43.7, 42.4, 36.8, 35.4, 27.4, 21.7 ppm. HRMS-ESI ( $m/z$ ):  $[\text{M} + \text{H}]^+$  calculated for  $\text{C}_{17}\text{H}_{18}\text{O}_2$   $[\text{M}+\text{H}]^+$ : 255.1307, found 255.1305.

### 3',4'-dihydrospiro[bicyclo[3.3.1]nonane-9,1'-pyrano[3,4-*b*]benzofuran] 54j

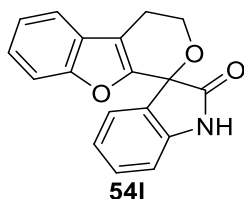


Synthesized via procedure C, 15.8 mg, 56%.  $^1\text{H}$  NMR (500 MHz, Chloroform-*d*)  $\delta$  7.51 – 7.44 (m, 2H), 7.29 – 7.19 (m, 2H), 4.03 (t,  $J = 5.6$  Hz, 2H), 2.79 (t,  $J = 5.6$  Hz, 2H), 2.51 (ttd,  $J = 12.1, 6.6, 5.7, 2.9$  Hz, 2H), 2.26 (dddd,  $J = 18.1, 9.4, 4.7, 2.0$  Hz, 2H), 2.10 – 1.87 (m, 4H), 1.85 – 1.72 (m, 3H), 1.59 – 1.54 (m, 1H), 1.51 (ddq,  $J = 13.9, 6.9, 1.3$  Hz, 2H) ppm.  $^{13}\text{C}$  NMR (126 MHz, Chloroform-*d*)  $\delta$  159.1, 154.2, 128.2, 123.8, 122.7, 119.2, 111.6, 111.4, 76.9, 58.1, 36.1, 29.1, 27.8, 23.1, 21.5, 20.9 ppm. HRMS-ESI ( $m/z$ ):  $[\text{M} + \text{H}]^+$  calculated for  $\text{C}_{19}\text{H}_{22}\text{O}_2$   $[\text{M}+\text{H}]^+$ : 283.1620, found 283.1617.

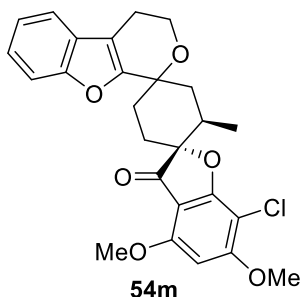
### 3',4'-dihydrospiro[chromane-4,1'-pyrano[3,4-*b*]benzofuran] 54k



Synthesized via procedure C, 8.4 mg, 29%.  $^1\text{H}$  NMR (400 MHz, Chloroform-*d*)  $\delta$  7.60 (d,  $J = 8.2$  Hz, 1H), 7.43 (s, 1H), 7.20 – 7.09 (m, 4H), 6.90 (dd,  $J = 8.2, 1.1$  Hz, 1H), 6.81 (d,  $J = 8.2$  Hz, 1H), 6.72 – 6.68 (m, 1H), 4.57 (ddd,  $J = 10.6, 9.0, 6.2$  Hz, 1H), 4.37 – 4.20 (m, 1H), 4.16 – 3.95 (m, 2H), 2.99 (dd,  $J = 15.4, 6.8$  Hz, 1H), 2.87 (ddd,  $J = 15.4, 6.8, 4.6$  Hz, 1H), 2.40 – 2.23 (m, 2H) ppm.  $^{13}\text{C}$  NMR (176 MHz, Chloroform-*d*)  $\delta$  155.7, 136.9, 136.3, 131.3, 131.0, 127.5, 124.7, 122.9, 121.3, 121.0, 119.4, 118.0, 111.9, 110.9, 70.5, 63.1, 60.8, 34.6, 23.1 ppm. HRMS-ESI ( $m/z$ ):  $[\text{M} + \text{H}]^+$  calculated for  $\text{C}_{19}\text{H}_{16}\text{O}_3$   $[\text{M}+\text{H}]^+$ : 293.1099, found 293.1100.

3',4'-dihydrospiro[indoline-3,1'-pyrano[3,4-*b*]benzofuran]-2-one **54l**

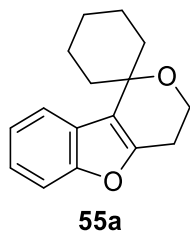
Synthesized via procedure C, 17.8 mg, 61%. **<sup>1</sup>H NMR** (700 MHz, Chloroform-*d*)  $\delta$  7.77 (s, 1H), 7.60 – 7.47 (m, 2H), 7.36 – 7.28 (m, 2H), 7.26 – 7.24 (m, 1H), 7.18 (d,  $J$  = 7.4 Hz, 1H), 7.03 (t,  $J$  = 7.5 Hz, 1H), 6.93 (d,  $J$  = 7.9 Hz, 1H), 4.86 (ddd,  $J$  = 11.3, 9.6, 3.9 Hz, 1H), 4.28 (ddd,  $J$  = 11.4, 5.4, 2.7 Hz, 1H), 3.13 (ddd,  $J$  = 15.3, 9.6, 5.4 Hz, 1H), 2.92 (dt,  $J$  = 15.8, 3.4 Hz, 1H) ppm. **<sup>13</sup>C NMR** (176 MHz, Chloroform-*d*)  $\delta$  174.5, 154.0, 146.8, 140.2, 129.8, 127.0, 126.2, 124.6, 123.6, 122.3, 121.9, 118.3, 113.8, 110.7, 109.4, 75.0, 61.1, 20.9 ppm. **HRMS-ESI** ( $m/z$ ):  $[M + H]^+$  calculated for C<sub>18</sub>H<sub>13</sub>O<sub>3</sub>N  $[M+H]^+$ : 292.0895, found 292.0891.

(2*R*,2'*R*)-7-chloro-4,6-dimethoxy-2'-methyl-3'',4''-dihydro-3*H*-dispiro[benzofuran-2,1'-cyclohexane-4',1''-pyrano[3,4-*b*]benzofuran]-3-one **54m**

Synthesized via procedure C, 37.9 mg, 81%. **<sup>1</sup>H NMR** (400 MHz, Chloroform-*d*)  $\delta$  7.54 – 7.40 (m, 2H), 7.25 – 7.17 (m, 2H), 6.09 (s, 1H), 4.07 – 3.92 (m, 8H), 2.87 – 2.63 (m, 5H), 2.44 (ddd,  $J$  = 14.1, 12.9, 4.2 Hz, 1H), 2.02 – 1.74 (m, 3H), 0.83 (d,  $J$  = 6.3 Hz, 3H) ppm. **<sup>13</sup>C NMR** (126 MHz, Chloroform-*d*)  $\delta$  198.9, 168.7, 164.3, 158.0, 156.5, 154.8, 128.3, 124.0, 122.8, 119.2, 112.0, 110.4, 106.3, 92.6, 89.1, 73.4, 60.0, 57.2, 56.6, 37.1, 33.6, 28.6, 28.5, 27.3, 23.0, 15.1 ppm. **HRMS-ESI** ( $m/z$ ):  $[M + H]^+$  calculated for C<sub>26</sub>H<sub>25</sub>O<sub>6</sub>Cl  $[M+H]^+$ : 469.1340 and 471.1310, found 469.1341 and 471.1309.

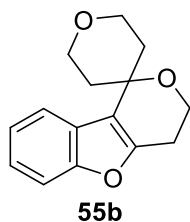
## Experimental

### 3',4'-dihydrospiro[cyclohexane-1,1'-pyrano[4,3-*b*]benzofuran] **55a**



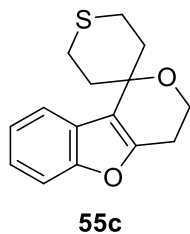
Synthesized via procedure C, 22.0 mg, 91%. **<sup>1</sup>H NMR** (700 MHz, Chloroform-*d*)  $\delta$  7.51 – 7.47 (m, 1H), 7.47 – 7.42 (m, 1H), 7.25 – 7.19 (m, 2H), 4.03 (t,  $J$  = 5.5 Hz, 2H), 2.84 (t,  $J$  = 5.5 Hz, 2H), 1.98 – 1.88 (m, 4H), 1.86 – 1.72 (m, 3H), 1.66 – 1.56 (m, 3H), 1.40 – 1.32 (m, 1H) ppm. **<sup>13</sup>C NMR** (176 MHz, Chloroform-*d*)  $\delta$  154.6, 150.9, 126.1, 123.4, 122.7, 119.9, 119.4, 111.6, 74.1, 58.9, 35.1, 25.9, 25.7, 21.6 ppm. **HRMS-ESI** ( $m/z$ ):  $[M + H]^+$  calculated for C<sub>16</sub>H<sub>18</sub>O<sub>2</sub>  $[M+H]^+$ : 243.1307, found 243.1305.

### 2,3,3',4',5,6-hexahydrospiro[pyran-4,1'-pyrano[4,3-*b*]benzofuran] **55b**



Synthesized via procedure C, 18.1 mg, 74%. **<sup>1</sup>H NMR** (500 MHz, Chloroform-*d*)  $\delta$  7.59 – 7.53 (m, 1H), 7.51 – 7.45 (m, 1H), 7.30 – 7.22 (m, 2H), 4.06 (t,  $J$  = 5.4 Hz, 2H), 4.00 – 3.80 (m, 4H), 2.88 (t,  $J$  = 5.4 Hz, 2H), 2.36 (ddd,  $J$  = 14.0, 12.2, 5.8 Hz, 2H), 1.85 – 1.76 (m, 2H) ppm. **<sup>13</sup>C NMR** (126 MHz, Chloroform-*d*)  $\delta$  154.7, 151.3, 125.8, 123.8, 123.0, 119.4, 118.5, 111.7, 71.8, 63.7, 59.2, 35.4, 25.4 ppm. **HRMS-ESI** ( $m/z$ ):  $[M + H]^+$  calculated for C<sub>15</sub>H<sub>16</sub>O<sub>3</sub>  $[M+H]^+$ : 245.1099, found 245.10992.

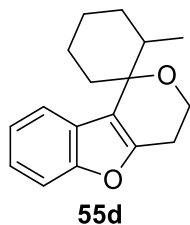
### 2',3,3',4,5',6'-hexahydrospiro[pyrano[4,3-*b*]benzofuran-1,4'-thiopyran] **55c**



Synthesized via procedure C, 17.7 mg, 68%. **<sup>1</sup>H NMR** (500 MHz, Chloroform-*d*)  $\delta$  7.66 – 7.54 (m, 1H), 7.53 – 7.42 (m, 1H), 7.33 – 7.20 (m, 2H), 4.04 (t,  $J$  = 5.5 Hz, 2H), 3.24 (t,  $J$  = 13.1 Hz, 2H),

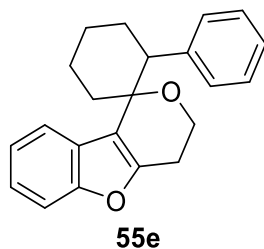
2.86 (t,  $J = 5.5$  Hz, 2H), 2.51 – 2.40 (m, 2H), 2.34 (ddd,  $J = 14.0, 12.9, 3.7$  Hz, 2H), 2.28 – 2.16 (m, 2H) ppm.  $^{13}\text{C NMR}$  (126 MHz, Chloroform-*d*)  $\delta$  154.6, 150.9, 125.7, 123.8, 123.0, 119.6, 119.5, 111.7, 72.8, 58.9, 36.1, 25.3, 23.9 ppm. **HRMS-ESI** ( $m/z$ ):  $[\text{M} + \text{H}]^+$  calculated for  $\text{C}_{15}\text{H}_{16}\text{O}_2\text{S}$   $[\text{M} + \text{H}]^+$ : 261.0871, found 261.0873.

2-methyl-3',4'-dihydrospiro[cyclohexane-1,1'-pyrano[4,3-*b*]benzofuran] **55d**



Synthesized via procedure C, 18.2 mg, 71%.  $^1\text{H NMR}$  (500 MHz, Chloroform-*d*)  $\delta$  7.51 – 7.40 (m, 2H), 7.25 – 7.13 (m, 2H), 4.20 – 4.07 (m, 1H), 3.91 (td,  $J = 11.2, 3.5$  Hz, 1H), 2.99 (ddd,  $J = 16.1, 11.0, 6.1$  Hz, 1H), 2.60 (ddd,  $J = 16.2, 3.5, 1.1$  Hz, 1H), 2.17 – 2.09 (m, 2H), 1.86 – 1.77 (m, 1H), 1.77 – 1.66 (m, 2H), 1.65 – 1.57 (m, 2H), 1.50 – 1.39 (m, 1H), 0.65 (d,  $J = 6.7$  Hz, 3H) ppm.  $^{13}\text{C NMR}$  (126 MHz, Chloroform-*d*)  $\delta$  154.7, 151.8, 126.1, 123.5, 122.7, 119.7, 118.7, 111.6, 76.7, 59.0, 39.7, 34.1, 29.9, 26.8, 25.3, 21.7, 16.2 ppm. **HRMS-ESI** ( $m/z$ ):  $[\text{M} + \text{H}]^+$  calculated for  $\text{C}_{17}\text{H}_{20}\text{O}_2$   $[\text{M} + \text{H}]^+$ : 257.1463, found 257.1462.

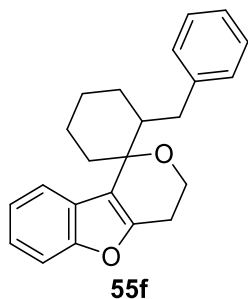
2-phenyl-3',4'-dihydrospiro[cyclohexane-1,1'-pyrano[4,3-*b*]benzofuran] **55e**



Synthesized via procedure C, 20.7 mg, 65%.  $^1\text{H NMR}$  (500 MHz, Chloroform-*d*)  $\delta$  7.66 (dd,  $J = 7.7, 1.3$  Hz, 1H), 7.34 (dt,  $J = 7.9, 0.7$  Hz, 1H), 7.29 – 7.24 (m, 2H), 7.21 (ddd,  $J = 8.5, 7.4, 1.3$  Hz, 1H), 7.05 – 6.89 (m, 5H), 4.06 (ddd,  $J = 11.2, 5.4, 1.8$  Hz, 1H), 3.82 (ddd,  $J = 11.2, 10.1, 3.9$  Hz, 1H), 3.21 (dd,  $J = 13.0, 3.6$  Hz, 1H), 2.52 – 2.35 (m, 2H), 2.30 (qd,  $J = 13.0, 3.6$  Hz, 1H), 2.17 (ddt,  $J = 13.1, 4.2, 2.0$  Hz, 1H), 2.01 – 1.91 (m, 2H), 1.87 (tt,  $J = 13.2, 3.5$  Hz, 1H), 1.78 – 1.70 (m, 1H), 1.70 – 1.62 (m, 1H), 1.62 – 1.50 (m, 2H) ppm.  $^{13}\text{C NMR}$  (126 MHz, Chloroform-*d*)  $\delta$  154.4, 151.7, 143.1, 129.4, 127.3, 126.4, 126.2, 123.3, 122.8, 119.8, 118.1, 111.6, 76.7, 59.5, 52.1, 34.6, 28.6, 26.7, 25.0, 21.7 ppm. **HRMS-ESI** ( $m/z$ ):  $[\text{M} + \text{H}]^+$  calculated for  $\text{C}_{22}\text{H}_{22}\text{O}_2$   $[\text{M} + \text{H}]^+$ : 319.1620, found 319.1617.

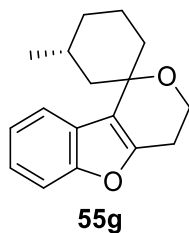
## Experimental

### 2-benzyl-3',4'-dihydrospiro[cyclohexane-1,1'-pyrano[4,3-b]benzofuran] **55f**



**<sup>1</sup>H NMR** (500 MHz, Chloroform-*d*)  $\delta$  7.56 (dd,  $J = 5.8, 3.2$  Hz, 1H), 7.50 – 7.45 (m, 1H), 7.28 (q,  $J = 3.4, 2.8$  Hz, 1H), 7.13 (dd,  $J = 8.1, 6.6$  Hz, 2H), 7.10 – 7.04 (m, 1H), 6.86 (dd,  $J = 6.9, 1.8$  Hz, 2H), 4.23 – 4.15 (m, 1H), 3.97 (td,  $J = 11.3, 3.5$  Hz, 1H), 3.05 (ddd,  $J = 16.9, 11.2, 6.2$  Hz, 1H), 2.66 (ddd,  $J = 16.3, 3.5, 1.0$  Hz, 1H), 2.44 (dd,  $J = 13.3, 2.7$  Hz, 1H), 2.30 (dd,  $J = 13.4, 10.8$  Hz, 1H), 2.24 – 2.14 (m, 2H), 1.82 – 1.65 (m, 3H), 1.64 – 1.48 (m, 5H) ppm. **<sup>13</sup>C NMR** (126 MHz, Chloroform-*d*)  $\delta$  153.4, 150.6, 140.8, 128.2, 126.9, 124.5, 124.3, 122.3, 121.5, 118.3, 117.0, 110.3, 75.8, 57.6, 45.9, 35.8, 32.7, 25.1, 24.7, 24.0, 20.3 ppm **HRMS-ESI** ( $m/z$ ): [M + H]<sup>+</sup> calculated for C<sub>23</sub>H<sub>24</sub>O<sub>2</sub> [M+H]<sup>+</sup>: 333.1776, found 333.1773.

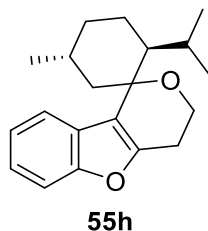
### (3*R*)-3-methyl-3',4'-dihydrospiro[cyclohexane-1,1'-pyrano[4,3-*b*]benzofuran] **55g**



Synthesized via procedure C, 19.5 mg, 76%. **<sup>1</sup>H NMR** (700 MHz, Chloroform-*d*)  $\delta$  7.49 – 7.46 (m, 1H), 7.46 – 7.42 (m, 1H), 7.25 – 7.18 (m, 2H), 4.08 – 3.92 (m, 2H), 2.90 – 2.74 (m, 2H), 1.93 (tdd,  $J = 14.6, 4.5, 2.5$  Hz, 3H), 1.88 – 1.75 (m, 3H), 1.67 – 1.52 (m, 3H), 1.08 – 0.98 (m, 1H), 0.93 (d,  $J = 6.5$  Hz, 3H) ppm. **<sup>13</sup>C NMR** (176 MHz, Chloroform-*d*)  $\delta$  154.6, 150.9, 126.1, 123.4, 122.7, 119.6, 119.6, 111.6, 74.9, 59.0, 44.0, 34.8, 34.5, 27.7, 25.4, 22.9, 21.6 ppm. **HRMS-ESI** ( $m/z$ ): [M + H]<sup>+</sup> calculated for C<sub>17</sub>H<sub>20</sub>O<sub>2</sub> [M+H]<sup>+</sup>: 257.1463, found 257.1463.

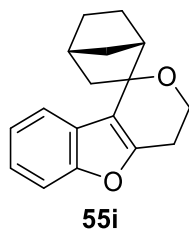


(2*S*,5*R*)-2-isopropyl-5-methyl-3',4'-dihydrospiro[cyclohexane-1,1'-pyrano[4,3-*b*]benzofuran] **55h**



Synthesized via procedure C, 20.0 mg, 67%. **<sup>1</sup>H NMR** (500 MHz, Chloroform-*d*)  $\delta$  7.48 – 7.40 (m, 2H), 7.26 – 7.17 (m, 2H), 4.09 – 3.96 (m, 1H), 3.89 (ddd,  $J = 11.4, 8.2, 4.4$  Hz, 1H), 2.94 – 2.78 (m, 1H), 2.72 – 2.61 (m, 1H), 2.53 (dt,  $J = 4.1, 1.4$  Hz, 1H), 2.45 – 2.34 (m, 1H), 2.27 (dp,  $J = 9.7, 1.9$  Hz, 1H), 2.19 (ddd,  $J = 12.9, 4.6, 3.0$  Hz, 1H), 2.08 – 1.98 (m, 1H), 1.98 – 1.86 (m, 1H), 1.70 – 1.49 (m, 1H), 1.49 – 1.32 (m, 2H), 1.31 – 1.22 (m, 1H) ppm. **<sup>13</sup>C NMR** (126 MHz, Chloroform-*d*)  $\delta$  156.5, 154.5, 153.3, 126.9, 122.5, 117.8, 110.5, 107.8, 80.8, 60.9, 45.1, 43.7, 42.4, 36.8, 35.4, 27.4, 21.7 ppm. **HRMS-ESI** ( $m/z$ ):  $[M + H]^+$  calculated for C<sub>20</sub>H<sub>26</sub>O<sub>2</sub>  $[M+H]^+$ : 299.1933, found 299.1930.

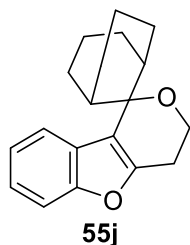
(1*S*,4*R*)-3',4'-dihydrospiro[bicyclo[2.2.1]heptane-2,1'-pyrano[4,3-*b*]benzofuran] **55i**



**<sup>1</sup>H NMR** (500 MHz, Chloroform-*d*)  $\delta$  7.63 – 7.49 (m, 1H), 7.49 – 7.39 (m, 1H), 7.24 – 7.14 (m, 2H), 4.25 – 4.05 (m, 2H), 3.08 (dddd,  $J = 16.7, 13.0, 11.0, 7.2$  Hz, 1H), 2.71 – 2.42 (m, 4H), 2.10 – 1.99 (m, 2H), 1.78 – 1.62 (m, 3H), 1.34 – 1.20 (m, 2H) ppm. **<sup>13</sup>C NMR** (126 MHz, Chloroform-*d*)  $\delta$  154.7, 152.6, 127.8, 123.4, 120.7, 116.9, 111.7, 83.5, 60.8, 46.7, 43.7, 38.2, 30.4, 29.1, 25.1, 24.8, 22.6 ppm. **HRMS-ESI** ( $m/z$ ):  $[M + H]^+$  calculated for C<sub>17</sub>H<sub>18</sub>O<sub>2</sub>  $[M+H]^+$ : 255.1307, found 255.1306.

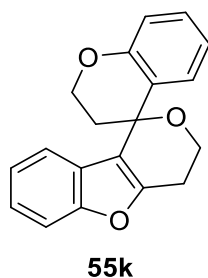
## Experimental

### 3',4'-dihydrospiro[bicyclo[3.3.1]nonane-9,1'-pyrano[4,3-*b*]benzofuran] **55j**

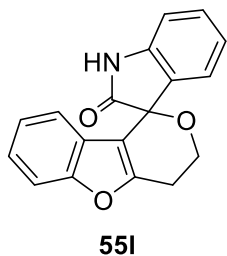


Synthesized via procedure C, 9.8 mg, 35%. **<sup>1</sup>H NMR** (500 MHz, Chloroform-*d*)  $\delta$  7.60 (dd,  $J = 7.3$ , 2.0 Hz, 1H), 7.52 – 7.48 (m, 1H), 7.45 – 7.40 (m, 1H), 7.26 – 7.15 (m, 2H), 6.52 (q,  $J = 0.9$  Hz, 1H), 4.00 (td,  $J = 5.9$ , 2.2 Hz, 2H), 3.05 (td,  $J = 6.2$ , 0.9 Hz, 1H), 2.90 (t,  $J = 5.7$  Hz, 1H), 2.51 (tdd,  $J = 14.9$ , 9.3, 3.8 Hz, 1H), 2.46 – 2.40 (m, 2H), 2.36 – 2.19 (m, 3H), 2.10 – 2.00 (m, 3H), 1.93 (ddd,  $J = 27.1$ , 13.5, 7.1 Hz, 1H), 1.88 – 1.78 (m, 1H), 1.48 (ddq,  $J = 13.9$ , 6.9, 1.3 Hz, 1H) ppm. **<sup>13</sup>C NMR** (126 MHz, Chloroform-*d*)  $\delta$  155.9, 153.9, 128.7, 123.6, 122.7, 120.5, 111.0, 103.7, 79.0, 60.8, 56.3, 46.6, 37.0, 34.4, 32.1, 28.5, 25.9, 21.1, 20.7 ppm. **HRMS-ESI** ( $m/z$ ): [M + H]<sup>+</sup> calculated for C<sub>19</sub>H<sub>22</sub>O<sub>2</sub> [M+H]<sup>+</sup>: 283.1620, found 283.1617.

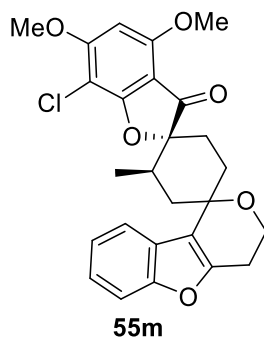
### 3',4'-dihydrospiro[chromane-4,1'-pyrano[4,3-*b*]benzofuran] **55k**



Synthesized via procedure C, 11.7 mg, 40%. **<sup>1</sup>H NMR** (400 MHz, Chloroform-*d*)  $\delta$  7.53 (d,  $J = 8.1$  Hz, 1H), 7.40 (s, 1H), 7.17 – 7.00 (m, 4H), 6.85 (dd,  $J = 8.1$ , 1.2 Hz, 1H), 6.73 (d,  $J = 8.1$  Hz, 1H), 6.70 – 6.61 (m, 1H), 4.51 (ddd,  $J = 10.7$ , 9.1, 6.4 Hz, 1H), 4.33 – 4.19 (m, 1H), 4.10 – 3.88 (m, 2H), 2.91 (dd,  $J = 15.4$ , 6.4 Hz, 1H), 2.72 (dd,  $J = 15.3$ , 6.4 Hz, 1H), 2.32 – 2.20 (m, 2H) ppm. **<sup>13</sup>C NMR** (176 MHz, Chloroform-*d*)  $\delta$  155.0, 136.2, 136.0, 132.7, 130.2, 127.1, 123.9, 122.2, 121.0, 122.4, 118.8, 117.6, 111.3, 110.4, 70.0, 62.7, 60.2, 34.1, 22.3 ppm. **HRMS-ESI** ( $m/z$ ): [M + H]<sup>+</sup> calculated for C<sub>19</sub>H<sub>16</sub>O<sub>3</sub> [M+H]<sup>+</sup>: 293.1099, found 293.1097.

3',4'-dihydrospiro[indoline-3,1'-pyrano[4,3-*b*]benzofuran]-2-one **55l**

Synthesized via procedure C, 19.8 mg, 68%. **<sup>1</sup>H NMR** (700 MHz, Chloroform-*d*)  $\delta$  7.90 (s, 1H), 7.44 (d,  $J = 8.2$  Hz, 1H), 7.32 (td,  $J = 7.7, 1.2$  Hz, 1H), 7.20 – 7.11 (m, 2H), 7.03 – 6.93 (m, 3H), 6.58 (d,  $J = 7.8$  Hz, 1H), 5.02 (ddd,  $J = 11.2, 9.8, 4.1$  Hz, 1H), 4.31 (ddd,  $J = 11.5, 6.0, 2.2$  Hz, 1H), 3.26 (ddd,  $J = 16.2, 9.9, 6.0$  Hz, 1H), 2.97 (ddd,  $J = 16.6, 4.1, 2.2$  Hz, 1H) ppm. **<sup>13</sup>C NMR** (176 MHz, Chloroform-*d*)  $\delta$  177.3, 154.8, 153.7, 140.9, 130.9, 129.3, 126.1, 125.1, 124.2, 123.8, 123.2, 118.6, 111.6, 110.9, 110.5, 76.6, 61.7, 24.7 ppm. **HRMS-ESI** ( $m/z$ ):  $[M + H]^+$  calculated for C<sub>18</sub>H<sub>13</sub>O<sub>3</sub>N  $[M+H]^+$ : 292.0895, found 292.0891.

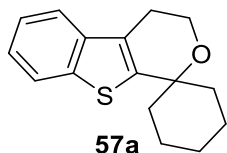
(2*R*,2'*R*)-7-chloro-4,6-dimethoxy-2'-methyl-3'',4''-dihydro-3*H*-dispiro[benzofuran-2,1'-cyclohexane-4',1''-pyrano[4,3-*b*]benzofuran]-3-one **55m**

**<sup>1</sup>H NMR** (400 MHz, Chloroform-*d*)  $\delta$  8.13 – 8.00 (m, 1H), 7.47 – 7.38 (m, 1H), 7.30 – 7.24 (m, 2H), 6.11 (s, 1H), 4.10 – 3.93 (m, 9H), 2.95 – 2.66 (m, 5H), 2.49 (ddd,  $J = 14.1, 13.0, 4.2$  Hz, 1H), 2.00 – 1.73 (m, 3H), 0.83 (d,  $J = 6.5$  Hz, 3H) ppm. **<sup>13</sup>C NMR** (126 MHz, Chloroform-*d*)  $\delta$  198.7, 168.5, 163.7, 157.2, 156.0, 154.3, 128.1, 123.7, 121.9, 118.7, 111.5, 110.0, 105.6, 92.1, 88.6, 73.0, 59.8, 56.5, 56.1, 36.8, 33.2, 28.3, 28.0, 26.8, 22.6, 14.8 ppm. **HRMS-ESI** ( $m/z$ ):  $[M + H]^+$  calculated for C<sub>26</sub>H<sub>25</sub>O<sub>6</sub>Cl  $[M+H]^+$ : 469.1340 and 471.1310, found 469.1339 and 471.1307.

## Experimental

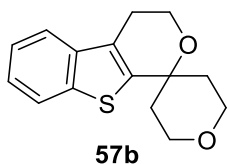
### TETRAHYDROPYRANO BENZOTHIOPHENES

#### 3,4-dihydrospiro[benzo[4,5]thieno[2,3-c]pyran-1,1'-cyclohexane] **57a**



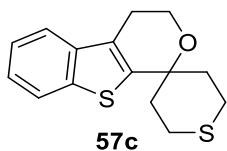
Synthesized via procedure C, 25.6 mg, 99%. **<sup>1</sup>H NMR** (700 MHz, Chloroform-*d*)  $\delta$  7.81 (dt,  $J$  = 8.0, 0.9 Hz, 1H), 7.60 (dt,  $J$  = 7.9, 1.0 Hz, 1H), 7.36 (ddd,  $J$  = 8.0, 7.1, 1.1 Hz, 1H), 7.30 (ddd,  $J$  = 8.2, 7.1, 1.2 Hz, 1H), 4.06 (t,  $J$  = 5.5 Hz, 2H), 2.84 (t,  $J$  = 5.5 Hz, 2H), 2.15 – 2.07 (m, 2H), 1.81 – 1.73 (m, 3H), 1.70 (td,  $J$  = 13.2, 3.8 Hz, 2H), 1.62 (dq,  $J$  = 13.0, 3.3 Hz, 2H), 1.37 – 1.31 (m, 1H) ppm. **<sup>13</sup>C NMR** (176 MHz, Chloroform-*d*)  $\delta$  144.5, 139.1, 138.4, 126.8, 124.1, 124.1, 122.5, 120.9, 74.6, 58.8, 38.0, 25.4, 24.9, 21.6 ppm. **HRMS-ESI** ( $m/z$ ):  $[M + H]^+$  calculated for C<sub>16</sub>H<sub>18</sub>OS  $[M+H]^+$ : 259.1078, found 259.1075.

#### 2',3,3',4,5',6'-hexahydrospiro[benzo[4,5]thieno[2,3-c]pyran-1,4'-pyran] **57b**



Synthesized via procedure C, 20.0 mg, 77%. **<sup>1</sup>H NMR** (700 MHz, Chloroform-*d*)  $\delta$  7.82 (d,  $J$  = 8.0 Hz, 1H), 7.64 – 7.59 (m, 1H), 7.39 – 7.36 (m, 1H), 7.32 (td,  $J$  = 7.5, 7.0, 1.2 Hz, 1H), 4.07 (t,  $J$  = 5.5 Hz, 2H), 3.97 – 3.79 (m, 4H), 2.86 (t,  $J$  = 5.5 Hz, 2H), 2.16 – 2.07 (m, 2H), 1.96 (dd,  $J$  = 14.1, 2.1 Hz, 2H) ppm. **<sup>13</sup>C NMR** (176 MHz, Chloroform-*d*)  $\delta$  141.7, 137.8, 137.4, 126.5, 123.4, 123.2, 121.6, 120.0, 71.2, 62.5, 58.1, 37.0, 23.8 ppm. **HRMS-ESI** ( $m/z$ ):  $[M + H]^+$  calculated for C<sub>15</sub>H<sub>16</sub>O<sub>2</sub>S  $[M+H]^+$ : 261.0871, found 261.0869.

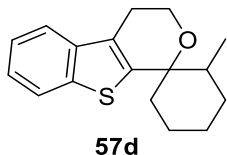
#### 2',3,3',4,5',6'-hexahydrospiro[benzo[4,5]thieno[2,3-c]pyran-1,4'-thiopyran] **57c**



Synthesized via procedure C, 20.7 mg, 75%. **<sup>1</sup>H NMR** (700 MHz, Chloroform-*d*)  $\delta$  7.82 (d,  $J$  = 8.0 Hz, 1H), 7.61 (d,  $J$  = 7.9 Hz, 1H), 7.37 (t,  $J$  = 7.5 Hz, 1H), 7.35 – 7.28 (m, 1H), 4.05 (t,  $J$  = 5.5 Hz, 2H), 3.20 (ddd,  $J$  = 14.4, 12.9, 2.4 Hz, 2H), 2.84 (t,  $J$  = 5.5 Hz, 2H), 2.43 (dd,  $J$  = 14.0, 3.8 Hz, 2H), 2.34 (dt,  $J$  = 14.2, 3.3 Hz, 2H), 2.08 (td,  $J$  = 13.5, 3.6 Hz, 2H) ppm. **<sup>13</sup>C NMR** (176 MHz, 186

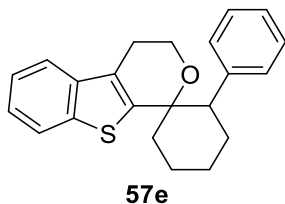
Chloroform-*d*)  $\delta$  142.2, 137.8, 137.4, 126.0, 123.4, 123.2, 121.6, 120.0, 71.9, 57.8, 37.4, 23.7, 22.7 ppm. **HRMS**-ESI (*m/z*): [M + H]<sup>+</sup> calculated for C<sub>15</sub>H<sub>16</sub>OS<sub>2</sub> [M+H]<sup>+</sup>: 277.0643, found 277.0640.

2'-methyl-3,4-dihydrospiro[benzo[4,5]thieno[2,3-*c*]pyran-1,1'-cyclohexane] **57d**



Synthesized via procedure C, 18.5 mg, 68%. **<sup>1</sup>H NMR** (700 MHz, Chloroform-*d*)  $\delta$  7.76 (dt, *J* = 8.2, 1.0 Hz, 1H), 7.53 (dt, *J* = 8.2, 1.0 Hz, 1H), 7.27 (ddd, *J* = 8.2, 7.3, 1.0 Hz, 1H), 7.19 (ddd, *J* = 8.2, 7.3, 1.0 Hz, 1H), 4.11 – 3.95 (m, 2H), 2.84 – 2.70 (m, 2H), 2.10 – 1.99 (m, 2H), 1.89 – 1.82 (m, 1H), 1.77 – 1.70 (m, 2H), 1.63 – 1.52 (m, 2H), 1.32 (dd, *J* = 13.5, 12.0 Hz, 1H), 1.00 – 0.91 (m, 1H), 0.90 (d, *J* = 6.5 Hz, 3H) ppm. **<sup>13</sup>C NMR** (176 MHz, Chloroform-*d*)  $\delta$  144.2, 138.4, 137.9, 126.2, 124.0, 123.7, 122.1, 119.9, 75.0, 57.8, 45.9, 37.3, 34.1, 26.9, 24.1, 22.2, 19.6 ppm. **HRMS**-ESI (*m/z*): [M + H]<sup>+</sup> calculated for C<sub>17</sub>H<sub>20</sub>OS [M+H]<sup>+</sup>: 273.1235, found 273.1234.

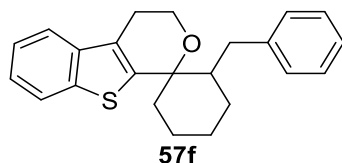
2'-phenyl-3,4-dihydrospiro[benzo[4,5]thieno[2,3-*c*]pyran-1,1'-cyclohexane] **57e**



Synthesized via procedure C, 17.4 mg, 52%. **<sup>1</sup>H NMR** (500 MHz, Chloroform-*d*)  $\delta$  7.69 (dd, *J* = 7.7, 1.3 Hz, 1H), 7.37 (dt, *J* = 7.7, 0.7 Hz, 1H), 7.32 – 7.27 (m, 2H), 7.24 (ddd, *J* = 8.5, 7.4, 1.3 Hz, 1H), 7.08 – 6.92 (m, 5H), 4.09 (ddd, *J* = 11.2, 5.4, 1.8 Hz, 1H), 3.85 (ddd, *J* = 11.2, 10.1, 3.9 Hz, 1H), 3.24 (dd, *J* = 13.0, 3.6 Hz, 1H), 2.55 – 2.38 (m, 2H), 2.33 (qd, *J* = 13.0, 3.6 Hz, 1H), 2.20 (ddt, *J* = 13.1, 4.2, 2.0 Hz, 1H), 2.04 – 1.94 (m, 2H), 1.90 (tt, *J* = 13.2, 3.5 Hz, 1H), 1.81 – 1.73 (m, 1H), 1.73 – 1.65 (m, 1H), 1.65 – 1.53 (m, 2H) ppm. **<sup>13</sup>C NMR** (126 MHz, Chloroform-*d*)  $\delta$  155.9, 153.2, 144.8, 130.9, 128.8, 127.9, 127.9, 125.0, 124.3, 121.3, 119.6, 113.1, 78.2, 61.1, 53.6, 36.3, 30.2, 28.4, 26.5, 23.2 ppm. **HRMS**-ESI (*m/z*): [M + H]<sup>+</sup> calculated for C<sub>22</sub>H<sub>22</sub>OS [M+H]<sup>+</sup>: 335.1391, found 355.1390.

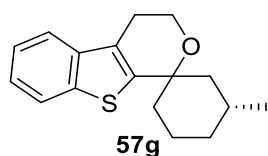
## Experimental

### 2'-benzyl-3,4-dihydrospiro[benzo[4,5]thieno[2,3-c]pyran-1,1'-cyclohexane] **57f**



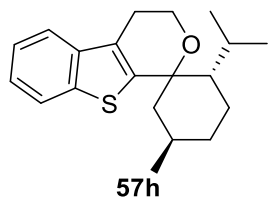
Synthesized via procedure C, 21.9 mg, 63%. **<sup>1</sup>H NMR** (500 MHz, Chloroform-*d*)  $\delta$  7.49 (dd,  $J$  = 5.8, 3.2 Hz, 1H), 7.43 – 7.38 (m, 1H), 7.20 (q,  $J$  = 3.2, 2.8 Hz, 2H), 7.06 (dd,  $J$  = 8.1, 6.2 Hz, 2H), 7.03 – 6.96 (m, 1H), 6.79 (dd,  $J$  = 6.9, 1.8 Hz, 2H), 4.16 – 4.08 (m, 1H), 3.90 (td,  $J$  = 11.3, 3.2 Hz, 1H), 2.98 (ddd,  $J$  = 16.9, 11.2, 6.2 Hz, 1H), 2.59 (ddd,  $J$  = 16.3, 3.5, 1.0 Hz, 1H), 2.37 (dd,  $J$  = 13.3, 2.7 Hz, 1H), 2.23 (dd,  $J$  = 13.4, 10.8 Hz, 1H), 2.17 – 2.07 (m, 2H), 1.75 – 1.58 (m, 4H), 1.57 – 1.40 (m, 6H) ppm. **<sup>13</sup>C NMR** (126 MHz, Chloroform-*d*)  $\delta$  153.3, 150.5, 140.9, 128.2, 126.9, 124.4, 124.4, 122.2, 121.6, 118.2, 116.8, 110.4, 75.9, 57.7, 46.0, 35.8, 32.7, 25.9, 24.7, 23.7, 20.2 ppm. **HRMS-ESI** ( $m/z$ ):  $[M + H]^+$  calculated for C<sub>23</sub>H<sub>24</sub>OS  $[M+H]^+$ : 349.1548, found 349.1550.

### (3'*R*)-3'-methyl-3,4-dihydrospiro[benzo[4,5]thieno[2,3-c]pyran-1,1'-cyclohexane] **57g**



Synthesized via procedure C, 19.3 mg, 71%, d.r. 8:1. **<sup>1</sup>H NMR** (700 MHz, Chloroform-*d*)  $\delta$  7.81 (dt,  $J$  = 8.0, 0.9 Hz, 1H), 7.60 (dt,  $J$  = 7.9, 1.0 Hz, 1H), 7.36 (ddd,  $J$  = 8.0, 7.1, 1.1 Hz, 1H), 7.30 (ddd,  $J$  = 8.2, 7.1, 1.2 Hz, 1H), 4.10 – 4.00 (m, 2H), 2.89 – 2.78 (m, 2H), 2.14 – 2.06 (m, 2H), 1.96 – 1.87 (m, 1H), 1.83 – 1.73 (m, 2H), 1.67 – 1.57 (m, 2H), 1.35 (dd,  $J$  = 13.7, 12.1 Hz, 1H), 1.04 – 0.94 (m, 1H), 0.93 (d,  $J$  = 6.7 Hz, 3H) ppm. **<sup>13</sup>C NMR** (176 MHz, Chloroform-*d*)  $\delta$  144.4, 139.1, 138.4, 126.8, 124.1, 124.0, 122.5, 120.9, 75.2, 58.9, 46.7, 37.3, 34.2, 27.7, 24.9, 22.5, 21.6 ppm. **HRMS-ESI** ( $m/z$ ):  $[M + H]^+$  calculated for C<sub>17</sub>H<sub>20</sub>OS  $[M+H]^+$ : 273.1235, found 273.1239.

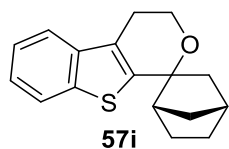
### (2'*S*,5'*R*)-2'-isopropyl-5'-methyl-3,4-dihydrospiro[benzo[4,5]thieno[2,3-c]pyran-1,1'-cyclohexane] **57h**



Synthesized via procedure C, 23.3 mg, 74%. **<sup>1</sup>H NMR** (500 MHz, Chloroform-*d*)  $\delta$  7.71 (d,  $J$  = 7.8 Hz, 1H), 7.45 (d,  $J$  = 7.8 Hz, 1H), 7.23 (dt,  $J$  = 28.2, 7.8 Hz, 2H), 4.19 (d,  $J$  = 17.0 Hz, 1H), 4.00

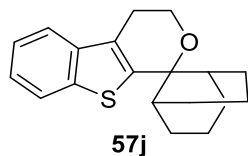
(d,  $J = 22.5$  Hz, 1H), 3.12 (d,  $J = 32.8$  Hz, 1H), 2.72 (d,  $J = 15.5$  Hz, 1H), 2.29 – 2.15 (m, 1H), 1.99 (d,  $J = 12.5$  Hz, 1H), 1.90 (s, 2H), 1.84 – 1.70 (m, 1H), 1.62 – 1.59 (m, 3H), 1.29 (td,  $J = 12.8, 3.7$  Hz, 1H), 0.94 (d,  $J = 6.4$  Hz, 3H), 0.89 (d,  $J = 6.8$  Hz, 3H), 0.71 (d,  $J = 6.8$  Hz, 3H) ppm.  $^{13}\text{C NMR}$  (126 MHz, Chloroform-*d*)  $\delta$  136.7, 133.5, 127.8, 124.0, 123.7, 120.1, 117.9, 110.8, 81.2, 59.4, 51.5, 46.6, 37.6, 28.3, 28.1, 26.2, 25.9, 24.7, 21.7, 20.8 ppm. **HRMS-ESI** ( $m/z$ ):  $[\text{M} + \text{H}]^+$  calculated for  $\text{C}_{20}\text{H}_{26}\text{OS}$   $[\text{M} + \text{H}]^+$ : 315.1704, found 315.1703.

(1'*S*,4'*R*)-3,4-dihydrospiro[benzo[4,5]thieno[2,3-*c*]pyran-1,2'-bicyclo[2.2.1]heptane] **57i**



Synthesized via procedure C, 14.3 mg, 53%.  $^1\text{H NMR}$  (700 MHz, Chloroform-*d*)  $\delta$  7.79 (t,  $J = 8.2$  Hz, 1H), 7.59 (dd,  $J = 8.0, 3.9$  Hz, 1H), 7.38 – 7.33 (m, 1H), 7.32 – 7.28 (m, 1H), 4.16 – 4.02 (m, 1H), 3.95 (ddd,  $J = 11.4, 8.3, 4.6$  Hz, 1H), 2.91 (ddd,  $J = 15.8, 8.3, 5.6$  Hz, 1H), 2.80 – 2.71 (m, 1H), 2.55 (d,  $J = 3.7$  Hz, 1H), 2.38 (dt,  $J = 18.2, 4.8$  Hz, 1H), 2.11 (ddd,  $J = 13.4, 4.4, 2.9$  Hz, 1H), 2.09 – 1.97 (m, 2H), 1.70 – 1.61 (m, 2H), 1.51 (ddt,  $J = 10.7, 3.6, 1.7$  Hz, 1H), 1.41 (dtdd,  $J = 33.3, 12.2, 5.4, 3.0$  Hz, 2H) ppm.  $^{13}\text{C NMR}$  (176 MHz, Chloroform-*d*)  $\delta$  143.1, 137.7, 137.3, 125.3, 123.2, 123.0, 121.2, 119.7, 81.8, 60.3, 47.4, 47.0, 38.1, 35.3, 26.8, 23.4, 21.7 ppm. **HRMS-ESI** ( $m/z$ ):  $[\text{M} + \text{H}]^+$  calculated for  $\text{C}_{17}\text{H}_{18}\text{OS}$   $[\text{M} + \text{H}]^+$ : 271.1078, found 271.1077.

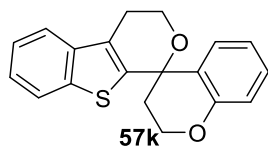
3,4-dihydrospiro[benzo[4,5]thieno[2,3-*c*]pyran-1,9'-bicyclo[3.3.1]nonane] **57j**



Synthesized via procedure C, 18.2 mg, 61%.  $^1\text{H NMR}$  (500 MHz, Chloroform-*d*)  $\delta$  7.43 – 7.36 (m, 2H), 7.21 – 7.12 (m, 2H), 3.95 (t,  $J = 5.6$  Hz, 2H), 2.71 (t,  $J = 5.6$  Hz, 2H), 2.43 (tt,  $J = 12.1, 6.6, 5.7, 2.9$  Hz, 2H), 2.18 (dddd,  $J = 18.1, 9.4, 4.7, 2.0$  Hz, 2H), 2.02 – 1.80 (m, 4H), 1.70 (ddt,  $J = 13.7, 6.7, 1.4$  Hz, 3H), 1.51 – 1.46 (m, 1H), 1.43 (ddq,  $J = 13.9, 6.9, 1.3$  Hz, 2H) ppm.  $^{13}\text{C NMR}$  (126 MHz, Chloroform-*d*)  $\delta$  157.2, 153.7, 126.9, 122.8, 121.6, 118.6, 110.0, 110.2, 75.6, 56.3, 34.3, 27.7, 26.6, 21.9, 20.7, 19.3 ppm. **HRMS-ESI** ( $m/z$ ):  $[\text{M} + \text{H}]^+$  calculated for  $\text{C}_{19}\text{H}_{22}\text{OS}$   $[\text{M} + \text{H}]^+$ : 299.1391, found 299.1391.

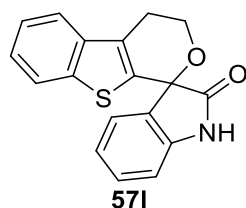
## Experimental

### 3,4-dihydrospiro[benzo[4,5]thieno[2,3-*c*]pyran-1,4'-chromane] **57k**



Synthesized via procedure C, 10.1 mg, 33%. **<sup>1</sup>H NMR** (500 MHz, Chloroform-*d*)  $\delta$  8.03 (s, 1H), 7.37 (d,  $J$  = 8.0 Hz, 1H), 7.19 (dddd,  $J$  = 38.1, 8.0, 7.1, 1.5 Hz, 2H), 7.03 – 6.93 (m, 3H), 6.89 (d,  $J$  = 8.0 Hz, 1H), 6.74 (td,  $J$  = 7.4, 1.2 Hz, 1H), 4.63 (ddd,  $J$  = 13.2, 10.8, 2.0 Hz, 1H), 4.42 (ddd,  $J$  = 10.8, 4.4, 2.2 Hz, 1H), 4.23 – 4.06 (m, 2H), 3.08 (ddd,  $J$  = 15.8, 6.8, 5.0 Hz, 1H), 2.92 (dt,  $J$  = 15.8, 5.0 Hz, 1H), 2.72 (ddd,  $J$  = 14.6, 13.5, 4.4 Hz, 1H), 2.30 (dt,  $J$  = 14.6, 2.1 Hz, 1H) ppm. **<sup>13</sup>C NMR** (126 MHz, Chloroform-*d*)  $\delta$  154.1, 134.2, 132.8, 128.3, 124.5, 123.3, 120.0, 119.4, 118.2, 118.0, 116.4, 112.8, 109.1, 70.3, 61.0, 57.6, 32.7, 26.3, 23.9 ppm. **HRMS-ESI** ( $m/z$ ): [M + H]<sup>+</sup> calculated for C<sub>19</sub>H<sub>16</sub>O<sub>2</sub>S [M+H]<sup>+</sup>: 309.0871, found 309.0870.

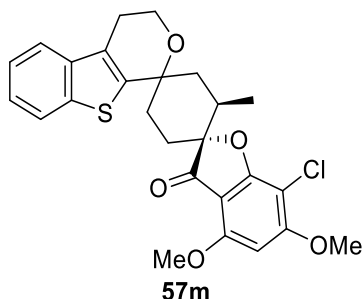
### 3,4-dihydrospiro[benzo[4,5]thieno[2,3-*c*]pyran-1,3'-indolin]-2'-one **57l**



Synthesized via procedure C, 20.9 mg, 68%. **<sup>1</sup>H NMR** (700 MHz, Chloroform-*d*)  $\delta$  7.90 (s, 1H), 7.44 (d,  $J$  = 8.2 Hz, 1H), 7.32 (td,  $J$  = 7.7, 1.2 Hz, 1H), 7.20 – 7.11 (m, 2H), 7.03 – 6.93 (m, 3H), 6.58 (d,  $J$  = 7.8 Hz, 1H), 5.02 (ddd,  $J$  = 11.2, 9.8, 4.1 Hz, 1H), 4.31 (ddd,  $J$  = 11.5, 6.0, 2.2 Hz, 1H), 3.26 (ddd,  $J$  = 16.2, 9.9, 6.0 Hz, 1H), 2.97 (ddd,  $J$  = 16.6, 4.1, 2.2 Hz, 1H) ppm. **<sup>13</sup>C NMR** (176 MHz, Chloroform-*d*)  $\delta$  176.0, 153.4, 152.4, 139.6, 129.5, 128.0, 124.7, 123.7, 122.8, 122.5, 121.9, 117.3, 110.3, 109.6, 109.1, 75.2, 60.3, 23.3 ppm. **HRMS-ESI** ( $m/z$ ): [M + H]<sup>+</sup> calculated for C<sub>18</sub>H<sub>13</sub>O<sub>2</sub>NS [M+H]<sup>+</sup>: 308.0667, found 308.0669.



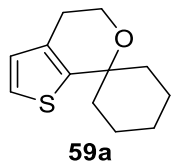
(2*R*,2'*R*)-7-chloro-4,6-dimethoxy-2'-methyl-3'',4''-dihydro-3H-dispiro[benzofuran-2,1'-cyclohexane-4',1''-benzo[4,5]thieno[2,3-*c*]pyran]-3-one **57m**



Synthesized via procedure C, 41.2 mg, 85%. **<sup>1</sup>H NMR** (400 MHz, Chloroform-*d*)  $\delta$  8.13 – 8.00 (m, 1H), 7.47 – 7.38 (m, 1H), 7.30 – 7.24 (m, 1H), 6.11 (s, 1H), 4.10 – 3.93 (m, 8H), 2.95 – 2.66 (m, 3H), 2.49 (ddd,  $J$  = 14.1, 13.0, 4.2 Hz, 1H), 2.00 – 1.73 (m, 2H), 0.83 (d,  $J$  = 6.5 Hz, 3H) ppm. **<sup>13</sup>C NMR** (126 MHz, Chloroform-*d*)  $\delta$  199.7, 169.4, 162.8, 158.1, 137.5, 132.3, 126.0, 124.1, 121.7, 121.5, 118.0, 111.2, 107.6, 95.4, 89.9, 75.2, 59.2, 57.7, 57.2, 37.9, 34.2, 33.3, 30.4, 29.0, 25.1, 15.7 ppm. **HRMS-ESI** ( $m/z$ ):  $[M + H]^+$  calculated for C<sub>26</sub>H<sub>25</sub>O<sub>5</sub>SCl  $[M+H]^+$ : 485.1111 and 487.1082, found 485.1115 and 487.1083.

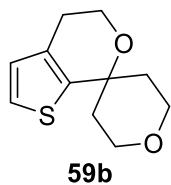
#### TETRAHYDROPYRANO THIOPHENES

4',5'-dihydrospiro[cyclohexane-1,7'-thieno[2,3-*c*]pyran] **59a**



Synthesized via procedure D, 17.7 mg, 85%. **<sup>1</sup>H NMR** (400 MHz, Chloroform-*d*)  $\delta$  7.10 (d,  $J$  = 5.0 Hz, 1H), 6.76 (d,  $J$  = 5.0 Hz, 1H), 3.92 (t,  $J$  = 5.5 Hz, 2H), 2.69 (t,  $J$  = 5.5 Hz, 2H), 2.14 – 1.97 (m, 2H), 1.80 – 1.66 (m, 3H), 1.60 (ddt,  $J$  = 13.4, 11.0, 3.5 Hz, 5H), 1.40 – 1.22 (m, 1H) ppm. **<sup>13</sup>C NMR** (176 MHz, Chloroform-*d*)  $\delta$  142.5, 131.2, 124.7, 123.6, 71.4, 42.1, 36.2, 30.2, 25.2 ppm. **HRMS-ESI** ( $m/z$ ):  $[M + H]^+$  calculated for C<sub>12</sub>H<sub>16</sub>OS  $[M+H]^+$ : 209.0922, found 209.0924.

2,3,4',5,5',6-hexahydrospiro[pyran-4,7'-thieno[2,3-*c*]pyran] **59b**

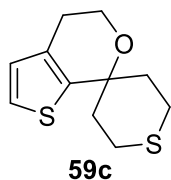


Synthesized via procedure D, 14.5 mg, 69%. **<sup>1</sup>H NMR** (700 MHz, Chloroform-*d*)  $\delta$  7.15 (s, 1H), 6.77 (s, 1H), 3.93 (s, 2H), 3.84 (d,  $J$  = 46.8 Hz, 4H), 2.70 (s, 2H), 2.01 (d,  $J$  = 31.0 Hz, 2H), 1.92

## Experimental

(s, 2H) ppm. **<sup>13</sup>C NMR** (176 MHz, Chloroform-*d*)  $\delta$  140.8, 132.0, 125.9, 121.6, 71.3, 62.7, 58.3, 37.9, 25.5 ppm. **HRMS-ESI** (*m/z*): [M + H]<sup>+</sup> calculated for C<sub>11</sub>H<sub>14</sub>O<sub>2</sub>S [M+H]<sup>+</sup>: 211.0715, found 211.0714.

### 2',3',4,5,5',6'-hexahydrospiro[thieno[2,3-c]pyran-7,4'-thiopyran] **59c**



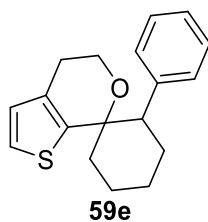
Synthesized via procedure D, 13.8 mg, 61%. **<sup>1</sup>H NMR** (400 MHz, Chloroform-*d*)  $\delta$  7.13 (d, *J* = 5.0 Hz, 1H), 6.76 (d, *J* = 5.0 Hz, 1H), 3.91 (d, *J* = 5.5 Hz, 2H), 3.16 (t, *J* = 12.9 Hz, 2H), 2.68 (d, *J* = 5.5 Hz, 2H), 2.35 (dd, *J* = 40.2, 14.1 Hz, 4H), 2.12 – 1.89 (m, 2H) ppm. **<sup>13</sup>C NMR** (101 MHz, Chloroform-*d*)  $\delta$  142.6, 132.7, 127.1, 122.7, 73.2, 59.2, 39.5, 26.7, 24.1 ppm. **HRMS-ESI** (*m/z*): [M + H]<sup>+</sup> calculated for C<sub>11</sub>H<sub>14</sub>OS<sub>2</sub> [M+H]<sup>+</sup>: 227.0486, found 227.0483.

### 2-methyl-4',5'-dihydrospiro[cyclohexane-1,7'-thieno[2,3-c]pyran] **59d**



Synthesized via procedure D, 13.1 mg, 59%. **<sup>1</sup>H NMR** (400 MHz, Chloroform-*d*)  $\delta$  7.02 (d, *J* = 5.0 Hz, 1H), 6.72 – 6.62 (m, 1H), 3.90 – 3.77 (m, 2H), 2.67 – 2.50 (m, 2H), 2.05 – 1.92 (m, 2H), 1.79 (tddd, *J* = 13.4, 11.9, 6.6, 3.3 Hz, 1H), 1.69 – 1.59 (m, 2H), 1.35 (s, 3H), 0.82 (d, *J* = 6.7 Hz, 4H) ppm. **<sup>13</sup>C NMR** (101 MHz, Chloroform-*d*)  $\delta$  143.7, 132.5, 127.0, 122.1, 75.6, 59.3, 47.8, 38.4, 34.4, 28.0, 27.2, 26.8, 22.7, 21.9 ppm. **HRMS-ESI** (*m/z*): [M + H]<sup>+</sup> calculated for C<sub>13</sub>H<sub>18</sub>OS [M+H]<sup>+</sup>: 223.1078, found 223.1073.

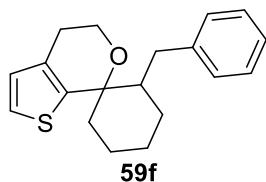
### 2-phenyl-4',5'-dihydrospiro[cyclohexane-1,7'-thieno[2,3-c]pyran] **59e**



Synthesized via procedure D, 18.5 mg, 65%. **<sup>1</sup>H NMR** (700 MHz, Chloroform-*d*)  $\delta$  7.24 – 7.19 (m, 2H), 7.11 – 7.03 (m, 3H), 7.01 (d, *J* = 5.0 Hz, 1H), 6.50 (d, *J* = 5.0 Hz, 1H), 3.99 (ddd, *J* = 11.1,

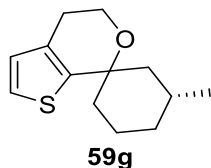
5.3, 1.6 Hz, 1H), 3.70 (td,  $J = 11.1, 3.0$  Hz, 1H), 2.85 (dd,  $J = 12.8, 3.7$  Hz, 1H), 2.37 – 2.30 (m, 1H), 2.30 – 2.16 (m, 3H), 1.93 – 1.82 (m, 2H), 1.74 – 1.69 (m, 1H), 1.69 – 1.62 (m, 2H), 1.51 (qt,  $J = 13.0, 3.8$  Hz, 1H) ppm.  $^{13}\text{C NMR}$  (176 MHz, Chloroform- $d$ )  $\delta$  141.7, 140.6, 133.0, 128.4, 125.9, 125.4, 124.8, 120.6, 58.9, 55.1, 37.6, 28.1, 25.3, 25.2, 20.7 ppm. **HRMS-ESI** ( $m/z$ ):  $[\text{M} + \text{H}]^+$  calculated for  $\text{C}_{18}\text{H}_{20}\text{OS}$   $[\text{M} + \text{H}]^+$ : 285.1235, found 285.1237.

2-benzyl-4',5'-dihydrospiro[cyclohexane-1,7'-thieno[2,3- $c$ ]pyran] **59f**



Synthesized via procedure D, 23.3 mg, 78%.  $^1\text{H NMR}$  (400 MHz, Chloroform- $d$ )  $\delta$  7.14 – 7.08 (m, 3H), 7.03 (td,  $J = 7.0, 6.6, 1.4$  Hz, 1H), 7.00 – 6.95 (m, 2H), 6.69 (d,  $J = 5.0$  Hz, 1H), 4.01 – 3.92 (m, 1H), 3.76 (td,  $J = 11.4, 3.2$  Hz, 1H), 2.83 – 2.68 (m, 1H), 2.50 – 2.36 (m, 2H), 2.30 – 2.13 (m, 2H), 1.72 (td,  $J = 10.8, 4.8, 2.5$  Hz, 1H), 1.66 – 1.55 (m, 2H), 1.46 – 1.36 (m, 4H), 1.21 – 1.08 (m, 1H) ppm.  $^{13}\text{C NMR}$  (101 MHz, Chloroform- $d$ )  $\delta$  142.6, 142.2, 134.5, 129.5, 128.3, 128.2, 127.1, 125.7, 122.6, 78.0, 59.6, 51.7, 38.0, 36.8, 26.9, 26.5, 22.0 ppm. **HRMS-ESI** ( $m/z$ ):  $[\text{M} + \text{H}]^+$  calculated for  $\text{C}_{19}\text{H}_{22}\text{OS}$   $[\text{M} + \text{H}]^+$ : 299.1391, found 299.1390.

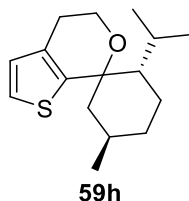
3-methyl-4',5'-dihydrospiro[cyclohexane-1,7'-thieno[2,3- $c$ ]pyran] **59g**



Synthesized via procedure D, 18.2 mg, 82%, d.r. 13:1.  $^1\text{H NMR}$  (700 MHz, Chloroform- $d$ )  $\delta$  7.11 (d,  $J = 5.0$  Hz, 1H), 6.75 (dd,  $J = 5.0, 0.5$  Hz, 1H), 3.97 – 3.86 (m, 2H), 2.74 – 2.64 (m, 2H), 2.07 (dddt,  $J = 19.8, 13.7, 4.8, 2.1$  Hz, 2H), 1.87 (ddtq,  $J = 15.6, 12.1, 6.8, 3.5$  Hz, 1H), 1.77 – 1.68 (m, 2H), 1.62 – 1.54 (m, 1H), 1.50 (td,  $J = 13.7, 4.4$  Hz, 1H), 1.25 (dd,  $J = 13.6, 12.1$  Hz, 1H), 0.99 – 0.92 (m, 1H), 0.90 (d,  $J = 6.7$  Hz, 3H) ppm.  $^{13}\text{C NMR}$  (176 MHz, Chloroform- $d$ )  $\delta$  143.5, 132.3, 126.8, 121.9, 75.3, 59.1, 47.6, 38.1, 34.2, 27.8, 26.6, 22.5, 21.7 ppm. **HRMS-ESI** ( $m/z$ ):  $[\text{M} + \text{H}]^+$  calculated for  $\text{C}_{13}\text{H}_{18}\text{OS}$   $[\text{M} + \text{H}]^+$ : 223.1078, found 223.1077.

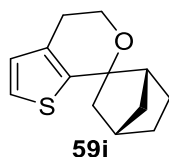
## Experimental

### (2*S*,5*R*)-2-isopropyl-5-methyl-4',5'-dihydrospiro[cyclohexane-1,7'-thieno[2,3-*c*]pyran] **59h**



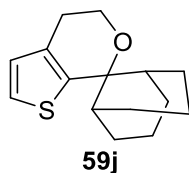
Synthesized via procedure D, 20.3 mg, 77%. **<sup>1</sup>H NMR** (400 MHz, Chloroform-*d*)  $\delta$  7.12 (d,  $J$  = 5.0 Hz, 1H), 6.76 (d,  $J$  = 5.0 Hz, 1H), 3.98 (d,  $J$  = 16.1 Hz, 1H), 3.76 (s, 1H), 2.78 (d,  $J$  = 32.8 Hz, 1H), 2.51 (d,  $J$  = 20.0 Hz, 1H), 2.25 (d,  $J$  = 19.8 Hz, 1H), 1.80 (d,  $J$  = 32.0 Hz, 2H), 1.74 – 1.59 (m, 1H), 1.55 (d,  $J$  = 29.7 Hz, 2H), 1.42 (d,  $J$  = 16.2 Hz, 1H), 1.09 (d,  $J$  = 12.0 Hz, 1H), 1.06 – 0.94 (m, 1H), 0.92 – 0.83 (m, 6H), 0.78 (d,  $J$  = 7.0 Hz, 3H) ppm. **<sup>13</sup>C NMR** (101 MHz, Chloroform-*d*)  $\delta$  143.2, 133.9, 126.9, 122.2, 79.9, 59.3, 53.6, 47.4, 35.3, 28.2, 27.4, 26.9, 24.1, 22.4, 21.2, 18.9 ppm. **HRMS-ESI** ( $m/z$ ):  $[M + H]^+$  calculated for C<sub>16</sub>H<sub>24</sub>OS  $[M+H]^+$ : 265.1548, found 265.1544.

### (1*R*,4*S*)-4',5'-dihydrospiro[bicyclo[2.2.1]heptane-2,7'-thieno[2,3-*c*]pyran] **59i**



Synthesized via procedure D, 16.7 mg, 76%. **<sup>1</sup>H NMR** (400 MHz, Chloroform-*d*)  $\delta$  7.00 (d,  $J$  = 5.1 Hz, 1H), 6.68 (d,  $J$  = 5.1 Hz, 1H), 3.94 – 3.82 (m, 2H), 3.73 (ddd,  $J$  = 11.4, 8.9, 4.5 Hz, 1H), 2.78 – 2.66 (m, 1H), 2.57 – 2.50 (m, 1H), 2.30 – 2.24 (m, 1H), 1.98 – 1.88 (m, 4H), 1.60 – 1.52 (m, 3H), 1.44 – 1.38 (m, 1H) ppm. **<sup>13</sup>C NMR** (101 MHz, Chloroform-*d*)  $\delta$  131.96, 126.84, 122.13, 83.23, 61.74, 49.63, 48.30, 39.09, 38.26, 36.35, 28.08, 26.35, 22.68 ppm. **HRMS-ESI** ( $m/z$ ):  $[M + H]^+$  calculated for C<sub>13</sub>H<sub>16</sub>OS  $[M+H]^+$ : 221.0922, found 221.0921.

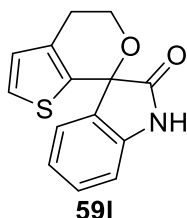
### 4',5'-dihydrospiro[bicyclo[3.3.1]nonane-9,7'-thieno[2,3-*c*]pyran] **59j**



Synthesized via procedure D, 8.4 mg, 34%. **<sup>1</sup>H NMR** (700 MHz, Chloroform-*d*)  $\delta$  7.06 (d,  $J$  = 5.2 Hz, 1H), 6.76 (d,  $J$  = 5.1 Hz, 1H), 3.90 (t,  $J$  = 5.9 Hz, 2H), 2.69 (t,  $J$  = 5.9 Hz, 2H), 2.39 (tddd,  $J$  = 15.1, 7.4, 4.8, 2.2 Hz, 2H), 2.25 – 2.16 (m, 2H), 1.97 – 1.87 (m, 3H), 1.81 (ddq,  $J$  = 20.5, 13.7,

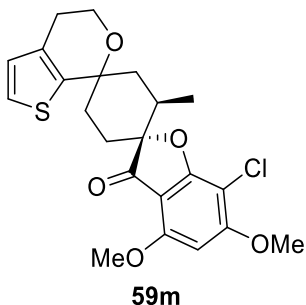
7.1 Hz, 1H), 1.72 (ddq,  $J = 15.6, 7.5, 1.2$  Hz, 2H), 1.58 (dt,  $J = 14.8, 7.6$  Hz, 1H), 1.49 (dt,  $J = 14.6, 7.4$  Hz, 1H), 1.41 (ddq,  $J = 13.8, 7.1, 1.2$  Hz, 2H) ppm.  $^{13}\text{C}$  NMR (176 MHz, Chloroform-*d*)  $\delta$  138.2, 132.8, 125.5, 121.0, 77.4, 56.0, 35.0, 27.7, 26.6, 25.8, 19.3, 19.2 ppm. HRMS-ESI ( $m/z$ ):  $[\text{M} + \text{H}]^+$  calculated for  $\text{C}_{15}\text{H}_{20}\text{OS}$   $[\text{M} + \text{H}]^+$ : 249.1235, found 2489.1235.

4',5'-dihydrospiro[indoline-3,7'-thieno[2,3-*c*]pyran]-2-one **59I**



Synthesized via procedure D, 14.9 mg, 58%.  $^1\text{H}$  NMR (500 MHz, Chloroform-*d*)  $\delta$  7.28 (td,  $J = 7.7, 1.3$  Hz, 1H), 7.24 – 7.15 (m, 2H), 7.03 (td,  $J = 7.6, 1.0$  Hz, 1H), 6.95 – 6.85 (m, 2H), 4.88 (ddd,  $J = 11.5, 10.0, 3.9$  Hz, 1H), 4.18 (ddd,  $J = 11.4, 5.7, 2.7$  Hz, 1H), 3.05 (ddd,  $J = 15.8, 10.0, 5.7$  Hz, 1H), 2.86 (ddd,  $J = 16.1, 3.9, 2.7$  Hz, 1H) ppm.  $^{13}\text{C}$  NMR (126 MHz, Chloroform-*d*)  $\delta$  177.4, 140.6, 136.3, 131.6, 130.6, 127.0, 125.6, 125.0, 123.5, 110.4, 77.6, 61.6, 25.6 ppm. HRMS-ESI ( $m/z$ ):  $[\text{M} + \text{H}]^+$  calculated for  $\text{C}_{14}\text{H}_{11}\text{NO}_2\text{S}$   $[\text{M} + \text{H}]^+$ : 258.0510, found 258.0509.

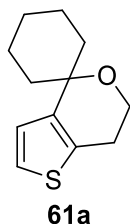
(2*R*,2'*R*)-7-chloro-4,6-dimethoxy-2'-methyl-4'',5''-dihydro-3H-dispiro[benzofuran-2,1'-cyclohexane-4',7''-thieno[2,3-*c*]pyran]-3-one **59m**



Synthesized via procedure D, 30.0 mg, 69%.  $^1\text{H}$  NMR (400 MHz, Chloroform-*d*)  $\delta$  7.08 (d,  $J = 5.0$  Hz, 1H), 6.69 (d,  $J = 5.0$  Hz, 1H), 6.01 (s, 1H), 3.93 (s, 3H), 3.91 (s, 3H), 3.90 – 3.83 (m, 2H), 2.62 (dtd,  $J = 17.1, 6.4, 4.6$  Hz, 3H), 2.55 – 2.28 (m, 3H), 2.06 – 1.79 (m, 2H), 1.67 (ddd,  $J = 12.8, 3.8, 2.7$  Hz, 1H), 1.35 (s, 1H), 0.73 (d,  $J = 6.8$  Hz, 3H) ppm.  $^{13}\text{C}$  NMR (151 MHz, Chloroform-*d*)  $\delta$  198.7, 168.0, 163.7, 157.1, 140.4, 132.0, 124.2, 121.5, 105.2, 96.3, 92.5, 88.0, 74.1, 59.0, 56.4, 55.8, 37.9, 33.3, 30.1, 27.4, 24.7, 14.0 ppm. HRMS-ESI ( $m/z$ ):  $[\text{M} + \text{H}]^+$  calculated for  $\text{C}_{22}\text{H}_{23}\text{ClO}_5\text{S}$   $[\text{M} + \text{H}]^+$ : 435.0955 and 437.0925, found 435.0945 and 437.0921.

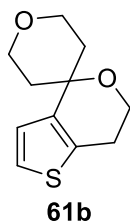
## Experimental

### 6',7'-dihydrospiro[cyclohexane-1,4'-thieno[3,2-c]pyran] **61a**



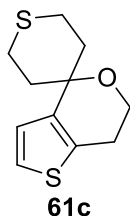
Synthesized via procedure D, 16.9 mg, 81%. **<sup>1</sup>H NMR** (400 MHz, Chloroform-*d*)  $\delta$  6.98 (dd,  $J = 5.2, 0.8$  Hz, 1H), 6.69 (d,  $J = 5.2$  Hz, 1H), 3.86 (t,  $J = 5.4$  Hz, 2H), 2.74 (t,  $J = 5.4$  Hz, 2H), 1.82 (ddt,  $J = 15.6, 11.4, 4.8$  Hz, 2H), 1.65 (tdd,  $J = 14.2, 5.1, 2.8$  Hz, 3H), 1.56 – 1.44 (m, 4H), 1.29 – 1.08 (m, 1H) ppm. **<sup>13</sup>C NMR** (176 MHz, Chloroform-*d*)  $\delta$  142.5, 132.4, 124.7, 122.3, 76.2, 59.4, 45.5, 36.0, 26.2, 21.8 ppm. **HRMS-ESI** ( $m/z$ ):  $[M + H]^+$  calculated for C<sub>12</sub>H<sub>16</sub>OS  $[M+H]^+$ : 209.0922, found 209.0921.

### 2,3,5,6,6',7'-hexahydrospiro[pyran-4,4'-thieno[3,2-c]pyran] **61b**



Synthesized via procedure D, 13.9 mg, 66%. **<sup>1</sup>H NMR** (700 MHz, Chloroform-*d*)  $\delta$  7.15 (s, 1H), 6.77 (s, 1H), 3.93 (s, 2H), 3.84 (d,  $J = 46.8$  Hz, 4H), 2.70 (s, 2H), 2.01 (d,  $J = 31.0$  Hz, 2H), 1.92 (s, 2H) ppm. **<sup>13</sup>C NMR** (176 MHz, Chloroform-*d*)  $\delta$  140.8, 132.0, 125.9, 121.6, 71.3, 62.7, 58.3, 37.9, 25.5 ppm. **HRMS-ESI** ( $m/z$ ):  $[M + H]^+$  calculated for C<sub>11</sub>H<sub>14</sub>O<sub>2</sub>S  $[M+H]^+$ : 211.0715, found 211.0716.

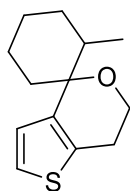
### 2',3',5',6,6',7-hexahydrospiro[thieno[3,2-c]pyran-4,4'-thiopyran] **61c**



Synthesized via procedure D, 10.4 mg, 46%. **<sup>1</sup>H NMR** (400 MHz, Chloroform-*d*)  $\delta$  7.06 – 6.97 (m, 1H), 6.72 (d,  $J = 5.2$  Hz, 1H), 3.85 (t,  $J = 5.4$  Hz, 2H), 3.09 (ddd,  $J = 13.8, 12.7, 2.5$  Hz, 2H), 2.75 (t,  $J = 5.4$  Hz, 2H), 2.31 (dddd,  $J = 13.8, 4.1, 2.9, 1.5$  Hz, 2H), 2.17 – 2.02 (m, 2H), 1.90 (ddd,  $J = 196$

14.0, 12.8, 3.8 Hz, 2H) ppm.  $^{13}\text{C}$  NMR (176 MHz, Chloroform-*d*)  $\delta$  141.2, 132.8, 123.5, 122.3, 71.5, 64.6, 58.2, 37.7, 21.3 ppm. HRMS-ESI ( $m/z$ ):  $[\text{M} + \text{H}]^+$  calculated for  $\text{C}_{11}\text{H}_{14}\text{OS}_2$   $[\text{M}+\text{H}]^+$ : 227.0486, found 227.0484.

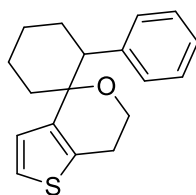
2-methyl-6',7'-dihydrospiro[cyclohexane-1,4'-thieno[3,2-*c*]pyran] **61d**



**61d**

Synthesized via procedure D, 11.3 mg, 51%.  $^1\text{H}$  NMR (700 MHz, Chloroform-*d*)  $\delta$  7.07 (d,  $J = 5.2$  Hz, 1H), 6.77 (d,  $J = 5.2$  Hz, 1H), 4.03 – 3.81 (m, 2H), 2.84 (qt,  $J = 15.8, 5.4$  Hz, 2H), 1.92 (tt,  $J = 16.0, 1.9$  Hz, 2H), 1.87 (dtd,  $J = 12.2, 6.5, 5.9, 2.7$  Hz, 1H), 1.75 (tdt,  $J = 16.8, 13.2, 3.7$  Hz, 2H), 1.61 – 1.58 (m, 1H), 1.51 (td,  $J = 13.6, 4.3$  Hz, 1H), 1.31 – 1.24 (m, 1H), 0.99 – 0.93 (m, 1H), 0.91 (d,  $J = 6.5$  Hz, 3H) ppm.  $^{13}\text{C}$  NMR (176 MHz, Chloroform-*d*)  $\delta$  142.2, 132.0, 124.4, 121.9, 75.8, 59.0, 45.2, 35.6, 34.4, 27.6, 25.9, 22.6, 21.5 ppm. HRMS-ESI ( $m/z$ ):  $[\text{M} + \text{H}]^+$  calculated for  $\text{C}_{13}\text{H}_{18}\text{OS}$   $[\text{M}+\text{H}]^+$ : 223.1078, found 223.1078.

2-phenyl-6',7'-dihydrospiro[cyclohexane-1,4'-thieno[3,2-*c*]pyran] **61e**

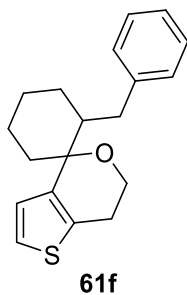


**61e**

Synthesized via procedure D, 19.0 mg, 67%.  $^1\text{H}$  NMR (700 MHz, Chloroform-*d*)  $\delta$  7.03 – 6.93 (m, 5H), 6.91 (d,  $J = 5.2$  Hz, 1H), 6.79 (d,  $J = 5.2$  Hz, 1H), 3.90 (ddd,  $J = 11.1, 5.3, 1.6$  Hz, 1H), 3.60 (td,  $J = 11.0, 3.1$  Hz, 1H), 2.79 (dd,  $J = 12.9, 3.6$  Hz, 1H), 2.29 (dt,  $J = 15.7, 2.4$  Hz, 1H), 2.25 – 2.12 (m, 2H), 2.11 – 2.05 (m, 1H), 1.86 – 1.70 (m, 2H), 1.64 – 1.51 (m, 2H), 1.41 (qt,  $J = 13.1, 3.7$  Hz, 1H), 1.21 – 1.17 (m, 1H) ppm.  $^{13}\text{C}$  NMR (176 MHz, Chloroform-*d*)  $\delta$  141.8, 139.2, 132.1, 128.3, 125.8, 124.7, 123.4, 120.4, 76.7, 58.8, 52.8, 34.8, 27.3, 25.4, 24.5, 20.5 ppm. HRMS-ESI ( $m/z$ ):  $[\text{M} + \text{H}]^+$  calculated for  $\text{C}_{18}\text{H}_{20}\text{OS}$   $[\text{M}+\text{H}]^+$ : 285.1235, found 285.1236.

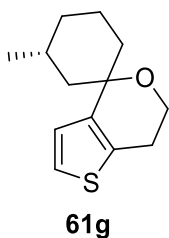
## Experimental

### 2-benzyl-6',7'-dihydrospiro[cyclohexane-1,4'-thieno[3,2-c]pyran] **61f**



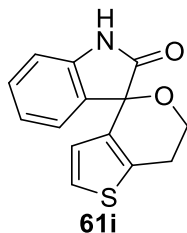
Synthesized via procedure D, 11.9 mg, 40%. **<sup>1</sup>H NMR** (400 MHz, Chloroform-*d*)  $\delta$  7.37 – 7.32 (m, 2H), 7.29 – 7.23 (m, 1H), 7.23 – 7.18 (m, 2H), 6.91 (d,  $J$  = 5.0 Hz, 1H), 4.25 – 4.13 (m, 1H), 3.98 (td,  $J$  = 11.4, 3.2 Hz, 1H), 3.02 – 2.91 (m, 1H), 2.72 – 2.58 (m, 2H), 2.50 – 2.37 (m, 2H), 1.94 (tdd,  $J$  = 10.8, 4.8, 2.5 Hz, 1H), 1.86 – 1.79 (m, 2H), 1.70 – 1.61 (m, 5H), 1.42 – 1.33 (m, 1H) ppm. **<sup>13</sup>C NMR** (101 MHz, Chloroform-*d*)  $\delta$  141.2, 141.0, 133.0, 128.1, 127.6, 126.1, 124.4, 121.9, 77.1, 58.1, 50.5, 37.7, 35.4, 25.7, 25.4, 25.7, 21.2 ppm. **HRMS-ESI** ( $m/z$ ): [M + H]<sup>+</sup> calculated for C<sub>19</sub>H<sub>22</sub>OS [M+H]<sup>+</sup>: 299.1391, found 299.1390.

### (3*R*)-3-methyl-6',7'-dihydrospiro[cyclohexane-1,4'-thieno[3,2-c]pyran] **61g**

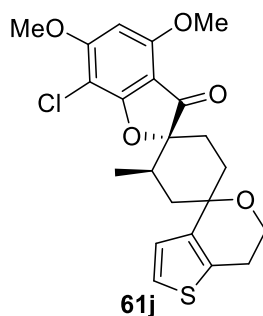


Synthesized via procedure D, 16.0 mg, 72%, d.r. 15:1. **<sup>1</sup>H NMR** (700 MHz, Chloroform-*d*)  $\delta$  7.07 (d,  $J$  = 5.2 Hz, 1H), 6.77 (d,  $J$  = 5.2 Hz, 1H), 4.03 – 3.81 (m, 2H), 2.84 (qt,  $J$  = 15.8, 5.4 Hz, 2H), 1.92 (tt,  $J$  = 16.0, 1.9 Hz, 2H), 1.87 (dtd,  $J$  = 12.2, 6.5, 5.9, 2.7 Hz, 1H), 1.75 (tdt,  $J$  = 16.8, 13.2, 3.7 Hz, 2H), 1.61 – 1.58 (m, 1H), 1.51 (td,  $J$  = 13.6, 4.3 Hz, 1H), 1.31 – 1.24 (m, 1H), 0.99 – 0.93 (m, 1H), 0.91 (d,  $J$  = 6.5 Hz, 3H) ppm. **<sup>13</sup>C NMR** (176 MHz, Chloroform-*d*)  $\delta$  142.2, 132.0, 124.4, 121.9, 75.8, 59.0, 45.2, 35.6, 34.4, 27.6, 25.9, 22.6, 21.5 ppm. **HRMS-ESI** ( $m/z$ ): [M + H]<sup>+</sup> calculated for C<sub>13</sub>H<sub>18</sub>OS [M+H]<sup>+</sup>: 223.1078, found 223.1076.



6',7'-dihydrospiro[indoline-3,4'-thieno[3,2-c]pyran]-2-one **61i**

Synthesized via procedure D, 17.5 mg, 68%. **<sup>1</sup>H NMR** (500 MHz, Chloroform-*d*)  $\delta$  8.57 (s, 1H), 7.21 – 7.16 (m, 1H), 7.05 (dd,  $J = 7.5, 1.3$  Hz, 1H), 6.97 (d,  $J = 5.2$  Hz, 1H), 6.92 (td,  $J = 7.5, 1.0$  Hz, 1H), 6.82 (d,  $J = 7.8$  Hz, 1H), 6.27 (d,  $J = 5.2$  Hz, 1H), 4.78 (ddd,  $J = 11.3, 9.5, 3.9$  Hz, 1H), 4.17 (ddd,  $J = 11.3, 5.4, 3.1$  Hz, 1H), 3.12 (dddd,  $J = 16.0, 9.5, 5.4, 0.9$  Hz, 1H), 2.92 (dt,  $J = 16.2, 3.5$  Hz, 1H) ppm. **<sup>13</sup>C NMR** (126 MHz, Chloroform-*d*)  $\delta$  178.0, 140.8, 135.6, 131.3, 131.1, 130.2, 123.7, 123.5, 123.3, 110.4, 78.5, 61.8, 26.9, 25.0 ppm. **HRMS-ESI** ( $m/z$ ):  $[M + H]^+$  calculated for C<sub>14</sub>H<sub>11</sub>NO<sub>2</sub>S  $[M+H]^+$ : 258.0510, found 258.0509.

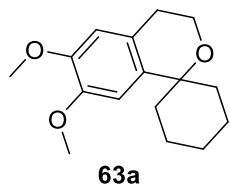
(2*R*,2'*R*)-7-chloro-4,6-dimethoxy-2'-methyl-6'',7''-dihydro-3H-dispiro[benzofuran-2,1'-cyclohexane-4',4''-thieno[3,2-c]pyran]-3-one **61j**

Synthesized via procedure D, 36.9 mg, 85%. **<sup>1</sup>H NMR** (600 MHz, Chloroform-*d*)  $\delta$  6.99 (d,  $J = 5.1$  Hz, 1H), 6.90 (d,  $J = 5.2$  Hz, 1H), 5.99 (s, 1H), 3.91 (s, 3H), 3.89 (s, 3H), 3.89 – 3.81 (m, 2H), 2.82 – 2.68 (m, 2H), 2.56 (dq,  $J = 13.5, 6.8, 4.1$  Hz, 1H), 2.47 (td,  $J = 14.2, 4.1$  Hz, 1H), 2.39 (dd,  $J = 14.2, 12.9$  Hz, 1H), 2.32 (td,  $J = 13.5, 4.1$  Hz, 1H), 1.87 – 1.78 (m, 1H), 1.75 (ddd,  $J = 14.2, 4.1, 2.6$  Hz, 1H), 1.64 (ddd,  $J = 12.9, 4.0, 2.6$  Hz, 1H), 0.70 (d,  $J = 6.8$  Hz, 3H) ppm. **<sup>13</sup>C NMR** (151 MHz, Chloroform-*d*)  $\delta$  199.0, 168.4, 164.0, 157.5, 140.9, 132.3, 124.7, 122.2, 105.9, 97.2, 92.7, 88.7, 74.9, 59.3, 56.9, 56.2, 39.3, 33.7, 30.5, 28.7, 25.8, 14.7 ppm. **HRMS-ESI** ( $m/z$ ):  $[M + H]^+$  calculated for C<sub>22</sub>H<sub>23</sub>ClO<sub>5</sub>S  $[M+H]^+$ : 435.0955 and 437.0925, found 435.0945 and 437.0934.

## Experimental

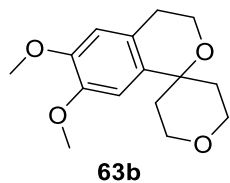
### SPIRO CHROMANS

#### 6',7'-dimethoxyspiro[cyclohexane-1,1'-isochromane] **63a**



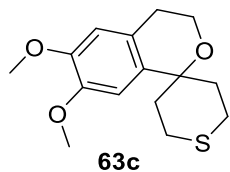
Synthesized via procedure C, 23.9 mg, 91%. **<sup>1</sup>H NMR** (500 MHz, Chloroform-*d*)  $\delta$  6.59 (s, 1H), 6.56 (s, 1H), 3.87 (d,  $J$  = 6.7 Hz, 5H), 3.84 (s, 3H), 2.73 (t,  $J$  = 5.5 Hz, 2H), 1.97 – 1.88 (m, 2H), 1.72 (qd,  $J$  = 12.6, 11.9, 5.8 Hz, 3H), 1.66 – 1.53 (m, 4H), 1.31 – 1.23 (m, 1H) ppm. **<sup>13</sup>C NMR** (126 MHz, Chloroform-*d*)  $\delta$  147.5, 147.5, 135.7, 125.9, 111.6, 108.9, 75.0, 59.1, 56.4, 56.1, 37.4, 29.5, 25.9, 22.1 ppm. **HRMS-ESI** ( $m/z$ ):  $[M + H]^+$  calculated for C<sub>16</sub>H<sub>22</sub>O<sub>3</sub>  $[M+H]^+$ : 263.1569, found 263.1564.

#### 6,7-dimethoxy-2',3',5',6'-tetrahydrospiro[isochromane-1,4'-pyran] **63b**



Synthesized via procedure C, 18.5 mg, 70%. **<sup>1</sup>H NMR** (700 MHz, Chloroform-*d*)  $\delta$  6.63 (s, 1H), 6.57 (s, 1H), 3.91 – 3.81 (m, 12H), 2.75 (t,  $J$  = 5.5 Hz, 2H), 2.09 – 2.01 (m, 2H), 1.82 – 1.75 (m, 2H) ppm. **<sup>13</sup>C NMR** (176 MHz, Chloroform-*d*)  $\delta$  146.5, 145.9, 132.6, 124.8, 110.3, 107.5, 71.3, 62.9, 58.1, 55.1, 54.9, 36.3, 28.1 ppm. **HRMS-ESI** ( $m/z$ ):  $[M + H]^+$  calculated for C<sub>15</sub>H<sub>20</sub>O<sub>4</sub>  $[M+H]^+$ : 265.1362, found 265.1365.

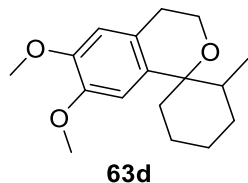
#### 6,7-dimethoxy-2',3',5',6'-tetrahydrospiro[isochromane-1,4'-thiopyran] **63c**



Synthesized via procedure C, 23.3 mg, 83%. **<sup>1</sup>H NMR** (400 MHz, Chloroform-*d*)  $\delta$  6.59 (s, 1H), 6.54 (d,  $J$  = 0.9 Hz, 1H), 3.84 (dd,  $J$  = 9.2, 5.2 Hz, 8H), 3.16 (ddd,  $J$  = 13.7, 12.6, 2.6 Hz, 2H), 2.74 – 2.67 (m, 2H), 2.42 – 2.29 (m, 2H), 2.20 – 2.07 (m, 2H), 1.99 (ddd,  $J$  = 13.9, 12.7, 3.7 Hz, 2H) ppm. **<sup>13</sup>C NMR** (126 MHz, Chloroform-*d*)  $\delta$  145.3, 144.7, 133.3, 124.9, 110.3, 107.8, 74.3,

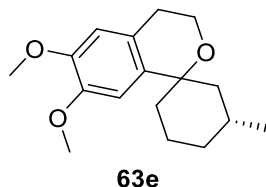
57.9, 55.2, 54.3, 38.5, 28.5, 21.0 ppm. **HRMS-ESI** ( $m/z$ ):  $[M + H]^+$  calculated for  $C_{15}H_{20}O_3S$   $[M+H]^+$ : 281.1133, found 281.1130.

6',7'-dimethoxy-2-methylspiro[cyclohexane-1,1'-isochromane] **63d**



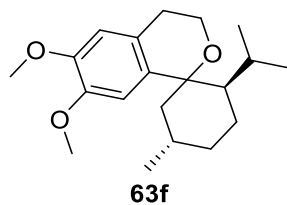
Synthesized via procedure C, 8.0 mg, 29%.  **$^1H$  NMR** (700 MHz, Chloroform-*d*)  $\delta$  6.57 (s, 1H), 6.54 (s, 1H), 3.95 (ddd,  $J = 11.2, 5.7, 1.5$  Hz, 1H), 3.91 – 3.82 (m, 6H), 3.77 (td,  $J = 11.5, 2.8$  Hz, 1H), 2.92 (dddd,  $J = 15.7, 11.8, 5.7, 1.0$  Hz, 1H), 2.43 (dt,  $J = 15.2, 2.2$  Hz, 1H), 2.12 (dq,  $J = 13.9, 2.6$  Hz, 1H), 1.85 – 1.73 (m, 2H), 1.69 – 1.48 (m, 4H), 1.48 – 1.35 (m, 1H), 1.35 – 1.24 (m, 1H), 0.59 (d,  $J = 6.7$  Hz, 3H) ppm.  **$^{13}C$  NMR** (176 MHz, Chloroform-*d*)  $\delta$  146.5, 145.9, 133.3, 126.0, 110.0, 107.3, 76.1, 58.0, 55.1, 54.8, 40.7, 35.1, 29.0, 28.3, 25.3, 20.7, 14.5 ppm. **HRMS-ESI** ( $m/z$ ):  $[M + H]^+$  calculated for  $C_{17}H_{24}O_3$   $[M+H]^+$ : 277.1725, found 277.1726.

(3*R*)-6',7'-dimethoxy-3-methylspiro[cyclohexane-1,1'-isochromane] **63e**



Synthesized via procedure C, 22.7 mg, 82%, d.r. 12:1.  **$^1H$  NMR** (400 MHz, Chloroform-*d*)  $\delta$  6.51 (s, 1H), 6.49 (d,  $J = 1.0$  Hz, 1H), 3.85 – 3.74 (m, 8H), 2.77 – 2.54 (m, 2H), 1.91 – 1.73 (m, 3H), 1.74 – 1.60 (m, 2H), 1.55 – 1.38 (m, 2H), 1.23 – 1.13 (m, 1H), 0.97 – 0.85 (m, 1H), 0.83 (d,  $J = 6.5$  Hz, 3H) ppm.  **$^{13}C$  NMR** (176 MHz, Chloroform-*d*)  $\delta$  145.8, 144.9, 132.7, 124.6, 111.1, 106.2, 75.8, 57.5, 55.0, 53.9, 40.0, 33.9, 29.0, 25.9, 24.3, 19.8, 13.7 ppm. **HRMS-ESI** ( $m/z$ ):  $[M + H]^+$  calculated for  $C_{17}H_{24}O_3$   $[M+H]^+$ : 277.1725, found 277.1724.

(2*R*,5*S*)-2-isopropyl-6',7'-dimethoxy-5-methylspiro[cyclohexane-1,1'-isochromane] **63f**

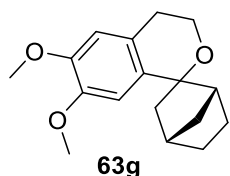


Synthesized via procedure C, 13.7 mg, 43%.  **$^1H$  NMR** (500 MHz, Chloroform-*d*)  $\delta$  6.45 (s, 1H), 6.39 (d,  $J = 0.9$  Hz, 1H), 3.73 (dd,  $J = 9.2, 5.2$  Hz, 8H), 3.76 (s, 1H), 2.75 (d,  $J = 32.8$  Hz, 1H),

## Experimental

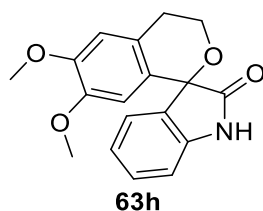
2.41 (d,  $J = 20.0$  Hz, 1H), 2.20 (d,  $J = 19.8$  Hz, 1H), 1.74 (d,  $J = 32.0$  Hz, 2H), 1.70 – 1.49 (m, 1H), 1.45 (d,  $J = 29.7$  Hz, 2H), 1.40 (d,  $J = 16.2$  Hz, 1H), 1.07 (d,  $J = 12.0$  Hz, 1H), 1.05 – 0.91 (m, 1H), 0.88 – 0.80 (m, 5H), 0.74 (d,  $J = 7.0$  Hz, 3H) ppm.  $^{13}\text{C}$  NMR (126 MHz, Chloroform- $d$ )  $\delta$  146.5, 146.1, 134.7, 124.8, 110.9, 106.9, 74.6, 58.8, 55.6, 53.9, 47.3, 35.1, 28.0, 27.3, 25.8, 23.4, 21.9, 21.0, 18.2 ppm. HRMS-ESI ( $m/z$ ):  $[\text{M} + \text{H}]^+$  calculated for  $\text{C}_{20}\text{H}_{30}\text{O}_3$   $[\text{M} + \text{H}]^+$ : 319.2195, found 319.2195.

(1*R*,4*S*)-6',7'-dimethoxyspiro[bicyclo[2.2.1]heptane-2,1'-isochromane] **63g**



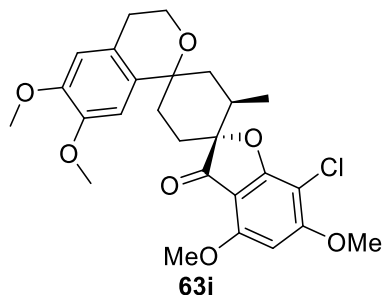
Synthesized via procedure C, 10.7 mg, 39%.  $^1\text{H}$  NMR (400 MHz, Chloroform- $d$ )  $\delta$  6.77 (s, 1H), 6.64 – 6.51 (m, 1H), 3.99 – 3.90 (m, 1H), 3.88 – 3.84 (m, 6H), 3.01 (ddtd,  $J = 16.3, 10.8, 6.9, 1.0$  Hz, 1H), 2.67 – 2.52 (m, 2H), 2.52 – 2.34 (m, 2H), 2.18 (ddd,  $J = 13.5, 4.5, 2.8$  Hz, 1H), 2.05 (dp,  $J = 9.4, 2.0$  Hz, 1H), 2.00 – 1.85 (m, 3H), 1.80 – 1.51 (m, 3H) ppm.  $^{13}\text{C}$  NMR (126 MHz, Chloroform- $d$ )  $\delta$  148.3, 146.9, 136.8, 126.7, 111.4, 106.7, 76.2, 58.0, 57.3, 55.9, 36.3, 26.9, 24.9, 24.2, 23.2, 21.7, 20.9 ppm. HRMS-ESI ( $m/z$ ):  $[\text{M} + \text{H}]^+$  calculated for  $\text{C}_{17}\text{H}_{22}\text{O}_3$   $[\text{M} + \text{H}]^+$ : 275.1569, found 275.1569.

6',7'-dimethoxyspiro[indoline-3,1'-isochroman]-2-one **63h**



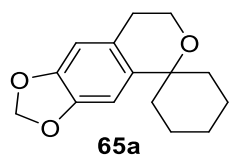
Synthesized via procedure C, 21.2 mg, 68%.  $^1\text{H}$  NMR (500 MHz, Chloroform- $d$ )  $\delta$  7.63 (s, 1H), 7.28 (td,  $J = 7.7, 1.3$  Hz, 1H), 7.16 – 7.06 (m, 1H), 7.02 (td,  $J = 7.5, 1.0$  Hz, 1H), 6.91 (dt,  $J = 7.8, 0.8$  Hz, 1H), 6.69 (s, 1H), 6.04 (s, 1H), 4.80 (ddd,  $J = 11.3, 9.9, 3.7$  Hz, 1H), 4.21 – 4.07 (m, 1H), 3.87 (s, 3H), 3.60 (s, 3H), 3.21 – 3.06 (m, 1H), 2.83 (dt,  $J = 16.0, 3.5$  Hz, 1H) ppm.  $^{13}\text{C}$  NMR (126 MHz, Chloroform- $d$ )  $\delta$  178.2, 148.8, 148.0, 140.9, 132.6, 130.1, 127.2, 125.5, 124.4, 123.5, 111.6, 110.0, 108.3, 78.5, 61.6, 55.9, 27.9, 26.9 ppm. HRMS-ESI ( $m/z$ ):  $[\text{M} + \text{H}]^+$  calculated for  $\text{C}_{18}\text{H}_{17}\text{O}_4\text{N}$   $[\text{M} + \text{H}]^+$ : 312.1158, found 312.1142.

(2*R*,2'*R*)-7-chloro-4,6,6'',7''-tetramethoxy-2'-methyl-3*H*-dispiro[benzofuran-2,1'-cyclohexane-4',1''-isochroman]-3-one **63i**



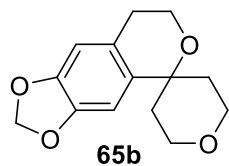
Synthesized via procedure C, 41.0 mg, 84%. **<sup>1</sup>H NMR** (700 MHz, Chloroform-*d*)  $\delta$  6.87 (s, 1H), 6.60 (s, 1H), 6.15 (s, 1H), 6.00 – 5.91 (m, 2H), 4.51-4.40 (m, 2H), 4.23 (s, 3H), 4.01 (s, 3H), 3.99 – 3.82 (m, 4H), 2.90 – 2.75 (m, 3H), 2.72 – 2.47 (m, 3H), 1.99 (ddt,  $J$  = 14.0, 4.3, 2.5 Hz, 1H), 1.90 (ddd,  $J$  = 14.0, 4.3, 2.5 Hz, 1H), 1.81 (ddd,  $J$  = 12.8, 4.3, 2.5 Hz, 1H), 0.86 (d,  $J$  = 6.9 Hz, 3H) ppm. **<sup>13</sup>C NMR** (176 MHz, Chloroform-*d*)  $\delta$  199.2, 168.3, 163.5, 157.1, 147.8, 146.4, 145.3, 135.1, 127.0, 108.3, 106.1, 100.0, 97.5, 92.5, 88.8, 75.1, 57.2, 56.6, 56.0, 40.2, 33.7, 31.4, 29.5, 28.4, 26.9, 14.0 ppm. **HRMS-ESI** ( $m/z$ ): [M + H]<sup>+</sup> calculated for C<sub>26</sub>H<sub>29</sub>O<sub>7</sub>Cl [M+H]<sup>+</sup>: 489.1602 and 491.1572, found 489.1602 and 491.1572.

7',8'-dihydrospiro[cyclohexane-1,5'-[1,3]dioxolo[4,5-*g*]isochromene] **65a**



Synthesized via procedure C, 19.7 mg, 80%. **<sup>1</sup>H NMR** (500 MHz, Chloroform-*d*)  $\delta$  6.61 (s, 1H), 6.53 (s, 1H), 5.89 (s, 2H), 3.84 (s, 2H), 2.70 (s, 2H), 1.94 – 1.83 (m, 2H), 1.67 (s, 3H), 1.54 (s, 4H), 1.29-1.22 (m, 1H) ppm. **<sup>13</sup>C NMR** (126 MHz, Chloroform-*d*)  $\delta$  145.9, 145.6, 136.6, 126.7, 108.4, 105.6, 100.7, 75.0, 58.6, 37.1, 29.7, 25.6, 21.8 ppm. **HRMS-ESI** ( $m/z$ ): [M + H]<sup>+</sup> calculated for C<sub>15</sub>H<sub>18</sub>O<sub>3</sub> [M+H]<sup>+</sup>: 247.1256, found 247.1259.

2,3,5,6,7',8'-hexahydrospiro[pyran-4,5'-[1,3]dioxolo[4,5-*g*]isochromene] **65b**

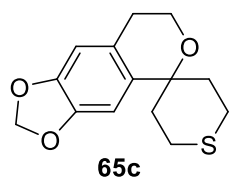


Synthesized via procedure C, 16.6 mg, 67%. **<sup>1</sup>H NMR** (700 MHz, Chloroform-*d*)  $\delta$  6.63 (s, 1H), 6.55 (s, 1H), 5.90 (s, 2H), 3.91 – 3.75 (m, 6H), 2.73 (t,  $J$  = 5.5 Hz, 2H), 2.05 – 1.93 (m, 2H), 1.80

## Experimental

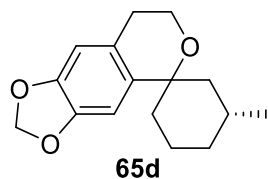
– 1.72 (m, 2H) ppm. **<sup>13</sup>C NMR** (176 MHz, Chloroform-*d*)  $\delta$  145.2, 144.9, 133.8, 126.0, 107.4, 104.6, 99.8, 71.6, 62.8, 58.0, 36.3, 28.7 ppm. **HRMS-ESI** (*m/z*): [M + H]<sup>+</sup> calculated for C<sub>14</sub>H<sub>16</sub>O<sub>4</sub> [M+H]<sup>+</sup>: 249.1049, found 249.1047.

2,3,5,6,7',8'-hexahydrospiro[thiopyran-4,5'-[1,3]dioxolo[4,5-*g*]isochromene] **65c**



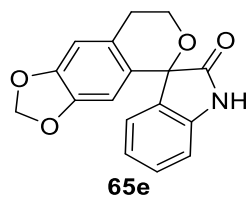
Synthesized via procedure C, 21.7 mg, 82%. **<sup>1</sup>H NMR** (700 MHz, Chloroform-*d*)  $\delta$  6.63 (s, 1H), 6.54 (d, *J* = 0.8 Hz, 1H), 5.90 (s, 2H), 3.84 (t, *J* = 5.5 Hz, 2H), 3.22 – 3.09 (m, 2H), 2.70 (t, *J* = 5.5 Hz, 2H), 2.44 – 2.32 (m, 2H), 2.13 (dtd, *J* = 13.0, 3.4, 1.9 Hz, 2H), 1.96 (ddd, *J* = 13.9, 12.8, 3.7 Hz, 2H) ppm. **<sup>13</sup>C NMR** (176 MHz, Chloroform-*d*)  $\delta$  145.1, 144.9, 134.5, 125.4, 107.5, 104.4, 99.8, 72.2, 57.6, 36.8, 28.5, 22.9 ppm. **HRMS-ESI** (*m/z*): [M + H]<sup>+</sup> calculated for C<sub>14</sub>H<sub>16</sub>O<sub>3</sub>S [M+H]<sup>+</sup>: 265.0820, found 265.0818.

(3*R*)-3-methyl-7',8'-dihydrospiro[cyclohexane-1,5'-[1,3]dioxolo[4,5-*g*]isochromene] **65d**



Synthesized via procedure C, 19.8 mg, 76%, d.r. 14:1. **<sup>1</sup>H NMR** (700 MHz, Chloroform-*d*)  $\delta$  6.60 (s, 1H), 6.57 – 6.51 (m, 1H), 5.90 – 5.87 (m, 2H), 3.92 – 3.77 (m, 2H), 2.88 – 2.65 (m, 3H), 2.05 – 1.97 (m, 1H), 1.94 – 1.81 (m, 3H), 1.77 – 1.68 (m, 1H), 1.35 – 1.21 (m, 3H), 0.91 – 0.87 (m, 3H) ppm. **<sup>13</sup>C NMR** (176 MHz, Chloroform-*d*)  $\delta$  144.9, 144.5, 135.3, 125.7, 107.4, 104.6, 99.7, 74.7, 57.7, 45.1, 35.4, 33.4, 28.7, 26.7, 21.6, 20.7 ppm. **HRMS-ESI** (*m/z*): [M + H]<sup>+</sup> calculated for C<sub>16</sub>H<sub>20</sub>O<sub>3</sub> [M+H]<sup>+</sup>: 261.1412, found 261.1410.

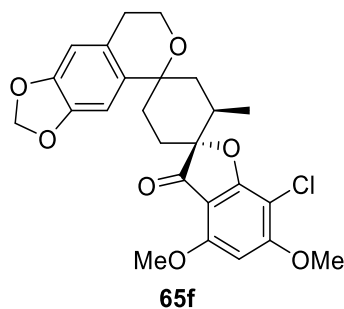
7',8'-dihydrospiro[indoline-3,5'-[1,3]dioxolo[4,5-*g*]isochromen]-2-one **65e**



Synthesized via procedure C, 15.6 mg, 53%. **<sup>1</sup>H NMR** (500 MHz, Chloroform-*d*)  $\delta$  7.94 (s, 1H), 7.28 (dd, *J* = 7.7, 1.3 Hz, 1H), 7.11 (dd, *J* = 7.5, 1.3 Hz, 1H), 7.02 (td, *J* = 7.5, 0.9 Hz, 1H), 6.90

(dt,  $J = 7.8, 0.8$  Hz, 1H), 6.67 (s, 1H), 6.08 (s, 1H), 5.86 (dd,  $J = 8.8, 1.4$  Hz, 2H), 4.78 (ddd,  $J = 11.3, 9.8, 3.7$  Hz, 1H), 4.12 (ddd,  $J = 11.3, 5.3, 3.4$  Hz, 1H), 3.17 – 3.03 (m, 1H), 2.82 (dt,  $J = 16.2, 3.6$  Hz, 1H) ppm.  $^{13}\text{C}$  NMR (126 MHz, Chloroform- $d$ )  $\delta$  178.4, 147.3, 146.5, 140.9, 132.7, 130.1, 128.4, 125.6, 125.4, 123.5, 110.2, 108.9, 105.5, 101.0, 78.9, 61.6, 28.4 ppm. HRMS-ESI ( $m/z$ ):  $[\text{M} + \text{H}]^+$  calculated for  $\text{C}_{17}\text{H}_{13}\text{O}_4\text{N}$   $[\text{M} + \text{H}]^+$ : 296.0845, found 296.0845.

(2*R*,2'*R*)-7-chloro-4,6-dimethoxy-2'-methyl-7'',8''-dihydro-3H-dispiro[benzofuran-2,1'-cyclohexane-4',5''-[1,3]dioxolo[4,5-*g*]isochromen]-3-one **65f**



Synthesized via procedure C, 42.0 mg, 89%.  $^1\text{H}$  NMR (700 MHz, Chloroform- $d$ )  $\delta$  6.96 (s, 1H), 6.52 (s, 1H), 6.09 (s, 1H), 5.92 – 5.86 (m, 2H), 4.00 (d,  $J = 9.3$  Hz, 6H), 3.93 – 3.78 (m, 2H), 2.82 – 2.61 (m, 3H), 2.61 – 2.37 (m, 3H), 1.92 (ddt,  $J = 14.3, 4.4, 2.6$  Hz, 1H), 1.85 (ddd,  $J = 14.2, 4.2, 2.5$  Hz, 1H), 1.72 (ddd,  $J = 12.8, 4.1, 2.6$  Hz, 1H), 0.79 (d,  $J = 6.8$  Hz, 3H) ppm.  $^{13}\text{C}$  NMR (176 MHz, Chloroform- $d$ )  $\delta$  198.1, 167.4, 162.9, 156.5, 145.2, 144.9, 134.0, 125.6, 107.1, 105.1, 99.7, 96.2, 91.7, 87.7, 73.8, 56.0, 55.8, 55.2, 39.4, 32.9, 30.5, 28.6, 27.9, 25.9, 13.7 ppm. HRMS-ESI ( $m/z$ ):  $[\text{M} + \text{H}]^+$  calculated for  $\text{C}_{25}\text{H}_{25}\text{O}_7\text{Cl}$   $[\text{M} + \text{H}]^+$ : 473.1289 and 475.1259, found 473.1288 and 475.1257.

## Experimental

### 5.2.4. DEAROMATISATION

#### GENERAL PROCEDURE E: $\gamma$ -PYRONE ANNULATION

An argon flushed round-bottom flask was charged with the corresponding indole substrate (1.0 eq.). After dissolving the starting material in anhydrous  $\text{CH}_2\text{Cl}_2$  (1 M), 2-(bromomethyl)-3-((tert-butyldimethylsilyl)oxy)-4H-pyran-4-one (2.0 eq.) dissolved in TFE (0.32 M) was added. The reaction mixture was heated to 50 °C and continuously stirred for 30 min. After complete conversion indicated by TLC and LC-MS analysis, the solvent was removed *in vacuo* and directly applied to the next step.

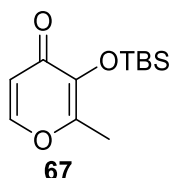
#### GENERAL PROCEDURE F: ACETYLATION

The crude indolenine (1.0 eq.) was dissolved in anhydrous  $\text{CH}_2\text{Cl}_2$  (2 ml) under argon atmosphere. After catalytic amounts of DMAP (0.1 eq.) and  $\text{Et}_3\text{N}$  (3.0 eq.) were added, the mixture was stirred (5 min at 0 °C).  $(\text{Ac})_2\text{O}$  (2.4 eq.) was added and the dark reaction mixture was stirred for at 22 °C. After complete conversion, the reaction was quenched with  $\text{NaHCO}_3$  (5 ml) and the aqueous layer was extracted with EtOAc (3 x 5 ml). The combined organic layers were dried over  $\text{NaSO}_4$  and the solvent was removed *in vacuo*. The crude product was purified either by flash column chromatography (CH/EtOAc 100% v/v) or gel perfusion chromatography to isolate the desired compound.

#### GENERAL PROCEDURE G: REDUCTION TO INDOLINES

The acetylated spiro-indolenine was dissolved in anhydrous methanol (0.5 mL) under argon atmosphere. After the addition of  $\text{NaBH}_3\text{CN}$  (1.5 eq.), the reaction was stirred for 15 min at 22 °C. The reaction mixture was quenched with brine (3 mL) and the aqueous layer was extracted with EtOAc (3 x 5ml). The combined organic layers were dried over  $\text{NaSO}_4$  and the solvent was removed *in vacuo*. The crude product was purified by flash column chromatography (CH/EtOAc 40-80% v/v) to afford the desired compound. The yield was determined over three steps.

3-((tert-butyldimethylsilyl)oxy)-2-methyl-4H-pyran-4-one **67**

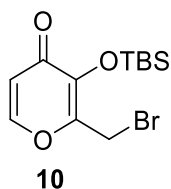


Maltol (5.08 g, 40.28 mmol, 1.0 eq.) was dissolved in DMF (80 mL) in an oven-dried 500 ml round-bottom flask under an argon atmosphere. TBSCl (7.10 g, 47.13 mmol, 1.17 eq.) was added and the resulting mixture was stirred for 5 min. After the addition of imidazole (5.48 g, 80.56 mmol, 206



2.0 eq), the solution was stirred for another 2.5 h at 22 °C. After completion, the reaction was quenched by the addition of sodium hydrogen carbonate (NaHCO<sub>3</sub>, 120 ml). The aqueous phase was extracted with cyclohexane (3 x 50 ml) and the combined organic phases were subsequently dried over sodium sulfate (NaSO<sub>4</sub>). The resulting suspension was filtrated and the remaining solvent was evaporated to dryness to give the desired compound **67** as white crystals (9.54 g, 99%). **<sup>1</sup>H NMR** (400 MHz, Chloroform-*d*) δ 7.57 (dt, *J* = 5.6, 1.5 Hz, 1H), 6.29 (ddd, *J* = 5.6, 2.2, 1.3 Hz, 1H), 2.31 (s, 3H), 0.96 (s, 9H), 0.26 (s, 6H). **<sup>13</sup>C NMR** (100 MHz, Chloroform-*d*) δ 174.2, 154.7, 151.9, 142.0, 115.3, 25.9, 18.7, 14.7, 3.8 ppm. **HRMS-ESI** (*m/z*) calculated for C<sub>12</sub>H<sub>21</sub>O<sub>3</sub>Si [M+H]<sup>+</sup>: 241.1254, found 241.1252.

2-(bromomethyl)-3-((*tert*-butyldimethylsilyl)oxy)-4*H*-pyran-4-one **10**

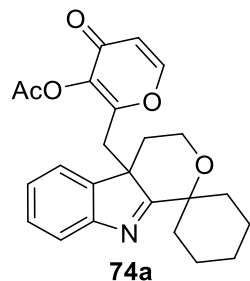


The reactive maltol species was prepared freshly before every annulation experiment. To an oven dried high pressure flask 3-((*tert*-butyldimethylsilyl)oxy)-2-methyl-4*H*-pyran-4-one (150 mg, 0.62 mmol, 1.0 eq.) was added under an argon atmosphere. After the subsequent addition of DMC (3 ml), NBS (116.62 mg, 0.66 mmol, 1.05 eq.) and AIBN (13.32 mg, 0.08 mmol, 0.13 eq.), the resulting suspension was submitted to a microwave irradiator (105 °C, 1 min). The reaction mixture was cooled to 22 °C and quenched with NaHCO<sub>3</sub> (5 ml). The aqueous layer was extracted with cyclohexane (3 x 3 ml) and the combined organic phases were dried over NaSO<sub>4</sub>. The solvent was removed *in vacuo* and the crude product **10** was stored under reduced pressure. **<sup>1</sup>H NMR** (400 MHz, Chloroform-*d*) δ 7.66 (d, *J* = 5.6 Hz, 1H), 6.33 (d, *J* = 5.6 Hz, 1H), 4.43 (s, 2H), 0.99 (s, 9H), 0.31 (s, 6H) ppm. **<sup>13</sup>C NMR** (176 MHz, Chloroform-*d*) δ ppm: 174.5, 153.5, 151.2, 143.5, 115.9, 25.8, 23.2, 18.9, -3.4 ppm. **HRMS-ESI** (*m/z*): [M + H]<sup>+</sup> calculated for C<sub>12</sub>H<sub>20</sub>BrO<sub>3</sub>Si [M+H]<sup>+</sup>: 319.0360, found 319.0365.

## Experimental

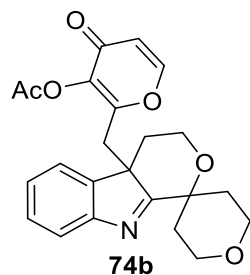
### INDOLENINE

(S)-2-((3',4'-dihydro-4a'H-spiro[cyclohexane-1,1'-pyrano[3,4-b]indol]-4a'-yl)methyl)-4-oxo-4H-pyran-3-yl acetate **74a**



White amorph solid (78%). **<sup>1</sup>H NMR** (700 MHz, Chloroform-*d*)  $\delta$  7.56 (d,  $J = 7.7$  Hz, 1H), 7.37 (d,  $J = 5.6$  Hz, 1H), 7.30 (t,  $J = 7.3$  Hz, 1H), 7.14 (q,  $J = 7.3$  Hz, 2H), 6.22 (d,  $J = 5.6$  Hz, 1H), 4.09 (dt,  $J = 11.9, 8.0$  Hz, 1H), 3.80 (ddd,  $J = 11.7, 8.1, 3.2$  Hz, 1H), 3.52 (d,  $J = 15.1$  Hz, 1H), 3.38 (d,  $J = 15.0$  Hz, 1H), 2.57 (ddd,  $J = 13.2, 7.3, 3.2$  Hz, 1H), 2.32 (s, 3H), 2.18 (d,  $J = 13.4$  Hz, 1H), 2.05 – 1.95 (m, 2H), 1.88 (td,  $J = 13.2, 3.7$  Hz, 1H), 1.79 – 1.68 (m, 2H), 1.68 – 1.53 (m, 4H), 1.43 – 1.35 (m, 1H) ppm. **<sup>13</sup>C NMR** (176 MHz, Chloroform-*d*)  $\delta$  189.8, 171.5, 167.3, 158.1, 153.8, 141.3, 139.3, 128.7, 125.8, 122.3, 120.9, 116.9, 78.0, 56.3, 55.2, 34.7, 34.0, 33.3, 33.2, 25.4, 25.3, 21.4, 21.2, 20.5 ppm. **HRMS-ESI** ( $m/z$ ):  $[M + H]^+$  calculated for  $C_{24}H_{26}NO_5$   $[M+H]^+ = 408.1806$ , found 408.1802.

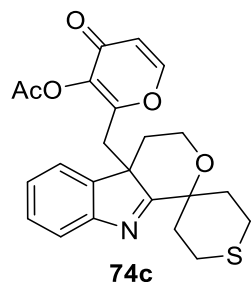
(S)-2-((2,3,3',4',5,6-hexahydro-4a'H-spiro[pyran-4,1'-pyrano[3,4-b]indol]-4a'-yl)methyl)-4-oxo-4H-pyran-3-yl acetate **74b**



Yellow solid (79%). **<sup>1</sup>H NMR** (700 MHz, Chloroform-*d*)  $\delta$  7.58 (s, 1H), 7.36 (s, 1H), 7.32 (s, 1H), 7.17 (d,  $J = 16.8$  Hz, 2H), 6.23 (s, 1H), 4.11 (q,  $J = 7.3$  Hz, 1H), 3.94 (dt,  $J = 11.3, 3.7$  Hz, 1H), 3.89 (td,  $J = 11.1, 3.1$  Hz, 1H), 3.83 (m, 3H), 3.47 (s, 1H), 3.38 (s, 1H), 2.58 (dd,  $J = 13.8, 2.5$  Hz, 1H), 2.47 (m, 1H), 2.32 (s, 3H), 2.17 (m, 2H), 1.86 (m, 1H), 1.63 (m, 1H) ppm. **<sup>13</sup>C NMR** (176 MHz, Chloroform-*d*)  $\delta$  186.7, 171.4, 167.3, 157.6, 154.1, 153.8, 141.4, 139.3, 128.9, 126.2, 122.1,

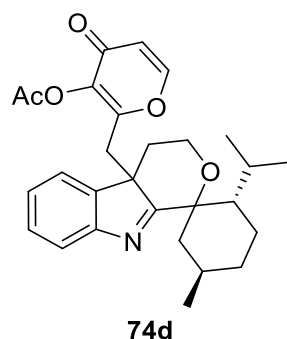
121.2, 116.9, 75.4, 63.6, 62.8, 56.8, 55.0, 35.8, 34.3, 33.7, 33.3, 21.2, 20.5 ppm. **HRMS-ESI** ( $m/z$ ):  $[M + H]^+$  calculated for  $C_{23}H_{24}NO_6$   $[M+H]^+ = 410.1598$ , found 410.1596.

(*S*)-2-((2',3,3',4,5',6'-hexahydro-4a*H*-spiro[pyrano[3,4-*b*]indole-1,4'-thiopyran]-4a-yl)methyl)-4-oxo-4H-pyran-3-yl acetate **74c**



White amorph solid (26%).  **$^1H$  NMR** (700 MHz, Chloroform-*d*)  $\delta$  7.60 (d,  $J = 7.7$  Hz, 1H), 7.37 (d,  $J = 5.7$  Hz, 1H), 7.33 (t,  $J = 7.6$  Hz, 1H), 7.17 (m, 2H), 6.23 (d,  $J = 5.7$  Hz, 1H), 4.11 (t,  $J = 7.0$  Hz, 1H), 3.83 (ddd,  $J = 11.7, 8.1, 3.3$  Hz, 1H), 3.51 (d,  $J = 15.1$  Hz, 1H), 3.39 (d,  $J = 15.1$  Hz, 1H), 3.17 (t,  $J = 11.7$  Hz, 1H), 3.03 (t,  $J = 12.2$  Hz, 1H), 2.58 (m, 2H), 2.47 (m, 3H), 2.33 (s, 3H), 2.24 (m, 2H), 1.57 (dt,  $J = 14.1, 8.4$  Hz, 1H) ppm.  **$^{13}C$  NMR** (176 MHz, Chloroform-*d*)  $\delta$  187.9, 171.3, 167.2, 157.6, 153.6, 140.9, 139.2, 128.8, 126.0, 122.1, 121.0, 116.8, 76.3, 56.2, 54.9, 35.3, 34.0, 34.0, 33.0, 26.9, 23.3, 23.0, 20.4 ppm. **HRMS-ESI** ( $m/z$ ):  $[M + H]^+$  calculated for  $C_{23}H_{24}NO_5S$   $[M+H]^+ = 426.1370$ , found 426.1368.

2-(((2*S*,4a'*S*,5*R*)-2-isopropyl-5-methyl-3',4'-dihydro-4a'*H*-spiro[cyclohexane-1,1'-pyrano[3,4-*b*]indol]-4a'-yl)methyl)-4-oxo-4H-pyran-3-yl acetate **74d**

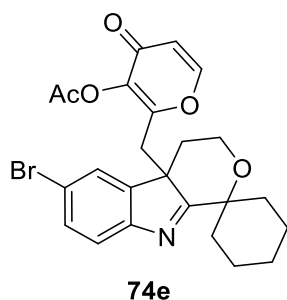


White pale solid (36%).  **$^1H$  NMR** (700 MHz, Chloroform-*d*)  $\delta$  7.59 (d,  $J = 7.7$  Hz, 1H), 7.42 (d,  $J = 5.7$  Hz, 1H), 7.32 (t,  $J = 7.6$  Hz, 1H), 7.15 (t,  $J = 7.4$  Hz, 1H), 7.05 (d,  $J = 7.4$  Hz, 1H), 6.26 – 6.23 (m, 1H), 4.16 (td,  $J = 12.1, 2.1$  Hz, 1H), 3.94 (dd,  $J = 12.0, 4.7$  Hz, 1H), 3.46 (d,  $J = 14.8$  Hz, 1H), 3.07 (d,  $J = 14.7$  Hz, 1H), 2.44 (d,  $J = 13.7$  Hz, 1H), 2.41 – 2.36 (m, 1H), 2.25 (s, 3H), 2.15 – 2.10 (m, 1H), 1.87 – 1.78 (m, 2H), 1.80 – 1.74 (m, 1H), 1.72 (td,  $J = 13.1, 5.2$  Hz, 1H), 1.59 (td,  $J =$

## Experimental

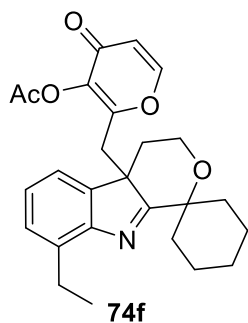
10.2, 8.5, 3.1 Hz, 2H), 1.25 – 1.19 (m, 1H), 1.03 (dtd,  $J = 15.8, 7.4, 6.7, 4.4$  Hz, 1H), 0.93 (t,  $J = 6.8$  Hz, 6H), 0.77 (d,  $J = 6.9$  Hz, 3H) ppm.  $^{13}\text{C}$  NMR (176 MHz, Chloroform-*d*)  $\delta$  185.6, 171.3, 167.1, 157.6, 153.7, 141.1, 139.5, 128.8, 125.7, 121.8, 120.9, 116.8, 82.8, 57.2, 54.8, 47.8, 41.8, 35.4, 34.6, 33.9, 27.8, 27.6, 26.9, 23.7, 22.4, 21.3, 20.3, 18.7. HRMS-ESI ( $m/z$ ):  $[\text{M} + \text{H}]^+$  calculated for  $\text{C}_{28}\text{H}_{34}\text{NO}_5$   $[\text{M} + \text{H}]^+ = 464.2432$ , found 464.2431 (-0.9372 ppm).

(*S*)-2-((6'-bromo-3',4'-dihydro-4a'H-spiro[cyclohexane-1,1'-pyrano[3,4-b]indol]-4a'-yl)methyl)-4-oxo-4H-pyran-3-yl acetate **74e**



Yellow solid (56 %).  $^1\text{H}$  NMR (700 MHz, Chloroform-*d*)  $\delta$  7.45 (d,  $J = 1.5$  Hz, 2H), 7.41 (d,  $J = 5.7$  Hz, 1H), 7.29 (s, 1H), 6.27 (d,  $J = 5.7$  Hz, 1H), 4.09 (dt,  $J = 12.3, 7.7$  Hz, 1H), 3.81 (ddd,  $J = 11.9, 8.2, 3.5$  Hz, 1H), 3.50 (d,  $J = 15.0$  Hz, 1H), 3.37 (d,  $J = 15.0$  Hz, 1H), 2.55 (ddd,  $J = 13.8, 7.4, 3.4$  Hz, 1H), 2.36 (s, 3H), 2.18 (d,  $J = 12.9$  Hz, 1H), 2.01 (td,  $J = 13.3, 12.5, 4.0$  Hz, 1H), 1.96 (d,  $J = 12.0$  Hz, 1H), 1.87 (td,  $J = 13.1, 4.0$  Hz, 1H), 1.79 – 1.73 (m, 2H), 1.70 – 1.66 (m, 1H), 1.66 – 1.62 (m, 1H), 1.62 – 1.54 (m, 2H), 1.40 (ddd,  $J = 16.1, 8.1, 3.8$  Hz, 1H) ppm.  $^{13}\text{C}$  NMR (176 MHz, Chloroform-*d*)  $\delta$  190.4, 171.3, 167.1, 157.1, 153.6, 143.3, 139.4, 131.8, 125.9, 121.9, 119.5, 116.9, 77.9, 56.0, 55.6, 34.3, 33.5, 33.3, 33.2, 25.2, 21.2, 21.0, 20.4 ppm. HRMS-ESI ( $m/z$ ):  $[\text{M} + \text{H}]^+$  calculated for  $\text{C}_{24}\text{H}_{25}\text{BrNO}_5$   $[\text{M} + \text{H}]^+ = 486.0911$ , found 486.0910.

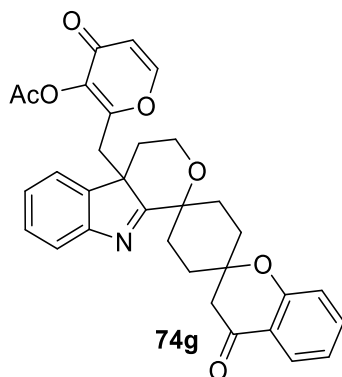
(*S*)-2-((8'-ethyl-3',4'-dihydro-4a'H-spiro[cyclohexane-1,1'-pyrano[3,4-b]indol]-4a'-yl)methyl)-4-oxo-4H-pyran-3-yl acetate **74f**



Yellow solid (55%).  $^1\text{H}$  NMR (700 MHz, Chloroform-*d*)  $\delta$  7.37 (d,  $J = 5.7$  Hz, 1H), 7.12 (d,  $J = 7.5$  Hz, 1H), 7.06 (t,  $J = 7.5$  Hz, 1H), 6.93 (d,  $J = 7.3$  Hz, 1H), 6.23 (d,  $J = 5.7$  Hz, 1H), 4.08 (dt,  $J =$

12.2, 7.8 Hz, 1H), 3.79 (ddd,  $J = 11.7, 8.0, 3.5$  Hz, 1H), 3.49 (d,  $J = 15.0$  Hz, 1H), 3.32 (d,  $J = 14.8$  Hz, 1H), 2.95 (ddt,  $J = 34.4, 14.1, 7.3$  Hz, 2H), 2.53 (ddd,  $J = 13.7, 7.2, 3.6$  Hz, 1H), 2.32 (s, 3H), 2.15 (d,  $J = 13.7$  Hz, 1H), 2.11 – 2.06 (m, 1H), 1.92 (t,  $J = 12.4$  Hz, 2H), 1.79 – 1.73 (m, 2H), 1.65 – 1.60 (m, 2H), 1.56 (dt,  $J = 13.8, 8.3$  Hz, 1H), 1.43 (qd,  $J = 12.0, 3.7$  Hz, 1H), 1.25 (t,  $J = 7.6$  Hz, 3H) ppm.  $^{13}\text{C NMR}$  (176 MHz, Chloroform-*d*)  $\delta$  187.5, 171.5, 167.2, 158.2, 153.6, 141.3, 139.2, 136.8, 128.1, 125.6, 119.5, 116.7, 78.0, 56.2, 54.9, 34.4, 34.1, 33.4, 33.3, 25.3, 25.1, 24.3, 21.4, 21.2, 20.4, 15.4 ppm. **HRMS-ESI** ( $m/z$ ):  $[\text{M} + \text{H}]^+$  calculated for  $\text{C}_{25}\text{H}_{28}\text{NO}_6$   $[\text{M} + \text{H}]^+ = 438.1912$ , found 436.2115.

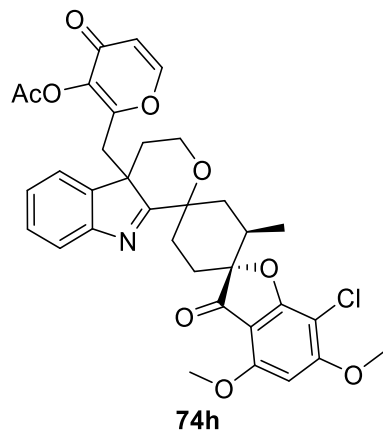
(*S*)-4-oxo-2-((4-oxo-3",4"-dihydro-4a"H-dispiro[chromane-2,1'-cyclohexane-4',1"-pyrano[3,4-b]indol]-4a"-yl)methyl)-4H-pyran-3-yl acetate **74g**



White pale solid (68%).  $^1\text{H NMR}$  (400 MHz, Chloroform-*d*)  $\delta$  7.87 (dd,  $J = 7.8, 1.7$  Hz, 1H), 7.62 (d,  $J = 7.8$  Hz, 1H), 7.50 (ddd,  $J = 8.8, 7.2, 1.8$  Hz, 1H), 7.38 (d,  $J = 5.7$  Hz, 1H), 7.33 (td,  $J = 7.8, 7.4, 1.8$  Hz, 1H), 7.16 (m, 3H), 7.00 (m, 1H), 6.22 (d,  $J = 5.7$  Hz, 1H), 4.10 (ddd,  $J = 12.2, 8.7, 7.2$  Hz, 1H), 3.78 (ddd,  $J = 11.8, 7.9, 3.6$  Hz, 1H), 3.51 (d,  $J = 15.0$  Hz, 1H), 3.41 (d,  $J = 15.0$  Hz, 1H), 2.75 (s, 2H), 2.59 (m, 2H), 2.32 (m, 4H), 2.13 (m, 3H), 1.94 (m, 2H), 1.77 (td,  $J = 14.0, 4.1$  Hz, 1H), 1.60 (dt,  $J = 13.9, 8.2$  Hz, 1H) ppm.  $^{13}\text{C NMR}$  (101 MHz, Chloroform-*d*)  $\delta$  192.3, 188.6, 171.4, 167.3, 159.5, 157.7, 153.8, 141.2, 139.3, 136.4, 128.9, 126.6, 126.2, 122.3, 121.1, 121.0, 120.8, 118.8, 116.9, 78.5, 56.7, 55.2, 48.9, 34.5, 33.3, 29.4, 29.4, 29.4, 28.2, 20.5 ppm. **HRMS-ESI** ( $m/z$ ):  $[\text{M} + \text{H}]^+$  calculated for  $\text{C}_{32}\text{H}_{30}\text{NO}_7$   $[\text{M} + \text{H}]^+ = 540.2017$ , found 540.2011.

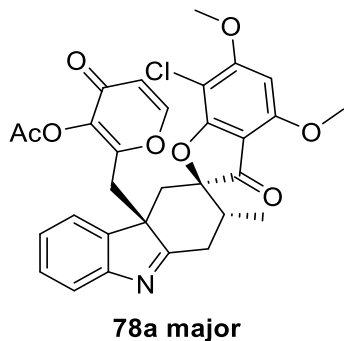
## Experimental

2-(((2*R*,2'*R*,4*a*'*S*)-7-chloro-4,6-dimethoxy-2'-methyl-3-oxo-3'',4''-dihydro-3*H*,4*a*''*H*-dispiro [benzofuran-2,1'-cyclohexane-4',1''-pyrano[3,4-*b*]indol]-4*a*''-yl)methyl)-4-oxo-4*H*-pyran-3-yl acetate **74h**



White amorph solid (69%); **dr** = 0.85:0.15 (major/minor diastereomer). **<sup>1</sup>H NMR** (700 MHz, Chloroform-*d*)  $\delta$  7.61 (d, *J* = 7.7 Hz, 1H), 7.42 (d, *J* = 5.7 Hz, 1H), 7.31 (t, *J* = 7.4 Hz, 1H), 7.16 (m, 2H), 6.21 (d, *J* = 5.7 Hz, 1H), 6.09 (s, 1H), 4.09 (m, 1H), 4.00 (s, 3H), 3.97 (s, 3H), 3.81 (ddd, *J* = 11.2, 7.1, 3.2 Hz, 1H), 3.50 (d, *J* = 15.2 Hz, 1H), 3.44 (d, *J* = 15.2 Hz, 1H), 3.00 (td, *J* = 14.5, 4.0 Hz, 1H), 2.71 (m, 1H), 2.58 (m, 2H), 2.33 (s, 4H), 2.25 (m, 1H), 2.07 (m, 1H), 1.83 (m, 1H), 1.64 (dt, *J* = 13.9, 8.3 Hz, 1H), 0.86 (d, *J* = 6.8 Hz, 3H) ppm. **<sup>13</sup>C NMR** (176 MHz, Chloroform-*d*)  $\delta$  198.2, 186.7, 171.5, 168.3, 167.4, 164.0, 157.8, 154.2, 154.0, 141.5, 139.2, 128.8, 126.0, 122.0, 121.4, 116.9, 106.0, 97.2, 92.0, 89.1, 77.5, 57.0, 56.8, 56.5, 55.0, 36.1, 33.4, 33.0, 28.7, 28.1, 20.5, 14.9 ppm. **HRMS-ESI** (*m/z*): [M + H]<sup>+</sup> calculated for C<sub>34</sub>H<sub>33</sub>ClNO<sub>9</sub> [M+H]<sup>+</sup> = 634.1766, found 634.1838.

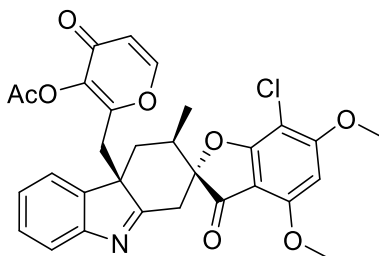
2-(((2*R*,2'*R*,4*a*'*S*)-7-chloro-4,6-dimethoxy-2'-methyl-3-oxo-1',2'-dihydro-3*H*-spiro[benzofuran-2,3'-carbazol]-4*a*'(4'*H*)-yl)methyl)-4-oxo-4*H*-pyran-3-yl acetate **78a major**



White crystalline solid (99%). **<sup>1</sup>H NMR** (500 MHz, Chloroform-*d*)  $\delta$  7.56 (d, *J* = 7.8 Hz, 1H), 7.33 (m, 1H), 7.27 (s, 1H), 7.24 (d, *J* = 6.9 Hz, 1H), 7.19 (t, *J* = 7.4 Hz, 1H), 6.15 (s, 1H), 6.15 (d, *J* =

5.5 Hz, 1H), 4.04 (s, 3H), 4.03 (d,  $J = 8.4$  Hz, 1H), 3.98 (s, 3H), 3.65 (dd,  $J = 12.9, 5.4$  Hz, 1H), 3.28 (d,  $J = 14.6$  Hz, 1H), 2.86 (d,  $J = 12.7$  Hz, 1H), 2.48 (m, 1H), 2.39 (m, 1H), 2.29 (s, 3H), 2.08 (d,  $J = 15.1$  Hz, 1H), 1.00 (d,  $J = 7.2$  Hz, 3H) ppm.  $^{13}\text{C}$  NMR (126 MHz, Chloroform-*d*)  $\delta$  195.4, 183.5, 171.5, 167.1, 166.9, 164.5, 158.2, 157.4, 154.0, 153.5, 141.8, 139.3, 129.0, 125.9, 122.4, 120.7, 116.6, 104.6, 97.8, 91.8, 89.6, 57.2, 56.6, 56.1, 40.6, 39.4, 34.5, 34.0, 20.6, 13.5 ppm. HRMS-ESI ( $m/z$ ):  $[\text{M} + \text{H}]^+$  calculated for  $\text{C}_{30}\text{H}_{27}\text{ClNO}_8$   $[\text{M} + \text{H}]^+ = 564.1420$ , found 564.1416.

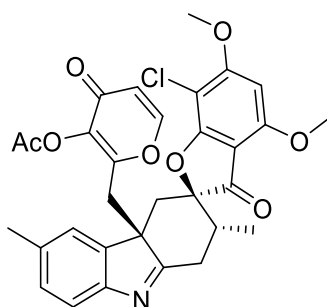
2-(((2*R*,3'*R*,4*a'**R*)-7-chloro-4,6-dimethoxy-3'-methyl-3-oxo-3',4'-dihydro-3H-spiro[benzofuran-2,2'-carbazol]-4*a'*(1*H*)-yl)methyl)-4-oxo-4H-pyran-3-yl acetate **78b minor**



**78b minor**

White crystalline solid (92%).  $^1\text{H}$  NMR (700 MHz, Chloroform-*d*)  $\delta$  7.50 (d,  $J = 7.6$  Hz, 1H), 7.28 (m, 1H), 7.22 (d,  $J = 5.7$  Hz, 1H), 7.15 (m, 2H), 6.15 (s, 1H), 6.10 (d,  $J = 5.7$  Hz, 1H), 4.28 (d,  $J = 14.8$  Hz, 1H), 4.03 (s, 3H), 3.98 (s, 3H), 3.37 (d,  $J = 15.0$  Hz, 1H), 3.35 (m, 1H), 3.11 (dd,  $J = 13.7, 4.4$  Hz, 1H), 2.70 (m, 1H), 2.37 (m, 1H), 2.29 (s, 3H), 2.12 (m, 1H), 0.53 (d,  $J = 7.3$  Hz, 3H) ppm.  $^{13}\text{C}$  NMR (176 MHz, Chloroform-*d*)  $\delta$  195.6, 183.5, 171.4, 166.9, 166.5, 164.4, 158.2, 157.9, 154.2, 153.7, 140.4, 138.9, 128.6, 125.7, 123.0, 120.6, 116.4, 104.5, 97.7, 92.3, 89.5, 61.4, 57.0, 56.4, 46.1, 34.4, 31.4, 25.6, 20.4, 9.7 ppm. HRMS-ESI ( $m/z$ ):  $[\text{M} + \text{H}]^+$  calculated for  $\text{C}_{30}\text{H}_{27}\text{ClNO}_8$   $[\text{M} + \text{H}]^+ = 564.1420$ , found 564.1417.

2-(((2*R*,2'*R*,4*a'**S*)-7-chloro-4,6-dimethoxy-2',6'-dimethyl-3-oxo-1',2'-dihydro-3H-spiro[benzofuran-2,3'-carbazol]-4*a'*(4'*H*)-yl)methyl)-4-oxo-4H-pyran-3-yl acetate **78c**



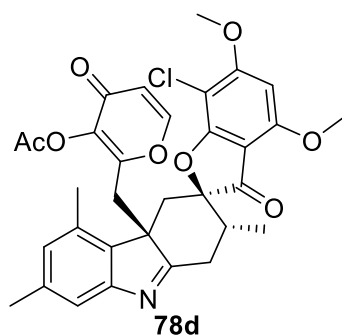
**78c**

Yellow pale solid (78%).  $^1\text{H}$  NMR (500 MHz, Chloroform-*d*)  $\delta$  7.44 (d,  $J = 7.8$  Hz, 1H), 7.31 (d,  $J = 5.8$  Hz, 1H), 7.13 (d,  $J = 7.9$  Hz, 1H), 7.02 (s, 1H), 6.16 (d,  $J = 5.8$  Hz, 1H), 6.15 (s, 1H), 4.04

## Experimental

(s, 3H), 3.98 (s, 3H), 3.98 (d,  $J = 14.5$  Hz, 1H), 3.63 (dd,  $J = 13.0, 5.3$  Hz, 1H), 3.28 (d,  $J = 14.6$  Hz, 1H), 2.86 (d,  $J = 12.5$  Hz, 1H), 2.47 (m, 1H), 2.36 (s, 3H), 2.36 (m, 1H), 2.28 (s, 3H), 2.08 (d,  $J = 15.3$  Hz, 1H), 0.99 (d,  $J = 7.2$  Hz, 3H) ppm.  $^{13}\text{C NMR}$  (126 MHz, Chloroform-*d*)  $\delta$  195.3, 180.9, 171.4, 166.8, 166.8, 164.3, 158.1, 157.3, 153.9, 150.9, 141.7, 139.2, 135.7, 129.5, 123.1, 119.9, 116.5, 104.4, 97.7, 91.7, 89.5, 57.0, 56.4, 55.7, 40.5, 39.2, 34.4, 33.7, 21.5, 20.4, 13.3 ppm. **HRMS-ESI** ( $m/z$ ):  $[\text{M} + \text{H}]^+$  calculated for  $\text{C}_{31}\text{H}_{29}\text{ClNO}_8$   $[\text{M} + \text{H}]^+ = 578.1576$  found 578.1574.

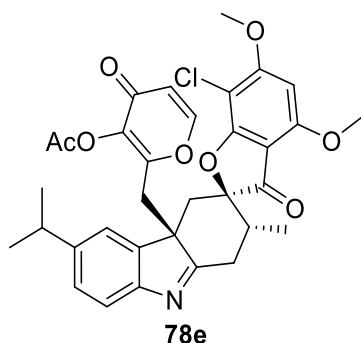
2-(((2*R*,2'*R*,4*a*'*S*)-7-chloro-4,6-dimethoxy-2',5',7'-trimethyl-3-oxo-1',2'-dihydro-3*H*-spiro [benzofuran-2,3'-carbazol]-4*a*'(4'*H*)-yl)methyl)-4-oxo-4*H*-pyran-3-yl acetate **78d**



Orange amorph solid (95%).  $^1\text{H NMR}$  (500 MHz, Chloroform-*d*)  $\delta$  7.26 (d,  $J = 3.4$  Hz, 1H), 7.14 (s, 1H), 6.75 (s, 1H), 6.15 (s, 1H), 6.13 (d,  $J = 5.8$  Hz, 1H), 4.09 (d,  $J = 14.8$  Hz, 1H), 4.03 (s, 3H), 3.98 (s, 3H), 3.62 (dd,  $J = 13.0, 5.3$  Hz, 1H), 3.36 (d,  $J = 14.6$  Hz, 1H), 2.79 (d,  $J = 11.7$  Hz, 1H), 2.50 (dd,  $J = 15.2, 1.6$  Hz, 1H), 2.44 (m, 1H), 2.33 (s, 3H), 2.32 (s, 3H), 2.32 (s, 3H), 2.19 (d,  $J = 15.1$  Hz, 1H), 0.97 (d,  $J = 7.3$  Hz, 3H) ppm.  $^{13}\text{C NMR}$  (126 MHz, Chloroform-*d*)  $\delta$  195.6, 182.7, 171.4, 167.0, 166.8, 164.4, 158.1, 157.4, 154.3, 153.9, 139.2, 138.8, 136.3, 132.9, 128.5, 118.9, 116.4, 104.5, 97.7, 91.8, 89.4, 57.1, 56.4, 56.3, 39.9, 38.3, 33.7, 33.0, 21.4, 20.5, 18.1, 13.3 ppm. **HRMS-ESI** ( $m/z$ ):  $[\text{M} + \text{H}]^+$  calculated for  $\text{C}_{32}\text{H}_{31}\text{ClNO}_8$   $[\text{M} + \text{H}]^+ = 592.1733$  found 592.1731.

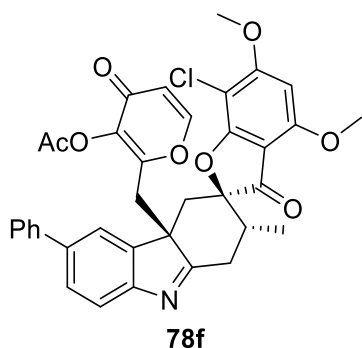


2-(((2*R*,2'*R*,4*a*'*S*)-7-chloro-6'-isopropyl-4,6-dimethoxy-2'-methyl-3-oxo-1',2'-dihydro-3*H*-spiro [benzofuran-2,3'-carbazol]-4*a*'(4'*H*)-yl)methyl)-4-oxo-4*H*-pyran-3-yl acetate **78e**



Yellow pale solid (77%). **<sup>1</sup>H NMR** (700 MHz, Chloroform-*d*)  $\delta$  7.44 (d,  $J$  = 8.0 Hz, 1H), 7.25 (d,  $J$  = 5.7 Hz, 1H), 7.16 (dd,  $J$  = 8.1, 1.6 Hz, 1H), 7.09 (d,  $J$  = 1.5 Hz, 1H), 6.15 (s, 1H), 6.13 (d,  $J$  = 5.7 Hz, 1H), 4.04 (s, 3H), 3.98 (s, 3H), 3.91 (d,  $J$  = 14.5 Hz, 1H), 3.62 (dd,  $J$  = 13.0, 5.4 Hz, 1H), 3.29 (d,  $J$  = 14.6 Hz, 1H), 2.90 (hept,  $J$  = 6.8 Hz, 1H), 2.82 (d,  $J$  = 12.9 Hz, 1H), 2.45 (m, 1H), 2.37 (dd,  $J$  = 15.2, 1.9 Hz, 1H), 2.28 (s, 3H), 2.08 (d,  $J$  = 15.2 Hz, 1H), 1.21 (dd,  $J$  = 9.4, 6.9 Hz, 6H), 0.99 (d,  $J$  = 7.3 Hz, 3H) ppm. **<sup>13</sup>C NMR** (176 MHz, Chloroform-*d*)  $\delta$  195.5, 182.5, 171.4, 167.2, 167.0, 164.5, 158.2, 157.7, 153.9, 151.7, 146.8, 141.9, 139.3, 127.1, 120.4, 120.2, 116.6, 104.6, 97.9, 92.0, 89.6, 57.1, 56.5, 56.0, 40.5, 39.4, 34.6, 34.3, 33.9, 24.4, 24.2, 20.5, 13.4 ppm. **HRMS-ESI** ( $m/z$ ):  $[M + H]^+$  calculated for  $C_{33}H_{33}ClNO_8$   $[M+H]^+ = 606.1889$  found 606.1886.

2-(((2*R*,2'*R*,4*a*'*S*)-7-chloro-4,6-dimethoxy-2'-methyl-3-oxo-6'-phenyl-1',2'-dihydro-3*H*-spiro [benzofuran-2,3'-carbazol]-4*a*'(4'*H*)-yl)methyl)-4-oxo-4*H*-pyran-3-yl acetate **78f**

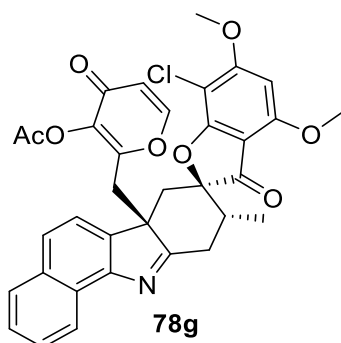


Yellow pale solid (90%). **<sup>1</sup>H NMR** (500 MHz, Chloroform-*d*)  $\delta$  7.62 (d,  $J$  = 7.9 Hz, 1H), 7.55 (ddd,  $J$  = 7.2, 5.2, 2.7 Hz, 3H), 7.44 (m, 3H), 7.35 (d,  $J$  = 7.3 Hz, 1H), 7.30 (d,  $J$  = 5.8 Hz, 1H), 6.16 (d,  $J$  = 5.6 Hz, 2H), 4.06 (d,  $J$  = 19.4 Hz, 1H), 4.05 (s, 3H), 3.99 (s, 3H), 3.69 (dd,  $J$  = 13.0, 5.3 Hz, 1H), 3.33 (d,  $J$  = 14.5 Hz, 1H), 2.90 (d,  $J$  = 12.7 Hz, 1H), 2.50 (m, 1H), 2.43 (m, 1H), 2.18 (s, 3H), 2.15 (d,  $J$  = 13.4 Hz, 1H), 1.02 (d,  $J$  = 7.3 Hz, 3H) ppm. **<sup>13</sup>C NMR** (126 MHz, Chloroform-*d*)  $\delta$

## Experimental

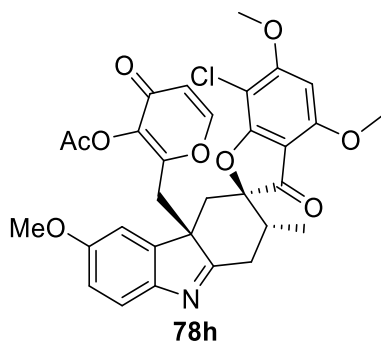
195.2, 183.7, 171.3, 166.9, 166.8, 164.4, 158.1, 157.1, 153.9, 152.5, 142.3, 140.9, 139.3, 128.8, 128.1, 127.4, 127.2, 121.4, 120.6, 116.5, 104.4, 97.7, 91.6, 89.5, 57.0, 56.4, 56.1, 40.5, 39.3, 34.6, 33.9, 20.3, 13.4 ppm. **HRMS-ESI** ( $m/z$ ):  $[M + H]^+$  calculated for  $C_{36}H_{31}ClNO_8$   $[M+H]^+ = 640.1733$ , found 640.1732.

2-(((2*R*,6*b'**S*,9'*R*)-7-chloro-4,6-dimethoxy-9'-methyl-3-oxo-9',10'-dihydro-3*H*-spiro[benzofuran-2,8'-benzo[*a*]carbazole]-6*b'*(7'*H*)-yl)methyl)-4-oxo-4*H*-pyran-3-yl acetate **78g**



White pale solid (58%). **<sup>1</sup>H NMR** (700 MHz, Chloroform-*d*)  $\delta$  8.56 (d,  $J = 8.2$  Hz, 1H), 7.87 (d,  $J = 8.2$  Hz, 1H), 7.71 (d,  $J = 8.2$  Hz, 1H), 7.58 (t,  $J = 7.5$  Hz, 1H), 7.51 (t,  $J = 7.5$  Hz, 1H), 7.37 (d,  $J = 8.3$  Hz, 1H), 7.15 (d,  $J = 5.3$  Hz, 1H), 6.16 (s, 1H), 6.05 (d,  $J = 5.7$  Hz, 1H), 4.08 (d,  $J = 14.7$  Hz, 1H), 4.05 (s, 3H), 3.98 (s, 3H), 3.74 (dd,  $J = 13.0, 5.2$  Hz, 1H), 3.39 (d,  $J = 14.7$  Hz, 1H), 3.00 (d,  $J = 10.7$  Hz, 1H), 2.53 (s, 1H), 2.48 (d,  $J = 15.3$  Hz, 1H), 2.29 (s, 3H), 2.06 (d,  $J = 15.2$  Hz, 1H), 1.01 (d,  $J = 7.2$  Hz, 3H) ppm. **<sup>13</sup>C NMR** (176 MHz, Chloroform-*d*)  $\delta$  195.4, 183.5, 171.3, 167.0, 166.9, 164.4, 158.1, 157.3, 153.7, 149.5, 139.1, 138.4, 134.1, 128.0, 127.3, 126.5, 126.2, 126.1, 123.6, 119.5, 116.5, 104.5, 97.8, 91.7, 89.5, 57.0, 56.4, 42.6, 40.8, 39.5, 34.1, 34.0, 20.4, 13.3 ppm. **HRMS-ESI** ( $m/z$ ):  $[M + H]^+$  calculated for  $C_{34}H_{29}ClNO_8$   $[M+H]^+ = 614.1576$  found 614.1578.

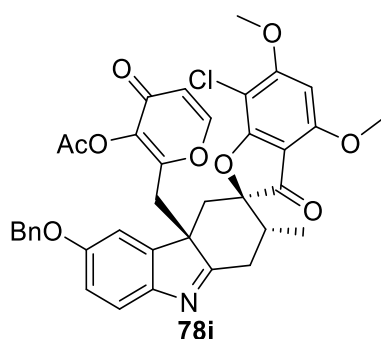
2-(((2*R*,2'*R*,4*a'**S*)-7-chloro-4,6,6'-trimethoxy-2'-methyl-3-oxo-1',2'-dihydro-3*H*-spiro [benzofuran-2,3'-carbazol]-4*a'*(4'*H*)-yl)methyl)-4-oxo-4*H*-pyran-3-yl acetate **78h**



Yellow pale solid (72%). **<sup>1</sup>H NMR** (700 MHz, Chloroform-*d*)  $\delta$  7.45 (d,  $J = 8.5$  Hz, 1H), 7.32 (d,  $J = 5.7$  Hz, 1H), 6.84 (dd,  $J = 8.5, 2.5$  Hz, 1H), 6.79 (d,  $J = 2.4$  Hz, 1H), 6.17 (d,  $J = 5.8$  Hz, 1H), 216

6.15 (s, 1H), 4.04 (s, 3H), 4.01 (m, 1H), 3.98 (s, 3H), 3.79 (s, 3H), 3.61 (dd,  $J = 13.0, 5.3$  Hz, 1H), 3.26 (d,  $J = 14.6$  Hz, 1H), 2.81 (d,  $J = 12.5$  Hz, 1H), 2.45 (m, 2H), 2.33 (d,  $J = 15.3$  Hz, 1H), 2.28 (s, 3H), 2.07 (d,  $J = 15.2$  Hz, 1H), 0.99 (d,  $J = 7.3$  Hz, 3H) ppm.  $^{13}\text{C NMR}$  (176 MHz, Chloroform- $d$ )  $\delta$  195.3, 181.0, 171.3, 166.9, 166.8, 164.3, 158.2, 158.1, 157.3, 153.9, 146.9, 143.3, 139.2, 120.8, 116.5, 113.3, 109.3, 104.4, 97.7, 91.7, 89.5, 57.0, 56.4, 56.0, 55.7, 40.4, 39.2, 34.5, 33.7, 20.4, 13.3 ppm. **HRMS**-ESI ( $m/z$ ):  $[\text{M} + \text{H}]^+$  calculated for  $\text{C}_{31}\text{H}_{29}\text{ClNO}_9$   $[\text{M} + \text{H}]^+ = 594.1525$  found 594.1527.

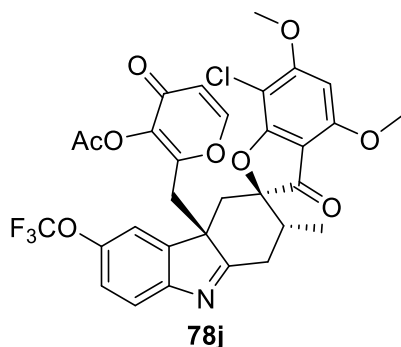
2-(((2*R*,2'*R*,4*a*'*S*)-6'-(benzyloxy)-7-chloro-4,6-dimethoxy-2'-methyl-3-oxo-1',2'-dihydro-3*H*-spiro [benzofuran-2,3'-carbazol]-4*a*'(4*H*)-yl)methyl)-4-oxo-4*H*-pyran-3-yl acetate **78i**



Yellow pale solid (yield = 90%).  $^1\text{H NMR}$  (500 MHz, Chloroform- $d$ )  $\delta$  7.47 (d,  $J = 8.4$  Hz, 1H), 7.40 (m, 4H), 7.34 (m, 1H), 7.26 (s, 1H), 6.92 (dd,  $J = 8.5, 2.4$  Hz, 1H), 6.88 (d,  $J = 2.4$  Hz, 1H), 6.17 (d,  $J = 5.7$  Hz, 1H), 6.15 (s, 1H), 5.05 (s, 2H), 4.04 (s, 3H), 4.04 (d,  $J = 14.8$  Hz, 1H), 3.98 (s, 3H), 3.63 (dd,  $J = 13.1, 5.4$  Hz, 1H), 3.24 (d,  $J = 14.7$  Hz, 1H), 2.88 (d,  $J = 12.7$  Hz, 1H), 2.47 (m, 1H), 2.33 (dd,  $J = 15.1, 2.0$  Hz, 1H), 2.29 (s, 3H), 2.10 (d,  $J = 15.2$  Hz, 1H), 1.00 (d,  $J = 7.3$  Hz, 3H) ppm.  $^{13}\text{C NMR}$  (126 MHz, Chloroform- $d$ )  $\delta$  195.4, 181.8, 171.5, 167.0 (d,  $J = 15.1$  Hz), 164.5, 158.2, 157.7, 157.2, 154.0, 143.3, 139.4, 136.8, 128.8, 128.3, 127.7, 120.8, 116.7, 114.4, 110.6, 104.5, 97.8, 91.8, 89.6, 70.7, 57.2, 56.6, 56.2, 40.7, 39.4, 34.7, 33.8, 20.6, 13.5 ppm. **HRMS**-ESI ( $m/z$ ):  $[\text{M} + \text{H}]^+$  calculated for  $\text{C}_{37}\text{H}_{33}\text{ClNO}_9$   $[\text{M} + \text{H}]^+ = 670.1838$  found 670.1839.

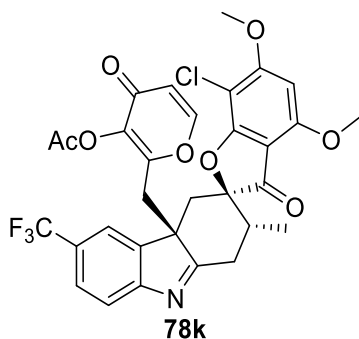
## Experimental

2-(((2*R*,2'*R*,4*a*'*S*)-7-chloro-4,6-dimethoxy-2'-methyl-3-oxo-6'-(trifluoromethoxy)-1',2'-dihydro-3*H*-spiro [benzofuran-2,3'-carbazol]-4*a*'(4*H*)-yl)methyl)-4-oxo-4*H*-pyran-3-yl acetate **78j**



Yellow pale solid (92%). **<sup>1</sup>H NMR** (500 MHz, Chloroform-*d*)  $\delta$  7.56 (d,  $J = 8.5$  Hz, 1H), 7.27 (d,  $J = 5.6$  Hz, 1H), 7.21 (d,  $J = 8.5$  Hz, 1H), 7.15 (s, 1H), 6.16 (m, 2H), 4.08 (d,  $J = 14.5$  Hz, 1H), 4.05 (s, 3H), 3.99 (s, 3H), 3.66 (dd,  $J = 13.0, 5.4$  Hz, 1H), 3.23 (d,  $J = 14.6$  Hz, 1H), 2.85 (dd,  $J = 12.9, 1.9$  Hz, 1H), 2.50 (dd,  $J = 7.2, 5.5$  Hz, 1H), 2.38 (dd,  $J = 15.2, 1.8$  Hz, 1H), 2.31 (s, 3H), 2.10 (d,  $J = 15.1$  Hz, 1H), 0.99 (d,  $J = 7.3$  Hz, 3H) ppm. **<sup>13</sup>C NMR** (126 MHz, Chloroform-*d*)  $\delta$  195.0, 184.8, 171.2, 167.0, 166.7, 164.5, 158.1, 156.5, 153.8, 151.8, 147.1, 143.3, 139.3, 122.0, 121.2, 119.4, 116.6, 115.9, 104.3, 97.7, 91.3, 89.6, 57.1, 56.7, 56.4, 40.4, 39.0, 34.5, 33.9, 20.3, 13.3 ppm. **HRMS-ESI** ( $m/z$ ):  $[M + H]^+$  calculated for  $C_{31}H_{26}ClF_3NO_9$   $[M+H]^+ = 648.1243$  found 648.1242.

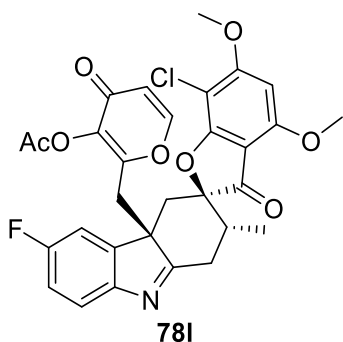
2-(((2*R*,2'*R*,4*a*'*S*)-7-chloro-4,6-dimethoxy-2'-methyl-3-oxo-6'-(trifluoromethyl)-1',2'-dihydro-3*H*-spiro[benzofuran-2,3'-carbazol]-4*a*'(4*H*)-yl)methyl)-4-oxo-4*H*-pyran-3-yl acetate **78k**



Yellow pale solid (75%). **<sup>1</sup>H NMR** (700 MHz, Chloroform-*d*)  $\delta$  7.64 (m, 2H), 7.54 (s, 1H), 7.30 (d,  $J = 5.7$  Hz, 1H), 6.16 (m, 2H), 4.10 (d,  $J = 14.5$  Hz, 1H), 4.05 (s, 3H), 3.99 (s, 3H), 3.71 (dd,  $J = 13.0, 5.4$  Hz, 1H), 3.29 (d,  $J = 14.6$  Hz, 1H), 2.89 (dd,  $J = 13.0, 2.1$  Hz, 1H), 2.51 (dd,  $J = 7.3, 5.4$  Hz, 1H), 2.43 (dd,  $J = 15.2, 1.9$  Hz, 1H), 2.28 (s, 3H), 2.10 (d,  $J = 15.2$  Hz, 1H), 0.98 (d,  $J = 7.3$  Hz, 3H) ppm. **<sup>13</sup>C NMR** (176 MHz, Chloroform-*d*)  $\delta$  194.8, 186.7, 171.1, 166.9, 166.7, 164.5, 158.1, 156.3, 156.1, 153.8, 142.3, 139.4, 126.6, 125.0, 123.4, 120.7, 119.6, 116.6, 104.3, 97.7, 218

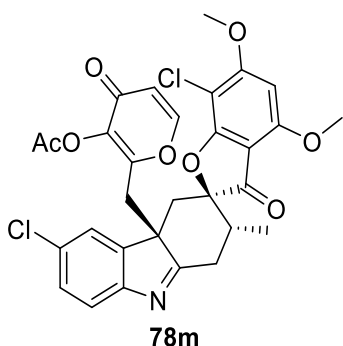
91.2, 89.6, 57.0, 56.6, 56.4, 40.5, 39.0, 34.6, 34.1, 20.2, 13.3 ppm. **HRMS-ESI** ( $m/z$ ):  $[M + H]^+$  calculated for  $C_{31}H_{26}ClF_3NO_8$   $[M+H]^+ = 632.1294$  found 632.1295.

2-(((2*R*,2'*R*,4*a*'*S*)-7-chloro-6'-fluoro-4,6-dimethoxy-2'-methyl-3-oxo-1',2'-dihydro-3H-spiro [benzofuran-2,3'-carbazol]-4*a*'(4'*H*)-yl)methyl)-4-oxo-4H-pyran-3-yl acetate **78l**



Yellow pale solid (94%). **<sup>1</sup>H NMR** (500 MHz, Chloroform-*d*)  $\delta$  7.50 (dd,  $J = 8.5, 4.5$  Hz, 1H), 7.32 (d,  $J = 5.8$  Hz, 1H), 7.04 (td,  $J = 8.8, 2.4$  Hz, 1H), 6.97 (dd,  $J = 7.7, 2.5$  Hz, 1H), 6.18 (d,  $J = 5.8$  Hz, 1H), 6.16 (s, 1H), 4.07 (d,  $J = 14.6$  Hz, 1H), 4.04 (s, 3H), 3.99 (s, 3H), 3.65 (dd,  $J = 13.0, 5.3$  Hz, 1H), 3.23 (d,  $J = 14.6$  Hz, 1H), 2.84 (d,  $J = 11.9$  Hz, 1H), 2.48 (m, 1H), 2.36 (dd,  $J = 15.1, 1.8$  Hz, 1H), 2.31 (s, 3H), 2.08 (d,  $J = 15.1$  Hz, 1H), 0.99 (d,  $J = 7.3$  Hz, 3H) ppm. **<sup>13</sup>C NMR** (126 MHz, Chloroform-*d*)  $\delta$  195.0, 183.4, 171.3, 166.9, 166.7, 164.4, 162.2, 160.2, 158.1, 156.7, 149.3, 143.6, 139.3, 121.3, 116.6, 115.6, 110.3, 104.3, 97.7, 91.4, 89.5, 57.1, 56.5, 56.4, 40.4, 39.0, 34.5, 33.8, 20.4, 13.3 ppm. **HRMS-ESI** ( $m/z$ ):  $[M + H]^+$  calculated for  $C_{30}H_{26}ClFNO_8$   $[M+H]^+ = 582.1326$  found 582.1323.

2-(((2*R*,2'*R*,4*a*'*S*)-6',7-dichloro-4,6-dimethoxy-2'-methyl-3-oxo-1',2'-dihydro-3H-spiro [benzofuran-2,3'-carbazol]-4*a*'(4'*H*)-yl)methyl)-4-oxo-4H-pyran-3-yl acetate **78m**

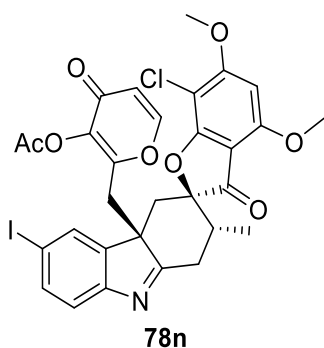


Colourless solid (89%). **<sup>1</sup>H NMR** (500 MHz, Chloroform-*d*)  $\delta$  7.46 (d,  $J = 8.4$  Hz, 1H), 7.34 (d,  $J = 5.6$  Hz, 1H), 7.31 (dd,  $J = 8.2, 2.0$  Hz, 1H), 7.24 (d,  $J = 2.0$  Hz, 1H), 6.18 (d,  $J = 5.6$  Hz, 1H), 6.16

## Experimental

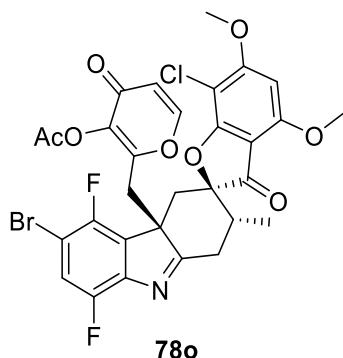
(s, 1H), 4.07 (d,  $J = 14.6$  Hz, 1H), 4.04 (s, 3H), 3.98 (s, 3H), 3.65 (dd,  $J = 13.0, 5.4$  Hz, 1H), 3.23 (d,  $J = 14.5$  Hz, 1H), 2.82 (dd,  $J = 13.0, 1.8$  Hz, 1H), 2.47 (dd,  $J = 7.1, 5.4$  Hz, 1H), 2.35 (m, 1H), 2.31 (s, 3H), 2.08 (d,  $J = 15.1$  Hz, 1H), 0.97 (d,  $J = 7.2$  Hz, 3H) ppm.  $^{13}\text{C}$  NMR (126 MHz, Chloroform-*d*)  $\delta$  195.0, 183.8, 171.2, 166.9, 166.7, 164.4, 158.1, 156.6, 153.9, 152.1, 143.5, 139.3, 131.6, 129.1, 123.0, 121.4, 116.6, 104.3, 97.7, 91.4, 89.6, 57.1, 56.5, 56.4, 40.4, 38.9, 34.6, 33.9, 20.4, 13.3 ppm. HRMS-ESI ( $m/z$ ):  $[\text{M} + \text{H}]^+$  calculated for  $\text{C}_{30}\text{H}_{26}\text{Cl}_2\text{NO}_8$   $[\text{M} + \text{H}]^+ = 598.1030$  found 598.1030.

2-(((2*R*,2'*R*,4*a*'*S*)-7-chloro-6'-iodo-4,6-dimethoxy-2'-methyl-3-oxo-1',2'-dihydro-3*H*-spiro [benzofuran-2,3'-carbazol]-4*a*'(4'*H*)-yl)methyl)-4-oxo-4*H*-pyran-3-yl acetate **78n**



Yellow pale solid (59%).  $^1\text{H}$  NMR (700 MHz, Chloroform-*d*)  $\delta$  7.66 (dd,  $J = 8.2, 1.6$  Hz, 1H), 7.59 (d,  $J = 1.6$  Hz, 1H), 7.34 (d,  $J = 5.7$  Hz, 1H), 7.30 (d,  $J = 8.2$  Hz, 1H), 6.18 (d,  $J = 5.8$  Hz, 1H), 6.16 (m, 1H), 4.04 (m, 4H), 3.99 (s, 3H), 3.64 (dd,  $J = 13.1, 5.4$  Hz, 1H), 3.21 (d,  $J = 14.5$  Hz, 1H), 2.81 (dd,  $J = 13.0, 1.9$  Hz, 1H), 2.47 (dd,  $J = 7.2, 5.4$  Hz, 1H), 2.34 (dd,  $J = 15.1, 1.9$  Hz, 1H), 2.34 (s, 3H), 2.08 (d,  $J = 15.2$  Hz, 1H), 0.97 (d,  $J = 7.3$  Hz, 3H) ppm.  $^{13}\text{C}$  NMR (176 MHz, Chloroform-*d*)  $\delta$  194.9, 183.6, 171.2, 166.9, 166.7, 164.4, 158.1, 156.6, 153.9, 153.3, 144.2, 139.3, 137.9, 131.8, 122.3, 116.6, 104.3, 97.7, 91.4, 90.5, 89.6, 57.0, 56.5, 56.4, 40.4, 38.9, 34.6, 33.9, 20.6, 13.3 ppm. HRMS-ESI ( $m/z$ ):  $[\text{M} + \text{H}]^+$  calculated for  $\text{C}_{30}\text{H}_{26}\text{IClNO}_8$   $[\text{M} + \text{H}]^+ = 690.0386$  found 690.0388.

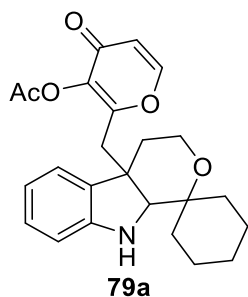
2-(((2*R*,2'*R*,4*a*'*S*)-6'-bromo-7-chloro-5',8'-difluoro-4,6-dimethoxy-2'-methyl-3-oxo-1',2'-dihydro-3*H*-spiro[benzofuran-2,3'-carbazol]-4*a*'(4*H*)-yl)methyl)-4-oxo-4*H*-pyran-3-yl acetate **78o**



Yellow pale solid (48%). **<sup>1</sup>H NMR** (500 MHz, Chloroform-*d*)  $\delta$  7.46 (d, *J* = 5.8 Hz, 1H), 7.31 (dd, *J* = 8.2, 5.2 Hz, 1H), 6.23 (d, *J* = 5.6 Hz, 1H), 6.16 (s, 1H), 4.10 (d, *J* = 14.5 Hz, 1H), 4.05 (s, 3H), 3.99 (s, 3H), 3.67 (dd, *J* = 13.0, 5.1 Hz, 1H), 3.53 (d, *J* = 14.5 Hz, 1H), 2.85 (dd, *J* = 13.0, 2.1 Hz, 1H), 2.57 (d, *J* = 15.3 Hz, 1H), 2.50 (m, 1H), 2.32 (s, 3H), 2.23(m, 1H), 0.99 (d, *J* = 7.2 Hz, 3H) ppm. **<sup>13</sup>C NMR** (126 MHz, Chloroform-*d*)  $\delta$  194.7, 184.9, 171.2, 167.0, 166.7, 164.5, 158.2, 156.2, 154.1, 150.4, 141.7, 139.5, 121.5, 121.3, 116.8, 104.3, 97.8, 90.9, 89.6, 89.3, 58.2, 57.1, 56.5, 40.4, 38.0, 34.0, 33.4, 29.7, 20.3, 13.4 ppm. **HRMS-ESI** (*m/z*): [M + H]<sup>+</sup> calculated for C<sub>33</sub>H<sub>24</sub>BrClF<sub>2</sub>NO<sub>8</sub> [M+H]<sup>+</sup> = 678.0336 found 678.0338.

#### INDOLINE

4-oxo-2-((3',4',9',9*a*'-tetrahydro-4*a*'H-spiro[cyclohexane-1,1'-pyrano[3,4-*b*]indol]-4*a*'-yl)methyl)-4*H*-pyran-3-yl acetate **79a**

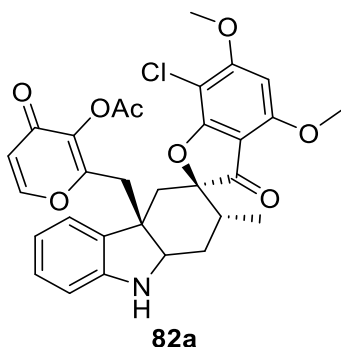


White amorph solid (16 mg, 40%). **<sup>1</sup>H NMR** (600 MHz, Methanol-*d*<sub>4</sub>)  $\delta$  7.90 (d, *J* = 3.8 Hz, 1H), 7.03 (t, *J* = 7.6 Hz, 1H), 6.90 (d, *J* = 7.2 Hz, 1H), 6.68 (t, *J* = 7.2 Hz, 1H), 6.63 (d, *J* = 7.7 Hz, 1H), 6.40 (d, *J* = 5.7 Hz, 1H), 3.67 (dt, *J* = 12.1, 4.8 Hz, 1H), 3.45 (ddd, *J* = 12.4, 9.7, 3.6 Hz, 1H), 3.21 (s, 1H), 3.07 (d, *J* = 14.3 Hz, 1H), 2.92 (d, *J* = 14.1 Hz, 1H), 2.20 (s, 3H), 2.06 (m, 2H), 1.63 (m, 5H), 1.47 (d, *J* = 12.7 Hz, 2H), 1.38 (m, 1H), 1.20 (m, 1H) ppm. **<sup>13</sup>C NMR** (151 MHz, Methanol-*d*<sub>4</sub>)

## Experimental

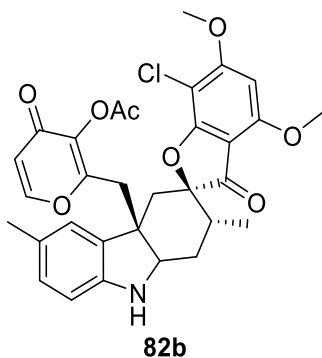
$\delta$  172.4, 166.8, 160.0, 155.2, 149.0, 138.9, 127.4, 120.7, 117.6, 114.8, 108.5, 74.4, 69.0, 55.4, 45.8, 38.2, 35.6, 30.8, 28.0, 24.6, 20.5, 19.9, 18.0 ppm. **HRMS-ESI** ( $m/z$ ):  $[M + H]^+$  calculated for  $C_{24}H_{28}NO_5$   $[M+H]^+ = 410.1962$ , found 410.1958.

2-(((2*R*,2'*R*,4*a*'*S*)-7-chloro-4,6-dimethoxy-2'-methyl-3-oxo-1',2',9',9*a*'-tetrahydro-3*H*-spiro[benzofuran-2,3'-carbazol]-4*a*'(4'*H*)-yl)methyl)-4-oxo-4*H*-pyran-3-yl acetate **82a**



White amorph solid (22 mg, 48%). **<sup>1</sup>H NMR** (400 MHz, Chloroform-*d*)  $\delta$  7.36 (d,  $J = 5.7$  Hz, 1H), 6.99 (td,  $J = 7.6, 1.3$  Hz, 1H), 6.87 (ddd,  $J = 7.5, 1.3, 0.6$  Hz, 1H), 6.67 (t,  $J = 7.5$  Hz, 1H), 6.59 (d,  $J = 7.9$  Hz, 1H), 6.22 (d,  $J = 5.7$  Hz, 1H), 6.03 (s, 1H), 3.94 (s, 3H), 3.88 (s, 3H), 3.83 (m, 1H), 3.56 (d,  $J = 14.6$  Hz, 1H), 2.90 (d,  $J = 14.6$  Hz, 1H), 2.30 (d,  $J = 15.2$  Hz, 1H), 2.22 (s, 3H), 2.06 (d,  $J = 9.8$  Hz, 1H), 1.98 (m, 1H), 1.85 (m, 2H), 1.02 (d,  $J = 7.0$  Hz, 3H) ppm. **<sup>13</sup>C NMR** (176 MHz, Chloroform-*d*)  $\delta$  196.6, 172.0, 167.5, 167.5, 164.1, 159.5, 158.0, 154.5, 140.6, 133.7, 129.3, 128.5, 126.0, 123.7, 116.7, 110.6, 105.1, 97.4, 92.8, 89.3, 61.5, 57.1, 56.5, 47.7, 38.3, 37.5, 34.5, 32.2, 20.5, 16.2 ppm. **HRMS-ESI** ( $m/z$ ):  $[M + H]^+$  calculated for  $C_{30}H_{29}ClNO_8$   $[M+H]^+ = 566.1576$  found 566.1575.

2-(((2*R*,2'*R*,4*a*'*S*)-7-chloro-4,6-dimethoxy-2',6'-dimethyl-3-oxo-1',2',9',9*a*'-tetrahydro-3*H*-spiro[benzofuran-2,3'-carbazol]-4*a*'(4'*H*)-yl)methyl)-4-oxo-4*H*-pyran-3-yl acetate **82b**

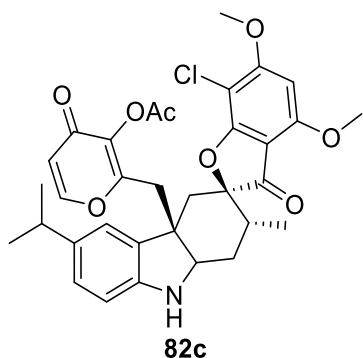


White amorph solid (30 mg, 52%). **<sup>1</sup>H NMR** (700 MHz, Methanol-*d*<sub>4</sub>)  $\delta$  7.82 (d,  $J = 5.6$  Hz, 1H), 6.82 (d,  $J = 7.9$  Hz, 1H), 6.75 (s, 1H), 6.51 (d,  $J = 7.6$  Hz, 1H), 6.36 (m, 2H), 4.03 (s, 3H), 3.93 (s,



3H), 3.77 (t,  $J = 7.0$  Hz, 1H), 3.44 (d,  $J = 14.4$  Hz, 1H), 3.04 (d,  $J = 14.4$  Hz, 1H), 2.33 (d,  $J = 15.2$  Hz, 1H), 2.21 (s, 3H), 2.19 (s, 3H), 2.15 (m, 1H), 2.08 (d,  $J = 15.1$  Hz, 1H), 1.92 (t,  $J = 7.1$  Hz, 2H), 0.96 (d,  $J = 7.0$  Hz, 3H) ppm.  $^{13}\text{C}$  NMR (176 MHz, Methanol- $d_4$ )  $\delta$  198.7, 174.5, 168.9 (d,  $J = 11.4$  Hz), 166.2, 162.5, 159.5, 157.4, 148.3, 141.1, 134.6, 129.7, 129.4, 128.9, 125.3, 116.9, 111.2, 105.9, 97.7, 94.1, 91.0, 63.5, 57.7, 56.8, 49.6, 39.3, 35.9, 33.6, 21.1, 20.3, 16.1 ppm. HRMS-ESI ( $m/z$ ):  $[\text{M} + \text{H}]^+$  calculated for  $\text{C}_{31}\text{H}_{31}\text{ClNO}_8$   $[\text{M} + \text{H}]^+ = 580.1733$  found 580.1729.

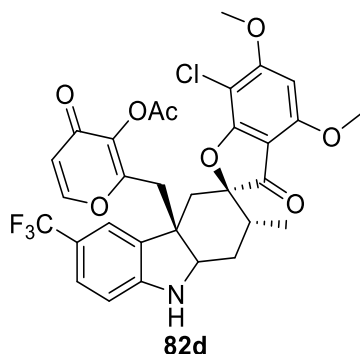
2-(((2*R*,2'*R*,4*a'**S*)-7-chloro-6'-isopropyl-4,6-dimethoxy-2'-methyl-3-oxo-1',2',9',9*a'*-tetrahydro-3*H*-spiro[benzofuran-2,3'-carbazol]-4*a'*(4'*H*)-yl)methyl)-4-oxo-4*H*-pyran-3-yl acetate **82c**



White amorph solid (18 mg, 21%).  $^1\text{H}$  NMR (700 MHz, Methanol- $d_4$ )  $\delta$  7.79 (d,  $J = 5.5$  Hz, 1H), 6.87 (d,  $J = 7.9$  Hz, 1H), 6.77 (s, 1H), 6.55 (d,  $J = 5.6$  Hz, 1H), 6.36 (s, 1H), 6.34 (d,  $J = 5.6$  Hz, 1H), 4.03 (s, 3H), 3.92 (s, 3H), 3.77 (t,  $J = 6.9$  Hz, 1H), 3.42 (d,  $J = 14.3$  Hz, 1H), 3.06 (d,  $J = 14.3$  Hz, 1H), 2.74 (p,  $J = 6.8$  Hz, 1H), 2.34 (d,  $J = 15.0$  Hz, 1H), 2.19 (s, 3H), 2.15 (q,  $J = 7.1$  Hz, 1H), 2.11 (d,  $J = 15.0$  Hz, 1H), 1.94 (t,  $J = 6.9$  Hz, 2H), 1.14 (d,  $J = 6.8$  Hz, 6H), 0.97 (d,  $J = 7.0$  Hz, 3H) ppm.  $^{13}\text{C}$  NMR (176 MHz, Methanol- $d_4$ )  $\delta$  198.6, 174.5, 169.0, 168.7, 166.1, 162.5, 159.6, 157.4, 148.5, 141.1, 140.6, 134.2, 127.2, 122.6, 116.9, 111.1, 105.9, 97.8, 94.1, 91.0, 63.9, 57.7, 56.8, 49.7, 39.2, 39.0, 35.9, 35.0, 33.7, 24.9, 24.9, 20.3, 16.1 ppm. HRMS-ESI ( $m/z$ ):  $[\text{M} + \text{H}]^+$  calculated for  $\text{C}_{33}\text{H}_{35}\text{ClNO}_8$   $[\text{M} + \text{H}]^+ = 608.2046$  found 608.2043.

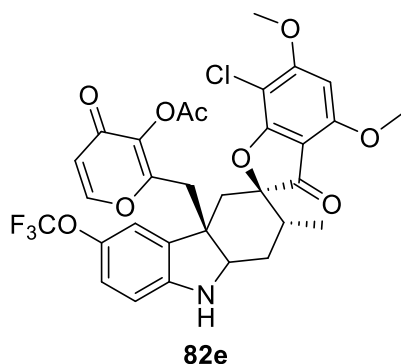
## Experimental

2-(((2*R*,2'*R*,4*a*'*S*)-7-chloro-4,6-dimethoxy-2'-methyl-3-oxo-6'-(trifluoromethyl)-1',2',9',9*a*'-tetrahydro-3*H*-spiro[benzofuran-2,3'-carbazol]-4*a*'(4'*H*)-yl)methyl)-4-oxo-4*H*-pyran-3-yl acetate **82d**



White amorph solid (22 mg, 31%). **<sup>1</sup>H NMR** (700 MHz, Methanol-*d*<sub>4</sub>) δ 7.81 (d, *J* = 5.5 Hz, 1H), 7.26 (d, *J* = 8.2 Hz, 1H), 7.23 (s, 1H), 6.60 (d, *J* = 8.2 Hz, 1H), 6.36 (m, 2H), 4.03 (s, 3H), 3.92 (s, 3H), 3.89 (m, 1H), 3.46 (d, *J* = 14.5 Hz, 1H), 3.09 (d, *J* = 14.5 Hz, 1H), 2.36 (d, *J* = 15.1 Hz, 1H), 2.23 (s, 3H), 2.14 (m, 2H), 2.01 (d, *J* = 6.0 Hz, 1H), 1.94 (dt, *J* = 17.6, 11.4 Hz, 2H), 0.97 (d, *J* = 6.9 Hz, 3H) ppm. **<sup>13</sup>C NMR** (176 MHz, Methanol-*d*<sub>4</sub>) δ 196.4, 172.2, 166.8, 166.7, 164.1, 159.8, 157.5, 155.2, 139.0, 132.2, 125.0, 120.0, 118.2, 114.9, 107.2, 103.7, 95.6, 91.5, 88.9, 61.2, 55.6, 54.7, 47.1, 36.9, 36.8, 33.6, 31.3, 25.8, 18.2, 13.9 ppm. **HRMS-ESI** (*m/z*): [M + H]<sup>+</sup> calculated for C<sub>31</sub>H<sub>28</sub>ClF<sub>3</sub>NO<sub>8</sub> [M+H]<sup>+</sup> = 634.1450 found 634.1448.

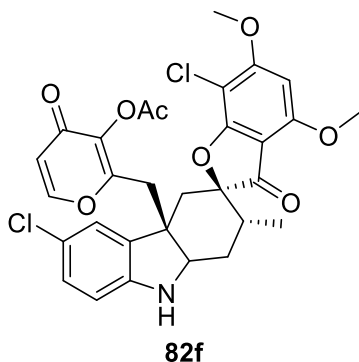
2-(((2*R*,2'*R*,4*a*'*S*)-7-chloro-4,6-dimethoxy-2'-methyl-3-oxo-6'-(trifluoromethoxy)-1',2',9',9*a*'-tetrahydro-3*H*-spiro[benzofuran-2,3'-carbazol]-4*a*'(4'*H*)-yl)methyl)-4-oxo-4*H*-pyran-3-yl acetate **82e**



White amorph solid (12 mg, 30%). **<sup>1</sup>H NMR** (700 MHz, Methanol-*d*<sub>4</sub>) δ 7.80 (d, *J* = 5.7 Hz, 1H), 6.90 (d, *J* = 8.8 Hz, 1H), 6.88 (s, 1H), 6.58 (d, *J* = 8.4 Hz, 1H), 6.36 (m, 2H), 4.03 (s, 3H), 3.92 (s, 3H), 3.81 (t, *J* = 6.7 Hz, 1H), 3.48 (d, *J* = 14.4 Hz, 1H), 3.02 (d, *J* = 14.5 Hz, 1H), 2.37 (d, *J* = 15.1 Hz, 1H), 2.23 (s, 3H), 2.13 (m, 2H), 1.96 (m, 2H), 0.97 (d, *J* = 7.0 Hz, 3H) ppm. **<sup>13</sup>C NMR** (176 MHz, Methanol-*d*<sub>4</sub>) δ 198.5, 174.4, 168.9, 168.8, 166.2, 161.9, 159.6, 157.3, 149.9, 142.4, 141.2,

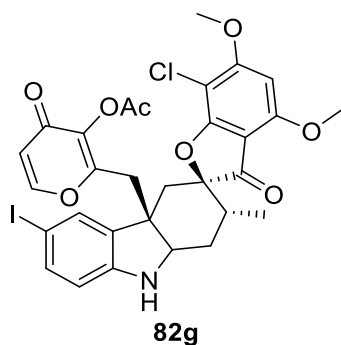
135.4, 122.5, 118.9, 117.0, 110.6, 105.9, 97.7, 93.6, 91.0, 63.9, 57.7, 56.8, 49.8, 38.9, 38.5, 35.9, 33.2, 20.3, 16.0 ppm. **HRMS-ESI** ( $m/z$ ):  $[M + H]^+$  calculated for  $C_{31}H_{28}ClF_3NO_9$   $[M+H]^+ = 650.1399$  found 650.1397.

2-(((2*R*,2'*R*,4*a*'*S*)-6',7-dichloro-4,6-dimethoxy-2'-methyl-3-oxo-1',2',9',9*a*'-tetrahydro-3*H*-spiro[benzofuran-2,3'-carbazol]-4*a*'(4'*H*)-yl)methyl)-4-oxo-4*H*-pyran-3-yl acetate **82f**



White amorph solid (5 mg, 7%).  **$^1H$  NMR** (700 MHz, Methanol- $d_4$ )  $\delta$  7.87 (d,  $J = 5.6$  Hz, 1H), 6.96 (m, 2H), 6.53 (d,  $J = 8.7$  Hz, 1H), 6.38 (d,  $J = 5.7$  Hz, 1H), 6.37 (s, 1H), 4.03 (s, 3H), 3.93 (s, 3H), 3.80 (t,  $J = 6.9$  Hz, 1H), 3.43 (d,  $J = 14.4$  Hz, 1H), 3.03 (d,  $J = 14.5$  Hz, 1H), 2.36 (d,  $J = 15.1$  Hz, 1H), 2.24 (s, 3H), 2.15 (m, 2H), 1.93 (p,  $J = 9.5$  Hz, 2H), 0.95 (d,  $J = 6.9$  Hz, 3H) ppm.  **$^{13}C$  NMR** (176 MHz, Methanol- $d_4$ )  $\delta$  198.6, 174.5, 168.9, 168.8, 166.2, 162.0, 159.6, 157.5, 149.6, 141.2, 136.1, 129.0, 125.0, 123.6, 117.0, 111.6, 105.9, 97.7, 93.7, 91.0, 63.5, 57.7, 56.8, 49.8, 39.3, 38.8, 35.9, 33.4, 20.4, 16.0 ppm. **HRMS-ESI** ( $m/z$ ):  $[M + H]^+$  calculated for  $C_{30}H_{28}Cl_2NO_8$   $[M+H]^+ = 600.1186$  found 600.1185.

2-(((2*R*,2'*R*,4*a*'*S*)-7-chloro-6'-iodo-4,6-dimethoxy-2'-methyl-3-oxo-1',2',9',9*a*'-tetrahydro-3*H*-spiro[benzofuran-2,3'-carbazol]-4*a*'(4'*H*)-yl)methyl)-4-oxo-4*H*-pyran-3-yl acetate **82g**



White amorph solid (19 mg, 25%).  **$^1H$  NMR** (700 MHz, Methanol- $d_4$ )  $\delta$  7.87 (m, 1H), 7.27 (d,  $J = 8.3$  Hz, 1H), 7.24 (s, 1H), 6.39 (m, 3H), 4.03 (s, 3H), 3.94 (s, 3H), 3.79 (t,  $J = 6.8$  Hz, 1H), 3.42

## Experimental

(d,  $J = 14.5$  Hz, 1H), 3.02 (d,  $J = 14.4$  Hz, 1H), 2.34 (d,  $J = 15.1$  Hz, 1H), 2.25 (s, 3H), 2.15 (m, 1H), 2.09 (d,  $J = 15.1$  Hz, 1H), 1.93 (t,  $J = 6.8$  Hz, 2H), 0.96 (d,  $J = 6.9$  Hz, 3H) ppm.  $^{13}\text{C}$  NMR (176 MHz, Methanol- $d_4$ )  $\delta$  198.6, 174.4, 169.0, 168.8, 166.2, 162.0, 159.6, 157.4, 150.7, 141.2, 138.0, 137.1, 133.7, 117.0, 112.8, 105.9, 97.8, 93.8, 91.1, 78.8, 63.3, 57.7, 56.9, 49.7, 39.3, 38.9, 35.8, 33.4, 20.5, 16.0 ppm. **HRMS-ESI** ( $m/z$ ):  $[\text{M} + \text{H}]^+$  calculated for  $\text{C}_{30}\text{H}_{28}\text{ClINO}_8$   $[\text{M} + \text{H}]^+ = 692.0543$  found 692.0541.

### 5.3. MATERIALS FOR BIOLOGICAL EXPERIMENTS

#### BUFFERS AND SOLUTIONS

Buffer/ Solution	Composition
Lysis Buffer	50 mM PIPES, 50 mM NaCl, 5 mM EGTA, 5 mM MgCl <sub>2</sub> , 0,1 % NP-40, 0,1 % Triton X-100, 0,1 % Tween
Mitochondrial Assay Solution	220 mM Mannitol, 70 mM Sucrose, 10 mM KH <sub>2</sub> PO <sub>4</sub> , 5 mM MgCl <sub>2</sub> , 2 mM HEPES, 1 mM EGTA, pH 7.4 at 37 °C
PBS	137 mM NaCl, 2.7 mM KCl, 10 mM Na <sub>2</sub> HPO <sub>4</sub> , 2.0 mM KH <sub>2</sub> PO <sub>4</sub> , pH 7.4
PBS-T	PBS with 0.1% Tween
SDS loading buffer (5x)	50% v/v Glycerol, 250 mM Tris (pH 6.8), 10% w/v SDS, 500 mM DTE, 360 µM bromophenol blue
Transfer Buffer	14.41 g/l glycine, 3.03 g/l Tris, 20% v/v MeOH
Tris-buffer	50 mM Tris, pH 7.5

#### SOFTWARE

EnsoChemLab Version 5.0.8 Enso Software GmbH, Erbach, Germany

IncuCyte® ZOOM Version 2016A, Essen BioScience, Ann Arbor, USA

Llama<sup>[74]</sup>, University of Leeds, UK

Maestro Version 10.5, Schrödinger LLC, New York, USA

MestReNova Version 6.0.3-5604, Mestrelab Research, Santiago de Compostela, Spain

MetaMorph Offline Version 7.7.0.0 Molecular Devices, Biberach, Germany

Tecan i-control Version 3.4.2.0 Tecan AG, Männedorf, CH

## Experimental

### INSTRUMENTS

AxioVert 200M fluorescence microscope, Carl Zeiss Microscopy GmbH

Centrifuge 5415R, Eppendorf

Centrifuge 5425R, Eppendorf

Centrifuge 5430, Eppendorf

Centrifuge, Minispin, Eppendorf

ChemiDoc™ MP Imaging System, BioRad

Countess™ II Automated Cell Counter, Thermo Fisher Scientific

IncuCyte® S3, Essen BioScience

Infinite M200 Plate Reader, Tecan

Leica DM IRB inverted research microscope, Leica

Mastercycler ep gradient S, Eppendorf

Mini-PROTEAN® Tetracell Electrophoresis System, Bio-Rad

NuAire NU-437-400E or NuAire NU-447-400E biosafety cabinet, ibs tecnomara

NuAire NU-5500E incubator, ibs integra biosciences

pH-Meter, Mettler Toledo

Spark multimode microplate reader, Tecan

Seahorse XFp Analyzer, Agilent

Sonorex Super ultrasound bath, Bandelin

Thermomixer comfort 5355, Eppendorf

Vortex-gene 2, Scientific Industries

## 5.4. BIOLOGICAL METHODS

### CELL CULTURE OF MAMMALIAN CELLS

Experiments with living mammalian cells were conducted in a sterile environment employing cell culture-approved clean benches, sterile equipment and media. All cells lines were cultured in a humidified atmosphere at 37 °C and 5% CO<sub>2</sub>. Waste generated during the work with cells was collected and sterilized with an autoclave (134 °C, 15 min).

Human breast cancer MCF7 cells were cultured in Eagle's dulbecco's modified eagle medium (DMEM) (PAN Biotech, cat# P04-03550) with the addition of 10% fetal bovine serum (FBS) (Invitrogen, cat# 10500-084), 1% sodium pyruvate (PAN Biotech, cat# P04-43100), 1% nonessential amino acids (PAN Biotech, cat# P08-32100), and 0.01 mg/mL bovine insulin (Sigma Aldrich, cat# I9278). The stably transfected MCF7 cells with eGFP-LC3 (MCF7/LC3) were incubated under the same conditions, but with the addition of 200 µg/mL G418 (Sigma Aldrich, Cat. No.: G8168) in the medium.

HeLa cells were cultivated in DMEM supplemented with 10% FBS, 1% sodium pyruvate and 1% non-essential amino acids.

### PASSAGING OF MAMMALIAN CELLS

All solutions, including the respective media, were prewarmed to 37 °C in a water bath. After the cells were grown to 70-80% confluence in culture flasks (75 cm<sup>2</sup>), the old medium was removed and the cells were washed with PBS (10 mL). For detachment, the cells were treated with the addition of a trypsin/EDTA solution (2 mL, 37 °C, 2 min). When the cells were detached, fresh medium was added and a desired volume of the cell suspension was transferred into a new tissue flask (75 cm<sup>2</sup>). The final volume in the flask was set to 10 mL and was accordingly filled up with medium.

### CRYO-CONSERVATION AND THAWING OF CRYO-CONSERVED CELLS AND

For cryo-conservation, the cells were cultured in a tissue culture flask (175 cm<sup>2</sup>) until they grew to confluence. After trypsinization and centrifugation (350 g, 5 min), the cell pellet was resuspended in the respective medium (6 mL) with DMSO (5% v/v). The suspension was distributed into cryo-conservation vials and transferred into a cell freezing container (CoolCell® LX) and kept at -80 °C overnight. For long-term storage the cells were stored in liquid nitrogen.

## Experimental

Cryo-conserved cells were rapidly thawed in a water bath (37 °C, 2 min) and subsequently transferred to the respective medium (10 mL). After centrifuging the suspension (350 g, 5 min), the supernatant was removed and the cell pellet was resuspended in fresh medium (10 mL). The cells were transferred to tissue culture flasks (25 cm<sup>2</sup>).

### AUTOMATED CELL COUNTING

The cell count was performed employing the automated cell counter Countess™ II Automated Cell Counter according to the manufacturer's instructions. Cells were diluted with Trypan blue (ratio 1:1) for the identification of dead cells, 10 µL of the suspension were transferred to a Countess® Cell Counting Chamber Slide (Thermo Fisher Scientific, Cat. No. C10228) and the slide was inserted to the machine to directly give the cell number.

### GFP-LC3 PUNCTA FORMATION ASSAY

The GFP-LC3 puncta formation assay was performed by the COMAS in a medium throughput manner. Stably transfected MCF7 cells expressing eGFP-LC3 were seeded with a density of 400 cells/well in a volume of 25 µL per well in 384 well-plates (Greiner: cat# 781080, lid cat# 656191). After incubation overnight (37 °C, 5% CO<sub>2</sub>), the cells were washed with PBS (Biotek, ELx405, 3x). For the compound treatment, the stock solution (10 mM in DMSO, 25 µL) is added to the cells employing an echo dispenser (Labcyte). The respective medium (25 µL EBSS with chloroquine (50 µM) or standard medium supplemented with chloroquine (50 µM) and rapamycin (Biomol, cat# Cay13346, 100 nM)) was added using a Multidrop Combi (Thermo Scientific) to induce autophagy. After the incubation (3 h, 37 °C, 5% CO<sub>2</sub>), the cells were fixed with the addition of 25 µL of a fixing solution containing formaldehyde/PBS (1:4) and nuclei were stained with 1:500 Hoechst (stock: 1 mg/ml, Sigma Aldrich cat# B2261-25mg) at ambient temperature for 20 min. The cells were washed three times with PBS and subsequently fluorescent pictures were taken by an ImageXpress Micro XL (Molecular Devices, 4 sites per well, 20x magnification). The granularity setting of MetaXpress Software (Molecular Devices) was employed for an automated image analysis.

### IMMUNOBLOTT FOR AUTOPHAGY MARKERS

MCF7/LC3 cells were seeded in 6-well plates (300,000 cells/ 2 mL medium) and cultivated overnight in an incubator (37 °C, 5% CO<sub>2</sub>). The medium was substituted by fresh medium or EBSS for starvation conditions. After compound addition (2 µL of the respective DMSO solution), the cells were incubated (3 h, 37 °C, 5% CO<sub>2</sub>). The cultivated cells were washed with PBS (1x



1 mL) and trypsinated to collect the cell with a cell scraper. After the centrifugation (4000 rpm, 5 min) followed by washing with PBS (1 mL), 50  $\mu$ L lysis buffer (50 mM PIPES, 50 mM NaCl, 5 mM EGTA, 5 mM MgCl<sub>2</sub>, 0.1% NP-40, 0.1%TX-100, 0.1% Tween at pH=7.4) was added to the cells. The suspension was incubated for 30 min on ice while inverting the tube every 10 min. After another centrifugation (20 min, 14000 rpm, 4 °C), the supernatant was collected and the protein concentration was determined via DC assay according to the “DC protein assay instruction manual”. The BSA standard curve was detected for protein concentrations between 0 mg/mL – 2.5 mg/mL. The absorbance was measured at 750 nm by a Tecan plate reader.

The samples were diluted with SDS loading buffer (5x, 50% v/v Glycerol, 250 mM Tris (pH 6.8), 10% w/v SDS, 500 mM DTE, 360  $\mu$ M bromophenol blue) to a final concentration of 2% w/v and desaturated by heating them to 95 °C for 5 min. Until their use for separation on the SDS-PAGE followed by western blot, the samples were stored at -80 °C.

To separate the proteins according to their size a sodium dodecyl sulfate–polyacrylamide gel electrophoresis (SDS-PAGE) was performed using a Mini-PROTEAN® Tetra Cell chamber (Bio Rad) according to the standard method<sup>[124]</sup>. The desaturated samples were loaded onto the SDS-gel (separation gel: 12.5%). The PageRuler™ Plus Prestained Protein Ladder (Thermo Fisher Scientific, Cat. No. 26619) was used as marker. The gel was initially run at a constant voltage of 80 V for 30 min and afterwards the electric voltage was increased to 120 V for another 60 min.

Afterwards, the separated proteins were transferred to a polyvinylidene fluoride (PVDF) membrane. For this purpose, the membrane was shortly activated in methanol and afterwards together with the SDS-gel equilibrated in transfer buffer for 15 min. The filter paper was also soaked in transfer buffer before transferring the parts to the Trans-Blot® SD Semi-Dry Transfer Cell (Bio-Rad) system, where it was blotted according to the manufactures instructions (25 V, 25 min).

The membrane was washed with water and subsequently stained employing Ponceau S to check for the protein transfer. The staining was removed by repeatedly washing the membrane with water. The membrane was subsequently blocked with blocking buffer for 1 h at ambient temperature. The primary antibody in blocking solution (5 % w/v milk powder in PBS-T) was added and the membrane was incubated overnight at 4 °C (see table below). The primary antibody solution was removed, the membrane was washed (3x 5 mL PBS-T, 10 min), and incubated with secondary coupled to a near-infrared dye (IRDye 680RD or IRDye 800CW, Licor) antibody in blocking solution (see table below). After the membrane was washed (3x 5 mL PBS-T, 10 min), the protein band were visualized on the ChemiDoc™ MP Imaging System, BioRad.

## Experimental

The autophagy marker p62 and LC3 were detected and vinculin was chosen as a loading control.

antibody	host	dilution	supplier	Cat. No.
LC3	rabbit	1:1000	Cell Signaling	2775
p62	rabbit	1:10000	MBL international	PM045
vinculin	mouse	1:10000	Sigma Aldrich	V9131
IRDye 680RD anti rabbit	goat	1:10000	LI-COR	P/N 926-68071
IRDye 800CW goat anti-mouse	goat	1:10000	LI-COR	P/N 926-32210

### SELECTIVE VIABILITY ASSAY

5000 MCF7 cells per well were seeded in a volume of 100  $\mu$ L medium in clear flat-bottom 96 well plates and incubated overnight (37  $^{\circ}$ C, 5% CO<sub>2</sub>). The medium was removed and substituted by either 80  $\mu$ L fresh medium or medium without glucose, both containing propidium iodide (1:60). A series of nine different compound concentrations was prepared and 20  $\mu$ L were added to the cells. DMSO (0.1%) was used as negative control and nocodazole (10  $\mu$ M) as positive control. The cell growth was monitored for 72 h using the IncuCyte<sup>®</sup> ZOOM for 72 h, where two images per well are taken at 10-fold magnification every 2 h in the red and phase channel. The resulting images were analyzed with the IncuCyte<sup>®</sup> ZOOM software.

### MITO STRESS TEST

The Mito Stress Test was performed in the Seahorse XFp analyzer (Agilent, USA) employing the corresponding Cell Mito Stress Test kit (Agilent, USA, No. 103015-100) according to the manufacturer's protocol. 20,000 cells (HeLa or MCF7) in 100  $\mu$ L of the respective medium were seeded into the XFp cell culture plates (Agilent, USA) and incubated overnight (37  $^{\circ}$ C, 5% CO<sub>2</sub>). The XFp cartridges were hydrated with the XF Calibrant solution (Agilent, USA) and also incubated overnight at 37  $^{\circ}$ C without CO<sub>2</sub>.

The next day, the medium was exchanged for 180  $\mu$ L assay medium (XF base medium (pH 7.4, Agilent, USA), 2 mM GlutaMAX (ThermoFisher), 1 mM sodium pyruvate (PAN Biotech, Germany) and 25 mM glucose (Sigma-Aldrich, Germany)). Subsequently, the cells were equilibrated (45 min, 37  $^{\circ}$ C, no CO<sub>2</sub>) and the stock solutions of the kit were filled up with assay medium to give the desired concentrations of 50 mM for oligomycin and FCCP and 25  $\mu$ M for rotenone/antimycin A. The compounds were diluted in assay medium according their desired concentrations and loaded onto the respective injection ports. The plates were submitted to the Seahorse XFp analyzer and the oxygen consumption rate (OCR) and extracellular acidification rate (ECAR) were measured every 6 min. After the detection of five time cycles of the baseline, the test compounds

and DMSO as controls were added at the desired concentrations and measured for ten intervals. Afterwards oligomycin, FCCP and rotenone/antimycin A were injected and each addition was detected for three cycles. The results were analyzed with the Wave software, where the background was subtracted and normalized to the fifth base line measurement (=100%).

#### *IN-VITRO* TUBULIN POLYMERIZATION ASSAY

Porcine  $\alpha/\beta$ -tubulin (> 99% pure, Cytoskeleton, Denver, USA) was dissolved in buffer (80 mM Na-PIPES pH 6.9, 1 mM MgCl<sub>2</sub>, 1 mM EGTA and 0,88 mM Na-glutamate). The compounds were added at the respective concentrations and the mixture was incubated on ice for 30 min. The polymerization was started with the addition of GTP (0.4 mM) and followed by the detection of absorption at 340 nm in the Inifinite® M200 plate reader (Tecan, Grödig, Austria) at 37 °C for 75 min. The background was subtracted.

#### IN CELL HISTONE STAINING FOR THE MITOTIC ARREST

5000 HeLa cells per well were seeded in a volume of 100  $\mu$ L medium in clear flat-bottom 96 well plates (Corning) and incubated overnight (37 °C, 5% CO<sub>2</sub>). The medium was removed and substituted by 100  $\mu$ L medium with compound or controls and incubated for another 3 h (37 °C, 5% CO<sub>2</sub>). After the media was substituted by 100  $\mu$ L 3.7% formaldehyde in PBS and incubated for 10 min. For permeabilization 100  $\mu$ L of 0.1% Triton X-100 in PBS was added and incubated for 15 min. After the Triton solution was removed, the cells were washed with PBS-T and 100  $\mu$ L 2% BSA in PBS-T was added to the cells. After an incubation for 1 h, the corresponding antibodies were added in 40  $\mu$ L 2% BSA in PBS-T (see table below). The antibody solution was removed and the cells were washed once more with PBS-T. Subsequently, 100  $\mu$ L PBS-T were added for imaging. On the screening microscope the cells were imaged at 20-fold magnification in the 4', 6-diamidino-2-phenylindole, dihydrochloride (DAPI) and Texas Red channel. The resulting data were analyzed by quantifying the LysoTracker™ Red DND-99 staining with the software CellProfiler.

antibody/ compound	host	dilution	supplier	Cat. No.
DAPI	-	1:1000	Sigma Aldrich	D9542-10MG
Tubulin-FITC	mouse	1:500	Thermo Fisher Scientific	MA119581
Phospho Histone H3-AF594	rabbit	1:500	Cell Signalling	#8481

## Experimental

### LYSOTRACKER RED ASSAY FOR LYSOSOMOTROPIC COMPOUNDS

1000 MCF7 cells per well were seeded in a volume of 100  $\mu$ L medium in black, clear flat-bottom 96 well plates and incubated overnight (37 °C, 5% CO<sub>2</sub>). The medium was removed and substituted by 100  $\mu$ L medium with compound or controls and incubated for another 3 h (37 °C, 5% CO<sub>2</sub>). In the meantime, LysoTracker™ Red DND-99 [120] and Hoechst-33342 dilutions were prepared (8 mL DMEM + 80  $\mu$ L Hoechst-33342 + 8  $\mu$ L LysoTracker™ Red DND-99) and 100  $\mu$ L were added to each well. After mixing the solutions on the plate shaker for 1 min, the cells were incubated for 30 min (37 °C, 5% CO<sub>2</sub>). The cells were three-times washed with PBS, 100  $\mu$ L of 4% formaldehyde solution (10 mL PBS + 1.5 mL formaldehyde) was added to each well and the cells were incubated for 5 min in the dark. Subsequently the cells were washed once more with PBS and 100  $\mu$ L PBS were added for imaging. On the screening microscope the cells were imaged at 10-fold magnification in the TexasRed and DAPI channel. The resulting data were analyzed by quantifying the LysoTracker™ Red DND-99 staining with the software CellProfiler.

### 5.5.MORPHOLOGICAL PROFILING

The Cell Painting Assay was performed by the COMAS based on the method developed by Bray et al.[46] On a 384-well plate (PerkinElmer CellCarrier-384 Ultra) U2OS medium (5  $\mu$ L) was added to each well, followed by the addition of 1600 U2OS cells in 20  $\mu$ L medium. After short incubation at the ambient temperature (5 min), the cells were grown for 4 h in an incubator (37 °C, 5% CO<sub>2</sub>). For the compound treatment, an Echo 520 acoustic dispenser (Labcyte) was employed to generate the final concentrations of 1, 3, 10, 30 and 50  $\mu$ L. The samples were prepared in triplicates on different plates with shifted locations on the plate to reduce plate effects. After incubation for 20 h (37 °C, 5% CO<sub>2</sub>), the mitochondria were stained with Mito Tracker Deep Red (Thermo Fisher Scientific, Cat. No. M22426). The corresponding stock solution (1 mM) was diluted with prewarmed medium to a concentration of 100 nM. 15  $\mu$ L medium were removed from the wells leaving 10  $\mu$ L as residual volume and 25  $\mu$ L of the Mito Tracker solution were added to each well. After a 30 min incubation in the dark (37 °C, 5% CO<sub>2</sub>), the cells were fixed by the addition of formaldehyde in PBS (3.7%). The cells were incubated for another 20 min in the dark (37 °C, 5% CO<sub>2</sub>) and subsequently washed with PBS by the Biotek Washer Elx405 (3x 70  $\mu$ L). The U2OS cells were permeabilized with 25  $\mu$ L 0.1% Triton X-100 and incubated for 15 min (37 °C, 5% CO<sub>2</sub>). The cells were washed with PBS (3x 70  $\mu$ L) and a volume of 70  $\mu$ L was left in each well. A staining solution containing 1% BSA, 50  $\mu$ L phalloidin (Thermo Fisher Scientific, A12381), 25  $\mu$ g/ml concanavalin A (Thermo Fisher Scientific, Cat. No. C11252), 50  $\mu$ L/ml Hoechst

234

33342 (Sigma, Cat. No. B2261-25mg), 15  $\mu$ l/ml WGA-Alexa594 conjugate (Thermo Fisher Scientific, Cat. No. W11262) and 0.3  $\mu$ L/ml SYTO 14 solution (Thermo Fisher Scientific, Cat. No. S7576) was added to each well. After an incubation in the dark for 30 min (37 °C, 5% CO<sub>2</sub>), the cells were washed with PBS (3x 70  $\mu$ L) and the final 70  $\mu$ L were left in each well. The plates were sealed and subsequently centrifuged (1 min at 500 rpm).

The cells were imaged using a Micro XL High-Content Screening System (Molecular Devices, 5 channels, 9 sites per well, 20x magnification, binning 2). The microscope pictures were analyzed with a computing cluster of the Max Planck Society by employing the CellProfiler package (<https://cellprofiler.org/>) to extract 1716 features. Additional analyses were performed with custom Python scripts (<https://www.python.org/>) employing different data processing libraries (Pandas (<https://pandas.pydata.org/>) and Dask (<https://dask.org/>)).

Initially, the data was summarized as overall medians per well. A subset of 579 characteristic parameters that show high reproducibility were identified using the method published by Woehrmann et al.<sup>[125]</sup>

Z-scores were calculated for each feature by the following equation as the difference to the median of the controls divided by their MAD. The morphological profile of a compound represents a list of the z-scores of all parameters.

$$z\text{-score} = (\text{value}_{\text{meas.}} - \text{median}_{\text{controls}}) / \text{MAD}_{\text{controls}}$$

Additionally, the induction was calculated as a percentage of the number of significantly changed parameters compared to the controls.

$$\text{induction} = (\text{number of parameters with abs. values} > 3) / \text{total number of parameters}$$

Biosimilarities between morphological profiles were described as the correlation distances between two profiles (<https://docs.scipy.org/doc/scipy/reference/generated/scipy.spatial.distance.correlation.html>; Similarity = 1 - Correlation Distance).

## Experimental

### 5.5.1. COMPOUNDS USED FOR THE ANALYSIS (WELL IDS)

#### INDOFULVINS

##### $\gamma$ -Indofulvins (G-THPI-g)

409968:01:04\_10.00

409969:01:04\_10.00

409970:01:05\_10.00

408754:01:06\_10.00

410170:01:03\_10.00

409972:01:08\_30.00

409973:01:04\_10.00

410172:01:03\_10.00

410173:01:03\_10.00

409328:01:03\_10.00

410174:01:04\_10.00

##### $\beta$ -Indofulvins (G-THPI-b)

412373:01:02\_10.00

412370:01:03\_10.00

412366:01:02\_10.00

409966:01:11\_30.00

412374:01:02\_10.00

412371:01:02\_10.00

412372:01:03\_10.00

412367:01:02\_10.00

#### INDOLENINES

412356:01:05\_10.00

412344:01:03\_03.00

412355:01:05\_10.00

412354:01:06\_10.00

412351:01:03\_10.00

412352:01:03\_10.00

412353:01:03\_10.00

412349:01:03\_10.00  
412348:01:03\_10.00  
412343:01:03\_10.00  
412350:01:04\_10.00  
412356:01:02\_10.00  
412350:01:03\_10.00  
412355:01:02\_10.00

GRISEOFULVIN (G)

246980:07:08\_30.00  
246980:07:05\_50.00  
246980:01:04\_30.00  
246980:07:05\_30.00

GRISEOFULVIN INDOLES DERIVED FROM FISCHER INDOLE REACTION

Mayor regioisomers (G-I-1)

409697:01:06\_30.00  
408604:02:02\_10.00  
408579:01:04\_10.00  
409695:01:02\_10.00  
408590:01:10\_03.00  
409682:01:05\_50.00  
409689:01:09\_10.00  
408600:01:11\_10.00  
409680:01:02\_10.00  
408582:01:08\_03.00  
408647:01:05\_10.00  
408646:01:05\_10.00  
409693:01:02\_10.00  
409683:01:02\_10.00  
409078:01:04\_50.00  
409688:01:02\_10.00

## Experimental

409685:01:03\_10.00

### Minor regioisomers (G-I-2)

409079:01:04\_50.00

409673:01:04\_50.00

409694:01:11\_10.00

408596:01:08\_30.00

408602:01:06\_30.00

408648:01:06\_10.00

409696:01:08\_10.00

409692:01:02\_10.00

409681:01:02\_10.00

408591:01:05\_10.00

409081:01:05\_10.00

## ANNOTATED REFERENCE COMPOUNDS

### Lysosomotrop

347278:01:04\_10.00

247177:02:03\_10.00

246746:01:04\_30.00

247241:01:04\_30.00

246507:01:04\_30.00

280128:01:07\_03.00

247050:03:03\_10.00

391878:01:02\_02.00

392675:01:09\_02.00

246739:01:09\_03.00

247331:01:04\_30.00

246537:01:04\_30.00

281022:01:03\_30.00

247423:01:04\_30.00

247234:01:04\_30.00

247165:02:03\_10.00



280575:01:09\_03.00  
246344:01:04\_30.00  
247164:01:04\_10.00  
246940:01:04\_30.00  
280751:01:03\_30.00  
280660:01:03\_10.00  
280918:01:08\_03.00  
287906:02:15\_30.00  
392660:02:06\_03.00

HSP90

410608:01:03\_02.00  
410102:01:03\_02.00  
410702:01:03\_02.00  
410733:01:03\_02.00

AKT\_PI3K\_MTOR

392513:01:09\_02.00  
392538:01:10\_02.00  
392535:01:10\_02.00  
392483:01:10\_02.00  
392897:01:09\_10.00  
392514:01:10\_02.00  
392761:01:09\_02.00  
392764:01:09\_02.00  
392630:01:09\_02.00  
392708:01:09\_02.00  
392604:01:09\_02.00  
392761:01:09\_00.20  
392897:01:10\_03.00  
392893:01:08\_10.00  
392483:01:10\_00.20  
392616:01:09\_00.20

## Experimental

392634:01:09\_00.20

392638:01:09\_02.00

407972:01:04\_10.00

392563:01:10\_02.00

## DNA synth

247256:01:04\_10.00

247186:01:04\_10.00

280865:01:03\_10.00

407753:02:03\_02.00

247256:03:04\_10.00

280184:01:03\_30.00

280158:01:04\_30.00

247256:03:04\_06.00

246785:01:04\_10.00

280184:01:03\_10.00

407753:01:02\_10.00

246755:01:04\_10.00

280293:01:03\_10.00

246660:01:04\_30.00

280420:01:03\_10.00

246389:01:04\_10.00

246660:01:04\_10.00

247256:01:06\_03.00

246719:01:04\_10.00

408119:01:03\_10.00

280907:01:03\_30.00

246719:01:04\_30.00

280184:02:04\_10.00

392341:01:02\_00.20

247256:01:04\_30.00

392511:01:09\_02.00

280184:02:04\_06.00

246366:01:04\_10.00

247284:01:04\_30.00

#### HDAC

410069:01:03\_02.00

409838:01:04\_10.00

409947:01:03\_02.00

409879:01:04\_00.20

392651:01:09\_00.20

409879:01:05\_00.60

409879:01:05\_00.20

409879:01:02\_02.00

409879:01:04\_00.60

410069:01:06\_00.60

392651:01:09\_02.00

392531:01:09\_02.00

410069:01:05\_00.60

410679:01:03\_02.00

246890:01:04\_30.00

410122:01:05\_06.00

392789:01:10\_02.00

392664:01:09\_02.00

410668:01:03\_02.00

247167:11:04\_10.00

280708:01:03\_30.00

246514:02:04\_06.00

392717:02:03\_02.00

280973:01:03\_30.00

#### Tubulin

410065:01:03\_02.00

410613:01:03\_02.00

410072:01:03\_02.00

## Experimental

410074:01:03\_02.00

409915:01:02\_10.00

410129:01:03\_02.00

246967:02:06\_01.00

280897:07:06\_01.00

246557:01:07\_01.00

246972:01:08\_01.00

246967:02:06\_03.00

280630:01:11\_01.00

246994:01:07\_01.00

280954:01:07\_03.00

280630:01:11\_03.00

246980:07:05\_30.00

104614:02:17\_30.00

246980:07:05\_50.00

391925:03:05\_00.20

391925:03:04\_00.20

391925:03:04\_00.60

246972:12:05\_00.60

410753:01:04\_10.00

246876:01:04\_10.00

246876:01:04\_30.00

246967:01:04\_30.00

246557:01:04\_30.00

247208:01:05\_30.00

247133:01:04\_30.00

246702:01:04\_30.00

246898:01:04\_30.00

280954:01:03\_10.00

280428:01:03\_10.00

280418:01:03\_10.00

280418:01:03\_30.00

392625:01:09\_00.20

392542:01:09\_00.20

392286:01:02\_02.00

Uncoupler

404608:01:15\_10.00

404608:01:13\_10.00

280982:01:03\_10.00

280982:01:03\_30.00

280973:01:03\_10.00

246911:01:04\_30.00

392672:01:09\_02.00

392713:02:04\_10.00

Aurora

407889:01:03\_10.00

408573:01:04\_10.00

410632:01:03\_02.00

409875:01:02\_10.00

392522:02:03\_02.00

392321:03:03\_02.00

410128:01:03\_02.00

410084:01:04\_00.20

410084:01:05\_00.20

392321:02:09\_02.00

392522:01:09\_00.20

392643:01:09\_02.00

392522:01:09\_02.00

## ABBREVIATIONS

### A

Ac	acetyl group
Ac <sub>2</sub> O	acetic anhydride
ADP	adenosine diphosphate
Alog P	estimated hydrophobicity
AMP	adenosine monophosphate
AMPK	AMP activated protein kinase
AIBN	azobisisobutyronitrile
ATG	autophagy-related gene
ATP	adenosine triphosphate

### B

BF <sub>3</sub> ·Et <sub>2</sub> O	boron trifluoride etherate
BIOS	biology-oriented synthesis
Biosim.	biological similarity
Boc	<i>tert</i> -butyloxycarbonyl group
BSA	bovine serum albumin

### C

cAMP	cyclic adenosine monophosphate
chem. sim.	chemical similarity, Tanimoto similarity
ChEMBL	Chemical database of bioactive molecules of the European Molecular Biology Laboratory
CoA	Coenzyme A
COMAS	Compound Management and Screening Center
CoQ	ubiquinone
CPA	cell painting assay
CQ	chloroquine
CtD	complexity-to-diversity
CycHex	cyclohexane

**D**

d. r.	diastereomeric ratio
DAPI	4', 6-diamidino-2-phenylindole, dihydrochloride
DBDMH	1,3-dibromo-5,5-dimethylhydantoin
DCE	dichloroethane
DMEM	dulbecco's modified eagle medium
DMA	dimethylacetamide
DMAP	dimethylamino-pyridine
DMC	dimethyl carbonate
DMF	dimethylformamide
DMSO	dimethylsulfoxid
DNA	deoxyribonucleic acid
DOS	diversity-oriented synthesis

**E**

EBSS	Earle's balanced salt solution
ECAR	extracellular acidification rate
EDTA	ethylenediaminetetraacetic acid
eGFP	enhanced green fluorescent protein
EGTA	Ethylene glycol-bis( $\beta$ -aminoethyl ether)- <i>N,N,N',N'</i> -tetraacetic acid
eq.	equivalent
ESI	electrospray ionization
et al.	<i>lat. et alia, and others</i>
Et <sub>3</sub> N	triethylamine
EtOAc	ethyl acetate
Expl. Var.	explained variance

**F**

FAD	flavin adenine dinucleotide
FBDD	fragment-based drug design
FBS	fetal bovine serum
FCCP	cyanide-4 (trifluoromethoxy) phenylhydrazone
FDA	US Food and Drug Administration

## Abbreviations

### G

GABARAP	GABA <sub>A</sub> receptor associated protein
GFP	green fluorescent protein
G-I-1/2	griseofulvin indole from Fischer indole reaction
G-IE	griseofulvin indolenines
GPC	gel permeation chromatography
G-THPI-b	$\beta$ -tetrahydropyrano indoles
G-THPI-g	indofulvins, $\gamma$ -tetrahydropyrano indoles

### H

h	hours
HDAC	histone deacetylases
HeLa	Henrietta Lacks cells
HOPS	homotypic fusion and protein sorting
HPLC	high-performance liquid chromatography
HPLC-MS	high-performance liquid chromatography with mass spectrometry
HRMS	high-resolution mass spectrometry

### I

+I	positive inductive effect
-I	negative inductive effect
IC <sub>50</sub>	half maximal inhibitory concentration
IP <sub>3</sub>	1,4,5-trisphosphate

### L

LCMS	liquid chromatography with mass spectrometry
LC3	microtubule-associated proteins 1A/1B light chain 3B
LiAlH <sub>4</sub>	lithium aluminum hydride

### M

+M	positive mesomeric effect
-M	negative mesomeric effect
MAD	mean absolute deviation



MBH	Morita-Baylis-Hillman
MBP	median biosimilarity percentage
MCF7	Michigan Cancer Foundation-7 cells
Me	methyl
MeCN	acetonitrile
MEM	modified eagle medium
MeOH	methanol
MLCK1	myosin light chain kinases 1
min	minutes
MS	mass spectrometry
mTOR	mammalian target of rapamycin
mTORC1	mTOR complex 1
mw	microwave
MW	molecular weight

**N**

<i>n</i>	sample size
<i>N</i>	total sample size
N	unaltered natural product
NAD	nicotinamide adenine dinucleotide
NB	botanical drug
NBS	<i>N</i> -bromosuccinimide
ND	natural product derivative
NM	mimic of natural product
NMR	nuclear magnetic resonance
NP	natural product
NP-40	4-nonylphenyl-polyethylene glycol
O	
OCR	oxygen consumption rate

**P**

P	partition coefficient
p62	sequestosome 1
PBS	phosphate-buffered saline

## Abbreviations

PC	Principal Component
PCA	Principal Component Analysis
PE	phosphatidylethanolamine
PI3K	phosphatidylinositol 3-kinase
PMI	principal moments of inertia
pr.	profile
pseudo-NP	pseudo-natural product
pTs	p-toluenesulfonic acid
<b>Q</b>	
QD-C	quinidine chromanones
QD-I	quinidine indoles
QED	quantitative estimation of drug-likeness
QN-C	quinine chromanones
QN-I	quinine indoles
Quant.	quantitative
<b>R</b>	
RNA	ribonucleic acid
ROS	reactive oxygen species
<i>rt</i>	room temperature
<b>S</b>	
S	synthetic drug
S*	synthetic drug (NP pharmacophore)
SAG	Smoothened agonist
SAR	structure-activity-relationship
S-C	sinomenine chromanones
SCONP	structural classification of NPs
SDS	sodium dodecyl sulfate
S-I	sinomenine indoles
sim.	similarity
SiO <sub>2</sub>	silica
S <sub>N</sub> Ar	aromatic nucleophilic substitution reaction

SNAP	soluble NSF attachment proteins
SNARE	SNAP receptor proteins
<b>T</b>	
<i>t</i>	time
<i>T</i>	temperature
TBAF	<i>tetra</i> - <i>n</i> -butylammonium fluoride
TBS	<i>tert</i> -butyldimethylsilyl group
<i>t</i> BuOK	potassium <i>tert</i> -butoxide
TCA	tricarboxylic acid cycle
TFA	trifluoroacetic acid
TFE	trifluoroethanol
TfOH	triflic acid
TfOH·SiO <sub>2</sub>	triflic acid immobilized on silica
THF	tetrahydrofuran
TLC	thin-layer chromatography
TsCl	tosyl chloride
<b>U</b>	
U-2OS	human bone osteosarcoma epithelial cells
uHPLC	ultra-high-performance liquid chromatography
ULK1	Unc-51 like autophagy activating kinase
<b>V</b>	
VAMP8	vesicle-associated membrane protein 8
VSP34	vacuolar protein sorting-associated protein 34

## REFERENCES

- [1] P. I. H. B. E. Zamir, *Nat. Chem. Biol.* **2008**, *4*, 643-647.
- [2] M. C. Bohacek RS, Guida WC, *Med Res Rev* **1996**, *16*, 3–50.
- [3] D. J. Newman, G. M. Cragg, *J Nat Prod* **2020**, *83*, 770-803.
- [4] D. G. Kingston, *J Nat Prod* **2011**, *74*, 496-511.
- [5] H. van Hattum, H. Waldmann, *J Am Chem Soc* **2014**, *136*, 11853-11859.
- [6] D. B. Kell, *FEBS J* **2013**, *280*, 5957-5980.
- [7] a) W. R. Galloway, A. Isidro-Llobet, D. R. Spring, *Nat Commun* **2010**, *1*, 80; b) M. D. Burke, S. L. Schreiber, *Angew Chem Int Ed Engl* **2004**, *43*, 46-58.
- [8] a) S. L. Schreiber, *Science* **2000**, *287*, 1964-1969; b) S. Dandapani, L. A. Marcaurelle, *Curr Opin Chem Biol* **2010**, *14*, 362-370; c) C. Cordier, D. Morton, S. Murrison, A. Nelson, C. O'Leary-Steele, *Nat Prod Rep* **2008**, *25*, 719-737.
- [9] R. W. Huigens, 3rd, K. C. Morrison, R. W. Hicklin, T. A. Flood, Jr., M. F. Richter, P. J. Hergenrother, *Nat Chem* **2013**, *5*, 195-202.
- [10] a) R. J. Rafferty, R. W. Hicklin, K. A. Maloof, P. J. Hergenrother, *Angew Chem Int Ed Engl* **2014**, *53*, 220-224; b) N. G. Paciaroni, R. Ratnayake, J. H. Matthews, V. M. t. Norwood, A. C. Arnold, L. H. Dang, H. Luesch, R. W. Huigens, 3rd, *Chemistry* **2017**, *23*, 4327-4335.
- [11] E. Llabani, R. W. Hicklin, H. Y. Lee, S. E. Motika, L. A. Crawford, E. Weerapana, P. J. Hergenrother, *Nat Chem* **2019**, *11*, 521-532.
- [12] M. Grigalunas, A. Burhop, A. Christoforow, H. Waldmann, *Curr Opin Chem Biol* **2020**, *56*, 111-118.
- [13] A. S. M. A. Koch, M. Scheck, S. Wetzel, M. Casaulta, A. Odermatt, P. Ertl, H. Waldmann, *PNAS* **2005**, *102*, 17272–17277.
- [14] V. Praveen Kumar, R. Gajendra Reddy, D. D. Vo, S. Chakravarty, S. Chandrasekhar, R. Gree, *Bioorg Med Chem Lett* **2012**, *22*, 1439-1444.
- [15] A. P. Antonchick, S. Lopez-Tosco, J. Parga, S. Sievers, M. Schurmann, H. Preut, S. Hoing, H. R. Scholer, J. Sternecker, D. Rauh, H. Waldmann, *Chem Biol* **2013**, *20*, 500-509.
- [16] P. J. Hajduk, J. Greer, *Nat Rev Drug Discov* **2007**, *6*, 211-219.
- [17] H. Chen, X. Zhou, A. Wang, Y. Zheng, Y. Gao, J. Zhou, *Drug Discov Today* **2015**, *20*, 105-113.

- [18] W. Mao, M. Ning, Z. Liu, Q. Zhu, Y. Leng, A. Zhang, *Bioorg Med Chem* **2012**, *20*, 2982-2991.
- [19] B. Over, S. Wetzel, C. Grutter, Y. Nakai, S. Renner, D. Rauh, H. Waldmann, *Nat Chem* **2013**, *5*, 21-28.
- [20] G. Karageorgis, D. J. Foley, L. Laraia, H. Waldmann, *Nat Chem* **2020**, *12*, 227-235.
- [21] G. Karageorgis, E. S. Reckzeh, J. Ceballos, M. Schwalfenberg, S. Sievers, C. Ostermann, A. Pahl, S. Ziegler, H. Waldmann, *Nat Chem* **2018**, *10*, 1103-1111.
- [22] T. Schneidewind, S. Kapoor, G. Garivet, G. Karageorgis, R. Narayan, G. Vendrell-Navarro, A. P. Antonchick, S. Ziegler, H. Waldmann, *Cell Chem Biol* **2019**, *26*, 512-523 e515.
- [23] D. J. Foley, S. Zinken, D. Corkery, L. Laraia, A. Pahl, Y. W. Wu, H. Waldmann, *Angew Chem Int Ed Engl* **2020**.
- [24] W. H. B. Sauer, M. K. Schwarz, *J. Chem. Inf. Comput. Sci.* **2003**, *43*, 987-1003.
- [25] C. F. Stratton, D. J. Newman, D. S. Tan, *Bioorg Med Chem Lett* **2015**, *25*, 4802-4807.
- [26] J. Boström, D. G. Brown, R. J. Young, G. M. Keserü, *Nature Reviews Drug Discovery* **2018**, *17*, 709-727.
- [27] D. C. Blakemore, L. Castro, I. Churcher, D. C. Rees, A. W. Thomas, D. M. Wilson, A. Wood, *Nat Chem* **2018**, *10*, 383-394.
- [28] T. S. A. Pictet, *Ber. Dtsch. Chem. Ges.* **1911**, *44*, 2030-2036.
- [29] J. Stockigt, A. P. Antonchick, F. Wu, H. Waldmann, *Angew Chem Int Ed Engl* **2011**, *50*, 8538-8564.
- [30] H. P. H. J. Stöckigt, C. Kan-Fan, M. H. Zenk, *J. Chem. Soc. Chem. Commun.* **1977**, 164 – 166.
- [31] E. L. Larghi, T. S. Kaufman, *European Journal of Organic Chemistry* **2011**, *2011*, 5195-5231.
- [32] S.-X. Z. J.-Z. Deng, *J. Nat. Prod.* **1997**, *60*, 294–295.
- [33] S. N. Y. Li, B. Sun, S. Liu, X. Liu, Y. Che, *Org. Lett.* **2010**, *12*, 3144–3147.
- [34] M. A. Maskeri, A. C. Brueckner, T. Feoktistova, M. J. O'Connor, D. M. Walden, P. H.-Y. Cheong, K. A. Scheidt, *Chemical Science* **2020**, *11*, 8736-8743.
- [35] C. Zhao, S. B. Chen, D. Seidel, *J Am Chem Soc* **2016**, *138*, 9053-9056.
- [36] S. Das, L. Liu, Y. Zheng, M. W. Alachraf, W. Thiel, C. K. De, B. List, *J Am Chem Soc* **2016**, *138*, 9429-9432.
- [37] S. P. Roche, J. A. Porco, Jr., *Angew Chem Int Ed Engl* **2011**, *50*, 4068-4093.

## References

- [38] R. E. Ziegler, S. J. Tan, T. S. Kam, J. A. Porco, Jr., *Angew Chem Int Ed Engl* **2012**, *51*, 9348-9351.
- [39] C. S. Yeung, R. E. Ziegler, J. A. Porco, Jr., E. N. Jacobsen, *J Am Chem Soc* **2014**, *136*, 13614-13617.
- [40] M. C. C. o. S. Barradas, M. Gonzalez-Lopez, A. Latorre, A., Urbano, *Org. Lett.* **2007**, *9*, 5019-5022.
- [41] L. Laraia, H. Waldmann, *Drug Discov Today Technol* **2017**, *23*, 75-82.
- [42] R. S. Lokey, *Current Opinion in Chemical Biology* **2003**, *7*, 91-96.
- [43] S. Ziegler, V. Pries, C. Hedberg, H. Waldmann, *Angew Chem Int Ed Engl* **2013**, *52*, 2744-2792.
- [44] D. C. Swinney, J. Anthony, *Nat Rev Drug Discov* **2011**, *10*, 507-519.
- [45] J. Inglese, R. L. Johnson, A. Simeonov, M. Xia, W. Zheng, C. P. Austin, D. S. Auld, *Nat Chem Biol* **2007**, *3*, 466-479.
- [46] M. A. Bray, S. Singh, H. Han, C. T. Davis, B. Borgeson, C. Hartland, M. Kost-Alimova, S. M. Gustafsdottir, C. C. Gibson, A. E. Carpenter, *Nat Protoc* **2016**, *11*, 1757-1774.
- [47] E. H. Hinchcliffe, C. A. Day, K. B. Karanjeet, S. Fadness, A. Langfald, K. T. Vaughan, Z. Dong, *Nat Cell Biol* **2016**, *18*, 668-675.
- [48] G. H. P. J. Lippincott-Schwartz, **2003**, *300*, 87-91.
- [49] E. C. K. Wrobel, F. Segade, S. Ramos, P. S. Laze, *J. Immunol. Methods* **1996**, *189*, 243-249.
- [50] Y. Wang, A. Cornett, Fred J. King, Y. Mao, F. Nigsch, C. G. Paris, G. McAllister, Jeremy L. Jenkins, *Cell Chemical Biology* **2016**, *23*, 862-874.
- [51] S. J. Warchal, Unciti-Broceta, A. & O'Carraher, N., *Futur. Med. Chem.* **2016**, *8*, 1331-1347.
- [52] L. Laraia, G. Garivet, D. J. Foley, N. Kaiser, S. Müller, S. Zinken, T. Pinkert, J. Wilke, D. Corkery, A. Pahl, S. Sievers, P. Janning, C. Arenz, Y. Wu, R. Rodriguez, H. Waldmann, *Angewandte Chemie International Edition* **2020**, *59*, 5721-5729.
- [53] A. Christoforow, J. Wilke, A. Binici, A. Pahl, C. Ostermann, S. Sievers, H. Waldmann, *Angew Chem Int Ed Engl* **2019**, *58*, 14715-14723.
- [54] a) R. S. Hippman, I. Pavlinov, Q. Gao, M. K. Mavlyanova, E. M. Gerlach, L. N. Aldrich, *ChemBiochem* **2020**; b) B. Melillo, J. Zoller, B. K. Hua, O. Verho, J. C. Borghs, S. D. Nelson, Jr., M. Maetani, M. J. Wawer, P. A. Clemons, S. L. Schreiber, *J Am Chem Soc* **2018**, *140*, 11784-11790.

- [55] T. Schneidewind, A. Brause, A. Pahl, A. Burhop, T. Mejuch, S. Sievers, H. Waldmann, S. Ziegler, *ChemBioChem* **2020**.
- [56] J. L. Ochoa, W. M. Bray, R. S. Lokey, R. G. Linington, *J Nat Prod* **2015**, *78*, 2242-2248.
- [57] Michael A. Mancini, S. M. Gustafsdottir, V. Ljosa, K. L. Sokolnicki, J. Anthony Wilson, D. Walpita, M. M. Kemp, K. Petri Seiler, H. A. Carrel, T. R. Golub, S. L. Schreiber, P. A. Clemons, A. E. Carpenter, A. F. Shamji, *PLoS ONE* **2013**, *8*.
- [58] M. J. Wawer, K. Li, S. M. Gustafsdottir, V. Ljosa, N. E. Bodycombe, M. A. Marton, K. L. Sokolnicki, M. A. Bray, M. M. Kemp, E. Winchester, B. Taylor, G. B. Grant, C. S. Y. Hon, J. R. Duvall, J. A. Wilson, J. A. Bittker, V. Dan ik, R. Narayan, A. Subramanian, W. Winckler, T. R. Golub, A. E. Carpenter, A. F. Shamji, S. L. Schreiber, P. A. Clemons, *Proceedings of the National Academy of Sciences* **2014**, *111*, 10911-10916.
- [59] D. R. Green, Galluzzi, L., Kroemer, G., *Science* **2011**, *333*, 1109-1112.
- [60] D. R. Green, B. Levine, *Cell* **2014**, *157*, 65-75.
- [61] S. W. Ryter, S. M. Cloonan, A. M. K. Choi, *Molecules and Cells* **2013**, *36*, 7-16.
- [62] A. S. Limpert, L. J. Lambert, N. A. Bakas, N. Bata, S. N. Brun, R. J. Shaw, N. D. P. Cosford, *Trends Pharmacol Sci* **2018**, *39*, 1021-1032.
- [63] K. Jing, K. Lim, *Exp Mol Med* **2012**, *44*, 69-72.
- [64] a) A. M. Palhegyi, E. Seranova, S. Dimova, S. Hoque, S. Sarkar, *Front Cell Dev Biol* **2019**, *7*, 179; b) D. J. Klionsky, *Nat. Rev. Mol. Cell Biol.* **2007**, *8*, 931-937.
- [65] W. J. Liu, L. Ye, W. F. Huang, L. J. Guo, Z. G. Xu, H. L. Wu, C. Yang, H. F. Liu, *Cell Mol Biol Lett* **2016**, *21*, 29.
- [66] A. Matsuura, Tsukada, M., Wada, Y. & Ohsumi, Y., *Gene* **1997**, 245-250.
- [67] a) A. Caccamo, S. Majumder, A. Richardson, R. Strong, S. Oddo, *Journal of Biological Chemistry* **2010**, *285*, 13107-13120; b) P. Spilman, N. Podlutskaya, M. J. Hart, J. Debnath, O. Gorostiza, D. Bredesen, A. Richardson, R. Strong, V. Galvan, *PLoS One* **2010**, *5*, e9979.
- [68] P. Wipf, R. J. Halter, *Org Biomol Chem* **2005**, *3*, 2053-2061.
- [69] R. Bago, N. Malik, M. J. Munson, A. R. Prescott, P. Davies, E. Sommer, N. Shpiro, R. Ward, D. Cross, I. G. Ganley, D. R. Alessi, *Biochem J* **2014**, *463*, 413-427.
- [70] L. Robke, L. Laraia, M. A. Carnero Corrales, G. Konstantinidis, M. Muroi, A. Richters, M. Winzker, T. Engbring, S. Tomassi, N. Watanabe, H. Osada, D. Rauh, H. Waldmann, Y. W. Wu, J. Engel, *Angew Chem Int Ed Engl* **2017**, *56*, 8153-8157.
- [71] M. Mauthe, I. Orhon, C. Rocchi, X. Zhou, M. Luhr, K. J. Hijlkema, R. P. Coppes, N. Engedal, M. Mari, F. Reggiori, *Autophagy* **2018**, *14*, 1435-1455.

## References

- [72] S. P. Roche, J.-J. Youte Tendoung, B. Tréguier, *Tetrahedron* **2015**, *71*, 3549-3591.
- [73] F. L. C. A. Lipinski, B. W. Dominy, P. J. Feeney, *Advanced Drug Delivery Reviews* **2001**, *46*, 3-26.
- [74] I. Colomer, C. J. Empson, P. Craven, Z. Owen, R. G. Doveston, I. Churcher, S. P. Marsden, A. Nelson, *Chem Commun (Camb)* **2016**, *52*, 7209-7212.
- [75] M. Q. Zhang, B. Wilkinson, *Curr Opin Biotechnol* **2007**, *18*, 478-488.
- [76] a) J. C. Caicedo, S. Cooper, F. Heigwer, S. Warchal, P. Qiu, C. Molnar, A. S. Vasilevich, J. D. Barry, H. S. Bansal, O. Kraus, M. Wawer, L. Paavolainen, M. D. Herrmann, M. Rohban, J. Hung, H. Hennig, J. Concannon, I. Smith, P. A. Clemons, S. Singh, P. Rees, P. Horvath, R. G. Linington, A. E. Carpenter, *Nat Methods* **2017**, *14*, 849-863; b) S. M. Gustafsdottir, V. Ljosa, K. L. Sokolnicki, J. Anthony Wilson, D. Walpita, M. M. Kemp, K. Petri Seiler, H. A. Carrel, T. R. Golub, S. L. Schreiber, P. A. Clemons, A. E. Carpenter, A. F. Shamji, *PLoS One* **2013**, *8*, e80999.
- [77] O. Mendez-Lucio, J. L. Medina-Franco, *Drug Discov Today* **2017**, *22*, 120-126.
- [78] M. P. R. Pradhan, A. K. Behera, B. K. Mishrab, and, R. K. Behera, *Tetrahedron* **2006**, *62*, 771-778.
- [79] S. Schunk, K. Linz, S. Frommann, C. Hinze, S. Oberborsch, B. Sundermann, S. Zemolka, W. Englberger, T. Germann, T. Christoph, B. Y. Kogel, W. Schroder, S. Harlfinger, D. Saunders, A. Kless, H. Schick, H. Sonnenschein, *ACS Med Chem Lett* **2014**, *5*, 851-856.
- [80] a) I. Knappmann, D. Schepmann, B. Wunsch, *Bioorg Med Chem* **2016**, *24*, 4045-4055; b) J. R. Song, Z. Y. Li, G. D. Wang, N. Zhang, C. Chen, J. Chen, H. Ren, W. Pan, *Advanced Synthesis & Catalysis* **2019**, *362*, 500-505.
- [81] C. F. A. de Angelis, P. Ingallina, L. Montanari, M.G. Clerici, C. Carati, C. Perego, *Catalysis Today* **2001**, *65*, 363-371.
- [82] P. N. Liu, F. Xia, Q. W. Wang, Y. J. Ren, J. Q. Chen, *Green Chemistry* **2010**, *12*.
- [83] R. Sundberg, *Elsevier* **2012**, *Organic Chemistry; A Series of Monographs Band 18 von Organic chemistry*.
- [84] J. A. M. Joule, K. , *Heterocyclic Chemistry* **2010**, *5th ed*.
- [85] a) F. De Simone, J. Gertsch, J. Waser, *Angew Chem Int Ed Engl* **2010**, *49*, 5767-5770; b) S. Pan, N. Ryu, T. Shibata, *J Am Chem Soc* **2012**, *134*, 17474-17477; cZ. Ding, N. Yoshikai, *Beilstein J Org Chem* **2012**, *8*, 1536-1542.
- [86] M. M. Catellani, E.; Della Ca', N, *Acc. Chem. Res.* **2008**, *41*, 1512-1522.
- [87] T. Bach, L. Jiao, *Synthesis* **2013**, *46*, 35-41.



- [88] a) Z. Rong, K. Gao, L. Zhou, J. Lin, G. Qian, *RSC Advances* **2019**, *9*, 17975-17978; b) R. Zhou, W. Wang, Z. J. Jiang, K. Wang, X. L. Zheng, H. Y. Fu, H. Chen, R. X. Li, *Chem Commun (Camb)* **2014**, *50*, 6023-6026.
- [89] a) C. R. Reddy, M. D. Reddy, B. Srikanth, K. R. Prasad, *Org Biomol Chem* **2011**, *9*, 6027-6033; b) C. R. Reddy, A. G. Burra, K. K. Singarapu, R. Grée, *European Journal of Organic Chemistry* **2016**, *2016*, 5274-5281.
- [90] S. P. Park, S.-H. Ahn, K.-J. Lee, *Tetrahedron* **2010**, *66*, 3490-3498.
- [91] H. Vu, L. Pedro, T. Mak, B. McCormick, J. Rowley, M. Liu, A. Di Capua, B. Williams-Noonan, N. B. Pham, R. Pouwer, B. Nguyen, K. T. Andrews, T. Skinner-Adams, J. Kim, W. G. J. Hol, R. Hui, G. J. Crowther, W. C. Van Voorhis, R. J. Quinn, *ACS Infect Dis* **2018**, *4*, 431-444.
- [92] C. K. Ingold, *J Am Chem Soc* **1933**, 1120-1127.
- [93] M. M. N. Otero, R. A. Mosquera, *J. Phys. Chem. A* **2007**, *111*, 5557-5562.
- [94] M. Li, J. Xiong, Y. Huang, L.-J. Wang, Y. Tang, G.-X. Yang, X.-H. Liu, B.-G. Wei, H. Fan, Y. Zhao, W.-Z. Zhai, J.-F. Hu, *Tetrahedron* **2015**, *71*, 5285-5295.
- [95] S. J. Gharpure, V. Prasath, *Org Biomol Chem* **2014**, *12*, 7397-7409.
- [96] S. R. Peter Ertl, and Ansgar Schuffenhauer, *J. Chem. Inf. Model.* **2008**, *48*, 68-74.
- [97] v. Drugbank approved and experimental drugs, <https://www.drugbank.ca/releases/latest#structures> **2020**.
- [98] ChEMBL26, [ftp://ftp.ebi.ac.uk/pub/databases/chembl/ChEMBLdb/releases/chembl\\_26/](ftp://ftp.ebi.ac.uk/pub/databases/chembl/ChEMBLdb/releases/chembl_26/) **2020**, filtered for compounds from journal "J. Nat. Prod." or "J Nat Prod".
- [99] <http://www.rdkit.org>.
- [100] C. C. Loh, D. Enders, *Angew Chem Int Ed Engl* **2012**, *51*, 46-48.
- [101] M. J. James, P. O'Brien, R. J. Taylor, W. P. Unsworth, *Chemistry* **2016**, *22*, 2856-2881.
- [102] O. Domotor, S. Aicher, M. Schmidlehner, M. S. Novak, A. Roller, M. A. Jakupec, W. Kandioller, C. G. Hartinger, B. K. Keppler, E. A. Enyedy, *J Inorg Biochem* **2014**, *134*, 57-65.
- [103] M. K. Manibusan, M. Odin, D. A. Eastmond, *J Environ Sci Health C Environ Carcinog Ecotoxicol Rev* **2007**, *25*, 185-209.
- [104] S.-J. Tan, Y.-M. Choo, N. F. Thomas, W. T. Robinson, K. Komiyama, T.-S. Kam, *Tetrahedron* **2010**, *66*, 7799-7806.
- [105] M. A. B. Ferrer, H. Garcia, *Green Solvents I. Springer, Dordrecht* **2012**, 363-374.
- [106] S. J. M. A. F. Abdel-Magid, *Org. Process Res. Dev.* **2006**, *10*, 971-1031.

## References

- [107] A. D. Balgi, B. D. Fonseca, E. Donohue, T. C. Tsang, P. Lajoie, C. G. Proud, I. R. Nabi, M. Roberge, *PLoS One* **2009**, *4*, e7124.
- [108] D. J. Klionsky, K. Abdelmohsen, A. Abe, M. J. Abedin, H. Abeliovich, A. Acevedo Arozena, H. Adachi, C. M. Adams, P. D. Adams, K. Adeli, P. J. Adhietty, S. G. Adler, G. Agam, R. Agarwal, M. K. Aghi, M. Agnello, P. Agostinis, P. V. Aguilar, J. Aguirre-Ghiso, E. M. Airolidi, S. Ait-Si-Ali, T. Akematsu, E. T. Akporiaye, M. Al-Rubeai, G. M. Albaiceta, C. Albanese, D. Albani, M. L. Albert, J. Aldudo, H. Algul, M. Alirezaei, I. Alloza, A. Almasan, M. Almonte-Beceril, E. S. Alnemri, C. Alonso, N. Altan-Bonnet, D. C. Altieri, S. Alvarez, L. Alvarez-Erviti, S. Alves, G. Amadoro, A. Amano, C. Amantini, S. Ambrosio, I. Amelio, A. O. Amer, M. Amessou, A. Amon, Z. An, F. A. Anania, S. U. Andersen, U. P. Andley, C. K. Andreadi, N. Andrieu-Abadie, A. Anel, D. K. Ann, S. Anoopkumar-Dukie, M. Antonioli, H. Aoki, N. Apostolova, S. Aquila, K. Aquilano, K. Araki, E. Arama, A. Aranda, J. Araya, A. Arcaro, E. Arias, H. Arimoto, A. R. Ariosa, J. L. Armstrong, T. Arnould, I. Arsov, K. Asanuma, V. Askanas, E. Asselin, R. Atarashi, S. S. Atherton, J. D. Atkin, L. D. Attardi, P. Auburger, G. Auburger, L. Aurelian, R. Autelli, L. Avagliano, M. L. Avantaggiati, L. Avrahami, S. Awale, N. Azad, T. Bachetti, J. M. Backer, D. H. Bae, J. S. Bae, O. N. Bae, S. H. Bae, E. H. Baehrecke, S. H. Baek, S. Baghdiguan, A. Bagniewska-Zadworna, et al., *Autophagy* **2016**, *12*, 1-222.
- [109] a) N. Mizushima, T. Yoshimori, B. Levine, *Cell* **2010**, *140*, 313-326; b) F. Y. M. C. T. N. Campbell, *Mol. Biol. Today* **2001**, *2*, 1-4.
- [110] B. D. S. Marisan R. Mejillano, R. H. Himes, *Archives of Biochem. and Biophys.* **1996**, *336*, 130-138.
- [111] M. Grigalunas, A. Burhop, S. Zinken, A. Pahl, S. Sievers, D. Foley, H. Waldmann, *Nat. Commun.* **2020**, under revision.
- [112] L. Robke, Y. Futamura, G. Konstantinidis, J. Wilke, H. Aono, Z. Mahmoud, N. Watanabe, Y. W. Wu, H. Osada, L. Laraia, H. Waldmann, *Chem Sci* **2018**, *9*, 3014-3022.
- [113] L. Laraia, A. Friese, D. P. Corkery, G. Konstantinidis, N. Erwin, W. Hofer, H. Karatas, L. Klewer, A. Brockmeyer, M. Metz, B. Scholermann, M. Dwivedi, L. Li, P. Rios-Munoz, M. Kohn, R. Winter, I. R. Vetter, S. Ziegler, P. Janning, Y. W. Wu, H. Waldmann, *Nat Chem Biol* **2019**, *15*, 710-720.
- [114] a) K. Okamoto, N. Kondo-Okamoto, *Biochim Biophys Acta* **2012**, *1820*, 595-600; b) J. Lee, S. Giordano, J. Zhang, *Biochem J* **2012**, *441*, 523-540.
- [115] M. Graef, J. Nunnari, *EMBO J* **2011**, *30*, 2101-2114.
- [116] N. Kaiser, Corkery, D., Wu Y., Laraia, L., Waldmann H., *Bioorg. Med. Chem.* **2019**, *27*, 2444-2448.
- [117] J. A. S. R. M. Bertina, E. C. Slater, *Biochimica et Biophysica Acta (BBA) - Bioenergetics* **1974**, *368*, 279-297.
- [118] J. Zhang, Q. Zhang, *Methods Mol Biol* **2019**, *1928*, 353-363.
- [119] J. T. J. K. Chen, K. E. Young, T. Maiti, and P. A. Beachy, *PNAS* **2002**, *99*, 14071-14076.

- [120] A. Pierzynska-Mach, P. A. Janowski, J. W. Dobrucki, *Cytometry A* **2014**, *85*, 729-737.
- [121] a) A. E. Oxford;, H. Raistrick;, P. Simonart, *Biochem J* **1939**, *33* 240–248; b) G. V. B. R. D.Sloboda, W. A.Creasey, J. L.Rosenbaum, S. E. Malawista, *Biochemical and Biophysical Research Communications* **1982**, *105*, 882-888.
- [122] T. Voigt, C. Gerding-Reimers, T. T. Ngoc Tran, S. Bergmann, H. Lachance, B. Scholermann, A. Brockmeyer, P. Janning, S. Ziegler, H. Waldmann, *Angew Chem Int Ed Engl* **2013**, *52*, 410-414.
- [123] N. Kumar, *J. Bio. Chem.* **1981**, *256*, 10435-10441.
- [124] F. He, *Bio. Protocol* **2011**, *1*.
- [125] M. H. Woehrmann, W. M. Bray, J. K. Durbin, S. C. Nisam, A. K. Michael, E. Glassey, J. M. Stuart, R. S. Lokey, *Mol Biosyst* **2013**, *9*, 2604-2617.

## CURRICULUM VITAE (LEBENS LAUF)

### Personal Information

---

Surname	Burhop
Name	Annina
Date of Birth	09.03.1992
Place of Birth	Hoya (Weser) Lower Saxony, Germany
Citizenship	German

### Education

---

04/2017 – 11/2020	PhD student in Chemical Biology Max Planck Institute of Molecular Physiology, Dortmund, Germany  Thesis: Pseudo-Natural Products via Pictet-Spengler Reaction and Dearomatization Supervisor: Prof. Dr. Dr. h.c. Herbert Waldmann
10/2014 – 03/2017	Master of Science in Medicinal and Natural Product Chemistry Leibniz University Hannover, Hanover, Germany  Thesis: Untersuchung des Wasserstoff/Deuterium-Austausches von sekundären und tertiären Sulfonamiden mittels Iridium-katalysierter C-H-Aktivierung with Sanofi-Aventis Deutschland GmbH, Frankfurt am Main, Germany Supervisor: Prof. Dr. Mark Brönstrup, Prof. Dr. Andreas Kirschning, Dr. Jens Atzrodt, and Dr. Volker Derdau  Research stay: Imperial College London, London, United Kingdom Supervisor: Prof. Dr. Ed Tate

10/2011 – 09/2014

Bachelor of Science in Biochemistry

Leibniz University Hannover, Hanover, Germany

Thesis: Variation in host susceptibility in acute *Pseudomonas aeruginosa* infection

Supervisor: Dr. Lutz Wiehlmann, Dr. Antje Munder

# EIDESSTÄTLICHE VERSICHERUNG (AFFIDAVIT)

## Eidesstattliche Versicherung (Affidavit)

Burhop, Annina

200437

Name, Vorname  
(Surname, first name)

Matrikel-Nr.  
(Enrolment number)

**Belehrung:**

Wer vorsätzlich gegen eine die Täuschung über Prüfungsleistungen betreffende Regelung einer Hochschulprüfungsordnung verstößt, handelt ordnungswidrig. Die Ordnungswidrigkeit kann mit einer Geldbuße von bis zu 50.000,00 € geahndet werden. Zuständige Verwaltungsbehörde für die Verfolgung und Ahndung von Ordnungswidrigkeiten ist der Kanzler/die Kanzlerin der Technischen Universität Dortmund. Im Falle eines mehrfachen oder sonstigen schwerwiegenden Täuschungsversuches kann der Prüfling zudem exmatrikuliert werden, § 63 Abs. 5 Hochschulgesetz NRW.

Die Abgabe einer falschen Versicherung an Eides statt ist strafbar.

Wer vorsätzlich eine falsche Versicherung an Eides statt abgibt, kann mit einer Freiheitsstrafe bis zu drei Jahren oder mit Geldstrafe bestraft werden, § 156 StGB. Die fahrlässige Abgabe einer falschen Versicherung an Eides statt kann mit einer Freiheitsstrafe bis zu einem Jahr oder Geldstrafe bestraft werden, § 161 StGB.

Die oben stehende Belehrung habe ich zur Kenntnis genommen.

**Official notification:**

Any person who intentionally breaches any regulation of university examination regulations relating to deception in examination performance is acting improperly. This offence can be punished with a fine of up to EUR 50,000.00. The competent administrative authority for the pursuit and prosecution of offences of this type is the chancellor of the TU Dortmund University. In the case of multiple or other serious attempts at deception, the candidate can also be unenrolled, Section 63, paragraph 5 of the Universities Act of North Rhine-Westphalia.

The submission of a false affidavit is punishable.

Any person who intentionally submits a false affidavit can be punished with a prison sentence of up to three years or a fine, Section 156 of the Criminal Code. The negligent submission of a false affidavit can be punished with a prison sentence of up to one year or a fine, Section 161 of the Criminal Code.

I have taken note of the above official notification.

Dortmund,

Ort, Datum  
(Place, date)

Unterschrift  
(Signature)

Titel der Dissertation:  
(Title of the thesis):

Pseudo-Natural Products via Pictet-Spengler Reaction and Dearomatization

Ich versichere hiermit an Eides statt, dass ich die vorliegende Dissertation mit dem Titel selbstständig und ohne unzulässige fremde Hilfe angefertigt habe. Ich habe keine anderen als die angegebenen Quellen und Hilfsmittel benutzt sowie wörtliche und sinngemäße Zitate kenntlich gemacht.

Die Arbeit hat in gegenwärtiger oder in einer anderen Fassung weder der TU Dortmund noch einer anderen Hochschule im Zusammenhang mit einer staatlichen oder akademischen Prüfung vorgelegen.

I hereby swear that I have completed the present dissertation independently and without inadmissible external support. I have not used any sources or tools other than those indicated and have identified literal and analogous quotations.

The thesis in its current version or another version has not been presented to the TU Dortmund University or another university in connection with a state or academic examination.\*

\*Please be aware that solely the German version of the affidavit ("Eidesstattliche Versicherung") for the PhD thesis is the official and legally binding version.

Dortmund,

Ort, Datum  
(Place, date)

Unterschrift  
(Signature)